

Modeling and Identification of Linear
Parameter-Varying Systems
an Orthonormal Basis Function Approach

Cover: LPV system identification
R. Tóth, tothrola@ieee.org

**MODELING AND IDENTIFICATION
OF LINEAR PARAMETER-VARYING
SYSTEMS**
an Orthonormal Basis Function Approach

PROEFSCHRIFT

ter verkrijging van de graad van doctor
aan de Technische Universiteit Delft,
op gezag van de Rector Magnificus prof. dr. ir. J.T. Fokkema,
voorzitter van het College voor Promoties,
in het openbaar te verdedigen op
maandag 22 december 2008 om 12:30 uur

door

Roland TÓTH

Master of Engineering, University of Pannonia
geboren te Miskolc, Hongarije

Dit proefschrift is goedgekeurd door de promotor:

Prof. dr. ir. P. M. J. Van den Hof

Copromotor: Dr. P. S. C. Heuberger

Samenstelling promotiecommissie:

Rector Magnificus,	voorzitter
Prof. dr. ir. P. M. J. Van den Hof,	Technische Universiteit Delft, promotor
Dr. P. S. C. Heuberger,	Technische Universiteit Delft, copromotor
Prof. dr. C. W. Scherer,	Technische Universiteit Delft
Prof. dr. ir. J. C. Willems,	Katholieke Universiteit Leuven
Prof. dr. ir. M. Steinbuch,	Technische Universiteit Eindhoven
Prof. dr. ir. J. Schoukens,	Vrije Universiteit Brussel
Prof. dr. ir. B. Wahlberg,	Royal Institute of Technology, Stockholm
Prof. dr. ir. J. Hellendoorn,	Technische Universiteit Delft, reservelid

disc

The research reported in this thesis is part of the research program of the Dutch Institute of Systems and Control (DISC). The author has successfully completed the educational program of the Graduate School DISC.

The logo for the Netherlands Organisation for Scientific Research (NWO). It features the letters 'NWO' in a stylized, black, sans-serif font. A red swoosh or underline is positioned above the 'O', extending from the 'W' and curving under the 'O'.

This research was financially supported by the Netherlands Organisation for Scientific Research (NWO) in the framework of the Free Competition, project 613.000.306.

ISBN: 978-90-9023742-8

Copyright © 2008 by R. Tóth.

All rights reserved. No part of the material protected by this copyright notice may be reproduced or utilized in any form or by any means, electronic or mechanical, including photocopying, recording or by any information storage and retrieval system, without written permission from the copyright owner.

Printed in the Netherlands.

Acknowledgments

Looking back on the past four years, one thing is sure, time has slipped by so swiftly that it feels like yesterday when I first walked the corridors of the *Delft Center for Systems and Control* (DCSC). At the same time, I cherish all the countless memories that bound my heart to this place and to the people whom I worked with and walked those corridors with day by day. I owe many people a lot for their support, encouragement, and advice, which have contributed directly or indirectly to this thesis and the scientific research associated with it.

Besides these general words of gratitude, a number of people deserves special attention. First, I would like to express my thanks towards my supervisors Paul Van den Hof and Peter Heuberger for their excellent guidance and friendship over the years. They were always there helping to find the missing wheel or rejoicing in the success of a breakthrough. Their support both in terms of research and personal matters made my life a lot easier. I also would like to thank Carsten Scherer for many discussions. His ability to understand abstract ideas sharply from half words or bad notation always amazes me.

I would also like to thank many people for inspiration. Especially to Jan Willems, whose advice and vision about mathematical modeling helped me find a road leading to many results of this work. I am also thankful to Federico Felici for his earth-moving questions and discussions which made me aware of missing key points of *Linear Parameter-Varying* (LPV) system theory. I am also grateful to István Györi, who first taught me how to conduct research, to Katalin Hangos, who introduced me to the universe of control system theory, and to Dénes Fodor, who led my first adventure in LPV control. Without them, I would have never walked those corridors.

Furthermore, I want to thank all members of DCSC for the scientific conversations and the pleasant working atmosphere. Especially to Sjoerd Dietz who made some of my conferences an unforgettable adventure and to Zsófia Lendek, Lucian Busoniu, Hakan Köroğlu, and Tamás Keviczky with whom I always had excellent conversations in the coffee breaks. Special thanks go also to Rogier Blom, Diederick Joosten, Jan-Willem van Wingerden, Jorn van Doren, and to the man who is always ready for jokes: Eric Trottemant. I also thank to Hung Nguyen Tien for a fruitful cooperation. I am also grateful Karel Hinnen for providing me a beautiful style file for this thesis.

The financial support of NWO (The Netherlands Organization for Scientific

Research) is also gratefully acknowledged. The research presented in this thesis is part of the project: 613.000.306, *Identification and control of LPV systems using orthonormal basis functions*.

My family deserves major gratitude for their continuous support and motivation, which has helped me to shape my life as it is. My mother taught me to look in the future with hope and confidence and my father has always been an example for me in precision and persistency.

However, my greatest thanks go to my wife Andrea, whose tender love has been a miracle in my life. She was always there in these years, in every moment, supporting me to accomplish all that I was aiming at. She is more than I could ever wish for, as she is all that I would ever need. Last but not least, I thank our son Sándor for all the drawings and stamps he made on my manuscripts to make his father happy and also our daughter Lujza for the smiles to warm my heart. They always worked. It is to them whom I dedicate this thesis.

Delft, December 2008
Roland Tóth

Contents

Acknowledgments	v
1 Introduction	1
1.1 New challenges of system identification	1
1.2 The birth of LPV systems	3
1.3 The present state of LPV identification	4
1.3.1 The identification cycle	4
1.3.2 General picture of LPV identification	6
1.3.3 LPV-IO representation based methods	8
1.3.4 LPV-SS representation based methods	10
1.3.5 Similarity to other system classes	13
1.4 Challenges and open problems	13
1.5 Perspectives of OBF models	16
1.6 Problem statement	18
1.7 Overview of contents and results	21
2 LTI systems and OBFs	25
2.1 General class of LTI systems	25
2.1.1 Dynamical systems	25
2.1.2 Representations of continuous-time LTI systems	27
2.1.3 Representations of discrete-time LTI systems	31
2.1.4 Equivalence classes and relations	34
2.1.5 Stability of LTI systems	38
2.1.6 State-space canonical forms	42
2.1.7 Relation of state-space and input-output domains	51
2.1.8 Discretization of LTI system representations	56
2.2 Orthonormal basis functions	61

2.2.1	Signal spaces and inner functions	62
2.2.2	General class of orthonormal basis functions	63
2.3	Modeling and Identification of LTI systems	68
2.3.1	Concepts of the identification setting	68
2.3.2	Model structures	70
2.3.3	Properties	71
2.3.4	Linear regression	73
2.3.5	Identification with OBFs	73
2.3.6	Pole uncertainty of model estimates	76
2.3.7	Validation in the prediction error setting	81
2.4	The Kolmogorov n -width theory	81
2.5	Fuzzy clustering	84
2.6	Summary	88
3	LPV systems and representations	91
3.1	General class of LPV systems	91
3.1.1	Parameter varying dynamical systems	92
3.1.2	Representations of continuous-time LPV systems	95
3.1.3	Representations of discrete-time LPV systems	106
3.2	Equivalence classes and relations	114
3.3	Properties of LPV systems & representations	123
3.3.1	State-observability and reachability	123
3.3.2	Stability of LPV systems	136
3.3.3	Gramians of LPV state-space representations	141
3.4	Summary	142
4	LPV equivalence transformations	145
4.1	State-space canonical forms	145
4.1.1	The observability canonical form	146
4.1.2	Reachability canonical form	151
4.1.3	Companion canonical forms	155
4.1.4	Transpose of SS representations	156
4.1.5	LTI vs LPV state transformation	156
4.2	From state-space to the input-output domain	158
4.3	From the input-output to the state-space domain	162
4.4	Summary	172

5	LPV series expansion representations	175
5.1	Introduction	175
5.2	Impulse response representation of LPV systems	176
5.3	LPV series-expansion by OBFs	180
5.4	Series expansions and gain-scheduling	182
5.5	Summary	185
6	Discretization of LPV systems	187
6.1	The importance of discretization	187
6.2	Discretization of LPV system representations	189
6.3	Discretization of state-space representations	190
6.3.1	Approximative state-space discretization methods	193
6.4	Discretization errors and performance criteria	196
6.4.1	Local discretization errors	196
6.4.2	Global convergence and preservation of stability	199
6.4.3	Guaranteeing a desired level of discretization error	205
6.4.4	Switching effects	207
6.5	Properties of the discretization approaches	207
6.6	Discretization and dynamic dependence	208
6.7	Numerical example	210
6.8	Summary	212
7	LPV modeling of physical systems	215
7.1	Introduction	215
7.2	General questions of LPV modeling	216
7.3	Modeling of NL systems in the LPV framework	218
7.3.1	Linearization based approximation methods	220
7.3.2	Multiple model design procedures	223
7.3.3	Substitution based transformation methods	224
7.3.4	Automated model transformation	227
7.3.5	Summary of existing techniques	229
7.4	Translation of first principle models to LPV systems	230
7.4.1	Problem statement	231
7.4.2	The transformation algorithm	231
7.4.3	Handling non-factorizable terms	236
7.4.4	Properties of the transformation procedure	238
7.5	Summary	239

8	Optimal selection of OBFs	241
8.1	Perspectives of OBFs selection	241
8.2	Kolmogorov n -width optimality in the frozen sense	243
8.3	The Fuzzy-Kolmogorov c -Max clustering approach	245
8.3.1	The pole clustering algorithm	246
8.3.2	Properties of the FKcM	248
8.3.3	Simulation example	252
8.4	Robust extension of the FKcM approach	258
8.4.1	Questions of robustness	259
8.4.2	Basic concepts of hyperbolic geometry	260
8.4.3	Pole uncertainty regions as hyperbolic objects	264
8.4.4	The robust pole clustering algorithm	267
8.4.5	Properties of the robust FKcM	269
8.4.6	Simulation example	271
8.5	Summary	276
9	LPV identification via OBFs	279
9.1	Introduction	279
9.2	OBFs based LPV model structures	281
9.2.1	The LPV prediction error framework	281
9.2.2	The Wiener and the Hammerstein OBF models	285
9.2.3	Properties of Wiener and the Hammerstein OBF models	288
9.2.4	OBF models vs other model structures	290
9.2.5	Identification of W-LPV and H-LPV OBF models	293
9.3	Identification with static dependence	295
9.3.1	The identification setting	295
9.3.2	LPV identification with fixed OBFs	296
9.3.3	Local approach	297
9.3.4	Global approach	298
9.3.5	Properties	300
9.3.6	Examples	307
9.4	Approximation of dynamic dependence	312
9.4.1	Feedback-based OBF model structures	312
9.4.2	Properties of Wiener and Hammerstein feedback models	315
9.4.3	Identification by dynamic dependence approximation	316
9.4.4	Properties	320
9.4.5	Example	321
9.5	Extension towards MIMO systems	324
9.6	Summary	328

10 Conclusions and Recommendations	331
10.1 Conclusions	331
10.2 Contributions to the state-of-the-art	335
10.3 Recommendations for future research	337
A Proofs	339
A.1 Proofs of Chapter 3	339
A.2 Proofs of Chapter 5	341
A.3 Proofs of Chapter 8	344
A.4 Proofs of Chapter 9	351
Bibliography	353
Summary	367
Samenvatting	369
List of Symbols	371
List of Abbreviations	381
List of Publications	383
Curriculum Vitae	385

Introduction

The common need for accurate and efficient control of today's industrial applications is driving the system identification field to face the constant challenge of providing better models of physical phenomena. Systems encountered in practice are often nonlinear or have time-varying nature. Dealing with models of such kind without any structure is often found infeasible in practice. This rises the need for system descriptions that form an intermediate step between *Linear Time-Invariant* (LTI) systems and nonlinear/time-varying plants. To cope with these expectations, the model class of *Linear Parameter-Varying* (LPV) systems provides an attractive candidate. The philosophy of LPV systems is to represent the physical reality as a set of LTI systems from which one is selected at every time instance to describe the continuation of the signal trajectories. The LPV system class has a wide representation capability of physical processes and this framework is also supported by a well worked out and industrially reputed control theory. Despite the advances of the LPV control field, identification of such systems is still in its immature state, due to many open problems of LPV system theory. This thesis focusses on the development of a unified system theoretic view on general LPV systems. Using this unified framework, it proposes a novel way to identify LPV systems, as models of an underlying physical system. In this introductory chapter, the problem statement of this thesis is explained together with a brief overview of the state-of-the-art in the LPV field, underlying the need for improvement. This forms the starting point for motivating the followed research strategy. The chapter finishes with a brief overview of the context and the main contributions.

1.1 New challenges of system identification

Today, the need to optimize efficiency of plants in terms of performance or energy consumption and to improve reliability of automatization results in increas-

ing expectations towards automatic control applications. Engineers working in the control field have to face challenges in terms of operating industrial process in a more accurate way but at the same time with a lower cost in terms of used energy. For example in lithography, moving stages of wafer stepper machines today require fast and accurate positioning in the nanometer scale. In the emerging alternative energy field, the coupled nonlinear nature of wind turbines and the rapidly changing conditions of wind and grid load require more efficient and also easily reconfigurable control solutions. On the other hand, economical efficiency also drives the control field to replace existing control designs with solutions that require less sensors or actuators, but still provide the same performance. Like in the case of induction motors, high performance control based on less built-in sensors, like speed-sensorless drives, has great economical importance. To cope with these challenges, well applicable theoretical solutions have been developed like optimal, robust, and *nonlinear* (NL) control approaches, trying to refine and extend the results of *Linear Time-Invariant* (LTI) control theory, widely used in automatization. However to achieve the aimed objectives by these approaches, it is vital that an accurate, compact, and reliable mathematical description of the actual physical phenomenon is available.

First principle laws of physics, chemistry, biology etc. are commonly used to construct a dynamic model of the system of interest. However, such a procedure requires detailed process knowledge from specialists. Often it is a challenge to assemble the existing knowledge into a coherent and compact mathematical description. Usually, this results in a very complex model of the system dynamics, as it is hard to decide which effects are relevant and must be included in the final model and which are negligible. Such an approach is also often found to be very laborious and expensive. If the specialist's knowledge is lacking, like in case of poorly understood systems, the derivation of a model from first principles is even impossible. Moreover, certain quantities, like coefficients, rates, etc. required to build the model are often unknown, and have to be estimated by performing dedicated experiments.

Descriptions of systems can alternatively be derived by system identification, where the estimation of a dynamical model is accomplished directly from measured input-output data. The expert knowledge still has a major role, as it gives the basic source of information that is used in the decision on parameterization, model-structure selection, experiment design, and the actual way of deriving the estimate. This knowledge also helps in judging the quality and applicability of the obtained models. Even if system identification requires human intervention and expert knowledge to arrive at appropriate models, it also gives a general framework in which most of the steps can be automated, providing a less laborious and cost intensive modeling process.

Starting from frequency domain approaches in the early 1940s, over the years considerable attention has been given to the identification of LTI systems, which have proven their usefulness in many engineering applications. Today LTI system identification has become a strongly founded framework considering issues of uncertainty and closed-loop identification with a vast theory on experiment design (for an overview see Pintelon and Schoukens (2001)). But the need to operate

processes with higher accuracy/efficiency, has soon resulted in the realization that the commonly NL and *Time-Varying* (TV) nature of many physical systems must be handled by the control designs. This required better models, which initiated a significant research effort spent on identification and modeling of NL and *Linear Time-Varying* (LTV) systems (see Ginnakis and Serpedin (2001) and Niedźwiecki (2000) about the developed approaches). Despite many theoretical solutions, dealing with NL models without any structure has been found infeasible in practice both in terms of identification and control. Today, engineers working in the industry still prefer the application of LTI control-designs, due to the attractive approaches of optimal and robust control. These approaches are preferred as they guarantee high performance and reliability, have easy and quick design schemes, and engineers have a vast experience in their application. Additionally, it has been also observed in practice that many NL systems can be well approximated by multiple LTI models that describe the behavior of the plant around some operation points. The recognition manifested in the 1980s, that instead jumping into the deep-space of NL and TV systems, a model class is needed which can serve as an extension of the existing LTI control approaches, but is still able to incorporate NL and TV dynamical aspects. This recognition and the observation of multiple LTI modeling have led to the birth of *Linear Parameter-Varying* (LPV) systems through the idea of gain-scheduling (Shamma and Athans 1992).

1.2 The birth of LPV systems

In gain-scheduling, the basic concept is to linearize the NL system model at different operating points resulting in a collection of local LTI descriptions of the plant (see Figure 1.1). Then subsequently, LTI controllers are designed for each local aspect. These controllers are interpolated to give a global control solution to the entire operation regime (Rugh 1991). The used interpolation function is called the *scheduling function* in this framework and it is dependent on the current operating point of the plant. To describe the changes of the operating point, a signal is introduced, which is called the *scheduling signal* and often denoted by p . In this way, the parameters of the resulting controller are dependent on the varying signal p , hence the name *parameter-varying*, while the dynamic relation between the system signals is still *linear*. Due to many successful applications of this design methodology (Spong 1987; Whatley and Pot 1984; Stein 1980), gain-scheduling has become popular in industrial applications, even if guarantees for overall stability of the designed LPV controllers have not been available and the possibility of malfunction has existed. After 20 years, this has been resolved when interpolation based methods appeared that guarantee global stability (Stilwell and Rugh 2000; Korba and Werner 2001). Soon it has been realized that in general many NL systems can be converted into an LPV form. Approaches have appeared that provided direct LPV models for gain-scheduling without the laborious process of NL system modeling or identification (Milanese and Vicino 1991; Nemani et al. 1995; Carter and Shamma 1996; Tan 1997). LPV control has gained momentum during the 1990s, when the first results about the extension of \mathcal{H}_∞ and \mathcal{H}_2 optimal control through *Linear Matrix Inequalities* (LMIs) based optimization appeared (see Scherer (1996);

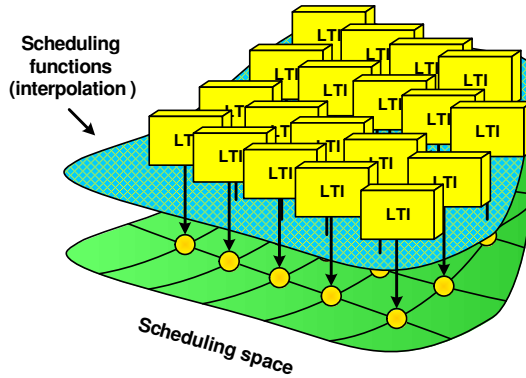


Figure 1.1: The mechanism of gain-scheduling: interpolation of local LTI models/controllers of the plant to approximate the global behavior on the entire operation regime, i.e. scheduling space.

Apkarian and Gahinet (1995); and Packard (1994) together with robust LTI control originated μ -synthesis approaches (Zhou and Doyle 1998). Contrary to the former methods, these approaches guarantee stability, optimal performance, and robustness over the entire operating regime of LPV models. Since then, the LPV field has evolved rapidly in the last 15 years and became a promising framework for modern industrial control with a growing number of applications like aircrafts (Marcos and Balas 2004; Verdult et al. 2004), wind turbines (Bianchi et al. 2007; Lescher et al. 2006), induction motors (Tóth and Fodor 2004; Prempain et al. 2002), compressors (Giarré et al. 2006), servo systems (Wijnheijmer et al. 2006), wafer steppers (Wassink et al. 2004; Steinbuch et al. 2003), internet web servers (Qin and Wang 2007), and CD-players (Dettori and Scherer 2001). Unfortunately, LPV system identification and modeling could barely keep up with the advances of the control field. Only very recently, initiatives have been taken to explore many open problems and questions in this area.

1.3 The present state of LPV identification

In the following, a general picture about the state-of-the-art in LPV system identification is presented. However, before going into details, we establish the key steps of the classical identification framework where the specifics of the LPV identification methods can be positioned and categorized.

1.3.1 The identification cycle

Identification of dynamical systems on the basis of experimentally measured data consists of several design steps, which need careful treatment in order to produce a desired model of the system. These steps are summarized in the so called identification cycle presented in Table 1.1. This set of steps is referred as a cycle, due to

Table 1.1: The identification cycle

Step 1.	Experiment design, data collection, and data manipulation.
Step 2.	Selection of model structure and parametrization.
Step 3.	Choice of the identification criterion.
Step 4.	Estimation of a model that is optimal with respect to the criterion.
Step 5.	Validation of the resulting model estimate.

the fact that several iterations might take place, using the knowledge gathered in the previous attempts, till the desired model is delivered. In the following a brief overview of each step is given based on Ljung (1999).

Step 1. Experiment design and data preprocessing

Experiment design focuses on the choice of the excitation of the system to be identified in order to maximize the information content in the measured signals. The design procedure is commonly accomplished with respect to a selected model class to minimize the variance, i.e. the estimation error, of the resulting model estimate. One of the most important problems, is how to choose input signals that are *Persistently Exciting* (PE), i.e. they result in output signals which have enough information content to describe the dynamical relation of the system. A similarly important notion is the use of *adequately exciting* inputs that result in *informative* data sets which have enough information content to distinguish between different models in the considered model class. White noise inputs are in general considered to be optimal, e.g. they excite all frequencies of an LTI system. As physical actuation by such signals is often infeasible, in practice random binary noises, frequency sweeps, and multisines are considered. Beside experiment design, data preprocessing is focusing on the attenuation of disturbances, noises or other defects in the measured data.

Step 2. Choice of the model structure

The choice of an appropriate model structure is the most crucial part of the identification cycle. It determines the set in which a suitable description of the system is searched for. General questions considered in this step are the selection of the model structure in terms of the representation form (*state-space* (SS), *input-output* (IO), *series-expansion*, etc.), parametrization, and the type of noise modeling. In terms of the well known bias/variance trade-off, the size of the model set is also important, like the number of parameters or order of the model structure. To obtain an adequate choice, the complexity of the algorithm delivering the model estimate or undesired local solutions of the estimation, non-uniqueness of the optimum, etc., also need to be considered.

Step 3. Choice of the identification criterion

Selection of the identification criterion, the mathematical formulation of the performance measure of the model estimates, defines the user's purpose or expectation towards the model of the plant. In the literature, many identification criteria are presented, but the most commonly applied is the mean squared error of the output prediction of the model estimate.

Step 4. Model Estimation

The model estimation phase is the consequence of the previous choices of the identification cycle. Commonly the algorithmic solution of the estimation problem, defined in terms of the model structure and the identification criterion, are considered here.

Step 5. Model (in)validation

A crucial question in identification is whether the obtained model is "good enough" for the intended purpose of the user. Prior knowledge and experimental data are both used to confront the estimated model for answering this question. By using experimental data, validation is often accomplished by comparing simulation results of the model estimates to the measurements or by analyzing the model as a predictor of future outputs of the system based on measured past data.

1.3.2 General picture of LPV identification

Next, the LPV identification problem is discussed, defining the notion of LPV systems and formulating the LPV model structures that are currently used in the literature. This sets the stage for the introduction of the state-of-the-art identification approaches.

LPV systems and the task of identification

Based on the original gain-scheduling principle, LPV systems are often viewed as a *linear dynamical relation* between input signals u and output signals y , where the relation itself is dependent on an external variable, the so called *scheduling signal* p . This provides the schematic view presented in Figure 1.2. The relation can be formalized as a convolution in terms of u and p , which reads in *discrete-time* (DT) as

$$y = \sum_{i=0}^{\infty} \mathbf{g}_i(p) q^{-i} u, \quad (1.1)$$

where q denotes the time shift operator, i.e. $q^{-i}u(k) = u(k-i)$, $u : \mathbb{Z} \rightarrow \mathbb{R}^{n_u}$ is the DT input, $y : \mathbb{Z} \rightarrow \mathbb{R}^{n_y}$ is the DT output, and $p : \mathbb{Z} \rightarrow \mathbb{P}$ is the DT scheduling signal of the system with a scheduling space $\mathbb{P} \subseteq \mathbb{R}^{n_p}$. The coefficients \mathbf{g}_i of (1.1) are

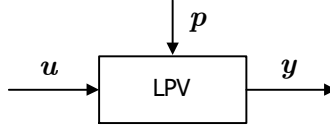


Figure 1.2: Input-output signal flow of LPV systems

functions of the scheduling variable and they define the varying linear dynamical relation between u and y . If the functions g_i are considered to be dependent only on the instantaneous value of the scheduling signal, i.e. $g_i : \mathbb{P} \rightarrow \mathbb{R}^{n_y \times n_u}$, then their functional dependence is called *static*. An important property of LPV systems is that for a constant scheduling signal, i.e. $p(k) = \bar{p}$ for all $k \in \mathbb{Z}$, (1.1) is equal to a convolution describing an LTI system as each $g_i(p)$ is constant. Thus, LPV systems can be seen to be similar to LTI systems, but their signal behavior is different due to the variation of the g_i parameters. Note that in the literature there are many formal definitions of LPV systems, commonly based on particular model structures and parameterizations. The convolution form (1.1) can be seen as their generalization.

In identification, we aim to estimate a dynamical model of the system based on measured data, which corresponds to the estimation of the coefficients g_i in (1.1). This estimation is formalized in terms of a model structure, an abstraction of (1.1), and an identification criterion.

Model structures in LPV identification, input-output models

One particular type of model structure, which is used in some LPV identification approaches, originates from the IO type of models of the LTI prediction-error setting. These LPV-IO models are commonly defined in a filter form

$$y = - \sum_{i=1}^{n_a} a_i(p)q^{-i}y + \sum_{j=0}^{n_b} b_j(p)q^{-j}u + e, \quad (1.2)$$

where e is a noise process, $n_a \geq 0$ and $n_b \geq 0$, and the coefficients $\{a_i\}_{i=1}^{n_a}$ and $\{b_j\}_{j=0}^{n_b}$ are functions of p with static dependence. e is commonly considered to be a zero-mean white noise.

Model structures in LPV identification, state-space models

Other type of model structures are inspired by the classical SS representation based LTI models. These so called LPV-SS models are often given with an innovation type of noise model:

$$qx = A(p)x + B(p)u + E_1(p)e, \quad (1.3a)$$

$$y = C(p)x + D(p)u + E_2(p)e, \quad (1.3b)$$

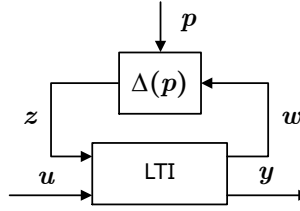


Figure 1.3: Input-output signal flow of LFT models

where $x : \mathbb{Z} \rightarrow \mathbb{R}^{n_x}$ is the state-variable, e is a vector of independent zero-mean white noise processes, and (A, B, C, D, E_1, E_2) are matrix functions with static dependence on p . It is commonly assumed that the noise part is not dependent on p , i.e. E_1 and E_2 are constants, however there are recent initiatives with varying noise models. Additionally, the matrices are often considered with linear dependence. In case of A , such a dependence is defined as

$$A(p) = A_0 + \sum_{l=1}^{n_p} A_l p_l, \quad (1.4)$$

where $A_l \in \mathbb{R}^{n_x \times n_x}$ and $p = [p_1 \ \dots \ p_{n_p}]^\top$. This type of dependence is called *affine*, and used as a core assumption in many LPV control-design approaches.

Alternatively, the process part of LPV-SS models is considered in an equivalent *Linear Fractional Transform* (LFT) realization, which originates from the robust control inspired μ -synthesis approaches. In this formalization, the scheduling dependence is extracted into a feedback gain, while the remaining part of the system is formulated as a LTI system (see Figure 1.3 for an upper LFT form). This formulation is described mathematically as:

$$\begin{bmatrix} qx \\ w \\ y \end{bmatrix} = \begin{bmatrix} A_1 & B_1 & B_2 \\ C_1 & D_{11} & D_{12} \\ C_2 & D_{21} & D_{22} \end{bmatrix} \begin{bmatrix} x \\ z \\ u \end{bmatrix}, \quad z = \Delta(p)w, \quad (1.5)$$

where w and z are auxiliary variables and $\{A_1, \dots, D_{22}\}$ are constant matrices, while Δ is a function of p with static dependence. An equivalent SS realization of (1.5) is defined as

$$\begin{aligned} A(p) &= A_1 + B_1 \Delta(p) (I - D_{11} \Delta(p))^{-1} C_1, \\ B(p) &= B_2 + B_1 \Delta(p) (I - D_{11} \Delta(p))^{-1} D_{12}, \\ C(p) &= C_2 + D_{21} \Delta(p) (I - D_{11} \Delta(p))^{-1} C_1, \\ D(p) &= D_{22} + D_{21} \Delta(p) (I - D_{11} \Delta(p))^{-1} D_{12}, \end{aligned}$$

if the matrix function $I - D_{11} \Delta(p)$ is invertible.

1.3.3 LPV-IO representation based methods

The existing LPV identification approaches are almost exclusively formulated in discrete-time, they assume static dependence, and they are mainly characterized

by the type of model structure LPV-IO or LPV-SS. In this way, the identification methods of the LPV field can be categorized based on the model structures. The resulting categories together with their main properties are summarized in Figure 1.4 and investigated in the following. First we treat LPV-IO approaches which extend the results of LTI prediction-error identification. A common mark of these methods that the approaches are derived only in the *Single-Input Single-Output* (SISO) case, i.e. when $n_Y = n_U = 1$. The following subcategories are distinguished:

A. Linear regression methods

Methods that fall into this category use the LPV-IO model structure (1.2) which corresponds to a noise model

$$v + \sum_{i=1}^{n_a} a_i(p)q^{-i}v = e, \quad (1.6)$$

where v is the additive output noise. This results in an *Auto-Regressive* model with *exogenous* input (ARX), well known in the LTI identification framework. However, in the LPV case, the coefficients are functions of a varying p . Additionally, the approaches use a linear parametrization of $\{a_i\}_{i=1}^{n_a}$ and $\{b_j\}_{j=0}^{n_b}$ with polynomial scheduling dependence. In case of $n_P = 1$, this reads for a_i as

$$a_i(p) = a_{i0} + \sum_{l=1}^n a_{il}p^l, \quad (1.7)$$

where $a_{il} \in \mathbb{R}$. As the resulting model is linear-in-the-parameters, the estimation of $\{a_{il}\}$ and $\{b_{jl}\}$ can be obtained by linear regression (see Wei and Del Re (2006); Wei (2006); Bamieh and Giarré (2000); and Bamieh and Giarré (1999)). In analogy, recursive least-squares or instrumental variable methods can also be applied to refine the estimate, building on the concepts of the LTI prediction-error identification framework (see Giarré et al. (2006) and Bamieh and Giarré (2002)). Extending the LTI concepts, some conditions of PE for LPV-ARX models are derived in Wei and Del Re (2006) and Bamieh and Giarré (2002). It is important to note that other popular model structure concepts of the LTI prediction error framework, like Box-Jenkins, Output-Error, etc. have not been used to identify LPV systems.

B. Nonlinear optimization methods

In this branch of IO approaches (see Figure 1.4), the coefficients $\{a_i\}$ and $\{b_j\}$ of the LPV-IO model (1.2) are estimated by using nonlinear optimization to minimize the mean-squared prediction error. The aim is to give better estimates than the linear regression methods by using a nonlinear parametrization

$$a_i(p) = a_{i0} + a_{i1}z, \quad (1.8)$$

where $a_{i0}, a_{i1} \in \mathbb{R}$ and z is the output of a feed-forward hidden layer neural network with inputs $\{y, q^{-1}y, \dots\}$, $\{u, q^{-1}u, \dots\}$, and $\{p, q^{-1}p, \dots\}$. The estimation

is accomplished via either a mixed linear/nonlinear procedure or by a separable least-squares approach. In the former case, the functional dependencies of the coefficients are identified through a neural-network approach while the linear part of the model is estimated by linear regression (Previdi and Lovera 2003, 2001, 1999). The approach is developed further in Previdi and Lovera (2004), where the parallel estimation problem of the neural-network model and the linear part is solved by a separable least-squares strategy.

1.3.4 LPV-SS representation based methods

Other type of approaches use the LPV-SS model structure (1.3a-b) or its LFT equivalent (1.5). In applications, these approaches are generally more appreciated, as LPV control theory requires a state-space representation and most of the LPV-SS identification methods can also easily handle MIMO plants. The methods of LPV-SS approaches fall into the following sub-categories (see Figure 1.4):

A. Gradient methods

These approaches formulate the estimation of the parameter-varying SS matrices as a NL optimization problem solved via gradient-search-based algorithms. Due to the nature of gradient-search optimization, the resulting estimate is often a locally optimal solution of the involved cost function. In Lee (1997) and Lee and Poolla (1996), an LFT type of SS model structure is used where the scheduling dependence is extracted as $\Delta(p) = \text{diag}(Ip_1, \dots, Ip_{n_p})$. The estimation of the linear part is formulated as a NL optimization, which is solved in an iterative scheme based on the gradients of the mean-squared output error. In every step of the estimation, the system matrices can be estimated in a different state basis, i.e. a family of matrix estimates can be given which are all related by state transformations. To eliminate the non-uniqueness of the estimation, in each iteration step, the matrix estimates are restricted to a specific structure. Identifiability issues of such LFT structures are investigated in Lee and Poolla (1997). Other methods have also been developed which use the same methodology, but on the LPV-SS form (1.3a-b) with radial-basis functions based scheduling dependence (Verdult et al. 2002, 2003). In this parametrization, the matrices are formulated as

$$A(p) = A_0 + \sum_{l=0}^n g_l(p)A_l \quad (1.9)$$

where $A_l \in \mathbb{R}^{n_x \times n_x}$ and each $g_l : \mathbb{P} \rightarrow [0, 1]$ is a radial basis function.

B. Full-state measurement approaches

These methods assume that the state x of the LPV-SS model, considered in the LFT form (1.5), is measurable. In this setting, if $\Delta(p)$ is parameterized linearly, the estimation problem reduces to a linear regression. In Nemani et al. (1995),

the one-dimensional case of this approach has been treated, assuming a white noise scheduling signal and using recursive least-squares to obtain the estimate. Conservative conditions of persistency of excitation have also been derived. In Mazzaro et al. (1999), the robust extension of the method has been worked out, while in Lovera et al. (1998) and Lovera (1997) the approach has been generalized to LFT structures with more complicated scheduling dependencies.

C. Multiple model approaches

These methods apply the classical gain-scheduling inspired approach: identification for constant scheduling and interpolation. However, this approach is often used in an intuitive manner. In some methods, the identified LTI models, or so called “frozen” models, are transformed into canonical SS forms (Wassink et al. 2004; van der Voort 2002; Young 2002; Steinbuch et al. 2003) or internally balanced modal form (Lovera and Mercère 2007) to perform interpolation on \mathbb{P} . Some of the methods also apply model reduction independently on the obtained LTI models before interpolation (Lovera and Mercère 2007; Steinbuch et al. 2003) or they use LTI discretization of the estimated frozen models (Wassink et al. 2004; Steinbuch et al. 2003). In other approaches, interpolation is accomplished via pole locations (Paijmans et al. 2008). As issues of noise and parametrization are dealt with in a local sense, i.e. by the applied LTI identification, these approaches focus on the question: how to accomplish interpolation in a more efficient sense. These approaches closely relate to the local-linear-modeling framework (Murray-Smith and Johansen 1997).

D. Linear-Matrix-Inequalities based optimization method

In Sznaier et al. (2000), identification of LPV-SS models is considered in a LFT form with a linear dependence: $\Delta(p) = \text{diag}(Ip_1, \dots, Ip_{n_p})$. The noise/disturbance v of the system is assumed to be output additive with a moving average structure

$$v = \sum_{i=0}^n E_i q^{-i} e, \quad (1.10)$$

where $E_i \in \mathbb{R}^r$ and e is a ℓ_∞ sequence. This noise model is considered to be known. Under this assumption, the estimation problem of the LTI part is formulated as a LMIs based optimization. Based on a similar mechanism, validation of a LFT model with a linearly parameterized dependence can be formulated as a LMI feasibility problem if norm bounds and structural properties of the noise are known.

E. Global subspace techniques

The family of these methods builds strongly on the concepts of the LTI *Multi-variable Output-Error State-Space* (MOESP) algorithm (see Verhaegen and Dewilde

(1992); Verhaegen (1994)). During the estimation process, a generalized data equation of the LPV-SS model (1.3a) is formulated to obtain both an estimate of the state evolution and the state-space matrices. In most methods, E_1 and E_2 are considered to be constant. The estimation is based on a discrete-time state-observability matrix of (1.3a) that is reconstructed from the measured data using a similar mechanism as in the MOESP algorithm. This identification strategy also enables the estimation of the system order, similar to the LTI case. Also common marks of the LPV subspace approaches are the assumption of affine scheduling dependence (see (1.4)) and the resemblance with bilinear system-identification methods.

- The early approaches have used certain approximations during the reconstruction of the state, possibly leading to biased estimates (Verdult and Verhaegen 2005; Verdult 2002; Verdult and Verhaegen 2002). The computational load of these methods has been found rather demanding in practice, as matrix dimensions quickly explode with an increasing number of scheduling variables and block dimensions. This has been the reason why the kernel method based modification has been proposed in Verdult and Verhaegen (2005) to regulate the computational load.
- To overcome the resulting bias, non-approximative methods have been derived by restricting the variation of the scheduling signals in the measured data to be periodic (Felici et al. 2007, 2006) or to be piece-wise constant (van Wingerden et al. 2007). While the former method is similar to periodic LTV identification like in Verhaegen and Yu (1995) and Liu (1997), the latter approach extends the approximative method of Verdult and Verhaegen (2004). For these special scheduling signals, it is possible to find parameter-varying state-transformations such that the states in the subspace calculation are at the same basis at every time instant. Thus, no approximation is needed for the state-reconstruction in the noiseless case. However, identifiability of SS models is not understood with such a restricted class of scheduling signals and problems concerning non-unique solutions of the estimation may result.
- In the work of dos Santos et al. (2007), LPV-SS models (1.3a-b) with affine dependence are formulated as LTI models by assuming white noise p , independent white noise u , and independent noise signals e_1 and e_2 in (1.3a) respectively (1.3b). Then the estimation is solved as a bilinear identification problem via a Picard type of iterative scheme. In this approach, the state is reconstructed by a Kalman filter at each time instant, where the filter is based on the model obtained in the previous time-steps. The disadvantage of the method is that it only provides a meaningful estimate in case the white noise assumptions of u and p are satisfied, which is hard to verify in practice.

F. Observer based grey-box techniques

These approaches like Gáspár et al. (2007, 2005) and Angelis (2001), formulate the LPV identification problem as a parameter estimation of a known NL model structure. In that case, it is possible to use an adaptive observer to find the unknown parameters of the model based on measured data. The used observer is

commonly an extended Kalman filter, which is applied on the augmented form of the NL model, where the state is extended with unknown parameters as variables. If the estimation has converged, then the obtained NL model is processed further, using the gain-scheduling approach to derive a LPV-SS form with affine coefficient dependence (Angelis 2001).

1.3.5 Similarity to other system classes

LPV systems are often considered to be similar in some aspects to other system classes. It has already been mentioned that LPV subspace techniques were inspired by the identification approaches of bilinear systems. These systems can be considered as LPV systems where the scheduling signal is equal to the input of the system.

LPV systems can also be seen as the extension of LTV systems. By restricting the coefficients of an LPV system to depend on a fixed linear trajectory of time, instead on a prior unknown trajectory of the scheduling variable, an LTV system results. Due to the undoubtable structural similarity, many LPV approaches have been inspired by the ideas of the LTV framework (IO methods, periodic identification) which do not exploit the prior known linear variation of the time trajectory.

In the fuzzy framework, *Takagi-Sugeno* (TS) dynamic fuzzy models with linear signal relation are often considered as LPV systems (Korba 2000). However, due to the if-then structure of the fuzzy rules, commonly LPV control cannot be applied on such systems and due to other structural differences such an equality of TS and LPV systems is dubious in the general sense. Thus, in the following, TS dynamic fuzzy models are treated as non-LPV systems.

1.4 Challenges and open problems

In the previous part, we have seen that a wide variety of identification methods is available, approaching the underlying LPV identification problem (see Section 1.3.2) from different viewpoints. Many of these approaches are built around an assumed model structure and focusing only on the estimation task, which is just one step of the classical identification cycle. Due to these and many other issues, several challenges and open problems exist, which deserve further research. The most crucial questions are collected into the following list:

- The current methods use different identification settings, model structures, and even different views about what an LPV system is. So it is an obvious question how these concepts and ideas can be brought to a common ground, where they can be analyzed, compared, and refined?
- Often, the validity of the used identification concepts is not investigated. For example in prediction-error methods, like the least-squares LPV-IO methods, the formulation of the predictor, or even description and analysis of the

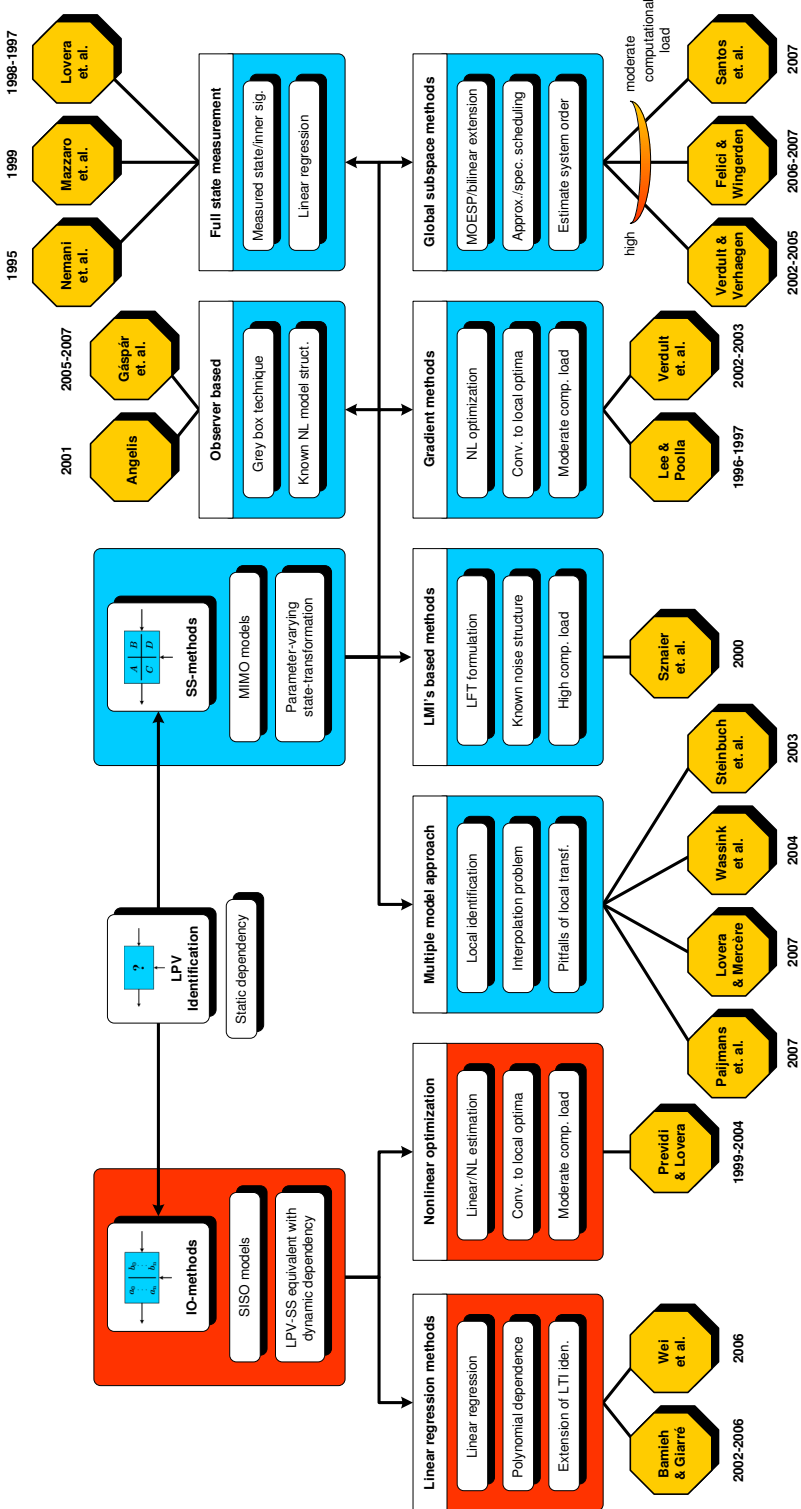


Figure 1.4: Available methods of LPV identification.

assumed noise structure of ARX models is omitted. Many approaches use linear regression, which is applied as an optimization tool instead of estimation in a stochastic sense. How to formulate the prediction-error setting in the LPV case and how to derive well-founded identification approaches that dwell on the concepts of the classical framework remain questions to be investigated.

- In the SS variants of the gain-scheduling principle based identification methods, state-transformations are applied independently on each LTI-SS model estimate. For example the frozen models are transformed to a canonical or balanced form and then they are interpolated. However, such transformed models do not have a common state, making the consequences of interpolation to be unpredictable. Similarly, the problem of local transformations applies when model reduction is used independently on the frozen models or the interpolation is based only on their pole locations. Unexpected problems can also occur in the interpolation process, if the *McMillan degree* of the local models changes at some interpolation points. Thus it is also important to investigate how the gain-scheduling principle can be used in identification such that the interpolation is well structured and issues of local transformations do not apply.
- Many LPV identification approaches, especially sub-space and gradient-search methods, have significant computational load which renders their practical use to be hopeless in case of large scale systems. To assist practical use, it is important to develop approaches that solve the estimation problem efficiently and which are less effected by the curse of dimensionality.
- Selection of model structure and parametrization is often entirely skipped. The way how possible first-principle knowledge about the data-generating system is transformed to a discrete-time LPV form to assist at least the order selection is generally ad-hoc. The main reasons are the absence of sound results on LPV discretization theory or on the conversion of NL differential equations to LPV representations.
- The cardinal question, concerning the choice of the scheduling variable for a given physical system is commonly not investigated. As the entire dynamics of LPV systems depends on this variable, its choice should also be part of model structure selection. This also implies the question when a given NL system can be efficiently described by a LPV model.
- In LTV system theory, it has been shown in discrete-time that equivalence transformations between SS and IO models result in coefficients that are constructed from time-shifted versions of the original coefficients (Guidorzi and Diversi 2003). If this is true for LTV systems, which can be considered as a special cases of LPV systems, may the same phenomenon hold in the LPV case? This would suggest that equivalent models in different representation forms depend on the time-shifted versions of the scheduling, which is called *dynamic dependence*.

- In LPV identification, many approaches build upon the assumption that LPV-SS and IO models with static dependence are equivalent representations of the same system. If in terms of the previous phenomenon, equivalence relations, like state-transformations and IO realization, result in dynamic dependence, then it becomes a cardinal question how this phenomenon effects the basic view of LPV identification and validity of the used approaches.
- In the view of the previous observation, further questions arise about how to define LPV systems, what kind of representations these systems have, what the equivalence relations are between these representations and how they correspond to the previously used concepts of LPV system theory. Answers to these questions are required to understand what LPV models correspond to, how they are related, what is the restriction of specific parameterizations and how the identification approaches can be compared.
- As LPV control is based on LPV-SS models it is also a question how to convert the model estimates to equivalent forms on which LPV control can be applied on directly.
- Beside these issues, it is a general mark of the LPV field that many approaches try to build intuitively on the concepts of the LTI theory. However, is it true that relations of the LTI framework apply directly to the LPV case? If not, then what are the merits of using the LTI concepts?

In conclusion, the current solutions of the field are not addressing the LPV identification problem in general well-founded sense due to the restricted class of model structures, the gaps of system theory, and the neglected steps of the identification cycle. This motivates the current thesis to fulfill some of these gaps and establish a well-posed identification setting of LPV systems.

1.5 Perspectives of OBF models

In view of the previous observations, a central problem of the field is the absence of a model structure which has good representation capabilities with a limited number of parameters, useful for control, and its identification represents a low complexity problem. The latter means for example that the model structure is either well applicable in a gain-scheduling type of approach, i.e. it is easily interpolatable without the need of local transformations, or its estimation is available through linear regression.

Perspectives of OBF models, gain-scheduling

From the gain-scheduling perspective, *Orthonormal Basis Functions* (OBF)s-based model representations offer an easily interpolatable structure with a well worked-out theory in the context of LTI system approximation and identification (Heuberger et al. 2005). The basis functions, that provide bases for the space \mathcal{H}_2

(Hilbert space of complex functions that are squared integrable on the unit circle), are generated by a cascaded network of stable all-pass filters, whose pole locations represent the prior knowledge about the system at hand. This approach characterizes the transfer function of a proper SISO LTI system as

$$F(z) = \sum_{i=0}^{\infty} w_i \phi_i(z), \quad (1.11)$$

where $\{w_i\}_{i=0}^{\infty}$ is the set of constant coefficients and $\Phi_{\infty} = \{\phi_i\}_{i=0}^{\infty}$ with $\phi_0 = 1$ represents the sequence of OBFs. This implies that every transfer function $F_{\bar{p}}$ that corresponds to (1.1) for constant scheduling $p(k) = \bar{p}$ can be represented as a linear combination of a given Φ_{∞} . In LTI identification, only a finite number of terms in (1.11) is used, like in *Finite Impulse Response* (FIR) models. In contrast with FIR structures, the OBF parametrization can achieve almost zero modeling error with a relatively small number of parameters, due to the infinite impulse-response characteristics of the basis functions. In this way, it is always possible to find a finite $\Phi_n \subset \Phi_{\infty}$, with a relatively small number of functions $n \in \mathbb{N}$, such that the representation error for all $F_{\bar{p}}$ is negligible. Then, based on experiments with constant p , frozen aspects of (1.1) can be identified in the form (1.11) with finitely many terms, resulting in a set of local basis coefficients. Due to the linearity of (1.11) in these coefficients, model interpolation can easily be accomplished on the scheduling space \mathbb{P} without the need of any local transformations, resulting in the LPV model:

$$\hat{y} = \sum_{i=0}^n w_i(p) \phi_i(q) u. \quad (1.12)$$

This type of interpolation would also be well structured against local changes of the McMillan degree as the coefficients in (1.11) are not related directly to the order of the system. By using SS realizations of the basis functions $\{\phi_i\}_{i=0}^n$ in (1.12) a direct LPV-SS realization of this model is available, which means that model estimates can be directly used for control.

Perspectives of OBF models, global identification

OBF-based model structures have many attractive properties in the LTI case. In the prediction-error framework, they correspond to output-error type of models with a linear-in-the-parameter property, which implies that their estimation is available through linear regression. They generally need less parameters than FIR models with similar properties. Non-asymptotic variance and bias bounds of the estimates are also available. These fruitful properties imply that direct identification of LPV systems may be beneficial in terms of the model structure (1.12) used in a prediction-error setting. In such a setting, parameterizing the coefficients as

$$w_i(p) = \sum_{l=0}^{n_{\psi}} \theta_{il} \psi_{il}(p), \quad (1.13)$$

where $\theta_{il} \in \mathbb{R}$ and ψ_{il} are prior chosen functions of p , would yield that estimation of $\{\theta_{il}\}_{i=0, \dots, n}^{l=0, \dots, n_\psi}$ is available by linear regression, based on experimental data with varying p . However, for the investigation of this approach, first an LPV prediction error framework needs to be established. This would provide an identification method with low complexity, like the IO approaches, but with direct SS realization of the model estimates.

Perspectives of OBF models, approximation

Based on the work of Boyd and Chua (1985), it has been proved for nonlinear Wiener models (LTI system followed by a static nonlinearity), that if the LTI part is an OBF filter bank Φ_n , then such models are general approximators of nonlinear systems with fading memory (NL dynamic systems with convolution representation). This means that, if the number of the OBFs in Φ_n approaches to infinity, then the best achievable approximation error of the output trajectories in terms of the choice of the static nonlinearity converges to zero in an arbitrary norm. It is obvious that (1.12) is similar to these general approximators, which means that, if the same property can be shown for the LPV case, then these models have a wide representation capability of LPV systems. Based on the general approximator property and the attractive identification properties of OBF models, successful identification approaches based on these structures have been introduced in the NL and the fuzzy field (see Gómez and Baeyens (2004) and Sbárbaro and Johansen (1997)). These methods provide low complexity and reliable estimates for the considered classes of systems, giving the hope that similar mechanisms could also be successfully applied in the LPV case.

It is well known in the LTI case that the approximation error, i.e. the resulting bias of the model estimate directly depends on how well the chosen basis functions Φ_n can represent the dynamics of the system. In terms of gain-scheduling, this refers to the size of the representation error of Φ_n with respect to each $F_{\bar{p}}$. This refers back to the observation that model structure selection has a prime importance in the LPV case, and as for other type of LPV models, this choice influences the achievable maximal accuracy of the estimates.

In conclusion, the above discussed perspectives yield the observation that identification of LPV systems with OBF models like (1.12) could provide answers to the current challenges of the identification field.

1.6 Problem statement

In the previous part, it has been shown that LPV modeling and system identification has many open issues and raises a lot of questions, which have not been answered yet. The underlying family of problems needs and deserves a unified treatment and much more research. Based on this observation, we formulate the aim of our research as the development of an effective LPV identification mechanism that overcomes the drawbacks of the existing state-of-the-art solutions (see

Section 1.4), but still delivers low complexity models in a computationally attractive way. The procedure is intended to handle the identification cycle from model structure selection until delivering the model estimate. This results in the following problem statement:

- Primary research objective -

Develop a framework and a structural approach for the identification of general LPV systems as models of an underlying physical process.

Based on our previous observations and in the view of this objective, we identify the following subgoals:

1. Investigate model-structure selection for LPV systems
 - (a) Explore how LPV models relate to each other. What is the role of dynamic dependence and what are the corresponding equivalence transformations. These investigations are needed to compare and analyze representation capabilities and choices of model parameterization.
 - (b) Study how first-principle information, like NL system descriptions can assist the choices of model structure.
 - (c) Due to the promising properties of OBF model structures, investigate how these structures approximate/describe general LPV systems. What are the representation capabilities and how can adequate selection of the OBFs be accomplished with respect to a LPV system.
2. Formulate the prediction-error framework for LPV identification
 - (a) Investigate how low complexity LTI identification approaches, like the OBFs-based method, can be extended to the LPV case.
 - (b) Investigate how the issues of noise, variance, and bias can be understood in this framework.
3. Based on the results of the previous investigations, possibly by the use of OBF models, develop estimation approaches that provide reliable LPV model estimates with low computation load.
 - (a) Investigate how the gain-scheduling principle can be effectively used for LPV identification without the need of local transformations.
 - (b) Explore how direct model estimates can be obtained using the prediction error framework.

These subgoals are explained in detail in the following subsections:

Subgoal 1, Model-structure selection

The first subgoal corresponds to the observation that model-structure selection in terms of representation capabilities and parameterizations must be well explored, i.e. clarified, before formulation of an LPV identification approach. It has been revealed that the main obstacle in the comparison of representation capabilities originates from the gaps of LPV system theory, i.e. absence of equivalence transformations between different models. It has also been observed that dynamic dependence may play an important role in such a relation. This has the consequence that the concept of LPV systems and representations must be reviewed and formally defined. In the LTI case, the behavioral approach (Polderman and Willems 1991) investigates these questions and gives a powerful framework where these concepts can be clearly formulated. This framework also incorporates most results of LTI system theory in a simple and efficient way. To give a unified system theoretical framework in the LPV case, which enables the investigation and comparison of model structures, the extension of the LTI behavioral approach has been considered. This theoretical framework is intended to serve as a tool in the formulation of a well-posed identification framework.

It has been also observed that to assist model-structure selection, a clear understanding how LPV systems correspond to NL systems must be obtained. Thus, a transformation procedure is required that can provide the best suitable LPV description of a given NL system. Based on first-principle knowledge, such an approach could provide vital information about parametrization, order selection, etc., all required to select a good model-structure candidate for identification. As first-principle models are commonly given in continuous-time, it is also vital to investigate how model discretization can be solved efficiently in the LPV case.

Using the observation that OBFs-based model structures might provide an attractive candidate to solve our primary objective, their representation capabilities and properties must be investigated in the planned LPV behavioral framework. A cardinal question that is to be understood, is whether a representation of LPV systems is available in terms of OBF series expansions, similar to the LTI case (see (1.11)). It must be investigated how adequate selection of OBFs can be accomplished based on measured data or a priori information in order to facilitate model-structure selection.

Subgoal 2, Prediction-error framework

From the studied LPV identification approaches and the classical identification framework, it can be concluded that low-complexity identification might be available in the prediction-error setting. However a formulation of this setting is missing in the current literature. Based on the promises that this setting may result in an approach that solves the primary objective, investigation and formulation of an LPV prediction-error setting is established as a secondary subgoal. It is planned that if OBF model structures are found adequate in the previous investigations, then the extension of the LTI-OBF identification framework is considered for the LPV case.

Subgoal 3, Estimation methods

Based on the results of the previous investigations, the actual formulation of the estimation methods is aimed for as the third subgoal. We intend to explore how the gain-scheduling approach of the current LTI identification literature can provide an answer to our primary research question. We also intend to seek out possible ways of direct estimation of the system using the prediction-error framework.

General remarks

In the following, we present a theory with new ideas of LPV behaviors, modeling, and identification methods, that have appealing properties and can be applied successfully to fulfill the aimed research objectives. Due to the vast number of problems this thesis addresses, we also leave many open ends and questions for future research. The exploration of all issues of the LPV identification cycle of general physical systems remains a problem, but the use of orthonormal basis functions opens interesting and promising perspectives to approach the identification of this system class efficiently.

1.7 Overview of contents and results

This thesis is divided into eight major chapters, next to this introduction and the conclusions in Chapter 10. See Figure 1.5 for an overview of the chapters and their relations.

The introductory Chapter 2 is devoted to the basic mathematical and system theoretical tools that are used in the remainder. This includes a brief overview of the behavioral approach of Polderman and Willems (1991) for LTI systems where we consider finite-dimensional differential/difference systems with input-output partitioning. Through this framework, we explore the definitions of representations, equivalence classes and transformations, and minimality together with issues of stability, state-observability and reachability, model balancing, and discretization theory with the purpose to extend these notions to LPV systems later on. We also present a short overview of the basic issues of identification, especially focusing on OBFs based methods. It is motivated that in the OBFs-based identification approach there is a prime emphasis on the model structure selection in terms of basis functions. To support this basis selection step in the LPV case, the theories of Kolmogorov n -widths and Fuzzy clustering are discussed.

In Chapter 3, we introduce an LPV behavioral approach that establishes a unified system theoretical framework, as a solution for the first research subgoal. In this framework, it becomes possible to understand basic relations of LPV models and it gives the basic tool to introduce OBFs based LPV model parameterizations later on.

In Chapter 4, we explore equivalence transformations between different representations of LPV systems. We investigate LPV-SS canonical forms and transformations between LPV-SS and IO representations. The explored relations give the tools to analyze and compare LPV model structures, fulfilling research goal 1.a. This chapter is based on the concepts of Tóth et al. (2007).

In Chapter 5, representation of LPV systems by OBF-based series-expansion is investigated. It is shown that finite truncation of these representations can be used as model structures for LPV system identification. Such structures also have wide approximation capabilities. This gives answers for research goal 1.c.

In Chapter 6, discretization of LPV systems is reviewed. New discretization approaches are introduced together with criteria to choose the discretization step size. The developed methods provide tools to derive solutions for research goal 1.b. This chapter is based on the paper Tóth et al. (2008).

In Chapter 7, the modeling of NL systems in a LPV form is investigated and the available solutions for this problem are studied. Using the framework of the LPV behavioral approach, a new mechanism is introduced that solves the LPV modeling issue of such systems. This approach is developed with the intention to assist the model-structure selection phase of the identification cycle based on first principle knowledge, fulfilling research goal 1.b.

In Chapter 8, the basis-selection problem of OBFs-based LPV model structures is considered, introducing a clustering algorithm, which is inspired by the previously presented fuzzy clustering and Kolmogorov n -width theory (see Chapter 2). The method is based on the clustering of sample poles that result from identification of the system with constant scheduling signals. The effect of noise on identification is also considered and a robust basis-selection procedure is developed based on hyperbolic-geometry results. This provides direct answers for research goal 1.c. The chapter is based on the papers Tóth et al. (2006b,a, 2008a,c).

In Chapter 9, the extension of the LTI OBFs-based identification approach to the LPV case is developed, relying heavily on the tools of the previous chapters. The prediction-error framework is established for the LPV case and the model structures of the current approaches are analyzed, fulfilling objective 2. Two identification approaches, a global and a local one, are formulated with static dependence of the coefficients. The former approach utilizes the gain-scheduling interpolation-based concept while the latter obtains a global estimate based on linear regression. To overcome the limiting assumption of static dependence, which is needed for the parametrization of these approaches, two alternative OBFs based model structures are also worked out. These structures enable approximation of dynamic dependence of the coefficients through a feedback with only static dependence. An identification approach of such feedback structures is also derived through a separable least-squares strategy. This concludes research objective 3. The presented results of the chapter are based on the papers Tóth et al. (2008b, 2007).

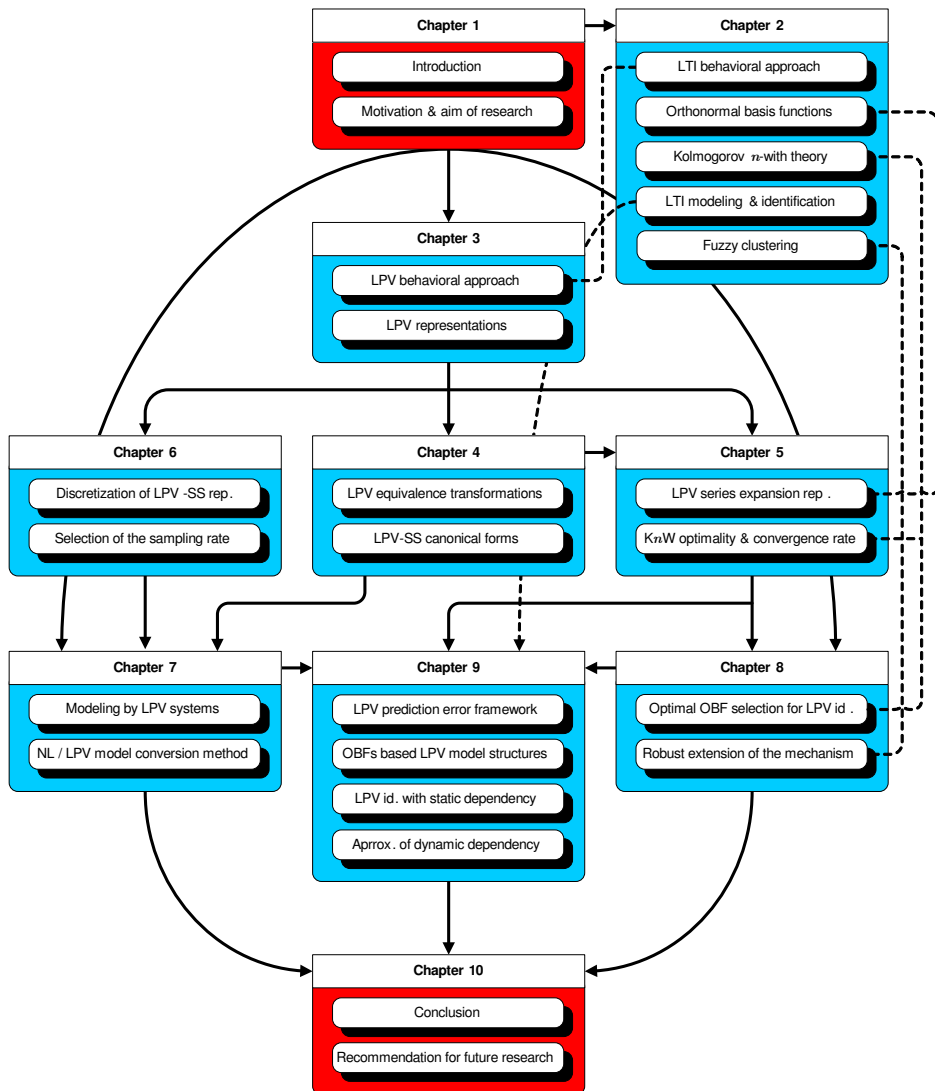


Figure 1.5: Structure of the thesis.

LTI systems and OBFs

This chapter is devoted to the introduction of a number of basic mathematical and system theoretical tools that are fundamental for the theory developed in the subsequent chapters. In the scope of this thesis, we consider dynamical systems based on the behavioral approach. Using this framework, in Section 2.1 we develop representations of LTI dynamical systems both in continuous and discrete-time and also introduce important system theoretical concepts. To investigate the connection of the continuous-time and the discrete-time domain, discretization theory of LTI systems is briefly covered in a zero-order-hold setting. Beside the system theoretical concepts, in Section 2.3 the basic theories of LTI system identification are introduced focusing on prediction error methods. The notion of *Orthonormal Basis Functions* (OBF)s is also developed in Section 2.2 with the brief coverage of their most important relations and properties. OBFs related parameterizations and the associated identification approaches are also introduced together with the optimality concept of OBF model structures in terms of the Kolmogorov n -width theory. At last in Section 2.5, the theory of fuzzy clustering is discussed, which is essential for the basis selection approach of Chapter 8.

2.1 General class of LTI systems

2.1.1 Dynamical systems

We consider definition of dynamical systems in the context of the behavioral approach, where systems are described as a set of possible signal trajectories that obey the underlying laws and restrictions of the physical phenomena.

Definition 2.1 (Dynamical system) (Polderman and Willems 1991) *A dynamical system \mathcal{G} is defined as a triple*

$$\mathcal{G} = (\mathbb{T}, \mathbb{W}, \mathfrak{B}), \quad (2.1)$$

with \mathbb{T} (often a subset of \mathbb{R}) called the time-axis, \mathbb{W} a set called the signal space, and \mathfrak{B} a subset of $\mathbb{W}^{\mathbb{T}}$ called the behavior ($\mathbb{W}^{\mathbb{T}}$ is the standard notation for the collection of all maps from \mathbb{T} to \mathbb{W}).

The set \mathbb{T} defines the time-axis¹ of the system, describing continuous, $\mathbb{T} = \mathbb{R}$, and discrete, $\mathbb{T} = \mathbb{Z}$, systems alike, while \mathbb{W} gives the range of the system signals. \mathfrak{B} defines the physical laws, the rules for selecting which trajectories of $\mathbb{W}^{\mathbb{T}}$ are possible and which are not. As it will be shown, this definition of dynamical systems is wide enough to contain popular system classes like *Linear Time-Invariant* (LTI) (Polderman and Willems 1991), *Linear Parameter-Varying* (LPV) (see Chapter 3), *Linear Time-Varying* (LTV) (Zerz 2006; Ilchmann and Mehrmann 2005), and even *nonlinear* (NL) systems (Polderman and Willems 1991; Pommaret 2001).

Two crucial properties of dynamical systems are linearity and time-invariance:

Definition 2.2 (Linear dynamical system) (Polderman and Willems 1991) *A dynamical system \mathcal{G} is called linear, if \mathbb{W} is a vector space and \mathfrak{B} is a linear subspace of $\mathbb{W}^{\mathbb{T}}$.*

Definition 2.3 (Time-invariant dynamical system) (Polderman and Willems 1991) *A dynamical system \mathcal{G} is called time-invariant, if \mathbb{T} is closed under addition and $q^{\tau}\mathfrak{B} = \mathfrak{B}$ for all $\tau \in \mathbb{T}$, where q is the forward time-shift operator, $q^{\tau}w(t) = w(t + \tau)$.*

A particularly important class of systems, which has both of these properties, are called LTI systems:

Definition 2.4 (LTI system) (Polderman and Willems 1991) *A dynamical system is called LTI if it is both linear and time-invariant.*

The class of LTI systems is considered to be the collection of the most simplest dynamical systems. Systems belonging to this class have been successfully used in countless engineering applications to describe or approximate a wide range of physical phenomena. In the sequel of the chapter, we recollect the major properties, representations, and identification theory of such systems with the intention to extend these concepts to the LPV case. In the remaining part, we restrict our attention to LTI dynamical systems which can be described by differential or difference equations that have finite order and finite signal dimension ($\mathbb{W} = \mathbb{R}^{n_{\mathbb{W}}}$, $n_{\mathbb{W}} \in \mathbb{N}$). We call these systems *Linear Time-Invariant Differential/Difference* systems and denote them with \mathcal{F} . A basic property of such systems is that their behaviors \mathfrak{B} are complete ($w \in \mathfrak{B} \Leftrightarrow w|_{[t_0, t_1]} \in \mathfrak{B}|_{[t_0, t_1]}, \forall [t_0, t_1] \subset \mathbb{T}$). In the sequel, if refer to LTI systems, we refer to this system class.

¹In general, \mathbb{T} can be more than just literally “time”, as it is defined to be a set of independent variables governing the system. For systems described by partial differential equations it can also involve space coordinates like position.

2.1.2 Representations of continuous-time LTI systems

In this section, we investigate the case when $\mathbb{T} = \mathbb{R}$, to which we refer as the *continuous-time* (CT) case. Consider the constant-coefficient *differential equation* (DE):

$$R\left(\frac{d}{dt}\right)w = 0, \quad R \in \mathbb{R}[\xi]^{n_r \times n_w}, \quad (2.2)$$

where $\mathbb{R}[\xi]^{n_r \times n_w}$ denotes the ring of real polynomial matrices in the indeterminate ξ with n_r rows and n_w columns. We denote by n_ξ the maximal power of ξ in $R(\xi)$, i.e. $\deg(R(\xi)) = n_\xi$. Define $\mathcal{L}_1^{\text{loc}}(\mathbb{R}, \mathbb{R}^{n_w})$, the space of locally integrable functions $w : \mathbb{R} \rightarrow \mathbb{R}^{n_w}$ satisfying:

$$\int_{\tau_1}^{\tau_2} \|w(t)\|_2 < \infty, \quad (2.3)$$

with $[\tau_1, \tau_2] \subset \mathbb{R}$ and $\|\cdot\|_2$ denoting the Euclidian norm on \mathbb{R}^{n_w} . Also define $\mathcal{C}^\infty(\mathbb{R}, \mathbb{R}^r)$ as the space of infinitely differentiable functions $w : \mathbb{R} \rightarrow \mathbb{R}^r$. Now we can formulate the definition of solutions we consider for (2.2). Restricting ourselves to \mathcal{C}^∞ would leave out important functions like steps. On the other hand, the space of distributions is too large to have the solution at every time instant well-defined. A vital alternative is $\mathcal{L}_1^{\text{loc}}$, which is large enough to accommodate steps, ramps, and so on and still concrete enough to avoid problems with distributions. Thus, the concept of solution is introduced in the following sense:

Definition 2.5 (Weak solution) We call $w \in \mathcal{L}_1^{\text{loc}}(\mathbb{R}, \mathbb{R}^{n_w})$ a *weak solution* of (2.2), if

$$\langle w, R^\top \left(-\frac{d}{dt}\right)\varphi \rangle := \int_{\mathbb{R}} w^\top R^\top \left(-\frac{d}{dt}\right)\varphi dt = 0 \quad (2.4)$$

holds for all smooth, so called *test function* $\varphi : \mathbb{R} \rightarrow \mathbb{R}^{n_r}$ with compact support.

Now we can give the differential equation or so called *kernel* (KR) representation of CT-LTI dynamic systems as follows:

Definition 2.6 (CT-KR-LTI representation) (Polderman and Willems 1991) The constant-coefficient differential equation (2.2) is called a *continuous-time kernel representation*, denoted by $\mathfrak{R}_K(\mathcal{F})$, of the LTI dynamical system $\mathcal{F} = (\mathbb{R}, \mathbb{R}^{n_w}, \mathfrak{B})$, if

$$\mathfrak{B} = \left\{ w \in \mathcal{L}_1^{\text{loc}}(\mathbb{R}, \mathbb{R}^{n_w}) \mid w \text{ is a weak solution of } R\left(\frac{d}{dt}\right)w = 0 \right\}. \quad (2.5)$$

Note that in the considered class of LTI systems, any system with $\mathbb{T} = \mathbb{R}$ has a KR representation. As a next step, we introduce the concept of rank with respect to matrix polynomials:

Definition 2.7 (Rank of matrix polynomials) The *row* (*column*) *rank* of a polynomial matrix $R \in \mathbb{R}[\xi]^{n_1 \times n_2}$ is the dimension of the row (*column*) space of R (the row space is the subspace of $\mathbb{R}[\xi]^{1 \times n_2}$ spanned by the rows of R). As $\mathbb{R}[\xi]^{\times \times}$ is an Euclidian ring, thus row and column ranks are equal, hence $\text{rank}(R)$, being the row or column rank of R , is well-defined.

The following theorem holds:

Theorem 2.1 (Existence of full row rank KR representation) (Polderman and Willems 1991) *Let \mathfrak{B} be given with a KR representation (2.2). Then, \mathfrak{B} can also be represented by a $R' \in \mathbb{R}[\xi]^{1 \times n_w}$ with full row rank.*

We postpone the further investigation of the properties of KR representations for a moment, to deduce other classical representations of LTI systems.

In many applications, in particular in control, it is necessary to group the signals of dynamical systems into sets of input signals $u : \mathbb{R} \rightarrow \mathbb{U}$ and output signals $y : \mathbb{R} \rightarrow \mathbb{Y}$. This is done to distinguish which of them we would like to (or we can) actuate as inputs in order to drive the remaining, so called output signals to a desired trajectory of \mathfrak{B} . The definition of such a IO partition of \mathcal{G} , which is commonly non-unique, is as follows:

Definition 2.8 (IO partition) (Polderman and Willems 1991) *Let $\mathcal{G} = (\mathbb{T}, \mathbb{R}^{n_w}, \mathfrak{B})$. The partition of the signal space as $\mathbb{R}^{n_w} = \mathbb{U} \times \mathbb{Y} = \mathbb{R}^{n_u} \times \mathbb{R}^{n_y}$ with $n_u, n_y > 0$ and partition of $w \in \mathcal{L}_1^{\text{loc}}(\mathbb{T}, \mathbb{R}^{n_w})$ correspondingly² as $w = \text{col}(u, y)$ with $u \in \mathcal{L}_1^{\text{loc}}(\mathbb{T}, \mathbb{U})$ and $y \in \mathcal{L}_1^{\text{loc}}(\mathbb{T}, \mathbb{Y})$ is called an IO partition of \mathcal{G} , if*

1. *u is free, i.e. for all $u \in \mathcal{L}_1^{\text{loc}}(\mathbb{T}, \mathbb{U})$, there exists a $y \in \mathcal{L}_1^{\text{loc}}(\mathbb{T}, \mathbb{Y})$ such that $\text{col}(u, y) \in \mathfrak{B}$.*
2. *y does not contain any further free component, i.e. given u , none of the components of y can be chosen freely (maximally free).*

In terms of Definition 2.8, if (u, y) is an IO partition of $\mathcal{F} = (\mathbb{R}, \mathbb{R}^{n_w}, \mathfrak{B})$, then there exist matrix-polynomials $R_y \in \mathbb{R}[\xi]^{n_y \times n_w}$ and $R_u \in \mathbb{R}[\xi]^{n_y \times n_u}$ with R_y full row rank, such that (2.2) can be written as

$$R_y \left(\frac{d}{dt} \right) y = R_u \left(\frac{d}{dt} \right) u, \quad (2.6)$$

and the corresponding behavior is

$$\mathfrak{B} = \left\{ w = \text{col}(u, y) \in \mathcal{L}_1^{\text{loc}}(\mathbb{R}, \mathbb{U} \times \mathbb{Y}) \mid R_y \left(\frac{d}{dt} \right) y = R_u \left(\frac{d}{dt} \right) u \text{ holds weakly} \right\}.$$

Furthermore, due to the maximum freedom of the input signal u , such a IO partition of an LTI system defines a causal mapping in case the solutions of (2.6) are restricted to have left compact support (zero initial conditions at $t = -\infty$). Otherwise, initial conditions do matter (Willems 2007). Those LTI systems which have no IO partition are conventionally called *autonomous* systems. In case $n_u = n_y = 1$, systems are referred as *Single-Input Single-Output (SISO)*, while systems with $n_u > 1, n_y > 1$ are called *Multiple-Input Multiple-Output (MIMO)* systems.

²col denotes column vector composition.

Definition 2.9 (CT-LTI-IO representation) (Polderman and Willems 1991) *The continuous-time IO representation of $\mathcal{F} = (\mathbb{R}, \mathbb{R}^{n_u+n_y}, \mathfrak{B})$ with IO partition (u, y) is denoted by $\mathfrak{R}_{\text{IO}}(\mathcal{F})$ and defined as a differential-equation system with order n_a :*

$$\sum_{i=0}^{n_a} a_i \frac{d^i}{dt^i} y = \sum_{j=0}^{n_b} b_j \frac{d^j}{dt^j} u, \quad (2.7)$$

where $a_j \in \mathbb{R}^{n_y \times n_y}$ and $b_j \in \mathbb{R}^{n_y \times n_u}$ with $a_{n_a} \neq 0$ and $b_{n_b} \neq 0$ are the coefficients of the matrix polynomials R_u and R_y satisfying (2.6) with R_y full row rank. Due to the maximum freedom of u , such polynomials exist with $n_a \geq n_b \geq 0$.

Full row rank of R_y and maximal freedom of u implies that $\det(R_y(\xi)) \neq 0$. Then, we call the rational matrix polynomial function

$$F(\xi) = R_y^{-1}(\xi)R_u(\xi), \quad (2.8)$$

the *transfer function* of $\mathfrak{R}_{\text{IO}}(\mathcal{F})$. Note that $n_b \leq n_a$, i.e. the order of the nominator polynomial is less than or equal to the order of the denominator polynomial. Such a transfer function F is called *proper* and it satisfies

$$\lim_{\xi \rightarrow \infty} [F(\xi)]_{ij} < \infty, \quad \forall i, j \quad (2.9)$$

where $[\cdot]_{ij}$ denotes the element of a matrix in the i^{th} row and j^{th} column. If $n_b < n_a$ holds, then we call F *strictly proper* and

$$\lim_{\xi \rightarrow \infty} [F(\xi)]_{ij} = 0. \quad (2.10)$$

It is well-known, that if we denote by $Y(s)$ and $U(s)$ the *Laplace transforms* of $(u, y) \in \mathfrak{B}$ respectively, where (u, y) have left compact support and $s \in \mathbb{C}$ denotes the *Laplace variable*, then

$$Y(s) = F(s)U(s). \quad (2.11)$$

Substitution of s in F by $i\omega$ gives the so called *frequency response* $F(i\omega)$ of the system, with $\omega \in \mathbb{R}$ as the frequency and $i = \sqrt{-1}$ as the imaginary unit. Additionally, let R'_y and R'_u be coprime polynomials such that $F(\xi) = (R'_y)^{-1}(\xi)R'_u(\xi)$. Then all $s \in \mathbb{C}$, for which $\det(R'_y(s)) = 0$, are called the *poles* of F , while all $s \in \mathbb{C}$ satisfying $\det(R'_u(s)) = 0$ are called the *zeros* of F . Furthermore, by applying a Laurent series-expansion of $F(s)$ around $s = \infty$, it can be shown, that there exists a sequence of constants $\{\mathbf{g}_i\}_{i=0}^{\infty} \subset \mathbb{R}^{n_y \times n_u}$, so called *Markov parameters*, such that

$$F(s) = \sum_{i=0}^{\infty} \mathbf{g}_i s^{-i}. \quad (2.12)$$

Such a sequence is unique for any $\mathfrak{R}_{\text{IO}}(\mathcal{F})$, therefore it is quite often used as a representation of \mathcal{F} . Moreover, the signal

$$h = \mathcal{L}^{-1} \left\{ \sum_{i=0}^{\infty} \mathbf{g}_i s^{-i} \right\}, \quad (2.13)$$

is called the *impulse response* of $\mathfrak{R}_{\text{IO}}(\mathcal{F})$ (\mathcal{L}^{-1} is the standard notation of the *inverse Laplace transformation*). Such a signal corresponds to the response of $\mathfrak{R}_{\text{IO}}(\mathcal{F})$ for an impulse input at $t = 0$ and it uniquely represents the IO behavior of \mathcal{F} .

Besides partitioning the signals of the system in an IO sense, we often need to introduce additional variables in most modeling exercises to express more conveniently the relationships of those signals which we are particularly interested in. This is motivated by the first principle laws of physics where we can often meet physically non-existing (virtual) variables like the potential field in the well-known Maxwell's equations. Also it can happen that we are just simply not interested in some "inner" variables of the system, like in the voltage drop on a resistor of a space shuttle, if we would like to control its motion around the planet. We call these other, auxiliary variables *latent variables*.

Definition 2.10 (Latent variable equivalent) (Polderman and Willems 1991) *The latent variable equivalent of a dynamical system $\mathcal{G} = (\mathbb{T}, \mathbb{W}, \mathfrak{B})$ is defined as a system $\mathcal{G}_L = (\mathbb{T}, \mathbb{W} \times \mathbb{W}_L, \mathfrak{B}_L)$ with \mathbb{T} the time-axis, \mathbb{W} the manifest signal space, \mathbb{W}_L the latent signal space, and $\mathfrak{B}_L \subseteq (\mathbb{W} \times \mathbb{W}_L)^\top$ the full behavior satisfying that*

$$\mathfrak{B} = \{w : \mathbb{T} \rightarrow \mathbb{W} \mid \exists w_L : \mathbb{T} \rightarrow \mathbb{W}_L \text{ such that } (w, w_L) \in \mathfrak{B}_L\}, \quad (2.14)$$

where \mathfrak{B} is called the manifest behavior of \mathfrak{B}_L .

Assuming that a continuous-time LTI system contains n_L latent and n_W manifest variables, then as a generalization of (2.2):

$$R\left(\frac{d}{dt}\right)w = R_L\left(\frac{d}{dt}\right)w_L, \quad (2.15)$$

where $w : \mathbb{R} \rightarrow \mathbb{R}^{n_W}$ is the manifest variable, $w_L : \mathbb{R} \rightarrow \mathbb{R}^{n_L}$ is the latent variable, $R(\xi) \in \mathbb{R}[\xi]^{n_r \times n_W}$ and $R_L(\xi) \in \mathbb{R}[\xi]^{n_r \times n_L}$ are polynomial matrices, and

$$\begin{aligned} \mathfrak{B}_L &= \{(w, w_L) \in \mathcal{L}_1^{\text{loc}}(\mathbb{R}, \mathbb{R}^{n_W} \times \mathbb{R}^{n_L}) \mid (w, w_L) \text{ satisfy (2.15) weakly}\}, \\ \mathfrak{B} &= \{w \in \mathcal{L}_1^{\text{loc}}(\mathbb{R}, \mathbb{R}^{n_W}) \mid \exists w_L \in \mathcal{L}_1^{\text{loc}}(\mathbb{R}, \mathbb{R}^{n_L}) \text{ s.t. } (w, w_L) \in \mathfrak{B}_L\}. \end{aligned}$$

Now we can introduce an important class of latent variables, the so called *state-variables*, which not only naturally show up in applications, but are also useful in the analysis and synthesis of dynamical systems. These variables often have a direct interpretation in terms of physical variables like positions, velocities, and masses and have a special property that distinguishes them from other latent variables:

Definition 2.11 (Property of state) (Polderman and Willems 1991) *Consider a latent variable system \mathcal{G}_L . Let $(w_1, w_{L,1}), (w_2, w_{L,2}) \in \mathfrak{B}_L$ and $t_0 \in \mathbb{T}$. In case of $\mathbb{T} = \mathbb{R}$, assume that $w_{L,1}$ and $w_{L,2}$ are continuous on \mathbb{R} . Define the concatenation of $(w_1, w_{L,1})$ and $(w_2, w_{L,2})$ at t_0 by $(w, w_L) = (w_1, w_{L,1}) \underset{t_0}{\wedge} (w_2, w_{L,2})$ with*

$$w(t) = \begin{cases} w_1(t), & t < t_0, \\ w_2(t), & t \geq t_0, \end{cases} \quad \text{and} \quad w_L(t) = \begin{cases} w_{L,1}(t), & t < t_0, \\ w_{L,2}(t), & t \geq t_0. \end{cases} \quad (2.16)$$

Then \mathfrak{B}_L is called a *state-space behavior*, and the latent variable w_L is called the *state*, if $w_{L,1}(t_0) = w_{L,2}(t_0)$ implies $(w, w_L) \in \mathfrak{B}_L$.

In this way, w_L with the property of state acts as the memory of \mathcal{G}_L . The following theorem holds:

Theorem 2.2 (State-kernel form) (Rapisarda and Willems 1997) *The latent variable w_L is a state, iff there exist matrices $r_w \in \mathbb{R}^{n_r \times n_w}$ and $r_0, r_1 \in \mathbb{R}^{n_r \times n_L}$ such that the full behavior \mathfrak{B}_L has the kernel representation:*

$$r_w w + r_0 w_L + r_1 \xi w_L = 0. \quad (2.17)$$

Based on Theorem 2.2, as a convention we assume that the state latent variables are chosen in such way that in (2.15), $\deg(R_L(\xi)) = 1$, while $\deg(R(\xi)) = 0$ and $R_L(\xi)$ is monic. In this way, a CT-LTI *state-space* (SS) behavior is always defined by a first-order constant-coefficient DE. Now we can give the definition of the so called SS representation of \mathcal{F} :

Definition 2.12 (CT-LTI-SS representation) (Polderman and Willems 1991) *The continuous-time state-space representation of $\mathcal{F} = (\mathbb{R}, \mathbb{R}^{n_u + n_y}, \mathfrak{B})$ is denoted by $\mathfrak{R}_{SS}(\mathcal{F})$ and defined as a first-order constant-coefficient differential equation system in the latent variable $x : \mathbb{R} \rightarrow \mathbb{X}$:*

$$\frac{d}{dt}x = Ax + Bu, \quad (2.18a)$$

$$y = Cx + Du, \quad (2.18b)$$

where (u, y) is the IO partition of \mathcal{F} , x is the state-vector, $\mathbb{X} = \mathbb{R}^{n_x}$ is the state-space,

$$\mathfrak{B}_{SS} = \{(u, x, y) \in \mathcal{L}_1^{\text{loc}}(\mathbb{R}, \mathbb{U} \times \mathbb{X} \times \mathbb{Y}) \mid (2.18a) \ \& \ (2.18b) \text{ are satisfied weakly}\},$$

is the full behavior of the manifest behavior \mathfrak{B} , and

$$\left[\begin{array}{c|c} A & B \\ \hline C & D \end{array} \right] \in \left[\begin{array}{c|c} \mathbb{R}^{n_x \times n_x} & \mathbb{R}^{n_x \times n_u} \\ \hline \mathbb{R}^{n_y \times n_x} & \mathbb{R}^{n_y \times n_u} \end{array} \right],$$

represents the SS matrices of $\mathfrak{R}_{SS}(\mathcal{F})$.

Note that in the full behavior \mathfrak{B}_{SS} , the latent variable x trivially fulfills the state property in terms of Theorem 2.2. An SS representation also has a transfer function in the form of

$$F(\xi) = D + C(\xi I - A)^{-1}B. \quad (2.19)$$

The transfer functions of $\mathfrak{R}_{SS}(\mathcal{F})$ and $\mathfrak{R}_{IO}(\mathcal{F})$ are equivalent and they describe the behavior of \mathcal{F} restricted to signal trajectories with compact left support. Moreover, their Markov parameters satisfy that $g_0 = D$ and $g_i = CA^{i-1}B$ for $i \geq 1$.

2.1.3 Representations of discrete-time LTI systems

Even if in the physical reality, the time-variation of systems, with a very few exceptions, is exclusively and inherently continuous, the class of *discrete-time* (DT) dynamical systems, where the time-axis is restricted to $\mathbb{T} = \mathbb{Z}$, is particularly important for engineering applications. Since the introduction of digital computation

operated on a DT scale, digital processors controlled systems have widespread in industry and have become a part of our daily life from coffee vendor machines to space shuttles. The essential interaction between the DT and CT world is accomplished or viewed through the so called *sampling* of physical continuous-time signals, observing them at specific points of the CT time-axis. With the restriction of periodic, equidistant sampling, we call $w' : \mathbb{Z} \rightarrow \mathbb{W}$

$$w'(k) = w(kT_d), \quad \forall k \in \mathbb{Z}, \quad (2.20)$$

the DT projection or discretization of the signal $w : \mathbb{R} \rightarrow \mathbb{W}$ with *sampling-time* or *discretization-step* $T_d \in \mathbb{R}^+$, where $\mathbb{R}^+ = \{x \in \mathbb{R} \mid x > 0\}$. In this way, we call $\mathcal{G}' = (\mathbb{Z}, \mathbb{W}, \mathfrak{B}')$ the DT equivalent of $\mathcal{G} = (\mathbb{R}, \mathbb{W}, \mathfrak{B})$ under sampling-time T_d , if

$$\mathfrak{B}' = \{w' \in \mathbb{W}^{\mathbb{Z}} \mid \exists w \in \mathfrak{B} \text{ such that (2.20) is fulfilled}\} \quad (2.21)$$

Note that the concept of sampling only provides a particular viewpoint for the understanding of the universe of DT systems. It is not guaranteed that a CT system has a DT equivalent for arbitrary T_d , nor that every DT system is an equivalent of a sampled CT system. It must be clear, that DT systems are a stand alone mathematical concept of modeling, however they have strong relation to the CT domain based on the concept of sampling.

In the remaining part of this section, we give the DT analog of the concepts of CT-LTI systems. Many of these concepts have been introduced in the way that by associating the indeterminate ξ with the forward time-shift operator q , the DT equivalent directly results.

Consider the constant-coefficient *difference equation* (DF):

$$R(q)w = 0, \quad R \in \mathbb{R}[\xi]^{n_r \times n_w}. \quad (2.22)$$

Definition 2.13 (DT-KR-LTI representation) (Polderman and Willems 1991) *The constant-coefficient difference equation (2.22) is called a discrete-time kernel (KR) representation, denoted by $\mathfrak{R}_K(\mathcal{F})$, of the LTI dynamical system $\mathcal{F} = (\mathbb{Z}, \mathbb{R}^{n_w}, \mathfrak{B})$ if*

$$\mathfrak{B} = \{w \in (\mathbb{R}^{n_w})^{\mathbb{Z}} \mid w \text{ is a solution of } R(q)w = 0\}. \quad (2.23)$$

Note that in the considered class of LTI systems, any system with $\mathbb{T} = \mathbb{Z}$ has a KR representation. In terms of Theorem 2.1, such representations can always be given with full row rank. We denote the discrete-time KR representation of a continuous-time LTI dynamical system $\mathcal{F} = (\mathbb{R}, \mathbb{R}^{n_w}, \mathfrak{B})$ by $\mathfrak{R}_K(\mathcal{F}, T_d)$, if the DT behavior \mathfrak{B}' of this representation is equivalent with \mathfrak{B} under T_d . Similar to the continuous-time case, we can give the definition of IO representations, based on a valid IO partition (u, y) of a discrete-time \mathcal{F} .

Definition 2.14 (DT-LTI-IO representation) (Polderman and Willems 1991) *The discrete-time IO representation of the LTI system $\mathcal{F} = (\mathbb{Z}, \mathbb{R}^{n_u+n_y}, \mathfrak{B})$ is denoted by $\mathfrak{R}_{IO}(\mathcal{F})$ and defined as a difference-equation system with order n_a :*

$$\sum_{i=0}^{n_a} a_i q^i y = \sum_{j=0}^{n_b} b_j q^j u, \quad (2.24)$$

where (u, y) is the IO partition of \mathcal{F} , $a_j \in \mathbb{R}^{n_y \times n_y}$ and $b_j \in \mathbb{R}^{n_y \times n_u}$ with $a_{n_a} \neq 0$ and $b_{n_b} \neq 0$ are the coefficients of the underlying matrix polynomials R_u, R_y with R_y being full row rank and $n_a \geq n_b \geq 0$.

By defining $u'(k) := u(kT_d)$ and $y'(k) := y(kT_d)$, the discrete-time IO representation, denoted by $\mathfrak{R}_{\text{IO}}(\mathcal{F}, T_d)$, of a continuous-time LTI system \mathcal{F} with IO partition (u, y) can be given, with equivalent behaviors under the sampling-time T_d .

Similar to the CT case, the transfer function $F(\xi)$ of an IO representation can be introduced. For a $\text{col}(u, y) \in \mathfrak{B}$ with left compact support, denote by $Y(z)$ and $U(z)$ the Z -transforms of u and y , defined on their appropriate region of convergence³ (ROC) with $z \in \mathbb{C}$ called the Z -variable. Then F satisfies that

$$Y(z) = F(z)U(z), \quad (2.25)$$

for any z in the intersection of the ROC of $Y(z)$ and $U(z)$. Substitution of z in $F(z)$ by $e^{i\omega T_d}$ gives the frequency response of the DT system. The Markov parameters of $F(z)$ are similarly deduced as in CT by a Laurent expansion around $z = \infty$, while the impulse response of $F(z)$ is given as

$$h = \mathcal{L}^{-1} \left\{ \sum_{i=0}^{\infty} \mathbf{g}_i z^{-i} \right\}, \quad (2.26)$$

where \mathcal{L}^{-1} represents the *inverse Z-transformation*.

For the discrete-time behavior \mathfrak{B} , we can also introduce latent variables in terms of Definition 2.10 with the property of state (see Definition 2.11). Based on these concepts, DT state-space representations of a \mathcal{F} are defined as follows:

Definition 2.15 (DT-LTI-SS representation) (Polderman and Willems 1991) *The SS representation $\mathfrak{R}_{\text{SS}}(\mathcal{F})$ of the LTI system $\mathcal{F} = (\mathbb{Z}, \mathbb{R}^{n_u+n_y}, \mathfrak{B})$ is defined as a first-order constant-coefficient difference-equation system in the latent variable $x : \mathbb{Z} \rightarrow \mathbb{X}$:*

$$qx = Ax + Bu, \quad (2.27a)$$

$$y = Cx + Du, \quad (2.27b)$$

where (u, y) is the I/O partition of \mathcal{F} , x is the state-vector, $\mathbb{X} = \mathbb{R}^{n_x}$ is the state-space,

$$\mathfrak{B}_{\text{SS}} = \{ (u, x, y) \in (\mathbb{U} \times \mathbb{X} \times \mathbb{Y})^{\mathbb{Z}} \mid (2.27a) \ \& \ (2.27b) \text{ are satisfied} \},$$

is the full behavior of the manifest behavior \mathfrak{B} , and

$$\left[\begin{array}{c|c} A & B \\ \hline C & D \end{array} \right] \in \left[\begin{array}{c|c} \mathbb{R}^{n_x \times n_x} & \mathbb{R}^{n_x \times n_u} \\ \hline \mathbb{R}^{n_y \times n_x} & \mathbb{R}^{n_y \times n_u} \end{array} \right],$$

represents the SS matrices of $\mathfrak{R}_{\text{SS}}(\mathcal{F})$.

³The region of convergence is the set of points in \mathbb{C} for which the Z -transform associated summation converges.

Again, the discrete-time SS representation of a continuous-time LTI dynamical system $\mathcal{F} = (\mathbb{R}, \mathbb{R}^{n_u + n_y}, \mathfrak{B})$ is denoted as $\mathfrak{R}_{\text{SS}}(\mathcal{F}, T_d)$, where the manifest behavior of $\mathfrak{R}_{\text{SS}}(\mathcal{F}, T_d)$ is equivalent with \mathfrak{B} under the sampling-time T_d . The transfer function of a discrete-time $\mathfrak{R}_{\text{SS}}(\mathcal{F})$ is similarly deduced as in the CT case (see equation (2.19)) and the same relation holds for the Markov parameters.

2.1.4 Equivalence classes and relations

In this subsection, we briefly cover the relation and the main properties of the introduced system representations. We require the introduction of these concepts as later we intend to extend this unified framework to LPV systems. First we concentrate on KR representations of a given \mathcal{F} . The following definition is important:

Definition 2.16 (Equal behaviors) (Polderman and Willems 1991) *Let $\mathfrak{B}_i \subseteq (\mathbb{R}^{n_w})^{\mathbb{T}}$, $i = 1, 2$. We call \mathfrak{B}_1 and \mathfrak{B}_2 equal if*

$$w \in \mathfrak{B}_1 \cap C^\infty(\mathbb{R}, \mathbb{R}^{n_w}) \Leftrightarrow w \in \mathfrak{B}_2 \cap C^\infty(\mathbb{R}, \mathbb{R}^{n_w}), \quad \text{for } \mathbb{T} = \mathbb{R}, \quad (2.28a)$$

$$w \in \mathfrak{B}_1 \Leftrightarrow w \in \mathfrak{B}_2, \quad \text{for } \mathbb{T} = \mathbb{Z}. \quad (2.28b)$$

As an abuse of notation, we introduce $\mathfrak{B}_1 = \mathfrak{B}_2$ to denote equality of \mathfrak{B}_1 and \mathfrak{B}_2 in terms of Definition 2.16. In analogy, the equivalence of KR representations follows as:

Definition 2.17 (Equivalent KR representations) (Polderman and Willems 1991) *Let $R_i \in \mathbb{R}[\xi]^{n_r \times n_w}$, $i = 1, 2$. Then the KR representations:*

$$R_1(\xi)w = 0 \quad \text{and} \quad R_2(\xi)w = 0, \quad (2.29)$$

where ξ is either $\frac{d}{dt}$ or q , are called equivalent, if they define the same (equal) behavior.

The existence of equivalent KR representations implies that such representations of dynamical systems are non-unique. To show this, introduce the concept of unimodular matrices:

Definition 2.18 (Unimodular matrix) *Let $M \in \mathbb{R}[\xi]^{n \times n}$. Then M is called an unimodular polynomial matrix if there exists a $M^\dagger \in \mathbb{R}[\xi]^{n \times n}$, such that $M^\dagger M = I$. In other words, $\det(M)$ is equal to a nonzero constant.*

Then, the following theorem holds:

Theorem 2.3 (Left-side unimodular transformation) (Polderman and Willems 1991) *Let $R \in \mathbb{R}[\xi]^{n_r \times n_w}$ and $M \in \mathbb{R}[\xi]^{n_r \times n_r}$ with M unimodular. Define $R' := MR$. Denote the behaviors corresponding to R and R' by \mathfrak{B} and \mathfrak{B}' respectively. Then $\mathfrak{B} = \mathfrak{B}'$.*

Furthermore, if $R \in \mathbb{R}[\xi]^{n_r \times n_w}$ is not full row rank, i.e. $\text{rank}(R) = n < n_r$, then there exists a unimodular $M \in \mathbb{R}[\xi]^{n_r \times n_r}$ such that

$$MR = \begin{bmatrix} R' \\ 0 \end{bmatrix}, \quad (2.30)$$

where $R' \in \mathbb{R}[\xi]^{n \times n_w}$ is full row rank and the corresponding behaviors are equivalent in terms of Theorem 2.3.

Theorem 2.4 (Right-side unimodular transformation) (Polderman and Willems 1991) *Let $R \in \mathbb{R}[\xi]^{n_r \times n_w}$ and $M \in \mathbb{R}[\xi]^{n_w \times n_w}$ with M unimodular. Denote the behaviors defined by R and RM as \mathfrak{B} and \mathfrak{B}' .*

- If $\mathbb{T} = \mathbb{R}$, then $\mathfrak{B} \cap \mathcal{C}^\infty(\mathbb{R}, \mathbb{R}^{n_w})$ and $\mathfrak{B}' \cap \mathcal{C}^\infty(\mathbb{R}, \mathbb{R}^{n_w})$ are isomorphic⁴.
- If $\mathbb{T} = \mathbb{Z}$, then \mathfrak{B} and \mathfrak{B}' are isomorphic.
- If M is constant (zero order polynomial), then \mathfrak{B} and \mathfrak{B}' are isomorphic even if $\mathbb{T} = \mathbb{R}$.

In other words, Theorem 2.4 implies that right-side unimodular transformations do not change the underlying relation between the system signals, but they do change the signals, the trajectories of the behavior in an isomorphic sense. There is an important form of LTI-KR representations that can be obtained via left and right-side unimodular transformations:

Theorem 2.5 (Smith-McMillan form) (Polderman and Willems 1991) *Let $R \in \mathbb{R}[\xi]^{n_r \times n_w}$ with $\text{rank}(R) = n$. Then, there exist unimodular matrices $M_1 \in \mathbb{R}[\xi]^{n_r \times n_r}$ and $M_2 \in \mathbb{R}[\xi]^{n_w \times n_w}$ such that*

$$M_1 R M_2 = \begin{bmatrix} R' & 0 \\ 0 & 0 \end{bmatrix},$$

where $R'(\xi) = \text{diag}(r_1, \dots, r_n)$ for some $0 \neq r_i \in \mathbb{R}[\xi]$.

The Smith-McMillan form gives a unique representation of the behavior associated with R and it is important for the characterization of the concept of minimality. Now it is possible to introduce the notion of *equivalence relation* based on Guidorzi (1981) and Kalman (1963):

Definition 2.19 (Equivalence relation) *Introduce the symbol \sim to denote the equivalence relation on $\bigcup \mathbb{R}[\xi]^{\cdot \times \cdot}$ (all polynomial matrices with finite dimensions). $R_1 \in \mathbb{R}[\xi]^{n_1 \times n_w}$ and $R_2 \in \mathbb{R}[\xi]^{n_2 \times n_w}$ with $n_1 \geq n_2$ are called equivalent, i.e. $R_1 \sim R_2$, if there exists a unimodular matrix $M \in \mathbb{R}[\xi]^{n_1 \times n_1}$ such that*

$$MR_1 = \begin{bmatrix} R_2 \\ 0 \end{bmatrix} \begin{array}{c} \updownarrow \\ \updownarrow \end{array} \begin{array}{c} n_2 \\ n_1 - n_2 \end{array}. \quad (2.31)$$

⁴An isomorphism is a bijective map f between two algebraic structures (groups, rings, or vector spaces) such that both f and its inverse f^{-1} preserve all the relevant structure; i.e. properties like identity elements, inverse elements, and binary operations (they are homomorphisms).

This implies that if $R_1 \sim R_2$, then the corresponding behaviors are equal.

Definition 2.20 (Equivalence class) *The set $\mathcal{E} \subseteq \bigcup \mathbb{R}[\xi]^{\cdot \times \cdot}$ is called an equivalence class, if it is a maximal subset of $\mathbb{R}[\xi]^{\cdot \times \cdot}$ such that $R_1, R_2 \in \mathcal{E}$ implies that $R_1 \sim R_2$.*

An equivalence class defines the set of all representations which have the same behavior. An important subset of an equivalence class are the so called minimal representations:

Definition 2.21 (Minimality) (Polderman and Willems 1991) *$R \in \mathbb{R}[\xi]^{n_r \times n_w}$ is called minimal if it has full row rank, i.e. $\text{rank}(R) = n_r$.*

We call $\sum_{i=1}^n \deg(r_i)$ in the Smith-McMillan form of a R associated with $\mathfrak{R}_K(\mathcal{F})$, the degree of all KR representations in the same equivalence class. This degree is often referred as the *McMillan degree* of \mathcal{F} . Note that for a minimal $\mathfrak{R}_K(\mathcal{F})$ with $n_w = 1$, the McMillan degree of \mathcal{F} is equal to $\deg(R) = n_\xi$.

To be able to uniquely specify or sort equivalence classes, we need a specially distinguished subclass of representations:

Definition 2.22 (Canonical forms) $\mathcal{E}_{\text{can}} \subset \bigcup \mathbb{R}[\xi]^{\cdot \times \cdot}$ is called a set of canonical forms, if each element of $\bigcup \mathbb{R}[\xi]^{\cdot \times \cdot}$ is equivalent under \sim with only one element of \mathcal{E}_{can} . (\mathcal{E}_{can} is the class representative of $\bigcup \mathbb{R}[\xi]^{\cdot \times \cdot}$ under \sim).

The introduced concepts generalize to IO representations as well. We can define equivalence relation on pairs of $\mathbb{R}[\xi]^{\cdot \times \cdot}$, which define an IO representation:

Definition 2.23 (Equivalence relation of IO representations) *Let $R_u, R'_u \in \mathbb{R}[\xi]^{n_y \times n_u}$ and $R_y, R'_y \in \mathbb{R}[\xi]^{n_y \times n_y}$ with R_y, R'_y full row rank, $\deg(R_y) \geq \deg(R_u)$, and $\deg(R'_y) \geq \deg(R'_u)$. We call (R_y, R_u) and (R'_y, R'_u) equivalent*

$$(R_y, R_u) \sim (R'_y, R'_u), \quad (2.32)$$

if there exists a unimodular matrix $M \in \mathbb{R}[\xi]^{n_y \times n_y}$ such that

$$R'_y = MR_y \quad \text{and} \quad R'_u = MR_u. \quad (2.33)$$

This implies the following concept of minimality for IO representations:

Definition 2.24 (Minimal IO representation) *An IO representation defined through R_y and R_u is called minimal, if there are no R'_u and R'_y polynomials with $\deg(R_y) < \deg(R'_y)$ such that*

$$(R_y, R_u) \sim (R'_y, R'_u).$$

Using the IO equivalence relation and minimality, the definitions of IO equivalence classes and canonical forms extend trivially. Note that for a minimal $\mathfrak{R}_{\text{IO}}(\mathcal{F})$ with $n_y = 1$, the McMillan degree of \mathcal{F} is equal to $\deg(R_y) = n_a$.

For SS representations $\mathfrak{R}_{\text{SS}}(\mathcal{F})$, the SS behavior is defined by a zero-order polynomial matrix $R \in \mathbb{R}[\xi]^{n_r \times (n_v + n_u)}$ and a first-order polynomial matrix $R_L \in \mathbb{R}[\xi]^{n_r \times n_x}$. Left-side multiplication of R and R_L by a unimodular matrix $M \in \mathbb{R}[\xi]^{n_r \times n_r}$ which does not change the order (to satisfy convention) of these polynomials, i.e. $\deg(MR) = \deg(R) = 0$ and $\deg(MR_L) = \deg(R_L) = 1$, is equal to a left-side multiplication by a nonsingular matrix $M_1 \in \mathbb{R}^{n_r \times n_r}$:

$$R' := M_1 R \quad \text{and} \quad R'_L := M_1 R_L. \quad (2.34)$$

However, such a multiplication results in a non-monic $R_L(\xi)$. To stress the monic convention of this polynomial, right-side multiplication of $R'_L(\xi)$ is done by a nonsingular $M_2 \in \mathbb{R}^{n_x \times n_x}$ to eliminate the non-monic term:

$$R''_L := M_1 R_L M_2. \quad (2.35)$$

By Theorem 2.4, we know that such a right-side multiplication does not change the manifest behavior of the resulting SS representation. However, it does change the SS behavior, altering it to an isomorphic group. As a result, the state trajectories of the system are altered, giving a new state variable. Moreover, it can be shown, that such a transformation requires a special structure of M_1 and M_2 . This structure is equivalent by appropriate left and right side multiplications of the SS matrices of $\mathfrak{R}_{\text{SS}}(\mathcal{F})$ with nonsingular matrices $T \in \mathbb{R}^{n_x \times n_x}$ and T^{-1} , called the *state-transformation* (see Rapisarda and Willems (1997) and Kailath (1980)). Based on the previous considerations, the following equivalence relation can be defined:

Definition 2.25 (Equivalence relation of SS representations) Let (A, B, C, D) and (A', B', C', D') be quadruplets of matrices in $\mathbb{R}^{\cdot \times \cdot}$ defining SS representations with $n_x \geq n'_x$. These SS representations are called *equivalent*,

$$\left[\begin{array}{c|c} A & B \\ \hline C & D \end{array} \right] \sim \left[\begin{array}{c|c} A' & B' \\ \hline C' & D' \end{array} \right], \quad (2.36)$$

if there exists a nonsingular matrix transformation $T \in \mathbb{R}^{n_x \times n_x}$ such that:

$$\begin{aligned} TAT^{-1} &= \begin{bmatrix} A' & 0 \\ * & * \end{bmatrix}, & TB &= \begin{bmatrix} B' \\ * \end{bmatrix}, & \begin{matrix} \updownarrow & n'_x \\ \updownarrow & n_x - n'_x \end{matrix} \\ CT^{-1} &= \begin{bmatrix} C' & 0 \end{bmatrix}, & D &= D'. \end{aligned} \quad (2.37)$$

Based on the previous considerations, the existence of a state-transformation T between the matrices of two SS representations implies that they have the same manifest behavior. Furthermore, the states are related as

$$Tx(t) = \begin{bmatrix} x'(t) \\ * \end{bmatrix}, \quad \begin{matrix} \updownarrow & n'_x \\ \updownarrow & n_x - n'_x \end{matrix} \quad \forall t \in \mathbb{T}. \quad (2.38)$$

It trivially follows that a state-transformation in the LTI case always implies algebraic equivalence of the state variables (Kalman 1963).

Definition 2.26 (Minimal SS representation) An SS representation defined through the (A, B, C, D) matrices is called minimal, if there exist no (A', B', C', D') such that

$$\left[\begin{array}{c|c} A & B \\ \hline C & D \end{array} \right] \sim \left[\begin{array}{c|c} A' & B' \\ \hline C' & D' \end{array} \right],$$

with $n'_x < n_x$.

Again, using the SS equivalence relation and minimality, definitions of SS equivalence classes and canonical forms can be established trivially. In addition, the state-dimension n_x of a minimal $\mathfrak{R}_{\text{SS}}(\mathcal{F})$ is equal to the McMillan degree of \mathcal{F} .

2.1.5 Stability of LTI systems

In this subsection, the stability concept of dynamical systems is introduced. Stability is a very common issue in many areas of engineering sciences and mathematics. Intuitively, stability implies that small causes produce small effects. There are several types of stability, but here we use the concept of *dynamical stability*.

Definition 2.27 (Dynamic stability) (Polderman and Willems 1991) *The autonomous LTI dynamical system $\mathcal{F} = (\mathbb{T}, \mathbb{R}^{n_w}, \mathfrak{B})$ is said to be stable, if $(w \in \mathfrak{B}) \Rightarrow (\exists \varepsilon \in \mathbb{R}_0^+)$ such that $\|w(t)\| \leq \varepsilon$ for all $t \geq 0$ (in an arbitrary norm $\|\cdot\|$). It is said to be unstable, if it is not stable; it is said to be asymptotically stable, if it is stable and $(w \in \mathfrak{B}) \Rightarrow (w(t) \rightarrow 0$ as $t \rightarrow \infty)$.*

This definition strongly builds on the linearity (the only fixed point of the dynamic relation is 0) and time-invariance of the system class (stability on $t \geq 0$ implies stability on $t \geq t_0$ for all $t_0 \in \mathbb{R}$). To check the stability of \mathcal{F} , consider the following theorem:

Theorem 2.6 (Stability by KR representation) (Polderman and Willems 1991) *Let $\mathfrak{R}_K(\mathcal{F})$ be the representation of $\mathcal{F} = (\mathbb{T}, \mathbb{R}^{n_w}, \mathfrak{B})$. Denote $R \neq 0$ the matrix polynomial associated with $\mathfrak{R}_K(\mathcal{F})$. Then, \mathcal{F} is*

1. *Asymptotically stable, iff all roots of $\det(R(\xi))$, denoted by $\{\lambda_i\}_{i=1}^n$, satisfy that:*

$$\begin{cases} \operatorname{Re}(\lambda_i) < 0, & \text{for } \mathbb{T} = \mathbb{R}; \\ |\lambda_i| < 1, & \text{for } \mathbb{T} = \mathbb{Z}. \end{cases} \quad (2.39)$$

2. *Stable, iff all $\{\lambda_i\}_{i=1}^n$ satisfy that:*

$$\begin{cases} \operatorname{Re}(\lambda_i) < 0 & \text{or} & \operatorname{Re}(\lambda_i) = 0, \ \& \ \lambda_i \text{ semisimple,} & \text{for } \mathbb{T} = \mathbb{R}; \\ |\lambda_i| < 1 & \text{or} & |\lambda_i| = 1, \ \& \ \lambda_i \text{ semisimple,} & \text{for } \mathbb{T} = \mathbb{Z}. \end{cases} \quad (2.40)$$

where λ_i is a semisimple root of $\det(R(\xi))$, if the dimension of $\ker(R(\lambda_i))$ is equal to the multiplicity of λ_i as a root of $\det(R(\xi))$.

3. *Unstable, iff it is not stable.*

In case of an IO partition of \mathcal{F} , the concept of dynamic stability is formulated around the autonomous part of the behavior (non-free signals) on the half line $[0, \infty)$, where $u = 0$. By considering the generalization of this theorem with respect to IO and SS representations of \mathcal{F} , the following well-know theorems result:

Theorem 2.7 (Stability by IO representation) (Polderman and Willems 1991) *Let $\mathfrak{R}_{\text{IO}}(\mathcal{F})$ be the IO representation of \mathcal{F} with polynomial matrices (R_y, R_u) such that $\deg(R_y) > 0$. Then \mathcal{F} is*

1. *Asymptotically stable, iff all roots of R_y , denoted by $\{\lambda_i\}_{i=1}^{n_a}$ satisfy (2.39).*
2. *Stable, iff all roots of R_y satisfy (2.40) and if λ_i is a semisimple root of R_y , then it is not a root of $R_y^{-1}R_u$.*

Theorem 2.8 (Stability by SS representation) (Polderman and Willems 1991) *Let $\mathfrak{R}_{\text{SS}}(\mathcal{F})$ be the SS representation of \mathcal{F} with state-space matrices (A, B, C, D) , where $A \neq 0$. The latent variable system defined by $\mathfrak{R}_{\text{SS}}(\mathcal{F})$ is*

1. *Asymptotically stable, iff all eigenvalues of A , denoted by $\{\lambda_i\}_{i=1}^{n_x}$ satisfy (2.39).*
2. *Stable, iff all eigenvalues of A satisfy (2.40), where λ_i is a semisimple eigenvalue of A , if the dimension of $\ker(\lambda_i I - A)$ is equal to the multiplicity of λ_i as a root of $\det(\xi I - A)$.*

It is important to note that the concept of dynamic stability implies IO stability (Bounded-Input Bounded-Output (BIBO) stability) in the (signal) ℓ_∞ norm, and asymptotic stability implies IO stability in the ℓ_τ norm, $1 \leq \tau < \infty$:

Definition 2.28 (BIBO stability) (Polderman and Willems 1991) *The LTI dynamical system $\mathcal{F} = (\mathbb{T}, \mathbb{R}^{n_w}, \mathfrak{B})$ with IO partition (u, y) is said to be BIBO stable in the ℓ_τ norm with $1 \leq \tau < \infty$, if*

$$(u, y) \in \mathfrak{B} \quad \text{and} \quad \begin{cases} \text{if } \mathbb{T} = \mathbb{R}, & \int_0^\infty \|u(t)\|^\tau dt < \infty \Rightarrow \int_0^\infty \|y(t)\|^\tau dt < \infty, \\ \text{if } \mathbb{T} = \mathbb{Z}, & \sum_{k=0}^\infty \|u(k)\|^\tau < \infty \Rightarrow \sum_{k=0}^\infty \|y(k)\|^\tau < \infty. \end{cases}$$

It is said to be BIBO stable in the ℓ_∞ norm if

$$(u, y) \in \mathfrak{B} \quad \text{and} \quad \sup_{t \geq 0} \|u(t)\| < \infty \Rightarrow \sup_{t \geq 0} \|y(t)\| < \infty.$$

The concept of *Bounded-Input Bounded-State* (BIBS) stability can be similarly defined for LTI systems with both IO partition and state variables. BIBS stability always implies BIBO stability.

Another approach of stability leads through the approach of Lyapunov, which is widely used for stability analysis of linear and nonlinear systems, with both

time-varying and time-invariant nature. While for LTI systems, the Lyapunov method gives an informative alternative approach, for LPV systems it is the most applicable way to characterize or test stability of a given SS representation (see Section 3.3.2). First we introduce the intuitive idea in the context of first-order differential/difference equations:

$$\xi w = f(w), \quad (2.41)$$

where $f : \mathbb{R}^{n_w} \rightarrow \mathbb{R}^{n_w}$ is a Lipschitz continuous function and ξ is either $\frac{d}{dt}$ or q . For notational convenience, assume that $f(0) = 0$, so the equilibrium of (2.41) is 0 for which we investigate the concept of stability. Note, that any isolated non-zero equilibrium point $\bar{w} \in \mathbb{R}^{n_w}$ of (2.41), i.e. $f(\bar{w}) = 0$, can be transferred to the origin by an exchange of variables $w' = w - \bar{w}$. We would like to find conditions ensuring that every solution $w : \mathbb{T} \rightarrow \mathbb{R}^{n_w}$ of (2.41) goes to zero as $t \rightarrow \infty$. Suppose that $\mathbb{T} = \mathbb{R}$ and a continuously partially differentiable function $\mathcal{V} : \mathbb{R}^{n_w} \rightarrow \mathbb{R}$ is given with $\mathcal{V}(0) = 0$ and $\mathcal{V}(\tau) > 0$ for $\tau \neq 0$. Assume that the derivative of \mathcal{V} along every solution of (2.41) is non-positive. Then $\mathcal{V}(w(t))$ is non-increasing for any w solution and under some additional requirements it implies that $w(t) \rightarrow 0$ for $t \rightarrow \infty$. To implement this idea, define the following:

Definition 2.29 (Definiteness of a function) *A real valued function $g : \mathbb{R}^n \rightarrow \mathbb{R}$ is*

- *positive semi-definit (denoted by $g \succeq 0$) if $g(\tau) \geq 0, \forall \tau \in \mathbb{R}^n$,*
- *positive definit (denoted by $g \succ 0$) if $g \succeq 0$ and $(g(\tau) = 0) \Leftrightarrow (\tau = 0)$,*
- *negative semi-definit (denoted by $g \preceq 0$) if $g(\tau) \leq 0, \forall \tau \in \mathbb{R}^n$,*
- *negative definit (denoted by $g \prec 0$) if $g \preceq 0$ and $(g(\tau) = 0) \Leftrightarrow (\tau = 0)$.*

Then based on the previously given considerations about \mathcal{V} , the following theorem holds:

Theorem 2.9 (Lyapunov stability) (Polderman and Willems 1991) *The origin is an asymptotically stable equilibrium point of (2.41) in a global sense, if there exists a so called Lyapunov function $\mathcal{V} : \mathbb{R}^{n_w} \rightarrow \mathbb{R}$ such that the following conditions are satisfied:*

1. $\mathcal{V} \succ 0$ (positive-definit),
2. If $\mathbb{T} = \mathbb{R}$, then \mathcal{V} is continuously partially differentiable and $\text{grad}[\mathcal{V}]f \prec 0$,
3. If $\mathbb{T} = \mathbb{Z}$, then \mathcal{V} is continuous at 0 and $(\mathcal{V} \circ f) - \mathcal{V} \prec 0$,
4. $\mathcal{V}(\tau) \rightarrow \infty$ as $\|\tau\| \rightarrow \infty$.

Similar conditions can be given for stability of the equilibrium point by relaxing Theorem 2.9 to require only semi-definiteness in the conditions. Instability condition of the equilibrium point can also be introduced in the similar sense as Theorem 2.9 by exchanging negative-definiteness of item 2 and 3 with positive-definiteness. However, Theorem 2.9 is non-constructive in the determination of the Lyapunov function which can be laborious in practice.

In the following, we focus on LTI systems in the context of the Lyapunov stability concept. Let $x \in \mathbb{X}^\top$ be the (weak) solution of the autonomous part of a SS representation $\mathfrak{R}_{\text{SS}}(\mathcal{F})$:

$$\xi x = Ax. \quad (2.42)$$

Consider the class of quadratic functions $\mathcal{V}(\tau) = \tau^\top P \tau$, where $\tau \in \mathbb{R}^{n_x}$, $P \in \mathbb{R}^{n_x \times n_x}$, and $P = P^\top$ (symmetric). For symmetric matrices, consider the concept of definiteness as the definiteness of $\tau^\top P \tau$ in terms of Definition 2.29. For a quadratic \mathcal{V} in continuous-time, using the chain rule of differentiation, it holds that

$$\frac{d}{dt} \mathcal{V}(x) = (\text{grad}[\mathcal{V}])(x) \cdot Ax = x^\top \underbrace{(A^\top P + PA)}_Q x, \quad (2.43)$$

where $Q \in \mathbb{R}^{n_x \times n_x}$ and symmetric. $Q = A^\top P + PA$ is called the CT Lyapunov equation. In discrete-time, using a quadratic Lyapunov function yields

$$\mathcal{V}(qx) - \mathcal{V}(x) = x^\top \underbrace{(A^\top PA - P)}_Q x, \quad (2.44)$$

where $Q \in \mathbb{R}^{n_x \times n_x}$ and symmetric. $Q = A^\top PA - P$ is called the DT Lyapunov equation. Based on Theorem 2.9, the following holds (Polderman and Willems 1991):

Theorem 2.10 (LTI Quadratic stability) (Polderman and Willems 1991) *Consider (2.42). Assume that A , $P = P^\top$, and $Q = Q^\top$ satisfy the corresponding Lyapunov equation (either in CT or in DT). Then*

- $(P \succ 0, Q \preceq 0) \Rightarrow ((2.42) \text{ is stable}).$
- $(P \succ 0, Q \preceq 0, \text{ and the } A\text{-invariant subspace in } \ker[Q] \text{ is } \{0\}) \Rightarrow ((2.42) \text{ is asymptotically stable}).$
- $(P \prec 0, Q \preceq 0, \text{ and the } A\text{-invariant subspace in } \ker[Q] \text{ is } \{0\}) \Rightarrow ((2.42) \text{ is unstable}).$

Note that in the last two items of Theorem 2.10, the additional condition results from the fact that if $Q \preceq 0$ it must be also guaranteed that $(\xi x = Ax, x^\top Q x = 0) \Rightarrow (x = 0)$ which corresponds to an observability condition. Note that Theorem 2.10 gives a constructive version of the Lyapunov theorem. For a given A and Q , under the condition that no two eigenvalues of A satisfy $\lambda_i + \lambda_j = 0$, the Lyapunov function can be constructed by solving the corresponding Lyapunov equation for P . Notice that such a construction can also be formulated without the specification of Q by solving the *Linear Matrix Inequalities* (LMI)s:

$$A^\top P + PA \prec 0, \quad \text{or} \quad A^\top PA - P \prec 0 \quad \text{with} \quad P \succ 0. \quad (2.45)$$

In terms of (2.45), finding P for a given A represents a *Linear Semi Definite Programming* (LSDP) problem that can be efficiently solved by a variety of (interior-point-based) solvers like SeDuMi (Sturm 1999) or CSDP. In case of LPV systems, this concept is successfully extended, giving an easily computable stability test. However as we will see, using quadratic Lyapunov functions with $P \in \mathbb{R}^{n_x \times n_x}$ in the LPV case only gives a sufficient stability condition of systems.

2.1.6 State-space canonical forms

Since the 1960s, state-space representations have been thoughtfully investigated to deduce informative and structurally attractive representatives of SS equivalence classes. Through these investigations many canonical forms have been introduced with special structures of the SS matrices. These structures are required to establish realization theory and equivalence transformations between SS and IO representations in the LTI and as we will see in the LPV case too. One set of these canonical forms is related to concepts of state-observability and state-reachability. Due to uniformity of these concepts in the LTI case, they are introduced without distinguishing between the CT and DT cases.

Definition 2.30 (Complete state-observability) (Polderman and Willems 1991) $\mathfrak{R}_{\text{SS}}(\mathcal{F})$ is called completely state-observable if (u, y) , with the laws of the system (state-space equations), determines x uniquely, i.e. for all $(u, x, y), (u, x', y) \in \mathfrak{B}_{\text{SS}}$ it holds that $x = x'$.

Definition 2.31 (Complete state-reachability) (Polderman and Willems 1991) $\mathfrak{R}_{\text{SS}}(\mathcal{F})$ is called completely state-reachable, if for any given two states $\mathbf{x}_1, \mathbf{x}_2 \in \mathbb{X}$, there exists an input signal u and an output signal y , such that $(u, x, y) \in \mathfrak{B}_{\text{SS}}$ with $x(t_1) = \mathbf{x}_1$ and $x(t_2) = \mathbf{x}_2$ for some $t_1, t_2 \in \mathbb{T}$.

The concepts of state-observability and state-reachability⁵ are important cornerstones of control theory and they are connected to the following informative matrices of SS representations:

Definition 2.32 (State-observability matrix) The state-observability matrix of $\mathfrak{R}_{\text{SS}}(\mathcal{F})$ is defined as $\mathcal{O}_{n_{\mathbf{x}}} \in \mathbb{R}^{(n_{\mathbf{y}} n_{\mathbf{x}}) \times n_{\mathbf{x}}}$ with

$$\mathcal{O}_{n_{\mathbf{x}}} = \begin{bmatrix} C^{\top} & A^{\top} C^{\top} & \dots & (A^{n_{\mathbf{x}}-1})^{\top} C^{\top} \end{bmatrix}^{\top}. \quad (2.46)$$

Definition 2.33 (State-reachability matrix) The state-reachability matrix of $\mathfrak{R}_{\text{SS}}(\mathcal{F})$ is defined as $\mathcal{R}_{n_{\mathbf{x}}} \in \mathbb{R}^{n_{\mathbf{x}} \times (n_{\mathbf{x}} n_{\mathbf{u}})}$ with

$$\mathcal{R}_{n_{\mathbf{x}}} = \begin{bmatrix} B & AB & \dots & A^{n_{\mathbf{x}}-1} B \end{bmatrix}. \quad (2.47)$$

These matrices have the following well-known property:

Theorem 2.11 (Induced complete state-observability/reachability) $\mathfrak{R}_{\text{SS}}(\mathcal{F})$ is completely state-observable (reachable), iff $\text{rank}(\mathcal{O}_{n_{\mathbf{x}}}) = n_{\mathbf{x}}$ (iff $\text{rank}(\mathcal{R}_{n_{\mathbf{x}}}) = n_{\mathbf{x}}$).

Corollary 2.1 If $\mathfrak{R}_{\text{SS}}(\mathcal{F})$ is completely state-observable (reachable), then at least $n_{\mathbf{x}}$ number of rows of $\mathcal{O}_{n_{\mathbf{x}}}$ (columns of $\mathcal{R}_{n_{\mathbf{x}}}$) are linearly independent, forming an invertible matrix. This implies that in the SISO case, $\mathcal{O}_{n_{\mathbf{x}}}$ (or $\mathcal{R}_{n_{\mathbf{x}}}$) is invertible.

⁵Note that in many text-books, reachability is also called controllability. As in DT, sometimes controllability is identified as state-stabilizability, usually much confusion rises around this term. To avoid this problem, here the terminology of reachability is used.

The following theorem is the consequence of the minimality concept of Proposition 2.26:

Theorem 2.12 (Induced SS minimality) (Polderman and Willems 1991) $\mathfrak{R}_{\text{SS}}(\mathcal{F})$ is minimal iff it is completely state-observable.

Note that, opposite to the orthodox LTI system theory, minimality in this context does not require⁶ state-reachability. However, when it is necessary to refer to original concept, we use the terminology of joint minimality:

Definition 2.34 (Joint minimality) If $\mathfrak{R}_{\text{SS}}(\mathcal{F})$ is minimal and completely state-reachable, then the representation is called jointly minimal.

In the sequel, \mathcal{O}_{n_x} and \mathcal{R}_{n_x} are used to develop canonical forms for LTI-SS representations.

Observability canonical form

Assume that $\mathfrak{R}_{\text{SS}}(\mathcal{F})$ is completely observable and SISO. Then, introduce a new state-basis with the transformation matrix

$$T_o = \mathcal{O}_{n_x}, \quad (2.48)$$

leading to a new state variable x_o , obtained as

$$x_o(t) = T_o x(t), \quad \forall t \in \mathbb{T}. \quad (2.49)$$

To derive an equivalent representation of \mathcal{F} in terms of the new state variable, T_o is applied to the system matrices in accordance with \sim , resulting in:

$$\left[\begin{array}{c|c} A_o = T_o A T_o^{-1} & B_o = T_o B \\ \hline C_o = C T_o^{-1} & D_o = D \end{array} \right] = \left[\begin{array}{cccc|c} 0 & 1 & \dots & 0 & \beta_{n_x-1}^o \\ \vdots & \vdots & \ddots & \vdots & \beta_{n_x-2}^o \\ 0 & 0 & \dots & 1 & \vdots \\ -\alpha_0^o & -\alpha_1^o & \dots & -\alpha_{n_x-1}^o & \beta_0^o \\ \hline 1 & 0 & \dots & 0 & \beta_{n_x}^o \end{array} \right].$$

The resulting representation

$$\mathfrak{R}_{\text{SS}}^o(\mathcal{F}) = \left[\begin{array}{c|c} A_o & B_o \\ \hline C_o & D_o \end{array} \right], \quad (2.50)$$

is called the *observability canonical state-space representation* of \mathcal{F} and it is equivalent with $\mathfrak{R}_{\text{SS}}(\mathcal{F})$. An important property of $\mathfrak{R}_{\text{SS}}^o(\mathcal{F})$, is that the associated observability matrix of this representation is an identity matrix.

Now assume that \mathcal{F} is a MIMO system. Then according to Luenberger (1967), the canonical form of a completely observable $\mathfrak{R}_{\text{SS}}(\mathcal{F})$ is realized by a mapping rule of three steps:

⁶Non-reachable systems are very common and they allow a state-minimal representation. Consider for instance autonomous systems. Such systems define an unique behavior, but their state representation is never state-reachable.

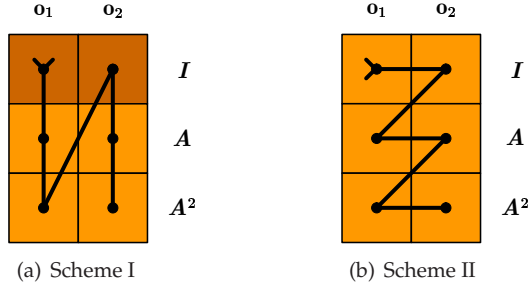


Figure 2.1: Young's selection scheme for \mathcal{O}_{n_x} : $n_x = 3$, $n_y = 2$. Vectors represented by dark cells must be selected if they are independent.

1. Choose n_x -independent rows of the full column-rank \mathcal{O}_{n_x} with a given ordering sequence.
2. Rearrange those n_x -independent rows with a fixed order to form a nonsingular state transformation matrix T_o .
3. By applying the equivalence transformation defined by T_o , compute the canonical representation.

Based on this, write \mathcal{O}_{n_x} as the sequence of vectors:

$$\mathcal{O}_{n_x} = [\mathbf{o}_1^\top \quad \dots \quad \mathbf{o}_{n_y}^\top \quad A^\top \mathbf{o}_1^\top \quad \dots \quad A^\top \mathbf{o}_{n_y}^\top \quad \dots]^\top, \quad (2.51)$$

where $C^\top = [\mathbf{o}_1^\top, \dots, \mathbf{o}_{n_y}^\top]$. According to the previous mapping strategy, the first step in the development of a MIMO observability canonical form is the selection of n_x linearly independent vectors from the $n_x \times n_y$ rows of (2.51), which form the state basis of the new representation. It can be shown, that due to the complete observability of the system, it is always possible to make a selection, but in general it is not unique (Luenberger 1967). Depending on the particular way of the selection procedure, different canonical forms can be obtained. In the following, such a selection procedure is used that reproduces the structure of the previously introduced SISO LTI observability canonical form. According to this, write the vectors defined by (2.51) in the following order

$$\{ \mathbf{o}_1, \mathbf{o}_2, \dots, \mathbf{o}_{n_y}, \mathbf{o}_1 A, \mathbf{o}_2 A, \dots, \mathbf{o}_{n_y} A, \dots \}, \quad (2.52)$$

which matches Young's selection scheme II presented in Figure 2.1. For the sake of simplicity, momentarily assume that $\text{rank}(C) = n_y$, meaning that $\{ \mathbf{o}_1, \mathbf{o}_2, \dots, \mathbf{o}_{n_y} \}$ are linearly independent. Define the index set $\mathbb{I}_{\tau_1}^{\tau_2} = \{ \tau \in \mathbb{Z} \mid \tau_1 \leq \tau \leq \tau_2 \}$. Then, the linear dependence of every vector from the ordered sequence (2.52) can be analyzed one after the other: if $\tau_i \in \mathbb{I}_1^{n_x}$ is the smallest number such that $\mathbf{o}_i A^{\tau_i}$ is linearly dependent on the previous vectors, then there exists a set of unique constants $\{ \alpha_{ijl}^o \}$, such that

$$\mathbf{o}_i A^{\tau_i} = \sum_{j=1}^{n_y} \sum_{l=0}^{\tau_{ij}-1} \alpha_{ijl}^o \mathbf{o}_j A^l, \quad (2.53)$$

where the ordering of the vectors implies that

$$\tau_{ij} = \begin{cases} \tau_i & \text{for } i = j, \\ \min(\tau_i + 1, \tau_j) & \text{for } i > j, \\ \min(\tau_i, \tau_j) & \text{for } i < j. \end{cases} \quad (2.54)$$

Once all dependent vectors belonging to all the n_Y output channels associated chains have been found, a total of $n_X = \sum_{i=1}^{n_Y} \tau_i$ independent vectors is selected due to the complete observability assumption. Furthermore, as the first n_Y vectors $\{\circ_1, \circ_2, \dots, \circ_{n_Y}\}$ are independent, they are automatically selected, implying that

$$\max_{i \in \mathbb{I}^{n_Y}} \tau_i = \tau_{\max} \leq n_X - n_Y + 1. \quad (2.55)$$

Moreover, the remaining linearly dependent relations (see (2.53)) are described by $\sum_{i=1}^{n_Y} \sum_{j=1}^{n_Y} \tau_{ij}$ number of constants $\{\alpha_{ijl}^o\}$. Finally, the new state basis is defined by

$$T_o^\top = \begin{bmatrix} \circ_1^\top & \dots & (A^{\tau_i-1})^\top \circ_1^\top & \dots & \circ_{n_Y}^\top & \dots & (A^{\tau_{n_Y}-1})^\top \circ_{n_Y}^\top \end{bmatrix}. \quad (2.56)$$

Due to the linear independence of the rows, T_o is invertible and by using the same argument as in the SISO case, it implies algebraic equivalence, defining an equivalence relation. This equivalence relation yields the following form of the transformed matrices of $\mathfrak{R}_{SS}^o(\mathcal{F})$:

$$\left[\begin{array}{c|c} A_o & B_o \\ \hline C_o & D_o \end{array} \right] = \left[\begin{array}{c|c} [A_{ij}^o], i, j \in \mathbb{I}^{n_Y} & \begin{array}{c} B_1^o \\ \vdots \\ B_{n_Y}^o \end{array} \\ \hline e_1 \quad 0_{n_Y \times (\tau_1-1)} \quad \dots \quad e_{n_Y} \quad 0_{n_Y \times (\tau_{n_Y}-1)} & D \end{array} \right],$$

where $[\cdot]$ denotes matrix composition, $\{e_i\}_{i=1}^{n_Y}$ is the standard basis of \mathbb{R}^{n_Y} , and

$$A_{ii}^o = \begin{bmatrix} 0 & \dots & 0 & -\alpha_{ii0}^o \\ 1 & \ddots & \vdots & -\alpha_{ii1}^o \\ \vdots & \ddots & 0 & \vdots \\ 0 & \dots & 1 & -\alpha_{ii(\tau_i-1)}^o \end{bmatrix}_{(\tau_i \times \tau_i)}^\top, \quad A_{ij}^o = \begin{bmatrix} 0 & \dots & 0 & -\alpha_{ij0}^o \\ \vdots & \vdots & \vdots & \vdots \\ \vdots & \vdots & \vdots & -\alpha_{ij(\tau_{ij}-1)}^o \\ \vdots & \vdots & \vdots & 0 \\ \vdots & \vdots & \vdots & \vdots \\ \vdots & \vdots & \vdots & \vdots \\ 0 & \dots & 0 & 0 \end{bmatrix}_{(\tau_i \times \tau_j)}^\top, \quad B_i^o = \begin{bmatrix} \beta_{i1(\tau_i-1)}^o & \dots & \beta_{in_U(\tau_i-1)}^o \\ \vdots & & \vdots \\ \beta_{i10}^o & \dots & \beta_{in_U0}^o \end{bmatrix}_{(\tau_i \times n_U)}, \quad D_o = \begin{bmatrix} \beta_{11\tau_1}^o & \dots & \beta_{1n_U\tau_1}^o \\ \vdots & & \vdots \\ \beta_{n_Y1\tau_{n_Y}}^o & \dots & \beta_{n_Yn_U\tau_{n_Y}}^o \end{bmatrix}_{(n_Y \times n_U)}$$

Based on this representation, the LTI system is separated to an interconnection of subsystems characterized by the A_{ii}^o and B_i^o matrices and the connection of these subsystems is defined through the A_{ij}^o matrices. In this way, using the constructed

state-space transformation T_o applied on $\mathfrak{R}_{SS}(\mathcal{F})$, we have constructed a canonical SS representation of \mathcal{F} . The following corollary holds for representations of \mathcal{F} with the structural form of (A_o, B_o, C_o, D_o) both in the SISO and the MIMO cases:

Corollary 2.2 $\mathfrak{R}_{SS}^o(\mathcal{F})$ is completely state-observable and hence minimal.

This corollary means that transformation to the canonical form preserves state-observability, i.e. a SS representation with this structure always completely state-observable. In case $\text{rank}(C) \neq n_y$, the observability canonical form does not exist in the previously introduced structure as C_o cannot be a matrix composed from zero vectors and standard bases. In this case, T_o is constructed by considering the system only with the independent output channels. Then, T_o is applied to the original matrices. The resulting C_o retains the structure of the conventional canonical form for the linearly independent channels (containing only zero vectors and standard bases), however it contains non-unit elements (the weights of the linear combination of the independent channels) in the rows corresponding to the dependent output channels.

Reachability canonical form

Similar to the previous part, assume that $\mathfrak{R}_{SS}(\mathcal{F})$ is SISO and completely reachable. We introduce a new state basis, using

$$T_r = \mathcal{R}_{n_x}^{-1}, \quad (2.57)$$

leading to a new state variable x_r , obtained as

$$x_r(t) = T_r x(t), \quad \forall t \in \mathbb{T}. \quad (2.58)$$

By applying the equivalence relation defined by T_r on $\mathfrak{R}_{SS}(\mathcal{F})$, the transformed matrices are given as (Guidorzi 1981; Kalman 1963):

$$\left[\begin{array}{c|c} A_r = T_r A T_r^{-1} & B_r = T_r B \\ \hline C_r = C T_r^{-1} & D_r = D \end{array} \right] = \left[\begin{array}{cccc|c} 0 & \dots & 0 & -\alpha_0^r & 1 \\ 1 & \ddots & \vdots & -\alpha_1^r & 0 \\ \vdots & \ddots & 0 & \vdots & \vdots \\ 0 & \dots & 1 & -\alpha_{n_x-1}^r & 0 \\ \hline \beta_{n_x-1}^r & \beta_{n_x-2}^r & \dots & \beta_0^r & \beta_{n_x}^r \end{array} \right].$$

Then,

$$\mathfrak{R}_{SS}^R(\mathcal{F}) = \left[\begin{array}{c|c} A_r & B_r \\ \hline C_r & D_r \end{array} \right], \quad (2.59)$$

is called the *reachability canonical state-space representation* of \mathcal{F} . Furthermore, the reachability matrix of $\mathfrak{R}_{SS}^R(\mathcal{F})$ is the identity matrix.

As a second step, the MIMO case is considered as an extension of the previously derived formulation. Similar to the observability case, \mathcal{R}_{n_x} is rewritten as

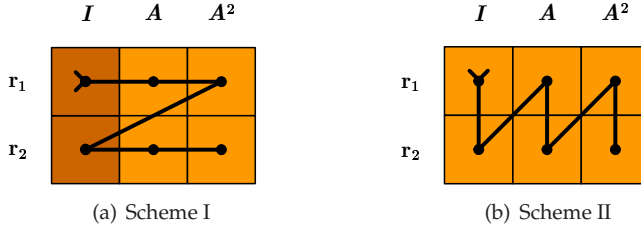


Figure 2.2: Young's selection scheme for \mathcal{R}_{n_x} : $n_x = 3$, $n_U = 2$. Vectors represented by dark cells must be selected if they are independent.

sequences of its column vectors. The selection of n_x linearly independent vectors from the $n_x \times n_U$ column vectors determine the state basis of the reachability form. In the following, such a selection procedure is used that reproduces the structure of the previously introduced SISO LTI reachability canonical form. According to this, define $B = [r_1, \dots, r_{n_U}]^\top$ and select the rows of \mathcal{R}_{n_x} in the order of

$$\{r_1, Ar_1, \dots, A^{n_x-1}r_1, r_2, Ar_2, \dots\},$$

which matches Young's selection scheme I presented in Figure 2.2. Temporally assume that $\text{rank}(B) = n_U$ meaning that $\{r_1, r_2, \dots, r_{n_U}\}$ are linearly independent. Then, the linear dependence of every vector from the ordered sequence can be analyzed one after the other just like in the observability case. However, in Young's selection scheme I, the vectors $\{r_1, r_2, \dots, r_{n_U}\}$ have to be selected to the state transformation matrix even if the ordering would indicate else. The explanation lies in that in the reachability canonical transform of B every row must be zero or a standard basis in $\mathbb{R}^{1 \times n_U}$, which needs that all $\{r_1, r_2, \dots, r_{n_U}\}$ must be the part of T_r . According to this, if $\tau_i \in \mathbb{I}_1^{n_x}$ is the smallest number such that $A^{\tau_i}r_i$ is linearly dependent on the previous vectors, then there exists a set of unique constants $\{\alpha_{ijl}^r\}$, such that

$$A^{\tau_i}r_i = \sum_{j=1}^i \sum_{l=0}^{\tau_{ij}-1} \alpha_{ijl}^r A^l r_j, \quad (2.60)$$

where, because of the ordering of the vectors, $\{\tau_{ij}\}$ satisfies (2.54). Once that all dependent vectors belonging all the n_U input channels associated chains have been found, a total of $n_x = \sum_{i=1}^{n_U} \tau_i$ independent vectors are selected due to the complete reachability assumption. Furthermore, by the selection scheme, the n_U number of vectors of $\{r_1, r_2, \dots, r_{n_U}\}$ are automatically selected, implying

$$\max_{i \in \mathbb{I}_1^{n_U}} \tau_i = \tau_{\max} \leq n_x - n_U + 1. \quad (2.61)$$

The remaining linearly dependent relations (see (2.60)) are described by $\sum_{i=1}^{n_U} \sum_{j=1}^i \tau_{ij}$ number of constants $\{\alpha_{ijl}^r\}$, and T_r is defined as:

$$T_r = [r_1 \quad \dots \quad A^{\tau_1-1}r_1 \quad \dots \quad r_{n_U} \quad \dots \quad A^{\tau_{n_U}-1}r_{n_U}]^{-1} \quad (2.62)$$

Again, linear independence of the selected rows assures the existence of the inverse. The T_r equivalence relation yields the following transformed matrices:

$$\left[\begin{array}{c|c} A_r & B_r \\ \hline C_r & D_r \end{array} \right] = \left[\begin{array}{c|c} [A_{ij}^r], i, j \in \mathbb{I}_1^{n_u} & \begin{array}{c} e_1^\top \\ 0_{(\tau_1-1) \times n_u} \\ \vdots \\ e_{n_u}^\top \\ 0_{(\tau_{n_y}-1) \times n_u} \end{array} \\ \hline C_1^r \ \dots \ C_{n_u}^r & D \end{array} \right],$$

where $\{e_i\}_{i=1}^{n_u}$ is the standard basis of $\mathbb{R}^{1 \times n_u}$ and

$$A_{ii}^r = \begin{bmatrix} 0 & \dots & 0 & -\alpha_{ii0}^r \\ 1 & \ddots & \vdots & -\alpha_{ii1}^r \\ \vdots & \ddots & 0 & \vdots \\ 0 & \dots & 1 & -\alpha_{ii(\tau_i-1)}^r \end{bmatrix}_{(\tau_i \times \tau_i)}$$

$$A_{ij}^r = \begin{bmatrix} 0 & \dots & 0 & -\alpha_{ij0}^r \\ \vdots & \vdots & \vdots & \vdots \\ \vdots & \vdots & -\alpha_{ij(\tau_{ij}-1)}^r & \vdots \\ \vdots & \vdots & \vdots & 0 \\ \vdots & \vdots & \vdots & \vdots \\ \vdots & \vdots & \vdots & \vdots \\ 0 & \dots & 0 & 0 \end{bmatrix}_{(\tau_i \times \tau_j)}$$

$$C_i^r = \begin{bmatrix} \beta_{1i(\tau_i-1)}^r & \dots & \beta_{1i0}^r \\ \vdots & & \vdots \\ \beta_{n_y i(\tau_i-1)}^r & \dots & \beta_{n_y i0}^r \end{bmatrix}_{(n_y \times \tau_i)}$$

$$D_r = \begin{bmatrix} \beta_{11\tau_1}^r & \dots & \beta_{1n_u\tau_1}^r \\ \vdots & & \vdots \\ \beta_{n_y 1\tau_{n_y}}^r & \dots & \beta_{n_y n_u\tau_{n_y}}^r \end{bmatrix}_{(n_y \times n_u)}$$

Again, $\mathfrak{R}_{SS}^R(\mathcal{F})$ is equivalent with $\mathfrak{R}_{SS}(\mathcal{F})$. The following corollary also holds:

Corollary 2.3 $\mathfrak{R}_{SS}^R(\mathcal{F})$ is completely reachable.

Furthermore, if $\mathfrak{R}_{SS}(\mathcal{F})$ is minimal, then the resulting $\mathfrak{R}_{SS}^R(\mathcal{F})$ by the given construction procedure is also minimal. In the case of dependent columns of B , the state-transformation is constructed based on the independent input channels.

Companion canonical forms

The observability and reachability canonical form can be given in an other so called *companion* or *phase-variable* form (Luenberger 1967). These are defined in the SISO case as:

$$\mathfrak{R}_{SS}^{O_c}(\mathcal{F}) = \left[\begin{array}{c|c} A_{co} & B_{co} \\ \hline C_{co} & D_{co} \end{array} \right] = \left[\begin{array}{c|c} 0 & \dots & 0 & -\alpha_0^{co} & \beta_0^{co} \\ 1 & \ddots & \vdots & -\alpha_1^{co} & \beta_1^{co} \\ \vdots & \ddots & 0 & \vdots & \vdots \\ 0 & \dots & 1 & -\alpha_{n_x-1}^{co} & \beta_{n_x-1}^{co} \\ \hline 0 & \dots & 0 & 1 & \beta_{n_x}^{co} \end{array} \right],$$

$$\mathfrak{R}_{\text{SS}}^{\mathcal{R}_c}(\mathcal{F}) = \left[\begin{array}{c|c} \frac{A_{\text{cr}}}{C_{\text{cr}}} & \frac{B_{\text{cr}}}{D_{\text{cr}}} \end{array} \right] = \left[\begin{array}{cccc|c} 0 & 1 & \dots & 0 & 0 \\ \vdots & \vdots & \ddots & \vdots & \vdots \\ 0 & 0 & \dots & 1 & 0 \\ -\alpha_0^{\text{cr}} & -\alpha_1^{\text{cr}} & \dots & -\alpha_{n_x-1}^{\text{cr}} & 1 \\ \hline \beta_0^{\text{cr}} & \beta_1^{\text{cr}} & \dots & \beta_{n_x-1}^{\text{cr}} & \beta_{n_x}^{\text{cr}} \end{array} \right],$$

with state-transformation matrices:

$$\begin{aligned} T_{\text{co}}^{-1} &= \left[\begin{array}{ccc} \circ & \dots & A^{n_x-1} \circ \end{array} \right], \\ T_{\text{cr}}^{\top} &= \left[\begin{array}{ccc} \mathbf{r}^{\top} & \dots & (A^{n_x-1})^{\top} \mathbf{r}^{\top} \end{array} \right]. \end{aligned}$$

Here \circ is the last column of $\mathcal{O}_{n_x}^{-1}$ and \mathbf{r} is the last row of $\mathcal{R}_{n_x}^{-1}$. In the MIMO case, the companion forms are generated by selecting the linearly independent rows (columns) based on a different ordering (Luenberger 1967). For the companion observability case, the ordering of the rows of \mathcal{O}_{n_x} matches with Young's selection scheme I presented in Figure 2.1, while in the companion reachability case, the ordering of the columns of \mathcal{R}_{n_x} matches with Young's selection scheme II of Figure 2.2. Similar to the previous canonical forms, the observability companion form is always observable and the reachability companion form is always reachable.

Transpose of SS representations

It is also important, that for a given SISO LTI system \mathcal{F} , it holds that

$$\mathfrak{R}_{\text{SS}}(\mathcal{F}) = \left[\begin{array}{c|c} A & B \\ \hline C & D \end{array} \right] \quad \text{and} \quad \mathfrak{R}_{\text{SS}}^{\top}(\mathcal{F}) = \left[\begin{array}{c|c} A^{\top} & C^{\top} \\ \hline B^{\top} & D \end{array} \right] \quad (2.63)$$

have equivalent manifest behaviors if they are both jointly minimal (Mason 1956). Here $\mathfrak{R}_{\text{SS}}^{\top}(\mathcal{F})$ is called the *transpose* of $\mathfrak{R}_{\text{SS}}(\mathcal{F})$. This implies that the transpose of $\mathfrak{R}_{\text{SS}}^{\mathcal{O}}(\mathcal{F})$ is equivalent with $\mathfrak{R}_{\text{SS}}^{\mathcal{R}}(\mathcal{F})$ in case of joint observability and reachability. Hence, the corresponding matrix coefficients are equal. If $\mathfrak{R}_{\text{SS}}^{\mathcal{O}}(\mathcal{F})$ or $\mathfrak{R}_{\text{SS}}^{\mathcal{R}}(\mathcal{F})$ is not jointly state-observable and state-reachable, then equality only holds for zero initial conditions, as non-observable states are transformed to non-controllable states. The same relation holds for the companion forms. In the MIMO case, the construction of the equivalent transpose form needs the computation of a state-transformation T (if it exists) such that $A^{\top}T = TA$.

Balanced SS realizations

In systems and control theory, complete state-observability and state-reachability are also frequently discussed involving observability and reachability gramians. These symmetric and positive semi-definit matrices also determine the state-observability or state-reachability of the SS representation:

Definition 2.35 (Gramians) *The observability gramian O and the reachability gramian R of an asymptotically stable $\mathfrak{R}_{SS}(\mathcal{F})$ are symmetric matrices which are defined as:*

$$O = \int_0^{\infty} e^{A^T \tau} C^T C e^{A \tau} d\tau \quad \text{and} \quad R = \int_0^{\infty} e^{A \tau} B B^T e^{A^T \tau} d\tau, \quad (2.64)$$

in continuous-time. In the discrete-time case, O and R of an asymptotically stable $\mathfrak{R}_{SS}(\mathcal{F})$ are defined as

$$O = \sum_{k=0}^{\infty} (A^T)^k C^T C A^k \quad \text{and} \quad R = \sum_{k=0}^{\infty} A^k B B^T (A^T)^k. \quad (2.65)$$

Theorem 2.13 (Induced observability/reachability) *The SS representation $\mathfrak{R}_{SS}(\mathcal{F})$, is completely state-observable (state-reachable), iff its observability (reachability) gramian is full rank.*

In practice, these gramians are computed by solving the following Lyapunov equations:

$$AR + RA^T = -BB^T \quad \text{and} \quad A^T O + OA = -C^T C, \quad (2.66)$$

in the CT case and

$$ARA^T + BB^T = R \quad \text{and} \quad A^T O A + C^T C = O, \quad (2.67)$$

in the DT case. Now we can introduce the concept of balancing:

Definition 2.36 (Balanced SS realization) *Let $\mathfrak{R}_{SS}(\mathcal{F})$ be an asymptotically stable SS representation of an LTI system \mathcal{F} with observability gramian O and reachability gramian R . If*

$$R = O = H \succeq 0, \quad (2.68)$$

where H is a diagonal matrix, then we call $\mathfrak{R}_{SS}(\mathcal{F})$ (internally) balanced w.r.t. H .

It is immediate that a balanced realization is jointly minimal, i.e. completely state-observable and reachable, if $H \succ 0$. The non-zero diagonal elements of $H = \text{diag}(\sigma_1, \dots, \sigma_{n_x})$ are called the *Hankel singular values*. It can be shown, that each non-autonomous LTI system has a jointly minimal balanced SS realization (Glover 1984). Balanced realizations are important tools for model reduction and as we will see, they play an important role for OBFs. To find the balanced realization of a given \mathcal{F} , the following theorem is important:

Theorem 2.14 (Balanced state transformation) (Glover 1984) *Let $\mathfrak{R}_{SS}(\mathcal{F})$ be an asymptotically stable and jointly minimal SS representation of an LTI system \mathcal{F} with observability gramian $O = L_o L_o^T$ and reachability gramian $R = L_r L_r^T$. Define the singular value decomposition of $L_r^T L_o$ as $L_r^T L_o = L_1 H^2 L_2^T$. Then the state-transformation*

$$T = H^{1/2} L_1 L_r^{-1} = H^{-1/2} L_2 L_o^T, \quad (2.69)$$

applied to $\mathfrak{R}_{SS}(\mathcal{F})$ gives a balanced realization of \mathcal{F} w.r.t. H .

2.1.7 Relation of state-space and input-output domains

In the previous part we have introduced SS and IO representations of LTI dynamical systems. In many areas of systems and control, it is an important question to find equivalent IO and SS representations of a given system. This means, that if a representation of an LTI system \mathcal{F} is available, e.g. a SS representation, how to find or characterize representations of the system in other domains, e.g. among IO representations, which define the same behavior. The theory for this, so called realization problem, is again introduced without making distinction between the CT and DT cases.

Input-output realization through elimination of the state

First consider the situation that the IO realization of a $\mathfrak{R}_{SS}(\mathcal{F})$ is sought. To establish IO realizations of SS representations, first it is shown that the state as a latent variable can always be eliminated without changing the manifest behavior:

Theorem 2.15 (Elimination of the latent variable) (Polderman and Willems 1991)
Given a latent representation of \mathcal{S} with manifest behavior \mathfrak{B} and polynomial matrices $R \in \mathbb{R}[\xi]^{n_r \times n_w}$, $R_L \in \mathbb{R}[\xi]^{n_r \times n_x}$. Let the unimodular matrix $M \in \mathbb{R}[\xi]^{n_r \times n_r}$ be such that

$$MR_L = \begin{bmatrix} R'_L \\ 0 \end{bmatrix}, \quad MR = \begin{bmatrix} R' \\ R'' \end{bmatrix}, \quad (2.70)$$

with R'_L of full row rank. Then, the manifest behavior defined by $R''(\xi)w = 0$ is equal with \mathfrak{B} .

Based on Theorem 2.15, the state vector as a latent variable can be eliminated from $\mathfrak{R}_{SS}(\mathcal{F})$ with an unimodular transformation. Due to Theorem 2.3 such a transformation does not change the manifest behavior, hence we call this latent variable elimination an *equivalence transformation*. The next step to establish an IO realization is to formulate the unimodular transformation and the resulting R'' as the combination of an output side polynomial R_y and an input side polynomial R_u . Consider the SISO case first:

Corollary 2.4 (IO Equivalence transformation) (Polderman and Willems 1991)
Let $\mathfrak{R}_{SS}(\mathcal{F})$ be a SISO state-space representation. Define $\bar{R}_y \in \mathbb{R}[\xi]$ and $\bar{R}_u \in \mathbb{R}[\xi]^{1 \times n_x}$ by

$$\bar{R}_y(\xi) = \det(I\xi - A), \quad \bar{R}_u(\xi) = \bar{R}_y(\xi)C(I\xi - A)^{-1}. \quad (2.71)$$

Let $R_{\text{com}} \in \mathbb{R}[\xi]$ be the greatest common divisor of \bar{R}_y and \bar{R}_u . Define

$$R_y(\xi) = \frac{\bar{R}_y(\xi)}{R_{\text{com}}(\xi)} \quad \text{and} \quad R_u(\xi) = \frac{\bar{R}_u(\xi)}{R_{\text{com}}(\xi)}B + DR_y(\xi). \quad (2.72)$$

Then the IO representation of \mathcal{F} , denoted by $\mathfrak{R}_{IO}(\mathcal{F})$, is given by

$$R_y(\xi)y = R_u(\xi)u. \quad (2.73)$$

The following property is important:

Property 2.1 (Polderman and Willems 1991) *Assume that $\mathfrak{R}_{SS}(\mathcal{F})$ is minimal, i.e. completely state-observable. Then the IO representation of \mathcal{F} is given as*

$$R_y(\xi) = \det(I\xi - A), \quad \text{and} \quad R_u(\xi) = R_y(\xi)C(I\xi - A)^{-1}B + DR_y(\xi). \quad (2.74)$$

In other words, for a minimal SS representation, the equivalence transformation simplifies, as dynamics related to non-observable states are not needed to be eliminated (\bar{R}_y and \bar{R}_u are coprime). In case of the previously introduced canonical forms, the state elimination results in the following conversion rules:

Corollary 2.5 (IO conversion rules) (Willems 2007) *The IO realization of minimal canonical SS representations of \mathcal{F} is given as*

	$\mathfrak{R}_{SS}^{\circ}(\mathcal{F})$	$\mathfrak{R}_{SS}^{\circ c}(\mathcal{F})$	$\mathfrak{R}_{SS}^{\text{r}}(\mathcal{F})$	$\mathfrak{R}_{SS}^{\text{rc}}(\mathcal{F})$
a_i	α_i°	$\alpha_i^{\circ c}$	α_i^{r}	α_i^{rc}
a_{n_x}	1	1	1	1
b_j	$\beta_j^{\circ} + \sum_{l=j}^{n_x-1} \alpha_l^{\circ} \beta_{n_x-l+j}^{\circ}$	$\beta_j^{\circ c} + \alpha_j^{\circ c} \beta_{n_x}^{\circ c}$	$\beta_j^{\text{r}} + \sum_{l=j}^{n_x-1} \alpha_l^{\text{r}} \beta_{n_x-l+j}^{\text{r}}$	$\beta_j^{\text{rc}} + \alpha_j^{\text{rc}} \beta_{n_x}^{\text{rc}}$
b_{n_x}	$\beta_{n_x}^{\circ}$	$\beta_{n_x}^{\circ c}$	$\beta_{n_x}^{\text{r}}$	$\beta_{n_x}^{\text{rc}}$

with $i, j \in \mathbb{I}_0^{n_x-1}$ and $n_a = n_b = n_x$.

In the MIMO case, the realization is computed by applying the algorithm defined by (2.71) and (2.72) for each output channel separately, i.e. for each $\bar{R}_y^{(i)} = \det(I\xi - A)$ and $\bar{R}_u^{(i)}(\xi) = e_i^{\top} \bar{R}_y^{(i)}(\xi)C(I\xi - A)^{-1}$, $i \in \mathbb{I}_1^{n_y}$ polynomials. The common divisor $R_{\text{com}}^{(i)}$ in this case is the greatest common divisor of $\bar{R}_y^{(i)}$ and $\bar{R}_u^{(i)}$.

State-space realization through cut & shift

Finding an equivalent SS representation of a given IO representation follows by constructing a state-mapping. This construction can be seen as the reverse operation of the previous latent variable elimination. The actual aim is to introduce a latent variable into (2.73) such that it satisfies the state-property, ergo it defines a SS representation of the original system via Theorem 2.2. The central idea of such a state-construction is the *cut-and-shift-map* $\varrho_- : \mathbb{R}[\xi]^{\times} \rightarrow \mathbb{R}[\xi]^{\times}$ that acts on polynomial matrices in the same way as the backward time-shift operator acts on time functions:

$$\varrho_- \underbrace{(r_0 + r_1\xi + \dots + r_n\xi^n)}_{R(\xi)} = r_1 + \dots + r_n\xi^{n-1}. \quad (2.75)$$

This operator can be seen as an intuitive way to introduce state-variables for a KR representation of \mathcal{F} associated with R , as $w_L = \varrho_-(R(\xi))w$ for a smooth w implies that

$$R(\xi)w = r_0w + \xi w_L. \quad (2.76)$$

Repeated use of ϱ_- and stacking the resulting polynomial matrices gives

$$\Sigma_-(R) = \begin{bmatrix} \varrho_-(R) \\ \varrho_-^2(R) \\ \vdots \\ \varrho_-^{n-2}(R) \\ \varrho_-^{n-1}(R) \end{bmatrix} = \begin{bmatrix} r_1 + \dots + r_n \xi^{n-1} \\ r_2 + \dots + r_n \xi^{n-2} \\ \vdots \\ r_{n-1} + r_n \xi \\ r_n \end{bmatrix}. \quad (2.77)$$

In case $R \in \mathbb{R}[\xi]^{n_r \times n_w}$ with $n_r = 1$, the rows Σ_- are independent, thus it can be shown that $X = \Sigma_-(R)$ defines a minimal state-map in the form of

$$x = X(\xi)w. \quad (2.78)$$

Later it is shown that such a state-map implies a unique SS representation. Before that, we characterize all possible minimal state-maps that lead to an equivalent SS representation.

We continue to consider the case $n_r = 1$. Denote the multiplication by ξ as ϱ_+ , which acts in the same way as the forward time-shift operator acts on time-functions:

$$\varrho_+(r_0 + r_1 \xi + \dots + r_n \xi^n) = r_0 \xi + r_1 \xi^2 + \dots + r_n \xi^{n+1}. \quad (2.79)$$

Note that $\varrho_- \varrho_+ = I$, while $\varrho_+(\varrho_-(R)) = R(\xi) - R(0)$. Consequently

$$\varrho_+ \left(\begin{bmatrix} \Sigma_-(R) \\ 0 \end{bmatrix} \right) = \begin{bmatrix} R \\ \Sigma_-(R) \end{bmatrix} - \begin{bmatrix} r_0 \\ r_1 \\ \vdots \\ r_n \end{bmatrix}. \quad (2.80)$$

Denote by $\text{span}_{\mathbb{R}}^{\text{row}}(P)$ the subspace spanned by the rows of $P \in \mathbb{R}[\xi]^{\cdot \times \cdot}$, viewed as a \mathbb{R} -vector space of polynomial vectors. Also introduce $\text{module}_{\mathbb{R}[\xi]}(R)$, the $\mathbb{R}[\xi]$ -module⁷ spanned by the rows of $R(\xi)$:

$$\text{module}_{\mathbb{R}[\xi]}(R) = \text{span}_{\mathbb{R}}^{\text{row}} \left(\begin{bmatrix} R \\ \varrho_+(R) \\ \vdots \end{bmatrix} \right). \quad (2.81)$$

This module represents the set of equivalence classes on $\text{span}_{\mathbb{R}}^{\text{row}}(\Sigma_-(R))$. Let $X \in \mathbb{R}[\xi]^{\cdot \times n_w}$ be a polynomial matrix with independent rows and such that

$$\text{span}_{\mathbb{R}}^{\text{row}}(X) \oplus \text{module}_{\mathbb{R}[\xi]}(R) = \text{span}_{\mathbb{R}}^{\text{row}}(\Sigma_-(R)) + \text{module}_{\mathbb{R}[\xi]}(R). \quad (2.82)$$

Then, X is a minimal state-map of the LTI system represented by the polynomial $R \in \mathbb{R}[\xi]^{1 \times n_w}$ and it defines a state variable by (2.78) (Willems 2007). This way it is possible to obtain all minimal equivalent SS realization of the system. The next step is to characterize these SS representations with respect to an IO partition.

⁷ $R' \in \text{module}_{\mathbb{R}[\xi]}(R)$ if and only if $\exists P \in \mathbb{R}[\xi]^{1 \times \cdot}$ such that $R' = PR$.

An input-output partition (u, y) associated with R is obtained by choosing a selector matrix⁸ $S_u \in \mathbb{R}^{n_w \times n_w}$ giving $u = S_u w$ and a complementary matrix $S_y \in \mathbb{R}^{n_w \times n_w}$ giving $y = S_y w$. Then it can be shown, that there exist unique matrices A, B, C, D and polynomial matrices $X_u(\xi), X_y(\xi)$ with appropriate dimensions such that

$$\xi X(\xi) = AX(\xi) + BS_u + X_u(\xi)R(\xi), \quad (2.83a)$$

$$S_y = CX(\xi) + DS_u + X_y(\xi)R(\xi). \quad (2.83b)$$

These imply that

$$\left[\begin{array}{c|c} A & B \\ \hline C & D \end{array} \right] \in \left[\begin{array}{c|c} \mathbb{R}^{n_x \times n_x} & \mathbb{R}^{n_x \times n_u} \\ \hline \mathbb{R}^{n_y \times n_x} & \mathbb{R}^{n_y \times n_u} \end{array} \right], \quad (2.84)$$

is a minimal state-representation of the LTI system represented by the polynomial $R \in \mathbb{R}[\xi]^{1 \times n_w}$.

The algorithm described by (2.83a-b) also gives insight into the realization of the classical SS canonical representations. Later we show that this mechanism can also be used in the LPV case. We continue to consider the SISO case. Assume that $\mathfrak{R}_{\text{IO}}(\mathcal{F})$ is given with polynomial matrices R_y and R_u , where R_y is monic. Then $\Sigma_{-}([\ R_y(\xi) \quad -R_u(\xi) \])$ gives:

$$\begin{bmatrix} a_1 + a_2\xi + \dots + \xi^{n_a-1} & -b_1 - b_2\xi - \dots - b_{n_b}\xi^{n_b-1} \\ a_2 + \dots + \xi^{n_a-2} & -b_2 - \dots - b_{n_b}\xi^{n_b-2} \\ \vdots & \vdots \\ a_{n_a-1} + \xi & \vdots \\ 1 & \vdots \end{bmatrix}. \quad (2.85)$$

This $n_a \times 2$ matrix has independent rows and the span of these rows is linearly independent from $\text{module}_{\mathbb{R}[\xi]}([\ R_y \quad -R_u \])$. In terms of (2.82), the construction of the state-map requires to choose $X \in \mathbb{R}[\xi]^{n_a \times 2}$ such that $\text{span}_{\mathbb{R}}^{\text{row}}(X)$ equals to the rowspan of (2.85). As all rows of (2.85) are independent, X can be easily constructed. The choice of selector matrices is also evident: $S_u = [\ 0 \ 1 \]$ and $S_y = [\ 1 \ 0 \]$. A convenient choice for X is to take the rows of (2.85) in the given order (top-to-bottom). Then, the algorithm defined by (2.83a-b) with such an X leads to the companion-observability canonical form $\mathfrak{R}_{\text{SS}}^{\text{OC}}(\mathcal{F})$. Another choice of X is

$$X(\xi) = \begin{bmatrix} 1 & -\beta_0^{\circ} \\ \xi & -\beta_1^{\circ} - \beta_0^{\circ}\xi \\ \vdots & \vdots \\ \xi^{n_a-2} & -\beta_{n_a-2}^{\circ} - \dots - \beta_0^{\circ}\xi^{n_a-2} \\ \xi^{n_a-1} & -\beta_{n_a-1}^{\circ} - \dots - \beta_0^{\circ}\xi^{n_a-1} \end{bmatrix}, \quad (2.86)$$

where the $\{\beta_j^{\circ}\}$ coefficients are computed from the expansion

$$\frac{R_u(\xi)}{R_y(\xi)} = \beta_{n_a}^{\circ} + \beta_{n_a-1}^{\circ}\xi^{-1} + \dots + \beta_0^{\circ}\xi^{-n_a} + \dots \quad (2.87)$$

⁸A matrix with one entry 1 in each row, at most one entry 1 in each column, and all other entries 0 is a selector matrix.

Claim 2.2 (Willems 2007) *The $\mathfrak{R}_{SS}^R(\mathcal{F})$ and $\mathfrak{R}_{SS}^{R_c}(\mathcal{F})$ SS realizations of a SISO $\mathfrak{R}_{IO}(\mathcal{F})$ via (2.89a-b) are completely state-reachable. They are also completely state-observable and hence minimal iff R_y and R_u are coprime.*

The direct coefficient relation of the canonical forms with the IO coefficients can also be obtained in case R_u and R_y are coprime:

	$\mathfrak{R}_{SS}^O(\mathcal{F})$	$\mathfrak{R}_{SS}^{O_c}(\mathcal{F})$	$\mathfrak{R}_{SS}^R(\mathcal{F})$	$\mathfrak{R}_{SS}^{R_c}(\mathcal{F})$
α_i	a_i	a_i	a_i	a_i
β_j	$b_j - \sum_{l=j}^{n_a-1} a_l \beta_{n_a-l+j}^o$	$b_j - a_j b_{n_a}$	$b_j - \sum_{l=j}^{n_a-1} a_l \beta_{n_a-l+j}^r$	$b_j - a_j b_{n_a}$
β_{n_x}	b_{n_a}	b_{n_a}	b_{n_a}	b_{n_a}

where $i, j \in \mathbb{I}_0^{n_x-1}$, $n_x = n_a$, and $b_j = 0$ if $j > n_b$. It is an important observation that the resulting relation of the coefficients is exactly the inverse of the previously derived conversion rules of the IO realization case. Moreover, due to the minimality of the state-map, all the obtained canonical forms are minimal and belong to the same equivalence class.

In the MIMO case, algorithm (2.83a-b) and (2.89a-b) also provides SS realization of IO representations, however with different selector matrices (due to the multi-dimension) and with a more complicated path to select independent rows from the shift-map for X . It is only guaranteed that at least n_a number of rows of the shift-map are independent, thus such selection is not evident. Similar to selection schemes generating SS canonical representations, only certain selection strategies for X lead to the MIMO observability and reachability canonical forms. Therefore, depending on the selection scheme, it is not guaranteed in the general sense that the obtained SS realization via algorithm (2.83a-b) or (2.89a-b) with the chosen X is minimal.

2.1.8 Discretization of LTI system representations

Similar to the representation problem discussed previously, it is important to find equivalent/adequate DT realizations of a given CT system. Such a transformation of continuous-time representations into a discrete-time counterpart is called discretization and it is highly motivated by both identification and controller implementation.

In the LTI framework, already extensive research has been dedicated to discretization methods. The developed techniques can be separated mainly into two distinct classes: isolated and non-isolated methods (see Hanselmann (1987) for an overview). Non-isolated techniques consider the discretization of a CT controller acting on a plant in a closed-loop setting and they aim at the preservation of the CT closed-loop performance. Isolated techniques consider the stand-alone discretization of a CT system aiming at only the preservation of the CT input-output behavior. While isolated approaches are applicable to any LTI system, the non-isolated techniques are only useful for controller discretization, but they generally result in a better closed-loop performance (Hanselmann 1987).

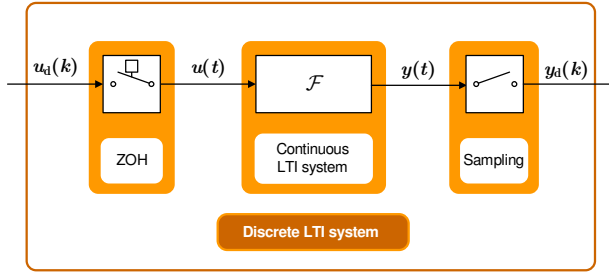


Figure 2.3: Zero-order hold discretization setting of general LTI systems.

In the following, a brief overview of the isolated discretization methods is given with the intention to extend the introduced methods for the discretization of LPV systems later on. To accomplish this, first the exact setting of the discretization problem has to be established. We consider an ideal *Zero-Order Hold* (ZOH) setting presented in Figure 2.3. In this formulation, we are given a CT-LTI system \mathcal{F} , with input-output partition (u, y) , and we would like to steer/describe \mathcal{F} in a discrete way. Thus, we choose that u is generated by a ideal ZOH⁹ device and y is sampled in a perfectly synchronized manner with sampling-time $T_d \in \mathbb{R}^+$. It is assumed that the ZOH and the instrument providing the output sampling have infinite resolution so there is no quantization error¹⁰ and their processing time is zero. In the following we use the notation u_d and y_d to denote the discrete-time counterparts of the continuous-time signals u and y satisfying (2.20) with sampling-time T_d . Based on this, for the signals of Figure 2.3 it holds that

$$u(t) := u_d(k), \quad \forall t \in [kT_d, (k+1)T_d), \quad (2.92a)$$

$$y_d(k) := y(kT_d), \quad (2.92b)$$

for each $k \in \mathbb{Z}$, meaning that u can only change at every sampling-time instant. However in Section 2.1.3, equivalence of CT and DT behaviors under a given sampling-time has been established without any restrictions on the variation of the input signal. But in order to compute/describe the effect of u on \mathcal{F} in a given sample interval, its variation must be restricted to a certain class of functions which is chosen here to be the piecewise constant (zero-order) class. By choosing this class wider, including linear, 2nd-order polynomial, etc., higher-order hold discretization settings of LTI systems can be derived (see Middleton and Goodwin (1990)). Moreover, ZOH based actuation is implemented in most actuation devices and such a setting is quite realistic in the sense how computer controlled physical systems behave (Hanselmann 1987).

⁹The ZOH device is a signal hold instrument providing a CT signal which is constant till the device is commanded to change it to a new value in a piecewise constant manner.

¹⁰Due to digital nature and physical limitation of the equipment, the ZOH device has finite resolution in reality, which means that it can only generate finite number of signal values. Moreover, sampling devices also store data digitally, making available only the representation of finite number of different measured values. The actuation and sampling error introduced by these problems is called quantization error. For more on quantization and its effects, see Gray and Neuhoff (1998).

Discretization of state-space representations

In order to find an equivalent DT-SS realization of a given $\mathfrak{R}_{\text{SS}}(\mathcal{F})$ under the ZOH setting, write the state equations (2.18a-b) as

$$\frac{d}{dt}x(t) = Ax(t) + Bu(kT_d), \quad (2.93a)$$

$$y(t) = Cx(t) + Du(kT_d), \quad (2.93b)$$

for $t \in [kT_d, (k+1)T_d)$ with initial condition $x(kT_d)$. These equations describe the state and output evolution of $\mathfrak{R}_{\text{SS}}(\mathcal{F})$ inside the k^{th} sampling interval. Then in the k^{th} interval, the *Ordinary Differential Equation* (ODE) defined by (2.93a) has the following solution:

$$x(t) = e^{A(t-kT_d)}x(kT_d) + \int_{\tau=0}^{t-kT_d} e^{A(t-kT_d-\tau)}Bu(kT_d) d\tau. \quad (2.94)$$

By substituting $t = (k+1)T_d$, $x_d(k) = x(kT_d)$, and $u_d(k) = u(kT_d)$, formula (2.94), under the restriction that A is invertible, results in:

$$x_d(k+1) = e^{AT_d}x_d(k) + A^{-1}(e^{AT_d} - I)Bu_d(k), \quad (2.95a)$$

$$y_d(k) = Cx_d(k) + Du_d(k), \quad (2.95b)$$

where $y_d(k) = y(kT_d)$ due to the ZOH setting. We call this discretization method the *complete method*, giving the following DT equivalent of $\mathfrak{R}_{\text{SS}}(\mathcal{F})$:

$$\mathfrak{R}_{\text{SS}}(\mathcal{F}, T_d) = \left[\begin{array}{c|c} e^{AT_d} & A^{-1}(e^{AT_d} - I)B \\ \hline C & D \end{array} \right]. \quad (2.96)$$

Approximative state-space discretization methods

In order to avoid the computation of e^{AT_d} , many different approximative methods have been introduced:

- *Rectangular (Euler's forward) method*

The simplest way of avoiding the computation of e^{AT_d} is to use a first-order approximation:

$$e^{AT_d} \approx I + AT_d. \quad (2.97)$$

Now introduce $f(x, u, t) = Ax(t) + Bu(t)$ as the left hand side of (2.18a). Then

$$\int_{\tau=kT_d}^{(k+1)T_d} f(x, u, \tau) d\tau = \int_{\tau=kT_d}^{(k+1)T_d} Ax(\tau) + Bu(kT_d) d\tau, \quad (2.98)$$

gives the solution of (2.93a) in $[kT_d, (k+1)T_d)$. By the *left-hand rectangular evaluation* of this Riemann integral, (2.98) is approximated as

$$x((k+1)T_d) \approx x(kT_d) + T_d Ax(kT_d) + T_d Bu(kT_d), \quad (2.99)$$

coinciding with the suggested matrix exponential approximation of (2.97). Based on this rectangular approach, the DT approximation of $\mathfrak{R}_{\text{SS}}(\mathcal{F})$ is given as:

$$\mathfrak{R}_{\text{SS}}(\mathcal{F}, T_d) \approx \left[\begin{array}{c|c} I + T_d A & T_d B \\ \hline C & D \end{array} \right]. \quad (2.100)$$

Another interpretation of this method can be derived from *Euler's forward discretization*, which uses that:

$$\frac{d}{dt}x(t) = \lim_{T_d \rightarrow 0} \frac{x(t + T_d) - x(t)}{T_d}. \quad (2.101)$$

Then, by using (2.101) as an approximation with $T_d > 0$ fixed:

$$\frac{d}{dt}x(t) \approx \frac{x((k+1)T_d) - x(kT_d)}{T_d}, \quad (2.102)$$

for $t \in [kT_d, (k+1)T_d)$. Substitution of (2.102) into (2.93a) yields the previously derived conversion rules.

- *Polynomial (Hanselmann) method*

Continuing the line of reasoning of the rectangular approach, it is possible to develop other methods that achieve better approximation of the complete case at the price of increasing complexity. As suggested by Hanselmann (1987), higher order Taylor expansions of the matrix exponential term:

$$e^{AT_d} \approx I + \sum_{l=1}^n \frac{T_d^l}{l!} A^l, \quad (2.103)$$

result in the so called *polynomial discretization methods*. Substituting (2.103) into (2.93a) gives:

$$\mathfrak{R}_{\text{SS}}(\mathcal{F}, T_d) \approx \left[\begin{array}{c|c} I + \sum_{l=1}^n \frac{T_d^l}{l!} A^l & T_d \left(I + \sum_{l=1}^{n-1} \frac{T_d^l}{l+1!} A^l \right) B \\ \hline C & D \end{array} \right]. \quad (2.104)$$

- *Trapezoidal (Tustin) method*

An alternative way to give a better approximation than the rectangular method is to use a different (approximative) evaluation of the integral (2.98):

$$x((k+1)T_d) \approx x(kT_d) + \frac{T_d}{2} [f(x, u, kT_d) + f(x, u, (k+1)T_d)], \quad (2.105)$$

which is the so called *trapezoidal evaluation* of the Riemann integral. This coincides with the *Extended Euler* method and the *1-step Adams-Moulton* method of numerical approximation of ODEs (Atkinson 1989) or the commonly used *Tustin* type of discretization. The derivation is as follows:

Assume that $(I - \frac{T_d}{2}A)$ is invertible and apply a change of variables

$$\check{x}_d(k) = \frac{1}{\sqrt{T_d}} \left(I - \frac{T_d}{2} A \right) x(kT_d) - \frac{\sqrt{T_d}}{2} B u(kT_d), \quad (2.106a)$$

which defines an invertible state-transformation. Then, substitution of (2.106a) into (2.105) gives

$$\mathfrak{R}_{\text{SS}}(\mathcal{F}, T_d) \approx \left[\begin{array}{c|c} (I + \frac{T_d}{2}A) (I - \frac{T_d}{2}A)^{-1} & \sqrt{T_d} (I - \frac{T_d}{2}A)^{-1} B \\ \hline \sqrt{T_d} C (I - \frac{T_d}{2}A)^{-1} & \frac{T_d}{2} C (I - \frac{T_d}{2}A)^{-1} B + D \end{array} \right].$$

It is important to note that the trapezoidal method only approximates the manifest behavior of $\mathfrak{R}_{\text{SS}}(\mathcal{F}, T_d)$, as it gives an approximative DT-SS representation in terms of the new latent variable \check{x}_d .

- *Multi-step methods*

As an other alternative, consider the state evolution as the solution of the DE defined by (2.18a). This solution can be numerically approximated via multi-step formulas like the Runge-Kutta, Adams-Moulton, or the Adams-Bashforth type of approaches (see Atkinson (1989)). In commercial engineering software packages, like Matlab Simulink, commonly variable step-size implementation of these algorithms assures accurate simulation of continuous-time systems. However in the considered ZOH discretization setting, the step size, i.e. the sampling rate, is fixed and sampled data is only available at past and present sampling instances. This immediately excludes multi-step implicit methods like the Adams-Moulton approaches. Moreover $f(x, u, t)$ can only be evaluated for integer multiples of the sampling-time, as the input only changes at these time instances and the resulting model must be realized as a single rate (not multi-rate) system. Therefore it is complicated to apply methods like the Runge-Kutta approach. The family of Adams-Bashforth methods does fulfill these requirements (see Atkinson (1989)). The 3-step version of this numerical approach uses the following approximation:

$$\begin{aligned} x((k+1)T_d) \approx x_d(k+1) = x(kT_d) + \frac{T_d}{12} [5f(x, u, (k-2)T_d) - \\ -16f(x, u, (k-1)T_d) + 23f(x, u, kT_d)]. \end{aligned} \quad (2.107)$$

Then, formulating this state-space equation in an augmented SS form with the new state-variable:

$$\check{x}_d(k) = \text{col}(x_d(k), f(x, u, (k-1)T_d), f(x, u, (k-2)T_d)), \quad (2.108)$$

gives that

$$\mathfrak{R}_{\text{SS}}(\mathcal{F}, T_d) \approx \left[\begin{array}{ccc|c} I + \frac{23T_d}{12}A & -\frac{16T_d}{12}I & \frac{5T_d}{12}I & \frac{23T_d}{12}B \\ A & 0 & 0 & B \\ 0 & I & 0 & 0 \\ \hline C & 0 & 0 & D \end{array} \right].$$

The resulting DT-SS representation is an approximation of $\mathfrak{R}_{\text{SS}}(\mathcal{F}, T_d)$ in terms of the new state variable \check{x}_d .

Discretization of input-output representations

In order to find the equivalent DT-IO realization of a given $\mathfrak{R}_{\text{IO}}(\mathcal{F})$ under the ZOH setting, commonly the transfer function $F(s)$ of $\mathfrak{R}_{\text{IO}}(\mathcal{F})$ is used for derivation.

Define:

$$F'(z) = \frac{z-1}{z} \mathcal{L} \left\{ \mathcal{L}^{-1} \left\{ \frac{1}{s} F(s) \right\} \right\} \Big|_{T_d}. \quad (2.109)$$

Then it can be shown that $\mathfrak{R}_{\text{IO}}(\mathcal{F}, T_d)$ with transfer function $F'(z)$ is the DT equivalent of $\mathfrak{R}_{\text{IO}}(\mathcal{F})$ in the ZOH setting under the sampling-time T_d (Neuman and Baradello 1979). Alternatively, discretization of IO representations can be carried out in the SS domain by finding an equivalent SS realization of $\mathfrak{R}_{\text{IO}}(\mathcal{F})$. Many approximative SS approaches have their equivalent formulation in terms of approximations of (2.109). These result in the well-known substitution formulas of s for $F(s)$ to approximate $F'(z)$.

Properties of approximative discretization methods

In the LTI case approximative discretization methods have been analyzed in many quantitative studies (see Hanselmann (1987)), while their numerical properties have been fully worked out by the numerical analysis community (see Atkinson (1989)). The main focus of these investigations concentrated around the introduced signal errors of the approximative DT projection and the numerical stability of the applied methods. During the extension of the LTI methods for LPV system, these properties will be revisited and thoughtfully investigated in Chapter 3.

2.2 Orthonormal basis functions

In LTI system theory, it is common to represent transfer functions of dynamical systems in a series-expansion form. The most simplest of these expansions is the Laurent expansion. Consider a DT-LTI system \mathcal{F} and its transfer function $F(z)$ associated with an IO partition (y, u) . Assume that \mathcal{F} is stable, so the domain of $F(z)$ is the exterior of the unit circle. Then, the Laurent expansion of $F(z)$ around $z = \infty$ is

$$F(z) = \sum_{i=0}^{\infty} \mathbf{g}_i z^{-i}. \quad (2.110)$$

We have already discussed that the constants $\{\mathbf{g}_i\}_{i=0}^{\infty}$ are called Markov parameters or expansion coefficients. These coefficients are unique with respect to the system, regarding the IO partition associated with $F(z)$. Note that in case of unstable systems, a Laurent expansion of $F(z)$ is available but around $z = 0$, which results in an expression in the positive powers of z . By substituting z^{-1} in (2.110) with the backward-shift operator q^{-1} , it holds that

$$y = \sum_{i=0}^{\infty} \mathbf{g}_i q^{-i} u, \quad (2.111)$$

for all $(u, y) \in \mathfrak{B}$ with left compact support. Thus (2.111) can be considered as a representation of the system itself and will be denoted by $\mathfrak{R}_{\text{IM}}(\mathcal{F})$. (2.111) has a direct relation with the impulse response of the system considering the IO partition

(y, u) (see (2.26)). Therefore (2.111) is called the *Impulse Response Representation* (IRR). Note that such a representation is available for unstable systems as well, but in terms of the forward-shift operator q .

Finite truncations of the IRR are known as *Finite Impulse Response* (FIR) models, which have proven their usefulness in many areas of engineering, ranging from signal processing to control design and also in approximative system identification. Despite numerous attractive properties of FIR models, these structures often require a large number of expansion terms to adequately approximate the original system dynamics. As an alternative, series-expansion models using general basis functions have been introduced:

$$y \approx \sum_{i=1}^n w_i \phi_i(q)u. \quad (2.112)$$

for a predefined set of rational basis functions $\{\phi_i\}_{i=1}^n$ with $\phi_0 = 1$ and constant coefficients $\{w_i\}_{i=0}^\infty$. Such models preserve all the advantages of FIR structures, but in general they require much less expansion terms for adequate approximation due to the *Infinite Impulse Response* (IIR) characteristics of the basis functions. In the following, the basic properties and the theory of *Orthonormal Basis Functions* (OBF) are introduced briefly with the intention to derive OBFs based representations/models of LPV systems later on. To simplify the following discussion, which is based on Heuberger et al. (2005); Ninness and Gustafsson (1997) and Heuberger et al. (1995), we restrict our attention to DT stable SISO systems, however some hints are also given later how the theory extends to MIMO or CT systems.

2.2.1 Signal spaces and inner functions

Before defining OBFs and their properties in system approximation, some preliminaries are needed to be briefly covered. We denote by $\mathbb{D} = \{z \in \mathbb{C} \mid |z| < 1\}$ the open unit disk on the complex plane and by $\mathbb{J} = \{z \in \mathbb{C} \mid |z| = 1\}$ the unit circle. Also introduce \mathbb{E} to represent the exterior of \mathbb{J} . The function space we frequently use in the sequel is the following:

Definition 2.37 (Hardy space on \mathbb{E}) Denote by $\mathcal{H}_2(\mathbb{E})$ the Hardy space of complex functions (transfer functions) $F : \mathbb{C} \rightarrow \mathbb{C}$, which are analytic (holomorphic) on \mathbb{E} , and squared integrable on \mathbb{J} :

$$\|F\|_{\mathcal{H}_2} := \sup_{1 < r} \sqrt{\frac{1}{2\pi} \int_0^{2\pi} |F(re^{i\omega})|^2 d\omega} < \infty, \quad (2.113)$$

where $\|\cdot\|_{\mathcal{H}_2}$ is a norm on $\mathcal{H}_2(\mathbb{E})$.

$\mathcal{H}_2(\mathbb{E})$ can be interpreted as the space of stable proper transfer functions. Additionally we denote by $\mathcal{H}_{2-}(\mathbb{E})$ the subspace of strictly proper functions in $\mathcal{H}_2(\mathbb{E})$. Introduce also $\mathcal{RH}_{2-}(\mathbb{E})$ as the subspace of transfer functions in $\mathcal{H}_{2-}(\mathbb{E})$ with real valued impulse response. $\mathcal{H}_2(\mathbb{E})$ is equipped with the following inner product:

Definition 2.38 (Inner product of $\mathcal{H}_2(\mathbb{E})$) The inner product of $F_1, F_2 \in \mathcal{H}_2(\mathbb{E})$ is defined as:

$$\langle F_1, F_2 \rangle := \frac{1}{2\pi} \int_{-\pi}^{+\pi} F_1(e^{i\omega}) F_2^*(e^{i\omega}) d\omega = \frac{1}{2i\pi} \oint_{\mathcal{J}} F_1(z) F_2^*\left(\frac{1}{z^*}\right) \frac{dz}{z}, \quad (2.114)$$

where $*$ denotes complex conjugation.

The norm of $F \in \mathcal{H}_2(\mathbb{E})$ satisfies

$$\|F\|_{\mathcal{H}_2} = \sqrt{\langle F, F \rangle}. \quad (2.115)$$

Two transfer functions $F_1, F_2 \in \mathcal{H}_2(\mathbb{E})$ are called orthonormal if the following conditions hold:

$$\langle F_1, F_2 \rangle = 0, \quad \|F_1\|_{\mathcal{H}_2} = \|F_2\|_{\mathcal{H}_2} = 1. \quad (2.116)$$

In this sense, the functions $\{z^{-k}\}_{k=1}^n$ in $\mathcal{H}_2(\mathbb{E})$ are orthonormal, as they trivially satisfy (2.116). Moreover, for a given transfer function $F \in \mathcal{H}_2(\mathbb{E})$, the Markov parameters can be computed as

$$\mathbf{g}_i = \langle F, z^{-i} \rangle, \quad (2.117)$$

yielding the Laurent series-expansion (2.110). This series-expansion is called convergent if

$$\|F\|_{\mathcal{H}_2} = \sqrt{\sum_{i=0}^{\infty} |\mathbf{g}_i|^2} < \infty. \quad (2.118)$$

Relation (2.118) implies that $\{z^{-i}\}_{i=1}^{\infty}$ are complete in $\mathcal{H}_{2-}(\mathbb{E})$. These functions, often referred as the *pulse basis*, are the most simple OBFs in $\mathcal{H}_{2-}(\mathbb{E})$ and they generate the IIR of stable dynamical systems.

We distinguish a special set of functions in $\mathcal{H}_2(\mathbb{E})$, the so called *inner* functions. A function $G \in \mathcal{H}_2(\mathbb{E})$ is called inner, if

$$G(z)G^*(1/z^*) = 1. \quad (2.119)$$

Such a function is completely determined, modulo the sign, by its poles $\Lambda_n = \{\lambda_i \in \mathbb{D}\}_{i=1}^n$:

$$G(z) = \pm \prod_{i=1}^n \frac{1 - \lambda_i^* z}{z - \lambda_i}, \quad (2.120)$$

often called a *Blaschke product*.

2.2.2 General class of orthonormal basis functions

First the class of DT stable basis functions is considered. Let $G_0 = 1$ and $\{G_i\}_{i=1}^{\infty}$ be a sequence of DT inner functions with McMillan degrees $\{n_i\}_{i=1}^{\infty}$. Let $(A_i, B_i,$

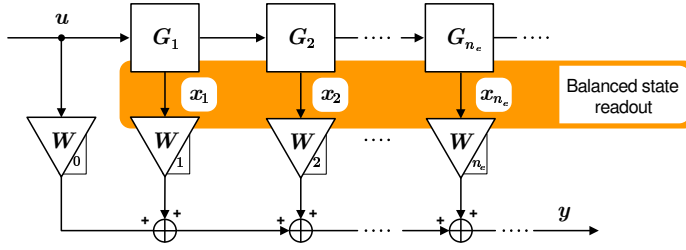


Figure 2.4: IO signal flow of OBFs based series-expansion models.

C_i, D_i) be a jointly minimal balanced DT-SS representation¹¹ of the transfer function G_i . Let $\{\lambda_1, \lambda_2, \dots\}$ denote the collection of all poles of the inner functions $\{G_i\}_{i=1}^{\infty}$. Under the completeness (Szász) condition that $\sum_{i=1}^{\infty} (1 - |\lambda_i|) = \infty$, the scalar elements of the sequence of vector functions

$$M_i(z) := (zI - A_i)^{-1} B_i \prod_{l=0}^{i-1} G_l(z), \quad i > 0, \quad (2.121)$$

constitute a basis for $\mathcal{H}_{2-}(\mathbb{E})$, and each element $\phi_{ij} = [M_i]_j$ is orthonormal in $\mathcal{H}_{2-}(\mathbb{E})$ with respect to the entire sequence. An important aspect of these basis functions $\{\phi_{ij}\}_{i=1, j=1}^{\infty, n_i}$ is that they are uniquely determined, modulo the sign, by the poles of the generating inner functions (see (2.120) and (2.121)). However, note that (2.121) is only a particular way to construct OBFs and hence the generated basis sequence is not unique with respect to $\{\lambda_1, \lambda_2, \dots\}$ (Heuberger et al. 2005).

Any $F \in \mathcal{H}_2(\mathbb{E})$ can be written as

$$F(z) = W_0 + \sum_{i=1}^{\infty} W_i M_i(z), \quad (2.122)$$

where $W_i^\top \in \mathbb{C}^{n_i}$ (if $F, G_i \in \mathcal{RH}_2(\mathbb{E})$, then $W_i^\top \in \mathbb{R}^{n_i}$) and it can be shown that the rate of convergence of this series is bounded. The IO relation of the OBF parametrization (2.122) is illustrated by Figure 2.4. Note that in this figure, the state signals $\{x_i\}_{i=1}^{\infty}$ are the state variables of the balanced SS realizations of $\{G_i\}_{i=1}^{\infty}$. Additionally, $x_i = M_i(q)u$, i.e. the states are equal to the output of the generated basis functions.

Basically, the class of OBFs generalized by (2.121) can be classified into five function sets represented in Figure 2.5. These categories, which hierarchically contain the smaller classes from pulse basis to the Takenaka-Malmquist class, are defined as follows (see Heuberger et al. (2005) for detailed overview on these classes):

¹¹Note, that only inner functions in $\mathcal{RH}_{2-}(\mathbb{E})$ have SS representations with real matrices. As an abuse of the previously introduced terminology, we allow here SS representations, i.e. their matrices to generalize to the complex case.

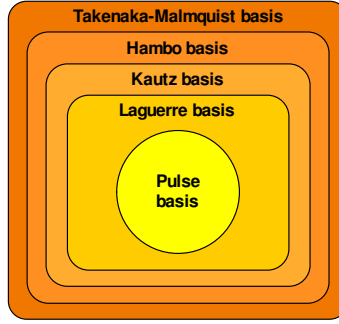


Figure 2.5: Classification of orthonormal basis functions.

Takenaka-Malmquist basis

The functions (2.121) are often referred to as the *Takenaka-Malmquist functions*. For a particular¹² balanced realization of the inner functions, it can be shown that the basis functions generated via (2.121) have the form of

$$\phi_{ij}(z) = \frac{\sqrt{1 - |\lambda_{ij}|}}{z - \lambda_{ij}} \left[\prod_{l=1}^{j-1} \frac{1 - z\lambda_{il}^*}{z - \lambda_{il}} \right] \left[\prod_{k=0}^{i-1} \prod_{l=1}^{n_k} \frac{1 - z\lambda_{kl}^*}{z - \lambda_{kl}} \right], \quad (2.123)$$

where $\{\lambda_{ij}\}_{j=1}^{n_i} \subset \mathbb{D}$ are the poles of the inner function G_i .

Hambo basis

The special cases when all G_i are equal, i.e. $G_i = G, \forall i > 0$, where G is an inner function with McMillan degree $n_g > 0$, are known as *Hambo functions* or *Generalized Orthonormal Basis Functions* (GOBFs). Let (A, B, C, D) be a jointly minimal balanced SS representation of G . Define

$$M_i^{AB}(z) := (zI - A)^{-1} B G^{i-1}(z), \quad (2.124a)$$

$$M_i^{AC}(z) := (zI - A^\top)^{-1} C^\top G^{i-1}(z). \quad (2.124b)$$

As system transposition is an equivalence transformation for jointly minimal systems, there exists a unitary¹³ $T \in \mathbb{C}^{n_g \times n_g}$ such that

$$M_1^{AB} = T M_1^{AC}. \quad (2.125)$$

Now by using $\phi_j = [M_1^{AB}]_j$, the Hambo basis consists of the functions

$$\Phi_{n_g}^\infty := \{\phi_j G^i\}_{j=1, \dots, n_g}^{i=0, \dots, \infty}. \quad (2.126)$$

¹²Note that a balanced state-space realization of an inner function is non-unique.

¹³A square matrix $T \in \mathbb{C}^{n \times n}$ is called unitary if $T T^* = T^* T = I$, where $*$ denotes conjugate transpose, also called Hermitian transpose.

We also introduce

$$\Phi_{n_g}^{n_e} := \{\phi_j G^i\}_{j=1, \dots, n_g}^{i=0, \dots, n_e}, \quad n_e \geq 0, \quad (2.127)$$

to denote the case when we talk only about a set of orthonormal functions generated by a finite extension of G . Note that by using M_1^{AC} to define ϕ_j , a different basis sequence $\tilde{\Phi}_{n_g}^\infty$ results. However, due to (2.125), these basis sequences can be considered equivalent. In the following we use the M_1^{AB} based construction if not indicated otherwise.

Similar to the previous generation method, G and hence $\Phi_{n_g}^\infty$ are completely determined by the poles of G , $\Lambda_{n_g} = \{\lambda_i, \dots, \lambda_{n_g}\}$ and any $F \in \mathcal{H}_2(\mathbb{E})$ can be written as

$$F(z) = w_{00} + \sum_{i=0}^{\infty} \sum_{j=1}^{n_g} w_{ij} \phi_j(z) G^i(z), \quad (2.128)$$

where w_{00} is associated with the unit gain $\phi_{00} = 1$. It can be shown, that the rate of convergence of this series-expansion is bounded by

$$\rho = \max_k |G(1/\lambda_k^{(0)})|, \quad (2.129)$$

where $\{\lambda_k^{(0)}\}$ are the poles of F . ρ is often called the *convergence rate* of the Hambo series-expansion and it is an essential measure of the approximation quality of the basis function set with respect to F . In the best case, where the poles of F are the same (with multiplicity) as the poles of G , only the terms with $i = 0$ in (2.128) are non-zero. Such a basis is commonly considered to be optimal for F .

Kautz basis

When $G_i = G$, $\forall i > 0$ with $n_g = 2$, the resulting OBFs are called *2-parameter Kautz functions*. Such basis sequences can be considered to be adequate for the expansion of systems with dominating second order modes.

Laguerre basis

The case when $G_i = G$, $\forall i > 0$ with $n_g = 1$ are called *Laguerre functions*. As this type of basis sequence in $\mathcal{RH}_{2-}(\mathbb{E})$ has only a real pole λ , therefore it can provide adequate basis for a $F \in \mathcal{RH}_{2-}(\mathbb{E})$ with a dominating first-order mode.

Pulse basis

The case when $G_i = z^{-1}$, $\forall i > 0$ are called *pulse functions*. Based on the expansion of the transfer functions of LTI dynamical systems in terms of the pulse basis, impulse response representation of LTI systems is available.

Orthonormal basis functions of MIMO systems

In the MIMO case, two approaches have been introduced for the construction of OBF functions in $\mathcal{H}_{2-}^{n_v \times n_v}(\mathbb{E})$. The generated functions provide a series-expansion of any $F \in \mathcal{H}_{2-}(\mathbb{E})^{n_v \times n_v}$. In one of the approaches, the key idea is to use MIMO functions that are composed from scalar basis sequences:

$$\check{\phi}_l(z) := \begin{bmatrix} \phi_{l11}(z) & \dots & \phi_{l1n_v}(z) \\ \vdots & \ddots & \vdots \\ \phi_{ln_v1}(z) & \dots & \phi_{ln_vn_v}(z) \end{bmatrix} \quad (2.130)$$

where each $\{\phi_{lij}\}_{l=1}^{\infty}$ corresponds to a basis of $\mathcal{H}_{2-}(\mathbb{E})$. Then any $F \in \mathcal{H}_{2-}^{n_v \times n_v}(\mathbb{E})$ can be represented as

$$F(z) = W_0 + \sum_{i=0}^{\infty} W_i \odot \check{\phi}_i(z), \quad (2.131)$$

where $W_i \in \mathbb{C}^{n_v \times n_v}$ and \odot denotes the element-by-element matrix product. Similar to the SISO case, with different basis sequences $\{\phi_{lij}\}_{l=1}^{\infty}$, different convergence rates of the series-expansion can be achieved. However, the degree of freedom in the basis selection is much higher in the MIMO case. Note, that it is not necessary to use different basis sequences in the generation of (2.130), which gives the possibility of several structural classifications of this type of MIMO bases (see van Donkelaar (2000)).

Another formulation of MIMO orthonormal basis functions follows by using a multivariable, specifically square, inner function $G \in \mathcal{H}_{2-}^{n_v \times n_v}(\mathbb{E})$. The derivation is the same as the state-space construction approach presented by (2.121), but in this case $\phi_i = M_i$ constitutes a basis for $\mathcal{H}_{2-}^{n_v \times n_v}(\mathbb{E})$ in the sense that any $F \in \mathcal{H}_{2-}^{n_v \times n_v}(\mathbb{E})$ can be written as

$$F(z) = W_0 + \sum_{i=1}^{\infty} W_i M_i(z), \quad (2.132)$$

where $W_i \in \mathbb{C}^{n_v \times n_v}$. An important issue here is the construction of the square all-pass function G . Where in the scalar case, G can be written as a Blaschke product and thus modulo the sign it is determined by the poles of the product, the multivariable-case is more involved and inhibits more freedom. Here also the structure and/or the dynamic directions are important (Heuberger et al. 2005). See van Donkelaar (2000) and Heuberger (1990) for more on MIMO-OBFs of this form.

Basis functions in continuous-time

All the results introduced so far are presented for DT systems as this time domain is used to formulate OBFs based identification of LPV systems later on. There is however a completely analogous theory for CT systems, where the Laplace transform is used instead of the Z-transform. The exterior of the unit disk \mathbb{E} is replaced

by the right half plane \mathbb{C}^+ and the inner product (2.114) is defined as integration over the imaginary axis:

$$\langle F_1, F_2 \rangle := \frac{1}{2i\pi} \int_{i\mathbb{R}} F_1(s) F_2^*(-s^*) ds. \quad (2.133)$$

It is possible to construct an explicit isomorphism between $\mathcal{H}_2(\mathbb{E})$ and $\mathcal{H}_2(\mathbb{C}^+)$ using the bilinear transformation

$$z \mapsto s = \gamma \frac{z-1}{z+1}, \quad \gamma > 0. \quad (2.134)$$

In this way, most of the introduced concepts extend trivially.

2.3 Modeling and Identification of LTI systems

When identifying a dynamical system on the basis of experimentally measured data records, the outline of the procedure is summarized in the so called identification cycle (see Table 1.1). The two most important steps of this cycle are the choices of an appropriate model set and the identification criterion. While the previous describes the set in which the suitable description of the system is sought, the latter defines the aimed performance of the model. The choice of the model set is crucial as it directly influences the maximum achievable accuracy or quality of the identified model in terms of the user-defined criterion. The model set should be as large as possible in order to contain as many candidate models as possible, which reduces the structural or bias error of the optimal model in the set. On the other hand, the number of parameters of the model should be kept as small as possible, because the variability of the identified models increases with increasing number of parameters. The conflict between these issues is the well-known bias/variance trade-off that is present in many estimation problems.

Model structures induced by orthonormal basis functions have attractive properties in terms of the variance/bias trade-off. When appropriately chosen, they require only a limited number of parameters to represent models that can accurately describe the dynamics of the considered system. The choice of basis functions then becomes a principle design issue. In this section, a brief coverage of DT prediction error system identification is given, based on Ljung (1999) and Heuberger et al. (2005). We focus on OBFs based model structures and concepts required for the derivation of the identification approaches of this thesis.

2.3.1 Concepts of the identification setting

As a framework, the black-box setting of Ljung (1999) is adopted. In this setting, identification of an unknown system is aimed at without the use of prior structural information. For simplicity, we assume that a predefined IO partition of the

system is given, so it is clear which signals we call inputs and outputs of the unknown system. An additional assumption is that the underlying, so called *data generating system*, is an LTI discrete-time SISO process:

$$y = F_0(q)u + v, \quad (2.135)$$

where $F \in \mathcal{H}_2(\mathbb{E})$, u is a *quasi-stationary* signal, and v is a stationary stochastic process (see Ljung (1999) for a definition of these properties). Furthermore v satisfies

$$v = Q_0(q)e, \quad (2.136)$$

with monic transfer function Q_0 such that $Q_0, Q_0^{-1} \in \mathcal{H}_2(\mathbb{E})$ and e is a zero-mean white noise process with variance σ_e^2 . Assume furthermore that data sequences $\mathcal{D}_{N_d} = \{u(k), y(k)\}_{k=0}^{N_d-1}$, generated by (2.135), are available. Under the given assumptions, the so called *one-step ahead prediction* of $y(k)$ based on $\{y(k-1), y(k-2), \dots\}$ and $\{u(k), u(k-1), \dots\}$ is

$$\hat{y} := (1 - Q_0(q)^{-1})y + Q_0(q)^{-1}F_0(q)u. \quad (2.137)$$

In prediction error identification, a parameterized model $(F(q, \theta), Q(q, \theta))$ is hypothesized where $\theta \subset \Theta$ represents the parameter vector, the coefficients of the model, and $\Theta \in \mathbb{R}^n$ is the allowed parameter space. This model structure leads to the one-step ahead predictor:

$$\hat{y}_\theta := (1 - Q(q, \theta)^{-1})y + Q(q, \theta)^{-1}F(q, \theta)u. \quad (2.138)$$

Then in the prediction error setting, we would like to choose θ such that the resulting \hat{y}_θ is a good approximation of y , i.e. the so called *prediction error*

$$\epsilon(k, \theta) := y(k) - \hat{y}_\theta(k), \quad (2.139)$$

is minimized. This is commonly performed by the minimization of the scalar valued *Least-Squares* (LS) identification criterion

$$\mathcal{W}_{N_d}(\theta, \mathcal{D}_{N_d}) = \frac{1}{N_d} \sum_{k=0}^{N_d-1} \epsilon^2(k, \theta), \quad (2.140)$$

resulting in

$$\hat{\theta}_{N_d} = \arg \min_{\theta \in \Theta} \mathcal{W}_{N_d}(\theta, \mathcal{D}_{N_d}), \quad (2.141)$$

based on the available data record \mathcal{D}_{N_d} . Other criteria based on different signal norms of ϵ can also be used or prefiltering can be applied on ϵ to deliver optimal estimates of θ based on certain considerations (see Ljung (1999)). Optimization of the identification criterion according to (2.141) is generally a non-convex optimization problem for which iterative (gradient) algorithms have to be applied. This also implies that convergence to a global optimum can not be easily guaranteed. However, in specific cases of parametrization, the optimization reduces to a convex problem with an analytical solution.

Table 2.1: Black-box model structures

	ARX	ARMAX	OE	FIR	BJ
$F(q, \theta)$	$\frac{R_B(q^{-1}, \theta)}{R_A(q^{-1}, \theta)}$	$\frac{R_B(q^{-1}, \theta)}{R_A(q^{-1}, \theta)}$	$\frac{R_B(q^{-1}, \theta)}{R_F(q^{-1}, \theta)}$	$R_B(q^{-1}, \theta)$	$\frac{R_B(q^{-1}, \theta)}{R_F(q^{-1}, \theta)}$
$Q(q, \theta)$	$\frac{1}{R_A(q^{-1}, \theta)}$	$\frac{R_C(q^{-1}, \theta)}{R_A(q^{-1}, \theta)}$	1	1	$\frac{R_C(q^{-1}, \theta)}{R_D(q^{-1}, \theta)}$

For dealing with quasi-stationary signals, we introduce the generalized expectation operator $\bar{\mathcal{E}}$ defined as

$$\bar{\mathcal{E}}\{y\} = \lim_{N \rightarrow \infty} \frac{1}{N} \sum_{k=0}^{N-1} \mathcal{E}\{y(k)\}, \quad (2.142)$$

where \mathcal{E} represents the mean value operator. The related (cross)-covariance functions are

$$\mathcal{C}_y(\tau) := \bar{\mathcal{E}}\{y(t)y(t-\tau)\}, \quad \mathcal{C}_{yu}(\tau) := \bar{\mathcal{E}}\{y(t)u(t-\tau)\}. \quad (2.143)$$

Additionally, the (cross)-power spectral densities are given as

$$\Phi_y(e^{i\omega}) := \sum_{\tau=-\infty}^{\infty} \mathcal{C}_y(\tau)e^{-i\omega\tau}, \quad \Phi_{yu}(e^{i\omega}) := \sum_{\tau=-\infty}^{\infty} \mathcal{C}_{yu}(\tau)e^{-i\omega\tau}. \quad (2.144)$$

2.3.2 Model structures

There are numerous different black-box model structures available for the parametrization of $F(q, \theta)$ and $Q(q, \theta)$. Most of them, collected in Table 2.1, parameterize the two transfer functions in terms of ratios of polynomials $R_A, \dots, R_F \in \mathbb{R}[\xi]$ in the backward time-shift operator q^{-1} . These structures are known under the acronyms given in the table. The parameter vector θ of these model structures contains the collection of the coefficients of the polynomials. Commonly, the denominator polynomials are assumed to be monic to ensure uniqueness of the parametrization. Every model structure or parametrization induces a set of predictor models, commonly called the *model set*:

$$\{(F(q, \theta), Q(q, \theta)) \in \mathcal{H}_2(\mathbb{E}) \times \mathcal{H}_2(\mathbb{E}) \mid \theta \in \Theta \subset \mathbb{R}^n\}. \quad (2.145)$$

This concept allows us to distinguish the following situations:

- The data generating system $(F_0(q), Q_0(q))$ is in the model set, i.e. an exact representation of the data generating system can be found by the applied model structure.
- $(F_0(q), Q_0(q))$ is not in the model set, i.e. no exact representation of the system exists by the model structure.

When the main attention is given to the IO dynamics of the system, i.e. the underlying deterministic behavior with respect to the considered IO partition, it is attractive to deal with the set of so called IO models:

$$\{F(q, \theta) \in \mathcal{H}_2(\mathbb{E}) \mid \theta \in \Theta \subset \mathbb{R}^n\}. \quad (2.146)$$

This leads to situations when the IO relation of the plant $F_0(q)$ can be or can not be captured within the chosen model set. Two important properties of the introduced model structures are the following

- For some model structures, the expression of the output predictor (2.138) is linear in the unknown parameters θ , i.e. both the terms $(1 - Q(q, \theta))^{-1}$ and $Q(q, \theta)^{-1}F(q, \theta)$ are polynomials. This property holds for the ARX and FIR structures and has the major benefit that the LS criterion can be minimized by solving a set of linear equations.
- If F and Q are independently parameterized, the two transfer functions can be estimated independently. This property holds for the FIR, OE, and BJ model structures.

From these viewpoints it is particularly attractive to consider the FIR model, where both these properties are satisfied.

2.3.3 Properties

Consistency and convergence

When applying the quadratic identification criterion (2.140), the asymptotic properties of the resulting parameter estimate can be derived in the situation when $N_d \rightarrow \infty$. If the noise in the measured data is normally distributed, the LS estimator is equivalent with a maximum likelihood (statistically optimal in an asymptotic sense) estimator (Ljung 1999). With other noise distributions, attractive properties also hold:

- *Convergence result* - For $N_d \rightarrow \infty$, the parameter estimate $\hat{\theta}_{N_d}$ converges, i.e. $\hat{\theta}_{N_d} \rightarrow \theta^*$, with probability 1. The convergence point θ^* is the minimizing argument of the expected value of the squared residual error, $\theta^* = \arg \min_{\theta \in \Theta} \bar{E}\{\epsilon^2(\theta)\}$. This implies that the asymptotic parameter estimate is independent from the particular noise realization in the data sequence.
- *Consistency result* - If u is *persistently exciting* (PE) of a sufficient order, then the asymptotic parameter estimate θ^* has the following properties:
 - If the data generating system is in the model set, then $F_0(q) = F(q, \theta^*)$ and $Q_0(q) = Q(q, \theta^*)$.
 - If $F_0(q)$ is in the IO model set and additionally $F(q, \theta)$ and $Q(q, \theta)$ are independently parameterized, then $F_0(q) = F(q, \theta^*)$. This means that consistency of the estimate F is also obtained if Q is misspecified.

Persistency of Excitation (PE) for an order n means in this context that the quasi-stationary u , used for excitation during the experiment, satisfy that

$$\det \begin{bmatrix} \mathcal{C}_u(0) & \mathcal{C}_u(1) & \dots & \mathcal{C}_u(n-1) \\ \mathcal{C}_u(1) & \mathcal{C}_u(0) & \dots & \mathcal{C}_u(n-2) \\ \vdots & \ddots & \ddots & \vdots \\ \mathcal{C}_u(n-1) & \dots & \mathcal{C}_u(1) & \mathcal{C}_u(0) \end{bmatrix} \neq 0. \quad (2.147)$$

This condition guarantees that enough information on the dynamics of F_0 is present in the measured y to approximate n parameters of a model. In the LTI case it is sufficient to require that $\Phi_u(e^{j\omega})$ has a non-zero contribution in the frequency range $-\pi < \omega \leq \pi$ in at least as many points as there are parameters to be estimated in $F(q, \theta)$.

Asymptotic bias and variance

In system identification, one also has to deal with estimation errors. This is due to the fact that information on the system to be estimated is only partially available: finite data records, effect of noise, etc. A well-accepted approach is to decompose the estimation error for $F(q, \hat{\theta}_{N_d})$ as:

$$F_0(q) - F(q, \hat{\theta}_{N_d}) = \underbrace{F_0(q) - F(q, \theta^*)}_{\text{bias}} + \underbrace{F(q, \theta^*) - F(q, \hat{\theta}_{N_d})}_{\text{variance}}. \quad (2.148)$$

In this decomposition, the first part is the *structural* or *bias error*, usually induced by the fact that the model set is not rich enough to exactly represent the plant. The second part is the *noise induced* or *variance error* which is due to noise contribution on the measured data. The bias can be characterized in terms of integral formulas over the frequency domain. Powerful formulas also exist to express variance error if both N_d and the model order tend to infinity (Ljung 1999).

One of the most basic results on variance error is formulated in terms of the variability of asymptotic parameter estimates. In the most general form, the characterization follows from the central limit theorem, proving that

$$\sqrt{N_d}(\hat{\theta}_{N_d} - \theta^*) \rightarrow \mathcal{N}(0, Q_\theta) \quad \text{as } N_d \rightarrow \infty, \quad (2.149)$$

i.e. the random variable $\sqrt{N_d}(\hat{\theta}_{N_d} - \theta^*)$ converges in distribution to a Gaussian probability density function with zero mean and covariance matrix Q_θ . Note that Q_θ can be calculated only in a limited number of situations. One of these is when the data generating system is in the model set, leading to the consistent estimate $\theta^* = \theta_0$. In this case:

$$Q_\theta = \sigma_e^2 (\bar{\mathcal{E}} \{ \varphi(k, \theta_0) \varphi^\top(k, \theta_0) \})^{-1}, \quad \text{with } \varphi(k, \theta_0) := -\frac{\partial}{\partial \theta} \epsilon(k, \theta) \Big|_{\theta=\theta_0}.$$

2.3.4 Linear regression

If the model structure has the property of being linear-in-the-parameters, then the LS problem (2.141) becomes a convex optimization problem with the analytic solution:

$$\hat{\theta}_{N_d} = \left[\frac{1}{N_d} \Gamma_{N_d}^\top \Gamma_{N_d} \right]^{-1} \left[\frac{1}{N_d} \Gamma_{N_d}^\top Y_{N_d} \right]. \quad (2.150)$$

where $Y_{N_d} = [y(0), \dots, y(N_d - 1)]^\top$ is the collection of the measured output samples and $\Gamma_{N_d} = [\gamma(0), \dots, \gamma(N_d - 1)]^\top$ contains the regressor vector γ that describes the data relation according to the one-step-ahead predictor: $\hat{y}_\theta(k) = \gamma^\top(k)\theta$. For the ARX case with $\deg(R_A) = n_a$ and $\deg(R_B) = n_b$, the regressor vector is

$$\gamma^\top(k) = [y(k-1) \quad \dots \quad y(k-n_a) \quad u(k) \quad \dots \quad u(k-n_b)],$$

while in the FIR case with $\deg(R_B) = n_b$, the regressor vector becomes

$$\gamma^\top(k) = [u(k) \quad \dots \quad u(k-n_b)].$$

Note that on the basis of numerical considerations regarding matrix inversion, the solution (2.150) is not computed directly, but via a QR-algorithm. Moreover, statistical analysis of this estimator results in non-asymptotic expressions of the bias and variance error, which provide important advantages of linear-in-the-parameter model structures over other model parameterizations.

2.3.5 Identification with OBFs

Considering the classical identification results described in the previous part, it appears that there are two attractive properties of model structures: linear-in-the-parameter property and independent parametrization of the process and noise models. Among the presented classical structures a combination of these two properties can only be found in the FIR structure. However, the main disadvantage of this structure is that it generally requires a large number of parameters to capture the dynamics of the physical system, which implies a relatively large variance of the estimate. Using OBFs instead of the pulse basis like in (2.112) can significantly decrease the number of required parameters and preserve all the attractive properties. In this section we focus on the model structures:

$$F(q, \theta) = \sum_{i=0}^n w_i \phi_i(q), \quad Q(q, \theta) = 1, \quad (2.151)$$

where $\{\phi_i\}_{i=1}^n$ with $\phi_0 = 1$ are orthonormal basis functions in $\mathcal{RH}_2(\mathbb{E})$ with pole locations $\Lambda_n = \{\lambda_i\}_{i=1}^n$. The unknown series-expansion coefficients of (2.151) are collected into the parameter vector

$$\theta = [w_0 \quad \dots \quad w_n] \subset \mathbb{R}^{n+1}.$$

In a general sense, different identification criteria and settings can be applied for OBFs based model structures, like for example frequency domain identification in $\mathcal{H}_2/\mathcal{H}_\infty$, resulting in attractive alternatives of LTI system identification (Heuberger et al. 2005). In the following we explore the LS prediction error setting to compare the properties of this model structure to the classical results of other structures. Later, these properties also form the basic motivation why this model structure with the LS prediction error setting yields an attractive candidate for LPV identification.

Least-squares identification

Due to the linear-in-the-parameter property of the OBF parametrization, estimation of the parameters in the LS setting similarly follows as in the FIR or ARX cases. The only difference with respect to these model structures is that the regression vector is

$$\gamma^\top(k) = [u(k) \quad (\phi_1(q)u)(k) \quad \dots \quad (\phi_n(q)u)(k)],$$

containing filtered versions of the input signal rather than delayed version of u or y . This form of the regressor implies that the LS parameter estimate of (2.151) can be obtained via (2.150). In terms of consistency/bias properties of the estimates all the classical results about FIR structures hold, if u is a white noise signal, i.e. $\Phi_u(e^{i\omega})$ is constant. This means, that if $F_0(q)$ is in the IO model set and the input is white noise, then the model estimate $F(q, \hat{\theta}_{N_d})$ is unbiased and consistent. This is the case when the true system has a finite series-expansion in terms of the used basis functions. In all other cases, the expansion coefficients of $F_0(q)$ in terms of the finite basis functions are estimated consistently, but a bias results due to the truncated tail of the required infinite expansion. Therefore there is a primal emphasis on the selection of appropriate basis functions, to reduce the bias by ensuring a fast convergence rate of the series-expansion.

A particularly interesting aspect results if the estimation of the parameters is formulated in state-space. As indicated in (2.124a-b), a basis functions based series-expansion model $F(q, \theta)$ can be realized efficiently in two SS forms:

$$\left[\begin{array}{c|c} A & B \\ \hline W & w_0 \end{array} \right] \quad \text{and} \quad \left[\begin{array}{c|c} A & (WT)^\top \\ \hline C & w_0 \end{array} \right], \quad (2.152)$$

where (A, B, C, D) is the jointly minimal balanced SS realization of the inner function G generating the basis functions $\{\phi_i\}_{i=1}^n$, $W = [w_1 \dots w_n]$, and $T \in \mathbb{R}^{n \times n}$ is a unitary matrix such that (2.125) is satisfied. The SS realization in the left is often called the AB-invariant while the representation in the right is recognized as the AC-invariant form. Due to property (2.125), estimation in a AB-invariant form results in a parameter estimate $\hat{\theta}_{N_d}$, whose elements are the linear combinations of a parameter estimate based on the AC-invariant form. An additional property is that the initial condition of the AC-invariant form can be easily formulated as the part of the parameter vector, due to the different formulation of the regressors in that case. Thus, estimation of the initial condition is available by linear regression

in the AC-invariant case. This property is important when, because of various reasons, the experiment providing the data record can not be accomplished on the system starting from zero initial state.

Asymptotic bias and variance

As indicated before, the classical results in terms of the FIR structure trivially extend to OBF model structures if the input sequence is a white noise signal. However, due to the fact that finite series expansions often result in the case where $F_0(q)$ is not in the IO model set, it is important to investigate how the estimated coefficients relate to the expansion coefficients of $F_0(q)$ in terms of the finite basis function set. It can be shown that, if u is white, then the expansion coefficients of $F_0(q)$ are identified consistently in the LS setting. This means that even if $F_0(q)$ can not be identified consistently due to the truncated tail of the expansion, the modeled dynamical part (the considered finite expansion) is consistently identified. Moreover, in this case θ^* obeys:

$$\theta^* = \arg \min_{\theta \in \Theta} \frac{1}{2\pi} \int_{-\pi}^{\pi} |F_0(e^{i\omega}) - F(e^{i\omega}, \theta)|^2 \frac{\Phi_u(e^{i\omega}) \sum_{i=0}^n |\phi_i(e^{i\omega})|^2}{|Q_0(e^{i\omega})|^2} d\omega, \quad (2.153)$$

which shows that the basis functions act as data prefilters, emphasizing the fit of the estimated model on the frequency domain where the gain of the basis functions is significant. The noise spectrum also does not appear in the expression due to the fixed noise model, thus the convergence of θ is not influenced by the noise just like in the case of FIR models. The bias, due to the undermodeling, can be directly computed via the theory of reproducing kernels (Heuberger et al. 2005). Furthermore, for specific transfer functions, like

$$F_0(z) = \sum_{j=1}^{n_0} \frac{b_j}{z - \lambda_j} \quad (2.154)$$

an upper bound on the approximation error can be computed with respect to $F(q, \theta^*)$ with basis functions $\{\phi_i\}_{i=1}^n$:

$$|F_0(e^{i\omega}) - F(e^{i\omega}, \theta^*)| \leq \sum_{j=1}^{n_0} \left| \frac{b_j}{e^{i\omega} - \lambda_j^{(0)}} \right| \underbrace{\left| \prod_{i=1}^n \frac{\lambda_j^{(0)} - \lambda_i}{1 - \lambda_i^* \lambda_j^{(0)}} \right|}_{\rho}, \quad (2.155)$$

where $\{\lambda_i\}_{i=1}^n$ are the poles of $\{\phi_i\}_{i=1}^n$. This expression shows a tight bound on the approximation error in terms of the bias. If for each pole of the system, there exists a matching pole of the basis $\lambda_j^{(0)} = \lambda_i$, then the upperbound is zero (F_0 has a finite series-expansion in terms of the basis). In the general case, the truncation error of the series-expansion is directly influenced by the convergence rate ρ (see (2.155)), which expresses the natural distance between the basis and the system poles. This implies that to minimize the bias, the poles of the basis should be as close to the poles of the system to be identified as possible.

The variance of the model estimate also obeys the classical results of FIR structures. In the frequency domain, if both $N_d, n \rightarrow \infty, n \ll N_d$, the variance of the estimate $F(q, \hat{\theta}_{N_d})$ reads

$$\text{var}\{F(q, \hat{\theta}_{N_d})\} \sim \frac{1}{N_d} \frac{\Phi_e(e^{i\omega})}{\Phi_u(e^{i\omega})} \sum_{i=1}^n |\phi_i(e^{i\omega})|^2, \quad (2.156)$$

where $\Phi_e(e^{i\omega})$ is the noise spectrum. This expression shows the classical result of FIR structures when the input is prefiltered. Note that by choosing the poles $\{\lambda_i\}_{i=1}^n$ of $\{\phi_i\}_{i=1}^n$ close to the poles of F_0 , the variance expression (2.156) peaks if $e^{i\omega}$ comes to the close neighborhood of λ_i . This corresponds to the variance/bias trade-off.

As discussed in this section, OBFs-based parametrization can be effectively used for LTI system representation with many fruitful properties, however it is required that the basis function set is “well chosen” with respect to system to be identified. In the next section, the concept of optimality of an OBF set with respect to a set of LTI systems is established, giving the key theorem to solve the basis selection problem of the identification scheme both in the LTI and in the LPV case later on. Before that, some additional aspects of identification are reviewed.

Identification in the MIMO case

In case of MIMO systems, identification follows similar guidelines as in the SISO case, except that the model structure (2.151) is formulated with MIMO basis functions. Due to FIR structure of OBFs models, the analytical solution of (2.141) is still obtained via a linear regression, however with a more extensive book keeping.

In case the MIMO basis are constructed from scalar basis functions (method 1), all properties in terms of identification trivially extend to MIMO case (Ninness and Gómez 1996). However, this model structure has a major disadvantage, namely that specific elements of $\{W_i\}$ can be insignificantly small for every $i > 0$, which can result in an over-parametrization, ergo in a significant bias of the estimate. MIMO basis sequences generated by square inner functions via (2.121) (method 2) are not affected by the previous disadvantage, however bias and variance properties of the estimates are not yet clearly understood. See van Donkelaar (2000) and Heuberger (1990) for more on identification properties of model structures based on this type of MIMO-OBFs.

2.3.6 Pole uncertainty of model estimates

In practical situations, identification is unavoidably effected by noise, resulting in uncertainty of the model estimates. The resulting model uncertainties can be characterized based on numerous concepts of uncertainty in the parameter or frequency domain. See Hakvoort and Van den Hof (1997); Ljung (1999); Ninness and Goodwin (1995) and Douma and Van den Hof (2005) for an overview on the available approaches. A well-known fact in the LTI case is that pole locations

of a model estimate are generally sensitive to parameter uncertainties, see e.g. Guillaume et al. (1989). In the following, some basic concepts of pole uncertainty regions are briefly introduced for DT model estimates in the LS setting. The developed concepts are essential for the formulation of the robust basis selection approach in Chapter 8.

In the literature, many approaches have been developed for the calculation of confidence bounds for the estimated parameters (for a survey see Pintelon and Schoukens (2001)). However, commonly the first-order Taylor approximation based ellipsoidal bounds are used, like in the Matlab System Identification Toolbox (Ljung 2006). Consider the LS setting with the model structures given in Table 2.1. In this case, if the data generating system is in the model set, then this implies that the parameter estimate $\hat{\theta}_{N_d}$ is consistent and has an asymptotically normal distribution with a covariance matrix \mathcal{Q}_θ (see Section 2.3.3). The previous properties provide that

$$(\hat{\theta}_{N_d} - \theta_0)^\top \mathcal{Q}_\theta^{-1} (\hat{\theta}_{N_d} - \theta_0) \rightarrow \chi^2(n), \quad \text{as } N_d \rightarrow \infty, \quad (2.157)$$

where $\chi^2(n)$ is a χ^2 -distribution with n -degrees of freedom and n is the number of parameters in θ . Let $[a_1, \dots, a_{n_a}]$ be the parameters in θ characterizing the denominator part of the process model and let $[b_0, \dots, b_{n_b}]$ be the denominator parameters. Denote $\Delta\theta := (\theta - \theta_0)$ for every $\theta \in \Theta$. Then for a given confidence level $\alpha \in [0, 1]$, the parameter uncertainty of $F(q, \hat{\theta}_{N_d})$ can be defined as an ellipsoid

$$\mathcal{E}_\theta(\mathcal{Q}_\theta, \alpha) := \{\theta \in \mathbb{R}^n \mid \Delta\theta^\top \mathcal{Q}_\theta^{-1} \Delta\theta \leq \chi_\alpha^2(n_\theta)\}, \quad (2.158)$$

where $\chi_\alpha^2(n)$ denotes the α -percentile of $\chi^2(n)$. This means that the probability of $\hat{\theta}_{N_d} \in \mathcal{E}_\theta(\mathcal{Q}_\theta, \alpha)$ is equal to α as $N_d \rightarrow \infty$. Note that often $\mathcal{E}_\theta(\mathcal{Q}_\theta, \alpha)$ is restricted to Θ .

In order to establish an uncertainty region of poles associated with each configuration of the parameters inside the derived ellipsoidal bound, a nonlinear transformation of the parameter confidence region $\mathcal{E}_\theta(\mathcal{Q}_\theta, \alpha)$ is needed. This transformation can be accomplished through the method of Vuerinckx et al. (2001), which gives a hypothesis test to decide whether a $\lambda \in \mathbb{C}$ is a pole location of a model with $\theta \in \mathcal{E}_\theta(\mathcal{Q}_\theta, \alpha)$.

Denote by $\Lambda_0 \subset \mathbb{C}$ the set of poles associated with $F(q, \theta_0)$ and define $\Delta\Lambda := \Lambda - \Lambda_0$ for every $\Lambda \in \mathbb{C}^{n_a}$. Let λ_0 be a real valued pole in Λ_0 with $n_a > 1$. Then, define the perturbation of this pole as $\lambda = \lambda_0 + \Delta\lambda$ such that a parameter vector $\theta \in \Theta$ exists whose associated pole vector contains λ . Note that θ is not unique because λ only determines the denominator parameters. If $\theta \in \Theta$ exists, then it can be chosen such that the numerator parameters $[b_0, \dots, b_{n_b}]$ of θ are equal to numerator parameters of θ_0 . Write $F(q, \theta)$ as

$$F(q, \theta) = F_1(q, \gamma)F_2(q, \check{\theta}), \quad (2.159)$$

with

$$F_1(q, \gamma) := \frac{1}{1 + \gamma q^{-1}} = \frac{1}{1 - \lambda q^{-1}} \quad \text{and} \quad F_2(q, \check{\theta}) := \frac{\sum_{j=0}^{n_b} b_j q^{-j}}{1 + \sum_{i=1}^{n_a-1} \check{a}_i q^{-i}},$$

where $\check{\theta}$ contains the parameters of F_2 . This factorization implies the existence of the transformation

$$\theta = T_1(\lambda)\check{\theta} + T_2(\lambda), \quad (2.160)$$

where $\gamma = -\lambda$ and

$$T_1(\lambda) = \left[\begin{array}{cccc|c} 1 & \dots & 0 & & 0 \\ \gamma & \ddots & \vdots & & 0 \\ \ddots & 1 & \vdots & & 0 \\ 0 & \dots & \gamma & & 0 \\ \hline 0 & \dots & 0 & I_{(n-n_a) \times (n-n_a)} & \end{array} \right]_{n \times (n-1)} \quad T_2(\lambda) = \begin{bmatrix} \gamma \\ 0 \\ \vdots \\ 0 \end{bmatrix}_{n \times 1}$$

In case of λ_0 is complex valued, define the perturbation of the complex pole pair λ_0, λ_0^* as $\lambda = \lambda_0 + \Delta\lambda$ and $\lambda^* = \lambda_0^* + \Delta\lambda^*$. Using the same mechanism, write $F(q, \theta)$ as

$$F(q, \check{\theta}) = F_1(q, \gamma_1, \gamma_2)F_2(q, \check{\theta}),$$

with

$$F_1(q, \gamma_1, \gamma_2) := \frac{1}{1 + \gamma_1 q^{-1} + \gamma_2 q^{-2}} = \frac{1}{1 - 2\text{Re}(\lambda)q^{-1} + |\lambda|^2 q^{-2}},$$

$$F_2(q, \check{\theta}) := \frac{\sum_{j=0}^{n_b} b_j q^{-j}}{1 + \sum_{i=1}^{n_a-2} \check{a}_i q^{-i}}.$$

Again, this factorization implies the existence of the transformation (2.160) with

$$T_1(\lambda) = \left[\begin{array}{cccc|c} 1 & 0 & \dots & 0 & 0 \\ \gamma_1 & 1 & \dots & 0 & 0 \\ \gamma_2 & \gamma_1 & \ddots & \vdots & 0 \\ 0 & \gamma_2 & \ddots & 1 & 0 \\ \vdots & \ddots & \ddots & \gamma_1 & \vdots \\ 0 & \dots & 0 & \gamma_2 & 0 \\ \hline 0 & 0 & \dots & 0 & I_{(n-n_a) \times (n-n_a)} \end{array} \right]_{n \times (n-2)} \quad T_2(\lambda) = \begin{bmatrix} \gamma_1 \\ \gamma_2 \\ 0 \\ \vdots \\ 0 \end{bmatrix}_{n \times 1}$$

where $\gamma_1 = -2\text{Re}(\lambda)$ and $\gamma_2 = |\lambda|^2$.

The above derived transformations qualify as a projection of a single pole or complex pole pair perturbation to the parameter domain Θ through the free parameter $\theta \in \mathbb{R}^{n-1}$ or $\check{\theta} \in \mathbb{R}^{n-2}$. In order to test that the parameter variation induced by $\Delta\lambda$ is inside the parameter uncertainty region $\mathcal{E}_\theta(\mathcal{Q}_\theta, \alpha)$, it is sufficient

to show that there exists a $\check{\theta} \in \mathbb{R}^{n-1}$ (or $\check{\theta} \in \mathbb{R}^{n-2}$) which minimizes

$$(T_1(\lambda)\check{\theta} + T_2(\lambda))^\top \mathcal{Q}_\theta^{-1} (T_1(\lambda)\check{\theta} + T_2(\lambda)), \quad (2.161)$$

and the minimum is smaller or equal than $\chi_\alpha^2(n_\theta)$ (see (2.158)). If this condition is not satisfied, then this proves the hypothesis that the pole perturbation cannot be associated with a parameter vector in $\mathcal{E}_\theta(\mathcal{Q}_\theta, \alpha)$. The minimization problem of (2.161) has an analytical solution:

$$\check{\theta} = \frac{T_1^\top(\lambda)\mathcal{Q}_\theta^{-1}\theta_0 - T_1^\top(\lambda)\mathcal{Q}_\theta^{-1}T_2(\lambda)}{T_1^\top(\lambda)\mathcal{Q}_\theta^{-1}T_1(\lambda)}. \quad (2.162)$$

Thus for a given pole perturbation $\Delta\lambda$, if $\check{\theta}$ resulting from (2.162) satisfies that (2.161) is smaller or equal than $\chi_\alpha^2(n)$, then λ can be the pole of the asymptotic model estimate with probability α .

Based on the derived hypothesis test, it is possible to calculate the pole uncertainty region

$$\mathcal{P}(\mathcal{Q}_\theta, \alpha) := \{\lambda \in \mathbb{C} \mid \exists \theta \in \mathcal{E}_\theta(\mathcal{Q}_\theta, \alpha) \text{ s.t. } \lambda \text{ is a pole of } F(q, \theta)\}, \quad (2.163)$$

associated with $\mathcal{E}_\theta(\mathcal{Q}_\theta, \alpha)$. Note that $\mathcal{P}(\mathcal{Q}_\theta, \alpha) \subset \mathbb{C}$ which means that the hyper ellipsoid $\mathcal{E}_\theta(\mathcal{Q}_\theta, \alpha)$ is projected to a lower dimensional space. This implies that for a pole location set Λ , associated with $\theta \in \mathcal{E}_\theta(\mathcal{Q}_\theta, \alpha)$, $\Lambda \in (\mathcal{P}(\mathcal{Q}_\theta, \alpha))^{n_a}$ holds. However, it is not true that any $\Lambda \in (\mathcal{P}(\mathcal{Q}_\theta, \alpha))^{n_a}$ can be associated with a $\theta \in \mathcal{E}_\theta(\mathcal{Q}_\theta, \alpha)$. So the projection is surjective. This is an advantage in the sense that with the given hypothesis test, $\mathcal{P}(\mathcal{Q}_\theta, \alpha)$ can be efficiently computed and visualized. However, the surjective property is also a disadvantage. Instead of representing all configuration of poles associated with $\mathcal{E}_\theta(\mathcal{Q}_\theta, \alpha)$, the complex region $\mathcal{P}(\mathcal{Q}_\theta, \alpha)$ characterizes the set of pole locations that can occur with the given probability level in the model estimates. In this way, the perimeter bounds of $\mathcal{P}(\mathcal{Q}_\theta, \alpha)$ describe the uncertain pole locations in a worst-case sense.

In practical situations, θ_0 can be substituted by $\hat{\theta}_{N_d}$ if N_d is large enough. Alternatively, using $\hat{\theta}_{N_d}$ instead of θ_0 results in the hypothesis test that the true poles of the system are in the uncertainty region of the estimated poles with a given confidence level. Note that the above given mechanism can be also used for the calculation of the uncertainty region associated with the zeros of the model, by varying the numerator part in (2.159) instead of the denominator.

Using this pole uncertainty concept, the uncertainty regions can take various shapes in \mathbb{C} , ranging from real segments (real pole) and ellipsoidal or banana shaped forms to butterfly figures (complex pole pairs) as illustrated in Example 2.1. Therefore, it is not guaranteed that they constitute convex regions in \mathbb{C} . The regions can be all connected or separated into small sets due to the fact that they are the nonlinear projection of a hyper dimensional ellipsoid. Increasing α often results in the merging of previously separated regions. For an increasing α , regions can also popup unexpectedly in \mathbb{C} , due to the higher possibility of parameter variation. This yields the need of special algorithms to ensure correct calculation of

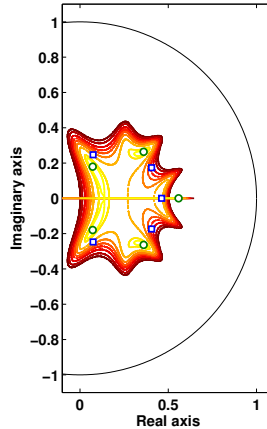


Figure 2.6: Pole-uncertainty regions $\mathcal{P}(\mathcal{Q}_\theta, \alpha)$ of estimated poles (green \circ) with different confidence levels α (deep red 0.99 \leftrightarrow bright yellow 0.01). The true pole locations Λ_0 are denoted by blue squares.

the regions. For this purpose, an algorithm is developed in Tóth et al. (2008c) that ensures calculation of possibly separated regions, unlike the existing solutions in the literature.

Note that other concepts of pole uncertainty regions have been developed in the literature as well. The commonly used ellipsoidal pole regions, also implemented in the identification toolbox of Matlab, are calculated using a first order Taylor approximation of the nonlinear projection of $\mathcal{E}_\theta(\mathcal{Q}_\theta, \alpha)$ to \mathbb{C} . This type of approximation can introduce significant errors in the calculation of $\mathcal{P}(\mathcal{Q}_\theta, \alpha)$, unlike the previously presented approach. Other approaches, like discussed in Mårtensson and Hjalmarsson (2007), focus more on the quantification of the variance of poles or zeros rather than on the actual calculation of their uncertainty regions. Based on these, the previously presented approach provides the state-of-the-art technique to calculate pole uncertainty regions associated with model estimates.

Example 2.1 (Pole uncertainty regions) Let the transfer function F_0 of a discrete-time asymptotically stable LTI system \mathcal{F} with IO partition (u, y) be given as

$$F(z) = \frac{1.4}{1 - 1.5z^{-1} + 0.83z^{-2} - 0.26z^{-3} + 0.05z^{-4} - 0.006z^{-5}} z^{-1}. \quad (2.164)$$

For this system \mathcal{F} , a 500 sample long data record has been collected with a white u based on a uniform distribution $\mathcal{U}(-1, 1)$ and an additive white output noise ϵ with normal distribution $\mathcal{N}(0, 0.15)$. The LS prediction error identification of F has been accomplished via OE parametrization with correct denominator and nominator orders. The resulting pole uncertainty regions $\mathcal{P}(\mathcal{Q}_\theta, \alpha)$ of the estimate $F(q, \hat{\theta}_{N_d})$ have been calculated with the approach of Section 2.3.6 using confidence levels (0.99 \leftrightarrow 0.01). The perimeter lines of these regions, calculated with the algorithm of Tóth et al. (2008c), are presented in Figure 2.6.

2.3.7 Validation in the prediction error setting

In the prediction error setting, commonly either simulation or prediction by the model estimate based on a measured data record is used for (in)validation. One approach is to investigate the correlation of the residual, i.e. the error of the prediction, with respect to the input or itself. In other cases, error measures of the difference between the measured y and the simulated output \hat{y} are calculated. These measures are used to decide on the validity of the model estimate. Some popular measures are the following:

Definition 2.39 (Mean squared error) (Ljung 1999) *The Mean Squared Error (MSE) is the expected value of the squared estimation error :*

$$\text{MSE} := \bar{\mathcal{E}}\{(y - \hat{y})^2\}. \quad (2.165)$$

Definition 2.40 (Best fit percentage) (Ljung 2006) *The Best Fit (BFT) percentage is defined as*

$$\text{BFT} := 100\% \cdot \max\left(1 - \frac{\|y - \hat{y}\|_2}{\|y - \bar{y}\|_2}, 0\right), \quad (2.166)$$

where \bar{y} is the mean of y .

Definition 2.41 (Variance accounted for) *The Variance Accounted For (VAF) percentage is the percentage of the output variation that is explained by the model:*

$$\text{VAF} := 100\% \cdot \max\left(1 - \frac{\text{var}\{y - \hat{y}\}}{\text{var}\{y\}}, 0\right). \quad (2.167)$$

Note that the MSE is equal to the LS criterion (2.140) evaluated for the simulated \hat{y} , instead of the predicted output signal. In this way, a high value indicates invalidity of the model. The BFT percentage is a relative measure, often used in the identification toolbox of Matlab, and a low value of this measure indicates invalidity of the model. The VAF measure describes how much of the output variation is explained by the model, disregarding possible bias of the estimates.

2.4 The Kolmogorov n -width theory

In the identification cycle, one of the key steps is the choice of an adequate model structure, i.e. the model set, which can represent the system to be identified with a relatively small number of statistically meaningful parameters. In the identification approach based on OBF model structures, finding an appropriate model set translates to the search for a set of basis functions $\Phi_{n_b}^{n_e}$, that gives a series-expansion of the system with a fast convergence rate ρ . In LTI system identification, one approach to find appropriate model sets is based on the n -width concept (Pinkus 1985), which has been shown to result in appropriate model sets for

robust modeling of linear systems (Mäkilä and Partington 1993). Using this concept, Oliveira e Silva (1996) showed that OBF model structures are optimal in the n -width sense for specific subsets of systems and finding the optimal OBF set for a given system set can be formulated as an optimization problem. In the following, the basic ingredients of this approach for discrete-time, stable, SISO systems are described. Later, this theory is used as the backbone of OBFs selection for the identification of LPV systems.

Let \mathcal{F} denote a set of LTI SISO systems with transfer functions $\{F(z)\} = \mathfrak{F} \subseteq \mathcal{H}_{2-}(\mathbb{E})$ that we want to approximate with a linear combination of n elements of $\mathcal{H}_{2-}(\mathbb{E})$. Let $\Phi_n = \{\phi_i\}_{i=1}^n$ be a sequence of n linearly independent elements of $\mathcal{H}_{2-}(\mathbb{E})$, and let $\mathcal{M}_n = \text{span}(\Phi_n)$. Note that \mathcal{M}_n describes all the possible linear combinations of Φ_n that can be used for the approximation of the elements of \mathfrak{F} . The distance $d_{\mathcal{H}_2}(F, \mathcal{M}_n)$ between a $F \in \mathcal{H}_{2-}(\mathbb{E})$ and \mathcal{M}_n is defined as

$$d_{\mathcal{H}_2}(F, \mathcal{M}_n) = \inf_{F' \in \mathcal{M}_n} \|F - F'\|_{\mathcal{H}_2}. \quad (2.168)$$

This distance describes the best possible approximation error of a given $F \in \mathcal{H}_{2-}(\mathbb{E})$ in terms of the \mathcal{H}_2 norm if the linear combination of Φ_n is used as an approximation. With respect to the transfer function set \mathfrak{F} , we can define the worst-case approximation error by Φ_n as the maximum of (2.168) on \mathfrak{F} . Now we can use this concept to look for a set Φ_n that has a minimal worst-case approximation error for \mathfrak{F} . This minimum is called the *Kolmogorov n -Width* (KnW) of \mathfrak{F} .

Definition 2.42 (Kolmogorov n -width) (Pinkus 1985) *Let \mathcal{M}_n be the collection of all n -dimensional subspaces of $\mathcal{H}_{2-}(\mathbb{E})$. The Kolmogorov n -width of a function set \mathfrak{F} in $\mathcal{H}_{2-}(\mathbb{E})$ is*

$$\pi_n(\mathfrak{F}, \mathcal{H}_{2-}(\mathbb{E})) = \inf_{\mathcal{M}_n \in \mathcal{M}_n} \sup_{F \in \mathfrak{F}} d_{\mathcal{H}_2}(F, \mathcal{M}_n). \quad (2.169)$$

In this way, $\pi_n(\mathfrak{F}, \mathcal{H}_{2-}(\mathbb{E}))$ describes the smallest possible $d_{\mathcal{H}_2}$ that can be achieved for all F in \mathfrak{F} by the linear combination of n independent elements of $\mathcal{H}_{2-}(\mathbb{E})$. The subspace $\mathcal{M}_n \in \mathcal{M}_n$, for which π_n is minimal, is called the optimal subspace in the KnW sense. This optimal subspace describes a Φ_n that can approximate \mathfrak{F} best in the worst-case sense. Now we can formulate this concept for OBFs.

Proposition 2.1 (n -width optimal OBFs) (Oliveira e Silva 1996) *Let $G \in \mathcal{H}_{2-}(\mathbb{E})$ be an inner function with McMillan degree $n_g > 0$, with poles Λ_{n_g} , and let $n_e \geq 0$. Consider the subspace*

$$\mathcal{M}_n = \text{span} \left\{ \phi_j(z) G^i(z) \right\}_{j=1, \dots, n_g}^{i=0, \dots, n_e} \quad (2.170)$$

where $\phi_j = [M_1]_j$ and M_1 is defined by (2.121) with respect to G . Then the subspace \mathcal{M}_n is optimal in the Kolmogorov n -width sense with $n = (n_e + 1)n_g$ for the set of systems with transfer functions \mathfrak{F} analytic in the complement of the region

$$\Omega(\Lambda_{n_g}, \rho) := \{z \in \mathbb{C} \mid |G(z^{-1})| \leq \rho\}, \quad (2.171)$$

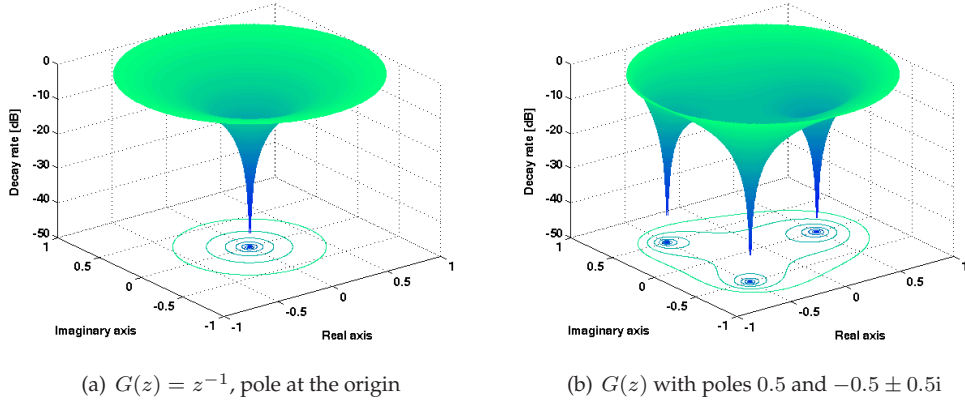


Figure 2.7: The plot of the function $|G(z^{-1})|$ for different choices of the inner function G and the convergence rate ρ (in dB). Level sets of $|G(z^{-1})|$ give the boundaries of the regions $\{z \in \mathbb{C}, |G(z^{-1})| \leq \rho\}$. Optimality of the G generated basis is ensured with a worst-case convergence rate ρ^{n_e+1} for systems with pole locations inside the regions defined by the level set boundaries.

and are square integrable on its boundary. The worst-case approximation error, i.e. $\sup_{F \in \mathfrak{F}} d_{\mathcal{H}_2}(F, \mathcal{M}_n)$, is proportional to ρ^{n_e+1} .

This remarkable result means that the set of OBFs $\Phi_{n_g}^{n_e} = \{\phi_j(z)G^i(z)\}_{j=1, \dots, n_g}^{i=0, \dots, n_e}$ is the best in the worst-case sense to approximate transfer functions with all pole locations in $\Omega(\Lambda_{n_g}, \rho)$. So if in an identification scenario it is known that the system poles lie in $\Omega(\Lambda_{n_g}, \rho)$, then the optimal choice of basis functions is the set of OBFs associated with the poles Λ_{n_g} . Additionally, Proposition 2.1 shows that for the specified region one can not improve on the worst-case error by adding new poles to the n_g basis poles. It also generalizes the well-known fact that the set of *pulse functions* $\{z^{-i}\}_{i=1}^n$ is optimal for the class of stable systems analytical outside the region $\Omega(\Lambda_{n_g}, \rho) = \{|z| \leq \rho\}$, $\rho > 0$. The boundary of $\Omega(\Lambda_{n_g}, \rho)$ is displayed in Figure 2.7a as a function of the convergence rate ρ . For a given $\rho > 0$, the boundary of the region results as the level set of this function, like the contour lines at the bottom of the figure. The worst-case approximation error in this case is proportional to ρ^n . This implies the optimality of FIR model structures with respect to the identification of such systems, which is a well-known result (Pinkus 1985). However, in case of arbitrary regions, like the regions in Figure 2.7b, the level sets are commonly non-circular, containing separate regions that merge for increasing values of ρ . For these regions, the optimal choice of a basis has to be found among general basis functions (OBF model structures).

In an OBFs-based identification scenario we are dealing with the opposite problem. We are given a rough idea about the possible pole locations of the system described as a region $\Omega_0 \subset \mathbb{D}$ and we want to find a fixed n number of OBFs that are optimal with respect to Ω_0 in the KnW sense. This problem is referred to

as the *inverse Kolmogorov problem*, where we want to find an inner function G to describe/approximate a given region of non-analyticity Ω_0 in the form $\Omega(\Lambda_{n_g}, \rho)$ with ρ as small as possible. The reason is that in terms of Proposition 2.1, the inner function G , associated with the best fitting $\Omega(\Lambda_{n_g}, \rho)$, generates the n_g -width optimal basis functions with respect to Ω_0 . Denote the inner function associated with the poles Λ_{n_g} as $G_{\Lambda_{n_g}}(z)$ and define

$$\kappa_{n_g}(z, \Lambda_{n_g}) := G_{\Lambda_{n_g}}(z^{-1}) = \prod_{j=1}^{n_g} \left| \frac{z - \lambda_j}{1 - z\lambda_j^*} \right|. \quad (2.172)$$

Then the solution of the inverse Kolmogorov problem for a given number of poles n_g , comes down to the min-max optimization problem:

$$\min_{\Lambda_{n_g} \subset \mathbb{D}} \max_{z \in \Omega} \kappa_{n_g}(z, \Lambda_{n_g}). \quad (2.173)$$

See (Heuberger et al. 2005) for details on this non-linear optimization problem and solution methods.

2.5 Fuzzy clustering

We will see in Chapter 8, that a key ingredient to develop a model structure, i.e. a basis selection tool for the identification of LPV systems, is to solve a particular data clustering¹⁴ problem. To tackle this problem, a weighting-function-based separation, so called *fuzzy clustering*, is used. In the following, the main idea of the conventional fuzzy clustering approach is briefly introduced.

Objective-function-based fuzzy clustering algorithms, such as the *Fuzzy c-Means* (FcM), have been used in a wide collection of applications like pattern recognition, data analysis, image processing and fuzzy modeling (see Bezdek (1981) and Kaymak and Setnes (2002)). These methods have become dominant over *hierarchical* and *graph-theoretical* methods as they offer quick and reliable separation of data. Generally, FcM partitions the data into overlapping groups, so called clusters, where each data element is associated with a set of membership levels with respect to these clusters. These indicate the strength of the association between that data element and a particular cluster. In this way, fuzzy clustering is a process of assigning these membership levels such that the resulting clusters describe the underlying structure within the data (Jain and Dubes 1988).

Let $n_c > 1$ be the number of clusters or data groups and let $Z = \{z_k\}_{k=1}^{N_z} \subset \mathbb{V}$, be the set of data points for clustering where \mathbb{V} denotes the clustering space (commonly a subset of \mathbb{R} or \mathbb{C}) and $N_z > 1$ is the number of data points. In fuzzy clustering, a cluster is defined by two ingredients: a center (or *prototype*) $v_i \in \mathbb{V}$, $i \in \mathbb{1}_1^{n_c}$ and a membership function $\mu_i : \mathbb{V} \rightarrow [0, 1]$. While the former defines the central point, the latter describes the “degree of membership” to the cluster for all

¹⁴Data clustering is the process of dividing data elements into classes or clusters so that items in the same class are as similar as possible, and items in different classes are as dissimilar as possible.

$\mathbf{z} \in \mathbb{V}$. Note that the shapes of fuzzy clusters are not described by hard borders but by the commonly bell-like shape of the membership functions on \mathbb{V} . Introduce also the so called dissimilarity measure $d := \mathbb{V} \times \mathbb{V} \rightarrow \mathbb{R}_0^+$, where \mathbb{R}_0^+ denotes the set of positive real numbers including 0. This dissimilarity measure is used to define the memberships of the clusters, i.e. how the function set $\{\mu_i\}_{i=1}^{n_c}$ is distributed on \mathbb{V} . Now we can formalize the clustering problem we consider:

Problem 2.1 (FcM clustering) *For a given data set Z and for a given number of clusters n_c , find a set of clusters, i.e. centers $\{v_i\}_{i=1}^{n_c}$ and membership functions $\{\mu_i\}$, and the maximum of $\varepsilon > 0$ such that the region $\{\mathbf{z} \in \mathbb{V} \mid \exists i \in \mathbb{1}^{n_c} \mu_i(\mathbf{z}) \geq \varepsilon\}$ contains Z and it describes the underlying distribution of Z in terms of a chosen dissimilarity measure d .*

In this problem, d represents a particular freedom to define the exact objective we would like to solve through FcM clustering. By choosing d to be different measures of \mathbb{V} , like in case of $\mathbb{V} = \mathbb{R}^n$ the Euclidian metric:

$$d(v, \mathbf{z}) = \|v - \mathbf{z}\|_2, \quad (2.174)$$

or other Minkowski, Mahalanobis, exponential, etc. metrics, different objectives of the clustering problem can be defined.

Denote $V = [v_i]_{i=1}^{n_c}$, and introduce the membership matrix $U = [\mu_{ik}]_{n_c \times N_z}$, where μ_{ik} is the degree of membership of \mathbf{z}_k to cluster i . Define also $d_{ik} := d(v_i, \mathbf{z}_k)$ as the distance between v_i and \mathbf{z}_k in terms of the dissimilarity measure d . In order to uniquely associate d_{ik} with a membership level μ_{ik} , the set of membership functions we consider must be constrained. A particular way is to restrict them to $\sum_{i=1}^{n_c} \mu_i(z) = 1$ for all $z \in \mathbb{V}$, i.e. requiring that $U \in \mathcal{U}_{n_c}^{N_z}$, where $\mathcal{U}_{n_c}^{N_z}$, defined as

$$\left\{ U \in [0, 1]^{n_c \times N_z} \mid \sum_{i=1}^{n_c} \mu_{ik} = 1, \forall k \in \mathbb{1}^{N_z}, \text{ and } 0 < \sum_{k=1}^{N_z} \mu_{ik}, \forall i \in \mathbb{1}^{n_c} \right\}, \quad (2.175)$$

characterizes the *fuzzy constraints*. Then, the solution of Problem 2.1 with a given choice of d , can be viewed as the minimization of the FcM-functional, $J_m(U, V) : \mathcal{U}_{n_c}^{N_z} \times \mathbb{V}^{n_c} \rightarrow \mathbb{R}_0^+$, which is formulated as

$$J_m(U, V) = \sum_{k=1}^{N_z} \sum_{i=1}^{n_c} \mu_{ik}^m d_{ik}^2. \quad (2.176)$$

The FcM-functional defines a cost function, a criterion of the expected solution and the design parameter¹⁵ $m \in (1, \infty)$ determines the “fuzziness”, the sharpness of separation of the resulting partition (U, V) . It can be observed, that (2.176) corresponds to a *mean-squared-error* criterion. The following theorem provides the ingredients to minimize (2.176), i.e. to solve the corresponding clustering problem:

¹⁵In FcM clustering only $m \geq 1$ is used as $m < 1$ gives unrealistic clustering of data sets. The $m = 1$ case is called hard clustering and treated separately due to minimization issues of the FcM functional Bezdek (1981). For these reasons, only $m \in (1, \infty)$ is considered in the sequel.

Theorem 2.16 (Optimal FcM Partition) (Bezdek 1981) Let $m > 1$, a data set $Z \subset \mathbb{V}$ with $N_z > 0$, and a fuzzy partition $(U, V) \in \mathcal{U}_{n_c}^{N_z} \times \mathbb{V}^{n_c}$ be given. Additionally, let $d_{ik} = d(v_i, z_k)$ be the dissimilarity measure of z_k with respect to v_i and $\mathcal{I}_k^\emptyset = \{i \in \mathbb{I}_1^{n_c} \mid d_{ik} = 0\}$ be the singularity set of z_k with $\text{card}(\mathcal{I}_k^\emptyset) = n_k^\emptyset$ (number of elements). Then (U, V) is a local minimum of J_m , if for any $(i, k) \in \mathbb{I}_1^{n_c} \times \mathbb{I}_1^{N_z}$:

$$\mu_{ik} = \begin{cases} \left[\sum_{j=1}^{n_c} \left(\frac{d_{jk}^2}{d_{jk}^2} \right)^{\frac{1}{m-1}} \right]^{-1} & \text{if } \mathcal{I}_k^\emptyset = \emptyset; \\ \frac{1}{n_k^\emptyset} & \text{if } i \in \mathcal{I}_k^\emptyset; \\ 0 & \text{if } i \notin \mathcal{I}_k^\emptyset \neq \emptyset; \end{cases} \quad (2.177a)$$

$$v_i = \frac{\sum_{k=1}^{N_z} \mu_{ik} z_k}{\sum_{k=1}^{N_z} \mu_{ik}}. \quad (2.177b)$$

To obtain an optimal partition, i.e. the solution of Problem 2.1 based on the choices of d , m , and the cost function J_m , minimization of (2.176) subject to (2.175) is usually tackled by alternating optimization (Picard iteration). This iterative optimization steers the solution towards a settling partition in the sense of Theorem 2.16. For the FcM, this yields the following algorithm, where V_l and U_l denote the actual fuzzy partition in iteration step l .

Algorithm 2.1 (FcM clustering)

- 0. Initialization:** Fix n_c and m ; and initialize $V_0 \in \mathbb{V}^{n_c}$, $l = 0$.
 - 1. Membership update:** With (2.177a), solve $U_{l+1} = \arg \min_{U \in \mathcal{U}_{n_c}^{N_z}} J_m(U, V_l)$.
 - 2. Cluster center update:** With (2.177b), solve $V_{l+1} = \arg \min_{V \in \mathbb{V}^{n_c}} J_m(U_{l+1}, V)$.
 - 3. Check of convergence:** If $J_m(U_{l+1}, V_{l+1})$ has converged, then stop, else $l = l + 1$ and goto Step 1.
-

The properties of the FcM algorithm have been extensively investigated by several authors (Bezdek 1981; Jain and Dubes 1988). Based on the fact that the FcM functional is bounded, monotonically decreasing and continuous both in V and U , it has been proved that Algorithm 2.1 always converges. The convergence point, which is directly dependent on the initial V^0 , can either be a local minimum or a saddle point of J_m , fulfilling Theorem 2.16. Therefore in a practical application, it is advisable to repeat the algorithm multiple times with different initial choices for V_0 to explore all possible local optima of (2.176).

To check the quality of the resulting (U, V) partition in terms of the goal of the clustering, several measures can be introduced that quantify the compactness, separation, and validity of (U, V) (see Backer and Jain (1981) and Davies

and Bouldin (1979)). A measure that can jointly express these concepts and give a common ground of comparison between different FcM partitions is the Xie-Beni validity index (Xie and Beni 1991):

$$\chi = \frac{1}{N_z} \frac{\sum_{k=1}^{N_z} \sum_{i=1}^{n_c} \mu_{ik}^2 d^2(v_i, z_k)}{\min_{i,j \in \mathbb{I}_1^{n_c}} d^2(v_i, v_j)}. \quad (2.178)$$

It can be proved that the smaller χ is, the better the corresponding fit of (U, V) with respect to Z is.

The determination of the number of “natural” groups in Z , i.e. the best suitable n_c for clustering, is important for the successful application of the FcM method. Similarity-based *Adaptive Cluster Merging* (ACM) is frequently used for this purpose (Kaymak and Setnes 2002), but other strategies like *cluster-splitting* (Jain and Dubes 1988; Schalkoff 1992) and supervised fuzzy clustering approaches (Setnes 1999) exist as well. ACM is more suitable for problems where little is known about the statistical properties of the data, like in the pole clustering case. The basic idea is the following: a measure of similarity is introduced with respect to cluster pairs. Then, in each iteration step of Algorithm 2.1, a cluster pair is merged when its similarity does not decrease between iterations and if also this pair is the most similar of all cluster pairs. However, merging is only applied if the similarity measure exceeds a certain threshold value, $\varepsilon_a \in [0, 1]$. In FcM clustering, most commonly the following similarity measure is applied:

Definition 2.43 (Inclusion similarity measure) (Kaymak and Setnes 2002) *The fuzzy-inclusion-similarity measure (given point-wise on Z) for two fuzzy clusters i and j is defined as*

$$[S_s]_{ij} := \frac{\sum_{k=1}^{N_z} \min(\mu_{ik}, \mu_{jk})}{\min\left(\sum_{k=1}^{N_z} \mu_{ik}, \sum_{k=1}^{N_z} \mu_{jk}\right)}. \quad (2.179)$$

For the theoretical details, see Kaymak and Setnes (2002). Denote in iteration step l the similarity matrix as $S_s^{(l)}$. Then, the most similar cluster pair in iteration step l is selected as

$$(\check{i}, \check{j}) = \arg \max_{(i,j) \in \mathbb{I}_1^{n_c} \times \mathbb{I}_1^{n_c}, i > j} \left\{ [S_s^{(l)}]_{ij} \right\}. \quad (2.180)$$

Merging is applied if $\left| [S_s^{(l-1)}]_{\check{i}, \check{j}} - [S_s^{(l)}]_{\check{i}, \check{j}} \right| < \varepsilon_s$, where $0 < \varepsilon_s \ll 1$ is a threshold value to judge the significance of decrease of cluster similarity between iterations. However as the partition converges, similarity changes a little between iterations, therefore merging is only applied if $[S_s^{(l)}]_{\check{i}, \check{j}} > \varepsilon_a^{(l)}$ where $\varepsilon_a^{(l)} \in [0, 1]$ is an adaptive threshold. In Kaymak and Setnes (2002), it is suggested to use $\varepsilon_a^{(l)} = (n_c^{(l)} - 1)^{-1}$ which has been observed empirically to work well if the initial number of clusters $n_c^{(0)}$ satisfies: $n_c^{(0)} < \frac{1}{2}N_z$.

In this way, the FcM algorithm with ACM gives the possibility to choose the number of needed clusters automatically based on Z . So by starting from a large n_c , the algorithm converges to a partition which contains only the necessary number of clusters representing the data. However, based on the initialization of the FcM algorithm, optimal partitions with different n_c can be attractive solutions of Algorithm 2.1 with ACM. To decide which of the solutions represents the underlying data-structure best, the separation of the clusters can give an indication. To quantify the quality of separation, commonly the *Normalized Entropy* is used (Bezdek 1981):

$$S_e = - \frac{\sum_{i=1}^{n_c} \sum_{k=1}^{N_z} \mu_{ik} \log\left(\frac{\mu_{ik}}{N_z}\right)}{N_z - n_c}. \quad (2.181)$$

The smaller S_e is, the more valid the hypothesis is that the clusters match with the natural data groups (if they exist).

In the literature, many different structural modifications for FcM algorithms has been developed, like *volume prototypes* (Kaymak and Setnes 2002) for dense data sets or kernel based dissimilarity measures leading to the theory of learning algorithms like *support vector machines* (Mizutani and Miyamoto 2005). Probabilistic FcM clustering, on which the kernel approaches are based, has been introduced to deal with stochastic data sets (Krishnapuram and Keller 2000). However, in this thesis we restrict our attention to conventional FcM clustering, as this framework gives an approach for the selection of OBFs based model structures for LPV systems.

2.6 Summary

In this introductory chapter, basic definitions, concepts, and mathematical tools have been introduced to establish a solid background for the research questions and problems this thesis addresses.

First, in Section 2.1, we have introduced the behavioral approach of LTI dynamical systems to give a clear framework where different concepts of system theory can be brought to a common ground. In this context we have defined several representations of dynamical systems both in continuous and discrete-time; we have established equivalence transformations between them which preserve the overall behavior; and we have investigated their properties in terms of stability, state-observability and reachability, and minimality. We have derived canonical and balanced state-space realizations and reviewed the zero-order hold based discretization theory of LTI systems. We have introduced all these concepts to enable their extension later to LPV systems, which is needed for the developed modeling and identification framework of this thesis. In Section 2.2, the concept of OBFs has been introduced and their role in the series-expansion representation of LTI systems has been investigated. This has served the purpose to motivate why finite truncations of such series expansions can be used as attractive model structures for the identification of both LTI and LPV systems. Then, in Section

2.3, the LTI prediction error identification framework has been introduced and analyzed with OBFs based model structures in the focus of the discussion. This framework has been set to provide the concept of model identification that is used for LPV systems later. Additionally, the concept of pole uncertainty regions has been developed with respect to model estimates. In the context of OBF model structures, the optimal choice of the model set has been discussed in Section 2.4, in terms of the Kolmogorov n -width concept. This theory serves as the backbone of the later developed OBF-model-structure-based model set selection approach for LPV systems. The previously introduced pole uncertainty concept will be an important ingredient for the robust formulation of this basis function selection mechanism. To provide a clustering tool which is needed to solve the model set selection problem in the LPV case, fuzzy c -means clustering has been introduced in Section 2.5.

In the next chapter, we return to the system theoretical concepts of Section 2.1, in order to extend them to the LPV system class. This contribution establishes the details of the system theory which are needed for the foundation of a strong LPV identification framework.

LPV systems and representations

In this chapter, we define the behavioral framework of LPV systems as an extension of the LTI behavioral approach introduced in Chapter 2. We do this with the intention to give a unified view on LPV system theory, that enables to approach LPV system identification in a well-founded system theoretic sense. First we define LPV dynamical systems from the behavioral point of view. Then we introduce the algebraic structure in which we formulate kernel, state-space, and input-output representations of LPV systems. We also analyze the properties of LPV systems in terms of state-observability, state-reachability, and dynamic stability.

3.1 General class of LPV systems

In this section, we establish the basics of a behavioral framework for *Linear Parameter-Varying* (LPV) systems where concepts of the existing LPV system theory can be brought to a common ground. Our main motivation is to set this framework as a tool for the analysis of LPV system identification in a well-founded sense.

One of the key concepts that is required to establish the LPV behavioral framework is an algebraic structure with elements describing *differential equations* (DE), like $\mathbb{R}[\xi]$ (the ring of polynomials with real constant coefficients) used in the LTI case. As we will see, the required structure in the LPV case is based on polynomials with coefficients that are functions of the scheduling variable p and its derivatives (continuous-time) or its time-shifts (discrete-time). The construction of this structure, which is the main contribution of this section to the state-of-the-art, enables to apply the results of the *Linear Time-Varying* (LTV) behavioral approach, worked out by Zerz (2006) and Ilchmann and Mehrmann (2005). We use these results to establish three key theorems: the existence of kernel representations, the existence of state-kernel forms, and later in Section 3.2 the concept of left/right unimodular transformations, similar to the LTI case. These theorems

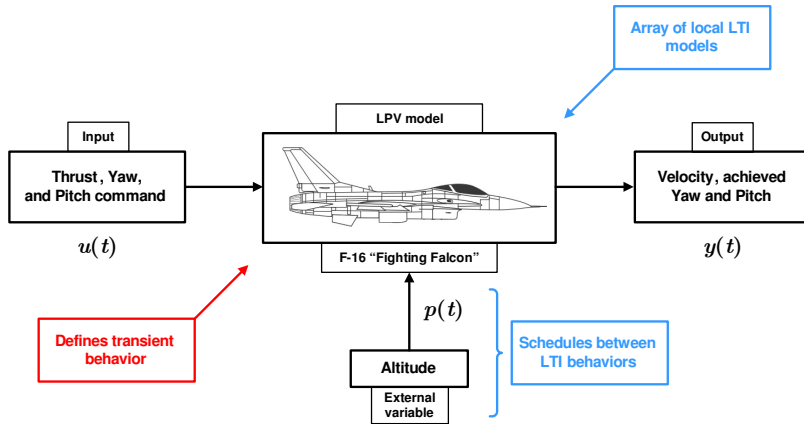


Figure 3.1: The LPV modeling concept of the F-16 Fighting Falcon.

set the stage for the derivation of equivalence transformations between LPV representations, treated in Chapter 4, which have paramount significance for system identification.

Before venturing into the mathematical concepts and definitions, let's investigate what we call an LPV system from the behavioral point of view and what kind of physical phenomena are represented by this modeling concept.

3.1.1 Parameter varying dynamical systems

In aerospace engineering, it is well-known that many airplanes, like the F-16 Fighting Falcon presented in Figure 3.1, are nonlinear dynamical systems, but at a constant altitude they can be well approximated as an LTI system (Stevens and Lewis 2003; Cook 1997). Then, by viewing the aircraft as a collection of LTI behaviors corresponding to different altitude levels and using the altitude variable as a *scheduling* between them, we can arrive at an approximation of the global behavior. In this context, the concept of scheduling means the selection of the LTI behavior associated with a specific altitude level. This behavior describes the possible continuation of signal trajectories during the time interval in which the aircraft remains at the same altitude. Thus, the resulting representation of the global behavior involves coefficients that are functions of the scheduling. Such a modeling approach, what we have already introduced in Chapter 1 as the *gain-scheduling* principle, defines a parameter-varying (due to scheduling) and linear (in signal relation) system. Such systems are referred as LPV. However, it is important that an LPV system is more than just an array of LTI systems, because the governing scheduling rules or functions also define the dynamical behavior between each scheduling point, i.e. altitude points of this example. The concept of scheduling functions and “frozen” LTI behaviors is an essential viewpoint on LPV systems and will be frequently used in the development of the identification approach of this thesis.

In the general *Parameter-Varying* (PV) framework, the scheduling variable, commonly denoted by p , is an external¹, so called free signal of the system, that governs the dynamical behavior. In this way, p is similar to time, however its trajectory is unknown in advance. This unknown trajectory of the scheduling variable makes LPV systems different from the LTV system class, where the variation of time follows a known linear trajectory. Based on this, by using the concept of dynamical systems (Definition 2.1), the class of PV systems can be defined as follows:

Definition 3.1 (Parameter-varying dynamical system) *A parameter-varying dynamical system \mathcal{G}_P is defined as a quadruple*

$$\mathcal{G}_P = (\mathbb{T}, \mathbb{P}, \mathbb{W}, \mathfrak{B}), \quad (3.1)$$

with \mathbb{T} the time-axis, \mathbb{P} the scheduling space, \mathbb{W} the signal space, and $\mathfrak{B} \subseteq (\mathbb{W} \times \mathbb{P})^{\mathbb{T}}$ the behavior.

The scheduling space \mathbb{P} is usually a closed subset of a vector space on which the scheduling variable p varies: $p \in \mathbb{P}^{\mathbb{T}}$. In our example, \mathbb{P} refers to the altitude range of the aircraft, which is a subset of \mathbb{R} , as the altitude of the aircraft must be positive. On the other hand, its altitude range is also bounded by a maximum height of operation, dependent on its engine and its aerodynamical construction. Often, the admissible trajectories of p are also restricted to a subset of $\mathbb{P}^{\mathbb{T}}$, as it is not possible for an aircraft to have discontinuous jumps in altitude. Therefore, this admissible set of scheduling trajectories is defined as the *projected scheduling behavior*:

$$\mathfrak{B}_{\mathbb{P}} = \{p \in \mathbb{P}^{\mathbb{T}} \mid \exists w \in \mathbb{W}^{\mathbb{T}} \text{ s.t. } (w, p) \in \mathfrak{B}\}. \quad (3.2)$$

Similarly we can define the projected signal behavior $\mathfrak{B}_{\mathbb{W}}$. For a given, fixed scheduling trajectory $p \in \mathfrak{B}_{\mathbb{P}}$, the projected behavior

$$\mathfrak{B}_p = \{w \in \mathbb{W}^{\mathbb{T}} \mid (w, p) \in \mathfrak{B}\}, \quad (3.3)$$

defines all the signal trajectories that are admissible with the fixed scheduling trajectory p . This important projected behavior gives the possible course of actions or maneuvers that the aircraft in our example can take to follow a fixed altitude trajectory. In case of a constant scheduling trajectory, $p \in \mathfrak{B}_{\mathbb{P}}$ with $p(t) = \bar{p}$ for all $t \in \mathbb{T}$ where $\bar{p} \in \mathbb{P}$, the projected behavior \mathfrak{B}_p is called a *frozen behavior* and denoted as

$$\mathfrak{B}_{\bar{p}} = \{w \in \mathbb{W}^{\mathbb{T}} \mid (w, p) \in \mathfrak{B} \text{ with } p(t) = \bar{p}, \forall t \in \mathbb{T}\}. \quad (3.4)$$

Building on the linearity and time-invariance concepts of the LTI system class, we can define LPV systems as follows:

¹Note that systems where p is an internal variable (like output, input, or state) are called *quasi parameter-varying systems*. Still, such systems are commonly treated as a PV system with external scheduling variable, therefore in the upcoming analysis, p is assumed to be an independent variable. For more on quasi-PV systems, see Chapter 7.

Definition 3.2 (LPV system) *The parameter-varying system \mathcal{G}_P is called LPV, if the following conditions are satisfied:*

- \mathbb{W} is a vector-space and \mathfrak{B}_p is a linear subspace of $\mathbb{W}^\mathbb{T}$ for all $p \in \mathfrak{P}$ (linearity).
- \mathbb{T} is closed under addition.
- For any $(w, p) \in \mathfrak{B}$ (a signal trajectory associated with a scheduling trajectory) and any $\tau \in \mathbb{T}$, it holds that $(w(\cdot + \tau), p(\cdot + \tau)) \in \mathfrak{B}$, in other words $q^\tau \mathfrak{B} = \mathfrak{B}$ (time-invariance).

Definition 3.2 does not imply that the dynamic system $\mathcal{G} = (\mathbb{T}, \mathbb{W}, \mathfrak{B}_p)$, associated with the projected behavior \mathfrak{B}_p , is also time-invariant. However, for a constant scheduling trajectory associated with $\bar{p} \in \mathfrak{P}$, time-invariance of \mathcal{G}_P implies time-invariance of $\mathcal{G} = (\mathbb{T}, \mathbb{W}, \mathfrak{B}_{\bar{p}})$. Based on this and the linearity condition of \mathfrak{B}_p , it holds for an LPV system that for each of its frozen behaviors $\mathfrak{B}_{\bar{p}}$ the associated system $\mathcal{G} = (\mathbb{T}, \mathbb{W}, \mathfrak{B}_{\bar{p}})$ is an LTI system. In this way, the projected behaviors of a given LPV system \mathcal{S} with respect to constant scheduling trajectories define a set of LTI systems:

Definition 3.3 (Frozen system set) *Let $\mathcal{S} = (\mathbb{T}, \mathfrak{P}, \mathbb{W}, \mathfrak{B})$ be an LPV system. The set of LTI systems*

$$\mathcal{F}_{\mathfrak{P}} = \{ \mathcal{F} = (\mathbb{T}, \mathbb{W}, \mathfrak{B}') \mid \exists \bar{p} \in \mathfrak{P} \text{ s.t. } \mathfrak{B}' = \mathfrak{B}_{\bar{p}} \} \quad (3.5)$$

is called the frozen system set of \mathcal{S} .

This set refers in our example to the LTI behaviors of the aircraft for constant altitude levels. We have already motivated that the LPV system concept is advantageous compared to nonlinear systems, as the relation of the signals is linear. Definition 3.2 also reveals the advantage of this system class over LTV systems: the variation of the system dynamics is not associated directly with time, but with the variation of a free signal. Thus, the LPV modeling concept, compared to LTV systems, is more suitable for non-stationary/coordinate dependent physical systems as it describes the underlying phenomena directly (see Example 3.1).

Example 3.1 (Varying mass on a spring) *To emphasize the advantage of LPV systems, let's investigate the modeling of the motion of a varying mass connected to a spring (see Figure 3.2). This problem is one of the typical phenomena occurring in systems with time-varying masses like in motion control (robotics, rotating crankshafts, rockets, conveyor systems, excavators, cranes), biomechanics, and in fluid-structure interaction problems. Denote by w_x the position of the varying mass m . Let $k_s > 0$ be the spring constant, introduce w_F as the force acting on the mass, and assume that there is no damping. By Newton's second law of motion, the following equation holds:*

$$\frac{d}{dt} \left(m \frac{d}{dt} w_x \right) = w_F - k_s w_x, \quad (3.6)$$

or equivalently

$$k_s w_x + \left(\frac{d}{dt} m \right) \frac{d}{dt} w_x + m \frac{d^2}{dt^2} w_x = w_F. \quad (3.7)$$

It is immediate that by taking m as a scheduling variable, the behavior of this plant can be described as an LPV system, preserving the physical insight of Newton's second law. On the other hand, viewing m as a time-varying parameter, whose trajectory is fixed in time, would result in a LTV system. Such a system would explain the behavior of the plant for only a fixed trajectory of the mass.

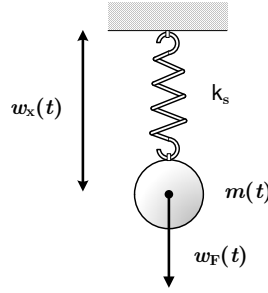


Figure 3.2: Varying-mass connected to a spring.

It also holds that for any constant scheduling trajectory $p(t) = \bar{p}$, i.e. constant m for all $t \in \mathbb{R}$, the set of admissible signal trajectories of (3.7) is defined as the weak solutions of

$$k_s w_x - w_F + \bar{p} \frac{d^2}{dt^2} w_x = 0. \quad (3.8)$$

This yields that the frozen system set is the collection of LTI systems represented by (3.8) for all $\bar{p} \in \mathbb{P}$, i.e. all possible constant m .

Similar to the discussion in the LTI case, we restrict our attention again to systems with finite dimensional and real signal space ($\mathbb{W} = \mathbb{R}^{n_w}$, $n_w \in \mathbb{N}$) and with finite dimensional, real, and closed scheduling space ($\mathbb{P} \subseteq \mathbb{R}^{n_p}$, $n_p \in \mathbb{N}$). In fact, we consider LPV systems described by finite order linear differential or difference equations with parameter-varying effects in the coefficients, and we call such systems *Linear Parameter-Varying Differential/Difference* systems and denote them with \mathcal{S} . A basic property of such systems is that their behaviors \mathfrak{B} are complete ($(w, p) \in \mathfrak{B} \Leftrightarrow (w, p)|_{[t_0, t_1]} \in \mathfrak{B}|_{[t_0, t_1], \forall [t_0, t_1] \subset \mathbb{T}$). In the sequel, if refer to LPV systems, we refer to this system class.

3.1.2 Representations of continuous-time LPV systems

In the following we introduce *kernel* (KR), *state-space* (SS) and *input-output* (IO) representations of *continuous-time* (CT) LPV systems. However, to define these representations, we first have to clarify the algebraic structure in which we consider PV differential equations. Similar to the LTI case, this requires two ingredients: the definition of the coefficients of these equations and the introduction of polynomials with such coefficients.

A. Coefficient functions

As stated, the coefficients of the representations of LPV systems are functions of the possibly multidimensional scheduling variable p . Thus, first we define the class of functional dependencies that we consider in the sequel. In fact, we establish an algebraic field of a wide class of multivariable functions. As a main contribution we show later that if the variables of these functions are assigned

to the elements of p and their derivatives, then equivalence transformations between different representation domains become possible. To formulate the class of multivariable functions that we consider, introduce the following definition:

Definition 3.4 (Real-meromorphic function) (Krantz 1999) *A real-meromorphic function $f : \mathbb{R}^n \rightarrow \mathbb{R}$, $n \in \mathbb{N}$, is a function in the form*

$$f = \frac{g}{h}, \quad (3.9)$$

where $g, h : \mathbb{R}^n \rightarrow \mathbb{R}$ are holomorphic (analytical) functions and $h \neq 0$ (not the zero function).

Meromorphic functions consist of all rational, polynomial functions, trigonometric expressions, rational exponential functions etc., however functions like $f(x) = \sin^{-1}(1/x)$ are not meromorphic ($x = 0$ is an accumulation point of the singularities). Therefore, this class contains the common functional dependencies that result during LPV modeling of physical systems (see Chapter 1 and 7). Next we formulate an algebraic field over all multivariable real-meromorphic functions.

Let \mathcal{R}_n denote the field of real-meromorphic functions with n variables. Denote the variables of a $r \in \mathcal{R}_n$ as ζ_1, \dots, ζ_n . Also define an operator \mathcal{U}_j on \mathcal{R}_n with $1 \leq j \leq n$ such that

$$\mathcal{U}_j(r(\zeta_1, \dots, \zeta_n)) := r(\zeta_1, \dots, \zeta_j, 0, \dots, 0). \quad (3.10)$$

Note that \mathcal{U}_j projects a meromorphic function to a lower dimensional domain. Introduce $\bar{\mathcal{R}}_n$, defined as

$$\bar{\mathcal{R}}_n = \{r \in \mathcal{R}_n \mid \mathcal{U}_{n-1}(r) \neq r\}. \quad (3.11)$$

It is clear that $\bar{\mathcal{R}}_n$ consist of all functions \mathcal{R}_n in which the variable ζ_n has a nonzero contribution, i.e. it plays a role in the function. Also define the operator $\mathcal{U}_* : (\cup_{i \geq 0} \mathcal{R}_i) \rightarrow (\cup_{i \geq 0} \bar{\mathcal{R}}_i)$, which associates a given $r \in \mathcal{R}_n$ with a $r' \in \bar{\mathcal{R}}_{n'}$, $n \geq n'$, i.e. $\mathcal{U}_*(r) = r'$, such that $\mathcal{U}_{n'}(r) = r'$ and n' is minimal. In this way, \mathcal{U}_* reduces the variables of a function till $\zeta_{n'}$ can not be left out from the expression because it has a nonzero contribution to the value of the function. Now define the collection of all real-meromorphic functions with finite many variables as

$$\mathcal{R} = \bigcup_{i \geq 0} \bar{\mathcal{R}}_i, \quad \text{with } \bar{\mathcal{R}}_0 = \mathbb{R}. \quad (3.12)$$

In the sequel we consider \mathcal{R} as the set of coefficient functions, giving the basic building blocks of PV differential equations. A basic ingredient that is required for this, is to show that \mathcal{R} is an algebraic field. Define the addition operator \boxplus and the multiplication operator \boxtimes on \mathcal{R} as

Definition 3.5 (Addition/Multiplication operator on \mathcal{R}) *Let $r_1, r_2 \in \mathcal{R}$ such that $r_1 \in \bar{\mathcal{R}}_i$ and $r_2 \in \bar{\mathcal{R}}_j$ with $i \geq j \geq 0$. Let $r'_2 \in \bar{\mathcal{R}}_i$ such that $\mathcal{U}_*(r'_2) = r_2$ where r'_2 is unique. Then*

$$r_1 \boxplus r_2 := \mathcal{U}_*(r_1 + r'_2), \quad (3.13a)$$

$$r_1 \boxtimes r_2 := \mathcal{U}_*(r_1 \cdot r'_2), \quad (3.13b)$$

where $+$ and \cdot are the Euclidean addition and multiplication operators of \mathcal{R}_i .

The following lemma holds:

Lemma 3.1 (Field property of \mathcal{R}) *The set \mathcal{R} is a field.*

The proof is given in Appendix A.1. Denote by \mathcal{R}^{\times} the matrices with elements in \mathcal{R} . Note that \mathcal{R}^{\times} is also a field. In the following, if it is not necessary to emphasize the difference between the Euclidean addition and \boxplus , we use $+$ to denote both operators in order to improve readability. The same abuse of notation is also introduced for \boxtimes .

The next step towards the formal definition of PV differential equations and the associated kernel representations, is to associate the variables of the coefficient functions with elements of p and its derivatives. This is required to handle multiplication of coefficients by time operators. Given the scheduling dimension $n_{\mathbb{P}} > 0$, denote the variables of $r \in \bar{\mathcal{R}}_n$ (n -dimensional function in \mathcal{R}) as:

$$\{\zeta_{ij}\}_{n_{\zeta}, n_{\mathbb{P}}, \tau} := \{\zeta_{01}, \zeta_{02}, \dots, \zeta_{0n_{\mathbb{P}}}, \zeta_{11}, \zeta_{12}, \dots, \zeta_{n_{\zeta}1}, \dots, \zeta_{n_{\zeta}\tau}\}, \quad (3.14)$$

where $n_{\zeta} \geq 0$ such that $n_{\zeta}n_{\mathbb{P}} + \tau = n$ and $0 < \tau \leq n_{\mathbb{P}}$. In this way, the first variable of r is denoted by ζ_{01} , the second is denoted by ζ_{02} , etc. Thus, (3.14) gives a unique labeling of the variables for each $\bar{\mathcal{R}}_n$ with $n \geq 1$. In continuous-time, associate each variable ζ_{ij} as

$$\zeta_{ij} = \frac{d^i}{dt^i} p_j \quad (3.15)$$

where p_j is the j^{th} element of the scheduling signal p . This association provides the description of parameter-varying coefficients in \mathcal{R} , where each coefficient is a meromorphic function of the elements of p and their finite order derivatives (see Example 3.2). We call such a coefficient dependence *dynamic*. To compare this dependency class to class of dependencies used in the state-of-the-art of LPV identification (see Chapter 1), define the subset of \mathcal{R} for a given $n_{\mathbb{P}}$ as $\mathcal{R}|_{n_{\mathbb{P}}} = \bigcup_{i=0}^{n_{\mathbb{P}}} \bar{\mathcal{R}}_i$. It is easy to show that $\mathcal{R}|_{n_{\mathbb{P}}}$ is a field and it consists of meromorphic coefficient functions dependent on the elements of p (without derivatives). This dependence type is called *static*. It has already been discussed in Chapter 1, that LPV representations based on coefficients in $\mathcal{R}|_{n_{\mathbb{P}}}$ are inequivalent. This is the main motivation to use coefficients in \mathcal{R} as the building blocks of representations, because with these, equivalency of representations can be re-established.

Example 3.2 (Coefficient function) *Let $p : \mathbb{R} \rightarrow \mathbb{R}^2$. Then the coefficient function*

$$r(p_1, p_2, \frac{d}{dt}p_1) = \frac{\cos(p_1)}{\sin(\frac{d}{dt}p_1)},$$

is a real-meromorphic function $r \in \bar{\mathcal{R}}_3$, with variables $\{\zeta_{01}, \zeta_{02}, \zeta_{11}\}$, i.e. $r(\zeta_{01}, \zeta_{02}, \zeta_{11}) = \frac{\cos(\zeta_{01})}{\sin(\zeta_{11})}$.

To define PV differential equations based on coefficient functions in \mathcal{R} , it is also required to evaluate a given coefficient function $r \in \mathcal{R}$ along a scheduling trajectory $p \in \mathfrak{B}_{\mathbb{P}}$ and its associated derivatives. For this purpose, define the operator $\diamond : (\mathcal{R}, \mathfrak{B}_{\mathbb{P}}) \rightarrow (\mathbb{R}^{\mathbb{R}})$ that associates r and p with a time function defined as:

$$r \diamond p = r \left(\left\{ \frac{d^i}{dt^i} p_j \right\}_{n_{\zeta}, n_{\mathbb{P}}, \tau} \right). \quad (3.16)$$

B. Polynomials over \mathcal{R}

In order to introduce representations of LPV systems, an other key ingredient is needed, namely the formulation of polynomials with meromorphic coefficient functions that have a finite number of variables. Polynomials of this type are used to define PV differential equations describing the behavior of CT-LPV systems. First we define the ring of such polynomials and we show that multiplication, which corresponds to differentiation, is non-commutative over this ring. We also analyze other key properties of this ring to show that the algebraic structure is the same as in the LTV behavioral approach of Zerz (2006). The latter property implies that key results of that framework also hold in the LPV case, enabling the introduction of LPV system representations relatively easily.

Introduce $\mathcal{R}[\xi]$ as the collection of all polynomials in the indeterminant ξ and with coefficients in \mathcal{R} . Note that it is a general property of polynomial spaces over a field, that they define a ring. Also introduce $\mathcal{R}[\xi]^{\times}$, the ring of matrix polynomial functions with elements in $\mathcal{R}[\xi]$. With $\mathcal{R}[\xi]$ formulated and operator \diamond defined, we are now able to define a parameter-varying differential equation with rows n_r and signal dimension $n_{\mathbb{W}}$ as follows:

$$\left(R \left(\frac{d}{dt} \right) \diamond p \right) w := \sum_{i=0}^{n_{\xi}} (r_i \diamond p) \frac{d^i}{dt^i} w = 0, \quad (3.17)$$

where $R \in \mathcal{R}[\xi]^{n_r \times n_{\mathbb{W}}}$, $\deg(R) = n_{\xi}$, and $r_i \in \mathcal{R}^{n_r \times n_{\mathbb{W}}}$ for all $i \in \mathbb{I}_0^{n_{\xi}}$. PV differential equations in the form of (3.17) are used to define the class of CT-LPV systems we consider in this thesis. It will be shown, that this class contains all the popular definitions of LPV state-space and IO models. Furthermore this mathematical structure also enables the transformation of a wide class of nonlinear systems to an LPV form by preserving physical insight (see Example 3.3 and Chapter 7).

Example 3.3 (PV differential equation) Consider the mass-spring system of Example 3.1. Let $p = m$ with a scheduling space $\mathbb{P} = [1, 2]$ and let $w = [w_x \quad w_F]^{\top}$ with $\mathbb{W} = \mathbb{R}^2$. Then the possible signal trajectories are defined as the solutions of

$$k_s w_1 - w_2 + \left(\frac{d}{dt} p \right) \frac{d}{dt} w_1 + p \frac{d^2}{dt^2} w_1 = 0. \quad (3.18)$$

and $\mathfrak{B}_{\mathbb{P}} = C^{\infty}(\mathbb{R}, \mathbb{P})$. Such a system equation can be written in the form (3.17) with $n_{\mathbb{W}} = 2$, $n_{\xi} = 1$, $n_{\mathbb{P}} = 1$, and

$$r_0 \diamond p = \begin{bmatrix} k_s & -1 \end{bmatrix}, \quad r_1 \diamond p = \begin{bmatrix} \frac{d}{dt} p & 0 \end{bmatrix}, \quad r_2 \diamond p = \begin{bmatrix} p & 0 \end{bmatrix}.$$

Due to its algebraic structure, it is possible to show that $\mathcal{R}[\xi]^{\cdot \times \cdot}$ is a domain, i.e. for all $R_1, R_2 \in \mathcal{R}[\xi]^{n_r \times n_w}$ it follows that

$$R_1 R_2 = 0 \quad \Rightarrow \quad R_1 = 0 \quad \text{or} \quad R_2 = 0. \quad (3.19)$$

On the other-hand, it is non-commutative due to the chain rule of differentiation. To show this, introduce the *dot* operator on \mathcal{R} to describe differentiation of parameter-varying coefficient functions.

Definition 3.6 (Dot operator) Let $r \in \bar{\mathcal{R}}_n$ be a n variable meromorphic function in \mathcal{R} . For a given $n_{\mathbb{P}} > 0$, denote the variables of r as $\{\zeta_{ij}\}_{n_{\zeta}, n_{\mathbb{P}}, \tau}$ based on (3.14). Then, in continuous-time, the dot operator on \mathcal{R} is introduced as

$$\dot{r} := \mathcal{U}_*(\check{r}), \quad (3.20)$$

where $\check{r} \in \bar{\mathcal{R}}_{n+n_{\mathbb{P}}}$ and is given by

$$\begin{aligned} \check{r}(\{\zeta_{ij}\}_{n_{\zeta}+1, n_{\mathbb{P}}, \tau}) &= \sum_{k=0}^{n_{\zeta}} \sum_{l=1}^{n_{\mathbb{P}}} \frac{\partial}{\partial \zeta_{kl}} r(\{\zeta_{ij}\}_{n_{\zeta}, n_{\mathbb{P}}, \tau}) \zeta_{(k+1)l} \\ &+ \sum_{l=1}^{\tau} \frac{\partial}{\partial \zeta_{n_{\zeta} l}} r(\{\zeta_{ij}\}_{n_{\zeta}, n_{\mathbb{P}}, \tau}) \zeta_{(n_{\zeta}+1)l}. \end{aligned} \quad (3.21)$$

Note that the chain rules of differentiation imply that the dot operator fulfills the following rules for any $r_1, r_2 \in \mathcal{R}$:

$$\begin{cases} \text{if } r = r_1 \pm r_2 & \text{then } \dot{r} = \dot{r}_1 \pm \dot{r}_2, \\ \text{if } r = r_1 r_2 & \text{then } \dot{r} = \dot{r}_1 r_2 + r_1 \dot{r}_2, \\ \text{if } r = \frac{r_1}{r_2} & \text{then } \dot{r} = \frac{\dot{r}_1 r_2 - r_1 \dot{r}_2}{r_2^2}. \end{cases}$$

Due to the differentiation to which (3.21) corresponds, the number of variables in the coefficient functions can grow, representing an increase in the order of derivatives of p in the functional dependence. Multiplication on $\mathcal{R}[\xi]$ with ξ now can be defined through the dot operator using the non-commutative rule:

$$\xi r = \dot{r} + r \xi, \quad (3.22)$$

where $r \in \mathcal{R}$ (see Example 3.4). Additionally, the ring $\mathcal{R}[\xi]$ is simple (i.e. the only ideals that are both right and left ideals are the trivial ones: 0 and $\mathcal{R}[\xi]$ itself) and it is a left and right principle domain (i.e. every left and right ideal can be generated by a single element). To show these properties, the argument similarly follows as in the case of polynomial rings with rational coefficient functions (Gooderal and Warfield 1989). In fact this ring is even a right and left Euclidian domain, which means that there exist a right and left division with remainder (Chon 1971). Based on these properties and with the non-commutative multiplication rule (3.22), it is possible to show that $\mathcal{R}[\xi]$ defines an Ore algebra (Chyzak and Salvy 1998). With these algebraic properties, there exists a categorical duality between the solution spaces of PV differential equations and the polynomial modules associated with

them, which is implied by a so called injective cogenerator property. This has been showed for the solution spaces of the polynomial ring over \mathcal{R}_1 by Zerz (2006). Due to the fact that all required algebraic properties are satisfied for $\mathcal{R}[\xi]$, the proof of the injective cogenerator property similarly follows in this case. Based on these facts, we will omit the rather heavy technicalities to prove certain theorems in the following discussion as all proofs similarly follows in $\mathcal{R}_1[\xi]$.

Example 3.4 (Non-commutativity and the dot operation) Consider again Example 3.1 and rewrite the differential equation (3.6) into the form:

$$\mathbf{k}_s w_x - w_F + \xi(r \diamond m)\xi w_x = 0, \quad (3.23)$$

with $\xi = \frac{d}{dt}$ and $r \in \mathcal{R}$ is the identity function: $r \diamond m = m$. Then due to the non-commutative multiplication rule (3.22), equation (3.23) is equivalent with

$$\mathbf{k}_s w_x - w_F + (\dot{r} \diamond m)\xi w_x + (r \diamond m)\xi^2 w_x = 0, \quad (3.24)$$

where $\dot{r} \diamond m = \frac{d}{dt}m$. Note that (3.24) is identical to (3.7), and by using the signal substitution $p = m$ and $w^\top = [w_x \quad w_F]$, it is in the identical polynomial form of (3.18).

C. Kernel representations

As a next step in the foundation of the LPV behavioral approach, we develop the concept of KR representations of CT-LPV systems and investigate some relating properties. To do so, first we define weak solutions of a PV differential equation. Then, based on this concept of solutions, we introduce KR representations of the LPV system behavior. Next, we clarify the concept of full row rank KR representations and their existence based on the result of Zerz (2006) for LTV systems. This requires the definition of the rank of polynomial matrices in $\mathcal{R}[\xi]^{\times}$ that we develop beforehand.

So far we have defined PV differential equations in the form of

$$\left(R\left(\frac{d}{dt}\right) \diamond p\right)w = 0, \quad (3.25)$$

which for a given p corresponds to an ordinary differential equation in the variable w . In the behavioral framework, a PV system is defined as the union of signal trajectories w that are the solution of a differential equation resulting from (3.25) for an admissible scheduling trajectory p . Thus to define a representation of a system in terms of a PV differential equation, we require the concept of admissible signal trajectories described by the PV differential equation. To define the admissible trajectories, we again use the concept of weak solutions over $\mathcal{L}_1^{\text{loc}}$ through the theory of distributions (see Section 2.1.2 for the motivation):

Definition 3.7 (Weak solution) We call $w \in \mathcal{L}_1^{\text{loc}}(\mathbb{R}, \mathbb{R}^{n_w})$ a weak solution of (3.17) for a given smooth scheduling trajectory $p \in \mathfrak{B}_{\mathbb{P}} \subseteq \mathcal{L}_1^{\text{loc}}(\mathbb{R}, \mathbb{R}^{n_{\mathbb{P}}})$, if

$$\langle w, (R^\dagger\left(\frac{d}{dt}\right) \diamond p)\varphi \rangle := \int_{\mathbb{R}} w^\top (R^\dagger\left(\frac{d}{dt}\right) \diamond p)\varphi dt = 0 \quad (3.26)$$

holds for every smooth, so called test function, $\varphi : \mathbb{R} \rightarrow \mathbb{R}^{n_r}$ with compact support, where R^\dagger is

$$R^\dagger(\xi) = \sum_{i=0}^{n_\xi} (-1)^i \xi^i r_i^\top. \quad (3.27)$$

In the following we only consider scheduling trajectories for which the coefficients of $R(\xi) \diamond p$ are bounded, so the set of solutions associated with R is well defined in terms of (3.26). Additionally, R^\dagger (also called the adjoint of R) results in the form of (3.27), due to integrations by parts of (3.17) to transfer all differential operators acting on w to differential operators acting on φ , similar to the LTI case (Evans 1998). Each integration by parts entails a multiplication by -1 . To compute R^\dagger in a form where the coefficients are right-side multiplied by ξ , repeated use of the multiplication rule (3.22) is required in (3.27) (see Example 3.5).

Example 3.5 (Weak solution) Consider the parameter-varying differential equation (3.18). Then

$$\begin{aligned} R^\dagger(\xi) &= r_0^\top - \xi r_1^\top + \xi^2 r_2^\top = (r_0^\top - \dot{r}_1^\top + \ddot{r}_2^\top) + (2\dot{r}_2^\top - r_1^\top) \xi + r_2^\top \xi^2, \\ R^\dagger(\xi) \diamond p &= \begin{bmatrix} \mathbf{k}_s \\ -1 \end{bmatrix} + \begin{bmatrix} \frac{d}{dt} p \\ 0 \end{bmatrix} \xi + \begin{bmatrix} p \\ 0 \end{bmatrix} \xi^2. \end{aligned}$$

Choose a particular scheduling trajectory $p(t) = \cos(t)$ and a test function $\varphi(t) = \cos(t)$. Then

$$(R^\dagger(\frac{d}{dt}) \diamond p)(t) \cdot \varphi(t) = \begin{bmatrix} \mathbf{k}_s \cos(t) + \sin^2(t) - \cos^2(t) \\ -\cos(t) \end{bmatrix},$$

which means that taking $w(t) = [\cos(t) \quad \mathbf{k}_s \cos(t) + \sin^2(t) - \cos^2(t)]^\top$ gives 0 for (3.26). It can be shown, that this holds for every φ , yielding that w is a weak solution. Substitution of w into (3.18) satisfies the differential equation with $p(t) = \cos(t)$ for all $t \in \mathbb{R}$. This implies that w is a strong solution (satisfies (3.18) for all $t \in \mathbb{R}$) of the varying-mass and spring system. However, taking $w(t) = [\frac{1}{\mathbf{k}_s \cos(t) - \cos^2(t) + \sin^2(t)} \quad \frac{1}{\cos(t)}]^\top$ also gives 0 for (3.26) with $\varphi(t) = \cos(t)$, but such a solution does not satisfies (3.18) for $\{k \cdot \pi\}_{k \in \mathbb{Z}}$ and as a result it can be only a weak solution. By considering other test functions, it can be shown that (3.26) is not satisfied in all cases, which proves that this choice of w is not a weak solution of (3.18).

Now we can give the definition of continuous-time KR representations of LPV dynamic systems as follows:

Definition 3.8 (CT-KR-LPV representation) The parameter-varying differential equation (3.17) is called a continuous-time kernel representation, denoted by $\mathfrak{R}_K(\mathcal{S})$, of the LPV dynamical system $\mathcal{S} = (\mathbb{R}, \mathbb{R}^{n_p}, \mathbb{R}^{n_w}, \mathfrak{B})$ with scheduling vector p and signals w , if

$$\mathfrak{B} = \left\{ (w, p) \in \mathcal{L}_1^{\text{loc}}(\mathbb{R}, \mathbb{R}^{n_w} \times \mathbb{R}^{n_p}) \mid (R(\frac{d}{dt}) \diamond p)w = 0 \text{ holds weakly} \right\}.$$

Note that in the LPV system class, we consider LPV systems with $\mathbb{T} = \mathbb{R}$ that have a KR representation, so existence of such a representation is explicitly assumed in the following. It is also important, that the trajectories of p are not described/restricted by (3.25) (only those trajectories are omitted where a coefficient becomes infinite) because p is assumed to be an external variable in the LPV modeling concept. One can also include further restrictions on $\mathfrak{B}_\mathbb{P}$, like description

of the admissible scheduling trajectories as solutions of a differential equation, etc. However, to preserve the generalism of the developed framework, we do not consider the latter case in the sequel.

An important concept to be established, is the concept of full row rank KR representations. In the LTI case, we have seen that such a concept have been required to introduce minimality and to handle equivalence transformations and relations. However to define full row rank KR representations, we first need to define the notion of division by remainder in $\mathcal{R}[\xi]^{\cdot \times \cdot}$.

Due to the fact that $\mathcal{R}[\xi]$ is a right and left Euclidean domain, there exist left and right division by remainder. This means, that if $R_1, R_2 \in \mathcal{R}[\xi]$ with $\deg(R_1) \geq \deg(R_2)$ and $R_2 \neq 0$, then there exist unique polynomials $R', R'' \in \mathcal{R}[\xi]$ such that

$$R_1 = R_2 R' + R'', \quad (3.28)$$

where $\deg(R_2) > \deg(R'')$. Here we call R'' the right-remainder. Furthermore, as $\mathcal{R}[\xi]$ is simple, the rank of a matrix polynomial $R \in \mathcal{R}[\xi]^{n_r \times n_w}$ is well-defined (Lam 2000). Denote by $\text{span}_{\mathcal{R}}^{\text{row}}(R)$ and $\text{span}_{\mathcal{R}}^{\text{col}}(R)$ the subspace spanned by the rows (columns) of $R \in \mathcal{R}[\xi]^{\cdot \times \cdot}$, viewed as a linear space of polynomial vector functions with coefficients in $\mathcal{R}^{\cdot \times \cdot}$. Then

$$\text{rank}(R) = \dim(\text{span}_{\mathcal{R}}^{\text{row}}(R)) = \dim(\text{span}_{\mathcal{R}}^{\text{col}}(R)). \quad (3.29)$$

Based on the concept of rank, the following theorem can be introduced:

Theorem 3.1 (Existence of full row rank KR representation) (Zerz 2006) *Let \mathfrak{B} be given with a KR representation (3.17). Then, \mathfrak{B} can also be represented by a $R' \in \mathcal{R}[\xi]^{\cdot \times n_w}$ with full row rank.*

Due to algebraic properties of $\mathcal{R}[\xi]$, the proof of this theorem similarly follows as in Zerz (2006). Just as for LTI systems, the concept of minimality for KR representations is based on the full row rank of the associated matrix polynomials. (see Chapter 3.2).

D. Input-output representations

Another key representation form is the IO representation, which we define from the behavioral point of view in this subsection. Before establishing our definition, we need the concept of IO partition for LPV systems.

In Section 2.1.2, the definition of IO partitions has been formulated for general dynamic systems. This applies to the LPV case as well:

Definition 3.9 (IO partition of a LPV system) *Let $\mathcal{S} = (\mathbb{T}, \mathbb{R}^{n_p}, \mathbb{R}^{n_w}, \mathfrak{B})$ be an LPV system. The partition of the signal space as $\mathbb{R}^{n_w} = \mathbb{U} \times \mathbb{Y} = \mathbb{R}^{n_u} \times \mathbb{R}^{n_y}$ with $n_u, n_y > 0$ and partition of $w \in \mathcal{L}_1^{\text{loc}}(\mathbb{T}, \mathbb{R}^{n_w})$ correspondingly with $u \in \mathcal{L}_1^{\text{loc}}(\mathbb{T}, \mathbb{U})$ and $y \in \mathcal{L}_1^{\text{loc}}(\mathbb{T}, \mathbb{Y})$ is called an IO partition of \mathcal{S} , if*

1. u is free, i.e. for all $u \in \mathcal{L}_1^{\text{loc}}(\mathbb{T}, \mathbb{U})$ and $p \in \mathfrak{B}_{\mathbb{P}}$, there exists a $y \in \mathcal{L}_1^{\text{loc}}(\mathbb{T}, \mathbb{Y})$ such that $(\text{col}(u, y), p) \in \mathfrak{B}$.
2. y does not contain any further free component, i.e. given u , none of the components of y can be chosen freely for every $p \in \mathfrak{B}_{\mathbb{P}}$ (maximally free).

An IO partition implies the existence of matrix-polynomial functions $R_y \in \mathcal{R}[\xi]^{n_y \times n_y}$ and $R_u \in \mathcal{R}[\xi]^{n_y \times n_u}$ with R_y full row rank, such that (3.17) can be written as

$$(R_y \left(\frac{d}{dt}\right) \diamond p)y = (R_u \left(\frac{d}{dt}\right) \diamond p)u, \quad (3.30)$$

with $n_w = n_u + n_y$. The corresponding behavior \mathfrak{B} is given by

$$\left\{ (u, y, p) \in \mathcal{L}_1^{\text{loc}}(\mathbb{R}, \mathbb{U} \times \mathbb{Y} \times \mathbb{P}) \mid (R_y \left(\frac{d}{dt}\right) \diamond p)y = (R_u \left(\frac{d}{dt}\right) \diamond p)u \text{ holds weakly} \right\},$$

with $\mathbb{U} = \mathbb{R}^{n_u}$ and $\mathbb{Y} = \mathbb{R}^{n_y}$. For those scheduling trajectories p , for which the maximum freedom of the input signal u holds in \mathfrak{B}_p , an IO partition defines a causal mapping in case the solutions of (3.30) are restricted to have left compact support. Otherwise, initial conditions also matter. Note that for some systems with IO partition (u, y) , it is not guaranteed for each $p \in \mathfrak{B}_{\mathbb{P}}$ that u is maximally free on \mathfrak{B}_p (see Definition 3.9). In other words, it can happen that some of the outputs become free for specific scheduling trajectories but not for all. However, such variables cannot be treated as general inputs. Similar to the LTI case, LPV systems with no IO partition are called autonomous. In case $n_u = n_y = 1$, systems are referred to as *Single-Input Single-Output* (SISO), while systems with $n_u > 1, n_y > 1$ are called *Multiple-Input Multiple-Output* (MIMO) systems.

Now it is possible to introduce IO representations of CT-LPV systems:

Definition 3.10 (CT-LPV-IO representation) *The continuous-time IO representation of $\mathcal{S} = (\mathbb{R}, \mathbb{P} \subseteq \mathbb{R}^{n_{\mathbb{P}}}, \mathbb{R}^{n_u+n_y}, \mathfrak{B})$ with scheduling vector p and IO partition (u, y) is denoted by $\mathfrak{R}_{\text{IO}}(\mathcal{S})$ and defined as a parameter-varying differential-equation system with order n_a :*

$$\sum_{i=0}^{n_a} (a_i \diamond p) \frac{d^i}{dt^i} y = \sum_{j=0}^{n_b} (b_j \diamond p) \frac{d^j}{dt^j} u, \quad (3.31)$$

where $a_j \in \mathcal{R}^{n_y \times n_y}$ and $b_j \in \mathcal{R}^{n_y \times n_u}$ with $a_{n_a} \neq 0$ and $b_{n_b} \neq 0$ are the meromorphic parameter-varying coefficients of the matrix polynomials R_u and R_y satisfying (3.30) with R_y full row rank. As u is maximally free, such polynomials exist with $n_a \geq n_b \geq 0$ and $n_a > 0$.

In terms of Theorem 3.1, any KR representation has a full row-rank equivalent, thus the existence of IO representations is guaranteed for any valid IO partition.

Example 3.6 (IO partition and representation) *In Example 3.1, the force w_F is free as it represents the inhomogeneous part of (3.6). Thus, $u = w_F$ can be considered as the input and $y = w_x$ as the output of the*

system. Let $w = [y \ u]^\top$ be the IO partition and $p = m$ be the scheduling signal. Then the behavior can be represented in the form of (3.30) with polynomials

$$R_y(\xi) \diamond p = \mathbf{k}_s + \left(\frac{d}{dt} p \right) \xi + p\xi^2, \quad R_u(\xi) \diamond p = 1, \quad (3.32)$$

Trivially, both R_y and R_u have full row rank. Then, (3.32) implies that the IO representation of the system is defined by

$$a_0 \diamond p = \mathbf{k}_s, \quad a_1 \diamond p = \frac{d}{dt} p, \quad a_2 \diamond p = p, \quad b_0 \diamond p = 1,$$

with $n_a = 1$ and $n_b = 0$.

In case of continuous-time LPV systems, the notion of transfer function or frequency response has no meaningful² interpretation. By using the approximative transfer function calculus of LTV systems (Matz and Hlawatsch 1998), some interpretation of these notions can be given for LPV systems. However, these concepts do not satisfy the relations of the LTI case. On the other hand, each element of the frozen system set $\mathcal{F}_\mathbb{P}$, is an LTI system. Therefore, each $\mathcal{F}_{\bar{p}} \in \mathcal{F}_\mathbb{P}$ has a transfer function $F_{\bar{p}}(s)$, a frequency response $F_{\bar{p}}(i\omega)$, and an impulse response $h_{\bar{p}}(t)$ with Markov parameters $\{\mathbf{g}_i^{(\bar{p})}\}_{i=0}^\infty$. The notion of frozen transfer function set or impulse response set can be established for any LPV system. The set of frozen poles or zeros follows similarly.

F. State-space representations

The introduction of latent variables and their associated representations are also essential for LPV systems as they give the mathematical concept of signals that corresponds to inner variables or states of the system. This interpretation of the global behavior directly follows the concept of the LTI case based on Definition 2.10. In the following we extend the definition of latent variables and the property of state to the LPV case. Then we introduce the state-kernel form, proving that all latent variable representations have a first order PV differential equation form. The latter property is used to define SS representations of LPV systems.

If the continuous-time LPV system contains n_L latent (eliminatable) and n_W manifest variables, then as a generalization of (3.17):

$$\left(R \left(\frac{d}{dt} \right) \diamond p \right) w = \left(R_L \left(\frac{d}{dt} \right) \diamond p \right) w_L \quad (3.33)$$

holds, where $w : \mathbb{R} \rightarrow \mathbb{R}^{n_W}$ is the manifest variable, $w_L : \mathbb{R} \rightarrow \mathbb{R}^{n_L}$ is the latent variable, $R \in \mathcal{R}[\xi]^{n_r \times n_w}$ and $R_L \in \mathcal{R}[\xi]^{n_r \times n_L}$ are polynomial matrices with meromorphic coefficients, and

$$\mathfrak{B}_L = \left\{ (w, w_L, p) \in \mathcal{L}_1^{\text{loc}}(\mathbb{R}, \mathbb{R}^{n_W} \times \mathbb{R}^{n_L} \times \mathbb{R}^{n_P}) \mid (3.33) \text{ holds weakly} \right\},$$

²Some authors (Wei 2006; Paijmans et al. 2006; Nichols et al. 1993) introduce LPV transfer functions with varying parameters. As they commonly refer only to the collection of transfer functions associated with $\mathcal{F}_\mathbb{P}$, this notion of the LPV transfer function is misleading.

is the full behavior of the latent representation (3.33), while the associated manifest behavior is defined as

$$\mathfrak{B} = \{(w, p) \in \mathcal{L}_1^{\text{loc}}(\mathbb{R}, \mathbb{R}^{n_w} \times \mathbb{R}^{n_p}) \mid \exists w_L \in \mathcal{L}_1^{\text{loc}}(\mathbb{R}, \mathbb{R}^{n_L}) \text{ s.t. } (w, w_L, p) \in \mathfrak{B}_L\}.$$

Based on the result of Zerz (2006) for LTV systems, it is possible to prove that elimination of latent variables is always possible on $\mathcal{R}[\xi]^{\times \cdot}$. This, so called, *elimination property* implies that if \mathfrak{B}_L corresponds to a LPV system, then \mathfrak{B} also corresponds to an LPV system. Now it is possible to extend the concept of state in terms of Definition 2.11 to LPV systems:

Definition 3.11 (Property of state for LPV systems) Consider a PV system \mathcal{G}_P with a latent variable w_L . Let $(w_1, w_{L,1}, p), (w_2, w_{L,2}, p) \in \mathfrak{B}_L$ and $t_0 \in \mathbb{T}$. In case $\mathbb{T} = \mathbb{R}$, assume that $w_{L,1}$ and $w_{L,2}$ are continuous on \mathbb{R} . Define

$$(w, w_L) = (w_1, w_{L,1}) \underset{t_0}{\wedge} ((w_2, w_{L,2}), \quad (3.34)$$

as the concatenation of $(w_1, w_{L,1})$ and $(w_2, w_{L,2})$ at t_0 (see (2.16)). If every $(w_1, w_{L,1}, p), (w_2, w_{L,2}, p) \in \mathfrak{B}_L$ with $w_{L,1}(t_0) = w_{L,2}(t_0)$ implies that $(w, w_L, p) \in \mathfrak{B}_L$, then \mathfrak{B}_L is called a *state-space behavior*, and the latent variable w_L is called the *state*.

In terms of Definition 3.11, w_L needs to qualify as a state for each scheduling trajectory of \mathfrak{B}_P .

Example 3.7 (Latent variable representation) By considering the system in Example 3.1 with scheduling $p = m$ and $\mathbb{P} = [1, 2]$, the following latent variable representation of the model has the same manifest behavior:

$$\begin{bmatrix} -k_s & 1 \\ 0 & 0 \\ 1 & 0 \end{bmatrix} \begin{bmatrix} w_x \\ w_F \end{bmatrix} = \begin{bmatrix} \frac{d}{dt} & 0 \\ -\frac{1}{p} & \frac{d}{dt} \\ 0 & 1 \end{bmatrix} w_L. \quad (3.35)$$

This can be proved by substituting the third row of (3.35) into the second row, giving

$$w_{L,1} = p \frac{d}{dt} w_F.$$

Substitution of the previous equation into the first row of (3.35) gives a PV difference equation (DF) in the variables w_x and w_F , which is equal to (3.18). Any $w_L \in \mathcal{L}_1^{\text{loc}}(\mathbb{R}, \mathbb{R}^2)$ satisfying weakly the previous equations, trivially fulfills the property of state.

To decide whether a latent variable is a state, the following theorem is important:

Theorem 3.2 (State-kernel form) The latent variable w_L is a state, iff there exist matrices $r_w \in \mathcal{R}^{n_r \times n_w}$ and $r_0, r_1 \in \mathcal{R}^{n_r \times n_L}$ such that the full behavior \mathfrak{B}_L has the kernel representation:

$$r_w w + r_0 w_L + r_1 \xi w_L = 0. \quad (3.36)$$

The proof is given in Appendix A.1. Again, as a convention, we assume that the state latent variables are chosen in such way that in (3.33), $\deg(R_L) = 1$, while $\deg(R) = 0$ and R_L is monic. In this way, a CT-LPV *state-space* (SS) behavior is defined by a first-order meromorphic-coefficient DE. Now we can give the definition of SS representations of a continuous-time \mathcal{S} :

Definition 3.12 (CT-LPV-SS representation) *The continuous-time state-space representation of $\mathcal{S} = (\mathbb{R}, \mathbb{P} \subseteq \mathbb{R}^{n_{\mathbb{P}}}, \mathbb{R}^{n_{\mathbb{U}} + n_{\mathbb{V}}}, \mathfrak{B})$ with scheduling vector p is denoted by $\mathfrak{R}_{\text{SS}}(\mathcal{S})$ and defined as a first-order parameter-varying differential equation system in the latent variable $x : \mathbb{R} \rightarrow \mathbb{X}$:*

$$\frac{d}{dt}x = (A \diamond p)x + (B \diamond p)u, \quad (3.37a)$$

$$y = (C \diamond p)x + (D \diamond p)u, \quad (3.37b)$$

where (u, y) is the IO partition of \mathcal{S} , x is the state-vector, $\mathbb{X} = \mathbb{R}^{n_{\mathbb{X}}}$ is the state-space,

$$\mathfrak{B}_{\text{SS}} = \{(u, x, y, p) \in \mathcal{L}_1^{\text{loc}}(\mathbb{R}, \mathbb{U} \times \mathbb{X} \times \mathbb{Y} \times \mathbb{P}) \mid (3.37a) \ \& \ (3.37b) \ \text{hold weakly}\},$$

is the full behavior of the manifest behavior \mathfrak{B} , and

$$\left[\begin{array}{c|c} A & B \\ \hline C & D \end{array} \right] \in \left[\begin{array}{c|c} \mathcal{R}^{n_{\mathbb{X}} \times n_{\mathbb{X}}} & \mathcal{R}^{n_{\mathbb{X}} \times n_{\mathbb{U}}} \\ \hline \mathcal{R}^{n_{\mathbb{Y}} \times n_{\mathbb{X}}} & \mathcal{R}^{n_{\mathbb{Y}} \times n_{\mathbb{U}}} \end{array} \right],$$

represents the meromorphic parameter-varying state-space matrices (matrix functions) of $\mathfrak{R}_{\text{SS}}(\mathcal{S})$.

Example 3.8 (SS representation) *Continuing Example 3.7, the LPV state-space representation of the model follows by taking $[y \ u]^{\top} = [w_{\mathbb{X}} \ w_{\mathbb{F}}]^{\top}$ as the IO partition and $x = w_{\mathbb{L}}$ as the state:*

$$\begin{aligned} \frac{d}{dt}x &= \begin{bmatrix} 0 & 0 \\ \frac{1}{p} & 0 \end{bmatrix} x + \begin{bmatrix} -k_{\text{S}} & 1 \\ 0 & 0 \end{bmatrix} \begin{bmatrix} y \\ u \end{bmatrix}, \\ y &= \begin{bmatrix} 0 & 1 \end{bmatrix} x. \end{aligned}$$

By substitution of the second equation into the first one, the state equation (3.37a) results, while the second equation gives the output equation (3.37b). Thus the corresponding SS representation is

$$\left[\begin{array}{c|c} A \diamond p & B \diamond p \\ \hline C \diamond p & D \diamond p \end{array} \right] = \left[\begin{array}{c|c} 0 & -k_{\text{S}} \\ \frac{1}{p} & 0 \\ \hline 0 & 1 \end{array} \right].$$

Note that in the full behavior \mathfrak{B}_{SS} , the latent variable x trivially fulfills the state property in terms of Theorem 3.2. Additionally, this behavioral type of definition of CT-SS representations includes the definition of LPV state-space models used in the state-of-the-art of LPV control. In those models, the dependence of the matrix functions are assumed to be rational and static, which is trivially included in \mathcal{R} . Similar to LPV-IO representations the notions of transfer function, frequency response, and impulse response can only be defined in a frozen sense for LPV-SS representations.

3.1.3 Representations of discrete-time LPV systems

The concept of *discrete-time* (DT) parameter-varying dynamical systems is also important for engineering applications. In the following we formulate the behavioral

framework for DT-LPV systems. First we investigate the concept of DT parameter-varying systems and then we define their KR, SS, IO representations. To do so, we use the previously developed ring of polynomials $\mathcal{R}[\xi]$ with meromorphic coefficient functions. Due to the time operator q substituted as the indeterminate of these polynomials in the DT case, we show that the non-commutative multiplication rule in $\mathcal{R}[\xi]$ is different than in CT case, but the algebraic structure remains the same. This property provides that the previously developed theories extend to the DT case.

A. The discrete-time parameter-varying concept

In discrete-time, the time-axis is restricted to $\mathbb{T} = \mathbb{Z}$. Signals on this axis can be viewed (but not necessarily) as observations of continuous-time signal trajectories at equidistant time points. This concept is called periodic, equidistant sampling that defines the DT projection of a CT signal $w : \mathbb{R} \rightarrow \mathbb{W}$ as $w' : \mathbb{Z} \rightarrow \mathbb{W}$ satisfying

$$w'(k) = w(kT_d), \quad \forall k \in \mathbb{Z}, \quad (3.38)$$

with discretization-step $T_d \in \mathbb{R}^+$. However in the parameter-varying case, the scheduling signal is also restricted to the DT time-axis as its observations are only available at the sampling instants. Thus, the DT projection of a CT scheduling signal $p : \mathbb{R} \rightarrow \mathbb{P}$ is defined as $p' : \mathbb{Z} \rightarrow \mathbb{P}$ satisfying

$$p'(k) = p(kT_d), \quad \forall k \in \mathbb{Z}. \quad (3.39)$$

In this way, we call $\mathcal{G}' = (\mathbb{Z}, \mathbb{W}, \mathbb{P}, \mathfrak{B}')$ the DT equivalent of $\mathcal{G} = (\mathbb{R}, \mathbb{W}, \mathbb{P}, \mathfrak{B})$ under the sampling time T_d if

$$\mathfrak{B}' = \{(w', p') \in (\mathbb{W} \times \mathbb{P})^{\mathbb{Z}} \mid \exists (w, p) \in \mathfrak{B} \text{ s.t. (3.38) \& (3.39) hold}\}. \quad (3.40)$$

Note that for arbitrary T_d it is not guaranteed that there exists a DT-LPV system such that (3.40) is satisfied. On the other hand, not every DT-LPV system is equivalent with a sampled CT-LPV system. Thus sampling provides only a particular viewpoint for understanding DT systems and it must be emphasized that DT-LPV systems are a stand alone mathematical concept of modeling just like in the LTI case. Additionally, the time projection is defined on the signals and not on their derivatives. This means that finding the DT equivalent of a $\mathcal{G} = (\mathbb{R}, \mathbb{W}, \mathbb{P}, \mathfrak{B})$, described by a differential equation with meromorphic coefficients dependent on p and its derivatives, is a non-trivial problem (see Section 6.2).

B. Polynomials over \mathcal{R}

In the following, the DT analog of the concepts introduced in the CT-LPV case is developed. Similar to the LTI case, the time operator that we use in the discrete-time PV case to define difference equations is the forward-time shift operator q . Such difference equations are used to describe the behavior of DT-LPV systems. However, the operator q has different properties than $\frac{d}{dt}$, used in the CT case.

Additionally, q being the time operator also implies that the coefficients in the DT case are dependent on p and its time-shifted versions. Due to these differences, in the following we reformulate concepts of coefficient dependence (association of coefficient variables with the scheduling) and commutation rules of multiplication in $\mathcal{R}[\xi]$ in order to define the analog of the concepts of the CT case.

As a first step, we define the variable association of the coefficient functions $r \in \mathcal{R}$ with elements of p and their forward and backward time-shifts. Note that in the DT case, dependence on both forward and backward time-shifts of p is required in order to establish equivalence transformations (state elimination/construction) between SS and IO representations of the system. Thus, labeling of the variables must contain positive and negative indexes as well.

For a fixed scheduling dimension $n_{\mathbb{P}} > 0$, denote the variables of a $r \in \bar{\mathcal{R}}_n$ (n -dimensional function in \mathcal{R}) as:

$$\{\zeta_{ij}\}_{n_{\zeta}, n_{\mathbb{P}}, \tau} := \{\zeta_{01}, \zeta_{02}, \dots, \zeta_{0\tau}\},$$

with $n_{\zeta} = 0$ and $\tau = n$ if $n \leq n_{\mathbb{P}}$. In case of $n > n_{\mathbb{P}}$, denote the variables as

$$\{\zeta_{ij}\}_{n_{\zeta}, n_{\mathbb{P}}, \tau} := \{\zeta_{0,1}, \dots, \zeta_{0,n_{\mathbb{P}}}, \zeta_{1,1}, \dots, \zeta_{1,n_{\mathbb{P}}}, \zeta_{-1,1}, \dots, \zeta_{-1,n_{\mathbb{P}}}, \zeta_{2,1}, \dots, \zeta_{\tau_1, \tau_2}\}$$

where $n = (2n_{\zeta} - 1)n_{\mathbb{P}} + \tau$ with $n_{\zeta} > 0$ and $0 < \tau \leq 2n_{\mathbb{P}}$ and

$$(\tau_1, \tau_2) = \begin{cases} (n_{\zeta}, \tau) & \text{if } \tau \leq n_{\mathbb{P}}; \\ (-n_{\zeta}, \tau - n_{\mathbb{P}}) & \text{if } \tau > n_{\mathbb{P}}. \end{cases} \quad (3.41)$$

The basic mechanism of this variable labeling scheme is presented in Figure 3.3 for $n_{\mathbb{P}} = 2$ and $n = 1, \dots, 6$. In this figure in each row, the yellow dots represent the labels of the variables for a n -variable coefficient function. Note that for all finite dimensions, this labeling sequence is unique.

Now we can associate the variables $\{\zeta_{ij}\}_{n_{\mathbb{P}}, n_{\zeta}, \tau}$ of a $r \in \mathcal{R}$ as

$$\zeta_{ij} = q^i p_j, \quad (3.42)$$

where p_j is the j^{th} element of p , $n_{\mathbb{P}}$ is the dimension of p , $n_{\zeta} \in \mathbb{N}$ is the maximal order of the shifted versions of p on which r is dependent. For an example of this variable association and the associated coefficient dependence see Example 3.9.

Example 3.9 (Coefficient function) Let $\mathbb{P} = \mathbb{R}^{n_{\mathbb{P}}}$ with $n_{\mathbb{P}} = 2$. Consider the real-meromorphic coefficient function $r : \mathbb{R}^3 \rightarrow \mathbb{R}$ defined as

$$r(\mathbf{x}_1, \mathbf{x}_2, \mathbf{x}_3) = \frac{1 + \mathbf{x}_3}{1 - \mathbf{x}_2}.$$

Associate $\{\zeta_{ij}\}_{1,2,1} = \{\zeta_{01}, \zeta_{02}, \zeta_{11}\}$ with $\{\mathbf{x}_1, \mathbf{x}_2, \mathbf{x}_3\}$. Then for a scheduling trajectory $p : \mathbb{R} \rightarrow \mathbb{R}^2$:

$$(r \diamond p)(k) = r(p_1, p_2, qp_1,)(k) = \frac{1 + p_1(k+1)}{1 - p_2(k)}.$$

In order to introduce PV difference equations in DT, it is required to evaluate a given coefficient function $r \in \mathcal{R}$ for a given scheduling trajectory $p \in \mathfrak{B}_{\mathbb{P}}$

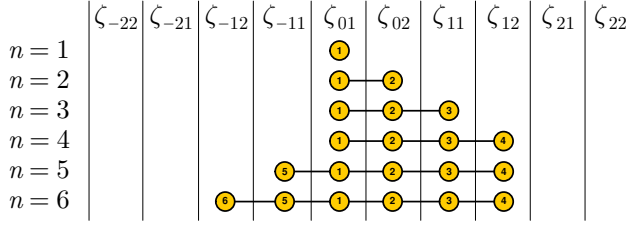


Figure 3.3: Labeling scheme for the variables of meromorphic coefficient functions $r : \bar{\mathcal{R}}_n$ for $n_{\mathbb{P}} = 2$ and $n = 1, \dots, 6$.

according to the association rule (3.42). For this purpose, define the operator $\diamond : (\mathcal{R}, \mathfrak{B}_{\mathbb{P}}) \rightarrow (\mathbb{R}^{\mathbb{Z}})$ in DT as:

$$r \diamond p = r \left(\left\{ q^i p_j \right\}_{n_{\zeta}, n_{\mathbb{P}}, \tau} \right) = r(p, qp, q^{-1}p, \dots). \quad (3.43)$$

With the association rule (3.42) and evaluation operator (3.43) in mind, we can use polynomial matrices in $\mathcal{R}^{n_r \times n_w}$ to define a parameter-varying difference equation with n_r rows and signal dimension n_w as follows:

$$(R(q) \diamond p)w = \sum_{i=0}^{n_{\xi}} (r_i \diamond p)q^i w = 0, \quad (3.44)$$

where $R \in \mathcal{R}[\xi]^{n_r \times n_w}$, $\deg(R) = n_{\xi}$, and $r_i \in \mathcal{R}^{n_r \times n_w}$ for all $i \in \mathbb{I}_0^{n_{\xi}}$. PV differential equations in the form (3.44) are used to define the class of DT-LPV systems we consider in this thesis. It will be shown, that this class contains all the popular definitions of LPV-SS and IO models used in LPV system identification.

Example 3.10 (PV difference equation) Consider again Example 3.1. Let $0 < T_d \ll 1$ and develop an approximation of the CT behavior of this system through the Euler type of approximation:

$$\frac{d}{dt}w \approx \frac{qw' - w'}{T_d}, \quad (3.45)$$

where $w'(k) = w(kT_d)$ for all $k \in \mathbb{Z}$. Repeated substitution of (3.45) for the derivatives of m , w_x , and w_F in (3.6) yields³

$$(T_d^2 \mathbf{k}_s + m(k))w_x(k) - (m(k+1) + m(k))w_x(k+1) + m(k+1)w_x(k+2) = T_d^2 w_F(k), \quad (3.46)$$

where the time index k denotes the values of the signals at kT_d on \mathbb{R} . We consider these signals as DT signals in the following. Let $p = m$ with a scheduling space $\mathbb{P} = [1, 2]$ and let $w = [w_x \ w_F]^T$. Then the difference equation (3.46), which defines the possible signal trajectories of the DT approximation of the mass-spring system, can be written in the form of (3.44) with $n_w = 2$, $n_{\xi} = 1$, $n_{\mathbb{P}} = 1$, and

$$p_0 \diamond p = \begin{bmatrix} T_d^2 \mathbf{k}_s + p & -T_d^2 \end{bmatrix}, \quad p_1 \diamond p = \begin{bmatrix} -qp - p & 0 \end{bmatrix}, \quad p_2 \diamond p = \begin{bmatrix} qp & 0 \end{bmatrix}.$$

So far we have used the polynomials of the ring $\mathcal{R}[\xi]^{n_r \times n_w}$ to define parameter-varying difference equations. Thus, by using the algebraic structure of this ring

³Note that applying the Euler derivative approximation on different representations (SS, IO, etc.) can result in inequivalent DT descriptions.

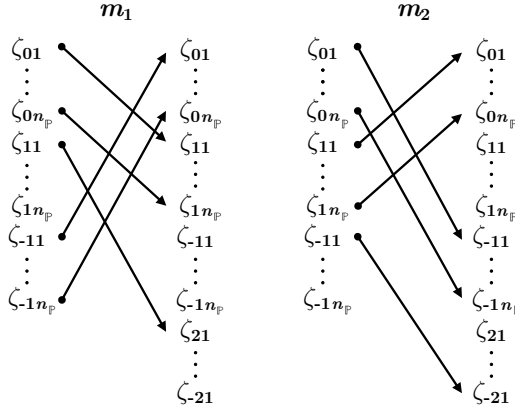


Figure 3.4: Variable assignment by the functions m_1 and m_2 in Definition 3.13.

we can develop the analog of the CT results using similar arguments. However, an important difference with the CT case is that multiplication in $\mathcal{R}[\xi]^{n_r \times n_w}$ obeys a different non-commutative rule in the DT case. To explore the non-commutative multiplication rule by $\xi = q$, first introduce the *shift operators* on \mathcal{R} , to describe time-shifts of parameter-varying coefficient functions:

Definition 3.13 (Shift operators) Let $r \in \bar{\mathcal{R}}_n$. For a given $n_p > 0$, denote the variables of r as $\{\zeta_{ij}\}_{n_\zeta, n_p, \tau}$ based on the previously introduced labeling. The forward-shift and backward-shift operators on \mathcal{R} are defined as

$$\vec{r} = \mathcal{U}_*(r \circ m_1), \quad (3.47a)$$

$$\overleftarrow{r} = \mathcal{U}_*(r \circ m_2), \quad (3.47b)$$

where \circ denotes the function concatenation, $m_1, m_2 \in \mathcal{R}_{n+2n_p}^n$, and m_1 assigns each variable ζ_{ij} to $\zeta_{(i+1)j}$, while m_2 assigns each variable ζ_{ij} to $\zeta_{(i-1)j}$ as depicted in Figure 3.4.

In other words, if $r \diamond p$ is dependent on for example p and qp , then \vec{r} is the “same” function (disregarding the number of variables) except it is now dependent on qp and q^2p . Similarly, \overleftarrow{r} is also the “same” as r except it is now dependent on $q^{-1}p$ and p . In this way, the shift operators describe time-shifts on the parameter-varying coefficient functions just like the dot operator describe differentiation in CT (see Example 3.11). The shift operators fulfill the following rules for any $r_1, r_2 \in \mathcal{R}$:

$$\left\{ \begin{array}{ll} \text{if } r = r_1 \pm r_2 & \text{then } \vec{r} = \vec{r}_1 \pm \vec{r}_2 \quad \text{and} \quad \overleftarrow{r} = \overleftarrow{r}_1 \pm \overleftarrow{r}_2, \\ \text{if } r = r_1 r_2 & \text{then } \vec{r} = \vec{r}_1 \vec{r}_2 \quad \text{and} \quad \overleftarrow{r} = \overleftarrow{r}_1 \overleftarrow{r}_2, \\ \text{if } r = \frac{r_1}{r_2} & \text{then } \vec{r} = \frac{\vec{r}_1}{\vec{r}_2} \quad \text{and} \quad \overleftarrow{r} = \frac{\overleftarrow{r}_1}{\overleftarrow{r}_2}. \end{array} \right.$$

Example 3.11 (Shift operators) Consider the coefficient function r given in Example 3.9. Then

$$\overrightarrow{r}(\{\zeta_{ij}\}_{2,2,1}) = \frac{1 + \zeta_{21}}{1 - \zeta_{12}}, \quad \overleftarrow{r}(\{\zeta_{ij}\}_{1,2,4}) = \frac{1 + \zeta_{01}}{1 - \zeta_{-12}}.$$

For a scheduling trajectory $p : \mathbb{R} \rightarrow \mathbb{R}^2$, it holds that

$$(\overrightarrow{r} \diamond p)(k) = \frac{1 + p_1(k+2)}{1 - p_2(k+1)}, \quad (\overleftarrow{r} \diamond p)(k) = \frac{1 + p_1(k)}{1 - p_2(k-1)}.$$

Multiplication on $\mathcal{R}[\xi]$ with ξ now can be defined through the forward-shift operator using the non-commutative rule:

$$\xi r = \overrightarrow{r} \xi, \quad (3.48)$$

where $r \in \mathcal{R}$. With the non-cumulative multiplication rule (3.48) it is possible to show that $\mathcal{R}[\xi]$ still defines an Ore algebra (Chyzak and Salvy 1998). Due to the fact that all required algebraic properties are still satisfied for $\mathcal{R}[\xi]$ the proof of the injective cogenerator property similarly follows in DT. The latter property implies that the theorems, introduced and used in Section 3.1.2, also hold in the DT case.

C. Kernel representations

As a next step, we develop the concept of KR representations of DT-LPV systems following the same line of discussion as in the CT case.

In discrete-time, all trajectories in $(\mathbb{W} \times \mathbb{P})^{\mathbb{Z}}$ that satisfy (3.44) are considered as solutions. Now we can give the definition of KR representations of LPV dynamic systems as follows:

Definition 3.14 (DT-KR-LPV representation) The parameter-varying difference equation (3.44) is called a discrete-time kernel representation, denoted by $\mathfrak{R}_K(\mathcal{S})$, of the LPV dynamical system $\mathcal{S} = (\mathbb{Z}, \mathbb{R}^{n_{\mathbb{P}}}, \mathbb{R}^{n_{\mathbb{W}}}, \mathfrak{B})$ with scheduling vector p and signals w , if

$$\mathfrak{B} = \{(w, p) \in (\mathbb{R}^{n_{\mathbb{W}}} \times \mathbb{R}^{n_{\mathbb{P}}})^{\mathbb{Z}} \mid (R(q) \diamond p)w = 0\}.$$

Note that in the LPV system class, we consider LPV systems with $\mathbb{T} = \mathbb{Z}$ that have a KR representation, so existence of such a representation is explicitly assumed in the following. We denote the DT-KR representation of a CT-LPV dynamical system $\mathcal{S} = (\mathbb{R}, \mathbb{P}, \mathbb{R}^{n_{\mathbb{W}}}, \mathfrak{B})$ by $\mathfrak{R}_K(\mathcal{S}, T_d)$, if the DT behavior \mathfrak{B}' of this representation is equivalent in terms of (3.40) with \mathfrak{B} under T_d .

The existence of full row rank representations follows directly:

Theorem 3.3 (Existence of full row rank KR representation) Let \mathfrak{B} be given with a KR representation (3.44). Then \mathfrak{B} can also be represented by a $R \in \mathcal{R}[\xi]^{\cdot \times n_{\mathbb{W}}}$ with full row rank.

The proof follows similarly as in Zerz (2006) due to the algebraic properties of $\mathcal{R}[\xi]$. This theorem has a crucial importance as the concept of minimality for KR representations is also based on the full row rank of the associated matrix polynomials R . (see Chapter 3.2).

D. Input-output representations

IO representations are also important for the DT behavioral framework of LPV systems. Beside system theoretical aspects, this type of representations connects the developed behavioral theory to IO models used in the-state-of-the-art of LPV system identification. In this way, it enables comparison and analysis of IO identification methods. In the following, we define DT-IO representations from the behavioral point of view, based on the same line of discussion as in the CT case.

For DT-LPV systems, IO partitions are also characterized by Definition 3.9. The existence of IO partition (u, y) implies the existence of matrix polynomials $R_y \in \mathcal{R}[\xi]^{n_y \times n_y}$ and $R_u \in \mathcal{R}[\xi]^{n_y \times n_u}$ with R_y full row rank, such that (3.44) can be written in a similar form as (3.30). Based on this, it is possible to introduce IO representations of DT-LPV systems as follows:

Definition 3.15 (DT-LPV-IO representation) *The discrete-time IO representation of $\mathcal{S} = (\mathbb{Z}, \mathbb{P} \subseteq \mathbb{R}^{n_p}, \mathbb{R}^{n_u+n_y}, \mathfrak{B})$ with IO partition (u, y) and scheduling vector p is denoted by $\mathfrak{R}_{\text{IO}}(\mathcal{S})$ and defined as a parameter-varying difference-equation system with order n_a :*

$$\sum_{i=0}^{n_a} (a_i \diamond p) q^i y = \sum_{j=0}^{n_b} (b_j \diamond p) q^j u, \quad (3.49)$$

where $a_j \in \mathcal{R}^{n_y \times n_y}$ and $b_j \in \mathcal{R}^{n_y \times n_u}$ with $a_{n_a} \neq 0$ and $b_{n_b} \neq 0$ are the meromorphic parameter-varying coefficients of the matrix polynomials R_u and full row rank R_y with $n_a \geq n_b \geq 0$ and $n_a > 0$.

Note that the coefficient dependencies in Definition 3.15 can be polynomial functions of p . Thus the behavioral definition of IO representations also contains the IO models used in LPV system identification (see Chapter 1). By defining $u(k) := u(kT_d)$ and $y(k) := y(kT_d)$, the DT-IO representation, denoted by $\mathfrak{R}_{\text{IO}}(\mathcal{S}, T_d)$, of a CT-LPV system \mathcal{S} with scheduling p and IO partition (u, y) can similarly be given with equivalent behaviors in terms of (3.40) under the sampling-time T_d . Note that the discrete-time projection with arbitrary T_d can change the validity of the IO partition as dynamic components of the system can be lost due to slow sampling. Thus, it is important to emphasize that existence of $\mathfrak{R}_{\text{IO}}(\mathcal{S}, T_d)$ is not guaranteed.

Example 3.12 (IO partition and representation) *In Example 3.10, the sampled force variable w_x is still a free variable as it represents the inhomogen part of difference equation (3.46). Thus the choice of $w = [y \quad u]^T = [w_x \quad w_F]^T$ yields a valid IO partition. With m being the scheduling signal, the discrete-time PV behavior can be represented in the form of (3.49) with polynomials*

$$R_y(\xi) = a_0 + a_1\xi + a_2\xi^2, \quad R_u(\xi) = b_0,$$

which have coefficients:

$$a_0 \diamond p = T_d^2 k_s + p, \quad a_1 \diamond p = -p - qp, \quad a_2 \diamond p = qp, \quad b_0 \diamond p = T_d^2.$$

Obviously, $R_y(\xi)$ have full row rank. This implies that $R_y(\xi)$ and $R_u(\xi)$ define an IO representation of the model with coefficients as above.

Similar to the CT-LPV case, the notion of transfer functions for DT-LPV systems is not well-defined. The introduction of a viable formulation can be tackled via the formal series approach of Kamen et al. (1985), constructed for DT-SS systems of the LTV case. However, the extension of this approximative transfer function calculus to the class of systems considered here is not available. The notion of frozen transfer functions, frequency responses, impulse responses, poles, and zeros can be similarly defined for the frozen system set as in the CT case.

F. State-space representations

For the discrete-time LPV behavior \mathfrak{B} , we can also introduce latent variables with the property of state (see Definition 3.11). Existence of latent variable representations with equivalent LPV manifest behaviors is guaranteed in the DT case as Theorem 3.2 holds regardless whether ξ is associated with q or $\frac{d}{dt}$ (see Example 3.13). Furthermore, the elimination property also applies for the DT case.

Example 3.13 (Latent variable representation) *By considering the DT system in Example 3.10 with scheduling $p = m$ and $\mathbb{P} = [1, 2]$, the following latent variable representation of the model has the same manifest behavior:*

$$\begin{bmatrix} T_d^2 k_s + p & -T_d^2 \\ (-p - q^{-1}p) & 0 \\ (-q^{-1}p) & 0 \end{bmatrix} \begin{bmatrix} w_x \\ w_F \end{bmatrix} = \begin{bmatrix} q & 0 \\ -1 & q \\ 0 & 1 \end{bmatrix} w_L. \quad (3.50)$$

This can be proved by substituting the third row of (3.50) into the second row, giving

$$w_{L,1} = (p + q^{-1}p)w - pqw.$$

Substitution of the previous equation into the first row of (3.50) gives a PV difference equation in the variables w_x and w_F , which is equal to (3.46). Note, that any $w_L \in (\mathbb{R}^2)^{\mathbb{Z}}$ satisfying (3.50) trivially fulfills the property of state.

Now we can introduce SS representations of DT-LPV systems as follows:

Definition 3.16 (DT-LPV-SS representation) *The discrete-time state-space representation of $\mathcal{S} = (\mathbb{Z}, \mathbb{P} \subseteq \mathbb{R}^{n_{\mathbb{P}}}, \mathbb{R}^{n_{\mathbb{U}} + n_{\mathbb{Y}}}, \mathfrak{B})$ with scheduling vector p is denoted by $\mathfrak{R}_{\text{SS}}(\mathcal{S})$ and defined as a first-order parameter-varying difference equation system in the latent variable $x : \mathbb{Z} \rightarrow \mathfrak{X}$:*

$$qx = (A \diamond p)x + (B \diamond p)u, \quad (3.51a)$$

$$y = (C \diamond p)x + (D \diamond p)u, \quad (3.51b)$$

where (u, y) is the IO partition of \mathcal{S} , x is the state-vector, $\mathfrak{X} \subseteq \mathbb{R}^{n_{\mathfrak{X}}}$ is the state-space,

$$\mathfrak{B}_{\text{SS}} = \{ (u, x, y, p) \in (\mathbb{U} \times \mathfrak{X} \times \mathbb{Y} \times \mathbb{P})^{\mathbb{Z}} \mid (3.51a) \ \& \ (3.51b) \ \text{holds} \},$$

is the full behavior of the manifest behavior \mathfrak{B} , and

$$\left[\begin{array}{c|c} A & B \\ \hline C & D \end{array} \right] \in \left[\begin{array}{c|c} \mathcal{R}^{n_{\mathfrak{X}} \times n_{\mathfrak{X}}} & \mathcal{R}^{n_{\mathfrak{X}} \times n_{\mathbb{U}}} \\ \hline \mathcal{R}^{n_{\mathbb{Y}} \times n_{\mathfrak{X}}} & \mathcal{R}^{n_{\mathbb{Y}} \times n_{\mathbb{U}}} \end{array} \right],$$

represents the parameter-varying state-space matrices of $\mathfrak{R}_{\text{SS}}(\mathcal{S})$.

Again in the full behavior \mathfrak{B}_{SS} , the latent variable x trivially fulfills the state property. Also the class of SS representations formulated by Definition 3.16 contains the SS models used in LPV system identification as the coefficient dependencies in the behavioral definition can be linear functions of p . This enables the analysis and comparison of the results of LPV-SS system identification. The DT-SS representation of a CT-LPV dynamical system $\mathcal{S} = (\mathbb{R}, \mathbb{P}, \mathbb{R}^{n_u + n_y}, \mathfrak{B})$ is denoted as $\mathfrak{R}_{\text{SS}}(\mathcal{S}, T_d)$, where the manifest behavior of $\mathfrak{R}_{\text{SS}}(\mathcal{S}, T_d)$ is equivalent in terms of (3.40) with \mathfrak{B} under the sampling-time T_d . As before, existence of such representations is not guaranteed for arbitrary T_d .

Example 3.14 (SS representation) Continuing Example 3.13, the LPV state-space representation of the model follows by taking $[y \ u]^T = [w_x \ w_F]^T$ as the IO partition and $x = w_L$ as the state:

$$qx = \begin{bmatrix} 0 & 0 \\ 1 & 0 \end{bmatrix} x + \begin{bmatrix} T_d^2 k_s - p & -1 \\ -p - q^{-1}p & 0 \end{bmatrix} \begin{bmatrix} y \\ u \end{bmatrix}, \quad (3.52)$$

$$y = \begin{bmatrix} 0 & \frac{1}{-q^{-1}p} \end{bmatrix} x. \quad (3.53)$$

By substitution of the second equation into the first one, the state equation in the form of (3.51a) results, while the second equation gives the output equation in the form of (3.51b). Thus, the corresponding SS representation is

$$\left[\begin{array}{c|c} A \diamond p & B \diamond p \\ \hline C \diamond p & D \diamond p \end{array} \right] = \left[\begin{array}{c|c} 0 & \frac{p - T_d^2 k_s}{q^{-1}p} \\ 1 & 1 + \frac{p}{q^{-1}p} \\ \hline 0 & \frac{-1}{q^{-1}p} \end{array} \middle| \begin{array}{c} -1 \\ 0 \\ 0 \end{array} \right].$$

Similar to LPV-IO representations, the notion of transfer function, frequency response, and impulse response can only be defined in a frozen sense for LPV-SS representations.

3.2 Equivalence classes and relations

In this section, we continue the introduction of the LPV behavioral framework by defining equivalence relations and classes for the introduced representation forms. These are essential aspects of the theory as they characterize which representations describe the same system, providing tools to compare and analyze representation capabilities/validity of LPV models for identification. In the upcoming discussion, we systematically extend the concepts introduced in Section 2.1.4. First we define equality of behaviors and investigate why this equality needs to be understood in an almost everywhere sense to express equivalence of representations. Then, we define equivalency, equivalence relations and equivalence classes of all representation forms together with the concept of minimality and canonical forms. To do so, we introduce key theorems of left/right side unimodular transformations based on the results of the LTV behavioral framework. To support these theorems, we also introduce the required concept of the Jacobson form (similar to the Smith-McMillan form in the LTI case).

The most important concept to begin with is to define equality with respect to behaviors of PV systems. Based on Definition 2.16, we introduce the following definition:

Definition 3.17 (Equal behaviors of PV systems) Let $\mathfrak{B}_1, \mathfrak{B}_2 \subseteq (\mathbb{W} \times \mathbb{P})^{\mathbb{T}}$ with $\mathbb{W} = \mathbb{R}^{n_{\mathbb{W}}}$, $\mathbb{P} \subseteq \mathbb{R}^{n_{\mathbb{P}}}$, and with \mathbb{T} equal to either \mathbb{R} or \mathbb{Z} . We call \mathfrak{B}_1 and \mathfrak{B}_2 equal, if in case of $\mathbb{T} = \mathbb{R}$:

$$(w, p) \in \mathfrak{B}_1 \cap \mathcal{C}^{\infty}(\mathbb{R}, \mathbb{W} \times \mathbb{P}) \Leftrightarrow (w, p) \in \mathfrak{B}_2 \cap \mathcal{C}^{\infty}(\mathbb{R}, \mathbb{W} \times \mathbb{P}), \quad (3.54)$$

or in the discrete-time case ($\mathbb{T} = \mathbb{Z}$):

$$(w, p) \in \mathfrak{B}_1 \Leftrightarrow (w, p) \in \mathfrak{B}_2. \quad (3.55)$$

Two systems are called equal if they have equal behaviors. However, it is important to remark that Definition 3.17 establishes the concept of equal behaviors in terms of internal, and hence not external equality. This means, that even if two LPV systems have the same behavior in terms of IO signals for a particular IO partition, they are not necessarily equal as their scheduling signals or latent variables can differ. In case of systems with latent variables, equality can be defined in terms of the equality of the manifest behaviors (see Definition 3.26). On the other hand, there also exist systems with equal signal behavior and isomorphic projected scheduling behavior (see Example 3.15). However, due to technical reasons, we do not consider such systems to be equal in the sequel.

Example 3.15 (Equal PV behaviors) Consider the varying-mass and spring system of Example 3.1 with m as the scheduling function. We have seen in Example 3.3, that the PV differential equation (KR representation)

$$k_s w_1 - w_2 + \left(\frac{d}{dt} p \right) \frac{d}{dt} w_1 + p \frac{d^2}{dt^2} w_1 = 0. \quad (3.56)$$

is basically the same as the differential equation (3.6) describing the behavior of the varying-mass and spring system. Based on the equivalence of the differential equations, the associated LPV behaviors are also equal. Now consider the image representation in Example 3.7. The behavior associated with (3.56) is not equal with the associated behavior of the image representation (3.35), as in the latter case the trajectories of the latent variable are part of the behavior. Another example of inequality is

$$k_s w_1 - w_2 - \left(\frac{d}{dt} \check{p} \right) \frac{d}{dt} w_1 + (1 - \check{p}) \frac{d^2}{dt^2} w_1 = 0. \quad (3.57)$$

with a scheduling variable $\check{p} = 1 - m$. In this case, the solution trajectories of w for this KR representation are the same as for (3.56), but the behaviors are not equivalent due to the different scheduling function.

In order to characterize equivalent representations of the same system, another key notion is required: the equality of behaviors in the *almost everywhere* sense. In the LPV framework, we have introduced representations that have meromorphic coefficient functions. Similar to the LTI framework, $R_1, R_2 \in \mathcal{R}[\xi]$ are expected to define an equal behavior if they are equivalent up to multiplication by a $r \in \mathcal{R}$, $r \neq 0$. However, r can be a rational function for which $(r \diamond p)(t) = \infty$ for some scheduling trajectories p and $t \in \mathbb{T}$. The behavior of a kernel representation is defined to contain only those trajectories of p for which a (weak) solution exists

and is well defined. The latter is guaranteed by the boundedness of $r \diamond p$. In this way, the behavior (solutions) of R_1 is equal with the behavior of $R_2 = rR_1$ except for those trajectories for which $r \diamond p$ is unbounded. This type of almost-everywhere-equality is what we use in the sequel to define equal behaviors.

Let a behavior $\mathfrak{B} \subseteq (\mathbb{W} \times \mathbb{P})^\top$ be given with $\mathfrak{B}_\mathbb{P}$ as its projected scheduling behavior. Let $\bar{\mathfrak{B}}_\mathbb{P} \subseteq \mathfrak{B}_\mathbb{P}$. Define the restriction of \mathfrak{B} to $\bar{\mathfrak{B}}_\mathbb{P}$ as

$$\mathfrak{B} \big|_{\bar{\mathfrak{B}}_\mathbb{P}} = \{(w, p) \in \mathfrak{B} \mid p \in \bar{\mathfrak{B}}_\mathbb{P}\}. \quad (3.58)$$

Then based on the previous considerations, the equivalence of LPV-KR representations is defined as follows:

Definition 3.18 (Equivalent KR representations) *Given a $R_1 \in \mathcal{R}[\xi]^{n_r \times n_w}$ and a behavior $\mathfrak{B}_1 \subseteq (\mathbb{W} \times \mathbb{P})^\top$ with $\mathbb{P} = \mathbb{R}^{n_p}$ and $\mathbb{W} = \mathbb{R}^{n_w}$ such that \mathfrak{B}_1 contains all the (weak) solutions that satisfy*

$$(R_1(\xi) \diamond p)w = 0. \quad (3.59)$$

Let $\mathfrak{B}_\mathbb{P} \subseteq \mathcal{L}^{\text{loc}}(\mathbb{R}, \mathbb{P})$ (continuous-time) or $\mathfrak{B}_\mathbb{P} \subseteq \mathbb{P}^\mathbb{Z}$ (discrete-time) be the projected scheduling behavior associated with \mathfrak{B} . Then the KR representation defined by $R_2 \in \mathcal{R}[\xi]^{n_r \times n_w}$:

$$(R_2(\xi) \diamond p)w = 0, \quad (3.60)$$

with behavior $\mathfrak{B}_2 \subseteq (\mathbb{W} \times \mathbb{P})^\top$ and projected scheduling behavior $\mathfrak{B}'_\mathbb{P}$ is called equivalent with (3.59), if \mathfrak{B}_1 and \mathfrak{B}_2 are equal almost everywhere, i.e. for the common scheduling behavior $\bar{\mathfrak{B}}_\mathbb{P} = \mathfrak{B}_\mathbb{P} \cap \mathfrak{B}'_\mathbb{P}$, the restricted behaviors $\mathfrak{B}_1 \big|_{\bar{\mathfrak{B}}_\mathbb{P}}$ and $\mathfrak{B}_2 \big|_{\bar{\mathfrak{B}}_\mathbb{P}}$ are equal in terms of Definition 3.17. If equality holds with $\mathfrak{B}'_\mathbb{P} = \mathfrak{B}_\mathbb{P}$, then the equivalence of the representations is called full equivalence.

Example 3.16 (Almost everywhere equivalence) *By continuing Example 3.15, the KR representation*

$$\frac{k_s}{p} w_1 - \frac{1}{p} w_2 - \frac{1}{p} \left(\frac{d}{dt} p \right) \frac{d}{dt} w_1 + \frac{d^2}{dt^2} w_1 = 0.$$

has the same weak solutions as (3.56) except for those trajectories of $p = m$, where $m(t) = 0$ for some $t \in \mathbb{T}$. Thus, this KR representation and (3.56) are equivalent in the almost everywhere sense.

The existence of equivalent KR equations implies that, similar to the LTI case, representations of PV dynamical systems are non-unique. Thus, we need to characterize when two KR representations define the same behavior. This characterization follows through left/right unimodular transformations just like in the LTI case. To derive these theories in the LPV case, we introduce the concept of unimodular matrices in $\mathcal{R}[\xi]^{\times \cdot}$ and the Jacobson form.

Definition 3.19 (Unimodular polynomial matrix function) *Let $M \in \mathcal{R}[\xi]^{n \times n}$. Then M is called unimodular, if there exists a $M^\dagger \in \mathcal{R}[\xi]^{n \times n}$, such that $M^\dagger(\xi)M(\xi) = I$ and $M(\xi)M^\dagger(\xi) = I$.*

It provides an important insight that any unimodular matrix operator in $\mathcal{R}[\xi]^{\times \cdot}$ is equivalent to the product of finite many elementary row and column operations:

1. Interchange row (column) i and row (column) j .
2. Multiply row (column) i by a $r \in \mathcal{R}, r \neq 0$.
3. For $i \neq j$, add to row (column) i row (column) j multiplied by $\xi^n, n > 0$.

Example 3.17 (Unimodular polynomial matrix function) *The matrix polynomials $M, M^\dagger \in \mathcal{R}[\xi]^{2 \times 2}$, defined as*

$$M = \begin{bmatrix} r_2 & r_2\xi \\ r_1\xi & r_1\xi^2 + r_1 \end{bmatrix}, \quad M^\dagger = \begin{bmatrix} r_1 + \xi^2 r_1 & -\xi r_2 \\ -\xi r_1 & r_2 \end{bmatrix} \frac{1}{r_1 r_2},$$

are unimodular as $MM^\dagger = M^\dagger M = I$. Note that $\xi r_1 \neq r_1 \xi$ due to the non-commutative multiplication rule of ξ on $\mathcal{R}[\xi]$.

Theorem 3.4 (Jacobson form) (Chon 1971) *Let $R \in \mathcal{R}[\xi]^{n_r \times n_w}$ with $n = \text{rank}(R)$. Then there exist unimodular matrices $M_1 \in \mathcal{R}[\xi]^{n_r \times n_r}$ and $M_2 \in \mathcal{R}[\xi]^{n_w \times n_w}$ such that*

$$M_1 R M_2 = \begin{bmatrix} R' & 0 \\ 0 & 0 \end{bmatrix},$$

where $R'(\xi) = \text{diag}(1, \dots, 1, r) \in \mathcal{R}[\xi]^{n \times n}$ for a $0 \neq r \in \mathcal{R}[\xi]$.

Due to the algebraic structure of $\mathcal{R}[\xi]^{\cdot \times \cdot}$, the proof of Theorem 3.4 similarly follows as in Chon (1971). The Jacobson form, also called Teichmüller-Nakayama form, gives a unique representation of the behavior, similar to the Smith-McMillan form in the LTI case. This form plays a key role in proofs over the ring $\mathcal{R}[\xi]^{\cdot \times \cdot}$ as it establishes the concept of isomorphism of behaviors, existence of full rank polynomials with equivalent behavior, the injective cogenerator property of modules in $\mathcal{R}[\xi]$, etc. (see Zerz (2006) and Ichmann and Mehrmann (2005)).

Example 3.18 (Jacobson form) (Zerz 2006) *Consider*

$$R = \begin{bmatrix} r + \xi & -1 & -1 \\ 1 - \frac{d}{dt}r & -\frac{1}{r} + \xi & -r \end{bmatrix} \in \mathcal{R}[\xi]^{2 \times 3},$$

where r is a meromorphic function and $\xi = \frac{d}{dt}$. Then the Jacobson form of R is

$$M_1 R M_2 = \begin{bmatrix} 1 & 0 & 0 \\ 0 & r - \frac{1}{r} + \xi & 0 \end{bmatrix},$$

with

$$M_1 = \begin{bmatrix} 1 & 0 \\ -r & 1 \end{bmatrix}, \quad M_2 = \begin{bmatrix} 0 & 0 & 1 \\ 0 & 1 & r \\ -1 & -1 & \xi \end{bmatrix}.$$

Based on the concept of unimodular matrices and Theorem 3.4, it is possible to show that the following theorem holds in the LPV case:

Theorem 3.5 (Left-side unimodular transformation) (Zerz 2006) *Let $R \in \mathcal{R}[\xi]^{n_r \times n_w}$ and $M \in \mathcal{R}[\xi]^{n_r \times n_r}$ with M unimodular. For a given $n_{\mathbb{P}} \in \mathbb{N}$, define $R' := MR$. Denote the behaviors corresponding to R and R' by \mathfrak{B} and \mathfrak{B}' with scheduling space $\mathbb{P} \subseteq \mathbb{R}^{n_{\mathbb{P}}}$ and signal space $\mathbb{W} = \mathbb{R}^{n_w}$. Then \mathfrak{B} and \mathfrak{B}' are equal (almost everywhere).*

Based on the Jacobson form, the proof similarly follows as in Zerz (2006) and Ilchmann and Mehrmann (2005). Furthermore, if $R \in \mathcal{R}[\xi]^{n_r \times n_w}$ is not full row rank, i.e. $\text{rank}(R) = n < n_r$, then there exists a unimodular $M \in \mathcal{R}[\xi]^{n_r \times n_r}$ such that

$$MR = \begin{bmatrix} R' \\ 0 \end{bmatrix}, \quad (3.61)$$

where $R' \in \mathcal{R}[\xi]^{n \times n_w}$ is full row rank and the corresponding behaviors are equivalent in terms of Theorem 3.5. Note that this theorem establishes the concept when two representations can be considered equivalent. However, to establish equivalence of SS representations or latent variable systems, we require the concept of right-side unimodular transformation just like in the LTI case. It can be showed that the following theorem holds:

Theorem 3.6 (Right-side unimodular transformation) (Zerz 2006) *Let $R \in \mathcal{R}[\xi]^{n_r \times n_w}$ and $M \in \mathcal{R}[\xi]^{n_w \times n_w}$ with M unimodular. Denote the behaviors defined by R and $R' := RM$ as \mathfrak{B} and \mathfrak{B}' with scheduling domain $\mathbb{P} \subseteq \mathbb{R}^{n_{\mathbb{P}}}$ and signal space $\mathbb{W} = \mathbb{R}^{n_w}$. If $\mathbb{T} = \mathbb{R}$, then $\mathfrak{B} \cap \mathcal{C}^\infty(\mathbb{R}, \mathbb{W} \times \mathbb{P})$ and $\mathfrak{B}' \cap \mathcal{C}^\infty(\mathbb{R}, \mathbb{W} \times \mathbb{P})$ are isomorphic in the almost everywhere sense. If $\mathbb{T} = \mathbb{Z}$, then \mathfrak{B} and \mathfrak{B}' are isomorphic in the almost everywhere sense.*

Again, the proof, based on the Jacobson form, similarly follows as in Zerz (2006) and Ilchmann and Mehrmann (2005). It is important that right-side unimodular transformations do not change the underlying relation between the system signals nor the projected scheduling behavior, but they do change the system signals, the trajectories of the behavior. An important difference with respect to the LTI case (see Theorem 2.4) is that if $M \in \mathcal{R}^{n_w \times n_w}$ (zero order polynomial), then only the \mathcal{C}^∞ part of \mathfrak{B} and \mathfrak{B}' are isomorphic for $\mathbb{T} = \mathbb{R}$, as M can introduce arbitrary finite order of derivatives on p .

As all the required tools are established, it is now possible to introduce the notion of equivalence relation for LPV kernel representations. Similar to the LTI case, this relation is the key to characterize the set of equivalent representations of the same behavior, which we call an equivalence class. In the LPV case, the scheduling dimension $n_{\mathbb{P}}$ plays an important role in $\mathcal{R}[\xi]$ as it defines the exact coefficient dependence and also how the dot or shift operators behave on \mathcal{R} . Thus, an equivalence relation must be dependent on $n_{\mathbb{P}}$. Based on this, the following definition is given:

Definition 3.20 (LPV Equivalence relation) *Introduce the symbol $\overset{n_{\mathbb{P}}}{\sim}$ to denote the equivalence relation on $\bigcup \mathcal{R}[\xi]^{n_1 \times n_2}$ (all polynomial matrices with finite dimension) for an $n_{\mathbb{P}}$ -dimensional scheduling space. $R_1 \in \mathcal{R}[\xi]^{n_1 \times n_w}$ and $R_2 \in \mathcal{R}[\xi]^{n_2 \times n_w}$ with $n_1 \geq n_2$ are called equivalent, i.e. $R_1 \overset{n_{\mathbb{P}}}{\sim} R_2$, if there exists a unimodular matrix function $M \in \mathcal{R}[\xi]^{n_1 \times n_1}$ such that*

$$MR_1 = \begin{bmatrix} R_2 \\ 0 \end{bmatrix} \begin{array}{c} \updownarrow \\ \updownarrow \end{array} \begin{array}{c} n_2 \\ n_1 - n_2 \end{array}. \quad (3.62)$$

This implies that if $R_1 \overset{n_{\mathbb{P}}}{\sim} R_2$, then the corresponding behaviors with $\mathbb{P} \subseteq \mathbb{R}^{n_{\mathbb{P}}}$ and $\mathbb{W} = \mathbb{R}^{n_w}$ are equal (almost everywhere). Using $\overset{n_{\mathbb{P}}}{\sim}$ we can define equivalence classes as follows:

Definition 3.21 (LPV Equivalence class) For a given $n_{\mathbb{P}} \in \mathbb{N}$, the set $\mathcal{E}^{n_{\mathbb{P}}} \subseteq \bigcup \mathcal{R}[\xi]^{\cdot \times \cdot}$ is called an equivalence class, if it is a maximal subset of $\mathcal{R}[\xi]^{\cdot \times \cdot}$ such that for all $R_1, R_2 \in \mathcal{E}^{n_{\mathbb{P}}}$ it holds that $R_1 \stackrel{n_{\mathbb{P}}}{\sim} R_2$.

An equivalence class defines the set of all KR representations which have equal behavior. An important subset of an equivalence class are the so called minimal representations:

Definition 3.22 (Minimality) Let $R \in \mathcal{R}[\xi]^{n_r \times n_w}$. Then R is called minimal if it has full row rank, i.e. $\text{rank}(R) = n_r$.

We call $\deg(r)$ in the Jacobson form of a R associated with $\mathfrak{R}_K(\mathcal{S})$, the degree of all KR representations in the same equivalence class. This degree can be considered as the order of \mathcal{S} , hence we call it *McMillan degree*. Note that for a minimal $\mathfrak{R}_K(\mathcal{S})$ with $n_w = 1$, the McMillan degree of \mathcal{S} is equal to $n_{\xi} = \deg(R)$. It is also important to consider the subclass of representations, so called canonical forms, that can uniquely identify each equivalence class:

Definition 3.23 (Canonical forms) For a given $n_{\mathbb{P}} \in \mathbb{N}$, $\mathcal{E}_{\text{can}}^{n_{\mathbb{P}}} \subset \bigcup \mathcal{R}[\xi]^{\cdot \times \cdot}$ is called a set of canonical forms, if each element of $\bigcup \mathcal{R}[\xi]^{\cdot \times \cdot}$ is equivalent under $\stackrel{n_{\mathbb{P}}}{\sim}$ with only one element of $\mathcal{E}_{\text{can}}^{n_{\mathbb{P}}}$. ($\mathcal{E}_{\text{can}}^{n_{\mathbb{P}}}$ is the class representative of $\bigcup \mathcal{R}[\xi]^{\cdot \times \cdot}$ under $\stackrel{n_{\mathbb{P}}}{\sim}$).

Example 3.19 (LPV equivalence relation and minimality) Let the KR representation $\mathfrak{R}_K(\mathcal{S})$ of an CT-LPV system \mathcal{S} with $\mathbb{P} \subseteq \mathbb{R}$ given by

$$R(\xi) \diamond p = \begin{bmatrix} (\sin(p)p - \cos(p)) \frac{d}{dt} p & 0 \\ p & \frac{1}{\cos(p)} \end{bmatrix} + \begin{bmatrix} -\cos(p)p & -1 \\ \frac{1}{\cos(p)} & 0 \end{bmatrix} \xi + \begin{bmatrix} -1 & 0 \\ 0 & 0 \end{bmatrix} \xi^2.$$

Then, there exists a unimodular matrix $M \in \mathcal{R}[\xi]^{2 \times 2}$ with

$$M(\xi) \diamond p = \begin{bmatrix} 0 & 1 \\ 1 & \cos(p)\xi - \sin(p) \frac{d}{dt} p \end{bmatrix} \quad \text{s.t.} \quad (M(\xi)R(\xi)) \diamond p = \begin{bmatrix} p + \frac{1}{\cos(p)}\xi & \frac{1}{\cos(p)} \\ 0 & 0 \end{bmatrix}.$$

Note that this result is obtained by using (3.22), i.e. $\xi r = \dot{r} + r\xi$, so

$$\xi \frac{1}{\cos(p)} = \frac{\sin(p)}{\cos^2(p)} \left(\frac{d}{dt} p \right) + \frac{1}{\cos(p)} \xi.$$

From Theorem 3.5 it follows that R' , defined as $\begin{bmatrix} (R')^{\top} & 0 \end{bmatrix}^{\top} = MR$, and R are equivalent for $n_{\mathbb{P}} = 1$. Furthermore, as R is equivalent with R' having row dimension 1, thus $\text{rank}(R) = 1$. This implies that R is not minimal in terms of Proposition 3.22. However, R' is trivially minimal. Hence, $\deg(R') = 1$ implies that the McMillan degree of \mathcal{S} is 1.

The introduced concepts generalize to LPV-IO representations as well:

Definition 3.24 (Equivalence relation of LPV-IO representations) Let $R_u, R'_u \in \mathcal{R}[\xi]^{n_y \times n_u}$ and $R_y, R'_y \in \mathcal{R}[\xi]^{n_y \times n_y}$ with R_y, R'_y are full row rank, $\deg(R_y) \geq \deg(R_u)$, and $\deg(R'_y) \geq \deg(R'_u)$. For a given $n_{\mathbb{P}} \in \mathbb{N}$, we call (R_y, R_u) and (R'_y, R'_u) equivalent

$$(R_y, R_u) \stackrel{n_{\mathbb{P}}}{\sim} (R'_y, R'_u), \quad (3.63)$$

if there exists a unimodular matrix $M \in \mathcal{R}[\xi]^{n_{\mathcal{Y}} \times n_{\mathcal{Y}}}$ such that

$$R'_{\mathcal{Y}} = MR_{\mathcal{Y}} \quad \text{and} \quad R'_{\mathcal{U}} = MR_{\mathcal{U}}. \quad (3.64)$$

Definition 3.25 (Minimal LPV-IO representation) An IO representation defined through $R_{\mathcal{Y}} \in \mathcal{R}[\xi]^{n_{\mathcal{Y}} \times n_{\mathcal{Y}}}$ and $R_{\mathcal{U}} \in \mathcal{R}[\xi]^{n_{\mathcal{Y}} \times n_{\mathcal{U}}}$ is called minimal for a given scheduling dimension $n_{\mathbb{P}}$, if there are no $R'_{\mathcal{Y}} \in \mathcal{R}[\xi]^{n_{\mathcal{Y}} \times n_{\mathcal{Y}}}$ and $R'_{\mathcal{U}} \in \mathcal{R}[\xi]^{n_{\mathcal{Y}} \times n_{\mathcal{U}}}$ polynomials with $\deg(R_{\mathcal{Y}}) < \deg(R'_{\mathcal{Y}})$ such that

$$(R_{\mathcal{Y}}, R_{\mathcal{U}}) \stackrel{n_{\mathbb{P}}}{\sim} (R'_{\mathcal{Y}}, R'_{\mathcal{U}}).$$

Using the IO equivalence relation and minimality, the definition of IO equivalence classes and canonical forms follows naturally. Note that for a minimal $\mathfrak{R}_{\text{IO}}(\mathcal{S})$ with $n_{\mathcal{Y}} = 1$, the McMillan degree of \mathcal{S} is equal to $\deg(R_{\mathcal{Y}})$.

Example 3.20 (LPV-IO equivalence relation and minimality) Let the IO representation $\mathfrak{R}_{\text{IO}}(\mathcal{S})$ of an CT-LPV system \mathcal{S} with $\mathbb{P} \subseteq \mathbb{R}$ be given by

$$\begin{aligned} R_{\mathcal{Y}}(\xi) \diamond p &= \begin{bmatrix} \sin^2(p)\xi & \sin^2(p)p \\ -2 \cot(p) \frac{d}{dt} p \xi - \xi^2 & (1-p)\xi - \frac{d}{dt} p (1 + 2 \cot(p)p) \end{bmatrix}, \\ R_{\mathcal{U}}(\xi) \diamond p &= \begin{bmatrix} \sin^2(p) \\ p - 2 \cot(p) \frac{d}{dt} p - \xi \end{bmatrix}. \end{aligned}$$

Then, there exists a unimodular matrix $M \in \mathcal{R}[\xi]^{2 \times 2}$ being equal to

$$M(\xi) \diamond p = \begin{bmatrix} \frac{1}{\sin^2(p)} & 0 \\ \frac{1}{\sin^2(p)} \xi & 1 \end{bmatrix} \quad \text{s.t.} \quad \begin{cases} (M(\xi)R_{\mathcal{Y}}(\xi)) \diamond p = \begin{bmatrix} \xi & p \\ 0 & \xi \end{bmatrix}, \\ (M(\xi)R_{\mathcal{U}}(\xi)) \diamond p = \begin{bmatrix} 1 \\ p \end{bmatrix}, \end{cases}$$

which can be verified by using

$$\frac{1}{\sin^2(p)} \xi \sin^2(p) = 2 \cot(p) \frac{d}{dt} p + \xi.$$

This implies that $(R'_{\mathcal{Y}}, R'_{\mathcal{U}}) = (MR_{\mathcal{Y}}, MR_{\mathcal{U}})$ and $(R_{\mathcal{Y}}, R_{\mathcal{U}})$ are equivalent for $n_{\mathbb{P}} = 1$ in terms of Theorem 3.5. From Proposition 3.25 it follows that $\mathfrak{R}_{\text{IO}}(\mathcal{S})$ is not minimal as $\deg(R_{\mathcal{Y}}) = 2$ is greater than $\deg(R'_{\mathcal{Y}}) = 1$. On the other hand, it is trivial that $(R'_{\mathcal{Y}}, R'_{\mathcal{U}})$ defines a minimal IO representation of \mathcal{S} . Hence $\deg(R'_{\mathcal{Y}}) = 1$ implies that the McMillan degree of \mathcal{S} is 1.

We can also generalize the introduced concepts to LPV-SS representations. To do so, we first have to clarify state-transformations in the LPV case which is the required ingredient to formulate equivalence relations of SS representations. As a contribution we prove that in the LPV case, state-transformations need dynamic dependence in order to define an equivalence relation of SS representations.

By definition, the full behavior of a $\mathfrak{R}_{\text{SS}}(\mathcal{S})$ is represented by a zero-order and a first-order polynomial matrix $R \in \mathcal{R}[\xi]^{n_{\mathcal{r}} \times (n_{\mathcal{Y}} + n_{\mathcal{U}})}$ and $R_{\text{L}} \in \mathcal{R}[\xi]^{n_{\mathcal{r}} \times n_{\mathcal{X}}}$ in the form of

$$(R(\xi) \diamond p) \text{col}(u, y) = (R_{\text{L}}(\xi) \diamond p)x \quad (3.65)$$

where ξ is either q or $\frac{d}{dt}$, (u, y) is an IO partition of \mathcal{S} , x is the state variable of $\mathfrak{R}_{\text{SS}}(\mathcal{S})$, and p is the scheduling signal. Similar to the LTI case, left and right side

multiplication of R and R_L with unimodular $M_1 \in \mathcal{R}[\xi]^{n_r \times n_r}$ and $M_2 \in \mathcal{R}[\xi]^{n_x \times n_x}$ leads to

$$R' = M_1 R, \quad R'_L = M_1 R_L M_2. \quad (3.66)$$

In terms of Theorem 3.5 and 3.6, the resulting polynomials R' and R'_L define an equivalent latent variable representation of \mathcal{S} . The new latent variable, given as

$$x' = (M_2^\dagger(\xi) \diamond p)x, \quad (3.67)$$

fulfills the property of state as M_2^\dagger is unimodular. To guarantee that the resulting latent variable representation qualifies as a SS representation, R'_L needs to be monic and $\deg(R') = 0$ with $\deg(R'_L) = 1$ must be satisfied. This implies that the unimodular matrices must have zero order, i.e. $M_1 \in \mathcal{R}^{n_r \times n_r}$ and $M_2 \in \mathcal{R}^{n_x \times n_x}$, and M_1 has a special structure in order to guarantee that R' and R'_L correspond to an equivalent SS representation. In that case, (3.67) is called a *state-transformation* and $T = M_2^\dagger$ is called the *state-transformation* matrix resulting in

$$x' = (T \diamond p)x. \quad (3.68)$$

As we have seen, state-transformation for LPV-SS representations can be similarly introduced as in the LTI case. However, a major difference with respect to LTI state-transformations is that in the LPV case, T is inherently dependent on p and this dependence is dynamic, i.e. $T \in \mathcal{R}^{n_x \times n_x}$.

An invertible $T \in \mathcal{R}^{n_x \times n_x}$ used as a state-transformation is always equivalent with a right and left-side multiplication by unimodular matrix functions yielding a valid SS representation of the LPV system. This is also proved by the algebraic equivalency, see (3.68), of the original and the new state variables (Silverman 1971). The converse, namely that the state variables of any two SS representations of the same LPV system are algebraically equivalent up to a state-transformation follows directly from Theorem 3.5 and 3.6.

Similar to the LTI case, the SS representation resulting from the state-transformation of $\mathfrak{R}_{SS}(\mathcal{S})$, can be analytically computed from the meromorphic matrices of $\mathfrak{R}_{SS}(\mathcal{S})$. However, different commutation rules in $\mathcal{R}[\xi]$ for the continuous and discrete-time cases yield different consequences with respect to the system matrices. Let $\mathfrak{R}_{SS}(\mathcal{S})$ be a given LPV-SS representation with $\mathcal{X} = \mathbb{R}^{n_x}$ and state-equation

$$\xi x = (A \diamond p)x + (B \diamond p)u. \quad (3.69)$$

Let $T \in \mathcal{R}^{n_x \times n_x}$ be an invertible matrix function and consider x' , given by (3.68), as a new state variable. It is immediate, that substitution of (3.68) into (3.69) yields

$$\xi(T^{-1} \diamond p)x' = (A \diamond p)(T^{-1} \diamond p)x' + (B \diamond p)u. \quad (3.70)$$

In the continuous-time case, the non-commutative multiplication by $\xi = \frac{d}{dt}$ in (3.70) gives that the state-equation in x' is:

$$\frac{d}{dt}x' = \left([TAT^{-1} + \dot{T}T^{-1}] \diamond p \right) x' + ([TB] \diamond p) u. \quad (3.71)$$

Here we use the fact that $\dot{T}T^{-1} = -T\dot{T}^{-1}$. In the discrete-time case, the non-commutative multiplication by $\xi = q$ in (3.70) yields:

$$qx' = \left(\left[\overrightarrow{T}AT^{-1} \right] \diamond p \right) x' + \left(\left[\overrightarrow{T}B \right] \diamond p \right) u. \quad (3.72)$$

In both cases, the new state-equation defines a LPV-SS representation with state-vector x' . Note that due to the different commutation rules of the time-operators, the transformation rules of the original system matrices are different in the CT and in the DT cases. Now we can give the following definition of equivalence classes:

Definition 3.26 (Equivalence relation of LPV-SS representations) *Let (A, B, C, D) and (A', B', C', D') be quadruplets of matrices in $\mathcal{R}^{\times \times}$ defining LPV-SS representations with $n_{\mathbb{X}} \geq n'_{\mathbb{X}}$ and with $n_{\mathbb{P}} \in \mathbb{N}$. These representations are called equivalent,*

$$\left[\begin{array}{c|c} A & B \\ \hline C & D \end{array} \right] \overset{n_{\mathbb{P}}}{\sim} \left[\begin{array}{c|c} A' & B' \\ \hline C' & D' \end{array} \right], \quad (3.73)$$

if there exists an invertible $T \in \mathcal{R}^{n_{\mathbb{X}} \times n_{\mathbb{X}}}$ such that in case of $\mathbb{T} = \mathbb{R}$ the following holds:

$$\begin{aligned} TAT^{-1} + \dot{T}T^{-1} &= \begin{bmatrix} A' & 0 \\ * & * \end{bmatrix}, & TB &= \begin{bmatrix} B' \\ * \end{bmatrix}, & \begin{array}{c} \updownarrow \\ n'_{\mathbb{X}} \\ \updownarrow \\ n_{\mathbb{X}} - n'_{\mathbb{X}} \end{array} \\ CT^{-1} &= \begin{bmatrix} C' & 0 \end{bmatrix}, & D &= D', \end{aligned} \quad (3.74a)$$

while in case of $\mathbb{T} = \mathbb{Z}$:

$$\begin{aligned} \overrightarrow{T}AT^{-1} &= \begin{bmatrix} A' & 0 \\ * & * \end{bmatrix}, & \overrightarrow{T}B &= \begin{bmatrix} B' \\ * \end{bmatrix}, & \begin{array}{c} \updownarrow \\ n'_{\mathbb{X}} \\ \updownarrow \\ n_{\mathbb{X}} - n'_{\mathbb{X}} \end{array} \\ CT^{-1} &= \begin{bmatrix} C' & 0 \end{bmatrix}, & D &= D'. \end{aligned} \quad (3.74b)$$

Based on the previous considerations, the existence of a state-transformation T between the matrices of two SS representations implies that they have the same manifest behavior. Furthermore, the states are related as

$$(T \diamond p)(t)x(t) = \begin{bmatrix} x'(t) \\ * \end{bmatrix}, \quad \begin{array}{c} n'_{\mathbb{X}} \\ \updownarrow \\ n_{\mathbb{X}} - n'_{\mathbb{X}} \end{array} \quad \forall t \in \mathbb{T}. \quad (3.75)$$

From the concept of LPV-SS equivalence the concept of minimality directly follows:

Definition 3.27 (Minimal LPV-SS representation) *For a given $n_{\mathbb{P}} > 0$, an SS representation defined through the matrix functions (A, B, C, D) is called minimal, if there exist no (A', B', C', D') such that*

$$\left[\begin{array}{c|c} A & B \\ \hline C & D \end{array} \right] \overset{n_{\mathbb{P}}}{\sim} \left[\begin{array}{c|c} A' & B' \\ \hline C' & D' \end{array} \right],$$

with $n'_{\mathbb{X}} < n_{\mathbb{X}}$.

Again, using the concept of SS equivalence relation and minimality, the definition of LPV-SS equivalence classes and canonical forms follows naturally. In addition, the state-dimension $n_{\mathcal{X}}$ of a minimal $\mathfrak{R}_{\text{SS}}(\mathcal{S})$ is equal to the McMillan degree of \mathcal{S} .

Example 3.21 (LPV-SS equivalence relation and minimality) Let the SS representation $\mathfrak{R}_{\text{SS}}(\mathcal{S})$ of an DT-LPV system \mathcal{S} with $\mathbb{P} \subseteq \mathbb{R}$ be given by

$$\left[\begin{array}{c|c} A & B \\ \hline C & D \end{array} \right] \diamond p = \left[\begin{array}{c|c|c} p & 1 & 1 \\ 0 & p & p \\ \hline 1 & \frac{1}{p} & p \end{array} \right].$$

It is possible to show that $\mathfrak{R}_{\text{SS}}(\mathcal{S})$ is minimal (see Example 3.33). Thus the McMillan degree of \mathcal{S} is $n_{\mathcal{X}} = 2$. Let $T \in \mathcal{R}^{2 \times 2}$ be an invertible state-transformation defined as

$$T \diamond p = \begin{bmatrix} \frac{1}{p} & p \\ 0 & 1 \end{bmatrix}.$$

Then

$$T^{-1} \diamond p = \begin{bmatrix} p & -p^2 \\ 0 & 1 \end{bmatrix}, \quad \vec{T} \diamond p = \begin{bmatrix} \frac{1}{qp} & qp \\ 0 & 1 \end{bmatrix},$$

implying

$$\left[\begin{array}{c|c} \vec{T}AT^{-1} & \vec{T}B \\ \hline CT^{-1} & D \end{array} \right] \diamond p = \left[\begin{array}{c|c|c} \frac{p^2}{qp} & \frac{1-p^3}{qp} + p(qp) & \frac{1}{qp} + p(qp) \\ 0 & p & p \\ \hline p & \frac{1}{p} - p^2 & p \end{array} \right].$$

The obtained SS representation is an equivalent minimal SS representation of \mathcal{S} as it is in an equivalence relation with $\mathfrak{R}_{\text{SS}}(\mathcal{S})$ and its state dimension is the same. As \mathcal{S} has no autonomous part, this can be easily checked by applying an impulsive input to the representations at time τ_0 , i.e. $u(\tau_0) = 1$ and $u(k) = 0$ for all $k \neq \tau_0$. Then the resulting output trajectory: $y(\tau_0) = (D \diamond p)(\tau_0)$, $y(\tau_0 + 1) = (C \diamond p)(\tau_0 + 1)(B \diamond p)(\tau_0)$, ... is the same for both representations for all $\tau_0 \in \mathbb{Z}$ and $p \in \mathfrak{B}_{\mathbb{P}}$, which yields equivalence (Brockett 1970).

3.3 Properties of LPV systems & representations

In the previous section we have developed the basics of a LPV behavioral framework. In order to use this framework as an analysis tool for LPV system identification, we also need to investigate key properties of systems and representations in terms of dynamic stability and state-observability/reachability. As a contribution, we analyze in this section these concepts using the results of LTV system theory. We also compare the developed results with their counterparts in the existing LPV theory. As the developed behavioral approach addresses a larger set of LPV systems than the state-of-the-art of LPV system theory, the existing LPV concepts follow as special cases of the theory presented in this section.

3.3.1 State-observability and reachability

The concepts of state-observability and reachability of LPV-SS system representations are important properties in the LPV case. They are not only key concepts for control and subspace-based identification, but they also provide the formulation

of special SS canonical forms. These so called observability or reachability canonical forms are strongly connected to the observability and reachability matrices of SS representations and they are required to develop equivalence transformation between different representation domains (see Chapter 4).

In the following discussion, we explore complete state-observability and reachability of LPV-SS representations both in CT and DT, based on concepts of the LTV system theory. We show that these properties are equivalent with the existence of invertible linear maps for all time instances and scheduling trajectories. Based on this, we define observability and reachability matrices of SS representations. We show that complete state-observability and reachability are very strong properties in the LPV case as only a rather restricted class of representations fulfills them. Moreover, they are not required for minimality nor the generation of observability or reachability canonical forms. We show that a weaker property, the so called structural state-observability/reachability, which defines the state-observability/reachability concept in an almost everywhere sense, is a necessary and sufficient property to generate these canonical forms.

As a first step, we extended Definitions 2.30 and 2.31 of complete state-observability and reachability to the LPV case:

Definition 3.28 (Complete LPV state-observability) $\mathfrak{R}_{\text{SS}}(\mathcal{S})$ is called completely state-observable, if for all $(u, x, y, p), (u, x', y, p) \in \mathfrak{B}_{\text{SS}}$ it holds that $x = x'$.

Definition 3.29 (Complete LPV state-reachability) $\mathfrak{R}_{\text{SS}}(\mathcal{S})$ is called completely state-reachable, if for any given two states $x_1, x_2 \in \mathbb{X}$ and any scheduling signal $p \in \mathfrak{B}_{\mathbb{P}}$, there exist an input signal u and an output signal y such that $(u, x, y, p) \in \mathfrak{B}_{\text{SS}}$ with $x(t_1) = x_1$ and $x(t_2) = x_2$ for some $t_1, t_2 \in \mathbb{T}$.

The main difference of these definitions with respect to the LTI case follows from the presence of the scheduling signal p that acts as an extra “time-axis” of the system. By freezing this axis, i.e. using a constant scheduling, these concepts coincide with Definitions 2.30 and 2.31.

To establish conditions when an LPV-SS representation is completely state-observable or reachable, as a next step, the concept of state-observability and reachability matrices is introduced. Appropriate conditions are derived to formulate when and in which sense the full rank of these matrices implies complete state-observability or reachability. However, the formulation of these matrices follows a different track than in the LTI case, due to the non-commutative multiplication on $\mathcal{R}[\xi]$.

A. State-observability in continuous-time

First the CT observability case is investigated based on the results of LTV system theory by Silverman and Meadows (1967) and Callier and Desoer (1991). Using these approaches, we establish the concept of state-observability of $\mathfrak{R}_{\text{SS}}(\mathcal{S})$ on a finite time interval and show that this property is equivalent with the existence of

an invertible linear map. Then we define this linear map as the state-observability matrix of $\mathfrak{R}_{\text{SS}}(\mathcal{S})$ and claim that state-observability (invertibility of the map) on any finite time interval implies complete state-observability.

For a given continuous-time LPV-SS representation $\mathfrak{R}_{\text{SS}}(\mathcal{S})$ with matrix functions (A, B, C, D) , define $\mathfrak{A}(t_1, t_0, p)$ as the *state transition matrix function* for $\dot{x} = (A \diamond p)x$. Then the state and output evolution of $\mathfrak{R}_{\text{SS}}(\mathcal{S})$ satisfy that

$$x(t_1) = \mathfrak{A}(t_1, t_0, p)x(t_0) + \int_{t_0}^{t_1} \mathfrak{A}(t_1, \tau, p)(B \diamond p)(\tau)u(\tau)d\tau, \quad (3.76a)$$

$$y(t_1) = (C \diamond p)(t_1)x(t_1), \quad (3.76b)$$

for all $t_1 \geq t_0$ along a given scheduling trajectory $p \in \mathfrak{B}_{\mathbb{F}}$. Note that for LPV-SS representations in general, the explicit form of $\mathfrak{A}(t_1, t_0, p)$ is hard to derive as it involves integration over the scheduling trajectory, while in the LTI case, $\mathfrak{A}(t_1, t_0) = e^{A(t_1-t_0)}$.

Complete state-observability of $\mathfrak{R}_{\text{SS}}(\mathcal{S})$ can be described using the concept of reconstructibility. For a given $p \in \mathfrak{B}_{\mathbb{F}}$, define the following linear map from \mathbb{X} to $\mathcal{L}_1^{\text{loc}}([t_0, t_1], \mathbb{Y})$:

$$y(t) = \underbrace{(C \diamond p)(t)}_{\mathfrak{C}(t)} \mathfrak{A}(t, t_0, p)x, \quad x \in \mathbb{X}, t \in [t_0, t_1]. \quad (3.77)$$

For the given $p \in \mathfrak{B}_{\mathbb{F}}$, the mapping $y(t) = \mathfrak{C}(t)x$ defines the output evolution of $\mathfrak{R}_{\text{SS}}(\mathcal{S})$ on the finite interval $[t_0, t_1] \subset \mathbb{R}$ with initial state $x(t_0) = x$ and with zero input signal $u = 0$. The state $x \in \mathbb{X}$ is said to be reconstructible on $[t_0, t_1]$, if x lies in the kernel of the linear map (3.77). This means that if (3.77) is injective, then every state is reconstructible on $[t_0, t_1]$. If (3.77) is injective for every $p \in \mathfrak{B}_{\mathbb{F}}$, then $\mathfrak{R}_{\text{SS}}(\mathcal{S})$ is called state-observable on $[t_0, t_1]$. It is easy to show that $\mathfrak{R}_{\text{SS}}(\mathcal{S})$ is completely state-observable, if it is state-observable for any finite interval of \mathbb{R} . Now we can introduce the following matrix function to describe the map (3.77):

Definition 3.30 (*n*-step CT state-observability matrix function) (Silverman and Meadows 1969) *In continuous-time, the *n*-step state-observability matrix function of $\mathfrak{R}_{\text{SS}}(\mathcal{S})$ is defined as $\mathcal{O}_n \in \mathcal{R}^{(nn_{\mathbb{Y}}) \times n_{\mathbb{X}}}$ with*

$$\mathcal{O}_n = [\mathfrak{o}_1^{\top} \quad \mathfrak{o}_2^{\top} \quad \dots \quad \mathfrak{o}_n^{\top}]^{\top}, \quad (3.78)$$

where $\mathfrak{o}_1 = C$ and

$$\mathfrak{o}_{i+1} = \mathfrak{o}_i A + \dot{\mathfrak{o}}_i, \quad i > 1. \quad (3.79)$$

The *n*-step state-observability matrix function has a similar role as the state-observability matrix for LTI representations, as in case of complete state-observability, it provides an invertible map for the reconstruction of the state from the derivatives of y .

Example 3.22 (CT state-observability matrix function) Let the SS representation $\mathfrak{R}_{\text{SS}}(S)$ of a CT-LPV system S with $\mathbb{P} \subseteq \mathbb{R}^+$ be given by

$$\left[\begin{array}{c|c} A & B \\ \hline C & D \end{array} \right] \diamond p = \left[\begin{array}{c|c|c} p & 1 & 1 \\ 0 & \frac{1}{p} & p \\ \hline 1 & p & p \end{array} \right].$$

Then the observability matrices of $\mathfrak{R}_{\text{SS}}(S)$ for $n = 1, 2, 3$ are as follows:

$$\mathcal{O}_1 \diamond p = \begin{bmatrix} 1 & p \end{bmatrix}, \quad \mathcal{O}_2 \diamond p = \begin{bmatrix} 1 & p \\ p & 2 + \frac{d}{dt}p \end{bmatrix}, \quad \mathcal{O}_3 \diamond p = \begin{bmatrix} 1 & p & p^2 \\ p & 2 + \frac{d}{dt}p & \frac{p^2+2+\frac{d}{dt}p}{p} + \frac{d^2}{dt^2}p \end{bmatrix}.$$

These matrices were computed by using:

$$\dot{\mathcal{O}}_1 \diamond p = \begin{bmatrix} 0 & \frac{d}{dt}p \end{bmatrix}, \quad \dot{\mathcal{O}}_2 \diamond p = \begin{bmatrix} \frac{d}{dt}p & \frac{d^2}{dt^2}p \end{bmatrix}.$$

Using the concept of observability matrices and intuition, based on the LTI case, one could expect that full rank of $\mathcal{O}_{n_{\mathcal{X}}}$, i.e. $\text{rank}(\mathcal{O}_{n_{\mathcal{X}}}) = n_{\mathcal{X}}$ (full rank in a functional sense), is the necessary and sufficient condition for complete state-observability. However, this not true in the LPV case. It can also be shown that instead of the functional full rank, full rank of $\mathcal{O}_{n_{\mathcal{X}}}$ for every time instance along every scheduling trajectory, i.e. $\text{rank}((\mathcal{O}_{n_{\mathcal{X}}} \diamond p)(t)) = n_{\mathcal{X}}$ for all $t \in \mathbb{R}$ and $p \in \mathfrak{B}_{\mathbb{P}}$, is a sufficient but not a necessary condition for complete state-observability. To show this and to derive the sufficient and necessary condition for complete state-observability, first introduce a weaker notion of state-observability:

Definition 3.31 (Structural state-observability) $\mathfrak{R}_{\text{SS}}(S)$ with state-dimension $n_{\mathcal{X}}$ is called *structurally state-observable* if its $n_{\mathcal{X}}$ -step observability matrix $\mathcal{O}_{n_{\mathcal{X}}}$ is full rank, i.e. $\text{rank}(\mathcal{O}_{n_{\mathcal{X}}}) = n_{\mathcal{X}}$.

Note that full rank in a functional sense, does not guarantee that $\mathcal{O}_{n_{\mathcal{X}}}$ is invertible for all $t \in \mathbb{R}$ and $p \in \mathfrak{B}_{\mathbb{P}}$. Therefore, for specific scheduling trajectories and time instances, reconstructibility of state \mathbf{x} by the linear map $\mathcal{O}_{n_{\mathcal{X}}}$ is not guaranteed. In this way, complete state-observability is not implied. Even if reconstructibility may fail for some scheduling trajectories, for the rest state-observability holds on \mathbb{R} . This gives that structural observability can be understood as complete state-observability in an almost everywhere sense. In the following we show that in fact structural state-observability is a necessary condition for complete state-observability.

To derive the appropriate conditions for complete state-observability the following lemma has a key importance:

Lemma 3.2 (Constant observability rank) (Silverman and Meadows 1969) Let a representation $\mathfrak{R}_{\text{SS}}(S)$ be given with a projected scheduling behavior $\mathfrak{B}_{\mathbb{P}}$ and observability matrices \mathcal{O}_n . For a scheduling trajectory $p \in \mathfrak{B}_{\mathbb{P}}$, it holds that, if there exists $n > 0$ such that

$$\text{rank}((\mathcal{O}_n \diamond p)(t)) = \text{rank}((\mathcal{O}_{n+1} \diamond p)(t)) = \gamma, \quad (3.80)$$

for all $t \in \mathbb{T}$, then $\text{rank}((\mathcal{O}_l \diamond p)(t)) = \gamma$ for all $l \geq n$ and $t \in \mathbb{T}$.

The proof is given in Silverman and Meadows (1969). The minimal $n > 0$, for which (3.80) holds, is called the observability radius of $\mathfrak{R}_{\text{SS}}(\mathcal{S})$ with respect to the scheduling trajectory p . This lemma has the obvious consequence that for a given $p \in \mathfrak{B}_{\mathbb{P}}$, if the ranks of $\mathcal{O}_n \diamond p$ and $\mathcal{O}_{n+1} \diamond p$ are constant and equal along the entire trajectory of p , then the rank of $\mathcal{O}_l \diamond p$ remains constant for all $l \geq n$. Contrary to the LTI case, it is not guaranteed that the rank of $\mathcal{O}_{n_{\mathcal{X}}} \diamond p$ is equal to the rank of $\mathcal{O}_{n_{\mathcal{X}}+1} \diamond p$ for all t , i.e. the observability radius is smaller or equal than $n_{\mathcal{X}}$. As the observability radius can vary for each trajectory of p , the introduction of the notion of constant observability rank representation is required:

Definition 3.32 (Constant observability rank representation) (Silverman and Meadows 1969) *A $\mathfrak{R}_{\text{SS}}(\mathcal{S})$ representation has constant observability rank, if there exist a $n \in \{1, \dots, n_{\mathcal{X}}\}$ and a $l > 0$ such that*

$$\text{rank}((\mathcal{O}_n \diamond p)(t)) = \text{rank}((\mathcal{O}_{n+1} \diamond p)(t)) = l \leq n_{\mathcal{X}}, \quad (3.81)$$

for all $p \in \mathfrak{B}_{\mathbb{P}}$ and $t \in \mathbb{T}$.

Example 3.23 (CT non-constant observability rank representation) *For Example 3.22 it holds, that $\text{rank}((\mathcal{O}_2 \diamond p)(t)) = 2$ for all possible scheduling signals and time instances, except when for a $t \in \mathbb{R}$ the scheduling signal satisfies $p^2(t) = 2 + \frac{d}{dt}p(t)$. At that time instant, $\text{rank}((\mathcal{O}_2 \diamond p)(t)) = 1$. Hence it is not a constant observability rank representation, but its minimal observability radius is 1. For a constant observability rank representation see Example 3.24.*

Using the previously introduced concepts the following theorem holds:

Theorem 3.7 (Induced complete LPV state-observability in CT) (Silverman and Meadows 1967) *The CT-LPV-SS representation $\mathfrak{R}_{\text{SS}}(\mathcal{S})$ is completely state-observable, iff for every $p \in \mathcal{C}^\infty(\mathbb{R}, \mathbb{P}) \cap \mathfrak{B}_{\mathbb{P}}$ there exists a $0 < n < \infty$ such that $\text{rank}((\mathcal{O}_n \diamond p)(\tau)) = n_{\mathcal{X}}$ for all $\tau \in \mathbb{R}$. If $\mathfrak{R}_{\text{SS}}(\mathcal{S})$ is a constant observability rank representation, then the condition is $\text{rank}((\mathcal{O}_{n_{\mathcal{X}}} \diamond p)(\tau)) = n_{\mathcal{X}}$ for all $\tau \in \mathbb{R}$.*

The proof follows similarly as in Silverman and Meadows (1967). The clear interpretation of this result is important. If a LPV-SS representation is completely state-observable, then it is not guaranteed that the reconstruction of the state is available for every time instance through the linear map $(\mathcal{O}_{n_{\mathcal{X}}} \diamond p)(\tau)$, as it is not injective. It can happen, that this property is only satisfied for $n > n_{\mathcal{X}}$. In case $\mathfrak{R}_{\text{SS}}(\mathcal{S})$ is a constant observability rank representation, then similar to the LTI case, full rank of $(\mathcal{O}_{n_{\mathcal{X}}} \diamond p)(\tau)$ along every $p \in \mathfrak{B}_{\mathbb{P}}$ guarantees complete state-observability. For an SS representation with complete state-observability, see Example 3.24.

It can be shown that the class of LPV-SS representations with constant observability rank includes the class of LTI-SS representations, similar to the LTV case (Silverman 1971). In LPV control design, instead of observability, the so called *detectability* of the state is investigated together with *stabilizability* (Lee 1997). These concepts are formulated in a quadratic sense, similar to quadratic Lyapunov stability (see later in Section 3.3.2). It can be shown, that if quadratic detectability is satisfied for a LPV-SS representation with static linear dependence, then it is a

necessary condition in terms of Theorem 3.7 for complete state-observability. In the existing LPV system theory, the notion of complete-state observability is only considered in Balas et al. (2003), where invariant observability subspaces of LPV-SS representations with static linear dependence are explored using the concepts of nonlinear system theory. However, the connection of these results to Theorem 3.7 needs further investigation.

Example 3.24 (CT complete state-observability) Let the SS representation $\mathfrak{R}_{\text{SS}}(\mathcal{S})$ of an CT-LPV system \mathcal{S} with $\mathbb{P} = [-\frac{1}{2}, \frac{1}{2}]$ be given by

$$\left[\begin{array}{c|c} A & B \\ \hline C & D \end{array} \right] \diamond p = \left[\begin{array}{cc|c} \tan(p) \frac{d}{dt} p & 0 & 1 \\ \sin(p) & 2 & 1 \\ \hline \cos(p) & 1 & 0 \end{array} \right].$$

Then it follows that

$$\mathcal{O}_2 \diamond p = \begin{bmatrix} \cos(p) & 1 \\ \sin(p) & 2 \end{bmatrix}.$$

As $\cos(p) \neq 2 \sin(p)$ on \mathbb{P} , \mathcal{O}_2 has a constant rank of 2 for all $p \in \mathfrak{B}_{\mathbb{P}}$ and $t \in \mathbb{R}$. This means that $\mathfrak{R}_{\text{SS}}(\mathcal{S})$ is completely state observable on \mathbb{P} .

In case $\text{rank}(\mathcal{O}_{n_{\mathcal{X}}}) = n_{\mathcal{X}}$ is satisfied, i.e. the SS representation is structurally state-observable, then it holds that $\text{rank}((\mathcal{O}_{n_{\mathcal{X}}} \diamond p)(\tau)) = n_{\mathcal{X}}$ for all $t \in \mathbb{R}$ except for some $p \in \mathcal{C}^{\infty}(\mathbb{R}, \mathbb{P}) \cap \mathfrak{B}_{\mathbb{P}}$. Then it is obvious that structural state-observability is a necessary condition for complete state-observability (see Example 3.25). This claim is also proved in Silverman (1971).

Example 3.25 (Structural state-observability) The representation defined in Example 3.22 has been shown to be not completely state-observable as $\min_{t \in \mathbb{R}} \text{rank}((\mathcal{O}_2 \diamond p)(t)) = 1$ for scheduling trajectories that satisfy $p^2(t) = 2 + \frac{d}{dt}p(t)$ for a $t \in \mathbb{R}$. However, it is obvious, that it is completely observable for all other scheduling trajectories, as $\text{rank}(\mathcal{O}_2) = 2$ in the functional sense. This implies complete state-observability of the representation in an almost everywhere sense, i.e. the representation defined in Example 3.22 is structurally state-observable.

To check complete state-observability of a given $\mathfrak{R}_{\text{SS}}(\mathcal{S})$, an iterative computation strategy must be applied in terms of Theorem 3.7, checking the rank of $\mathcal{O}_l \diamond p$ for increasing $l > 0$. In step l of this iterative scheme, computation of the minimum of $\text{rank}((\mathcal{O}_l \diamond p)(\tau))$ for all $p \in \mathfrak{B}_{\mathbb{P}}$ and $\tau \in \mathbb{R}$ is required which is usually an infinite dimensional and hence unsolvable optimization problem. An approximative solution may follow through the parametrization of p like polynomial, piecewise continuous, periodical, etc. and then using this parameterized scheduling to set up a feasibility problem for the full rank of the matrix function on a large interval of \mathbb{R} . If in iteration step l it holds that $\text{rank}((\mathcal{O}_l \diamond p)(\tau)) = \text{rank}((\mathcal{O}_{l-1} \diamond p)(\tau))$ for all $p \in \mathfrak{B}_{\mathbb{P}}$ and $t \in \mathbb{R}$, then the observability rank of the representation is found. As this condition cannot be checked in a non-conservative sense, the iterative scheme can only prove complete state-observability if full rank of $\mathcal{O}_l \diamond p$ can be showed in a computationally feasible number of steps.

On the other hand, the rank test for structural state-observability can be accomplished in the SISO case based on symbolic computation of the determinant of $\mathcal{O}_{n_{\mathcal{X}}}$. In case the result is a non-zero function, then structural state-observability

is satisfied. In the MIMO case, full rank of $\mathcal{O}_{n \times}$ can be checked by forming square matrices from the rows of $\mathcal{O}_{n \times}$ using all possible combinations and checking if any of the determinants of these matrices is non-zero.

B. State-reachability in continuous-time

The concepts introduced in the observability case can be similarly introduced in the reachability sense. The only difference is that to show the results, instead of state-reconstructibility, we need to introduce the so called *controllability map*. By introducing this map, we develop the analog of the results of the observability case.

In terms of Definition 3.29, reachability of an LPV representation represents the ability to transfer an arbitrary initial state to an arbitrary target state of \mathcal{X} in case of any scheduling trajectory. This can be explained using controllability maps between the space of input signals and the state-space \mathcal{X} . For a given $p \in \mathfrak{B}_{\mathbb{P}}$, define the following linear map from $\mathcal{L}_1^{\text{loc}}([t_0, t_1], \mathbb{U})$ to \mathcal{X} :

$$\mathbf{x} = \int_{t_0}^{t_1} \mathfrak{A}(t_1, \tau, p) B(p(\tau)) u(\tau) d\tau, \quad \mathbf{x} \in \mathcal{X}, \quad t \in [t_0, t_1]. \quad (3.82)$$

For the given p , the mapping (3.82) defines the state evolution of $\mathfrak{R}_{\text{SS}}(\mathcal{S})$ in the finite interval $[t_0, t_1]$ for an initial condition $x(t_0) = 0$ and input $u \in \mathcal{L}_1^{\text{loc}}([t_0, t_1], \mathbb{U})$. The state $\mathbf{x} \in \mathcal{X}$ is said to be controllable on $[t_0, t_1]$, if \mathbf{x} lies in the image of the linear map (3.82). Note that in case of initial condition $x(t_0) = \mathbf{x}_0$ and target state $x(t_1) = \mathbf{x}_1$, linearity of the signal behavior implies that the input $u \in \mathcal{L}_1^{\text{loc}}([t_0, t_1], \mathbb{U})$ which satisfies (3.82) for $\mathbf{x} = \mathbf{x}_1 - \mathfrak{A}(t_1, t_0, p)\mathbf{x}_0$, transfers the state \mathbf{x}_0 to \mathbf{x}_1 in $[t_0, t_1]$. This means that if (3.82) is surjective, then every state can be reached from an arbitrary state in the time-interval $[t_0, t_1]$. If (3.82) is surjective for every $p \in \mathfrak{B}_{\mathbb{P}}$, then $\mathfrak{R}_{\text{SS}}(\mathcal{S})$ is called state-reachable on $[t_0, t_1]$. It is easy to show that $\mathfrak{R}_{\text{SS}}(\mathcal{S})$ is completely state-reachable, if it is state-observable for any finite interval in \mathbb{R} . Now we can introduce the following matrix function to describe the linear map (3.82):

Definition 3.33 (*n*-step CT state-reachability matrix function) (Silverman and Meadows 1969) *In continuous-time, the *n*-step state-reachability matrix function of $\mathfrak{R}_{\text{SS}}(\mathcal{S})$ is defined as $\mathcal{R}_n \in \mathcal{R}^{n \times (n \nu)}$ with*

$$\mathcal{R}_n = [\mathbf{r}_1 \quad \mathbf{r}_2 \quad \dots \quad \mathbf{r}_n], \quad (3.83)$$

where $\mathbf{r}_1 = B$ and

$$\mathbf{r}_{i+1} = -A\mathbf{r}_i + \dot{\mathbf{r}}_i, \quad i > 1. \quad (3.84)$$

The *n*-step state-reachability matrix function has similar role as the state-reachability matrix for LTI representations.

Example 3.26 (CT state-reachability matrix function) Consider the LPV-SS representation $\mathfrak{R}_{\text{SS}}(S)$ defined in Example 3.22. The reachability matrices of $\mathfrak{R}_{\text{SS}}(S)$ for $n = 1, 2, 3$ are as follows:

$$\mathcal{R}_1 \diamond p = \begin{bmatrix} 1 \\ p \end{bmatrix}, \quad \mathcal{R}_2 \diamond p = \begin{bmatrix} 1 & -2p \\ p & \frac{d}{dt}p - 1 \end{bmatrix}, \quad \mathcal{R}_3 \diamond p = \begin{bmatrix} 1 & -2p & 1 + 2p^2 - 3\frac{d}{dt}p \\ p & \frac{d}{dt}p - 1 & \frac{1 - \frac{d}{dt}p}{p} + \frac{d^2}{dt^2}p \end{bmatrix}.$$

These matrices were computed by using:

$$\dot{\mathbf{r}}_1 \diamond p = \begin{bmatrix} 0 & \frac{d}{dt}p \end{bmatrix}^\top, \quad \dot{\mathbf{r}}_2 \diamond p = \begin{bmatrix} -2\frac{d}{dt}p & \frac{d^2}{dt^2}p \end{bmatrix}^\top.$$

We can also introduce the notion of structural state-reachability:

Definition 3.34 (Structural state-reachability) $\mathfrak{R}_{\text{SS}}(S)$ with state-dimension $n_{\mathcal{X}}$ is called *structurally state-reachable* if its $n_{\mathcal{X}}$ -step reachability matrix $\mathcal{R}_{n_{\mathcal{X}}}$ is full rank, i.e. $\text{rank}(\mathcal{R}_{n_{\mathcal{X}}}) = n_{\mathcal{X}}$.

Moreover it can be shown, that Lemma 3.2 holds also for \mathcal{R}_n implying all the properties that have been noted in the observability case (Silverman and Meadows 1969). Similarly we can introduce the reachability radius of a given SS representation with respect to a scheduling signal $p \in \mathfrak{B}_{\mathbb{P}}$. As the reachability radius can vary for each trajectory of p , thus the notion of constant reachability rank representation is introduced:

Definition 3.35 (Constant reachability rank representation) (Silverman and Meadows 1969) A $\mathfrak{R}_{\text{SS}}(S)$ representation has *constant reachability rank* if there exist a $n \in \{1, \dots, n_{\mathcal{X}}\}$ and a $l > 0$ such that

$$\text{rank}((\mathcal{R}_n \diamond p)(t)) = \text{rank}((\mathcal{R}_{n+1} \diamond p)(t)) = l \leq n_{\mathcal{X}}, \quad (3.85)$$

for all $p \in \mathfrak{B}_{\mathbb{P}}$ and $t \in \mathbb{T}$.

Example 3.27 (CT non-constant reachability rank representation) For Example 3.26 it holds, that $\text{rank}((\mathcal{R}_2 \diamond p)(t)) = 2$ for all possible scheduling signals and time instances, except when for a $t \in \mathbb{R}$ the scheduling signal satisfies $2p^2(t) = -\frac{d}{dt}p(t) + 1$. At that time instant, $\text{rank}((\mathcal{R}_2 \diamond p)(t)) = 1$. Hence it is not a constant reachability rank representation, but its minimal reachability radius is 1. For a constant reachability rank representation see Example 3.28.

Using the previously introduced concepts, the analog of Theorem 3.7 holds in the reachability case as well:

Theorem 3.8 (Induced complete LPV state-reachability in CT) (Silverman and Meadows 1967) The CT-LPV-SS representation $\mathfrak{R}_{\text{SS}}(S)$ is completely state-reachable, iff for any $p \in \mathcal{C}^\infty(\mathbb{R}, \mathbb{P}) \cap \mathfrak{B}_{\mathbb{P}}$ it holds that there exists a $0 < n < \infty$ such that $\text{rank}((\mathcal{R}_n \diamond p)(\tau)) = n_{\mathcal{X}}$ for all $\tau \in \mathbb{R}$. If $\mathfrak{R}_{\text{SS}}(S)$ has constant reachability rank, then the condition is $\text{rank}((\mathcal{R}_{n_{\mathcal{X}}} \diamond p)(\tau)) = n_{\mathcal{X}}$ for all $\tau \in \mathbb{R}$.

The proof follows similarly as in Silverman and Meadows (1967). The interpretation of this theorem is the same as in the observability case: an LPV-SS can be completely state-reachable, even if the n_x -step state-reachability matrix is not full rank along every scheduling trajectory. In case $\mathfrak{R}_{\text{SS}}(\mathcal{S})$ is a constant reachability rank representation, then similar to the LTI case, full rank of $(\mathcal{R}_{n_x} \diamond p)(\tau)$ along every $p \in \mathfrak{B}_{\mathbb{P}}$ guarantees complete state-reachability. For an SS representation with complete state-reachability, see Example 3.28.

It can be also shown that the class of LPV-SS representations with constant reachability rank includes the class of LTI-SS representations (see Silverman (1971)). It can be also shown, that if quadratic stabilizability (see Lee (1997)) is satisfied for a LPV-SS representation with static linear dependence, then it is a necessary condition in terms of Theorem 3.8 for complete state-reachability.

Example 3.28 (CT complete state-reachability) Let the SS representation $\mathfrak{R}_{\text{SS}}(\mathcal{S})$ of an CT-LPV system \mathcal{S} with $\mathbb{P} = [-\frac{1}{2}, \frac{1}{2}]$ be given by

$$\left[\begin{array}{c|c} A & B \\ \hline C & D \end{array} \right] \diamond p = \left[\begin{array}{cc|c} -\tan(p) \frac{d}{dt} p & \sin(p) & \cos(p) \\ 0 & 2 & 1 \\ \hline 1 & 1 & 0 \end{array} \right].$$

Then it follows that

$$\mathcal{R}_2 \diamond p = \begin{bmatrix} \cos(p) & \sin(p) \\ 1 & 2 \end{bmatrix}.$$

As $2 \cos(p) \neq \sin(p)$ on \mathbb{P} , thus \mathcal{R}_2 has rank 2 for all $p \in \mathfrak{B}_{\mathbb{P}}$ and $t \in \mathbb{R}$. This means that $\mathfrak{R}_{\text{SS}}(\mathcal{S})$ is completely state reachable on \mathbb{P} .

In case $\text{rank}(\mathcal{R}_{n_x}) = n_x$ is satisfied, i.e. the SS representation is structurally state-reachable, then it holds that $\text{rank}((\mathcal{R}_n \diamond p)(\tau)) = n_x$ for all $t \in \mathbb{R}$ except some $p \in \mathcal{C}^\infty(\mathbb{R}, \mathbb{P}) \cap \mathfrak{B}_{\mathbb{P}}$. Then similar to the previous case, it is obvious that structural state-reachability is a necessary condition for complete state-reachability. To check complete or structural state-reachability the computational considerations are the same as discussed for the observability case.

C. State-observability in discrete-time

The concept of state-observability can be similarly investigated in DT for a given LPV-SS representation $\mathfrak{R}_{\text{SS}}(\mathcal{S})$ with state and output equations (3.51a-b). By using a similar line of reasoning, we explore the previously introduced concepts based on the theory for DT-LTV systems in Gohberg et al. (1992). Define the state transition matrix as

$$\mathfrak{A}(k_1, k_0, p) = \begin{cases} \prod_{i=0}^{k_1-k_0-1} (A \diamond p)(k_1 - i), & \text{if } k_1 > k_0; \\ I, & \text{if } k_1 \leq k_0; \end{cases} \quad (3.86)$$

for $k_1, k_0 \in \mathbb{Z}$. Then, based on (3.51a-b), the state and output evolution of $\mathfrak{R}_{\text{SS}}(\mathcal{S})$ in the finite time interval $[k_0, k_1] \subset \mathbb{Z}$ satisfies

$$x(k_1) = \mathfrak{A}(k_1, k_0, p)x(k_0) + \sum_{i=k_0}^{k_1} \mathfrak{A}(k_1, i, p)(B \diamond p)(i)u(i), \quad (3.87a)$$

$$y(k_1) = (C \diamond p)(k_1)x(k_1), \quad (3.87b)$$

for all $k_1 \geq k_0$ along a scheduling trajectory $p \in \mathfrak{B}_{\mathbb{P}}$. Again, complete state-observability of $\mathfrak{R}_{\text{SS}}(\mathcal{S})$ can be considered as a reconstruction problem of any $x_0 = x(k_0)$ from a zero input response in the time interval $[k_0, k_1] \subset \mathbb{Z}$. Then state-observability on $[k_0, k_1]$ requires that the linear map

$$y(k) = (C \diamond p)(k)\mathfrak{A}(k, k_0, p)x, \quad x \in \mathfrak{X}, k \in [k_0, k_1], \quad (3.88)$$

from \mathfrak{X} to $\mathfrak{Y}^{[k_0, k_1]}$ is injective for every $p \in \mathbb{P}^{[k_0, k_1]}$. It can be shown again, that $\mathfrak{R}_{\text{SS}}(\mathcal{S})$ is completely state-observable if it is state-observable for any finite interval of \mathbb{Z} with $n_{\mathfrak{X}} \leq k_1 - k_0 < \infty$. Now we can introduce the following observability matrix in DT to describe the linear map (3.88):

Definition 3.36 (*n*-step DT state-observability matrix function) (Gohberg et al. 1992) *In discrete-time, the *n*-step state-observability matrix function $\mathcal{O}_n \in \mathbb{R}^{n_{\mathfrak{X}} \times n n_{\mathfrak{U}}}$ of $\mathfrak{R}_{\text{SS}}(\mathcal{S})$ is defined as (3.78) with*

$$o_1 = C, \quad o_{i+1} = \overrightarrow{o}_i A, \quad \forall i > 1. \quad (3.89)$$

The *n*-step state-observability matrix function has a similar role as the state-observability matrix for LTI representations, as in case of complete state-observability, it provides an invertible map for the reconstruction of the state from the samples of y . Note that the difference in the structure of the discrete-time *n*-step state-observability matrix with respect to its continuous-time counterpart is due to the different commutation rules for the $\frac{d}{dt}$ and q operators on $\mathcal{R}[\xi]$.

Example 3.29 (DT state-observability matrix function) *Consider the DT-LPV-SS representation $\mathfrak{R}_{\text{SS}}(\mathcal{S})$ of Example 3.21. This representation is given by*

$$\left[\begin{array}{c|c} A & B \\ \hline C & D \end{array} \right] \diamond p = \left[\begin{array}{cc|c} p & 1 & 1 \\ 0 & p & p \\ \hline 1 & \frac{1}{p} & p \end{array} \right],$$

with $\mathbb{P} = [\frac{1}{4}, \frac{3}{4}]$. Then the observability matrices of $\mathfrak{R}_{\text{SS}}(\mathcal{S})$ for $n = 1, 2, 3$ are as follows:

$$\mathcal{O}_1 \diamond p = \left[\begin{array}{c} 1 \\ \frac{1}{p} \end{array} \right], \quad \mathcal{O}_2 \diamond p = \left[\begin{array}{cc} 1 & \frac{1}{p} \\ p & 1 + \frac{p}{qp} \end{array} \right], \quad \mathcal{O}_3 \diamond p = \left[\begin{array}{cc} 1 & \frac{1}{p} \\ p & 1 + \frac{p}{qp} \\ p(qp) & p(1 + \frac{(qp)}{(q^2p)}) + qp \end{array} \right].$$

These matrices were computed by using:

$$\overrightarrow{o}_1 \diamond p = \left[\begin{array}{c} 0 \\ \frac{1}{qp} \end{array} \right], \quad \overrightarrow{o}_2 \diamond p = \left[\begin{array}{cc} qp & 1 + \frac{(qp)}{(q^2p)} \end{array} \right].$$

Again we can introduce structural state-observability in terms of Definition 3.31. Similarly, Lemma 3.2 also holds in the DT case and by using the concepts of n -step state-observability matrix and constant observability-rank representation, given by Definition 3.36 and 3.32, the induced complete state-observability, Theorem 3.7, can be shown to hold in DT as well:

Theorem 3.9 (Induced complete LPV state-observability in DT) (Gohberg et al. 1992) *The LPV-SS representation $\mathfrak{R}_{\text{SS}}(\mathcal{S})$ is completely state-observable, iff for any $p \in \mathfrak{B}_{\mathbb{P}}$ it holds that there exists a $0 < n < \infty$ such that $\text{rank}((\mathcal{O}_n \diamond p)(\tau)) = n_{\mathcal{X}}$ for all $\tau \in \mathbb{Z}$. If $\mathfrak{R}_{\text{SS}}(\mathcal{S})$ has constant observability rank, then the condition is $\text{rank}((\mathcal{O}_{n_{\mathcal{X}}} \diamond p)(\tau)) = n_{\mathcal{X}}$ for all $\tau \in \mathbb{Z}$.*

The proof follows similarly as in Gohberg et al. (1992). The consequences of this theorem are similar as in the CT case, also implying that discrete-time LPV-SS representations with constant observability rank include the class of DT-LTI-SS representations (see Gohberg et al. (1992)). Furthermore it can be shown, that structural state-observability is a necessary condition for complete state-observability also in the DT case. Again, basic DT results of the existing LPV system theory follow as special cases of Theorem 3.9.

Example 3.30 (DT complete state-observability) *Consider Example 3.29. It is trivial that $\det(\mathcal{O}_2 \diamond p) = \frac{p}{qp}$ can not be zero on $\mathbb{P} = [\frac{1}{4}, \frac{3}{4}]$, thus $\text{rank}((\mathcal{O}_2 \diamond p)(k)) = 2$ for all $p \in \mathfrak{B}_{\mathbb{P}}$ and $k \in \mathbb{Z}$. Naturally, the same holds for \mathcal{O}_3 . Hence the SS representation of Example 3.29 is completely state-observable.*

Again an iterative test can be applied to check complete state-observability in terms of Theorem 3.9. However in the DT case, computation of the minimal rank of $(\mathcal{O}_n \diamond p)(\tau)$ can be accomplished by the generalization of the *Popov-Belevitch-Hautus* (PBH) spectral test, resulting in an *almost eigenvalue* problem (Peters and Iglesias 1999). As computation of the almost eigenvalue/eigenvectors (Beauzamy 1988) is difficult in most general cases, even for representations with linear dependence, therefore in practice an approximative approach is suggested. By this approach, the full rank condition of $(\mathcal{O}_n \diamond p)(\tau)$ is checked for finite sequences of p , like $\{\bar{p}_0, \dots, \bar{p}_{N-1}\}$. Each shifted instance of p in \mathcal{O}_n , like $q^l p$, is associated with the appropriate element of the sequence, i.e. $q^l p = \bar{p}_l$. In this way, the full rank test of $(\mathcal{O}_n \diamond p)(\tau)$, can be formulated as a feasibility problem on \mathbb{P}^N , which can be solved via nonlinear optimization or by gridding. Note that this mechanism corresponds to a conservative rank test, as the feasibility is checked for arbitrary variations of p . To compute the actual rank of \mathcal{O}_n , the previous method is applied iteratively, checking the full rank of \mathcal{O}_l for increasing l . This yields an approach that is easily computable for small dimensions. To check structural state-observability, the same symbolic approach can be used as given in the CT case.

D. State-reachability in discrete-time

In discrete-time, the concept of complete state-reachability can be similarly investigated as in CT, except that in case of state-reachability on a discrete interval

$[k_0, k_1]$, it is required that the linear map

$$\mathbf{x} = \sum_{i=k_0}^k \mathfrak{A}(k, i, p)(B \diamond p)(i)u(i), \quad k \in [k_0, k_1], \quad (3.90)$$

from $\cup^{[k_0, k_1]}$ to \mathcal{X} is surjective for every $p \in \mathfrak{B}_p$. Then, $\mathfrak{R}_{SS}(\mathcal{S})$ is completely state-reachable, if it is state-reachable for any finite interval of \mathbb{Z} . Similar to the CT case, we can introduce the following matrix function to describe the linear map (3.90):

Definition 3.37 (n-step DT state-reachability matrix function) (Gohberg et al. 1992) *In discrete-time, the n-step state-reachability matrix function $\mathcal{R}_n \in \mathcal{R}^{n_{\mathcal{X}} \times n_{\text{nv}}}$ of $\mathfrak{R}_{SS}(\mathcal{S})$ is defined as (3.83) with*

$$\mathbf{r}_1 = B, \quad \mathbf{r}_{i+1} = A\overleftarrow{\mathbf{r}}_i, \quad \forall i > 1. \quad (3.91)$$

Similar to the previous part, the difference in the structure of the discrete-time n-step state-reachability matrix with respect to its continuous-time counterpart is due to the different commutation rules of the $\frac{d}{dt}$ and q operators on $\mathcal{R}[\xi]$.

Example 3.31 (DT state-reachability matrix function) *Consider the SS representation $\mathfrak{R}_{SS}(\mathcal{S})$ defined in Example 3.29. The observability matrices of $\mathfrak{R}_{SS}(\mathcal{S})$ for $n = 1, 2, 3$ are as follows:*

$$\begin{aligned} \mathcal{R}_1 \diamond p &= \begin{bmatrix} 1 \\ p \end{bmatrix}, \quad \mathcal{R}_2 \diamond p = \begin{bmatrix} 1 & p + q^{-1}p \\ p & p(q^{-1}p) \end{bmatrix}, \\ \mathcal{R}_3 \diamond p &= \begin{bmatrix} 1 & p + q^{-1}p & p(q^{-1}p) + (p + q^{-1}p)q^{-2}p \\ p & p(q^{-1}p) & p(q^{-1}p)(q^{-2}p) \end{bmatrix}. \end{aligned}$$

These matrices were computed by using:

$$\overleftarrow{\mathbf{r}}_1 = [0 \quad q^{-1}p]^\top, \quad \overleftarrow{\mathbf{r}}_2 = [q^{-1}p + q^{-2}p \quad q^{-1}p(q^{-2}p)]^\top.$$

Again we can introduce structural state-reachability in terms of Definition 3.34. Additionally, using the previously introduced concepts, the induced complete state-reachability, Theorem 3.8, holds in DT as well:

Theorem 3.10 (Induced complete LPV state-reachability in DT) (Gohberg et al. 1992) *The discrete-time LPV-SS representation $\mathfrak{R}_{SS}(\mathcal{S})$ is completely state-reachable, iff for any $p \in \mathfrak{B}_p$ it holds that there exists a $0 < n < \infty$ such that $\text{rank}((\mathcal{R}_n \diamond p)(\tau)) = n_{\mathcal{X}}$ for all $\tau \in \mathbb{Z}$. If $\mathfrak{R}_{SS}(\mathcal{S})$ has constant reachability rank, then the condition is $\text{rank}((\mathcal{R}_{n_{\mathcal{X}}} \diamond p)(\tau)) = n_{\mathcal{X}}$ for all $\tau \in \mathbb{Z}$.*

The proof follows similarly as in Gohberg et al. (1992). The consequences of this theorem are the same as in the CT case, also implying that discrete-time LPV-SS representations with constant reachability rank include the class of DT-LTI-SS representations (Gohberg et al. 1992). Furthermore it can be shown, that structural state-reachability is a necessary condition for complete state-reachability also in the DT case. Again, basic DT results of the existing LPV systems theory follow as special cases of Theorem 3.9. To check complete or structural state-reachability

in discrete-time the computational considerations are the same as given in the observability case.

Example 3.32 (DT complete state-reachability) Consider Example 3.31. $\det(\mathcal{R}_2 \diamond p) = -p^2$ implies that $\text{rank}((\mathcal{R}_2 \diamond p)(k)) = 2$ for all $p \in \mathfrak{B}_{\mathbb{P}}$ and $k \in \mathbb{Z}$. Trivially, the same holds for \mathcal{R}_3 . Hence the SS representation of Example 3.29 is completely state-reachable.

F. General properties and minimality

As a next step we show that structural state-observability/reachability are the necessary ingredients to develop observability and reachability canonical forms of SS representations which are similar to their LTI counterparts. Additionally, minimality of LPV-SS representations is implied by structural state-observability instead of the complete concept.

Based on the definition of structural state-observability/reachability, an important corollary is the following:

Corollary 3.1 *If $\mathfrak{R}_{\text{SS}}(\mathcal{S})$ is structurally state-observable (reachable), i.e. $\text{rank}(\mathcal{O}_{n_{\mathcal{X}}}) = n_{\mathcal{X}}$ ($\text{rank}(\mathcal{R}_{n_{\mathcal{X}}}) = n_{\mathcal{X}}$), then at least $n_{\mathcal{X}}$ number of rows of $\mathcal{O}_{n_{\mathcal{X}}}$ (columns of $\mathcal{R}_{n_{\mathcal{X}}}$) are linearly independent in the functional sense. This implies that in the SISO case, $\mathcal{O}_{n_{\mathcal{X}}}$ ($\mathcal{R}_{n_{\mathcal{X}}}$) is invertible.*

Based on this property, \mathcal{O}_n and \mathcal{R}_n can be used to define state-transformations in the behavioral framework and, by using similar argumentation as in the LTI case (see Section 2.1.6), to develop canonical forms for LPV-SS representations. Note that in case of complete state-observability/reachability, \mathcal{O}_n or \mathcal{R}_n are invertible for all scheduling trajectories and time instances, which is a much stronger property than the previous one. Thus by requiring this stronger property to generate canonical forms, we would exclude a large set of SS representations that have an equivalent (in the almost everywhere sense) observability/reachability canonical form (see Chapter 4).

A key theorem that enables construction of observability/reachability canonical forms in LPV case is the following:

Theorem 3.11 (Transformation of the state-observability/reachability structure) (Silverman and Meadows 1965) *If the matrices of two LPV-SS representations, with state dimensions $n_{\mathcal{X}}$ and with a common $n_{\mathbb{P}}$ dimensional scheduling space, fulfill the equivalence relation $\stackrel{\text{ne}}{\sim}$ via state-transformation $T \in \mathcal{R}^{n_{\mathcal{X}} \times n_{\mathcal{X}}}$, then for all $n \in \mathbb{N}$:*

$$\begin{cases} \text{for } \mathbb{T} = \mathbb{R}, & \mathcal{O}'_n = \mathcal{O}_n T^{-1}, & \mathcal{R}'_n = T \mathcal{R}_n \\ \text{for } \mathbb{T} = \mathbb{Z}, & \mathcal{O}'_n = \mathcal{O}_n T^{-1} & \mathcal{R}'_n = \overrightarrow{T} \mathcal{R}_n, \end{cases} \quad (3.92)$$

hold, where \mathcal{O}_n and \mathcal{O}'_n , respectively \mathcal{R}_n and \mathcal{R}'_n , are the corresponding n -step state-observability/reachability matrices of the representations.

The proof of this theorem similarly follows as in Silverman and Meadows (1965). This means that the state-observability/reachability structure of equivalent representations is projected through the state-transformation that connects them, which is the required property to develop canonical forms with special structure of \mathcal{O}_n or \mathcal{R}_n .

Similar to the LTI case, complete state-observability also implies minimality, however in the LPV case, minimality only implies structural state-observability:

Theorem 3.12 (Induced PV-SS minimality) *The representation $\mathfrak{R}_{SS}(\mathcal{S})$ is minimal iff it is structurally state-observable.*

The proof of this theorem similarly follows as in the LTI case. We can also define the concept of joint minimality, meaning that $\mathfrak{R}_{SS}(\mathcal{S})$ is jointly minimal if it is minimal and structurally state-reachable.

Example 3.33 (Induced minimality) *Consider Example 3.29 and 3.31. Then the DT-SS representation is minimal as it is completely state-observable. Additionally it is completely state-reachable, hence it is jointly minimal. In case of Example 3.22, structural observability of the representation holds even if it is not completely state-observable. Thus, this representation is also minimal.*

3.3.2 Stability of LPV systems

In this subsection we study stability of LPV systems, expanding the concepts introduced for the LTI case in Section 2.1.5. We follow a similar line of reasoning. First, we define dynamic stability in the behavioral point of view, then we explore its connections with IO stability concepts like *Bounded-Input Bounded-Output* (BIBO) stability. Then as a next step, we investigate stability in the Lyapunov sense and we show the connection of the derived theory with the existing results of LPV control design.

There exist various stability concepts of LPV systems, originating either from the concepts of stability along frozen, i.e. constant scheduling trajectories (frozen stability) or stability along arbitrary varying p (global stability). While the first aspect defines stability in the LTI sense of the frozen behaviors, the latter establishes this concept on the full behavior. In many works, LPV stability issues are only discussed for the state-space case with static dependence, involving the notion of state equilibrium points and Lyapunov functions (Scherer 1996; Apkarian and Gahinet 1995), or mixing the concepts of frozen and global stability by considering slow variations of p (Shamma 1990; Skoog and Lau 1972; Rosenbrock 1963). Here we intend to define stability in the developed behavioral framework, investigating dynamic, IO, and Lyapunov stability both in a global and frozen sense.

Global stability

Global stability is the natural concept of stability for LPV systems, as it means that small causes produce small effects for any scheduling trajectory. Historically, it

originates from LTV system theory (Halanay and Ionescu 1994; Sreedhar and Rao 1968) and robust control synthesis (Zhou and Doyle 1998), where the problem of stability over the variations of the system has been first encountered. From the behavioral point of view, this concept extends the notion of dynamic stability (see Definition 2.27) for LPV systems as follows:

Definition 3.38 (Global dynamic stability) *The autonomous LPV dynamical system $S = (\mathbb{T}, \mathbb{R}^{n_w}, \mathbb{P} \subseteq \mathbb{R}^{n_p}, \mathfrak{B})$ is said to be globally stable, if $((w, p) \in \mathfrak{B}) \Rightarrow (\exists \varepsilon \in \mathbb{R}_0^+$ such that $\|w(t)\| \leq \varepsilon$ for all $t \geq 0$) (in an arbitrary norm $\|\cdot\|$). It is said to be globally unstable, if it is not stable; it is said to be globally asymptotically stable, if $((w, p) \in \mathfrak{B}) \Rightarrow (w(t) \rightarrow 0$ as $t \rightarrow \infty$).*

The definition strongly builds on the linearity (the only fixed point of the dynamic relation is 0) and time-invariance (stability on $t \geq 0$ implies stability on $t \geq t_0$ for all $t_0 \in \mathbb{R}$) of the LPV system class. Note that in terms of Definition 3.38 any signal trajectory, i.e. signal evolution of the system on the half-line, is bounded no matter the scheduling trajectory it is associated with, and the bound depends on the particular solution w . It is obvious that global stability includes stability with respect to frozen behaviors, as boundedness of w must hold for constant scheduling trajectories as well. In this way, it generalizes the previously introduced LTI concept of Definition 2.27. This also emphasizes the difference between LPV and LTV systems, as in the latter case stability is defined with respect to only one, linear-trajectory of the scheduling ($p(t) = t$).

Contrary to the LTI case, conditions of global dynamic stability for LPV-KR representations can not be formulated in terms of eigenvalues or root conditions of polynomials in $\mathcal{R}[\xi]$. To show this, consider the following argument: In the CT-LTI case, $\frac{d}{dt}w = rw$ has solutions on the half-line in the form of $w(t) = e^r w(0)$, thus the condition $r < 0$ guarantees boundedness of the solutions. However in the CT-LPV case $\frac{d}{dt}w = (r \diamond p)w$ with $r \in \mathcal{R}$, has solutions on the half-line in the form of $w(t) = e^{(r \diamond p)(t)} w(0)$ only for constant p . Thus boundedness is not guaranteed by $(r \diamond p)(t) < 0, t \geq 0$. In fact, it is often possible to find a scheduling trajectory p such that the solution diverges even if $(r \diamond p)(t) < 0, t \geq 0$.

In case of an IO partition of S , the concept of dynamic stability is formulated around the autonomous part of the behavior on the half line $[0, \infty)$, where $u = 0$. Similarly, the notion of global dynamic stability generalizes for systems with state-variables. Furthermore, global dynamic stability of LPV systems with IO partition also implies BIBO stability in the ℓ_∞ norm, and global asymptotic stability implies BIBO stability in the ℓ_τ norm, $1 \leq \tau < \infty$:

Definition 3.39 (BIBO stability) *The LPV dynamical system $S = (\mathbb{T}, \mathbb{R}^{n_w}, \mathbb{P} \subseteq \mathbb{R}^{n_p}, \mathfrak{B})$ with IO partition (u, y) is said to be BIBO stable in the ℓ_τ norm with $1 \leq \tau < \infty$, if for all $(u, y, p) \in \mathfrak{B}$ it holds that*

$$\left\{ \begin{array}{l} \text{for } \mathbb{T} = \mathbb{R}, \quad \int_0^\infty \|u(t)\|^\tau dt < \infty \Rightarrow \int_0^\infty \|y(t)\|^\tau dt < \infty; \\ \text{for } \mathbb{T} = \mathbb{Z}, \quad \sum_{k=0}^\infty \|u(k)\|^\tau < \infty \Rightarrow \sum_{k=0}^\infty \|y(k)\|^\tau < \infty. \end{array} \right.$$

It is said to be BIBO stable in the ℓ_∞ norm, if for all $(u, y, p) \in \mathfrak{B}$ it holds that

$$\sup_{t \geq 0} \|u(t)\| < \infty \Rightarrow \sup_{t \geq 0} \|y(t)\| < \infty.$$

Dynamic stability implies BIBO stability in the ℓ_∞ norm as all trajectories of y are bounded in case of dynamic stability. This boundedness holds due to the fact that the autonomous part of the behavior is bounded and \mathfrak{B} fulfills the linearity and time-invariance properties in Definition 3.2. Similarly, asymptotic dynamic stability implies BIBO stability in an arbitrary ℓ_τ norm as all trajectories of y in the autonomous part of the behavior converge to zero. The concept of *Bounded-Input Bounded-State* (BIBS) stability can be defined for LPV systems with both IO partition and state variables in a similar manner as BIBO stability. Also in the LPV case, BIBS stability always implies BIBO stability.

Another notion of stability follows through the direct method of Lyapunov, extending the concepts that have been established in the LTI case (see Section 2.1.5). Let $x \in \mathbb{X}^\top$ be the solution of the autonomous part of a SS representation $\mathfrak{R}_{\text{SS}}(\mathcal{S})$ for a given scheduling trajectory $p \in \mathfrak{B}_{\mathbb{P}}$:

$$\xi x = (A \diamond p)x, \quad (3.93)$$

where ξ is either $\frac{d}{dt}$ or q . Similar to the discussion in the LTI case (see Section 2.1.5) we investigate dynamic stability of (3.93) by constructing a Lyapunov function that fulfills certain properties. Again, consider the class of quadratic functions as Lyapunov functions, but now assume that $P \in \mathcal{R}^{n_x \times n_x}$, so $\mathcal{V}(\tau, p) = \tau^\top (P \diamond p)\tau$, where $\tau \in \mathbb{R}^{n_x}$ and $P = P^\top$ (symmetric). Then in continuous-time, using the chain rule of differentiation, it holds that

$$\frac{d}{dt} \mathcal{V}(x, p) = x^\top \underbrace{((A^\top P + PA + \dot{P}) \diamond p)}_Q x, \quad (3.94)$$

where $Q \in \mathcal{R}^{n_x \times n_x}$ is symmetric. The term $Q = A^\top P + PA + \dot{P}$ is called the parameter-varying CT Lyapunov equation. In discrete-time, using a quadratic Lyapunov function yields

$$\mathcal{V}(qx, qp) - \mathcal{V}(x, p) = x^\top \underbrace{((A^\top \vec{P} A - P) \diamond p)}_Q x, \quad (3.95)$$

where $Q \in \mathcal{R}^{n_x \times n_x}$ is also symmetric. Here the term $Q = A^\top \vec{P} A - P$ is the parameter-varying DT Lyapunov equation. Similar to the LTI case, the concept of stability is formulated around the “definiteness” property of (3.94) or (3.95) and the quadratic Lyapunov function. In case of a quadratic parameter-varying function $\mathcal{V}(\tau, p) = \tau^\top (P \diamond p)\tau$ with symmetric $P \in \mathcal{R}^{n_x \times n_x}$, we can define for a given $p \in \mathfrak{B}_{\mathbb{P}}$ the positive definiteness of P . We call P positive definite for p , i.e. $(P \diamond p) \succ 0$, if there exists a $\varepsilon > 0$ such that $(P \diamond p)(t) \succeq \varepsilon I$ for all $t \geq 0$ ($P \diamond p$ is bounded away from 0). The definition of negative definit, semi definit, etc. similarly follows (see Definition 2.29). Then, based on Theorem 2.9, the following holds:

Theorem 3.13 (LPV Quadratic stability) Consider (3.93) and a projected scheduling behavior \mathfrak{B}_P . Assume that $P \in \mathcal{R}^{n_x \times n_x}$, $P = P^\top$, and $Q = Q^\top$ satisfy the corresponding Lyapunov equation (see (3.94) and (3.95)) and $P \diamond p$ is bounded for all $p \in \mathfrak{B}_P$. If for all $p \in \mathfrak{B}_P$ it holds that

- $(P \diamond p) \succ 0$ and $(Q \diamond p) \preceq 0$, then (3.93) is dynamically stable.
- $(P \diamond p) \succ 0$, $(Q \diamond p) \preceq 0$, and (A, Q) is completely state-observable, then (3.93) is dynamically asymptotically stable.
- $(P \diamond p) \prec 0$, $(Q \diamond p) \preceq 0$, and (A, Q) is completely state-observable, then (3.93) is dynamically unstable.

The proof of this theorem can be given according to Ravit et al. (1991) in CT and Anderson (1982) in DT. However, there are two important facts to be noted. First, complete state-observability is required to ensure that the behavior of all state trajectories are characterized by the Lyapunov function. In this way, as \mathcal{V} is bounded away from zero with a positive ε and its derivative (difference) is bounded away from zero with a non-positive ε along every state and scheduling trajectory, convergence of the state to the origin is ensured. However, checking complete state-observability of (A, Q) is a computationally difficult problem (see Section 3.3.1). Second, due to the freedom of the functional dependence of P , the theorem is non-constructive in the general case.

Based on the previous considerations, in practice $\mathcal{R}^{n_x \times n_x}$ can be found to be too general for Lyapunov function construction. Especially in LPV control, the search for quadratic Lyapunov functions is commonly restricted to either a constant matrix $P \in \mathcal{R}^{n_x \times n_x}$ or to rational functions with static dependence on p . This restriction introduces conservative use of the Lyapunov theorem: If such a $P \in \mathcal{R}^{n_x \times n_x}$ can be found that either of the first two items of Theorem 3.13 is satisfied, then stability of the system can be concluded, however, the lack of such a P does not necessarily imply instability. What we gain by the restriction of $P \in \mathcal{R}^{n_x \times n_x}$, is that the parameter-varying Lyapunov equations are modified as

$$\begin{cases} \text{for } \mathbb{T} = \mathbb{R}, & A^\top \diamond p P + P(A \diamond p) \prec 0, \\ \text{for } \mathbb{T} = \mathbb{Z}, & (A^\top \diamond p)P(A \diamond p) - P \prec 0. \end{cases} \quad (3.96)$$

By assuming that A has linear and static dependence on p , then the inequalities (3.96) become LMIs, defining an infinite dimensional *Linear Semi-Definite Programming* (LSDP) problem on \mathbb{P} for the synthesis of P . If additionally it is assumed that \mathbb{P} is a convex polytope⁴ in \mathbb{R}^{n_p} , then (3.96) reduces to a finite LSDP problem, where the feasibility of the Lyapunov equations is only checked at the vertices of the polytope \mathbb{P} (see Scherer (1996) and Apkarian and Gahinet (1995)). This gives the foundation of the traditional \mathcal{H}_2 and \mathcal{H}_∞ LPV control synthesis. Additionally, the use of full-block multipliers also enables to handle A with rational dependence through an LFT representation of the system (Scherer 2001). In some works, parameter-varying Lyapunov functions with rational (Wu and Dong 2006)

⁴A convex polytope is the convex hull of a finite set of points, i.e. it is the intersection of half-spaces.

or general (Apkarian and Adams 1998), static dependence are also considered to overcome the restrictions of searching for a constant P . In the most simple case, assuming linear dependence of both P and A on p and restricting the derivative of p to a polytopic set, gives that the parameter-varying Lyapunov equations (3.94) and (3.95) can be formulated as LMIs by the use of relaxations, which again translates to a finite LSDP problem.

Example 3.34 (Global LPV stability) Consider the DT-SS representation $\mathfrak{A}_{\text{SS}}(S)$, defined in Example 3.29. Choose a quadratic Lyapunov function

$$\mathcal{V}(\tau, p) = \tau^\top \underbrace{\begin{bmatrix} 0.1 & 0 \\ 0 & 1 \end{bmatrix}}_P \tau.$$

As all eigenvalues of P are positive, thus $P \succ 0$. By computing the DT Lyapunov equation, it follows that

$$Q \diamond p = (A^\top \vec{P} A - P) \diamond p = \frac{1}{10} \begin{bmatrix} p^2 - 1 & p \\ p & 10p^2 - 9 \end{bmatrix}.$$

Because $\mathbb{P} = [\frac{1}{4}, \frac{3}{4}]$, it holds that there exists a $\varepsilon < 0$ such that $(Q \diamond p)(k) \preceq \varepsilon I$ for all $k \in \mathbb{Z}$ and $p \in \mathfrak{B}_{\mathbb{P}}$. Furthermore (\vec{A}, \vec{Q}) is completely state-observable as the rank of Q is always 2 along any $p \in \mathfrak{B}_{\mathbb{P}}$. Thus the chosen Lyapunov function proves asymptotic stability of S .

Frozen stability

Another important aspect of LPV stability is the so called frozen stability. Stability analysis of the frozen behaviors has been in the focus of LPV control during the gain-scheduling area, before the appearance of global LPV control synthesis techniques. At that time, researchers concluded global stability of the system based on the stability of the frozen behaviors by assuming appropriately slowly varying scheduling signals (Yaz and Niu 1989; Skoog and Lau 1972; Rosenbrock 1963). This view has been found misleading as the term “appropriate” was not well-defined (see the arguments of Rugh (1991) and Shamma and Athans (1992)). Today, frozen stability is still important in LPV analysis as it is a necessary ingredient for global stability.

Definition 3.40 (Frozen stability) Let $\mathcal{F}_{\mathbb{P}}$ be the frozen system set (see Definition 3.3) of the LPV system S with scheduling space $\mathbb{P} \subseteq \mathbb{R}^{n_p}$. Then, in the frozen sense, S is

- Uniformly asymptotically stable, if for all $\bar{p} \in \mathbb{P}$ $\mathcal{F}_{\bar{p}} \in \mathcal{F}_{\mathbb{P}}$ is dynamically asymptotically stable.
- Uniformly stable, if for all $\bar{p} \in \mathbb{P}$, $\mathcal{F}_{\bar{p}}$ is dynamically stable.
- Non-uniformly stable, if it is not uniformly stable but there exists a $\bar{p} \in \mathbb{P}$ s.t. $\mathcal{F}_{\bar{p}}$ is dynamically stable.
- Uniformly unstable, if for all $\bar{p} \in \mathbb{P}$, $\mathcal{F}_{\bar{p}}$ is dynamically unstable.

Note that uniform frozen stability of \mathcal{S} does not imply global dynamic stability, though the converse is true. In terms of Definition 3.40, the stability of the frozen aspects of the system is checked separately for each frozen behavior. For example this means the construction of quadratic Lyapunov functions separately for each $\bar{p} \in \mathbb{P}$. If there exists such a common quadratic Lyapunov function which proves stability for all $\bar{p} \in \mathbb{P}$, where \mathbb{P} is convex, then in case of linear and static dependence of A , it also implies global stability in terms of Theorem 3.13. This makes an important distinction for systems with dynamic dependence, where the evaluation of A along a constant scheduling trajectory excludes the effect of the dependence on the derivatives/time shifts of p . For these systems, a common Lyapunov function of the frozen systems set does not imply global stability.

Example 3.35 (Frozen LPV stability) Consider again the DT-SS representation $\mathfrak{R}_{\text{SS}}(\mathcal{S})$, defined in Example 3.29. For every constant scheduling trajectory $p \in \mathfrak{B}_{\mathbb{P}}$, where $p(k) = \bar{p}, \forall k \in \mathbb{Z}$, it holds that the eigenvalues of $(A \diamond p)$ are equal to \bar{p} . As $\bar{p} < 1$ for all $\bar{p} \in \mathbb{P}$, thus uniform frozen asymptotic stability of \mathcal{S} holds. This is a not surprising discovery, as global asymptotic stability of \mathcal{S} , proved in Example 3.34, implies uniform frozen asymptotic stability of \mathcal{S} . Now consider the CT-SS representation defined in Example 3.24. For this representation, eigenvalues of $(A \diamond p)$ are $\{0, 2\}$ for any constant scheduling trajectory which proves uniform frozen instability of the represented system. Uniform frozen instability also implies global instability.

3.3.3 Gramians of LPV state-space representations

Gramians are also important concepts for LPV-SS representations, as they describe the complete state-observability and reachability properties and they can also characterize model reduction (see Wood et al. (1996)). Using the previously developed linear input-map (3.77) and linear output-map (3.82) of the CT case, and their DT equivalents (3.88) and (3.90), the concept of PV gramians is introduced as follows:

Definition 3.41 (PV gramians) In CT, the observability gramian O and the reachability gramian R of an asymptotically stable $\mathfrak{R}_{\text{SS}}(\mathcal{S})$ on the time interval $[t_0, t_1] \subset \mathbb{R}$ and along a scheduling trajectory $p \in \mathfrak{B}_{\mathbb{P}}$ are defined as:

$$O(t_1, t_0, p) = \int_{t_0}^{t_1} \mathfrak{A}^T(\tau, t_0, p)(C^\top \diamond p)(\tau)(C \diamond p)(\tau)\mathfrak{A}(\tau, t_0, p)d\tau, \quad (3.97a)$$

$$R(t_1, t_0, p) = \int_{t_0}^{t_1} \mathfrak{A}(t_1, \tau, p)(B \diamond p)(\tau)(B^\top \diamond p)(\tau)\mathfrak{A}^T(t_1, \tau, p)d\tau, \quad (3.97b)$$

while in DT, they are given on the time interval $[k_0, k_1] \subset \mathbb{Z}$ as:

$$O(k_1, k_0, p) = \sum_{i=k_0}^{k_1} \mathfrak{A}^T(i, k_0, p)(C^\top \diamond p)(i)(C \diamond p)(i)\mathfrak{A}(i, k_0, p), \quad (3.98a)$$

$$R(k_1, k_0, p) = \sum_{i=k_0}^{k_1} \mathfrak{A}(k_1, i, p)(B \diamond p)(i)(B^\top \diamond p)(i)\mathfrak{A}^T(k_1, i, p). \quad (3.98b)$$

Similar to the LTI case, the full rank property of gramians implies complete state-observability and reachability on the considered time interval and scheduling trajectory:

Theorem 3.14 (Induced PV observability/reachability) (Silverman and Meadows 1967) *The LPV-SS representation $\mathfrak{R}_{SS}(S)$, is completely state-observable/reachable) iff its observability/reachability gramian is full rank for any finite time interval and each scheduling trajectory of $\mathfrak{B}_{\mathbb{P}}$.*

See the proofs in (Silverman and Meadows 1967) for the CT case and in Gohberg et al. (1992) for the DT case.

3.4 Summary

In this chapter, we have developed a behavioral framework of LPV systems as an extension of the LTI behavioral approach introduced in Chapter 2. The introduced theory has been established to give a unified view on LPV system theory and to enable to approach LPV system identification in a well-founded system theoretic sense.

First in Section 3.1, we have introduced the behavioral concept of LPV systems, setting this system theoretical concept as a modeling approach in terms of the gain-scheduling principle. Then we have systematically built up the behavioral framework by introducing kernel, state-space, and input-output representations of LPV systems both in continuous and discrete-time. We have analyzed the notion of state and established three key theorems: the existence of kernel representations, the existence of state-kernel forms, and later in Section 3.2 the concept of left/right unimodular transformations based on the results of Zerz (2006) and Ilchmann and Mehrmann (2005). We have also shown that the behavioral definition of these representations includes the existing LPV-SS and IO model definitions of the literature. Our main contribution in this context is the development of an algebraic structure upon which the previous results are based on. By this structure, the behavior of LPV systems is described by polynomials in the time operators $\frac{d}{dt}$ (or q) and the coefficients of these polynomials are meromorphic functions of the scheduling variable p and its derivatives or time-shifts. This type of coefficient dependence has been introduced as dynamic dependence and it provides more freedom than the so called static dependence (dependence only on the instantaneous value of p) used in the models of the-state-of-the-art of the LPV literature. By establishing equivalence classes and relations of the introduced representations in Section 3.2, a major conclusion resulted that dynamic dependence is necessary to develop equivalent representations of the same system.

As a next step in Section 3.3, important properties of systems and representations have been investigated in terms dynamic stability and state-observability/reachability. Based on the results of LTV system theory, we have shown that complete state-observability and reachability are very strong properties in the LPV case as only a rather restricted class of representations fulfills them. Moreover,

they are not required for minimality nor the generation of observability or reachability canonical forms. We have shown that a weaker property, the so called structural state-observability/reachability, which defines the state-observability/reachability concept in an almost everywhere sense, is a necessary and sufficient property to generate these canonical forms or to imply minimality. After this, we have introduced dynamic stability of LPV systems in the behavioral sense and shown that BIBO stability is implied by this concept. Then we have explored Lyapunov stability of the considered LPV system class and we have shown that the developed theory includes the current Lyapunov theory of LPV control design as a special case.

In the next chapter, we continue by extending the concept of equivalence transformations between different representation domains, introduced in Section 2.1, to the LPV system class. This contribution gives the finishing details of the developed behavioral framework and enables the comparison of different LPV model structures.

LPV equivalence transformations

In this chapter, we continue the discussion of the LPV behavioral framework by establishing equivalence transformations between the state-space and the input-output representation domains. These equivalence transformations enable the comparison and analysis of LPV model structures and provide essential tools to formulate the identification approach of this thesis. First we define LPV canonical forms based on the concept of observability and reachability canonical forms of the LTI case and we give an algorithmic scheme to construct them from an existing SS representation of the system. Then, transformations are introduced which provide an equivalent IO representation of a SS representation and vice versa. In both cases, the introduced LPV canonical forms are special cases of the transformation problem, serving as a simple gateway between the representation domains.

4.1 State-space canonical forms

Specially structured canonical forms of state-space representations of LPV systems are essential ingredients to accommodate equivalence transformations between the *state-space* (SS) and the *input-output* (IO) representation domains. One set of these canonical forms are the so called observability/reachability canonical forms which are also used in the state-of-the-art of LPV identification and control design. In this section, LPV observability and reachability canonical forms are developed in the introduced LPV behavioral framework, using the same line of reasoning as in the LTI case (see Section 2.1.6).

The canonical forms in *continuous-time* (CT) and *discrete-time* (DT) are introduced through a transformation mechanism applied on a given SS representation of the LPV system. Using the concept of structural state-observability/reachability, i.e. the associated observability/reachability matrices, state-transformations are defined in the SISO case, that result in an equivalent SS representation with special structure in the system matrices. It is shown that this special

structure implies complete state-observability/reachability of the resulting representation and hence it is called a LPV observability/reachability canonical form. Additionally, the introduced canonical forms give a unique representation of their associated equivalence class. The applied transformation mechanism is based on the results of LTV systems theory and it can be seen as extension of the LTI canonical form construction approach given in Section 2.1.6.

Besides the derivation of observability/reachability canonical forms, a construction approach for their companion counterparts is also introduced. The concept of transposition of SS representations is also investigated, with the main conclusion, that contrary to the LTI case, the transpose of a SS representation in the LPV framework does not have an equal manifest behavior. This means that such a transformation alters the dynamical relation.

It is also investigated how the developed concept of canonical forms relates to applied theories of the current LPV literature. It is shown that the common practice to use LTI theory to compute canonical forms for LPV systems results in SS representations that do not have an equal manifest behavior. This underlines that the correct formulation of observability/reachability canonical forms is an essential contribution of this thesis to the general LPV systems theory.

4.1.1 The observability canonical form

At first, observability canonical forms are considered. It is assumed that a structurally state-observable state-space representation $\mathfrak{R}_{\text{SS}}(\mathcal{S})$ is given for the SISO LPV system \mathcal{S} . Due to the structural state-observability, i.e. the full rank of \mathcal{O}_{n_x} associated with $\mathfrak{R}_{\text{SS}}(\mathcal{S})$, it is possible to introduce a new state-basis for the representation with the parameter-varying transformation matrix, $T_o \in \mathcal{R}^{n_x \times n_x}$:

$$T_o := \mathcal{O}_{n_x}. \quad (4.1)$$

This leads to a new state variable x_o , obtained as

$$x_o := (T_o \diamond p)x, \quad \forall p \in \mathfrak{B}_{\mathbb{P}}. \quad (4.2)$$

Due to the full rank property of \mathcal{O}_{n_x} , T_o is invertible in $\mathcal{R}^{n_x \times n_x}$. If $\mathfrak{R}_{\text{SS}}(\mathcal{S})$ has constant observability rank and it is completely state-observable, then T_o is invertible for any scheduling trajectory and time instant. Thus in that case, (4.2) implies algebraic equivalence between x_o and x . If only structural observability holds, then invertibility is guaranteed in a functional sense, which means that (4.2) implies algebraic equivalence almost everywhere. However, the latter is a sufficient property for T_o to be a PV state-transformation, which leads to an equivalent SS representation of \mathcal{S} in terms of $\overset{n_{\mathbb{P}}}{\sim}$. Moreover, this transformation projects the observability structure in terms of Theorem 3.11 to the identity matrix ($\mathcal{O}_{n_x} \mathcal{O}_{n_x}^{-1} = I$). Thus, similar to the LTI case, we call the equivalent SS representation, resulting by the state transformation T_o , the observability canonical form.

To obtain the equivalent representation of \mathcal{S} in terms of the new state variable, T_o is applied to the system matrices in accordance with $\overset{n_{\mathbb{P}}}{\sim}$, resulting in a SS

representation with the following special structure:

$$\left[\begin{array}{c|c} A_o & B_o \\ \hline C_o & D_o \end{array} \right] := \left[\begin{array}{cccc|c} 0 & 1 & \dots & 0 & \beta_{n_x-1}^o \\ \vdots & \vdots & \ddots & \vdots & \beta_{n_x-2}^o \\ 0 & 0 & \dots & 1 & \vdots \\ -\alpha_0^o & -\alpha_1^o & \dots & -\alpha_{n_x-1}^o & \beta_0^o \\ \hline 1 & 0 & \dots & 0 & \beta_{n_x}^o \end{array} \right].$$

Then

$$\mathfrak{R}_{\text{SS}}^o(\mathcal{S}) := \left[\begin{array}{c|c} A_o & B_o \\ \hline C_o & D_o \end{array} \right] \in \left[\begin{array}{c|c} \mathcal{R}^{n_x \times n_x} & \mathcal{R}^{n_x \times 1} \\ \hline \mathcal{R}^{1 \times n_x} & \mathcal{R} \end{array} \right], \quad (4.3)$$

is called the *observability canonical state-space representation* of \mathcal{S} . Proof of that the invertible state-transformation based on (4.2) always results in the above given structure follows similarly as in the LTV case (see Silverman (1971) and Zenger and Ylinen (2005) for the CT case and Marcovitz (1964) and Guidorzi and Diversi (2003) for the DT case).

Example 4.1 (CT-LPV observability canonical form, SISO) Consider the structurally state-observable CT-LPV-SS representation $\mathfrak{R}_{\text{SS}}(\mathcal{S})$ of Example 3.22. By applying state-transformation (4.2) in terms of Definition 3.26, the resulting observability canonical form is as follows:

$$\mathfrak{R}_{\text{SS}}^o(\mathcal{S}) = \left[\begin{array}{cc|c} 0 & 1 & 1+p^2 \\ \frac{p \frac{d^2}{dt^2} p - (2+p^2 + \frac{d}{dt} p) \frac{d}{dt} p}{p^2 - 2 - \frac{d}{dt} p} - 1 & \frac{p^3 - 2p + p \frac{d}{dt} p - \frac{d^2}{dt^2} p}{p^2 - 2 - \frac{d}{dt} p} - \frac{1}{p} & 3p + p \frac{d}{dt} p \\ \hline 1 & 0 & p \end{array} \right].$$

Because the original representation $\mathfrak{R}_{\text{SS}}(\mathcal{S})$ is not completely state-observable, the resulting canonical representation $\mathfrak{R}_{\text{SS}}^o(\mathcal{S})$ is equivalent with $\mathfrak{R}_{\text{SS}}(\mathcal{S})$ only in the almost everywhere sense. Furthermore, $\mathfrak{R}_{\text{SS}}^o(\mathcal{S})$ is completely state-observable (its observability matrix is an identity matrix) even if $\mathfrak{R}_{\text{SS}}(\mathcal{S})$, used for its construction, is not.

It is important to note that due to the state-transformation (4.2), the complexity of the dependence of the meromorphic coefficients of $\mathfrak{R}_{\text{SS}}^o(\mathcal{S})$ can increase considerably. If in the representation $\mathfrak{R}_{\text{SS}}(\mathcal{S})$ all the coefficients/matrices are linear static functions of p , then the matrix functions defining $\mathfrak{R}_{\text{SS}}^o(\mathcal{S})$ can have rational dependence on p and its derivatives/forward time-shifts up to the order n_x . This property has been one of the reasons to define coefficient dependence of LPV systems over the field of meromorphic functions \mathcal{R} with variables associated with p and its derivatives/time-shifts in the introduced framework.

Example 4.2 (DT-LPV observability canonical form, SISO) As a DT example, we can consider the DT-LPV-SS representation defined in Example 3.29. Again, by applying state-transformation (4.2) in terms of Definition 3.26, the resulting observability canonical form of this representation is the following:

$$\mathfrak{R}_{\text{SS}}^o(\mathcal{S}) = \left[\begin{array}{cc|c} 0 & 1 & 1 + \frac{p}{qp} \\ - (qp^2) \frac{p}{q^2p} & qp + \frac{qp^2}{q^2p} & \frac{p(qp)}{q^2p} + p + qp \\ \hline 1 & 0 & p \end{array} \right].$$

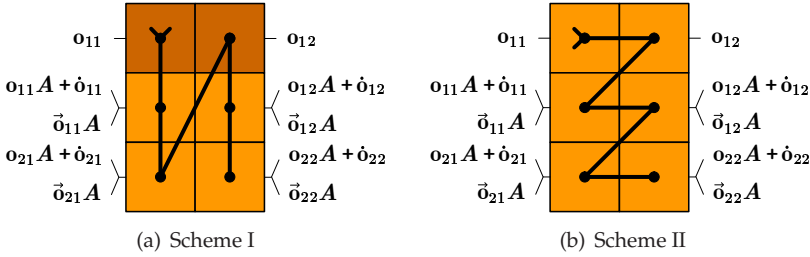


Figure 4.1: Young's PV selection scheme for \mathcal{O}_{n_x} : $n_x = 3$, $n_y = 2$. The rows of \mathcal{O}_{n_x} are indicated on the left and right side of the figures based on the generation rule in continuous (3.79) or discrete-time (3.89). The vector functions represented by dark cells must be selected if they are independent.

Due to the complete state-observability of the DT example, the resulting canonical form is fully equivalent with the original representation and it is also completely state-observable. Note that in the following, we restrict examples to the DT case to simplify the discussion.

As a next step the MIMO case is treated. According to theory given for LTV systems in Guidorzi and Diversi (2003), observability type of canonical forms with respect to a MIMO, structurally state-observable $\mathfrak{R}_{SS}(\mathcal{S})$ can be realized by a mapping rule of three steps, similar to the LTI case:

1. Choose n_x -independent rows of the full column-rank \mathcal{O}_{n_x} with a given ordering sequence.
2. Rearrange those n_x -independent rows with a fixed order to form a nonsingular state transformation matrix $T_o \in \mathcal{R}^{n_x \times n_x}$.
3. By applying the equivalence transformation defined via T_o , compute the canonical representation.

In the following, these steps form the line of reasoning for the introduction of a MIMO observability canonical form through its construction mechanism.

According to Step 1 of the previous algorithm, write \mathcal{O}_{n_x} as the sequence of row vectors:

$$\mathcal{O}_{n_x} = [o_{11}^\top \quad \dots \quad o_{n_y 1}^\top \quad o_{12}^\top \quad \dots \quad o_{n_y 2}^\top \quad \dots]^\top, \quad (4.4)$$

where $C = [o_{11}^\top \quad \dots \quad o_{n_y 1}^\top]^\top$. Each $o_j = [o_{ij}]_{i=1}^{n_y}$, $j > 1$ is defined similarly as (3.79) in the CT case and as (3.89) in the DT case. To complete Step 1 of the algorithm, the selection of n_x linearly independent vector functions from the $n_x \times n_y$ rows of (4.4) is needed, to form the new state-basis of the canonical representation. Due to the structural state-observability of the system, it is always possible to make such a selection, but in general it is not unique (Guidorzi and Diversi 2003; Luenberger 1967). Depending on the particular way of the selection procedure, different canonical forms can be obtained. In the following, the selection strategy

that reproduces the structure of the previously introduced SISO LPV observability canonical form is used. According to this, select the vectors of (4.4) in the order of

$$\{\circ_{011}, \circ_{021}, \dots, \circ_{n_Y 1}, \circ_{12}, \circ_{22}, \dots, \circ_{n_Y 2}, \dots\}, \quad (4.5)$$

which matches with the generalization of Young's selection scheme II, discussed in the LTI case (see Section 2.1.6). In the LPV case, this scheme is presented in Figure 4.1. For the sake of simplicity, temporarily assume that $\text{rank}(C) = n_Y$, meaning that $\{\circ_{011}, \circ_{021}, \dots, \circ_{n_Y 1}\}$ are linearly independent vector functions. Then, the linear dependence of every vector function from the ordered sequence (4.5) can be analyzed one after the other: if $\tau_i \in \mathbb{N}_1^{n_X}$ is the smallest number such that $\circ_{i\tau_i}$ is linearly dependent on the previous vectors, then there exists a set of unique functions $\{\alpha_{ijl}^\circ \in \mathcal{R}\}$, such that

$$\circ_{i\tau_i} = \sum_{j=1}^{n_Y} \sum_{l=0}^{\tau_{ij}-1} \alpha_{ijl}^\circ \circ_{jl}, \quad (4.6)$$

where the ordering of the vectors, similar to the LTI case, implies that τ_{ij} satisfies (2.54). Once all dependent vector functions have been found, a total of $n_X = \sum_{i=1}^{n_Y} \tau_i$ independent vectors is selected due to the full rank assumption of \mathcal{O}_{n_X} . Furthermore, as the first n_Y vectors $\{\circ_{011}, \circ_{021}, \dots, \circ_{n_Y 1}\}$ are independent, they are automatically selected, implying that τ_i satisfies (2.55). Moreover, the remaining linearly dependent relations are described by $\sum_{i=1}^{n_Y} \sum_{j=1}^{n_Y} \tau_{ij}$ number of functions $\{\alpha_{ijl}^\circ\}$. This accomplishes Step 1 of the algorithm.

Using the previously selected vectors, the new state-basis is defined by

$$T_o := \begin{bmatrix} \circ_{011}^\top & \dots & \circ_{01(\tau_1-1)}^\top & \dots & \circ_{n_Y 1}^\top & \dots & \circ_{n_Y(\tau_{n_Y}-1)}^\top \end{bmatrix}^\top. \quad (4.7)$$

Due to the linear independence of the rows, T_o is invertible and implies an equivalence relation in terms of Definition 3.26. This completes Step 2 of the algorithm.

As a final step, applying the previously constructed equivalence relation on $\mathfrak{R}_{SS}(\mathcal{S})$, yields the transformed matrices in the following form:

$$\left[\begin{array}{c|c} A_o & B_o \\ \hline C_o & D_o \end{array} \right] := \left[\begin{array}{c|c} [A_{ij}^\circ], i, j \in \mathbb{N}_1^{n_Y} & \begin{array}{c} B_1^\circ \\ \vdots \\ B_{n_Y}^\circ \end{array} \\ \hline e_1 \quad 0_{n_Y \times (\tau_1-1)} \quad \dots \quad e_{n_Y} \quad 0_{n_Y \times (\tau_{n_Y}-1)} & D \end{array} \right],$$

where $\{e_i\}_{i=1}^{n_Y}$ is the standard basis of \mathbb{R}^{n_Y} , and

$$A_{ii}^\circ = \begin{bmatrix} 0 & \dots & 0 & -\alpha_{ii0}^\circ \\ 1 & \ddots & \vdots & -\alpha_{ii1}^\circ \\ \vdots & \ddots & 0 & \vdots \\ 0 & \dots & 1 & -\alpha_{ii(\tau_i-1)}^\circ \end{bmatrix}_{(\tau_i \times \tau_i)}^\top \quad A_{ij}^\circ = \begin{bmatrix} 0 & \dots & 0 & -\alpha_{ij0}^\circ \\ \vdots & \vdots & \vdots & \vdots \\ \vdots & \vdots & -\alpha_{ij(\tau_{ij}-1)}^\circ & \vdots \\ \vdots & \vdots & 0 & \vdots \\ \vdots & \vdots & \vdots & \vdots \\ 0 & \dots & 0 & 0 \end{bmatrix}_{(\tau_i \times \tau_j)}^\top$$

$$B_i^o = \begin{bmatrix} \beta_{i1(\tau_i-1)}^o & \cdots & \beta_{in_U(\tau_i-1)}^o \\ \vdots & & \vdots \\ \beta_{i10}^o & \cdots & \beta_{in_U0}^o \end{bmatrix}_{(\tau_i \times n_U)} \quad D_o = \begin{bmatrix} \beta_{11\tau_1}^o & \cdots & \beta_{1n_U\tau_1}^o \\ \vdots & & \vdots \\ \beta_{n_Y1\tau_{n_Y}}^o & \cdots & \beta_{n_Yn_U\tau_{n_Y}}^o \end{bmatrix}_{(n_Y \times n_U)}$$

Proof of that the invertible state-transformation based on (4.7) always results in the above given structure follows similarly as in Guidorzi and Diversi (2003). Based on this representation, the LTI system is separated to an interconnection of subsystems characterized by the A_{ii}^o and B_i^o matrices and the connection of these subsystems is defined through the A_{ij}^o matrices. In this way, using the constructed state-space transformation T_o applied on $\mathfrak{R}_{SS}(\mathcal{S})$, we have constructed a canonical SS representation of \mathcal{S} . Due to the fact, that the projected $n_{\mathcal{X}}$ -step observability matrix of $\mathfrak{R}_{SS}^o(\mathcal{S})$ is the identity matrix (SISO case) or composed from zero row vectors and the standard basis of $\mathbb{R}^{1 \times n_{\mathcal{X}}}$ (MIMO case) such a canonical representation is always completely state-observable. Thus the following corollary holds for all representations of \mathcal{S} with the structural form of (A_o, B_o, C_o, D_o) both in the SISO and the MIMO cases:

Corollary 4.1 $\mathfrak{R}_{SS}^o(\mathcal{S})$ is completely state-observable and hence minimal.

In case $\text{rank}(C) \neq n_Y$, the observability canonical form does not exist in the previously introduced structure as C_o cannot be a matrix composed from zero vectors and standard bases. In this case, T_o is constructed by considering the system only with output channels which are associated with the independent rows of C . Then, T_o is applied to the original matrix functions. The resulting C_o retains the structure of the conventional canonical form for the linearly independent output channels (containing only zero vectors and standard bases), however it also contains meromorphic coefficient functions (the weights of the linear combination of the independent channels) in the rows corresponding to the dependent output channels. If the LPV-SS representation is not structurally state-observable, then computation of an equivalent observability canonical form by the presented algorithm requires to search for a SS representation of the LPV system with structural state-observability. Then, such a representation can be converted to an observability canonical form. As we will see in the Section 4.3, the construction of such a representation is always possible.

Example 4.3 (DT-LPV observability canonical form, MIMO) Let the SS representation $\mathfrak{R}_{SS}(\mathcal{S})$ of an DT-LPV system \mathcal{S} with $\mathbb{P} = [0.1, 0.3]$ be given by

$$\left[\begin{array}{c|c} A & B \\ \hline C & D \end{array} \right] \diamond p = \left[\begin{array}{cccc|cc} p & 0 & 0 & -0.5 & 1 & 1 \\ 0 & -p & 0 & 0 & p & p \\ 0 & 0 & -p & 0 & -1 & 0 \\ 0.5 & 0 & 0 & p & 0 & 1 \\ \hline 0 & p & 0 & 0 & 0 & 0 \\ 0 & 0 & 1 & p & 0 & 0 \\ p & 1 & 0 & 0 & 0 & 0 \end{array} \right].$$

By computing the 2-step observability matrix of $\mathfrak{R}_{\text{SS}}(\mathcal{S})$,

$$\mathcal{O}_2 \diamond p = \begin{bmatrix} 0 & p & 0 & 0 \\ 0 & 0 & 1 & p \\ \hline p & 1 & 0 & 0 \\ 0 & -p(qp) & 0 & 0 \\ 0.5qp & 0 & -p & p(qp) \\ p(qp) & -p & 0 & -0.5qp \end{bmatrix}$$

results. It is clear, that the first four rows of \mathcal{O}_2 are independent in the functional sense, thus $\mathfrak{R}_{\text{SS}}(\mathcal{S})$ is structurally state-observable. However, the first three rows and the sixth are independent along all possible scheduling trajectories on \mathbb{P} , thus $\mathfrak{R}_{\text{SS}}(\mathcal{S})$ is also completely state-observable. Note that in this case, computation of \mathcal{O}_4 is not necessary to show these properties. By calculating the observability canonical form $\mathfrak{R}_{\text{SS}}^{\text{O}}(\mathcal{S})$ of $\mathfrak{R}_{\text{SS}}(\mathcal{S})$ using the first three and the sixth rows of \mathcal{O}_2 , the resulting matrices are the following (the sub-matrices are denoted by dashed lines):

$$A_{\text{O}} \diamond p = \begin{bmatrix} qp & 0 & 0 \\ \hline -\frac{qp^2+4p^2+8p(qp)+4p^2(qp^2)}{2p^2(qp)} & p & -\frac{qp+4p^3+4p^2(qp)}{2p} & \frac{p(p+qp)}{2qp} \\ 0 & 0 & 0 & 1 \\ \hline -\frac{(qp)(q^2p)+4p^2(qp^2)+4p^3(q^3p)+8p^2(qp)(q^2p)}{4p^2(qp)} & 0 & \frac{(1+4p^2)q^2p}{4p} & -\frac{(p+qp)q^2p}{q^2p} \end{bmatrix}$$

$$B_{\text{O}} \diamond p = \begin{bmatrix} p(qp) & p(qp) \\ \hline -1 & qp \\ p+qp & p+qp \\ (q^2p-p)qp & \frac{2(q^2p-2p)qp-q^2p}{2} \end{bmatrix}, \quad C_{\text{O}} \diamond p = \begin{bmatrix} 1 & 0 & 0 & 0 \\ 0 & 1 & 0 & 0 \\ 0 & 0 & 1 & 0 \end{bmatrix}.$$

Note that the resulting LPV-SS representation is the interconnection of 3 subsystems, each associated with a specific output channel. Furthermore, this observability canonical form is not generated using Young's selection scheme as in that case the first 4 rows of \mathcal{O}_2 would have been selected for the transformation. In opposite with the used state-transformation, the transformation of the state, based on the first 4 rows, only provides an equivalent representation in the almost everywhere sense, as independence of the rows only holds in the functional sense. This underlines that in the MIMO case there is a freedom in the construction of observability canonical forms and the provided selection scheme is only one from the available possibilities.

4.1.2 Reachability canonical form

As a next step, we extend the previously introduced mechanism to the reachability case. Similar to the previous part, SISO systems are considered first. It is assumed that a structurally state-reachable state-space representation $\mathfrak{R}_{\text{SS}}(\mathcal{S})$ is given for the SISO LPV system \mathcal{S} . Due to the full rank of $\mathcal{R}_{n_{\mathcal{X}}}$ associated with $\mathfrak{R}_{\text{SS}}(\mathcal{S})$, it is possible to introduce a new state-basis for the representation by using

$$T_{\text{r}}^{-1} := \begin{cases} \mathcal{R}_{n_{\mathcal{X}}}, & \text{if } \mathbb{T} = \mathbb{R}, \\ \overleftarrow{\mathcal{R}_{n_{\mathcal{X}}}}, & \text{if } \mathbb{T} = \mathbb{Z}, \end{cases} \quad (4.8)$$

that leads to a new state variable x_{r} , obtained as

$$x_{\text{r}} := (T_{\text{r}} \diamond p)x, \quad \forall p \in \mathfrak{B}_{\mathbb{P}}. \quad (4.9)$$

Again, the full rank property of \mathcal{R}_{n_x} implies that T_r is invertible in $\mathcal{R}^{n_x \times n_x}$. Thus, (4.9) yields an equivalent SS representation of \mathcal{S} in terms of $\overset{n_p}{\sim}$. In case of complete state-reachability, (4.9) also implies algebraic equivalence of the original and the new states. Moreover, this state-transformation projects the reachability structure in terms of Theorem 3.11 to the identity matrix. Therefore, we call this equivalent SS representation the reachability canonical form.

By applying the transformation associated with T_r on the matrices of $\mathfrak{R}_{SS}(\mathcal{S})$ in accordance with $\overset{n_p}{\sim}$, the transformed matrices are given by:

$$\left[\begin{array}{c|c} A_r & B_r \\ \hline C_r & D_r \end{array} \right] := \left[\begin{array}{cccc|c} 0 & \dots & 0 & -\alpha_0^r & 1 \\ 1 & \ddots & \vdots & -\alpha_1^r & 0 \\ \vdots & \ddots & 0 & \vdots & \vdots \\ 0 & \dots & 1 & -\alpha_{n_x-1}^r & 0 \\ \hline \beta_{n_x-1}^r & \beta_{n_x-2}^r & \dots & \beta_0^r & \beta_{n_x}^r \end{array} \right].$$

Then,

$$\mathfrak{R}_{SS}^{\mathcal{R}}(\mathcal{S}) := \left[\begin{array}{c|c} A_r & B_r \\ \hline C_r & D_r \end{array} \right] \in \left[\begin{array}{c|c} \mathcal{R}^{n_x \times n_x} & \mathcal{R}^{n_x \times 1} \\ \hline \mathcal{R}^{1 \times n_x} & \mathcal{R} \end{array} \right], \quad (4.10)$$

is called the *reachability canonical state-space representation* of \mathcal{S} and it is equivalent with $\mathfrak{R}_{SS}(\mathcal{S})$. Proof of the above given matrix operations similarly follows as for LTV-SS representations (see Silverman (1971); Zenger and Ylinen (2005) for the CT case and Marcovitz (1964); Park and Verriest (1990) for the DT case).

Example 4.4 (LPV reachability canonical form, SISO) Consider the completely state-reachable DT-LPV-SS representation defined in Example 3.29. By applying state-transformation (4.9) in terms of Definition 3.26, the resulting reachability canonical form of this representation is the following:

$$\mathfrak{R}_{SS}^{\mathcal{R}}(\mathcal{S}) = \left[\begin{array}{cc|c} 0 & -q^{-1}p^2 & 1 \\ 1 & q^{-1}p + q^{-2}p & 0 \\ \hline 1 + \frac{q^{-1}p}{p} & \left(1 + \frac{q^{-2}p}{p}\right)q^{-1}p + q^{-2}p & p \end{array} \right].$$

Due to the complete state-reachability, the resulting canonical form is fully equivalent with the original representation.

Note that the previously introduced algorithm can also be applied to generate reachability-based MIMO canonical forms, but instead of the rows of \mathcal{O}_{n_x} , the columns of \mathcal{R}_{n_x} are used in this case. According to Step 1 of this mechanism, \mathcal{R}_{n_x} is rewritten as a sequence of its column vectors:

$$\mathcal{R}_{n_x} = \left[\begin{array}{cccccc} \mathbf{r}_{11} & \dots & \mathbf{r}_{n_{\nu}1} & \mathbf{r}_{12} & \dots & \mathbf{r}_{n_{\nu}2} & \dots \end{array} \right], \quad (4.11)$$

where $B = [\mathbf{r}_{11} \dots \mathbf{r}_{n_{\nu}1}]$ and each $\mathbf{r}_j = [\mathbf{r}_{ij}]_{i=1}^{n_{\nu}}$, $j > 1$ is defined similarly as (3.84) for CT and as (3.91) for DT. To accomplish Step 1, the selection of n_x linearly independent vectors from the $n_x \times n_{\nu}$ column vectors is required in order to determine the state-basis of the reachability canonical form. In the following, such a selection strategy is used that reproduces the structure of the previously introduced SISO

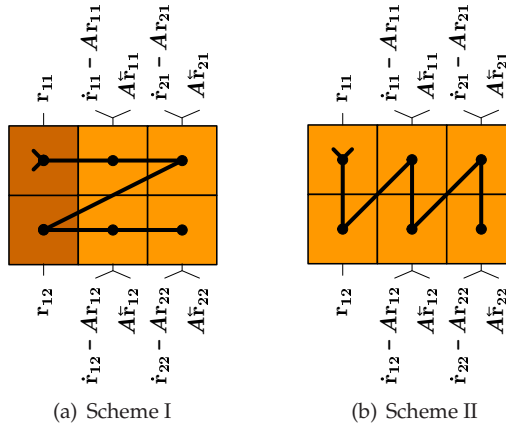


Figure 4.2: Young's PV selection scheme for \mathcal{R}_{n_x} : $n_x = 3$, $n_u = 2$. The columns of \mathcal{R}_{n_x} are indicated on the left and right side of the figures based on the generation rule in continuous (3.84) or discrete-time (3.91). Vectors represented by dark cells must be selected if they are independent.

LPV reachability canonical form. According to this, select the rows of \mathcal{R}_{n_x} in the order of

$$\{\mathbf{r}_{11}, \mathbf{r}_{12}, \dots, \mathbf{r}_{1(n_x n_u)}, \mathbf{r}_{21}, \mathbf{r}_{22}, \dots\},$$

which matches the extension of Young's selection scheme I presented in Figure 4.2. Temporally assume that $\text{rank}(B) = n_u$ which means that $\{\mathbf{r}_{11}, \mathbf{r}_{12}, \dots, \mathbf{r}_{1n_u}\}$ are linearly independent vector functions. Then, the linear dependence of every vector function from the ordered sequence can be analyzed one after the other just like in the observability case. However, in Young's selection scheme I, the vectors $\{\mathbf{r}_{11}, \mathbf{r}_{21}, \dots, \mathbf{r}_{n_u 1}\}$ have to be selected to the state transformation even if the ordering would indicate it else. The explanation follows similarly as in the LTI case. According to this selection scheme, if $\tau_i \in \mathbb{N}_1^{n_x}$ is the smallest number such that $\mathbf{r}_{i\tau_i}$ is linearly dependent on the previous vectors, then there exists a set of unique meromorphic functions $\{\alpha_{ijl}^r \in \mathcal{R}\}$, such that

$$\mathbf{r}_{i\tau_i} = \sum_{j=1}^i \sum_{l=0}^{\tau_{ij}-1} \alpha_{ijl}^r \mathbf{r}_{il}, \quad (4.12)$$

where $\{\tau_{ij}\}$ satisfies (2.54) because of the ordering of the vectors. Once that all dependent vector functions have been found, a total of $n_x = \sum_{i=1}^{n_u} \tau_i$ independent vector functions are selected due to the full rank assumption of \mathcal{R}_{n_x} . Furthermore, by the selection scheme, the n_u number of vectors of $\{\mathbf{r}_{11}, \mathbf{r}_{12}, \dots, \mathbf{r}_{1n_u}\}$ are automatically selected, thus τ_i satisfies the upperbound (2.61). The remaining linearly dependent relations are described by $\sum_{i=1}^{n_u} \sum_{j=1}^i \tau_{ij}$ rational functions $\{\alpha_{ijl}^r\} \in \mathcal{R}$, and T_r is defined as:

$$T_r^{-1} := \begin{cases} \begin{bmatrix} \mathbf{r}_{11} & \dots & \mathbf{r}_{1(\tau_1-1)} & \dots & \mathbf{r}_{n_u 1} & \dots & \mathbf{r}_{n_u(\tau_{n_u}-1)} \end{bmatrix}, & \text{if } \mathbb{T} = \mathbb{R}; \\ \begin{bmatrix} \overleftarrow{\mathbf{r}}_{11} & \dots & \overleftarrow{\mathbf{r}}_{1(\tau_1-1)} & \dots & \overleftarrow{\mathbf{r}}_{n_u 1} & \dots & \overleftarrow{\mathbf{r}}_{n_u(\tau_{n_u}-1)} \end{bmatrix}, & \text{if } \mathbb{T} = \mathbb{Z}. \end{cases}$$

which accomplishes Step 2. Again, linear independence of the selected vector functions assures the existence of the inverse, thus T_r implies an equivalence relation in terms of Definition 3.26. As a final step, applying the previously constructed equivalence relation on $\mathfrak{R}_{SS}(\mathcal{S})$, yields the transformed matrices in the following form:

$$\left[\begin{array}{c|c} A_r & B_r \\ \hline C_r & D_r \end{array} \right] := \left[\begin{array}{c|c} [A_{ij}^r], i, j \in \mathbb{I}_1^{n_u} & \begin{array}{c} e_1^\top \\ 0_{(\tau_1-1) \times n_u} \\ \vdots \\ e_{n_u}^\top \\ 0_{(\tau_{n_y}-1) \times n_u} \end{array} \\ \hline C_1^r \quad \dots \quad C_{n_u}^r & D \end{array} \right],$$

where $\{e_i\}_{i=1}^{n_u}$ is the standard basis of \mathbb{R}^{n_u} and

$$A_{ii}^r = \begin{bmatrix} 0 & \dots & 0 & -\alpha_{ii0}^r \\ 1 & \ddots & \vdots & -\alpha_{ii1}^r \\ \vdots & \ddots & 0 & \vdots \\ 0 & \dots & 1 & -\alpha_{ii(\tau_i-1)}^r \end{bmatrix}_{(\tau_i \times \tau_i)}$$

$$A_{ij}^r = \begin{bmatrix} 0 & \dots & 0 & -\alpha_{ij0}^r \\ \vdots & \vdots & \vdots & \vdots \\ \vdots & \vdots & \vdots & -\alpha_{ij(\tau_{ij}-1)}^r \\ \vdots & \vdots & \vdots & 0 \\ \vdots & \vdots & \vdots & \vdots \\ \vdots & \vdots & \vdots & \vdots \\ 0 & \dots & 0 & 0 \end{bmatrix}_{(\tau_i \times \tau_j)}$$

$$C_i^r = \begin{bmatrix} \beta_{1i(\tau_i-1)}^r & \dots & \beta_{1i0}^r \\ \vdots & & \vdots \\ \beta_{n_y i(\tau_i-1)}^r & \dots & \beta_{n_y i0}^r \end{bmatrix}_{(n_y \times \tau_i)}$$

$$D_r = \begin{bmatrix} \beta_{11\tau_1}^r & \dots & \beta_{1n_u\tau_1}^r \\ \vdots & & \vdots \\ \beta_{n_y 1\tau_{n_y}}^r & \dots & \beta_{n_y n_u\tau_{n_y}}^r \end{bmatrix}_{(n_y \times n_u)}$$

Proof of that the invertible state-transformation T_r always results in the above given structure follows similarly as in Park and Verriest (1990). Again, $\mathfrak{R}_{SS}^{\mathfrak{R}}(\mathcal{S})$ is equivalent with $\mathfrak{R}_{SS}(\mathcal{S})$ and characterizes the decomposition of $\mathfrak{R}_{SS}^{\mathfrak{R}}(\mathcal{S})$ into state-reachable subsystems associated with each output channels. Due to the fact, that the projected n_x -step reachability matrix of $\mathfrak{R}_{SS}^{\mathfrak{R}}(\mathcal{S})$ is the identity matrix (SISO case) or composed from zero column vectors and the standard basis of \mathbb{R}^{n_x} (MIMO case) the resulting canonical representation is always completely state-reachable. Thus the following corollary holds for all representations of \mathcal{S} with the structural form of (A_r, B_r, C_r, D_r) both in the SISO and the MIMO cases:

Corollary 4.2 $\mathfrak{R}_{SS}^{\mathfrak{R}}(\mathcal{S})$ is completely state-reachable.

Furthermore it also holds that if $\mathfrak{R}_{SS}(\mathcal{S})$ is minimal, then the resulting $\mathfrak{R}_{SS}^{\mathfrak{R}}(\mathcal{S})$ by the given construction procedure is also minimal. In the case of dependent columns of B , the state transformation is constructed based on the independent input channels. If the LPV-SS representation is not structurally state-reachable, then computation of an equivalent reachability canonical form is possible by finding an SS realization of the system which is structurally state-reachable. Similar to the observability case, such a realization always exists, if \mathcal{S} has no autonomous dynamics.

4.1.3 Companion canonical forms

The LPV observability and reachability canonical forms can also be given in an other, so called *companion* or *phase-variable* form. These representations $\mathfrak{R}_{\text{SS}}^{\text{O}_c}(\mathcal{S})$ and $\mathfrak{R}_{\text{SS}}^{\text{R}_c}(\mathcal{S})$ are defined in the SISO case as:

$$\mathfrak{R}_{\text{SS}}^{\text{O}_c}(\mathcal{S}) := \left[\begin{array}{c|c} A_{\text{co}} & B_{\text{co}} \\ \hline C_{\text{co}} & D_{\text{co}} \end{array} \right] = \left[\begin{array}{cccc|c} 0 & \dots & 0 & -\alpha_0^{\text{co}} & \beta_0^{\text{co}} \\ 1 & \ddots & \vdots & -\alpha_1^{\text{co}} & \beta_1^{\text{co}} \\ \vdots & \ddots & 0 & \vdots & \vdots \\ 0 & \dots & 1 & -\alpha_{n_x-1}^{\text{co}} & \beta_{n_x-1}^{\text{co}} \\ \hline 0 & \dots & 0 & 1 & \beta_{n_x}^{\text{co}} \end{array} \right],$$

$$\mathfrak{R}_{\text{SS}}^{\text{R}_c}(\mathcal{S}) := \left[\begin{array}{c|c} A_{\text{cr}} & B_{\text{cr}} \\ \hline C_{\text{cr}} & D_{\text{cr}} \end{array} \right] = \left[\begin{array}{cccc|c} 0 & 1 & \dots & 0 & 0 \\ \vdots & \vdots & \ddots & \vdots & \vdots \\ 0 & 0 & \dots & 1 & 0 \\ -\alpha_0^{\text{cr}} & -\alpha_1^{\text{cr}} & \dots & -\alpha_{n_x-1}^{\text{cr}} & 1 \\ \hline \beta_0^{\text{cr}} & \beta_1^{\text{cr}} & \dots & \beta_{n_x-1}^{\text{cr}} & \beta_{n_x}^{\text{cr}} \end{array} \right],$$

Again, it can be proved, based on Silverman (1966) and Weiss (2005), that every LPV system \mathcal{S} admits a state-variable representation in these forms and they are equivalent with all SS representations of \mathcal{S} . The state-transformations that lead to these canonical forms can be constructed as:

$$T_{\text{co}}^{-1} := \begin{cases} [\mathbf{r}_1, \mathbf{r}_2, \dots, \mathbf{r}_{n_x}], & \text{if } \mathbb{T} = \mathbb{R}; \\ [\overleftarrow{\mathbf{r}}_1, \overleftarrow{\mathbf{r}}_2, \dots, \overleftarrow{\mathbf{r}}_{n_x}], & \text{if } \mathbb{T} = \mathbb{Z}; \end{cases} \quad (4.13a)$$

$$T_{\text{cr}}^\top := [\mathbf{o}_1^\top, \mathbf{o}_2^\top, \dots, \mathbf{o}_{n_x}^\top], \quad (4.13b)$$

where \mathbf{r}_1 is the last column of $\mathcal{O}_{n_x}^{-1}$ which is additionally shifted forward in time in case of $\mathbb{T} = \mathbb{Z}$, \mathbf{o}_1 is the last row of $\mathfrak{R}_{n_x}^{-1}$ which is additionally shifted backward in time in case of $\mathbb{T} = \mathbb{Z}$, and \mathbf{r}_i , \mathbf{o}_i are generated recursively by (3.79) and (3.84) in continuous-time and by (3.89) and (3.91) in discrete-time. In the MIMO case, the companion forms are generated by selecting the linearly independent rows (columns) based on a different ordering. Similar to the LTI case, the ordering of the rows of \mathcal{O}_{n_x} by Young's extended selection scheme I presented in Figure 4.1 results in the companion observability canonical form, while the ordering of the columns of \mathfrak{R}_{n_x} by Young's extended selection scheme II of Figure 4.2 results in the companion reachability canonical form.

Example 4.5 (Companion canonical forms) Consider again the DT-LPV-SS representation defined in Example 3.29. By constructing the state-transformations (4.13a-b) and applying them to the original SS representation, the following companion canonical forms result.

$$T_{\text{co}} \diamond p = \begin{bmatrix} -\frac{p^2}{qp} & 0 \\ 1 & \frac{1}{p} \end{bmatrix} \Rightarrow \mathfrak{R}_{\text{SS}}^{\text{O}_c}(\mathcal{S}) = \left[\begin{array}{cc|c} 0 & -p\frac{qp^2}{q^2p} & -\frac{qp^2}{q^2p} \\ 1 & p + \frac{p^2}{qp} & 1 + \frac{p}{qp} \\ \hline 0 & 1 & p \end{array} \right],$$

$$T_{cr} \diamond p = \left[\begin{array}{c|c} \frac{1}{q^{-1}p} & -\frac{1}{q^{-1}p^2} \\ \hline 1 & 0 \end{array} \right] \Rightarrow \mathfrak{R}_{SS}^{\mathcal{R}_c}(\mathcal{S}) = \left[\begin{array}{cc|c} 0 & 1 & 0 \\ \hline -q^{-1}p^2 & p + q^{-1}p & 1 \\ -\frac{q^{-1}p^2}{p} & 1 + \frac{q^{-1}p}{p} & p \end{array} \right].$$

4.1.4 Transpose of SS representations

An important difference with respect to the LTI case is that transposed LPV-SS representations do not have an equal manifest behavior. To show this, consider the following argument:

Let $\mathfrak{R}_{SS}(\mathcal{S})$ be a state-space representation of a given SISO LPV system. Then the transposed SS representation, defined as

$$\mathfrak{R}_{SS}^{\top}(\mathcal{S}) := \left[\begin{array}{c|c} A^{\top} & C^{\top} \\ \hline B^{\top} & D \end{array} \right] \quad \text{when} \quad \mathfrak{R}_{SS}(\mathcal{S}) = \left[\begin{array}{c|c} A & B \\ \hline C & D \end{array} \right], \quad (4.14)$$

is not a SS representation of \mathcal{S} , because the associated output trajectories of these representations are not equal in case of a varying scheduling signal (see Example 4.6). This can be proved by computing the output responses of the representations for an impulsive input at $k = 0$, i.e. $u(0) = 1$, and zero initial state $x(0) = 0$. Denote the resulting output sequences by y for $\mathfrak{R}_{SS}(\mathcal{S})$ and y' for $\mathfrak{R}_{SS}^{\top}(\mathcal{S})$. Then these sequences reads as

$$\begin{aligned} y(0) &= (D \diamond p)(0), & y'(0) &= (D \diamond p)(0), \\ y(1) &= (C \diamond p)(1)(B \diamond p)(0), & y'(1) &= (B^{\top} \diamond p)(1)(C^{\top} \diamond p)(0), \\ y(2) &= (C \diamond p)(2)(A \diamond p)(1)(B \diamond p)(0), & y'(2) &= (B^{\top} \diamond p)(2)(A^{\top} \diamond p)(1)(C^{\top} \diamond p)(0), \end{aligned}$$

It is obvious that these sequences are not equal if p is not a constant signal. The reason for this phenomena is based on the non-commutativity of the multiplication on $\mathcal{R}[\xi]$.

Example 4.6 (LPV system transposition) *In this example, the connection between LPV canonical forms and their transpose is investigated. Consider the canonical forms derived in Example 4.2 and 4.4 which are equivalent with the DT-SS representation of Example 3.29. The transpose of these canonical forms have been obtained according to (4.14) by computing the transpose of the matrices. The output response of these transposed representations, the canonical forms, and the original SS representation have been calculated for*

$$u(k) = \sin\left(\frac{1}{4}k + \frac{\pi}{6}\right), \quad p(k) = \frac{1}{2} + \frac{1}{4}\sin\left(\frac{1}{4}k + \frac{\pi}{2}\right),$$

and with zero initial conditions of the state variables at $k = 0$. The results are presented in Figure 4.3. From the obtained signals one can conclude that the transposed forms are not equal to the original SS representation. This proves that transposition of SS representations changes the manifest behavior of LPV-SS representations in general.

4.1.5 LTI vs LPV state transformation

In the previous part, we have seen that through the developed behavioral framework, canonical forms of LPV systems can be similarly formulated as in the LTI

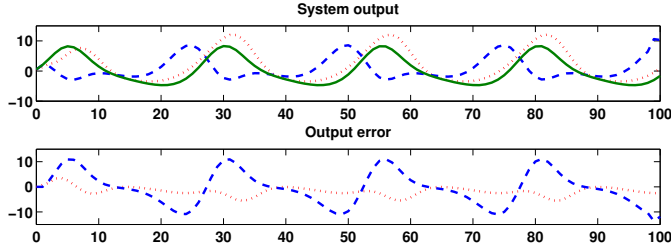


Figure 4.3: Comparison of the transpose of canonical representations given in Examples 4.2 and 4.4 in terms of their output response, i.e. their output error with respect to the original representation. Transposed canonical observability form (dashed blue), transposed canonical reachability form (dotted red), original representation (solid green).

case. It has also been emphasized how this framework extends the concepts of LTI system theory to LPV systems by proper handling of the time operators and their effect on scheduling-dependent coefficient functions. Comparing the introduced construction mechanism of LPV canonical forms to the state-of-the-art of the LPV literature, similar mechanisms can be found, which have been developed for CT-SS representations with linear dependence (see Kulcsár et al. (2008) as a notable approach). Thus the develop algorithm can be seen as a generalization of these approaches.

However in the general LPV literature, at many occasions the LTI theory is used intuitively, applying-state transformations in the form:

$$A' = T^{-1}AT, \quad (4.15)$$

where T is dependent on p . Such a state-transformation is equivalent to a state-transformation applied separately for every constant scheduling signal of $\mathfrak{B}_{\mathbb{F}}$. Based on Section 3.2, it is obvious that this transformation does not imply equivalence in any sense if T is not constant. It is also common, that canonical forms are usually “achieved” by generating \mathcal{O}_{n_x} and \mathcal{R}_{n_x} similar to the LTI case (see Definition 2.32 and 2.33). This corresponds to the observability/reachability matrices of the representation with respect to constant scheduling signals. Using independent rows (columns) of these matrices a state-transformation matrix T is formed. Then T is applied according to (4.15) to calculate the “canonical” form (see Wassink et al. (2004) and Steinbuch et al. (2003) as examples). It is not surprising that by this methodology the resulting structures resemble the observability/reachability canonical forms, however they are not equivalent in manifest behavior with the original system. To illustrate this see Example 4.7.

Example 4.7 (LTI vs LPV state transformation) Consider the canonical forms of the DT-SS representation derived in Example 4.2 and 4.4 for the DT-SS representation $\mathfrak{A}_{\text{SS}}(\mathcal{S})$ defined in Example 3.29. Let $\mathcal{O}_{n_x}^1$ and $\mathcal{R}_{n_x}^1$ denote the “observability” and “reachability” matrices constructed for $\mathfrak{A}_{\text{SS}}(\mathcal{S})$ in the LTI sense:

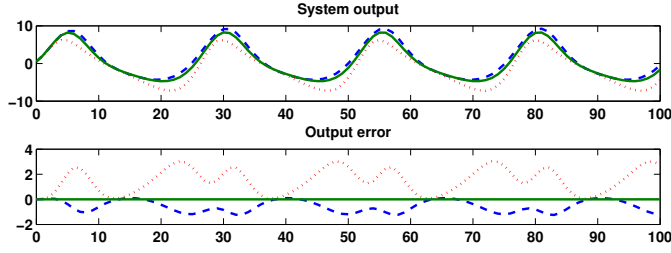


Figure 4.4: Comparison of global and frozen canonical representations of Example 4.7 in terms of their output response, i.e. their output error with respect to the original representation. $\mathfrak{R}_{SS}^{\mathcal{O}_{LTI}}(\mathcal{S})$ (dashed blue), $\mathfrak{R}_{SS}^{\mathcal{R}_{LTI}}(\mathcal{S})$ (dotted red), $\mathfrak{R}_{SS}^{\mathcal{O}}(\mathcal{S})$ (solid green), $\mathfrak{R}_{SS}^{\mathcal{R}}(\mathcal{S})$ (identical to green), original representation (identical to green).

$$\mathcal{O}_{n_x}^\dagger = [C^\top \quad A^\top C^\top]^\top, \quad \mathcal{R}_{n_x}^\dagger = [B \quad AB]$$

$$\mathcal{O}_{n_x}^\dagger \diamond p = \begin{bmatrix} 1 & \frac{1}{p} \\ p & 2 \end{bmatrix}, \quad \mathcal{R}_{n_x}^\dagger \diamond p = \begin{bmatrix} 1 & 2p \\ p & p^2 \end{bmatrix}.$$

Now compute what would result by applying the state transformation (4.15) with $T = \mathcal{O}_{n_x}^\dagger$ or $T^{-1} = \mathcal{R}_{n_x}^\dagger$ just like in the LTI case. This intuitive approach produces the following so called “frozen” canonical forms:

$$\mathfrak{R}_{SS}^{\mathcal{O}_{LTI}}(\mathcal{S}) = \left[\begin{array}{cc|c} 0 & 1 & p \\ -p & -p & -p^2 \\ \hline 1 & 0 & p \end{array} \right], \quad \mathfrak{R}_{SS}^{\mathcal{R}_{LTI}}(\mathcal{S}) = \left(\mathfrak{R}_{SS}^{\mathcal{O}_{LTI}}(\mathcal{S}) \right)^\top$$

Generally in the literature some follow this approach (see Wassink et al. (2004); Steinbuch et al. (2003)). It is important to note that the two sets of LPV representations derived here and in Example 4.2 and 4.4 are equivalent for constant scheduling trajectories, but they are unequal globally. To show this phenomenon, the output response of these frozen canonical representations, the global canonical forms, and the original SS representation have been calculated for the signals p and u indicated in Example 4.6. The results are presented in Figure 4.4. As can be seen, the global canonical forms $\mathfrak{R}_{SS}^{\mathcal{O}}(\mathcal{S})$ and $\mathfrak{R}_{SS}^{\mathcal{R}}(\mathcal{S})$ completely reproduce the original output with zero error. However, $\mathfrak{R}_{SS}^{\mathcal{O}_{LTI}}(\mathcal{S})$ and $\mathfrak{R}_{SS}^{\mathcal{R}_{LTI}}(\mathcal{S})$ have a relatively huge representation error in the magnitude of 35% even for these very smooth and slowly varying p and u , which mainly comes from a scheduling dependent phase and gain lag with respect to y .

4.2 From state-space to the input-output domain

Equivalence transformations between SS and IO representations in the LPV behavioral framework are of paramount importance. Such transformations are not only necessary to provide representations of a given system in these domains, but they are also the key elements to compare LPV model structures in terms of representation capabilities, to compare identified models in different representation domains, and also to convert results of IO identification approaches to SS models applicable for control.

As one of the main contributions of this thesis, in the following we develop these transformations. We show that they generalize the theory presented for LTI systems in case the coefficient dependence on the scheduling vector is meromorphic and dynamic. It is also shown that the canonical forms, developed in the

previous part, give special cases of the transformation problem, thus they serve as a simple gateway between the SS and the IO representation domains. Again, it is proved that the common practice of the current LPV literature, namely to apply LTI theory to convert IO models to SS models, provides results which have an unequal manifest behavior.

At first the equivalence transformation from the SS to the IO representation domain is considered. The equivalence transformation in this context means the search for an equivalence class of IO realizations with the same manifest behavior. To derive such a transformation, it is first shown that the state as a latent variable can always be eliminated without changing the manifest behavior. Then a specific algorithm is established which provides a minimal realization of a given SS representation in the IO domain. According to this plan, consider the following theorem:

Theorem 4.1 (Elimination of the latent variable in the LPV case) (Zerz 2006) *Given a latent representation (see (3.33)) of \mathcal{S} with manifest behavior \mathfrak{B} and polynomial matrices $R \in \mathcal{R}[\xi]^{n_r \times n_w}$, $R_L \in \mathcal{R}[\xi]^{n_r \times n_x}$. Let the unimodular matrix $M \in \mathcal{R}[\xi]^{n_r \times n_r}$ be such that*

$$MR_L = \begin{bmatrix} R'_L \\ 0 \end{bmatrix}, \quad MR = \begin{bmatrix} R' \\ R'' \end{bmatrix}, \quad (4.16)$$

with R'_L of full row rank. The manifest behavior defined by $(R''(\xi) \diamond p)w = 0$ is equal (almost everywhere) with \mathfrak{B} .

Due to the algebraic structure of $\mathcal{R}[\xi]$, the proof of this theorem follows similarly as in Zerz (2006). Based on Theorem 4.1, the state vector as a latent variable can be eliminated from a given $\mathfrak{R}_{SS}(\mathcal{S})$ with an unimodular transformation. Note that due to the latent nature of the eliminated variable, this elimination is always possible. Furthermore, Theorem 3.5 implies that such a transformation does not change the manifest behavior, hence in analogy with the LTI case, this transformation is an *equivalence transformation*.

The next step to establish an IO realization is to formulate the unimodular transformation of Theorem 4.1 and the resulting R'' in the form of an output side polynomial R_y and an input side polynomial R_u . Write the LPV state-space representation $\mathfrak{R}_{SS}(\mathcal{S})$ with matrix functions (A, B, C, D) into the latent form (3.33):

$$\underbrace{\begin{bmatrix} I\xi - A \\ -C \end{bmatrix}}_{R_L(\xi)} x = \underbrace{\begin{bmatrix} 0 & B \\ -I & D \end{bmatrix}}_{R(\xi)} \begin{bmatrix} y \\ u \end{bmatrix}. \quad (4.17)$$

The resulting polynomials $R \in \mathcal{R}[\xi]^{(n_x+n_y) \times (n_y+n_u)}$ and $R_L \in \mathcal{R}[\xi]^{(n_x+n_y) \times n_x}$ give an equivalent representation of the full behavior of $\mathfrak{R}_{SS}(\mathcal{S})$. Now by applying Theorem 4.1, we are looking for a unimodular matrix $M \in \mathcal{R}[\xi]^{(n_x+n_y) \times (n_x+n_y)}$ such that

$$\underbrace{\begin{bmatrix} M_{11}(\xi) & M_{12}(\xi) \\ M_{21}(\xi) & M_{22}(\xi) \end{bmatrix}}_{M(\xi)} \begin{bmatrix} I\xi - A \\ -C \end{bmatrix} = \begin{bmatrix} * \\ 0 \end{bmatrix}, \quad (4.18)$$

where $\deg(M_{22}) = n_X$ and $\deg(M_{21}) \leq n_X - 1$. Note that there is a particular freedom in choosing M to satisfy (4.18), however by restricting $M_{22}(\xi)$ to be monic, $M_{21}(\xi)$ and $M_{22}(\xi)$ can be uniquely determined. Multiplying (4.17) with the resulting $M(\xi)$ yields

$$\begin{bmatrix} * \\ 0 \end{bmatrix} x = \begin{bmatrix} * & * \\ -M_{21}(\xi) & M_{21}(\xi)B + M_{22}(\xi)D \end{bmatrix} \begin{bmatrix} y \\ u \end{bmatrix}, \quad (4.19)$$

from which the polynomials of a equivalent IO representation can be trivially determined.

Corollary 4.3 (IO Equivalence transformation) *Let $\mathfrak{R}_{SS}(\mathcal{S})$ be a state-space representation with manifest behavior \mathfrak{B} and system matrices (A, B, C, D) . Then there exists a unique monic polynomial $\bar{R}_y \in \mathcal{R}[\xi]^{n_Y \times n_Y}$ with $\deg(\bar{R}_y) = n_X$ and a unique $\bar{R}_u \in \mathcal{R}[\xi]^{n_Y \times n_X}$ with $\deg(\bar{R}_u) \leq n_X - 1$ such that*

$$\bar{R}_y(\xi)C = \bar{R}_u(I\xi - A). \quad (4.20)$$

Let $R_{\text{com}} = \text{diag}(r_1, \dots, r_{n_Y})$, $r_i \in \mathcal{R}[\xi]$, be the greatest common divisor of \bar{R}_y and \bar{R}_u such that there exist $R_y, R_u \in \mathcal{R}[\xi]$ satisfying

$$\bar{R}_y(\xi) = R_{\text{com}}(\xi)R_y(\xi) \quad \text{and} \quad R_{\text{com}}(\xi)R_u(\xi) = \bar{R}_u(\xi)B + \bar{R}_y(\xi)D. \quad (4.21)$$

Then the IO representation of \mathcal{S} , denoted by $\mathfrak{R}_{IO}(\mathcal{S})$, is given by

$$(R_y(\xi) \diamond p)y = (R_u(\xi) \diamond p)u. \quad (4.22)$$

In this way, similar to Corollary 2.4 in the LTI case, an equivalent, minimal IO representation of \mathcal{S} is obtained, based on the given SS representation $\mathfrak{R}_{SS}(\mathcal{S})$ (see Example 4.8). Note that the algorithm defined by (4.20) and (4.21) is more complicated than in the LTI case, as it involves multiplication with the time operators on the coefficients. Thus, this transformation can result in an increased complexity of the coefficient functions in the equivalent IO representation, e.g. if $\mathfrak{R}_{SS}(\mathcal{S})$ has a static dependence on p , then its equivalent IO realization commonly has dynamic dependence on p . The following property also holds in the LPV case:

Corollary 4.4 *Assume that $\mathfrak{R}_{SS}(\mathcal{S})$ is minimal, i.e. structurally state-observable. Then the polynomials \bar{R}_u and \bar{R}_y satisfying (4.20) are left-coprime (their greatest common divisor R_{com} is 1).*

Corollary 4.4 means that the equivalence transformation between the SS and IO domain results in the elimination of dynamics related to unobservable states. Thus in case of a structurally state-observable SS representation, like the observability canonical forms, the equivalence transformation simplifies. However, dynamics related to unreachable states are preserved. This underlines the validity of the proposed minimality concept of LPV-SS representations, namely that minimality is equivalent with structural state-observability.

Example 4.8 (IO realization of a LPV-SS representation) Consider the observability canonical form given in Example 4.2. Note that

$$A_o = \begin{bmatrix} 0 & 1 \\ -\alpha_0^o & -\alpha_1^o \end{bmatrix} \quad \text{and} \quad I\xi - A_o = \begin{bmatrix} \xi & -1 \\ \alpha_0^o & \xi + \alpha_1^o \end{bmatrix},$$

with $\alpha_0^o \diamond p = p \frac{qp^2}{q^2p}$ and $\alpha_1^o \diamond p = -qp - \frac{qp^2}{q^2p}$. In terms of (4.20), we are looking for a $\bar{R}_u \in \mathcal{R}[\xi]^{1 \times 2}$ with $\deg(\bar{R}_u) = 1$ and a monic polynomial $\bar{R}_y \in \mathcal{R}[\xi]$ with $\deg(\bar{R}_y) = 2$. Parameterize these polynomials as

$$\bar{R}_y(\xi) = \xi^2 + a_1\xi + a_0, \quad \bar{R}_u(\xi) = [b_{11}\xi + b_{12} \quad b_{21}\xi + b_{22}].$$

Then in terms of (4.20):

$$(\xi^2 + a_1\xi + a_0) \begin{bmatrix} 1 & 0 \end{bmatrix} = \begin{bmatrix} b_{11}\xi + b_{12} & b_{21}\xi + b_{22} \end{bmatrix} \begin{bmatrix} \xi & -1 \\ \alpha_0^o & \xi + \alpha_1^o \end{bmatrix}.$$

Solving this equation system it follows that

$$\begin{aligned} a_1 &= \alpha_1^o, & b_{11} &= 1, & b_{12} &= \alpha_1^o, \\ a_0 &= \alpha_0^o, & b_{21} &= 0, & b_{22} &= 1. \end{aligned}$$

The resulting polynomials \bar{R}_u and \bar{R}_y are left coprime, hence

$$\begin{aligned} R_y(\xi) &= \bar{R}_y(\xi) = \xi^2 + \alpha_1^o\xi + \alpha_0^o \\ R_u(\xi) &= \bar{R}_u(\xi)B_o + \bar{R}_y(\xi)D_o = \overrightarrow{\beta_2^o}\xi^2 + (\alpha_1^o\overrightarrow{\beta_2^o} + \overrightarrow{\beta_1^o})\xi + \alpha_0^o\beta_2^o + \alpha_1^o\beta_1^o + \beta_0^o, \end{aligned}$$

where $\beta_2^o \diamond p = p$, $\beta_1^o \diamond p = 1 + \frac{p}{qp}$, and $\beta_0^o \diamond p = p \frac{qp}{q^2p} + p + qp$. The above given polynomials provide an IO representation of S with coefficients

$$\begin{aligned} a_2 \diamond p &= 1 & b_2 \diamond p &= q^2p, \\ a_1 \diamond p &= -qp \left(1 + \frac{qp}{q^2p}\right), & b_1 \diamond p &= (1 - qp^2) \left(1 + \frac{qp}{q^2p}\right), \\ a_0 \diamond p &= p \frac{qp^2}{q^2p}, & b_0 \diamond p &= qp^2 \frac{p^2 - 1}{q^2p}. \end{aligned}$$

After this simplified example, consider the DT-LPV-SS representation defined in Example 3.29, which is equivalent with the above considered observability canonical form. In this case

$$A \diamond p = \begin{bmatrix} p & 1 \\ 0 & p \end{bmatrix} \quad \text{and} \quad (I\xi - A) \diamond p = \begin{bmatrix} \xi - p & -1 \\ 0 & \xi - p \end{bmatrix}.$$

In terms of (4.20), we are again looking for a $\bar{R}_u \in \mathcal{R}[\xi]^{1 \times 2}$ with $\deg(\bar{R}_u) = 1$ and a monic polynomial $\bar{R}_y \in \mathcal{R}[\xi]$ with $\deg(\bar{R}_y) = 2$. By using the previously introduced parametrization of these polynomials, (4.20) reads as

$$((\xi^2 + a_1\xi + a_0) \diamond p) \begin{bmatrix} 1 & \frac{1}{p} \end{bmatrix} = (\begin{bmatrix} b_{11}\xi + b_{12} & b_{21}\xi + b_{22} \end{bmatrix} \diamond p) \begin{bmatrix} \xi - p & -1 \\ 0 & \xi - p \end{bmatrix}.$$

Solving this equation system it follows that

$$\begin{aligned} a_1 \diamond p &= -qp \left(1 + \frac{qp}{q^2p}\right), & b_{11} \diamond p &= 1, & b_{12} \diamond p &= -\frac{qp^2}{q^2p}, \\ a_0 \diamond p &= p \frac{qp^2}{q^2p}, & b_{21} \diamond p &= \frac{1}{q^2p}, & b_{22} \diamond p &= 0. \end{aligned}$$

Additionally, \bar{R}_u and \bar{R}_y are left coprime and they result in exactly the same IO realization as the previous example.

Contrary to the LTI case, closed formula on the conversion rules between the parameters of the previously introduced canonical forms and the resulting IO realization can only be given for the observability canonical form and its companion version in DT. Even if the algorithm defined by (4.20) and (4.21) is always solvable for the reachability canonical forms, the resulting formulas of the $\{b_j\}$ coef-

ficients are complicated rational functions of the original matrix coefficients. The reason of this phenomenon is again the non-commutativity of multiplication by ξ on $\mathcal{R}[\xi]$. In CT, the chain-rule of differentiation gives also complicated expressions. Therefore the conversion rules are only stated for the observability forms in discrete-time:

Corollary 4.5 (IO conversion rules) *The IO realization of canonical SS representations of the discrete-time SISO LPV system \mathcal{S} is given by*

	$\mathfrak{R}_{SS}^{\circ}(\mathcal{S})$	$\mathfrak{R}_{SS}^{\circ c}(\mathcal{S})$
a_i	α_i°	$[\alpha_i^{\circ c}]^{(i)}$
a_{n_x}	1	1
b_j	$[\beta_j^{\circ}]^{(j)} + \sum_{l=j}^{n_x-1} \alpha_l^{\circ} [\beta_{n_x-l+j}^{\circ}]^{(j)}$	$[\beta_j^{\circ c} + \alpha_j^{\circ c} \beta_{n_x}^{\circ c}]^{(j)}$
b_{n_x}	$[\beta_{n_x}^{\circ}]^{(n_x)}$	$[\beta_{n_x}^{\circ c}]^{(n_x)}$

with $[\cdot]^{(n)}$ denoting the forward-shift operation applied to the coefficients n times, $i, j \in \mathbb{I}_{0}^{n_x-1}$, and $n_a = n_b = n_x$.

Note that in the reachability and reachability companion cases, the conversion formulas are the same for all parameters except $\{b_j\}_{j=0}^{n_x-1}$.

4.3 From the input-output to the state-space domain

As a next step, the equivalence transformation from the IO to the SS representation domain is considered. To derive such a transformation, a vital ingredient is to construct a state-map for a given IO representation that defines an equivalent SS representation. This construction can be seen as the reverse operation of the previous latent variable elimination. The actual aim is to introduce a latent variable into (4.22) such that it satisfies the state-property, ergo it defines a SS representation of the original system via Theorem 3.2.

Generation of a state-map is more involved in the LPV case than for time-invariant systems as the scheduling dependence of the coefficients does not commute with time operators as integration, derivation, and time-shift. In order to improve readability of the upcoming rather technical discussion, we first investigate the intuitive idea behind the used state-construction mechanism, the so called *cut-and-shift* operation. Then this operation is formally defined over the ring $\mathcal{R}[\xi]$ both in CT and in DT. As a next step, state-maps generated by the cut-and-shift procedure are constructed and it is shown that they introduce latent variables satisfying the state property. Minimality of the resulting state kernel forms is also shown in the SISO case. Finally, algorithms are derived that provide realization of a given IO representation in terms of the previously introduced canonical forms.

The idea of recursive state-construction

The central idea of state-construction for LPV-IO representations is the extension of the previously introduced cut-and-shift mechanism of the LTI case (see Section 2.1.7). However, before venturing into the technicalities, we explain the intuitive idea of the cut-and-shift-map based state-construction through a simple example. Assume that, in continuous-time, a kernel representation $\mathfrak{R}_K(\mathcal{S})$ with $\mathbb{P} = \mathbb{R}$ is given. $\mathfrak{R}_K(\mathcal{S})$ is described by $R \in \mathcal{R}[\xi]$, providing the differential equation

$$(r_0 \diamond p)w + (r_1 \diamond p)\frac{d}{dt}w + (r_2 \diamond p)\frac{d^2}{dt^2}w = 0. \quad (4.23)$$

In the following, we construct an equivalent SS representation of $\mathfrak{R}_K(\mathcal{S})$. This requires a state-construction, where our aim is the elimination of the derivatives of w in (4.23) through the introduction of state-variables. Introduce the latent variable $x_1 : \mathbb{R} \rightarrow \mathbb{R}$, defined by

$$x_1 = ((r_1 - \dot{r}_2) \diamond p)w + (r_2 \diamond p)\frac{d}{dt}w. \quad (4.24)$$

Then equation (4.23) can be rewritten as

$$\frac{d}{dt}x_1 + ((r_0 - \dot{r}_1 + \ddot{r}_2) \diamond p)w = 0, \quad (4.25)$$

using the rule of chain-derivation. It is obvious, that the resulting equations (4.24) and (4.25) define the same manifest behavior as (4.23). In this way, we have eliminated the derivatives of w from (4.23), however the resulting extra equation (4.24) still contains a first order derivative of w . Thus, introduce the latent variable $x_2 : \mathbb{R} \rightarrow \mathbb{R}$ such that

$$x_2 = (r_2 \diamond p)w. \quad (4.26)$$

Then, equation (4.24) can be rewritten as

$$\frac{d}{dt}x_2 - x_1 + ((r_1 - 2\dot{r}_2) \diamond p)w = 0. \quad (4.27)$$

We have arrived at the following equation system

$$-\left(\begin{bmatrix} r_0 - \dot{r}_1 + \ddot{r}_2 \\ r_1 - 2\dot{r}_2 \\ r_2 \end{bmatrix} \diamond p\right)w = \begin{bmatrix} \frac{d}{dt} & 0 \\ -1 & \frac{d}{dt} \\ 0 & -1 \end{bmatrix} \begin{bmatrix} x_1 \\ x_2 \end{bmatrix}, \quad (4.28)$$

which is equivalent with (4.23). Due to the fact that the left side is a zero-order while the right side is first-order polynomial, (4.28) is a state-kernel form and $x = [x_1 \ x_2]^\top$ trivially fulfills the property of state (see Theorem 3.2). Additionally, the algebraic equivalence of the introduced state-relations (4.24) and (4.26) implies that there exists an unimodular transformation in terms of Theorem 4.1, which can eliminate x from (4.28) such that (4.23) is reobtained. Thus, the manifest behavior of (4.28) is equivalent with the behavior of $\mathfrak{R}_K(\mathcal{S})$. Note that in this way, we have defined an equivalent state-map of the original system. Using this state-map, one

choice of SS realization follows through the use of (4.26) as the output equation and by the substitution of this equation into (4.28). This results in the state-space representation

$$\frac{d}{dt}x = \left(\begin{bmatrix} 0 & -\frac{r_0 - \dot{r}_1 + \ddot{r}_2}{r_2} \\ 1 & -\frac{r_1 - 2\dot{r}_2}{r_2} \end{bmatrix} \diamond p \right) x, \quad (4.29a)$$

$$w = \left(\begin{bmatrix} 0 & \frac{1}{r_2} \end{bmatrix} \diamond p \right) x, \quad (4.29b)$$

which is a companion observability canonical form if $r_2 = 1$, i.e. if R is monic. This SS realization is equivalent with (4.23) only for those scheduling trajectories where $(r_2 \diamond p)(t) \neq 0$ (see (4.26)). Thus, (4.29a-b) is equivalent in an almost everywhere sense with (4.23). If r_2 is unequal to zero for all scheduling trajectories, then full equivalence holds.

The intuitive idea behind the state construction that we exposed in this example can be formalized as the following recursive scheme. For a given continuous-time SISO kernel representation $\mathfrak{R}_K(\mathcal{S})$, the behavior is described by

$$(R_0 \left(\frac{d}{dt} \right) \diamond p)w = 0. \quad (4.30)$$

Let $l = 1$ and define a latent variable as

$$x_l := (R_l \left(\frac{d}{dt} \right) \diamond p)w, \quad \text{s.t.} \quad R_{(l-1)}(\xi) := \bar{R}_l + \xi R_l(\xi), \quad (4.31)$$

where $\bar{R}_l \in \mathcal{R}$, $R_l \in \mathcal{R}[\xi]$, and due to the multiplication rules, \bar{R}_0 is chosen as:

$$\bar{R}_0 := r_0 + \sum_{i=1}^{n_\xi} (-1)^i \dot{r}_i^{(i)}, \quad (4.32)$$

where $\dot{r}^{(i)}$ denotes the dot operation applied to $r \in \mathcal{R}$ for i -times (see equations (4.25) and (4.27) as examples). According to this mechanism

$$\begin{cases} \text{for } l = 1, & \frac{d}{dt}x_1 = -(\bar{R}_0 \diamond p)w, \\ \text{for } 1 < l \leq n_\xi, & \frac{d}{dt}x_l = x_{l-1} - (\bar{R}_{l-1} \diamond p)w. \end{cases} \quad (4.33)$$

holds and (4.31) with (4.33) give a latent variable representation of \mathcal{S} . Repeat these steps recursively on (4.31) till $l = n_\xi$ which results in $R_{n_\xi}(\xi) = 0$. Then the obtained polynomials $\{R_l(\xi)\}_{l=1}^{n_\xi}$ define a state map and $\{\bar{R}_l\}_{l=1}^{n_\xi}$ give the coefficients of the associated SS representation, as it holds that

$$\begin{cases} \text{for } 1 \leq l < n_\xi, & \frac{d}{dt}x_{(l+1)} = x_l - (\bar{R}_l \diamond p)w, \\ \text{for } l = n_\xi, & (\bar{R}_{n_\xi} \diamond p)w = x_{n_\xi}. \end{cases} \quad (4.34)$$

The procedure, defined by (4.31), gives the algorithm of state-construction which we call the parameter-varying cut-and-shift map $\varrho_- : \mathcal{R}[\xi]^{\times} \rightarrow \mathcal{R}[\xi]^{\times}$. In this terminology, \bar{R}_l corresponds to the cut term while $\xi R_l(\xi)$ is the shift term. Similar to the LTI case, the PV cut-and-shift operator ϱ_- acts on polynomial matrices but

with meromorphic coefficient functions. Another difference with the LTI case is that the cut-and-shift-map is defined differently for the CT and DT time-axis, due to the different non-commutative multiplication rules of derivation and time-shift with respect to the scheduling dependent coefficients. In the following, the technical definition of ϱ_- is given both in the CT and DT cases, using the idea of the recursive scheme introduced before.

Cut-and-shift in continuous-time

In the CT case, the indeterminant ξ is associated with $\frac{d}{dt}$, implying that multiplication with ξ on $\mathcal{R}[\xi]^{\times}$ gives the non-commutative rule of (3.22). The reverse operation, multiplication by ξ^{-1} , results in integration, which yields:

$$\xi^{-1} \left[r\xi^i + (-1)^i \dot{r}^{(i)} \right] = \sum_{j=0}^{i-1} (-1)^j \dot{r}^{(j)} \xi^{i-j-1}. \quad (4.35)$$

This operation is the same as what is used in (4.31). Based on this, the cut-and-shift-map in continuous-time is defined on $\mathcal{R}[\xi]^{\times}$ as

$$\varrho_- \left(\underbrace{r_0 + r_1\xi + \dots + r_n\xi^n}_{R(\xi)} \right) = \underbrace{r'_1 + \dots + r'_n\xi^{n-1}}_{R'(\xi)}, \quad (4.36)$$

where $R, R' \in \mathcal{R}[\xi]^{\times}$ and each new meromorphic coefficient function of R' is computed as the result of elementary cut-and-shift operations:

$$\varrho_-(r\xi^i) = \begin{cases} \sum_{j=0}^{i-1} (-1)^j \dot{r}^{(j)} \xi^{i-j-1}, & \text{if } i > 1; \\ 0, & \text{if } i = 0. \end{cases} \quad (4.37)$$

This yields that

$$r'_i = \sum_{j=0}^{n-i} (-1)^j \dot{r}_{i+j}^{(j)}. \quad (4.38)$$

Cut-and-shift in discrete-time

In the DT case, ξ is associated with the forward time-shift operator q , implying that multiplication with ξ on $\mathcal{R}[\xi]^{\times}$ gives the non-commutative rule of (3.42). The reverse operation, multiplication by ξ^{-1} , results in backward time-shift, giving:

$$\xi^{-1} [r\xi^i] = \overleftarrow{r} \xi^{i-1}. \quad (4.39)$$

This implies that in discrete-time, the cut-and-shift-map is defined on $\mathcal{R}[\xi]^{\times}$ in the form of (4.36), where each new meromorphic coefficient function is computed

as the result of elementary cut-and-shift operations:

$$\varrho_-(r\xi^i) = \begin{cases} \overleftarrow{r} \xi^{i-1}, & \text{if } i > 1; \\ 0, & \text{if } i = 0. \end{cases} \quad (4.40)$$

giving that $r'_i = \overleftarrow{r}_i$ where $\overleftarrow{\cdot}$ is the backward shift operation on \mathcal{R} .

State-maps and polynomial modules

As a next step we formulate the construction of a state-map, i.e. the generation of state variables, for a given kernel representation, as the recursive use of the cut-and-shift operation on the polynomials of $\mathcal{R}[\xi]$. This procedure is the analog of the introduced recursive-scheme of state-construction in the CT case (see (4.33)). The resulting state-map characterizes a state-kernel representation of the system, which is minimal in the SISO case. In order to describe all equivalent (minimal) state-kernel representations of the system, equivalence classes of the state-map are established in terms of polynomial modules over $\mathcal{R}[\xi]$.

Let $R \in \mathcal{R}[\xi]^{n_r \times n_w}$ be the associated polynomial of the kernel presentation $\mathfrak{R}_K(\mathcal{S})$. Assume that R is monic and given as

$$R(\xi) = r_0^{[0]} + r_1^{[0]}\xi + \dots + r_n^{[0]}\xi^n, \quad (4.41)$$

where superscript $\cdot^{[0]}$ denotes an additional index of the coefficients. Repeated use of ϱ_- on R and stacking the resulting polynomial matrices leads to

$$\Sigma_-(R) = \begin{bmatrix} \varrho_-(R) \\ \varrho_-^2(R) \\ \vdots \\ \varrho_-^{n-2}(R) \\ \varrho_-^{n-1}(R) \end{bmatrix} = \begin{bmatrix} r_1^{[1]} + \dots + r_{n-1}^{[1]}\xi^{n-2} + \xi^{n-1} \\ r_2^{[2]} + \dots + r_{n-1}^{[2]}\xi^{n-3} + \xi^{n-2} \\ \vdots \\ r_{n-1}^{[n-1]} + \xi \\ 1 \end{bmatrix}. \quad (4.42)$$

where each coefficient function $r_i^{[j]}$ is computed according to the local cut-and-shift rules based on $\{r_i^{[j-1]}\}_{i=n-j+1}^n$ recursively. It is obvious, that if $n_r = 1$ (SISO case if additionally $n_w = 2$), the rows of Σ_- are independent, thus it can be shown that $X = \Sigma_-(R)$ defines a minimal state-map in the form of

$$x = (X(\xi) \diamond p)w. \quad (4.43)$$

Later it is shown, that such a state-map implies a unique SS representation. Before that, we characterize all possible minimal state-maps that lead to an equivalent SS representation.

Denote the multiplication by ξ as ϱ_+ , which acts in the same way as as defined

by (3.22) and (3.42): Consequently

$$\varrho_+ \left(\begin{bmatrix} \Sigma_-(R) \\ 0 \end{bmatrix} \right) = \begin{bmatrix} R \\ \Sigma_-(R) \end{bmatrix} - \begin{bmatrix} r_0^{[0]} \\ r_1^{[1]} \\ \vdots \\ 1 \end{bmatrix}. \quad (4.44)$$

Note that $\varrho_-\varrho_+ = I$, while $\varrho_+(\varrho_-(R)) = R(\xi) - R(0)$.

Following a similar path as in the LTI case, denote by $\text{span}_{\mathcal{R}}^{\text{row}}(R)$ the subspace spanned by the rows of $R \in \mathcal{R}[\xi]^{\times \times}$, viewed as a linear space of polynomial vector functions with coefficients in $\mathcal{R}^{\times \times}$. Also introduce $\text{module}_{\mathcal{R}[\xi]}(R)$ as the left-module in $\mathcal{R}[\xi]^{n_r \times n_w}$ spanned by the rows of $R \in \mathcal{R}[\xi]^{n_r \times n_w}$:

$$\text{module}_{\mathcal{R}[\xi]}(R) = \mathcal{R}[\xi]^{1 \times n_w} / \mathcal{R}[\xi]^{1 \times n_r} R, \quad (4.45a)$$

$$= \text{span}_{\mathcal{R}}^{\text{row}} \left(\begin{bmatrix} R \\ \varrho_+(R) \\ \vdots \end{bmatrix} \right). \quad (4.45b)$$

This module represents the set of equivalence classes on $\text{span}_{\mathcal{R}}^{\text{row}}(\Sigma_-(R))$. Let $X \in \mathcal{R}[\xi]^{n_r \times n_w}$ be a polynomial matrix with independent rows (full row-rank) and such that

$$\text{span}_{\mathcal{R}}^{\text{row}}(X) \oplus \text{module}_{\mathcal{R}[\xi]}(R) = \text{span}_{\mathcal{R}}^{\text{row}}(\Sigma_-(R)) + \text{module}_{\mathcal{R}[\xi]}(R). \quad (4.46)$$

Then similar to the LTI case, it is possible to show that X is a minimal state-map of the LPV system \mathcal{S} and it defines a state variable by (4.43). This way it is possible to obtain all minimal SS realizations of \mathcal{S} that are equivalent with the kernel representation associated with R .

State-maps based on kernel representations

In the previous part, we have established state-map constructions for kernel representations based on the cut-and-shift operation and characterized the class of all state-maps that result in an equivalent SS representation. The next step is to characterize these SS representations with respect to an IO partition. We develop an algorithm which, based on a given state-map, provides a SS realization of a kernel representation for a chosen IO partition. We show that, for specific choices of the state-map, the algorithm provides the SS realization in terms of the previously introduced observability and companion observability canonical forms.

For a given kernel representation $\mathfrak{R}_K(\mathcal{S})$ associated with the polynomial $R \in \mathcal{R}[\xi]^{n_r \times n_w}$, the input-output partition of R is characterized by choosing a selector matrix $S_u \in \mathbb{R}^{\times \times n_w}$ giving $u = S_u w$ and a complementary matrix $S_y \in \mathbb{R}^{\times \times n_w}$ giving $y = S_y w$. In case of an unknown IO partition, the construction of S_u follows by computing the subspace of $\mathcal{R}^{1 \times n_w}$ consisting of the \mathcal{R} -span of the elements with degree zero in $\text{span}_{\mathcal{R}}^{\text{row}}(\Sigma_-(R)) + \text{module}_{\mathcal{R}[\xi]}(R)$ and choosing S_u such that

the rows of S_u span a complement of this subspace relative to \mathcal{R}^{n_w} . Then, S_y is chosen complementary to S_u .

Assume that a full row rank $X \in \mathcal{R}[\xi]^{n_w \times n_w}$ is given which satisfies (4.46). Then the matrix polynomial X and the matrix S_u jointly lead to the direct sum decomposition:

$$\begin{aligned} \text{span}_{\mathcal{R}}^{\text{row}}(I_{n_w \times n_w}) + \text{span}_{\mathcal{R}}^{\text{row}}(\Sigma_-(R)) + \text{module}_{\mathcal{R}[\xi]}(R) = \\ \text{span}_{\mathcal{R}}^{\text{row}}(\Sigma_-(S_u)) \oplus \text{span}_{\mathcal{R}}^{\text{row}}(\Sigma_-(X)) \oplus \text{module}_{\mathcal{R}[\xi]}(R). \end{aligned} \quad (4.47)$$

From (4.44), it follows that

$$\begin{aligned} \text{span}_{\mathcal{R}}^{\text{row}}(\varrho_+(\Sigma_-(X))) \subseteq \text{span}_{\mathcal{R}}^{\text{row}}(I_{n_w \times n_w}) + \\ \text{span}_{\mathcal{R}}^{\text{row}}(\Sigma_-(R)) + \text{module}_{\mathcal{R}[\xi]}(R), \end{aligned} \quad (4.48)$$

which implies

$$\text{span}_{\mathcal{R}}^{\text{row}}(\varrho_+(X)) \subseteq \text{span}_{\mathcal{R}}^{\text{row}}(X) \oplus \text{span}_{\mathcal{R}}^{\text{row}}(S_u) \oplus \text{module}_{\mathcal{R}[\xi]}(R). \quad (4.49)$$

On the other hand, S_y gives

$$\text{span}_{\mathcal{R}}^{\text{row}}(S_y) \subseteq \text{span}_{\mathcal{R}}^{\text{row}}(X) \oplus \text{span}_{\mathcal{R}}^{\text{row}}(S_u) \oplus \text{module}_{\mathcal{R}[\xi]}(R). \quad (4.50)$$

These inclusions imply, that there exist unique matrix functions (A, B, C, D) in $\mathcal{R}^{\times \cdot}$ and polynomial matrix functions $X_u, X_y \in \mathcal{R}[\xi]^{\cdot \times \cdot}$ with appropriate dimensions such that

$$\xi X = AX + BS_u + X_u R, \quad (4.51a)$$

$$S_y = CX + DS_u + X_y R. \quad (4.51b)$$

Then

$$\left[\begin{array}{c|c} A & B \\ \hline C & D \end{array} \right] \in \left[\begin{array}{c|c} \mathcal{R}^{n_x \times n_x} & \mathcal{R}^{n_x \times n_w} \\ \hline \mathcal{R}^{n_y \times n_x} & \mathcal{R}^{n_y \times n_w} \end{array} \right], \quad (4.52)$$

is a minimal state-representation of the LPV system \mathcal{S} . This algorithm provides an SS realization of both LPV-IO and LPV-KR representations.

As a next step, we show that specific choices of X lead to the construction of the observability and the reachability canonical forms via algorithm (4.51a-b). Consider the SISO case. Assume that $\mathfrak{R}_{\text{IO}}(\mathcal{S})$ is given with polynomial matrices $R_y, R_u \in \mathcal{R}$:

$$R_y(\xi) = a_0^{[0]} + a_1^{[0]}\xi + \dots + a_{n_a}^{[0]}\xi^{n_a}, \quad (4.53)$$

$$R_u(\xi) = b_0^{[0]} + b_1^{[0]}\xi + \dots + b_{n_b}^{[0]}\xi^{n_b}. \quad (4.54)$$

where $n_a = n_b$. Additionally, let R be monic, i.e. $a_{n_a}^{[0]} = 1$, otherwise redefine the polynomials by dividing by the coefficient function $a_{n_a}^{[0]}$. Then $\Sigma_-([R_y \quad -R_u])$

gives:

$$\begin{bmatrix} a_1^{[1]} + \dots + a_{n_a-1}^{[1]} \xi^{n_a-2} + \xi^{n_a-1} & -b_1^{[1]} - \dots - b_{n_a-1}^{[1]} \xi^{n_a-1} \\ a_2^{[2]} + \dots + a_{n_a-1}^{[2]} \xi^{n_a-3} + \xi^{n_a-2} & -b_2^{[2]} - \dots - a_{n_a-1}^{[2]} \xi^{n_a-2} \\ \vdots & \vdots \\ a_{n_a-1}^{[n_a-1]} + \xi & -b_{n_a-1}^{[n_a-1]} - b_{n_a}^{[n_a-1]} \xi \\ 1 & -b_{n_a}^{[n_a]} \end{bmatrix}. \quad (4.55)$$

Obviously, this $n_a \times 2$ matrix has independent rows and the span of these rows is linearly independent from $\text{module}_{\mathcal{R}[\xi]}([R_y \quad -R_u])$. Thus, the construction of the state-map in terms of (4.46) requires to choose $X \in \mathcal{R}[\xi]^{n_a \times 2}$ such that $\text{span}_{\mathcal{R}}^{\text{row}}(X)$ equals the rowspan of (4.55). As all rows of (4.55) are independent, therefore X can be easily constructed. The selector matrices are also evident: $S_u = [0 \quad 1]$ and $S_y = [1 \quad 0]$.

A convenient choice for X is to take the rows of (4.55) in the given order (top-to-bottom). Application of the algorithm defined by (4.51a-b) with such a X leads to the companion-observability canonical form $\mathfrak{R}_{\text{SS}}^{\text{O}}(\mathcal{S})$. This can be shown by solving the corresponding equation system of (4.51a-b). Note that the resulting conversion rules in DT are exactly the same as in Corollary 4.5.

To derive a realization in terms of the observability canonical form, define $\beta_0, \dots, \beta_{n_a} \in \mathcal{R}$ such that

$$R_u(\xi) = \beta_{n_a}^{[0]} R_y(\xi) + \beta_{n_a-1}^{[0]} \xi^{-1} R_y(\xi) + \dots + \beta_0^{[0]} \xi^{-n_a} R_y(\xi) + \dots \quad (4.56)$$

These functions are the resulting expansion coefficients (left-fractions) of R_u in terms of R_y . Then, by choosing X as

$$X(\xi) = \begin{bmatrix} 1 & -\beta_{n_a}^{[n_a]} \\ \xi & -\beta_{n_a-1}^{[n_a-1]} - \beta_{n_a}^{[n_a-1]} \xi \\ \vdots & \vdots \\ \xi^{n_a-2} & -\beta_2^{[2]} - \dots - \beta_{n_a}^{[2]} \xi^{n_a-2} \\ \xi^{n_a-1} & -\beta_1^{[1]} - \dots - \beta_{n_a}^{[1]} \xi^{n_a-1} \end{bmatrix}, \quad (4.57)$$

results in $\mathfrak{R}_{\text{SS}}^{\text{O}}(\mathcal{S})$ via the algorithm defined by (4.51a-b). The resulting coefficients in this case are

$$\alpha_i^{\text{o}} = a_i^{[0]}, \quad \beta_j^{\text{o}} = \beta_j^{[j]}, \quad (4.58)$$

where $i, j \in \llbracket 1^{n_a} \rrbracket$, $n_{\mathcal{X}} = n_a$, $\beta_{n_a}^{\text{o}} = b_{n_a}^{[n_a]}$. Again, it can be shown that the resulting conversion rules in DT are exactly the same as in Corollary 4.5.

The following claim obviously holds in the LPV case as well:

Claim 4.1 *The $\mathfrak{R}_{\text{SS}}^{\text{O}}(\mathcal{S})$ and $\mathfrak{R}_{\text{SS}}^{\text{O}^c}(\mathcal{S})$ SS realizations of a SISO $\mathfrak{R}_{\text{IO}}(\mathcal{S})$ via (4.51a-b) are completely state-observable and hence minimal. They are also structurally state-reachable iff R_y and R_u are left-coprime on $\mathcal{R}[\xi]$.*

State-maps based on image-representations

The previously developed algorithm provides SS realizations based on kernel representations. However it is also possible to derive another algorithm that is based on state-maps generated from the so called image representations. In this part, we develop this algorithm and we show that for specific choices of the state-map it provides the SS realization in terms of the previously introduced reachability and companion reachability canonical forms.

To deduce reachability canonical forms, investigate $\mathfrak{R}_{\text{IO}}(S)$ with matrix polynomial functions R_u and monic R_y in the following, so called *image representation*:

$$\begin{bmatrix} u \\ y \end{bmatrix} = \left(\underbrace{\begin{bmatrix} R_u(\xi) \\ R_y(\xi) \end{bmatrix}}_{\check{X}(\xi)} \diamond p \right) w_L. \quad (4.59)$$

with ξ either equal to $\frac{d}{dt}$ or q . Note that any LPV system has an image representation in the form of (4.59) with equal manifest behavior (see Zerz (2006) for a proof). Applying the cut-and-shift based state-construction mechanism on (4.59) with system variables (w_L, u, y) leads to

$$\Sigma_-([\check{X} \quad I_{2 \times 2}]) = [\Sigma_-(\check{X}) \quad 0 \quad 0],$$

where

$$\Sigma_-(\check{X}) = \begin{bmatrix} a_1^{[1]} + a_2^{[1]}\xi + \dots + \xi^{n_a-1} \\ b_1^{[1]} + b_2^{[1]}\xi + \dots + b_{n_b}^{[1]}\xi^{n_b-1} \\ a_2^{[2]} + \dots + \xi^{n_a-2} \\ b_2^{[2]} + \dots + b_{n_b}^{[2]}\xi^{n_b-2} \\ \vdots \\ 1 \\ b_{n_a}^{[n_a]} \end{bmatrix}.$$

A minimal state for (4.59) is therefore given by

$$x = (X(\xi) \diamond p) w_L, \quad (4.60)$$

where $X \in \mathcal{R}[\xi]^{n_a \times 1}$ has independent rows and satisfies

$$\text{span}_{\mathcal{R}}^{\text{row}}(X) = \text{span}_{\mathcal{R}}^{\text{row}}(\Sigma_-(\check{X})). \quad (4.61)$$

The input is given as $u = S_u(\check{X}(\xi) \diamond p) w_L$ with S_u a selector matrix such that $\text{span}_{\mathcal{R}}^{\text{row}}(X)$ and $\text{span}_{\mathcal{R}}^{\text{row}}(S_u \check{X})$ are direct summands. This implies that $S_u = [0 \quad 1]$ and $S_y = [1 \quad 0]$. Then again, it can be seen that

$$\text{span}_{\mathcal{R}}^{\text{row}}(\varrho_+(X)) \subseteq \text{span}_{\mathcal{R}}^{\text{row}}(X) \oplus \text{span}_{\mathcal{R}}^{\text{row}}(S_u \check{X}), \quad (4.62a)$$

$$\text{span}_{\mathcal{R}}^{\text{row}}(S_y \check{X}) \subseteq \text{span}_{\mathcal{R}}^{\text{row}}(X) \oplus \text{span}_{\mathcal{R}}^{\text{row}}(S_u \check{X}). \quad (4.62b)$$

These inclusions imply the existence of unique matrices (A, B, C, D) in $\mathcal{R}^{\times \times}$ and a polynomial matrix $X \in \mathcal{R}[\xi]^{\times \times}$ with appropriate dimensions such that

$$\xi X = AX + BS_u \check{X}, \quad (4.63a)$$

$$S_y \check{X} = CX + DS_u \check{X}, \quad (4.63b)$$

giving a state-representation of the LPV system \mathcal{S} .

Consider again the SISO case. By choosing X as

$$X(\xi) = [1 \quad \xi \quad \dots \quad \xi^{n_a-2} \quad \xi^{n_a-1}]^\top, \quad (4.64)$$

algorithm (4.63a-b) results in the companion-reachability canonical form $\mathfrak{R}_{SS}^{\mathcal{R}_c}(\mathcal{S})$, while, using

$$X = \begin{bmatrix} a_1^{[1]} + \dots + \xi^{n_a-1} \\ a_2^{[2]} + \dots + \xi^{n_a-2} \\ \vdots \\ a_{n_a-1}^{[n_a-1]} + \xi \\ 1 \end{bmatrix}, \quad (4.65)$$

gives $\mathfrak{R}_{SS}^{\mathcal{R}}(\mathcal{S})$. Unfortunately, due to the same reasons as in the state-elimination case, closed formulas of the coefficient relations can not be given for the reachability and its companion canonical forms. However, the transformed coefficients can always be uniquely obtained through algorithm (4.63a-b). The following claim also holds:

Claim 4.2 *The $\mathfrak{R}_{SS}^{\mathcal{R}}(\mathcal{S})$ and $\mathfrak{R}_{SS}^{\mathcal{R}_c}(\mathcal{S})$ SS realizations of a SISO $\mathfrak{R}_{IO}(\mathcal{S})$ via (4.63a-b) are completely state-reachable. They are also structurally state-observable and hence minimal iff R_y and R_u are coprime.*

State-construction in the MIMO case

In the MIMO case, algorithms (4.51a-b) and (4.63a-b) also provide SS realization of IO representations, however with different selector matrices (due to the multi-dimension) and with a more complicated path to select independent rows from the shift-map for X . It is only guaranteed that at least n_a number of rows of the shift-map are independent, thus such selection is not evident. Similar to the selection schemes generating the SS MIMO canonical representations, only certain selection strategies for X lead to the MIMO observability and reachability canonical forms. Thus minimality of the obtained SS realizations via algorithm (4.51a-b) and (4.63a-b) is not guaranteed in the general sense.

Example 4.9 (SS realization of LPV-IO representations) *Consider the following DT-LPV-IO representation $\mathfrak{R}_{IO}(\mathcal{S})$:*

$$y + pq^{-1}y + pq^{-2}y = pq^{-1}u,$$

with $\mathbb{P} = [1, 2]$. Then the polynomial form of this representation is characterized as

$$R(\xi) \diamond p = \begin{bmatrix} R_y(\xi) \diamond p & -R_u(\xi) \diamond p \end{bmatrix} = \begin{bmatrix} \xi^2 + (q^2 p)\xi + q^2 p & -(q^2 p)\xi \end{bmatrix}.$$

In the following we derive a SS realization of this representation in an observability canonical form. According to (3.42), associate the involved scheduling dependencies as

$$\zeta_{01} = p, \quad \zeta_{11} = qp, \quad \zeta_{21} = q^2 p.$$

In terms of these variables, R reads as

$$R(\xi) = \begin{bmatrix} R_y(\xi) & -R_u(\xi) \end{bmatrix} = \begin{bmatrix} \xi^2 + \zeta_{21}\xi + \zeta_{21} & -\zeta_{21}\xi \end{bmatrix}.$$

By solving (4.56), it follows that

$$\beta_2^{[0]} = 0, \quad \beta_1^{[0]} = \zeta_{21}.$$

Then, by generating $X(\xi)$ in terms of (4.57), we obtain

$$X(\xi) = \begin{bmatrix} 1 & 0 \\ \xi & -\zeta_{11} \end{bmatrix}.$$

Now with $S_y = \begin{bmatrix} 1 & 0 \end{bmatrix}$ and $S_u = \begin{bmatrix} 0 & 1 \end{bmatrix}$, equations (4.51a-b) read as

$$\underbrace{\begin{bmatrix} \xi & 0 \\ \xi^2 & -\zeta_{21}\xi \end{bmatrix}}_{\xi X(\xi)} = \underbrace{\begin{bmatrix} \alpha_{11} & \alpha_{12} \\ \alpha_{21} & \alpha_{22} \end{bmatrix}}_A \cdot \underbrace{\begin{bmatrix} 1 & 0 \\ \xi & -\zeta_{11} \end{bmatrix}}_{X(\xi)} + \underbrace{\begin{bmatrix} 0 & \beta_1 \\ 0 & \beta_2 \end{bmatrix}}_{BS_u} + \underbrace{\begin{bmatrix} X_{u1}(\xi) \\ X_{u2}(\xi) \end{bmatrix}}_{X(\xi)} R(\xi),$$

$$\underbrace{\begin{bmatrix} 1 & 0 \end{bmatrix}}_{S_y} = \underbrace{\begin{bmatrix} c_1 & c_2 \end{bmatrix}}_C \cdot \underbrace{\begin{bmatrix} 1 & 0 \\ \xi & -\zeta_{11} \end{bmatrix}}_{X(\xi)} + \underbrace{\begin{bmatrix} 0 & d_1 \end{bmatrix}}_{DS_u} + X_y(\xi)R(\xi),$$

These give the following

$$\begin{aligned} \xi &= \alpha_{11} + \alpha_{12}\xi + X_{u1}(\xi)R_y(\xi), & \Rightarrow & X_{u1}(\xi) = 0, \alpha_{11} = 0, \alpha_{12} = 1, \\ 0 &= -\zeta_{11}\alpha_{12} + \beta_1 - X_{u1}(\xi)R_u(\xi), & \Rightarrow & \beta_1 = \zeta_{11}, \\ \xi^2 &= \alpha_{21} + \alpha_{22}\xi + X_{u2}(\xi)R_y(\xi), & \Rightarrow & X_{u2}(\xi) = 1, \alpha_{21} = \alpha_{22} = -\zeta_{21}, \\ -\zeta_{21}\xi &= -\zeta_{11}\alpha_{22} + \beta_2 - X_{u2}(\xi)R_u(\xi), & \Rightarrow & \beta_2 = -\zeta_{11}\zeta_{21}, \\ 1 &= c_1 + c_2\xi + X_y(\xi)R_y(\xi), & \Rightarrow & X_y(\xi) = 0, c_1 = 1, c_2 = 0, \\ 0 &= -\zeta_{11}c_2 + d_1 - X_y(\xi)R_u(\xi), & \Rightarrow & d_1 = 0. \end{aligned}$$

Then, the observability canonical form results as

$$\mathfrak{R}_{SS}^O(S) = \left[\begin{array}{cc|c} 0 & 1 & qp \\ -q^2 p & -q^2 p & -(qp)(q^2 p) \\ \hline 1 & 0 & 0 \end{array} \right].$$

Similarly, the reachability canonical form can be obtained, giving

$$\mathfrak{R}_{SS}^R(S) = \left[\begin{array}{cc|c} 0 & -q^{-1}p & 1 \\ 1 & -q^{-1}p & 0 \\ \hline p & -p(q^{-1}p) & 0 \end{array} \right].$$

4.4 Summary

In this chapter, we have established equivalence transformations between the state-space and the input-output representation domains. These transformations have been introduced to enable comparison of LPV model structures and identified models later on and also to provide essential tools for the identification approach of this thesis. Additionally, we have defined observability and reachability

canonical SS representations of LPV systems and we have shown that they provide a simple gateway for the conversion between the representation domains.

First in Section 4.1, we introduced the observability/reachability canonical SS representation through a transformation mechanism applied on a given SS representation of the LPV system. It has been shown that in case of structural state-observability/reachability of the SS representation, state-transformations can be computed both in the SISO and in the MIMO case that result in observability/reachability canonical representations. It has been pointed out that the matrix structure of these canonical forms imply complete state-observability/reachability and the canonical forms provide a unique representation of their associated equivalence class. This means that, using the weak property of structural observability/reachability of the given SS representation, such representations of the system can be computed that have these properties in the complete-sense. The latter property is a consequence of the almost-everywhere-equality concept of the equivalence relations introduced in Section 3.2.

Besides the observability/reachability canonical forms, their companion counterparts have also been introduced. Furthermore, it has been shown that the transpose of a LPV-SS representation does not have the same manifest behavior, which is a notable difference with respect to the LTI theory. This property also proves that coefficients of canonical forms that structurally seem to be the transpose of each other (like the reachability and observability forms), are not equal. The connection of the introduced canonical forms with the applied theories of the current LPV literature has been also investigated. This has resulted in the conclusion that the common practice to use LTI theory to compute canonical forms for LPV systems yields SS representations that do not have an equal manifest behavior. Thus, the correct formulation of observability/reachability canonical forms is an essential contribution of this thesis to the general LPV systems theory.

In Section 4.2, we have introduced an equivalence transformation from the SS to the IO representation domain, extending the results of the LTI case. Using the concept of latent variable elimination, we have derived an algorithm that results in a minimal IO realization of a given SS representation. Using the algorithm, we have also provided simple conversion rules between the coefficients of observability and companion observability canonical forms and the resulting IO representation.

Continuing the line of reasoning, in Section 4.3 we have introduced an equivalence transformation from the IO to the SS representation domain as a reverse operation of the previously used latent variable elimination. We have studied a recursive scheme of state variable construction using elementary operations called cut-and-shift. Then, we constructed state-maps based on this mechanism, and formalized the equivalence class of all equivalent (minimal) SS representations. Using the previously developed concepts, we have introduced algorithms which, for special choices of the state-maps, result in the introduced canonical forms. In this way, simple conversion between the representation domains is accomplished.

LPV series expansion representations

In this chapter, series-expansion representations of LPV systems for a given IO partition are developed using the framework of the behavioral approach. In fact, expansion of DT asymptotically stable LPV systems is considered in terms of OBFs and the connection between this type of expansion and the gain-scheduling principle is explored. It is shown that this series-expansion representation is unique and always exists for the considered system class and in some cases only a finite number of the expansion coefficients are nonzero. This implies that finite truncation of a OBFs-based series-expansion can be used as a model structure for the identification of asymptotically stable DT-LPV systems just like in the LTI case.

5.1 Introduction

In the LTI framework, series-expansion representations have proved their usefulness in a number of contexts. They not only characterize a unique representation of the *input-output* (IO) system dynamics, like impulse-response representations, but they also provide model structures, like *Orthonormal Basis Functions* (OBFs)-based models, that provide an efficient alternative for LTI system identification. Using such model structures for the identification of LPV systems has a number of attractive properties and it would also allow the extension of the OBFs based identification approaches to the LPV case (see the argument of Chapter 1). Based on this, we develop in this chapter the concept of series-expansion of LPV systems in terms of OBFs, providing a unique perspective on the representation of the system dynamics with respect to an IO partition. This contribution of the thesis enables the introduction of model structures as the finite truncation of a OBF series-expansion with respect to a LPV system. These model structures are vital ingredients of the LPV identification approach developed later.

To simplify the discussion and to avoid cases that are complicated but unimportant for our identification approach, we restrict the discussion to *discrete-time*

(DT) asymptotically-stable LPV systems. For this type of systems, we first develop in Section 5.2 the series-expansion representation for a given IO partition in terms of the pulse basis. We investigate convergence of the expansion and we show that it uniquely characterizes the behavior for signals with left compact support. Next in Section 5.3, by using basic relations of OBFs with respect to the pulse basis, we develop LPV series-expansion representations in terms of general LTI orthonormal basis functions. We claim that these representations also uniquely characterize the behavior and the convergence rate of the OBFs expansion depends on the used basis sequence. As a next step in Section 5.4, we explore the connection between series-expansion representations and the gain-scheduling principle, showing that the expansion coefficients characterizes the scheduling function part of the LPV system, while the basis functions are strongly related to the frozen system set. It is also shown, that *Kolmogorov n-Width* (KnW) optimality of the OBFs, with respect to the transfer functions of the frozen system set, implies optimal convergence rate of the basis sequence based series-expansion of the LPV system for constant scheduling trajectories. Furthermore, it is motivated that for systems with minimal *input-output* (IO) representation having static dependence, the optimal convergence rate of the series-expansion with respect to such basis also holds for arbitrary scheduling trajectories. We will see later, that these observations enable to accommodate OBFs-based model structure selection in practice for LPV identification.

5.2 Impulse response representation of LPV systems

As a first step, we develop the series-expansion representation of DT asymptotically stable LPV systems based on a pulse basis (see Section 2.2 for the definition of pulse basis). LPV systems can not be handled in the frequency domain, thus we develop the concept of series-expansion in terms of the time operator form of the pulse basis. To do so, we first introduce the filter form of an LPV-IO representation. Then we generate the expansion in terms of the pulse basis by recursive substitution of the filter form. We show the uniqueness and the convergence of the resulting expansion coefficients. Additionally we briefly cover how this series-expansion can be generalized to unstable and *continuous-time* (CT) systems.

Filter form of LPV-IO representations

Based on the previously given line of discussion, first the filter form of LPV-IO representations is introduced. Let a discrete-time LPV system $\mathcal{S} = (\mathbb{Z}, \mathbb{P}, \mathbb{W}, \mathfrak{B})$ be given with a IO partition $w = \text{col}(u, y)$ and scheduling variable p . Assume that \mathcal{S} is asymptotically dynamically stable and that a minimal IO representation $\mathfrak{R}_{\text{IO}}(\mathcal{S})$ of \mathcal{S} is given, characterized by the polynomial $R_u \in \mathcal{R}[\xi]^{n_y \times n_u}$ and the full row rank $R_y \in \mathcal{R}[\xi]^{n_y \times n_y}$ with $\deg(R_y) = n_a \geq n_b = \deg(R_u)$. In this way, the

behavior \mathfrak{B} is described by the relation

$$\sum_{i=0}^{n_a} (a_i \diamond p) q^i y = \sum_{j=0}^{n_b} (b_j \diamond p) q^j u. \quad (5.1)$$

for every $(u, y, p) \in \mathfrak{B}$ with left compact support. Without loss of generality, assume that R_y is monic and multiply (5.1) by q^{-n_a} according to the non-commutative multiplication rules in discrete-time (see Definition 3.13). The resulting expression reads as

$$y = - \sum_{i=0}^{n_a-1} ([a_i]^{n_a} \diamond p) q^{i-n_a} y + \sum_{j=0}^{n_b} ([b_j]^{n_a} \diamond p) q^{j-n_a} u, \quad (5.2)$$

where $[\cdot]^{n_a}$ denotes the backward shift operator applied on the coefficient function for n_a times. As only the backward time-shifted versions of y appear on the right side of (5.2), the relation (5.2) is called the filter form of (5.1).

Series expansion by pulse basis

Assume that $n_a = n_b$, which can be realized by including extra coefficients $\{b_j\}_{j=n_b+1}^{n_a}$ that are zero functions. By substituting the relation (5.2) recursively into itself to eliminate the shifted versions of y we obtain:

$$y = (\mathfrak{g}_0 \diamond p)u + (\mathfrak{g}_1 \diamond p)q^{-1}u + (\mathfrak{g}_2 \diamond p)q^{-2}u + \dots \quad (5.3)$$

where

$$\begin{aligned} \mathfrak{g}_0 &= [b_{n_a}]^{n_a}, \\ \mathfrak{g}_1 &= [b_{n_a-1}]^{n_a} - [a_{n_a-1}]^{n_a} [b_{n_a}]^{n_a+1}, \\ \mathfrak{g}_2 &= [b_{n_a-2}]^{n_a} - [a_{n_a-1}]^{n_a} [b_{n_a-1}]^{n_a+1} - [a_{n_a-2}]^{n_a} [b_{n_a}]^{n_a+2} + \\ &\quad + [a_{n_a-1}]^{n_a} [a_{n_a-1}]^{n_a+1} [b_{n_a}]^{n_a+2}. \end{aligned}$$

It is obvious that $\{\mathfrak{g}_0, \mathfrak{g}_1, \mathfrak{g}_2, \dots\}$ are meromorphic coefficient functions. Furthermore, they are backward-shifted combinations of the coefficients of $\mathfrak{R}_{\text{IO}}(\mathcal{S})$ and due to the minimality of $\mathfrak{R}_{\text{IO}}(\mathcal{S})$ they are unique with respect to the considered IO partition of \mathcal{S} . In addition, the signal trajectories $(u, y, p) \in \mathfrak{B}$ described by (5.1) have left-compact support. This means, that there exists a $n \in \mathbb{N}$, such that after n substitutions of the relation (5.2) recursively into itself, y vanishes from the expression (5.3). This shows, that by this recursive substitution we have obtained an infinite expansion of (5.2) in terms of the LTI pulse basis $\{1, q^{-1}, q^{-2}, \dots\}$ with coefficients $\mathfrak{g}_i \in \mathcal{R}^{n_v \times n_w}$ for $i = 1, 2, \dots$. If the coefficients of $\mathfrak{R}_{\text{IO}}(\mathcal{S})$ have static dependence or they are all dependent only on the backward shifted versions of p , then each \mathfrak{g}_i depends only on the past values of p .

Furthermore, in case of a given scheduling trajectory $p \in \mathfrak{B}_{\mathbb{P}}$, and a pulse input at $k = 0$, the output trajectory of \mathcal{S} satisfies

$$y(0) = (\mathfrak{g}_0 \diamond p)(0), \quad y(1) = (\mathfrak{g}_1 \diamond p)(1), \quad y(2) = (\mathfrak{g}_2 \diamond p)(2), \quad \dots$$

thus $\{g_i\}_{i=0}^{\infty}$ can be considered as the *impulse response coefficients* of \mathcal{S} for the considered IO partition. Additionally, the asymptotic stability of \mathcal{S} implies that

$$y(k) \rightarrow 0, \quad \text{as } k \rightarrow \infty, \quad (5.4)$$

which means that the sequence of coefficients $\{g_i\}_{i=0}^{\infty}$ converges to zero along every scheduling trajectory $p \in \mathfrak{B}_{\mathbb{P}}$. Thus

$$\lim_{i \rightarrow \infty} (g_i \diamond p)(i) = 0, \quad \forall p \in \mathfrak{B}_{\mathbb{P}}. \quad (5.5)$$

This implies that due to the shift-invariant property of \mathfrak{B} :

$$\lim_{i \rightarrow \infty} (g_i \diamond p) = 0, \quad \forall p \in \mathfrak{B}_{\mathbb{P}}, \quad (5.6)$$

holds, which means that the sequence of coefficient functions $\{g_0, g_1, g_2, \dots\}$ converges to the zero function with respect to $\mathfrak{B}_{\mathbb{P}}$. It is also important that asymptotic stability of \mathcal{S} implies BIBO stability in the ℓ_{∞} norm:

$$\sup_{k \geq 0} \|u(k)\| < \infty \Rightarrow \sup_{k \geq 0} \|y(k)\| < \infty.$$

As (5.3) holds for any $(u, y, p) \in \mathfrak{B}$ with left compact support,

$$\left(\sup_{k \geq 0} \|u(k)\| < \infty \quad \text{and} \quad \sup_{k \geq 0} \|y(k)\| < \infty \right) \Rightarrow \sup_{k \geq 0} \sum_{i=0}^{\infty} \|(g_i \diamond p)(k)\| < \infty. \quad (5.7)$$

These properties yield the following theorem:

Theorem 5.1 (Existence of series-expansion representation, pulse basis) *Any asymptotically stable, discrete-time LPV system $\mathcal{S} = (\mathbb{Z}, \mathbb{P}, \mathbb{W}, \mathfrak{B})$ with an IO partition (u, y) has a unique, convergent series-expansion in terms of the pulse-basis $\{q^{-i}\}_{i=0}^{\infty}$ and coefficients $g_i \in \mathcal{R}^{n_y \times n_u}$, such that*

$$y = \sum_{i=0}^{\infty} (g_i \diamond p) q^{-i} u, \quad (5.8)$$

is satisfied for all $(u, y, p) \in \mathfrak{B}_{\mathbb{P}}$ with left compact support.

For a proof see Appendix A.2. The LPV series-expansion in terms of the pulse basis is similar to the series-expansion in the LTI case (see (2.111)). This means that the LPV system has a convergent series-expansion in terms of an LTI basis, which has a strong connection to the gain-scheduling concept of LPV systems. Furthermore it is a general property of the expansion coefficients $\{g_i\}_{i=0}^{\infty}$ that they have dynamic dependence even if the original IO representation, used for their computation, has coefficients with static dependence.

Note that in case of a uniformly unstable LPV system (\mathcal{S} is unstable for every constant scheduling trajectory in $\mathfrak{B}_{\mathbb{P}}$), a series-expansion representation can also

be derived in terms of the pulse basis $\{q^1, q^2, q^3, \dots\}$. If the system is only non-uniformly stable, then the series-expansion follows by taking the two sided pulse basis $\{\dots, q^{-1}, 1, q^1, \dots\}$. These cases are not treated here as we consider only the identification of asymptotically-stable LPV systems in this thesis. Furthermore, the continuous-time case of series expansions is also not covered in the following. One of the reasons is that in the introduced behavioral framework it would be cumbersome to handle ξ^{-1} , which corresponds to an integral operator in CT. An additional problem is that the unit-step function, which is associated with $\xi^{-1} = s^{-1}$ in the LTI case, is not an \mathcal{H}_2 function, thus it does not correspond to a basis function sequence. Remember, that a CT basis is related to its DT counterpart by the bilinear transformation (2.134). Based on these considerations, we only treat the asymptotically stable DT case.

The impulse response representation

Based on Theorem 5.1, it is possible to define the series-expansion representation of \mathcal{S} in terms of the LTI pulse basis $\{1, q^{-1}, q^{-2}, \dots\}$ as follows:

Definition 5.1 (LPV series-expansion representation, pulse basis) *The pulse basis series-expansion representation of a discrete-time asymptotically stable $\mathcal{S} = (\mathbb{Z}, \mathbb{P} \subseteq \mathbb{R}^{n_p}, \mathbb{R}^{n_u + n_y}, \mathfrak{B})$ with scheduling signal p and IO partition (u, y) is denoted by $\mathfrak{R}_{\text{IM}}(\mathcal{S})$ and defined as:*

$$y = \sum_{i=0}^{\infty} (\mathbf{g}_i \diamond p) q^{-i} u \quad (5.9)$$

where $\mathbf{g}_i \in \mathcal{R}^{n_y \times n_u}$, $i \in \mathbb{N}_0^\infty$ are the meromorphic expansion coefficients.

In the following, we call this representation the *Impulse Response Representation* (IRR) of the LPV system. Note that $\mathfrak{R}_{\text{IM}}(\mathcal{S})$, similar to the IO representations, describes the behavior of \mathcal{S} restricted to signal trajectories with left-compact support. However, in contrast with other LPV representations, it is unique. It is also important that an equivalence transformation exists from IO representations to the IRR domain, i.e. $\mathfrak{R}_{\text{IO}}(\mathcal{S})$ can be always transformed to $\mathfrak{R}_{\text{IM}}(\mathcal{S})$ if \mathcal{S} is asymptotically stable, however realization of a IO representation from the IRR is unsolved yet. See Example 5.1 for the construction of a IRR.

Example 5.1 (Pulse basis series-expansion representation of an DT-LPV system) *Consider the DT-LPV-IO representation $\mathfrak{R}_{\text{IO}}(\mathcal{S})$ given in the following filter form:*

$$y = -0.1pq^{-1}y - 0.2pq^{-2}y + \sin(p)q^{-1}u,$$

with $\mathbb{P} = [0, 1]$. By recursive substitution of this equation for $q^{-1}y, q^{-2}y, \dots$, the following series-expansion in terms of the pulse basis functions $\{q^{-1}, q^{-2}, \dots\}$ results:

$$y = \underbrace{\sin(p)q^{-1}u}_{\mathbf{g}_1 \diamond p} + \underbrace{(-0.1 \sin(q^{-1}p))q^{-2}u}_{\mathbf{g}_2 \diamond p} + \underbrace{(0.02p(q^{-1}p) - 0.2) \sin(q^{-2}p)q^{-3}u \dots}_{\mathbf{g}_3 \diamond p}$$

The resulting expansion coefficients are uniquely defined by the above expression with $\mathbf{g}_0 = 0$. As $\mathfrak{R}_{\text{IO}}(\mathcal{S})$ corresponds to an asymptotically stable behavior, the above series-expansion is convergent. This can be seen from the increasing power of -0.1 and -0.2 in the resulting expression.

5.3 LPV series-expansion by OBFs

As a next step, we generalize the series-expansion concept to general OBFs in $\mathcal{RH}_{2-}(\mathbb{E})$. To do so, we first show that each element of the pulse basis sequence can be written in a series-expansion form of an orthonormal basis Φ_∞ of $\mathcal{RH}_{2-}(\mathbb{E})$. By substituting each pulse function by its expansion in terms of a Φ_∞ , the series-expansion of a $\mathfrak{X}_{\text{IO}}(\mathcal{S})$ can be obtained for general orthonormal basis functions in a similar way as before.

Expansion of pulse functions by OBFs

Consider an OBF set $\Phi_\infty \subset \mathcal{RH}_{2-}(\mathbb{E})$. Then, based on the LTI transfer function theory, a pulse basis function q^{-i} , $i > 0$ has a unique series-expansion in terms of $\Phi_\infty = \{\phi_i\}_{i=1}^\infty$:

$$q^{-i} = \sum_{j=1}^{\infty} w_{ij} \phi_j(q), \quad (5.10)$$

where $w_{ij} \in \mathbb{R}$, $i, j \in \mathbb{I}_1^\infty$, are the expansion coefficients. This series-expansion is convergent and it is a well-known property that for all $i \in \mathbb{I}_1^\infty$, the sequence $\{w_{ij}\}_{j=1}^\infty$ is an ℓ_2 sequence. Additionally, the same property holds for each $\{w_{ij}\}_{i=1}^\infty$ sequence.

Series expansion by OBFs

As a next step, by using the relation derived in the previous part, we develop the series-expansion of a minimal $\mathfrak{X}_{\text{IO}}(\mathcal{S})$ in terms of an OBF set $\Phi_\infty = \{\phi_j\}_{j=1}^\infty$ in $\mathcal{RH}_{2-}(\mathbb{E})$. Let \mathcal{S} be asymptotically stable and assume that the pulse basis expansion of $\mathfrak{X}_{\text{IO}}(\mathcal{S})$ has been already derived in the form of (5.9). Then by substituting (5.10) into the expansion (5.9), we obtain

$$y = (\mathbf{g}_0 \diamond p)u + (\mathbf{g}_1 \diamond p) \sum_{j=1}^{\infty} w_{1j} \phi_j(q)u + (\mathbf{g}_2 \diamond p) \sum_{j=1}^{\infty} w_{2j} \phi_j(q)u + \dots$$

By rearranging this expression we arrive at

$$y = (\mathbf{g}_0 \diamond p)u + \underbrace{\left(\sum_{i=1}^{\infty} w_{i1} \mathbf{g}_i \diamond p \right)}_{w_1 \diamond p} \phi_1(q)u + \underbrace{\left(\sum_{i=1}^{\infty} w_{i2} \mathbf{g}_i \diamond p \right)}_{w_2 \diamond p} \phi_2(q)u + \dots$$

where $\{w_1, w_2, \dots\}$ are the coefficient functions of the new series-expansion in terms of the basis Φ_∞ . Note that for each $j \in \mathbb{I}_1^\infty$, $\{w_{ij}\}_{i=1}^\infty$ is an ℓ_2 sequence. Furthermore the expansion coefficients satisfy (5.6) and (5.7) for every $p \in \mathfrak{B}_\mathbb{F}$. Thus, each w_i exists and it is an element of $\mathcal{R}^{n_y \times n_u}$. Furthermore, zero convergence of all $\{w_{ij}\}_{j=1}^\infty$ and (5.7) implies that the sequence $\{w_1, w_2, \dots\}$ converges

to zero for every $p \in \mathfrak{B}_{\mathbb{P}}$ similarly as in the pulse-basis case. Based on this, the following theorem holds:

Theorem 5.2 (Existence of series-expansion representation, OBFs) *Any asymptotically stable, discrete-time LPV system $\mathcal{S} = (\mathbb{Z}, \mathbb{P}, \mathbb{W}, \mathfrak{B})$ with an IO partition (u, y) has a unique series-expansion in terms of a orthonormal basis sequence $\Phi_{\infty} = \{\phi_j\}_{j=1}^{\infty}$ in $\mathcal{RH}_{2-}(\mathbb{E})$ and coefficients $w_i \in \mathcal{R}^{n_y \times n_u}$, such that*

$$y = (w_0 \diamond p)u + \sum_{i=1}^{\infty} (w_i \diamond p)\phi_i(q)u, \quad (5.11)$$

is satisfied for all $(u, y, p) \in \mathfrak{B}_{\mathbb{P}}$ with left compact support.

For a proof see Appendix A.2. Note that the rate of convergence of the series-expansion directly depends on the basis sequence Φ_{∞} . Moreover, it is a general property of the expansion coefficients $\{w_i\}_{i=0}^{\infty}$ that they have dynamic dependence. In contrast with the LTI case, commonly the analytical computation of these coefficients is only available in an approximative manner by truncating their infinite sum relation with respect to the impulse response coefficients.

The OBF expansion representation

Based on the previously developed series-expansion concept, the following definition follows as the extension of Definition 5.1:

Definition 5.2 (DT-LPV series-expansion representation, OBFs) *Let $\Phi_{\infty} = \{\phi_i\}_{i=1}^{\infty}$ be a collection of orthonormal basis functions in $\mathcal{RH}_{2-}(\mathbb{E})$ with poles $\{\lambda_1, \lambda_2, \dots\}$ satisfying the completeness condition $\sum_{i=1}^{\infty} (1 - |\lambda_i|) = \infty$. Then, in terms of the basis Φ_{∞} , the series-expansion representation of a discrete-time asymptotically stable LPV system $\mathcal{S} = (\mathbb{Z}, \mathbb{P} \subseteq \mathbb{R}^{n_{\mathbb{P}}}, \mathbb{R}^{n_w + n_y}, \mathfrak{B})$ with scheduling vector p and IO partition (u, y) is denoted by $\mathfrak{R}_{\text{OBF}}(\mathcal{S}, \Phi_{\infty})$ and defined as:*

$$y = (w_0 \diamond p)u + \sum_{i=1}^{\infty} (w_i \diamond p)\phi_i(q)u, \quad (5.12)$$

where $w_i \in \mathcal{R}^{n_y \times n_u}$ are the meromorphic expansion coefficients.

In the following we call this representation the OBF *expansion representation* of the LPV system. Again, $\mathfrak{R}_{\text{OBF}}(\mathcal{S}, \Phi_{\infty})$ is unique and describes the behavior of \mathcal{S} restricted to signal trajectories with left-compact support. Similar to the IRR case, equivalence transformation from IO representations to the expansion representation domain exists, however realization in the other direction is unsolved. See Example 5.1 for the construction of a LPV expansion representation.

Example 5.2 (Hambo basis series-expansion representation of an LPV system) *Continue Example 5.1 to develop the series-expansion of the considered $\mathfrak{R}_{\text{IO}}(\mathcal{S})$ in terms of the Laguerre basis $\Phi_1^{\infty} = \{\phi_i\}_{i=1}^{\infty}$ with*

poles $\Lambda_1 = 0.5$. Based on the LTI transfer function theory, the pulse basis $\{q^{-1}, q^{-2}, \dots\}$ has the following series-expansion in terms of Φ_1^∞ :

$$\begin{aligned} q^{-1} &= 0.866\phi_1(q) - 0.433\phi_2(q) + 0.217\phi_3(q) + \dots \\ q^{-2} &= 0.433\phi_1(q) + 0.433\phi_2(q) - 0.541\phi_3(q) + \dots \\ q^{-3} &= 0.217\phi_1(q) + 0.541\phi_2(q) - 0.108\phi_3(q) + \dots \end{aligned}$$

Then by substituting these series expansions into the pulse basis expansion of Example 5.1, it follows that

$$\begin{aligned} y &= \underbrace{(0.866 \sin(p) - 0.0433 \sin(q^{-1}p) + 0.0433 (0.1p(q^{-1}p) - 1) \sin(q^{-2}p) + \dots)}_{w_1 \diamond p} \phi_1(q)u \\ &+ \underbrace{(-0.433 \sin(p) - 0.0433 \sin(q^{-1}p) + 0.1082 (0.1p(q^{-1}p) - 1) \sin(q^{-2}p) + \dots)}_{w_2 \diamond p} \phi_2(q)u \\ &+ \dots \end{aligned}$$

Note that the infinite sum expression of the coefficients $\{w_1, w_2, \dots\}$ converges as the expansion coefficients of each Laguerre basis $\phi_i(q)$ with respect to the pulse basis corresponds to an ℓ_2 sequence. In this way, the resulting expression is the series-expansion of $\mathfrak{R}_{\text{IO}}(\mathcal{S})$ in terms of Φ_1^∞ . Note that the coefficients $\{w_1, w_2, \dots\}$ of this new series-expansion are linear combinations of the coefficients of the IRR. The weights of these linear combinations are uniquely determined by the series-expansion of the pulse basis functions in terms of Φ_1^∞ .

Similar to the LTI case, expansion representations have the property that the relative contribution of the basis, i.e. the w_i functions, converge to the zero function on \mathfrak{B}_p as $i \rightarrow \infty$. In this way, for an asymptotically stable LPV system, it is always possible to find a finite $\Phi_n \subset \Phi_\infty$, i.e. the truncation of (5.12), with a relatively small number of functions, such that the representation error for all $(u, y, p) \in \mathfrak{B}$ is negligible. This provides an efficient approximation of the system. Based on this, finite truncation of an OBF based expansion representation can be used as a model structure for the identification of asymptotically stable DT-LPV systems. Similar to the LTI case, identification based on this type of model structure reduces to the estimation of the meromorphic coefficient functions $\{w_i\}_{i=0}^n$ which appear linearly in the dynamic relation. This vital result provides the basic concept for the identification approach of this thesis.

5.4 Series expansions and gain-scheduling

There is an interesting relation of the OBF expansion representation and the gain-scheduling principle. This relation helps to understand whether an orthonormal basis is adequate for the series-expansion of the LPV system, i.e. how the rate of convergence of the expansion can be characterized. In the following, we explore this relation by first showing that for constant scheduling trajectories the OBF expansion representation is equivalent with the series-expansion representations of the frozen system set. As a next step we show, that this equivalence implies that for some LPV systems, KnW optimality of the basis with respect to the frozen system set implies an optimal convergence rate of the series-expansion in the LPV case.

The role of gain-scheduling

Let $\mathfrak{R}_{\text{OBF}}(\mathcal{S}, \Phi_\infty)$ be the expansion representation of a discrete-time asymptotically stable \mathcal{S} in terms of an orthonormal basis $\Phi_\infty \subset \mathcal{RH}_2(\mathbb{E})$. Denote by $\mathcal{F}_{\bar{p}}$ the frozen system set of \mathcal{S} , and introduce \mathfrak{F} as the set of transfer functions associated with each $\mathcal{F}_{\bar{p}} \in \mathcal{F}_{\bar{p}}$ for the IO partition (u, y) . As \mathcal{S} is asymptotically stable, each $F_{\bar{p}} \in \mathfrak{F}$ is in $\mathcal{RH}_2(\mathbb{E})$ and its strictly proper part has a convergent series-expansion in terms of Φ_∞ . It is obvious, that in case of a constant scheduling signal $p(k) = \bar{p}$, the expansion coefficients $\{w_i\}_{i=0}^\infty$ of $\mathfrak{R}_{\text{OBF}}(\mathcal{S}, \Phi_\infty)$ satisfy that

$$w_i \diamond p = w_i^{(\bar{p})}, \quad (5.13)$$

where $w_i^{(\bar{p})} \in \mathbb{R}$, $i \in \mathbb{N}_0^\infty$ are the expansion coefficients of the transfer function $F_{\bar{p}}$ with respect to Φ_∞ . In this way, Φ_∞ with coefficients $\{w_i^{(\bar{p})}\}_{i=0}^\infty$ characterizes the behavior of each $\mathcal{F}_{\bar{p}} \in \mathcal{F}_{\bar{p}}$ in terms of an LTI expansion representation. We have already discussed that by the gain-scheduling principle, an LPV system can be viewed as a collection of LTI behaviors (frozen system set) and a scheduling signal dependent function set (scheduling functions) that selects one of the behaviors to describe the possible continuation of the signal trajectories at every time instant. From the previous observation it is clear, that the basis Φ_∞ with coefficients $w_i^{(\bar{p})}$ characterizes all frozen systems $\mathcal{F}_{\bar{p}}$, while the remaining part of the LPV dynamic relation is in the global expansion coefficients $\{w_i\}_{i=0}^\infty$. This provides the conclusion that from the gain-scheduling perspective, series-expansion separates the LPV system into a frozen behavior set, described as the linear combination of the basis functions, and a scheduling function set, which is represented by the coefficient functions.

Optimality of the basis in the frozen sense

Now we can use this insight to consider the question, how the basis should be chosen to achieve a fast convergence rate of the LPV series-expansion. This problem has a key importance in using truncated series expansions as model structures for LPV system identification as it formulates the optimality of a model structure with respect to a given system. To simplify the following discussion, we only investigate the SISO case.

Consider the optimality concept of OBFs in terms of the Kolmogorov n -width theory discussed in Section 2.4. By this concept, for a given transfer function set $\mathfrak{F} \subset \mathcal{RH}_2(\mathbb{E})$ with pole locations

$$\Omega = \{\lambda \in \mathbb{C} \mid \lambda \text{ is a pole of } F \in \mathfrak{F}\}, \quad (5.14)$$

the finite set of OBFs Φ_n is called optimal in the n -width sense, if the subspace

$$\mathcal{M}_n = \text{span}(\Phi_n), \quad (5.15)$$

has the minimal distance in terms of (2.168) for the worst-case $F \in \mathfrak{F}$. Denote by $\Phi_{n_g}^\infty$ the Hambo basis generated by the inner function G with n_g number of

poles and let $\Phi_{n_g}^{n_e}$ describe the Hambo functions obtained with n_e as the number of extensions of G (finite truncation of $\Phi_{n_g}^\infty$). It has been shown, that if $\Phi_{n_g}^{n_e}$ with $n_e \geq 0$ is optimal in the $n = (n_e + 1)n_g$ -width sense with respect to \mathfrak{F} , then the rate of convergence of the series-expansion of each $F \in \mathfrak{F}$ in terms of $\Phi_{n_g}^\infty$ is optimal and it is bounded by ρ^{n_e+1} where

$$\rho = \sup_{\lambda \in \Omega} |G(1/\lambda)|. \quad (5.16)$$

This means that in the series-expansion of any $F \in \mathfrak{F}$ with a $n = (n_e + 1)n_g$ -width optimal Hambo basis $\Phi_{n_g}^\infty = \{\phi_{ij}\}_{j=1, \dots, n_g}^{i=1, \dots, \infty}$, there exists a $\gamma > 0$ such that all expansion coefficients w_{ij} satisfy:

$$|w_{ij}| \leq \gamma \rho^{(n_e+1)(i+1)j}. \quad (5.17)$$

It is obvious that if \mathfrak{F} corresponds to the transfer function set of \mathcal{F}_p with respect to a given IO partition and the Hambo basis $\Phi_{n_g}^\infty$ is $n = (n_e + 1)n_g$ -width optimal with respect to \mathfrak{F} , then there exists a $\gamma > 0$ such that the expansion coefficients of the LPV system in terms of $\Phi_{n_g}^\infty$ with respect to the considered IO partition satisfy that

$$|(w_{ij} \diamond p)(k)| \leq \gamma \rho^{(n_e+1)(i+1)j} \quad \forall k \in \mathbb{Z}. \quad (5.18)$$

for any constant scheduling trajectory $p(k) = \bar{p}$. This means that if the basis is optimal with respect to the frozen behaviors of the LPV system, then fast convergence rate of the expansion coefficients holds in the frozen sense. However, this does not imply fast convergence for non-frozen scheduling trajectories in the general case. This leads to the conclusion, that to achieve a fast convergence rate for the expansion of general LPV systems, a necessary condition is to have fast convergence with respect to the frozen system set.

Optimality of the basis in the global sense

As a next step, we investigate when it is possible to characterize the convergence rate of the global expansion coefficients based on the KnW optimality in the frozen sense. Though, we have not been able yet to prove it, we strongly believe that optimality with respect to the frozen system set is also a sufficient condition if the LPV system has a IO representation with static coefficient dependence. This is formalized in the following conjecture:

Conjecture 5.1 (Optimal basis) *Given a discrete-time asymptotically stable SISO system $S = (\mathbb{Z}, \mathbb{P} \subseteq \mathbb{R}^{n_p}, \mathbb{R}^2, \mathfrak{B})$ with scheduling vector p and IO partition (u, y) . Assume that there exists a minimal $\mathfrak{R}_{IO}(S)$ such that all coefficient dependencies in $\mathfrak{R}_{IO}(S)$ are static. Denote by \mathcal{F}_p the frozen system set of S and let \mathfrak{F} be its associated transfer function set with respect to the IO partition (u, y) . Let $\Phi_{n_g}^\infty = \{\phi_{ij}\}_{j=1, \dots, n_g}^{i=1, \dots, \infty}$ be a Hambo basis which is $n = (n_e + 1)n_g$ -width optimal with respect to \mathfrak{F} with convergence rate ρ . Then, there exists a set of meromorphic expansion coefficients $w_{ij} \in \mathcal{R}$ and $\gamma > 0$, such that for*

all $(u, y, p) \in \mathfrak{B}$ with left compact support:

$$y = (w_{00} \diamond p)u + \sum_{i=0}^{\infty} \sum_{j=1}^{n_g} (w_{ij} \diamond p)\phi_{ij}(q)u, \quad (5.19)$$

and

$$|(w_{ij} \diamond p)(k)| \leq \gamma \rho^{(i+1)j(n_e+1)} \quad \forall p \in \mathfrak{B}_P \text{ and } \forall k \in \mathbb{Z}. \quad (5.20)$$

If additionally,

$$\mathfrak{F} \subseteq \text{span}\{\Phi_{n_g}^{n_e}\}, \quad (5.21)$$

is satisfied, then

$$w_{ij} \diamond p = 0, \quad (5.22)$$

for all $i > n_e$ and $j \in \mathbb{I}_1^{n_g}$.

Conjecture 5.1 is of crucial importance even if its proof is an open problem for the general case. By this concept, under the condition of a minimal IO representation with static dependence, the KnW optimality of the basis with respect to the frozen system set can imply optimality of the basis in the series-expansion of the LPV system. Optimality in the latter case means that the same convergence rate of the expansion coefficients is satisfied both in the global and in the frozen sense. Furthermore, an asymptotically stable LPV system can have a finite series-expansion in terms of a basis that can represent all the frozen transfer functions of the system by linear combinations. For example in case of LPV systems with a minimal SS representation where the A and B matrices are constant and the C and D matrices have static dependence, (5.21) is satisfied for a basis function set with poles equal to the eigenvalues of A . In that case, a series-expansion exists with finite nonzero expansion coefficients. This gives the conclusion, that to achieve a fast convergence rate for the expansion of this subclass of LPV systems, it is both a necessary and a sufficient condition to have fast convergence with respect to the frozen local system set.

5.5 Summary

In this chapter, series-expansion representations of DT asymptotically stable LPV systems for a given IO partition have been developed based on the concepts of the behavioral approach. We investigated expansions in terms of orthonormal basis functions with the intention to use finite truncation of these expansion representations as a model structure for the identification of asymptotically stable DT-LPV systems later on. This contribution enables the use of the LTI OBF-based identification approach in the LPV case, which is of crucial importance in providing an efficient and theoretically well-founded LPV identification method.

First in Section 5.2, we have develop series-expansion representations for DT asymptotically stable LPV systems in terms of the pulse basis, which uniquely characterizes the behavior for signals with left compact support. It has been

shown that such an expansion always exists for these systems and it can be uniquely generated from a minimal IO representation. Additionally, asymptotic stability of the system implies zero convergence of the expansion coefficients, which are meromorphic coefficient functions.

As a next step, in Section 5.3 we have develop LPV series-expansion representations in terms of general LTI orthonormal basis functions. We have shown that series-expansion of each element of the pulse basis in terms of arbitrary OBFs of $\mathcal{RH}_2(\mathbb{E})$ implies that OBFs expansion representations of LPV systems can always be generated uniquely from their pulse basis expansion. It has been shown that the resulting representations also uniquely characterize the behavior and the associated expansion coefficients are convergent with respect to the projected scheduling behavior.

As a next step in Section 5.4, the connection between series-expansion representation and the gain-scheduling principle has been explored, showing that the expansion coefficients of the basis sequence characterizes the scheduling function part of the LPV system, while the basis functions are strongly related to the frozen system set. Based on this connection, it has been proved that KnW optimality of the basis sequence with respect to the frozen system set associated transfer functions implies optimal convergence rate of the LPV series-expansion with these basis functions for every constant scheduling trajectory. It has been also motivated that for systems with minimal IO representations having static coefficient dependence, optimal convergence rate of the LPV series-expansion with such basis also holds for every scheduling trajectories. These properties have a paramount importance for OBFs-based model structure selection in LPV identification.

Discretization of LPV systems

This chapter is devoted to the discretization of LPV systems through the discrete-time projection of their state-space representations. Both exact and approximative approaches are developed in a zero-order hold setting, where the continuous-time input and scheduling trajectories are restricted to be piecewise constant. Primary attention is given to the discretization of state-space representations with static coefficient dependence. For this case, criteria are derived to assist the choice of the sampling-time in terms of preservation of frozen dynamic stability and acceptable upperbound on the discretization error. Discretization of representations with dynamic dependence is briefly investigated with the main conclusion that their adequate discretization requires a higher-order hold setting with respect to the scheduling variable. In such a setting, the scheduling trajectories are restricted to be piecewise polynomial with a given order.

6.1 The importance of discretization

Transformation between LPV systems represented on the *continuous-time* (CT) and the *discrete-time* (DT) axis, has primary importance both for control and identification in the LPV framework:

Implementation of LPV control designs in physical hardware often meets significant difficulties, as CT control design approaches (see Packard and Becker (1992) and Scherer (1996)) are preferred in the literature over DT solutions (see Apkarian and Gahinet (1995) and Packard (1994)). The main motivation for this preference is that stability and performance requirements for LPV systems can be expressed significantly easier in CT, like in a mixed sensitivity setting (Zhou and Doyle (1998)). As a result, the current design tools focus on continuous-time LPV *state-space* (SS) controller synthesis, requiring efficient discretization of such representations for implementation purposes.

In the LPV modeling framework, first principle LPV models of nonlinear systems are also often derived in a CT form. In LPV system identification, such models serve as a primary source of information to assist adequate model structure selection in terms of order, type of coefficient dependence, etc. However, current LPV identification methods are developed exclusively for DT. This means that DT projection of first principle LPV models is required to assist model structure selection for practical identification.

These issues imply that general discretization of LPV representations is a crucial topic, which must be well explored and analyzed. However, the existing literature about LPV discretization is very limited. In the early work of Apkarian (1997), three different approaches have been introduced based on an *isolated* (stand-alone discretization of a CT system aiming at only the preservation of the CT input-output behavior) *zero-order-hold* (variation of free CT signals is restricted to be piecewise-constant) setting. These approaches: the complete, the rectangular, and the trapezoidal methods have been developed for the discretization of LPV-SS representations by extending the concepts of the LTI framework (see Section 2.1.8). However, only a limited discussion on the discretization error of the introduced approaches and on their applicability for specific LPV systems has been provided. In Hallouzi et al. (2006), an attempt has been made to characterize the discretization error of the rectangular method by expressing the approximation error of the involved state-space matrices. Other types of discretization techniques or criteria for the selection of sampling-time have not been investigated, leaving the-state-of-the-art of LPV discretization incomplete.

In this chapter, we aim to complete the extension of the isolated discretization approaches of the LTI framework (see Section 2.1.8). Additionally, we aim to compare the properties of the resulting methods with questions of sampling-time choice, preservation of stability, and discretization errors. Our main purpose is to give tools for the use of CT first principle knowledge in the model structure selection of DT-LPV identification approaches.

First in Section 6.2, we clarify the *zero-order-hold* (ZOH) discretization setting in the LPV case and we motivate why such a setting is adequate for the discretization of LPV representations with static dependence. Focusing on LPV-SS representations with static dependence, in Section 6.3 we develop the extension of both exact and approximative discretization methods of the ZOH setting, which have been discussed in the LTI case (see Section 2.1.8). To give these extensions an important assumption is made, namely that the switching behavior of the signal trajectories takes place smoothly in the ZOH setting. As a next step, in Section 6.4 we analyze the discretization error and numerical properties of the derived methods based on the results of the numerical analysis field (see Atkinson (1989)). Using the introduced concepts, we derive criteria for the choice of sampling-time in terms of preservation of dynamic stability of the discretized representation and guaranteed upperbound of the discretization error. This contribution enables the use of the developed discretization methods to assist the adequate choice of a model structure in the LPV identification framework. Additionally, important properties of the discretization approaches are also discussed in Section 6.5 from the viewpoint of identification and control. In Section 6.4.4, the result of the assump-

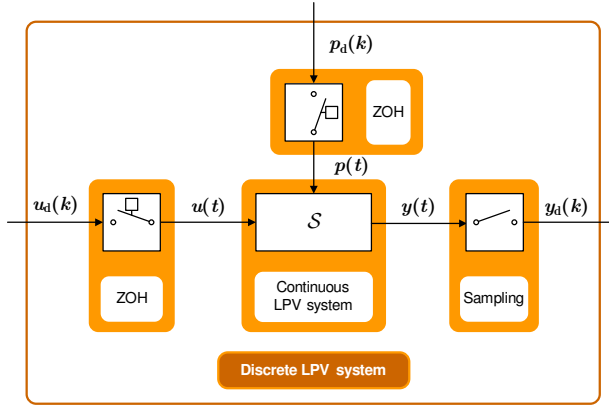


Figure 6.1: Ideal zero-order hold discretization setting of general LPV systems.

tion about the smooth switching behavior is analyzed, with the main conclusion that this assumption has no significant consequences in practical situations. As a final step in Section 6.6, it is investigated how the introduced theory can be applied to the discretization of LPV-IO or LPV-SS representations with dynamic dependence. It is concluded that adequate discretization of such representations requires a higher-order hold setting with respect to the scheduling variable. In that setting, the scheduling trajectories are restricted to be piecewise polynomial with a given order. To illustrate the introduced methods and the applicability of the derived criteria, a numerical example is presented.

6.2 Discretization of LPV system representations

As a first step of the previously given line of discussion, the exact characterization of the applied discretization setting is given. Similar to the LTI case, we consider an isolated approach in an ideal ZOH setting presented in Figure 6.1 where the following assumption holds:

Assumption 6.1 *We are given a CT-LPV system S , with input-output partition (u, y) and with scheduling signal p , where u and p are generated by an ideal ZOH and y is sampled in a perfectly synchronized manner with $T_d \in \mathbb{R}^+$. The ZOH and the instrument providing the output sampling have infinite resolution (no quantization error) and their processing time is zero.*

In this way, the problem we intend to solve in the following part is to find the DT equivalent of a given CT-LPV system according to Assumption 6.1. Introduce subscript “ $_d$ ” to denote sampled/discretized signals. Then it holds for the signals of Figure 6.1 that

$$u(t) := u_d(k), \quad \forall t \in [kT_d, (k+1)T_d), \quad (6.1a)$$

$$p(t) := p_d(k), \quad \forall t \in [kT_d, (k+1)T_d), \quad (6.1b)$$

$$y_d(k) := y(kT_d), \quad (6.1c)$$

for each $k \in \mathbb{Z}$, meaning that u and p can only change at every sampling-time instant. However, in the LPV framework p is considered to be a measurable external/environmental effect (general-LPV) or some function of the states or outputs of the system \mathcal{S} (quasi-LPV). Therefore, possibly it can not be fully influenced by the digitally controlled actuators of the plant which contain the ZOH. Furthermore in Section 3.1.3, equivalence of CT and DT behaviors under a given sampling-time has been established without any restrictions on the variation of u or p .

On the other hand, the variation of u and p inside a sample interval must be restricted to exactly characterize the effect of these signals on the plant. The reason is similar as in the LTI case. In DT, observations of the CT signals u and p are only available at each sampling-time instant. Thus there is no information about the trajectory of these signals during the sample interval. This means that the output signal can not be uniquely determined, unless the variation of the signals u and p is restricted to a certain class of functions. In the ZOH setting, this function class is chosen to be the piecewise constant (zero-order) class. It is also possible to choose this class wider, including linear, 2nd-order polynomial, etc., functions and in this way to define higher-order hold discretization settings of LPV systems. However, in conclusion it holds true that in any LPV discretization setting, the variation of the scheduling signals must be restricted.

By applying the ZOH setting for the discretization of a given LPV representation, the piecewise-constant variation of p implies that coefficients with dynamic dependence simplify as the derivatives of p are zero inside the sampling interval. This means, that unless the representation has static dependence, the ZOH setting may result in the loss of certain parts of the original behavior. Based on this, we assume that the CT representation to be discretized has static coefficient dependence. Later we explore how this limitation can be overcome, i.e. how the discretization of representations with dynamic dependence can be properly handled.

In conclusion, the introduced discretization setting coincides with the conventional setting of the LTI framework. Moreover, the presented setting is also applicable to closed-loop controllers in the structure given in Figure 6.2. This closed-loop setting has also been used in Apkarian (1997). Note that the assumption that the scheduling vector of the continuous LPV controller is affected by the ZOH setting, i.e. it can only vary in piece-wise manner, also holds in this case.

6.3 Discretization of state-space representations

Based on the previously introduced discretization setting, the isolated approaches of the LTI framework are extended to the LPV case. We only give this extension with respect to LPV-SS representations. In case the system description is available in the form of an other representation, using the equivalence transformations developed in Chapter 4, an equivalent SS realization can always be obtained. Additionally, we assume that the SS representation has only static coefficient dependence. Investigation of the discretization errors and other properties is postponed

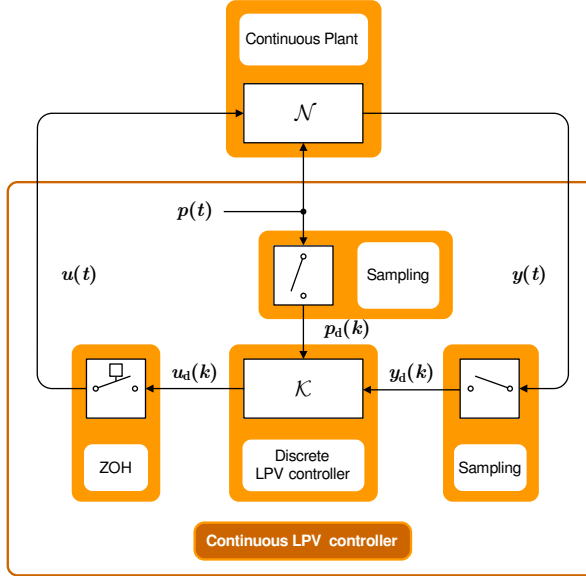


Figure 6.2: Ideal ZOH discretization setting of closed-loop LPV controllers.

till Sections 6.4 and 6.5. Before venturing into the derivation of discretization methods, consider the following phenomenon:

For the continuous-time signals u, p defined through (6.1a-b) it holds that

$$u(t) = \sum_{k=-\infty}^{\infty} 1(t - kT_d) [u_d(k) - u_d(k-1)], \quad (6.2a)$$

$$p(t) = \sum_{k=-\infty}^{\infty} 1(t - kT_d) [p_d(k) - p_d(k-1)], \quad (6.2b)$$

where $1(t)$ is the unit-step function (positive zero assumption based Heaviside function) defined as

$$1(t) := \begin{cases} 0, & \text{if } t < 0; \\ 1, & \text{if } t \geq 0. \end{cases} \quad (6.3)$$

The result of $1(t - kT_d)$ on $\mathfrak{R}_{SS}(\mathcal{S})$ in every sampling period is called the switching effect of the ZOH actuation. Based on this, the following important assumption is made:

Assumption 6.2 *The switching behavior of the ZOH actuation has no effect on the CT plant, i.e. the switching of the signals is assumed to take place smoothly.*

The analysis of the consequence of this assumption is postponed till Section 6.4.

Complete method

First the complete signal evolution approach of the LTI framework is extended to the LPV case. Let a continuous-time $\mathfrak{R}_{\text{SS}}(\mathcal{S})$ be given in the ZOH setting. Based on Assumption 6.1, i.e. p and u are constant signals inside each sampling interval, the state-equations (3.37a-b) of $\mathfrak{R}_{\text{SS}}(\mathcal{S})$ can be written as

$$\dot{x}(t) = (A \diamond p)(kT_d) x(t) + (B \diamond p)(kT_d) u(kT_d), \quad (6.4a)$$

$$y(t) = (C \diamond p)(kT_d) x(t) + (D \diamond p)(kT_d) u(kT_d), \quad (6.4b)$$

for $t \in [kT_d, (k+1)T_d)$ with initial condition $x(kT_d)$. Assume that, $\{A, B, C, D\}$ have static dependence on p . Then the DT signal p_d satisfies that

$$\begin{aligned} (A \diamond p)(kT_d) &= (A \diamond p_d)(k), & (B \diamond p)(kT_d) &= (B \diamond p_d)(k), \\ (C \diamond p)(kT_d) &= (C \diamond p_d)(k), & (D \diamond p)(kT_d) &= (D \diamond p_d)(k). \end{aligned} \quad (6.5)$$

The state-equation (6.4a), associated with the k^{th} sampling interval, is an *Ordinary Differential Equation* (ODE) which has the following solution:

$$x(t) = e^{(t-kT_d)(A \diamond p_d)(k)} x(kT_d) + \int_{\tau=0}^{t-kT_d} e^{(t-kT_d-\tau)(A \diamond p_d)(k)} (B \diamond p_d)(k) u(kT_d) d\tau.$$

By substituting $t = (k+1)T_d$, $x_d(k) = x(kT_d)$, and $u_d(k) = u(kT_d)$, the previous formula results in

$$x_d(k+1) = e^{T_d(A \diamond p_d)(k)} x_d(k) + e^{T_d(A \diamond p_d)(k)} \int_{\tau=0}^{T_d} e^{-\tau(A \diamond p_d)(k)} (B \diamond p_d)(k) u_d(k) d\tau.$$

Assume that $A(\bar{p})$ is invertible¹ for $\forall \bar{p} \in \mathbb{P}$. Then by evaluating the integral it follows that

$$q x_d = e^{T_d(A \diamond p_d)} x_d + (A^{-1} \diamond p_d) \left[e^{T_d(A \diamond p_d)} - I \right] (B \diamond p_d) u_d, \quad (6.6a)$$

$$y_d = (C \diamond p_d) x_d + (D \diamond p_d) u_d, \quad (6.6b)$$

where $x_d(k) = x(kT_d)$ and $y_d(k) = y(kT_d)$. Then the complete method gives that the DT equivalent of $\mathfrak{R}_{\text{SS}}(\mathcal{S})$ under Assumptions 6.1 and 6.2 is (Apkarian 1997):

$$\mathfrak{R}_{\text{SS}}(\mathcal{S}, T_d) := \left[\begin{array}{c|c} \frac{e^{T_d A}}{C} & \frac{A^{-1} (e^{T_d A} - I) B}{D} \end{array} \right]. \quad (6.7)$$

Example 6.1 (Complete discretization) Consider the CT-SS representation

$$\mathfrak{R}_{\text{SS}}(\mathcal{S}) = \left[\begin{array}{cc|c} 2p-1 & p & 0 \\ 0 & -1 & 1 \\ \hline 1 & p & 0 \end{array} \right]$$

with $\mathbb{P} = [-1, 1]$. The above representation has static linear dependence and it can be shown that it is uniformly frozen stable. By applying the complete method to $\mathfrak{R}_{\text{SS}}(\mathcal{S})$, it follows that the DT equivalent of this

¹Due to the assumed static dependence of A , i.e. $A \in \mathcal{R}_{n_{\bar{p}}^{\times} \times n_{\bar{p}}}$, it holds that $(A \diamond p)(t) = A(p(t))$.

representation under the sampling-time T_d is

$$\mathfrak{R}_{SS}(\mathcal{S}, T_d) = \left[\begin{array}{cc|c} e^{T_d(2p_d-1)} & \frac{1}{2}e^{T_d(2p_d-1)} - \frac{1}{2}e^{-T_d} & \frac{e^{T_d(2p_d-1)} + (2p_d-1)e^{-T_d} - 2p_d}{4p_d-2} \\ 0 & e^{-T_d} & 1 - e^{-T_d} \\ \hline 1 & p_d & 0 \end{array} \right].$$

Even for this simple LPV state-space representation, the DT projection results in a complicated rational/exponential dependence on the samples of the scheduling signal.

6.3.1 Approximative state-space discretization methods

The complete method is commonly not favored in the LPV literature as it introduces heavy nonlinear dependence on p_d , like $e^{T_d A}$, which is the main drawback of this approach. Many identification and control design techniques build on the assumption of linear or polynomial static dependence on p , and hence it is required to develop approximative discretization methods that try to achieve good representation of the original behavior, but with a low complexity of the coefficient dependence. To do that, we systematically extend the approximative discretization methods of the LTI case, by using different approximations of the integral that describes the state-evolution inside the sample-interval.

Rectangular (Euler's forward) method

The simplest way to avoid the appearance of $e^{T_d A}$ is to apply a first-order approximation:

$$e^{T_d(A \diamond p_d)(k)} \approx I + T_d(A \diamond p_d)(k). \quad (6.8)$$

Introduce $f(x, u, p, t)$ as the right hand side of (3.37a). Under Assumptions 6.1 and 6.2 it holds that

$$\int_{\tau=kT_d}^{(k+1)T_d} f(x, u, p, \tau) d\tau = \int_{\tau=kT_d}^{(k+1)T_d} (A \diamond p_d)(k)x(\tau) + (B \diamond p_d)(k)u(kT_d) d\tau, \quad (6.9)$$

which defines the solution of (6.4a) in $[kT_d, (k+1)T_d)$. Left-hand rectangular evaluation of the integral (6.9) gives

$$x((k+1)T_d) \approx x(kT_d) + T_d(A \diamond p_d)(k)x(kT_d) + T_d(B \diamond p_d)(k)u(kT_d), \quad (6.10)$$

coinciding with the suggested matrix exponential approximation of (6.8). Based on this rectangular approach, the DT approximation of $\mathfrak{R}_{SS}(\mathcal{S})$ is:

$$\mathfrak{R}_{SS}(\mathcal{S}, T_d) \approx \left[\begin{array}{c|c} \frac{I + T_d A}{C} & \frac{T_d B}{D} \end{array} \right]. \quad (6.11)$$

Another interpretation of this method follows from Euler's forward discretization formula (2.102) substituted into (6.4a) (see Apkarian (1997)).

Example 6.2 (Rectangular discretization) Continuing Example 6.1, the rectangular discretization method applied to $\mathfrak{R}_{SS}(S)$ results in

$$\mathfrak{R}_{SS}(S, T_d) \approx \left[\begin{array}{cc|c} 2T_d p_d + 1 - T_d & T_d p_d & 0 \\ 0 & 1 - T_d & T_d \\ \hline 1 & p_d & 0 \end{array} \right].$$

Comparing this DT approximation with the result of the complete method given in Example 6.1 illustrates well the difference in complexity of the resulting coefficient dependencies.

Polynomial (Hanselmann) method

It is also possible to develop other methods that achieve better approximation of the complete case but with increasing complexity. One way leads through the use of higher order Taylor expansion of the matrix exponential term:

$$e^{T_d(A \diamond p_d)(k)} \approx I + \sum_{l=1}^n \frac{T_d^l}{l!} (A^l \diamond p_d)(k), \quad (6.12)$$

This results in the extension of the LTI polynomial discretization methods (see Section 2.1.8). Substituting (6.12) into (6.6a) gives the following SS representation:

$$\mathfrak{R}_{SS}(S, T_d) \approx \left[\begin{array}{c|c} I + \sum_{l=1}^n \frac{T_d^l}{l!} A^l & T_d \left(I + \sum_{l=1}^{n-1} \frac{T_d^l}{l+1!} A^l \right) B \\ \hline C & D \end{array} \right]. \quad (6.13)$$

Example 6.3 (Polynomial discretization) Approximating the LPV-SS representation of Example 6.1 by the 2nd-order polynomial method results in

$$\mathfrak{R}_{SS}(S, T_d) \approx \left[\begin{array}{cc|c} 1 + T_d(2p_d - 1) + \frac{1}{2}T_d^2(2p_d - 1)^2 & (T_d - T_d^2)p_d + T_d^2 p_d^2 & \frac{1}{2}T_d^2 p_d \\ 0 & 1 - T_d + \frac{1}{2}T_d^2 & T_d - \frac{1}{2}T_d^2 \\ \hline 1 & p_d & 0 \end{array} \right].$$

Due to the polynomial approximation, the originally linear coefficient dependencies are transformed to polynomial functions with order 2.

Trapezoidal (Tustin) method

An alternative way of approximation leads through the extension of the Tustin method. By using a trapezoidal evaluation of integral (6.9) we obtain:

$$x((k+1)T_d) \approx x(kT_d) + \frac{T_d}{2} [f(x, u, p, kT_d) + f(x, u, p, (k+1)T_d)], \quad (6.14)$$

Using this approximation, the derivation of the LPV Tustin method can be given similarly as in Apkarian (1997). The key concept is to apply a change of variables:

$$\check{x}_d(k) = \frac{1}{\sqrt{T_d}} \left[I - \frac{T_d}{2} (A \diamond p_d)(k) \right] x(kT_d) - \frac{\sqrt{T_d}}{2} (B \diamond p_d)(k) u_d(k). \quad (6.15)$$

If $[I - \frac{T_d}{2}A(\bar{p})]$ is invertible for $\forall \bar{p} \in \mathbb{P}$, then substitution of (6.15) into (6.14) gives a DT state-equation after some algebraic manipulations. Based on this state-equation, the resulting SS representation reads as

$$\mathfrak{R}_{SS}(\mathcal{S}, T_d) \approx \left[\begin{array}{c|c} (I + \frac{T_d}{2}A) (I - \frac{T_d}{2}A)^{-1} & \sqrt{T_d} (I - \frac{T_d}{2}A)^{-1} B \\ \hline \sqrt{T_d} C (I - \frac{T_d}{2}A)^{-1} & \frac{T_d}{2} C (I - \frac{T_d}{2}A)^{-1} B + D \end{array} \right].$$

It is important to note that, like in the LTI case, the trapezoidal method approximates only the manifest behavior of $\mathfrak{R}_{SS}(\mathcal{S}, T_d)$, as it gives an approximative DT-SS representation in terms of the new state variable \check{x}_d .

Example 6.4 (Trapezoidal discretization) Applying the trapezoidal method to the LPV-SS representation of Example 6.1 results in

$$\mathfrak{R}_{SS}(\mathcal{S}, T_d) \approx \left[\begin{array}{c|c} \frac{2+2T_d p_d - T_d}{2-2T_d p_d + T_d} & \frac{4T_d p_d}{(2-2T_d p_d + T_d) \cdot (2+T_d)} \\ \hline 0 & \frac{2-T_d}{2+T_d} \\ \hline \frac{2\sqrt{T_d}}{2-2T_d p_d + T_d} & 4\sqrt{T_d} p_d \frac{T_d + 1 - T_d p_d}{(2-2T_d p_d + T_d) \cdot (2+T_d)} \end{array} \left| \begin{array}{c} \frac{2T_d^{3/2} p_d}{(2-2T_d p_d + T_d) \cdot (2+T_d)} \\ \frac{2\sqrt{T_d}}{2+T_d} \\ \hline 2T_d p_d \frac{T_d + 1 - T_d p_d}{(2-2T_d p_d + T_d) \cdot (2+T_d)} \end{array} \right].$$

Due to the discretization method, the originally linear coefficient dependencies are transformed to rational functions.

Multi-step methods

Next, the multistep approximation of the LTI case is extended. Consider the state evolution as the solution of the DE defined by (3.37a), where all the coefficients are assumed to have static dependence. Then, this solution can be numerically approximated via multi-step formulas. Due to the reasons discussed in Section 2.1.8, in the ZOH setting of the LPV case, the family of Adams-Bashforth methods represent a viable approach for such a discretization method. The 3-step version of this type of numerical approach yields the following approximation:

$$x((k+1)T_d) \approx x_d(k+1) = x(kT_d) + \frac{T_d}{12} [5f(x, u, p, (k-2)T_d) - 16f(x, u, p, (k-1)T_d) + 23f(x, u, p, kT_d)]. \quad (6.16)$$

Then, formulating this state-space equation in an augmented SS form with the new state-variable:

$$\check{x}_d(k) = \text{col}(x_d(k), f(x_d, u, p, (k-1)T_d), f(x_d, u, p, (k-2)T_d)), \quad (6.17)$$

leads to

$$\mathfrak{R}_{SS}(\mathcal{S}, T_d) \approx \left[\begin{array}{c|c} I + \frac{23T_d}{12}A & -\frac{16T_d}{12}I & \frac{5T_d}{12}I & \frac{23T_d}{12}B \\ A & 0 & 0 & B \\ \hline 0 & I & 0 & 0 \\ \hline C & 0 & 0 & D \end{array} \right].$$

The resulting DT-SS representation is an approximation of $\mathfrak{R}_{\text{SS}}(\mathcal{S}, T_d)$ in terms of the new state variable \check{x}_d . Note that multi-step discretization results in linear conversion rules but the state-dimension is increased.

Example 6.5 (3-step Adams-Bashforth discretization) Applying the 3-step Adams-Bashforth method to the LPV-SS representation of Example 6.1, results in

$$\left[\begin{array}{ccccccc|c} 1 + \frac{23}{6}T_d p_d - \frac{23}{12}T_d & \frac{23}{12}T_d p_d & -\frac{16}{12}T_d & 0 & \frac{5}{12}T_d & 0 & 0 & 0 \\ 0 & 1 - \frac{23}{12}T_d & 0 & -\frac{16}{12}T_d & 0 & \frac{5}{12}T_d & \frac{23}{12}T_d & \frac{23}{12}T_d \\ 2p_d - 1 & p_d & 0 & 0 & 0 & 0 & 0 & 0 \\ 0 & -1 & 0 & 0 & 0 & 0 & 0 & 1 \\ 0 & 0 & 1 & 0 & 0 & 0 & 0 & 0 \\ 0 & 0 & 0 & 1 & 0 & 0 & 0 & 0 \\ \hline 1 & p_d & 0 & 0 & 0 & 0 & 0 & 0 \end{array} \right].$$

As expected, the obtained DT projection preserves the originally linear coefficient dependence. However, the resulting DT representation has a 6 dimensional state-variable compared to the 2-dimensional state-variable of the original CT representation.

6.4 Discretization errors and performance criteria

In the following part, as a main contribution, the introduced methods are investigated in terms of the generated discretization error, numerical convergence, and numerical stability. These are used to derive upperbounds on the sampling-time T_d , that guarantee a user-defined bounded discretization error and stability preservation with respect to the original CT system. Moreover, the influence of the assumption that no switching effects result from the ZOH actuation is investigated.

6.4.1 Local discretization errors

Characterization of the discretization error for each of the introduced approaches is important in order to study how adequate the used approximation is with respect to the original CT behavior. It has been already emphasized that, due to the considered assumptions, the complete method theoretically gives errorless discretization in terms of the ZOH setting. For other approaches we investigate the discretization error in terms of the *Local Unit Truncation* (LUT) error, which is often applied in numerical analysis (see Atkinson (1989)). This concept describes the error that results in each sampling interval due to discretization. Thus in this section, we define LUT error with respect to all approaches and introduce the concept of consistency in terms of this error. We claim that consistency holds for all approaches and we also derive upperbounds on the LUT error.

As a first step, the LUT error, denoted by $\varepsilon_k \in \mathbb{R}$, is formally introduced. Let $\mathfrak{R}_{\text{SS}}(\mathcal{S})$ be the SS representation of the CT-LPV system \mathcal{S} , with $\mathbb{P} \subseteq \mathbb{R}^{n_{\mathbb{P}}}$ and with

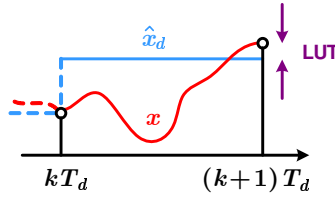


Figure 6.3: Local unit truncation error of the discretized representation associated state-signal \hat{x}_d with respect to the CT state-signal x at the time-step $(k + 1)T_d$.

meromorphic matrix functions

$$\left[\begin{array}{c|c} A & B \\ \hline C & D \end{array} \right] \in \left[\begin{array}{c|c} (\mathcal{R}|_{n_{\mathbb{P}}})^{n_x \times n_x} & (\mathcal{R}|_{n_{\mathbb{P}}})^{n_x \times n_u} \\ \hline (\mathcal{R}|_{n_{\mathbb{P}}})^{n_y \times n_x} & (\mathcal{R}|_{n_{\mathbb{P}}})^{n_y \times n_u} \end{array} \right],$$

defining static dependence on p . Denote by (A_d, B_d, C_d, D_d) the SS matrices of the DT representation resulting by the discretization methods of Section 6.3.1 applied to $\mathfrak{R}_{\text{SS}}(S)$. Note that, due to static dependence of the original representation, these matrix functions also have static dependence on p_d . In the rectangular and the polynomial case, the state-basis of this representation is equal to the state-basis of the original CT representation. However, in the trapezoidal and in the multi-step cases, the resulting DT projection also includes a state-transformation. In order to formulate the approximation error of the discretization methods based on the error of the approximation of the state evolution, those discretization results which involve state transformation must be brought back to the original state-basis. Introduce the matrix polynomials $R_x \in \mathcal{R}[\xi]^{n_x \times n_x}$ and $R_u \in \mathcal{R}[\xi]^{n_x \times n_u}$, that formulate the discrete-time state update of the DT approximations on the same state-basis as in $\mathfrak{R}_{\text{SS}}(S)$. In the rectangular and the polynomial case, $R_x(q) = A_d$ and $R_u(q) = B_d$, but in the other cases, they also include the appropriate state-transformation. For example in the trapezoidal case, (6.14) implies that:

$$R_x(q) = \left(I + \frac{T_d}{2} A \right) \left(I - \frac{T_d}{2} \overrightarrow{A} \right)^{-1}, \quad (6.18)$$

$$R_u(q) = \frac{T_d}{2} \left(I - \frac{T_d}{2} \overrightarrow{A} \right)^{-1} \left(B + \overrightarrow{B} q \right). \quad (6.19)$$

Then for each sampling interval, ε_k is defined by

$$T_d \varepsilon_{k+1} := [q x_d - (R_x(q) \diamond p_d) x_d - (R_u(q) \diamond p_d) u_d](k). \quad (6.20)$$

Note, that LUT represents the relative approximation error of the sampled state signal x_d of the CT representation by the state \hat{x}_d of the DT representation, when past samples of x_d and u_d are used to calculate \hat{x}_d via the DT state-equation (see Figure 6.3). Hence the name "local". In the theory of numerical approximation of differential equations, ε_k is considered as the measure of accuracy. The following definition is important:

Definition 6.1 (N-consistency) (based on Atkinson (1989)) Let $\mathfrak{R}_{\text{SS}}(\mathcal{S})$ be the SS representation of the LPV system \mathcal{S} with full behavior \mathfrak{B}_{SS} . The discrete-time approximation of the state-space equation (3.37a) is called numerically consistent, if for any $(u, x, y, p) \in \mathfrak{B}_{\text{SS}}$, it holds that

$$\lim_{T_d \rightarrow 0} \sup_{k \in \mathbb{Z}} \|\varepsilon_k\| = 0. \quad (6.21)$$

This means that - in case of N-consistency - the local approximation error reduces with decreasing T_d . However, this does not imply that the supremum of the global approximation error,

$$\eta_{k+1} = [qx_d - (R_x(q) \diamond p_d) \hat{x}_d - (R_u(q) \diamond p_d) u_d](k), \quad (6.22)$$

where \hat{x}_d is the discrete-time approximation of the state, decreases/converges to zero too. As a next step, the LUT error of each discretization method is investigated together with the N-consistency.

LUT error of the rectangular method

For the rectangular method, (6.20) gives

$$x((k+1)T_d) = [I + T_d(A \diamond p_d)(k)]x(kT_d) + T_d(B \diamond p_d)(k)u(kT_d) + T_d\varepsilon_{k+1}. \quad (6.23)$$

Define the first-order Taylor approximation of x around the time instant kT_d as

$$x(t) = x(kT_d) + \left(\frac{d}{dt}x\right)(kT_d) \cdot (t - kT_d) + \frac{1}{2} \left(\frac{d^2}{dt^2}x\right)(\tau), \quad \tau \in (kT_d, t), \quad (6.24)$$

for $t > kT_d$. Substraction of (6.24) for $t = (k+1)T_d$ from (6.23) yields that $T_d\varepsilon_{k+1}$ is equal to the residual term, giving

$$\varepsilon_{k+1} = \frac{T_d}{2} \left(\frac{d^2}{dt^2}x\right)(\tau) \quad \tau \in (kT_d, (k+1)T_d). \quad (6.25)$$

This shows that in the ZOH setting, the rectangular method is consistent in first-order (in T_d) if $\left\|\left(\frac{d^2}{dt^2}x\right)(t)\right\| < \infty$ for all $x \in \mathfrak{B}_X$ and $t \in \mathbb{R}$, where \mathfrak{B}_X denotes the projected signal behavior of \mathfrak{B}_{SS} on the variable x . As the meromorphic coefficients functions in (3.37a) are partially differentiable in p , the state evolution $f(x, u, p, t)$ is partially differentiable in each variable. Then

$$\frac{d^2}{dt^2}x = \underbrace{\frac{\partial f}{\partial x} \frac{d}{dt}x}_f + \frac{\partial f}{\partial u} \frac{d}{dt}u + \frac{\partial f}{\partial p} \frac{d}{dt}p. \quad (6.26)$$

Due to Assumptions 6.1 and 6.2, it holds true that $\left(\frac{d}{dt}u\right)(t) = 0$ and $\left(\frac{d}{dt}p\right)(t) = 0$ in each sampling interval. Thus, (6.26) gives that for $\tau \in (kT_d, (k+1)T_d)$:

$$\begin{aligned} \left\|\left(\frac{d^2}{dt^2}x\right)(\tau)\right\| &= \|(A \diamond p_d)(\tau) \cdot f(x, u, p, \tau)\| \\ &\leq \max_{\bar{p} \in \mathbb{P}, x \in \mathfrak{X}, u \in \mathbb{U}} \|A^2(\bar{p})x + A(\bar{p})B(\bar{p})u\|, \end{aligned} \quad (6.27)$$

where $\|\cdot\|$ is an arbitrary norm. Note that in (6.27), \mathbb{X} and \mathbb{U} must be bounded sets to be able to compute an upperbound. If this is not the case, then commonly \mathbb{X} and \mathbb{U} can be restricted to a bounded subset corresponding to the image of the typical trajectories of the system variables. Then the previous bound can be formulated for this region of interest. In the sequel, we denote the upperbound (6.27) by $M^{(1)}$ and call it the first-order *numerical sensitivity* (N-sensitivity) constant. Note, that $M^{(1)}$ can be computed via nonlinear optimization or alternatively it can be approximated through gridding. In case of an approximation, gridding of the sets \mathbb{P} , \mathbb{X} , and \mathbb{U} can be demanding, requiring significant computational power.

The derived result can also be compared with the existing error characterization of the rectangular method given in Hallouzi et al. (2006). In this work, an upperbound on the matrix approximation error of (6.8) has been introduced using basic algebra. This bound describes the discretization error also in the local sense, however it can not describe directly the approximation error of the state evolution. The latter is essentially needed to derive useful criteria for choosing adequate sampling-times (see Section 6.4.3). Therefore, the error concept of Hallouzi et al. (2006) is not considered here.

LUT error of other approximative methods

Using similar arguments, the LUT error of other discretization methods can be formulated based on Atkinson (1989). The results are given in the first row of Table 6.1, showing that each method is consistent with varying orders. Moreover, using (6.26) and the chain rule of differentiation, higher order N-sensitivity constants can be derived:

$$M^{(n)} = \max_{\bar{p} \in \mathbb{P}, \bar{x} \in \mathbb{X}, \bar{u} \in \mathbb{U}} \|A^{n+1}(\bar{p}) \bar{x} + A^n(\bar{p}) B(\bar{p}) \bar{u}\|. \quad (6.28)$$

6.4.2 Global convergence and preservation of stability

So far, only the LUT error of the introduced methods has been investigated, giving basic proofs of consistency. As a next step, we investigate global convergence of approximative methods together with their *numerical stability* (N-stability). The latter concept means that small errors in the initial condition of the discrete-time approximation do not cause the solution to diverge. We show that for the single-step approximative discretization methods, N-stability is identical with the preservation of the frozen stability of the original representation. This means that in case of numerical stability, the discretization method does not change the frozen stability properties of the discretized model, which is a prime requirement of a successful DT approximation of a CT system. To derive adequate criteria for the largest sampling-time for which this property holds (N-stability radius), each method is analyzed and computable formulas are derived.

According to the previously explained line of discussion, we introduce the following concepts:

Table 6.1: Local truncation error ε_k with $\tau \in ((k-1)T_d, kT_d)$, sampling boundary of stability \check{T}_d , and sampling upperbound of performance \hat{T}_d of LPV-SS ZOH discretization methods.

	Rectangular	n^{th} -polynomial
ε_k	$\frac{T_d}{2} \left(\frac{d^2}{dt^2} x \right) (\tau)$	$\frac{T_d^n}{(n+1)!} \left(\frac{d^{n+1}}{dt^{n+1}} x \right) (\tau)$
\check{T}_d	$\min_{\bar{p} \in \mathbb{P}} \min_{\lambda \in \sigma(A(\bar{p}))} -\frac{2\text{Re}(\lambda)}{ \lambda ^2}$	$\arg \min_{T_d \in \mathbb{R}_0^+} \left \max_{\bar{p} \in \mathbb{P}} \bar{\sigma} \left(\sum_{l=0}^n \frac{T_d^l}{l!} A^l(\bar{p}) \right) - 1 \right $
\hat{T}_d	$\sqrt{2 \frac{\varepsilon_{\max} M_x^{\max}}{M(1)}}$	$n+1 \sqrt{\frac{\varepsilon_{\max} M_x^{\max} (n+1)!}{M(n)}}$

	Trapezoidal	Adams-Bashforth (3-step)
ε_k	$\frac{5}{12} T_d^2 \left(\frac{d^3}{dt^3} x \right) (\tau)$	$\frac{3}{8} T_d^3 \left(\frac{d^4}{dt^4} x \right) (\tau)$
\check{T}_d	$\max_{\bar{p} \in \mathbb{P}} \max_{\lambda \in \sigma(A(\bar{p})), \text{Im}(\lambda)=0} \frac{2}{\text{Re}(\lambda)}$	$\arg \min_{T_d \in \mathbb{R}_0^+} \left \max_{\bar{p}_0, \dots, \bar{p}_n \in \mathbb{P}} \bar{\lambda} \left(\check{R}_{\bar{p}_0, \dots, \bar{p}_n}(\xi, T_d) \right) - 1 \right $
\hat{T}_d	$\sqrt[3]{\frac{12\varepsilon_{\max} M_x^{\max}}{5M(2)}}$	$\sqrt[4]{\frac{8\varepsilon_{\max} M_x^{\max}}{3M(3)}}$

Definition 6.2 (N-convergence) (based on Atkinson (1989)) Let $\mathfrak{R}_{\text{SS}}(\mathcal{S})$ be the SS representation of the LPV system \mathcal{S} with state-signal x and projected state behavior \mathfrak{B}_x , and let \hat{x}_d denote the DT approximation of x with $T_d \in \mathbb{R}^+$. Then a discretization method is called numerically convergent, if for any $x \in \mathfrak{B}_x$, the approximation \hat{x}_d satisfies that

$$\lim_{T_d \rightarrow 0} \sup_{k \in \mathbb{Z}_0} \|\hat{x}_d(k) - x(kT_d)\| = 0, \quad (6.29)$$

implies

$$\lim_{T_d \rightarrow 0} \sup_{k \in \mathbb{Z}^+} \|\hat{x}_d(k) - x(kT_d)\| = 0. \quad (6.30)$$

Note that in the trapezoidal and multi-step cases, \hat{x}_d is the appropriate state-transform of \check{x}_d with respect to x . In terms of Definition 6.2, N-convergence means that the discretized solution of the state-equation can get arbitrary close to the original CT behavior by decreasing T_d (see Figure 6.4).

Definition 6.3 (N-stability) (based on Atkinson (1989)) A discretization method is called numerically stable, if for sufficiently small values of T_d and ϵ , any two state-trajectories \hat{x}_d, \hat{x}'_d of the discretized representation associated with the same input-trajectory on the half line \mathbb{Z}^+ , satisfy that $\|\hat{x}'_d(0) - \hat{x}_d(0)\| < \epsilon$ implies the existence of a $\gamma \geq 0$ such that $\|\hat{x}'_d(k) - \hat{x}_d(k)\| < \gamma\epsilon$ for $\forall k \in \mathbb{Z}^+$.

The notion of N-stability means that small errors in the initial condition do not cause divergence as the solution is iterated (see Figure 6.5). For the approximative

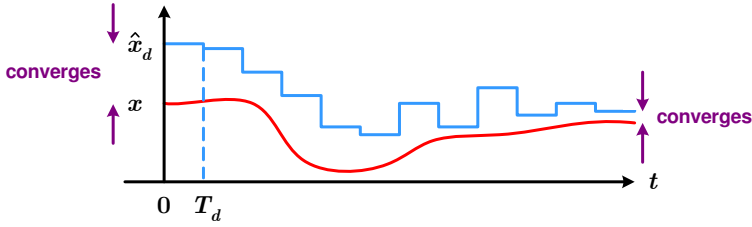


Figure 6.4: N-convergence of the DT approximation. The DT state-signal \hat{x}_d converges to the CT state-signal x of the approximated representation, if the error on the initial conditions (past) of the approximation converges to zero.

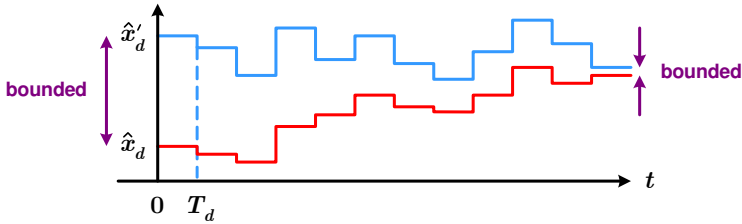


Figure 6.5: N-stability of the DT approximation. If the difference between the initial conditions of two state trajectories \hat{x}_d and \hat{x}'_d , provided by the approximation method for the same input on the half line \mathbb{Z}^+ , is bounded, then the difference of the two trajectories on \mathbb{Z}^+ is also bounded.

methods, N-convergence and N-stability are questions of main importance. To analyze these notions for the introduced discretization approaches, first consider the single-step methods. Introduce the characteristic polynomial $\check{R}_{\bar{p}} \in \mathbb{R}[\xi]$ of the frozen aspects of $\mathfrak{A}_{SS}(\mathcal{S})$ as

$$\check{R}_{\bar{p}}(\xi, T_d) = \det(\xi I - A \diamond p), \quad p(t) = \bar{p}, \quad \forall t \in \mathbb{R}, \quad (6.31)$$

where the indeterminant ξ is associated with q . Due to the multi-step nature of the Adams-Bashforth method - to avoid conservatism of the upcoming analysis - \check{R} is defined to reflect the multi-step nature of the state-evolution. In the n -step Adams-Bashforth case, the state evolution with respect to discretized original state x_d is characterized by

$$\xi^n I - T_d \sum_{l=0}^{n-1} \gamma_l \xi^l A, \quad (6.32)$$

with $\{\gamma_l\}_{l=1}^{n-1} \subset \mathbb{R}$ the Adams-Bashforth approximation coefficients (values of these coefficients for any $n > 0$ are given in Atkinson (1989)). The form of (6.32) results due to the augmented state vector \check{x}_d . However, even if $\mathfrak{A}_{SS}(\mathcal{S})$ has static dependence, the resulting polynomial in (6.32) becomes dynamically dependent on p_d . To express this, the following local characteristic polynomial is introduced

in the “frozen” sense for a scheduling sequence $\bar{p}_0, \dots, \bar{p}_n \in \mathbb{P}$:

$$\check{R}_{\bar{p}_0, \dots, \bar{p}_n}(\xi, T_d) = \det \left(\xi^n I - T_d \sum_{l=0}^{n-1} \gamma_l A(\bar{p}_l) \xi^l \right), \quad (6.33)$$

Now we can formulate the following theorem to characterize N-stability of the introduced discretization methods:

Theorem 6.1 (Strong root-condition) (based on Atkinson (1989)) *Discretization methods are N-convergent and N-stable, if for all $\lambda \in \mathbb{C}$ satisfying*

$$\exists \bar{p}_1, \dots, \bar{p}_n \in \mathbb{P} \text{ such that } \check{R}_{\bar{p}_0, \dots, \bar{p}_n}(\lambda, 0) = 0, \quad (6.34)$$

it holds that $|\lambda| \leq 1$ and if $|\lambda| = 1$, then $\frac{\partial}{\partial \xi} \check{R}_{\bar{p}_0, \dots, \bar{p}_n}(\lambda, 0) \neq 0$.

Note that for the single-step formulas $n = 1$ in Theorem 6.1. It can be shown, that all of the introduced LPV-SS discretization methods satisfy Theorem 6.1, as the proofs given in Atkinson (1989) also hold in this case. This means that all methods discussed in the previous part are N-convergent and N-stable. Now we can extend the root-condition to compute an exact upperbound \check{T}_d of the “sufficiently small” T_d that provides N-stability (see Definition 6.3):

Definition 6.4 (N-Stability-radius) (Atkinson 1989) *The N-stability radius \check{T}_d is defined as the largest $T_d \in \mathbb{R}_0^+$ for which all $\lambda \in \mathbb{C}$ with $\exists \bar{p}_1, \dots, \bar{p}_n \in \mathbb{P}$ such that*

$$\check{R}_{\bar{p}_0, \dots, \bar{p}_n}(\lambda, T_d) = 0, \quad (6.35)$$

satisfy that $|\lambda| \leq 1$.

This theorem has an interesting consequence for the discretization of LPV-SS representations. Namely, that through the characteristic polynomial \check{R} , it implies that, if $T_d \leq \check{T}_d$, then in the single-step cases, the resulting DT representation defines a uniformly frozen stable system (see Section 3.3.2), as for this T_d it is satisfied that

$$\max_{\bar{p} \in \mathbb{P}} \bar{\sigma}(A_d(\bar{p})) \leq 1, \quad (6.36)$$

where $\bar{\sigma}(\cdot) = \max |\sigma(\cdot)|$ is the spectral radius and $\sigma(\cdot)$ is the eigenvalue operator. If the original CT system \mathcal{S} is globally stable (dynamic, BIBO, etc.), then commonly it is desirable that its DT approximation is also globally stable. For such a property, it is needed that uniform frozen stability of $\mathfrak{R}_{SS}(\mathcal{S})$:

$$\max_{\bar{p} \in \mathbb{P}} \max_{\lambda \in \sigma(A(\bar{p}))} \operatorname{Re}\{\lambda\} < 0, \quad (6.37)$$

is preserved, resulting in the uniform frozen stability of the DT representation. This gives the important observation that, for the introduced single-step discretization methods, preservation of global stability of the original system and N-stability of the discretization method both require uniform frozen stability of the resulting

DT representation. For N-stability it is a sufficient, for preservation of global stability of S it is a necessary condition. Note, that this condition of N-stability is sufficient only for representations with static dependence. In the following, we analyze the N-stability radius of each discretization method to give computable bounds for the selection of T_d by which the discretization method preserves frozen stability of the original system, i.e. it has N-stability.

Stability radius of the rectangular method

In case of the rectangular method, (6.36) is equivalent with

$$\max_{\bar{p} \in \mathbb{P}} \bar{\sigma}(I + T_d A(\bar{p})) \leq 1. \quad (6.38)$$

Due to the basic properties of eigenvalues, it can be shown that (6.38) holds iff

$$\max_{\bar{p} \in \mathbb{P}} \max_{\lambda \in \sigma(A(\bar{p}))} \left| \frac{1}{T_d} + \lambda \right| < \frac{1}{T_d}. \quad (6.39)$$

From (6.39), the stability radius is

$$\check{T}_d = \min_{\bar{p} \in \mathbb{P}} \min_{\lambda \in \sigma(A(\bar{p}))} - \frac{2\operatorname{Re}(\lambda)}{|\lambda|^2}. \quad (6.40)$$

Note that $\check{T}_d = 0$ in case of non-uniformly frozen stable $\mathfrak{R}_{SS}(S)$, meaning that the rectangular DT approximation of non-uniformly frozen stable systems is not N-stable. Computation of the bound (6.40) is a nonlinear optimization problem for which an approximative solution may follow by the gridding of \mathbb{P} .

Stability radius of the polynomial method

In case of the polynomial method, (6.36) translates to

$$\max_{\bar{p} \in \mathbb{P}} \bar{\sigma} \left(I + \sum_{l=1}^n \frac{T_d^l}{l!} A^l(\bar{p}) \right) \leq 1. \quad (6.41)$$

From (6.41), the stability radius reads as

$$\check{T}_d = \arg \min_{T_d \in \mathbb{R}_0^+} \left| \max_{\bar{p} \in \mathbb{P}} \bar{\sigma} \left(\sum_{l=0}^n \frac{T_d^l}{l!} A^l(\bar{p}) \right) - 1 \right|. \quad (6.42)$$

Again, a possible approximation of \check{T}_d can be given by applying bisection based search in T_d on (6.42) over a grid of \mathbb{P} . Note, that in case of non-uniform frozen stability, $\check{T}_d = 0$ with this method as well.

Stability radius of the trapezoidal method

For the trapezoidal method, condition (6.36) becomes quite complicated due to the inverse term $[I - \frac{T_d}{2} A]^{-1}$ in A_d . First it must be guaranteed that this inverse

exists for all scheduling signals, meaning that

$$\det \left(I - \frac{T_d}{2} A(\bar{p}) \right) \neq 0, \quad \forall \bar{p} \in \mathbb{P}, \quad (6.43)$$

or equivalently

$$\min_{\bar{p} \in \mathbb{P}} \underline{\sigma} \left(I - \frac{T_d}{2} A(\bar{p}) \right) > 0, \quad (6.44)$$

where $\underline{\sigma}(\cdot) = \min |\sigma(\cdot)|$. Again, the eigenvalue properties yield that (6.44) is equivalent with

$$\min_{\bar{p} \in \mathbb{P}} \min_{\lambda \in \sigma(A(\bar{p}))} \left| \frac{2}{T_d} - \lambda \right| > 0,$$

which is guaranteed for every $0 \leq T_d < \check{T}_d$, where

$$\check{T}_d = \max_{\bar{p} \in \mathbb{P}} \max_{\lambda \in \sigma(A(\bar{p})), \text{Im}(\lambda)=0} \frac{2}{\text{Re}(\lambda)}. \quad (6.45)$$

Instead of N-stability, here \check{T}_d ensures the existence of the DT projection (existence of A_d). It is shown later, that if the DT projection exists, then N-stability and N-convergence hold. Note that, in case of $\text{Im}(\lambda) \neq 0$ for all $\lambda \in \sigma(A(\bar{p}))$ and $\bar{p} \in \mathbb{P}$, meaning that every frozen representation of the original CT system has only complex poles, condition (6.43) is guaranteed for arbitrary T_d , resulting in $\check{T}_d = \infty$. Similarly, uniform frozen stability of $\mathfrak{R}_{SS}(\mathcal{S})$, meaning that every frozen representation has poles with only negative or zero real part, gives $\check{T}_d = \infty$. In Apkarian (1997), the condition

$$T_d \leq \max_{\bar{p} \in \mathbb{P}} \frac{2}{\underline{\sigma}(A(\bar{p}))}, \quad (6.46)$$

was proposed to guarantee invertibility, which is a rather conservative upper-bound of (6.45). In case $0 \leq T_d < \check{T}_d$ holds and $\mathfrak{R}_{SS}(\mathcal{S})$ has uniform frozen stability, then (6.36) holds, as in this case

$$\max_{\bar{p} \in \mathbb{P}} \bar{\sigma} \left(\left[I + \frac{T_d}{2} A(\bar{p}) \right] \left[I - \frac{T_d}{2} A(\bar{p}) \right]^{-1} \right) \leq 1. \quad (6.47)$$

See Glover (1984) for the proof. Thus, for uniformly frozen stable LPV-SS representations with static dependence, the trapezoidal method always guarantees N-stability and N-convergence if T_d satisfies condition (6.45).

Stability radius of the Adams-Bashforth method

In case of the Adams-Bashforth method, the concept of N-stability means that for a given T_d ,

$$\max_{\bar{p}_0, \dots, \bar{p}_n \in \mathbb{P}} \bar{\lambda} \left(\check{R}_{\bar{p}_0, \dots, \bar{p}_n}(\xi, T_d) \right) \leq 1. \quad (6.48)$$

where

$$\bar{\lambda}(R(\xi)) = \max_{\lambda \in \mathcal{C}, R(\lambda)=0} |\lambda|. \quad (6.49)$$

A necessary condition for (6.48) is that the resulting DT representation has uniform frozen stability:

$$\max_{\bar{p} \in \mathbb{P}} \bar{\sigma}(A_d(\bar{p})) \leq 1. \quad (6.50)$$

This means, that in the multi-step case, preservation of frozen stability is not sufficient to imply N-stability. From (6.48) it follows that the N-stability radius reads as

$$\check{T}_d = \arg \min_{T_d \in \mathbb{R}_0^+} \left| \max_{\bar{p}_0, \dots, \bar{p}_n \in \mathbb{P}} \bar{\lambda} \left(\check{R}_{\bar{p}_0, \dots, \bar{p}_n}(\xi, T_d) \right) - 1 \right|, \quad (6.51)$$

which is a too complicated expression to be further analyzed. However in practice, it can be solved in an approximative manner based on gridding and bisection based search.

6.4.3 Guaranteeing a desired level of discretization error

In the previous part we have investigated the numerical properties of the introduced discretion methods and derived criteria on T_d in order to guarantee the preservation of frozen stability of the original CT system. However, the appropriate choice of T_d to arrive at a specific performance in terms of the discretization error is also important from a practical point of view. By utilizing the LUT error expressions developed in Section 6.4.1, in this section upperbounds of T_d are derived that guarantee a certain bound on the LUT error in terms of a chosen measure $\|\cdot\|$. Then it is investigated, how such expressions can be used to achieve a level of global discretization error.

As a first step, we formulate the concept of desired performance in terms of the LUT error. For a given continuous-time full behavior \mathfrak{B}_{SS} , which is approximated via a discretization method, define

$$\varepsilon_* := \sup_{x \in \mathfrak{B}_x} \sup_{k \in \mathbb{Z}} \|\varepsilon_k\| \quad (6.52)$$

as the maximal LUT error in a given, arbitrary norm $\|\cdot\|$. Note that his quantity describes the maximum of the truncation error with respect to all possible state trajectories of \mathfrak{B}_{SS} . Also introduce

$$M_x^{\max} := \sup_{x \in \mathfrak{B}_x} \max_{t \in \mathbb{R}} \|x(t)\| = \max_{x \in \mathfrak{X}} \|x\|, \quad (6.53)$$

as the maximum ‘‘amplitude’’ of the state signal for any u and p in \mathfrak{B}_{SS} . Denote ε_{\max} as the maximal acceptable relative local error of the discretization in terms of percentage. Then a $T_d \in \mathbb{R}^+$ is searched for, that satisfies

$$\varepsilon_* \leq \frac{\varepsilon_{\max} M_x^{\max}}{100 \cdot T_d}. \quad (6.54)$$

Here $1/T_d$ is introduced on the right side of (6.54) as ε_k is scaled by T_d (see (6.23)). Next, we formulate upperbounds of T_d with respect to each method, such that (6.54) is satisfied for the desired ε_{\max} percentage. Note that to derive these criteria,

(6.53) must be bounded, i.e. \mathcal{X} must be confined in a ball (bounded region) of \mathbb{R}^{n_x} . Such an assumption is not unrealistic in case of global asymptotic stability of \mathcal{S} and bounded \mathbb{P} and \mathbb{U} .

Performance criterion for the rectangular method

Based on (6.25), it holds in the rectangular case that

$$\varepsilon_* = \sup_{x \in \mathfrak{B}_x} \sup_{\tau \in \mathbb{R}} \frac{T_d}{2} \left\| \left(\frac{d^2}{dt^2} x \right) (\tau) \right\|. \quad (6.55)$$

By using the sensitivity constant $M^{(1)}$ (see (6.27)), inequality (6.54) holds for any $0 \leq T_d \leq \hat{T}_d$ where

$$\hat{T}_d = \sqrt{2 \frac{\varepsilon_{\max} M_x^{\max}}{100 \cdot M^{(1)}}}. \quad (6.56)$$

Criterion (6.56) gives an upperbound estimate of the required T_d , that achieves ε_{\max} percentage local discretization error of the state variable of the approximated representation in terms of a chosen measure $\| \cdot \|$.

Performance criteria of other approximative methods

Similar criteria can be developed for the other methods by using the LUT error expressions of Table 6.1 and the higher-order sensitivity constants $M^{(n)}$. These upperbounds are presented in Table 6.1. Note that similar expressions can also be worked out with respect to the approximation error of the output trajectories.

Guaranteeing bounds on the global error

In practical situations, one may be concerned about the maximum relative global error as a performance measure. Define

$$\eta_* := \sup_{x \in \mathfrak{B}_x} \sup_{k \in \mathbb{Z}} \|\eta_k\| \quad (6.57)$$

as the maximum global error (see (6.22) for the definition of η_k). Also define η_{\max} as the maximal acceptable relative global error of the discretization in terms of percentage. Then one would like to choose T_d , such that the global error η_k satisfies

$$\eta_* \leq \frac{\eta_{\max} M_x^{\max}}{100}. \quad (6.58)$$

Unfortunately, characterization of η_* for the introduced discretization methods requires the introduction of serious restrictions of the considered CT behaviors. However, in case of $T_d \leq \check{T}_d$ i.e. N-stability, ε_{\max} can be used as a good approximation of η_{\max} , therefore the performance bound \hat{T}_d can be used to approximate/guarantee a global error bound as well.

6.4.4 Switching effects

In the previous part, the effect of neglecting the switching phenomena of the ZOH actuation has not been considered. Here we investigate the case when the signals u and p described by (6.2a-b) are applied to $\mathfrak{R}_{SS}(\mathcal{S})$. First we show the effect of these discontinuous signals on the state evolution of $\mathfrak{R}_{SS}(\mathcal{S})$ inside a sample interval and the error that results by neglecting these terms. Then we motivate why this phenomenon is negligible in practical situations.

Consider the ODE corresponding to (3.37a) in the k^{th} sample interval. By using the bilateral Laplace transform of this differential equation with reference time $t_0 = kT_d$ and assuming that the dependence on p is commutative under addition², it follows that for a fixed k :

$$\begin{aligned} sX(s) &= x_d(k) + \left[\frac{(A \diamond p_d)(k) + (s-1)(A \diamond p_d)(k-1)}{s} \right] X(s) + \frac{(B \diamond p_d)(k)}{s} u_d(k) + \\ &+ \left[\frac{(B \diamond p_d)(k) + (s-1)(B \diamond p_d)(k-1)}{s} \right] u_d(k-1). \end{aligned} \quad (6.59)$$

where $X(s)$ is the Laplace transform of the solution of the ODE (the behavior of the state in the k^{th} sample interval). It is immediate that in the given sample interval, (6.59) does not correspond to (6.6a). (6.59) has a dynamic dependence, and it is not realizable as a LPV-SS representation directly without associating $q^{-1}u_d$ with a new state-variable. In this way, it becomes clear that neglecting the switching effects introduces discretization errors in the LPV case, which can be even more significant if T_d is decreased (more discontinuous switches in the dynamics). On the other hand, it is true that the discontinuous phenomenon which is described by (6.59) never happens in reality. One reason is that usually p is not actuated by ZOH and it changes smoothly/relatively slowly with respect to the actual dynamics of the plant. Additionally, ZOH actuation has a transient in practice as the underlying physical device needs to build up the new signal value, preventing sudden changes of the signals. In conclusion, for the considered class of LPV representations, the introduced discretization methods of this section give no step-invariant discretization in the ZOH setting (meaning equivalence even in case of switching effects), however they are well applicable methods for practical use. It is important to note that derivation of LPV discretization methods with step-invariant property is also possible, however the resulting discretization approaches are technical and their actual performance gain compared to the previously developed approaches is insignificant in practice.

6.5 Properties of the discretization approaches

Beside stability and discretization error characteristics, there are other properties of the derived discretization methods which could assist or hinder further use of the resulting DT model. With the previously obtained results, these vital

²Without this assumption, the formulation of the Laplace transform becomes complicated, but the core problem that results in the general case is illustrated well by (6.59).

Table 6.2: Properties of the derived discretization methods in terms of: (a) consistency/convergence; (b) preservation of stability/N-stability; (c) preservation of instability; (d) existence; (e) complexity; (f) preservation of linear dependence; (g) computational load; (h) system order.

Prop.	Complete	Rectangular	n^{th} -polynomial	Trapezoidal	Adams-Bash.
(a)	always	1 st -order	n^{th} -order	2 nd -order	3 rd -order
(b)	always global	frozen with \check{T}_d	frozen with \check{T}_d	always frozen	frozen with \check{T}_d
(c)	+	-	-	+	-
(d)	always	always	always	conditional	always
(e)	exponential	linear	polynomial	rational	linear
(f)	-	+	-	-	+
(g)	high	low	moderate	high	low
(h)	preserved	preserved	preserved	preserved	increased

properties are summarized in Table 6.2. From this table it is apparent that the complete method gives errorless conversion at the price of heavy nonlinear dependence of the DT model on p_d . As in LPV control synthesis low complexity of the p -dependence is assumed (like linear, polynomial, or rational functions, see Scherer (1996)), both for modeling and controller discretization purposes - beside the preservation of stability - the preservation of linear dependence over the scheduling is preferred. This favors approximative methods that give acceptable performance, but with less complexity of the new coefficient dependence on the scheduling. Complicated coefficient functions, like inversion or matrix exponential, also results in a serious increase of the computation time, which gives a preference towards the linear methods like the rectangular or the Adams-Bashforth approach. In the latter case, the order increase of the DT representation requires extra memory storage or more complicated controller design depending on the intended use. If the quality of the DT model has priority, then the trapezoidal and the polynomial methods are suggested due to their fast convergence and large stability radius. In terms of identification, linear dependence of the suggested model structures is also important as it simplifies parametrization.

6.6 Discretization and dynamic dependence

So far, the discretization of LPV-SS representations with static dependence has been considered in a ZOH setting. It has been already discussed that using the ZOH setting for the discretization of representations with dynamic dependence may result in the loss of significant parts of the original behavior. These parts, which are associated with the dynamic nature of the coefficient dependencies, are lost because in each sample interval the derivatives of p are assumed to be zero.

In this way, dynamic dependence of the original coefficients simplifies to a static dependence.

To show this phenomenon, consider the case when $A \diamond p = rp \frac{d}{dt}p$ with $r \in \mathbb{R}$ and $\mathbb{P} = \mathbb{R}$. Then in the ZOH setting, the following holds in each sample interval:

$$(A \diamond p)(t) = \begin{cases} 0, & \text{if } t \neq kT_d, k \in \mathbb{Z}; \\ \pm\infty, & \text{if } t = kT_d, k \in \mathbb{Z}; \end{cases} \quad (6.60)$$

If the switching effect is neglected, then A is approximated in DT as an identity matrix by all of the introduced discretization methods. Thus, the original behavior of the CT representation is lost due to the ZOH setting. However in practice, one would try to use the approximation

$$\frac{d}{dt}p(t) \approx \frac{p((k+1)T_d) - p(kT_d)}{T_d}, \quad (6.61)$$

for each $t \in [kT_d, (k+1)T_d)$. In fact, (6.61) means that p is assumed to be a linear function in the sample interval. Then, using this assumption, a better DT approximation of the original CT representation can be derived. This shows that in case of dynamic dependence, the ZOH assumption on p is not appropriate and instead of that, a first or higher order hold discretization setting is necessary for the scheduling variable.

Based on the previous example, consider the case when (u, y) are assumed to satisfy the ZOH setting, but p varies linearly in each sampling interval $t \in [kT_d, (k+1)T_d)$:

$$p(t) = \underbrace{\frac{p_d(k+1) - p_d(k)}{T_d}}_{\bar{p}_{1k}}(t - kT_d) + p_d(k). \quad (6.62)$$

Additionally, define $\bar{p}_{0k} = p_d(k) - kT_dp_d(k)$. This assumption on the scheduling is called the *first-order hold* setting. Let $\mathfrak{R}_{SS}(\mathcal{S})$ be a continuous-time LPV-SS representation and consider it in the above defined first-order hold setting. In case the matrices of $\mathfrak{R}_{SS}(\mathcal{S})$ are dependent on p and $\frac{d}{dt}p$, like $A \diamond p = A(p, \frac{d}{dt}p)$ (dynamic dependence), then the state-evolution in the k^{th} sampling interval satisfies:

$$\frac{d}{dt}x(t) = A(\bar{p}_{1k}t + \bar{p}_{0k}, \bar{p}_{1k})x(t) + B(\bar{p}_{1k}t + \bar{p}_{0k}, \bar{p}_{1k})u_d(k). \quad (6.63)$$

The solution of this ODE can be obtained in the time interval $t \in [kT_d, (k+1)T_d)$ for particular meromorphic functions A and B . Similarly to the complete method of the ZOH setting in Section 6.3, this analytical solution results in a complete type of discretization of the continuous-time LPV-SS representation. The resulting DT counterpart has also dynamic dependence on p_d and its time-shifted versions, and yields a better approximation of the CT representation than what would result in a pure ZOH setting. This suggests that for the discretization of LPV representations with dynamic dependence, the order of the hold setting with respect to p should be greater or equal than the maximal order of derivatives in the coefficient depen-

dencies. With some trivial modifications, the approximative methods treated in this paper, except the trapezoidal method, can be extended to this hybrid higher-order hold case, but the exact formulation of these extensions is not considered in this thesis. Unfortunately, for the extended approaches, the deduced formulas for the approximation error and the step-size bounds do not apply. Solving discretization of LPV representations with dynamic dependence in a general sense and giving compact formulas of discretization remains the objective of further research.

6.7 Numerical example

In the following a simple example is presented to visualize/compare the properties of the analyzed discretization methods and the performance of the sample-bound criteria. Consider the following state-space representation of a continuous-time SISO LPV system \mathcal{S} with IO partition (u, y) :

$$\mathfrak{R}_{\text{SS}}(\mathcal{S}) = \left[\begin{array}{c|c} A \diamond p & B \diamond p \\ \hline C \diamond p & D \diamond p \end{array} \right] = \left[\begin{array}{cc|c} 19.98p - 20 & 202 - 182p & 1 + p \\ 45p - 50 & 0 & 1 + p \\ \hline 1 + p & 1 + p & \frac{1+p}{10} \end{array} \right]$$

where $\mathbb{P} = [-1, 1]$. The above representation has static linear dependence on the scheduling signal p . Furthermore, for a constant scheduling $p(t) = \bar{p}$ for all $t \in \mathbb{R}$, $\mathfrak{R}_{\text{SS}}(\mathcal{S})$ is equivalent with an LTI representation that has poles

$$\sigma(A(\bar{p})) = 9.99\bar{p} - 10 \pm i\sqrt{10^4 - 17990.2\bar{p} + 8090.2\bar{p}^2}. \quad (6.64)$$

From (6.64), it is obvious that \mathcal{S} is uniformly frozen stable on \mathbb{P} .

Assume that \mathcal{S} is in a ZOH setting with sampling rate $T_d = 0.02$. By applying the discretization methods of Section 6.3, approximative discrete-time representations of \mathcal{S} have been calculated. In order to show the performance of the investigated discretization methods, the output of the original and its discrete approximations have been simulated on the $[0, 1]$ time interval for zero initial conditions and for 100 different realizations of white u_d and p_d with uniform distribution $\mathcal{U}(-1, 1)$. For fair comparison, the achieved MSE (see (2.165)) of the resulting output signals \hat{y}_d has been calculated with respect to the output y of $\mathfrak{R}_{\text{SS}}(\mathcal{S})$ and presented in Table 6.3. Beside the MSE of the output evolution, the relative worst-case maximum global error $\hat{\eta}_{\text{max}} = 100 \cdot \eta_*/M_x^{\text{max}}$ of the DT state-signals \hat{x}_d associated with the discrete-time SS representations has been also computed with respect to the state signal x of $\mathfrak{R}_{\text{SS}}(\mathcal{S})$ and presented in Table 6.3. From these error measures it is immediate that, except for the complete and the trapezoidal method, all approximations diverge. As expected, the error of the complete method is extremely small and the trapezoidal method gives a moderate, but acceptable performance. Note that the response of the original CT $\mathfrak{R}_{\text{SS}}(\mathcal{S})$ has been calculated via a 5th-order Runge-Kutta numerical approximation (see Atkinson (1989)) with step size 10^{-8} . This implies that the switching effect of the ZOH actuation does not show up in the calculated response.

Table 6.3: Discretization error of \mathcal{S} , given in terms of the achieved MSE and $\hat{\eta}_{\max} = 100 \cdot \eta_*/M_x^{\max}$ (relative worst-case η_k) for 100 simulations. (*) indicates unstable projection to the discrete domain.

MSE of y_d					
T_d	Complete	Rectangular	2^{nd} -polynom.	Trapezoidal	Adams-Bash.
$2 \cdot 10^{-2}$, (50Hz)	$1.68 \cdot 10^{-10}$	(*)	(*)	$1.97 \cdot 10^{-3}$	(*)
$5 \cdot 10^{-3}$, (0.2kHz)	$1.69 \cdot 10^{-10}$	(*)	$4.70 \cdot 10^{-4}$	$3.81 \cdot 10^{-5}$	$2.14 \cdot 10^{-1}$
10^{-4} , (10kHz)	$1.68 \cdot 10^{-10}$	$2.27 \cdot 10^{-6}$	$1.05 \cdot 10^{-10}$	$1.53 \cdot 10^{-8}$	$1.6 \cdot 10^{-8}$

$\hat{\eta}_{\max}$ of \hat{x}_d					
T_d	Complete	Rectangular	2^{nd} -polynom.	Trapezoidal	Adams-Bash.
$2 \cdot 10^{-2}$, (50Hz)	0.053%	(*)	(*)	106.12%	(*)
$5 \cdot 10^{-3}$, (0.2kHz)	0.060%	(*)	40.31%	8.02%	665.94%
10^{-4} , (10kHz)	0.063%	2.62%	0.06%	0.19%	0.76%

Table 6.4: Stability (\check{T}_d) and performance (\hat{T}_d) bounds provided by the criterion functions of Table 6.1. The results here are presented in terms of the Euclidian norm and $\varepsilon_{\max} = 1\%$.

Criteria				
	Rectangular	2^{nd} -polynomial	Trapezoidal	Adams-Bashforth
\check{T}_d	$2 \cdot 10^{-4}$, (5kHz)	$5.60 \cdot 10^{-3}$, (0.2kHz)	∞	$1.77 \cdot 10^{-3}$, (0.6kHz)
\hat{T}_d	$6.87 \cdot 10^{-5}$, (15kHz)	$1.73 \cdot 10^{-3}$, (0.6kHz)	$1.28 \cdot 10^{-3}$, (0.8kHz)	$1.21 \cdot 10^{-3}$, (0.8kHz)

As a second step, we calculate sampling bounds \check{T}_d and \hat{T}_d by choosing the Euclidian norm as an error measure and $\varepsilon_{\max} = 1\%$, with the intention to achieve $\eta_{\max} = 1\%$. The calculated sampling bounds are presented in Table 6.4. During the calculation of \hat{T}_d it has been assumed that $\mathcal{X} = [-0.1, 0.1]^2$, which has been verified by several simulations of $\mathfrak{R}_{SS}^c(\mathcal{S}_1, p)$ based on $u_d, p_d \in \mathcal{U}(-1, 1)$. By these results, the rectangular method needs a fast sampling rate to achieve a stable projection and even a faster sampling to obtain the required performance. The 2nd-order polynomial projection has significantly better bounds due to the 2nd-order accuracy of this method. For the trapezoidal case, the existence of the transformation is always guaranteed because $\mathfrak{R}_{SS}(\mathcal{S})$ is uniformly frozen stable. For comparison, the bound of Apkarian (1997) given by (6.46), would have resulted in $\check{T}_d = 0.2$.

Now we use the derived bounds to choose a new T_d for the calculation of the discrete projections. As the \check{T}_d bounds of Table 6.4 represent the boundary of stability, therefore $T_d < \check{T}_d$ is used as a new sampling-time in each case. Discretization of $\mathfrak{R}_{SS}(\mathcal{S})$ with $T_d = 0.005$, almost the stability bound of the polynomial method, provides the simulation results given in the second row of Table 6.3. The rectangular method again results in an unstable projection, while the Adams-Bashforth method is on the brink of instability due to frozen instability of A_d for some $\bar{p} \in \mathbb{P}$. The polynomial method gives a stable, convergent approximation, in accordance with its \check{T}_d bound. The trapezoidal method also improves significantly in performance. The achieved $\hat{\eta}_{\max}$ of each approximative method is above the aimed 1 % which is in accordance with their \hat{T}_d .

As a next step, discretizations of $\mathfrak{R}_{SS}(\mathcal{S})$ with $T_d = 10^{-4}$, the half of the \check{T}_d bound of the rectangular method, are calculated. The results are given in the third row of Table 6.3. Finally, the rectangular method converges and also the approximation capabilities of the other methods improve. By looking at the achieved $\hat{\eta}_{\max}$, all the methods, except the rectangular, obtain the aimed 1 % error performance which is in accordance with their \hat{T}_d bound, while in the rectangular case the achieved $\hat{\eta}_{\max}$ is larger than 1 % as 10^{-4} is larger than its \hat{T}_d bound. An interesting phenomenon is that the approximation error of the complete method is non-zero and it is slightly increasing by lowering the sampling-time. This increasing approximation error is due to numerical errors of the digital computation. However, the resulting approximation error is significantly less than the step size of the numerical approximation used for the simulation of $\mathfrak{R}_{SS}(\mathcal{S})$, thus it can be considered zero.

6.8 Summary

In this chapter, discretization of LPV state-space representations has been investigated in a zero-order hold setting, where the continuous-time input and scheduling trajectories are restricted to be piecewise constant. It has been shown that the ZOH setting provides an adequate discretization concept for SS representations with static dependence.

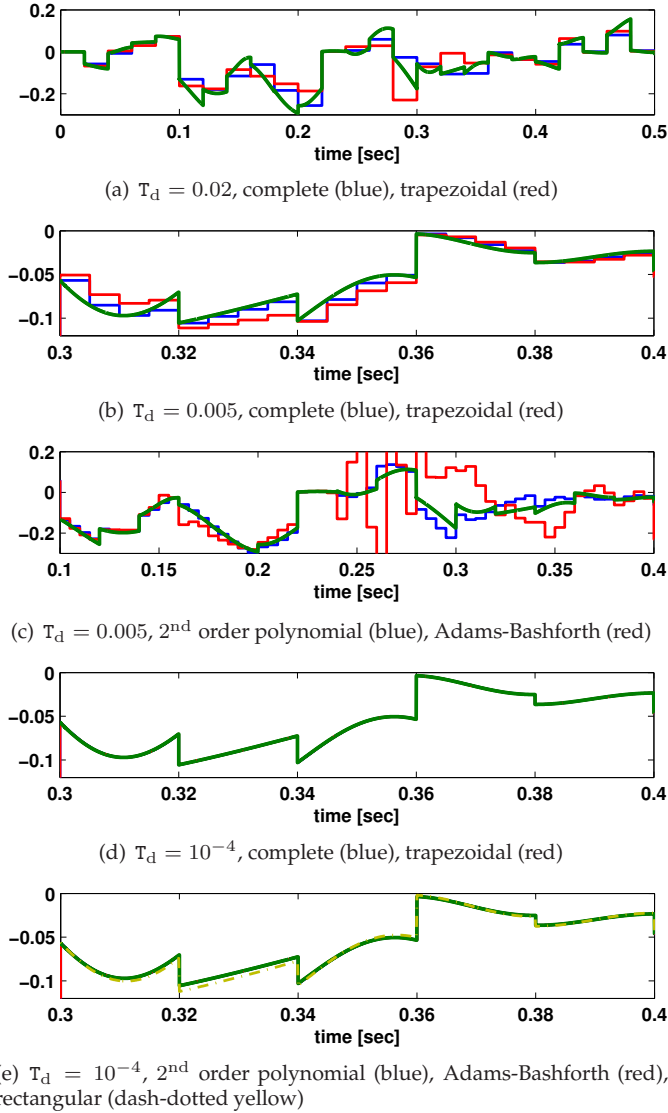


Figure 6.6: Output signal y of $\mathfrak{R}_{SS}(\mathcal{S})$ (green) in a ZOH setting with $T_d = 0.02$ and its discrete-time approximations with different sampling-times.

Extending the approaches of the LTI discretization theory introduced in Section 6.2, both exact and approximative methods have been developed in the ZOH setting for the discretization of LPV-SS representations with static dependence. These approaches have been developed for the LPV identification framework of this thesis to provide tools that assist model structure selection based on first-principle CT models.

Using the results of the numerical analysis field, the introduced methods have been investigated in terms of numerical consistency, convergence, and stability in Section 6.4.2. It has been shown that all methods fulfill these properties and for the single-step approximation methods numerical stability is equivalent with the preservation of the frozen stability of the original behavior. Powerful criteria have been developed to give upperbounds on the sampling-time for which numerical stability, i.e. preservation of frozen stability holds. Additionally, the approximation error of the introduced approaches has been analyzed in terms of the local truncation error in Section 6.4.1. Criteria have been developed in Section 6.4.3 for the choice of sampling-time that guarantees a user defined maximum of the truncation error. It has been also motivated how the developed criteria can be used to bound the global error of the approximation.

In Section 6.4.4, the result of the assumption of smooth switching behavior of the ZOH actuated signals has been analyzed. This assumption has been vital to enable the derivation of the introduced approaches. It has been shown that this assumption has no significant consequences in practical situations, as sharp steps of the input and scheduling signals seldom happen in reality. Additionally, important properties of the discretization approaches have been discussed in Section 6.5 from the viewpoint of identification and control. Comparing these properties, a clear trade-of has been identified between approximation quality and the complexity of coefficient dependencies of the resulting DT representation. It has been shown, that multi-step methods like the Adams-Bashforth approach provide simple and good quality of DT approximation at the expense of increased state-dimensions. Thus, for low order LPV systems, this method appears an attractive approach both for control and identification applications.

As a final step in Section 6.6, it has been investigated how the introduced theory can be applied to the discretization of LPV-SS representations with dynamic dependence. It has been shown that adequate discretization of such representations requires a higher-order hold setting with respect to the scheduling variable. In such a setting, the scheduling trajectories are restricted to be piecewise polynomial with a given order. It has also been pointed out that this order must be equal to the maximal order of the derivatives of the scheduling on which the coefficients of the original CT representation are dependent. To illustrate the introduced methods and the applicability of the derived criteria, a numerical example has been presented.

LPV modeling of physical systems

With the motivation to provide tools for model-structure selection in LPV identification, in this section, modeling of physical systems described by nonlinear differential equations is studied in the LPV framework. It is investigated how such a nonlinear system can be realized or approximated by a LPV system, giving models of the original behavior in terms of LPV representations. First an overview is presented of the available LPV modeling methods. Then, an algorithmic approach is introduced that ensures errorless conversion of nonlinear differential equations into LPV kernel representations. The approach explores adequate choices of the scheduling variable. Using the previously developed behavioral framework, equivalent realizations of the derived kernel form are available in the SS, IO, and OBF expansion representation domains. Based on these equivalent representations, an adequate choice of a model structure can be obtained for the LPV identification of the physical system.

7.1 Introduction

A crucial ingredient of any system identification procedure is the choice of model parametrization, that describes the model set in which the optimal candidate is to be found. If this structure is well-founded with respect to the system to be identified, then all other ingredients, like experiment design, criterion selection, estimation, etc. can contribute successfully to the validity of the end result. Commonly, a poor choice of the model set directly results in a poor estimate of the system.

LPV models have considerably more freedom in parametrization than the class of LTI models. This is due to the presence of functional and often dynamic dependence of the model parameters on the scheduling. Thus LPV model-structure selection is even a more sensitive question than in the LTI case. Furthermore, due

to the lack of a general LPV validation theory, mismodeled dynamics only show up in the performance loss of the designed controllers.

In LPV identification, methods that assist model-structure selection based on measured data have not been developed yet, thus the only source of information available for this decision is in the form of first principle laws or expert's knowledge. Such knowledge is most often presented in terms of nonlinear differential equations, which must be transformed to or approximated by an LPV representation to facilitate model structure selection in this setting. In this chapter, the concept of LPV modeling of nonlinear dynamical systems is investigated. The intention is to give a practical way of using first principle laws and knowledge in the decision process of LPV model structures, appropriate for the identification of the underlying system. Such a process is inevitable for successful identification in the general LPV framework, as it interprets key information about the order and type of functional dynamical dependencies on the scheduling signal and even about which signal(s) can be used for scheduling purposes.

First in Section 7.2, the general questions of LPV modeling are investigated and it is shown how the gain-scheduling principle has shaped LPV modeling of physical systems. It is also motivated why it has become necessary both for control and identification to explore approximation free LPV descriptions of the original behavior. Then in Section 7.3, existing LPV modeling techniques are studied and compared. This overview, which is also a contribution of the thesis, provides the conclusion that all of the available approaches are either too restricted or ad hoc to support LPV model structure selection in a general, well founded sense. Additionally, the result of these approaches is a *continuous-time* (CT) description, while existing techniques of LPV identification are based on *discrete-time* (DT). To fill this obvious gap of the identification cycle, an automated modeling procedure is proposed in Section 7.4, which uses the strength of the previously developed LPV behavioral framework and discretization approaches to deliver the required structural information. The developed technique is a crucial contribution for the general LPV framework as it can assist all identification methods of the field with structural information about the plant. The procedure is also a necessary ingredient of the identification approach of this thesis as it can assist the choice of *Orthonormal Basis Functions* (OBFs), adequate for the series-expansion representation of the system dynamics, and also the choice of the structure of functional dependencies for the parameterization of the expansion coefficients.

7.2 General questions of LPV modeling

Before the first papers on LPV identification methods appeared, modeling of physical systems in a LPV form had been dominated by the gain-scheduling principle (see Chapter 1). Motivated by the early approaches of LPV control, the available *nonlinear* (NL) description of the system was linearized in several operating/equilibrium points resulting in a collection of local LTI descriptions of the plant. Then these "local" descriptions were interpolated to obtain a global approximation of the physical system on the entire operation regime. However,

unknown coefficients/relations of the NL model still had to be estimated beforehand. This concept has resulted in many linearization-based LPV modeling approaches trying to approximate the NL system in a LPV *state-space* (SS) form.

For direct approximation of the NL system with an LPV model, LPV identification methods has appeared soon (see Chapter 1). However, these approaches only aim at the identification of an underlying “true LPV system” with completely known structural information. It has been seemingly forgotten that the true aim has always been the approximation of the NL physical system. Additionally, many of these approaches has followed the gain-scheduling principle by identifying local LTI models and interpolating them.

Due to higher performance demands and the still existing gap between LPV identification methods and practical application, a new generation of LPV modeling approaches have appeared, formulating LPV modeling from a different perspective than gain-scheduling. These approaches aim at the transformation of the original NL representation into a particular LPV form by using substitution or other mathematical manipulations. However, the resulting methods are only able to handle certain sub-classes of NL systems. So the natural question that what kind of systems can the LPV framework describe accurately has remained unanswered.

Till today, both the control and identification literature on LPV systems typically takes the existence of the plant in a LPV form as a starting point. It is commonly not pointed out how the underlying nonlinear system is transformed to this LPV form. On the other hand, the available LPV modeling approaches are focusing only on particular subclasses of LPV representations. The question that whether a significant loss of generality is introduced by the used assumptions usually remains uninvestigated. This shows that LPV modeling of NL systems deserves much more attention and research in order to understand what can be represented by LPV systems and how the best description for a given NL system can be found in the LPV system class. This is why we give in this section an overview on the available approaches, comparing and evaluating their modeling concepts.

To set the stage for the upcoming discussion we state the following questions that are intrinsic for the analysis or development of an LPV description with respect to a physical system:

- The scheduling variable, that governs the dynamics of LPV models, has a crucial role in the validity or in the approximation quality of the LPV description. Thus, in the process of formulating a LPV model, one of the most important questions is which variables of the original system can be selected as the scheduling variable in order to obtain an equivalent LPV description.
- Another question is that whether LPV modeling needs to be formulated in terms of systems or in terms of particular representations. The latter concept formulates LPV modeling as an approximation of a given state-space equation, which is a subjective description of the NL system. On the other hand, the former concept focuses on the approximatoion/description of the

original behavior. Thus the latter case provides more freedom and focuses on the “natural aim” of a modeling problem.

These general considerations are the guidelines by which we explore in the following how a reliable model-transformation approach can be formulated to support both identification and control design in the LPV framework.

7.3 Modeling of NL systems in the LPV framework

In the following, an overview is presented about the state-of-the-art methods of approximation/equivalent realization of NL systems by an LPV form. Our intention is to give a general picture about the difficulties and the available solutions of this task. To do so, first we define the class of NL systems we consider. These nonlinear systems characterize the first-principle laws of the behavior that we want to capture in the LPV framework. Then we define a particular class of LPV systems, the so called quasi-LPV systems, that commonly result in the presented modeling approaches. As a next step, we give a SS representation of the introduced NL systems. This representation is often the starting point of the existing LPV modeling methods. We also motivate that using such a representation as a starting point implies the assumption of prior chosen state variables and IO partition, which might restrict the generality of the resulting LPV description. After this, we systematically present the available approaches, sorted into categories.

As first principle laws are commonly (exclusively) available in continuous-time, we restrict our attention in the sequel to this domain. We consider real, finite dimensional, continuous-time NL systems in the following form:

Definition 7.1 (Nonlinear dynamic systems) *A dynamical system $\mathcal{G}_{\text{NL}} = (\mathbb{R}, \mathbb{W}, \mathfrak{B})$ is called a nonlinear, continuous-time, dynamical system, if $\mathbb{W} = \mathbb{R}^{n_{\mathbb{W}}}$, $\mathfrak{B} \subseteq \mathbb{W}^{\mathbb{T}}$, and there exists a nonlinear function $f : \mathbb{R}^{(n+1)n_{\mathbb{W}}} \rightarrow \mathbb{R}^{n_r}$, such that*

$$\mathfrak{B} = \left\{ w \in \mathcal{L}_1^{\text{loc}}(\mathbb{R}, \mathbb{W}) \mid f \left(w, \frac{d}{dt}w, \frac{d^2}{dt^2}w, \dots, \frac{d^n}{dt^n}w \right) = 0, \text{ holds weakly} \right\}.$$

Weak solutions of

$$f \left(w, \frac{d}{dt}w, \frac{d^2}{dt^2}w, \dots, \frac{d^n}{dt^n}w \right) = 0, \quad (7.1)$$

are defined in terms of distributions. Note that Definition 7.1 is wide enough to encompass of many physical systems and represent their dynamic behavior, however it does not describe every system which is non-LTI. This class of systems is considered with the main purpose to illustrate the problem of transformation of first-principle laws to LPV representations. In the sequel we consider the problem of finding an equivalent or a well approximating LPV system with respect to a given \mathcal{G}_{NL} . Without going into details, for the considered class of NL systems we can also define the set of free variables and IO partitions, similarly as in the LTI case. During transformation of these systems to an LPV form, such free signals

are the prime candidates for scheduling or input signals depending on their role in the nonlinear relationship (7.1).

In the LPV framework, models commonly originate from nonlinear dynamic system representations via the gain-scheduling approach. However, linearization of \mathcal{G}_{NL} at different operating points in \mathbb{W} and then interpolating the resulting LTI models by an operating point dependent function implies that the scheduling signal p of the obtained LPV description is dependent on w . In this way, the fundamental assumption of the LPV framework, namely the property of freedom for p does not hold in this case. Therefore, these descriptions are often referred to as *quasi-LPV* systems (see Leith and Leithhead (1999)). In the developed LPV framework, we define these systems in the following way:

Definition 7.2 (Quasi-LPV system) *A parameter-varying dynamical system $\mathcal{G}_P = (\mathbb{T}, \mathbb{P}, \mathbb{W}, \mathfrak{B})$ with signals w and scheduling variable p is called quasi-LPV, if it satisfies Definition 3.2 without p being a free variable, i.e. \mathfrak{B}_p is not a linear subspace of \mathbb{W}^T .*

Note that if some components of p are free signals, then the system is still considered to be quasi-LPV.

During the dawn of the gain-scheduling era, LPV systems have been defined with the concept of exogenous/external and thus free scheduling signal (see Shamma and Athans (1991)), opening the possibility of the later development of popular and theoretically well-founded optimal control solutions for such systems. However in the practical application, this assumption has been commonly neglected, treating LPV models with non-free scheduling signal as if their scheduling signal would be a free variable of the system (Becker et al. 1993). Even if such an assumption introduces conservatism into the model, and thus the control design applied to it, this masking of the dynamical relation made reliable control of many heavily nonlinear processes possible. In the upcoming analysis, we also intend to follow this tradition, by seeking out ways of transformation of NL systems into a quasi-LPV or a true LPV form.

In the existing literature on gain-scheduling based modeling, the class of NL systems of Definition 7.1 is often found to be too broad. Commonly a subclass of state-space realizations is investigated with a prior selection of the state variable x and the IO partition (u, y) :

$$\frac{d}{dt}x = f(x, u), \quad (7.2a)$$

$$y = g(x, u), \quad (7.2b)$$

where f and g are partially differentiable (smooth) functions and $w = \text{col}(u, y)$. Note that in our problem setting, where our goal is to obtain an equivalent or a well approximating LPV system with respect to a given \mathcal{G}_{NL} , prior selection of a state variable may severely restrict the search space, i.e. the transformation properties. Choosing a state variable or an IO partition in a priori sense is also not motivated from the viewpoint of first principle laws as in the laws of physics or chemistry there are no dedicated state variables, nor predefined inputs or outputs.

There are only system variables that are connected by algebraic and differential equations. Therefore, it must be pointed out that any latent-variable-based representation is just a particular and subjective description of the system. As we will see later, such a state-variable based description is not necessary to arrive at an equivalent LPV description of the considered NL system. Additionally, an important concept for the linearization based methods is the equilibrium point of (7.2a), which is defined as $(\mathbf{x}, \mathbf{u}) \in (\mathbb{X} \times \mathbb{U})$ satisfying:

$$0 = f(\mathbf{x}, \mathbf{u}). \quad (7.3)$$

Note that equilibrium points can be stable or unstable depending on the partial derivatives of f in their neighborhood.

Using the previously introduced concepts and notions, the existing LPV modeling approaches fall into the following categories:

7.3.1 Linearization based approximation methods

The family of these methods applies linearization theory on a given SS representation (7.2a-b) of the NL system to obtain local LTI models in a state-space form and then interpolates these models to derive an LPV approximation. Thus, the scheduling of the resulting LPV description is equal to those components of x and u that the linearization is based on. If we introduce selector matrices S_x and S_u , which select these components, then we can write that $p = \text{col}(S_x x, S_u u)$. The following subcategories of these methods are distinguished:

A. Linearization around a set of equilibrium points

Application of classical linearization theory requires that each linearization corresponds to an equilibrium of (7.2a). Thus it is a common approach in the LPV modeling process to use first-order (Jacobian) linearization of (7.2a-b) at a set of equilibrium points. This approach is followed in many works like Åström and Wittenmark (1989); Hyde and Glover (1993); Shamma and Athans (1990); Rugh (1991); Lawrence and Rugh (1995); and Leith and Leithhead (1999). Based on this concept, the LPV model is formulated as follows:

First, the equilibrium points $(\mathbf{x}_i, \mathbf{u}_i) \in (\mathbb{X} \times \mathbb{U})$, $i \in \mathbb{1}_n^r$ of (7.2a) are computed, then

$$A_i = \frac{\partial f}{\partial x}(\bar{\mathbf{p}}_i), \quad B_i = \frac{\partial f}{\partial u}(\bar{\mathbf{p}}_i), \quad C_i = \frac{\partial g}{\partial x}(\bar{\mathbf{p}}_i), \quad D_i = \frac{\partial g}{\partial u}(\bar{\mathbf{p}}_i), \quad (7.4)$$

are obtained with $\bar{\mathbf{p}}_i = \text{col}(\mathbf{x}_i, \mathbf{u}_i)$. Around the equilibrium point $\bar{\mathbf{p}}_i$, the state and output evolution are approximated by applying a first-order Taylor expansion of f and g :

$$\frac{d}{dt}x \approx A_i(x - \mathbf{x}_i) + B_i(u - \mathbf{u}_i), \quad (7.5a)$$

$$y \approx C_i(x - \mathbf{x}_i) + D_i(u - \mathbf{u}_i) + g(\bar{\mathbf{p}}_i). \quad (7.5b)$$

Then (7.5a-b) can be seen as a local LTI model of the system. Define $p = \text{col}(x, u)$ and $\mathbb{P} = \mathbb{X} \times \mathbb{U}$ with a set of normalized interpolation (scheduling) functions $\mathbf{g}_i : \mathbb{P} \rightarrow [0, 1]$, like radial basis, triangular functions, etc. with $\sum_{i=1}^n \mathbf{g}_i(\bar{p}) = 1$ for all $\bar{p} \in \mathbb{P}$. Then, the PV model is formulated as

$$\frac{d}{dt}\check{x} = \sum_{i=1}^n \mathbf{g}_i(p)A_i\check{x} + \sum_{i=1}^n \mathbf{g}_i(p)B_i u - \gamma_x(p), \quad (7.6a)$$

$$\check{y} = \sum_{i=1}^n \mathbf{g}_i(p)C_i\check{x} + \sum_{i=1}^n \mathbf{g}_i(p)D_i u - \gamma_y(p), \quad (7.6b)$$

where \check{x} and \check{y} are the approximations of the original x and y and the remainder terms are given as

$$\gamma_x(p) = \sum_{i=1}^n \mathbf{g}_i(p)(A_i x_i + B_i u_i), \quad (7.7a)$$

$$\gamma_u(p) = \sum_{i=1}^n \mathbf{g}_i(p)(C_i x_i + D_i u_i - g(\bar{p}_i)). \quad (7.7b)$$

It is obvious that for $p(t) = \bar{p}_i$, (7.6a-b) is equivalent with (7.5a-b), i.e. for each equilibrium point the global PV model is equal to the local LTI description. Note that in some cases all the partial derivatives in (7.4) are constants with respect to some elements of x and u . This means that these partial derivatives have the same value for all equilibrium points. This observation implies that the associated elements of x and u can be left out from p , i.e. from the interpolation space to formulate (7.6a-b).

Additionally, it is an important observation that the PV differential equation (7.6a-b) is not an LPV-SS representation as it contains the remainder terms γ_x and γ_u . These remainder terms can not be eliminated in general due to their time dependent nature. In many cases, the remainder terms are eliminated locally in (7.5a-b) by subtracting them from the signal variables (u, y, x) or they are just left out from the expression. Then, the locally altered LTI models are interpolated to obtain a global model. However, this results in an alteration of the state-space as, due to the local transformations, the local states do not have the same meaning any more. This may lead to a complete misfit of the approximation. An exceptional case is when $n = 1$, so the system is linearized in only one point. In such case no interpolation is needed, i.e. $\mathbf{g}_1 = 1$. Then by redefining the state as $\check{x} = x - x_1$, the input as $\check{u} = u - u_1$, and the output as $\check{y} = y - g(\bar{p}_1)$ an LTI-SS approximation of \mathcal{G}_{NL} results via (7.6a-b). Proper elimination of the remainder terms is only available in this case.

In the general sense, linearization in the equilibrium points is a serious restriction that may lead to poor transient performance and inability to preserve stability characteristics of (7.2a-b). Therefore, an adequate approximation capability requires the assumption of slowly varying scheduling. However, such an assumption is often unrealistic as x and u are not slowly varying signals. To improve the approximation capabilities of this approach many alternative linearization meth-

ods have been considered like higher order series-expansion based linearization (Banks and Al-Jurani 1996) or the reformulation of the mean value theorem (Boyd et al. 1994).

Furthermore, interpolation has its own pitfalls as well. If the local LTI models resulting from the linearization are transformed to a canonical form to accomplish interpolation, then the effect of local transformations can completely alter the behavior (see Nobakhti and Munro (2002) for an example). In this way, the resulting LPV representation may not even be able to reproduce basic dynamical aspects of the original NL form (see Example 7.1). Similar errors result if the interpolation is applied through the transfer functions of the local LTI models and then LTI realization theory is applied to obtain the LPV form (see Nichols et al. (1993) for an example).

Example 7.1 (Pitfalls of Interpolation) *In this example, one of the merits of local transformations is illustrated. Assume that the linearization of the NL system has resulted in two local LTI-SS representations*

$$\left[\begin{array}{c|c} \alpha_1 & 1 \\ \beta_1 & 0 \end{array} \right] \text{ if } \bar{p} = 0, \quad \left[\begin{array}{c|c} \alpha_2 & 1 \\ \beta_2 & 0 \end{array} \right] \text{ if } \bar{p} = 1,$$

with $\mathbb{P} = [0, 1]$. If \mathcal{S}_1 represents the LPV approximation of the considered NL system, then a $\mathfrak{R}_{\text{SS}}(\mathcal{S}_1)$ can be formulated as

$$\left[\begin{array}{c|c} A \diamond p & B \diamond p \\ C \diamond p & D \diamond p \end{array} \right] = \sum_{i=1}^2 \left[\begin{array}{c|c} \mathfrak{g}_i(p)\alpha_i & 0.5 \\ \mathfrak{g}_i(p)\beta_i & 0 \end{array} \right], \quad (7.8)$$

where $\mathfrak{g}_1(p) = 1 - p$ and $\mathfrak{g}_2(p) = p$ are the linear interpolation functions. The two local models can also be interpolated based on their IO representation. By using the same interpolation functions, the resulting $\mathfrak{R}_{\text{IO}}(\mathcal{S}_2)$ is

$$\frac{d}{dt}y - (a_0 \diamond p)y = (b_0 \diamond p)u, \quad (7.9)$$

with $a_0 = \sum_{i=1}^2 \mathfrak{g}_i \alpha_i$ and $b_0 = \sum_{i=1}^2 \mathfrak{g}_i \beta_i$. However, the IO representation of $\mathfrak{R}_{\text{SS}}(\mathcal{S}_1)$ reads as:

$$\frac{d}{dt}y - \left(\left(a_0 + \frac{b_0}{b_0} \right) \diamond p \right) y = (b_0 \diamond p)u. \quad (7.10)$$

One can conclude that $\mathfrak{R}_{\text{SS}}(\mathcal{S}_1)$ and $\mathfrak{R}_{\text{IO}}(\mathcal{S}_2)$ are the representations of two different LPV systems \mathcal{S}_1 and \mathcal{S}_2 . This phenomenon clearly emphasizes that interpolation must be carried out in the representation where the linearization was performed, otherwise unexpected alteration of the behavior can occur.

B. Multiple linearizations around a single equilibrium point

This approach originates from the Fuzzy control framework, where it is used to obtain linear *Takagi-Sugeno* (TS) dynamic fuzzy models, which can be viewed as quasi-LPV systems (Korba 2000). The basic idea is to linearize the NL-SS representation at multiple points of $\mathcal{X} \times \mathcal{U}$ around a single equilibrium point. Then the resulting local models are interpolated in a similar fashion as in the previous part. The method leads to a LPV model that performs well during transient operation, because the framework allows some of the local LTI models to be associated with transient operating regimes. If the system stays close to the used equilibrium point, no restrictions concerning slowly varying trajectories is needed. However, a principal disadvantage is that this approach is not suited for NL models with multiple equilibria.

C. Linearization along a nominal trajectory

This approach was introduced in the early 1990s when LPV controllers were typically scheduled in an open-loop sense based on a chosen reference trajectory (intended operation trajectory of the plant) or fixed auxiliary input variables (typical operation trajectories). These user-defined signals were used to describe a nominal trajectory of system operation. Linearizing the NL model along this nominal signal trajectory gives an LPV model (see Shamma and Athans (1990) and Leith and Leithhead (1999) for examples of this approach). It is an advantage of this approach that the resulting LPV description can cover transient operation of the plant along the used nominal trajectory, however such a description also suffers from the drawback that the performance may be poor when the system is operating far away from it. As the time-variation of the system is considered along a pre-chosen trajectory of scheduling variation, the resulting models resemble a LTV system rather than a LPV system.

D. Off-equilibrium linearization around a set of operating points

Linearization of the NL system at points of the state-space that may not be equilibria has been considered in numerous approaches (see (Hunt et al. 1997; Leith and Leithhead 1999; Murray-Smith and Johansen 1997) and Murray-Smith et al. (1999a)) The benefit of this concept is that the transient (off-equilibrium) dynamics of the LPV approximation may be significantly improved. The LPV model is obtained by selecting a set of linearization points $\bar{p}_i = \text{col}(x_i, u_i)$ with $(x_i, u_i) \in \mathbb{X} \times \mathbb{U}$, $i \in \mathbb{I}_1^N$ and using Jacobian linearization of the nonlinear functions f and g around these points in the sense of (7.5a-b). The only difference is that in (7.5a) an extra term $f(\bar{p}_i)$ appears if \bar{p}_i is not an equilibrium point. Then the local models are interpolated as described by (7.6a-b) and the remainder terms are neglected or locally eliminated to form a global LPV model. This approach has the same features as the equilibrium-points-based linearization with all the pitfalls of interpolation and local state transformations. An additional problem rises however from the selection of linearization points $\{\bar{p}_i\}_{i=1}^n$. Equidistant selection on the space $\mathbb{X} \times \mathbb{U}$ may seem tempting, but it might happen that due to the dynamical changes of \mathcal{G}_{NL} , a non-equidistant selection with dense samples in specific regions of $\mathbb{X} \times \mathbb{U}$ can lead to far better approximations (see Murray-Smith et al. (1999b) for details).

7.3.2 Multiple model design procedures

Multiple model design techniques investigate the LPV approximation of the NL system given by the state-space representation

$$\frac{d}{dt}x = A(x, u)x + B(x, u)u, \quad (7.11a)$$

$$y = C(x, u)x + D(x, u)u. \quad (7.11b)$$

The LPV modeling of (7.11a-b) is accomplished by selecting a set of interpolation functions $\{g_i\}_{i=1}^n$. Then the model approximation problem becomes a search for

a set of constant matrices $\{(A_i, B_i, C_i, D_i)\}_{i=1}^n$ such that the nonlinear functions (A, B, C, D) are approximated optimally by the weighted sum of the constant matrices, like

$$A(x, u) \approx \sum_{i=1}^n g_i(p) A_i, \quad \text{where } p = \text{col}(x, u). \quad (7.12)$$

However, these kind of techniques are most often considered to be model reduction tools rather than LPV model transformation methods as with the scheduling signal $p = \text{col}(x, u)$ the SS equations (7.11a-b) already define a quasi-LPV model. Notable approaches that fall into this category are the orthogonal decomposition based methods like Bos et al. (2005); Setnes and Babuška (2001) and Yen and Wang (1999), the convex polytope methods like Kanev (2006) and Korba (2000), and the radial basis functions based optimization techniques of Kiriakidis (2007) and Verdult (2002).

7.3.3 Substitution based transformation methods

Methods of this category use substitution techniques on an available SS representation of the NL system to generate a quasi-LPV model without the need of approximation. The PV coefficients appear as substituted functions of (x, u) and the resulting scheduling is $p = \text{col}(S_x x, S_u u)$, where S_x and S_u are the selector matrices of the components of (x, u) used for the substitution. The subcategories of these approaches are the following:

A. The “state-transformation” method

The “state-transformation” method was first introduced by Shamma and Cloutier (1993) followed by many successful applications in aerospace engineering (see Papageorgiou et al. (2000); Shin (2000) and Papageorgiou (1998)). A class of nonlinear systems that qualifies for this method is described by the following SS equation:

$$\frac{d}{dt} \begin{bmatrix} x_1 \\ x_2 \end{bmatrix} = \begin{bmatrix} f_1(x_1) \\ f_2(x_1) \end{bmatrix} + \begin{bmatrix} A_{11}(x_1) & A_{21}(x_1) \\ A_{21}(x_1) & A_{22}(x_1) \end{bmatrix} \begin{bmatrix} x_1 \\ x_2 \end{bmatrix} + \begin{bmatrix} B_1(x_1) \\ B_2(x_1) \end{bmatrix} u, \quad (7.13)$$

where $x = \text{col}(x_1, x_2)$, $(A_{11}, A_{12}, A_{21}, A_{22})$ and (B_1, B_2) are nonlinear matrix functions. Additionally, f_1, f_2 represent nonlinear matrix function terms which cannot be written as $f_1(x_1) = \tilde{f}_1(x_1)x_1$ with \tilde{f}_1 bounded in the origin. Assume that there exist differentiable functions γ_x and γ_u , such that:

$$\begin{bmatrix} 0 \\ 0 \end{bmatrix} = \begin{bmatrix} f_1(x_1) \\ f_2(x_1) \end{bmatrix} + \begin{bmatrix} A_{11}(x_1) & A_{12}(x_1) \\ A_{21}(x_1) & A_{22}(x_1) \end{bmatrix} \begin{bmatrix} x_1 \\ \gamma_x(x_1) \end{bmatrix} + \begin{bmatrix} B_1(x_1) \\ B_2(x_1) \end{bmatrix} \gamma_u(x_1), \quad (7.14)$$

holds for all $x_1 \in \mathcal{L}_1^{\text{loc}}(\mathbb{R}, \mathbb{R}^{n_1})$, which are the solutions of (7.13), i.e. for which there exist signals $(x_2, u) \in \mathcal{L}_1^{\text{loc}}(\mathbb{R}, \mathbb{R}^{n_2} \times \mathbb{U})$ such that (7.13) is satisfied. Subtracting

(7.14) from (7.13) with some rearrangement of the signals yields:

$$\begin{aligned} \frac{d}{dt} \begin{bmatrix} x_1 \\ \check{x}_2 \end{bmatrix} &= \begin{bmatrix} 0 & A_{12}(x_1) \\ 0 & A_{22}(x_1) - \frac{\partial \gamma_x(x_1)}{\partial x_1} A_{12}(x_1) \end{bmatrix} \begin{bmatrix} x_1 \\ \check{x}_2 \end{bmatrix} + \\ &+ \begin{pmatrix} B_1(x_1) \\ B_2(x_1) - \frac{\partial \gamma_x(x_1)}{\partial x_1} B_1(x_1) \end{pmatrix} \check{u}, \end{aligned} \quad (7.15)$$

where $\check{x}_2 = x_2 - \gamma_x(x_1)$ and $\check{u} = u - \gamma_u(x_1)$. In this way the state-transformation method has transformed the state-equation (7.13) into the quasi-LPV form (7.15) with scheduling signal $p = x_1$. Note that there are no approximations involved in this procedure, but it is only applicable to a limited class of NL-SS representations and often the resulting LPV representation is non-minimal. Furthermore, no constructive procedure to find γ_x and γ_u is available.

B. Substitution by virtual scheduling

Based on ad hoc mathematical treatment, some nonlinear equations in the form of (7.2a-b) can be rewritten as (7.11a-b). Then, assigning virtual scheduling signals for each nonlinear function element of the resulting matrix functions (A, B, C, D) , a quasi-LPV SS representation of the system results with static linear dependence. Due to the several possibilities of assignment, the result of the transformation is non-unique. Commonly, the methods that fall into this category can only be applied for specific NL systems without any generality. In most cases, the number of associated scheduling signals increases rapidly with the system order and it remains to the skill and insight of the modeler to find an economical representation. Despite its ad-hoc nature, this method is preferred for mildly-nonlinear systems as it involves no approximation of the system dynamics, delivering efficient modeling solutions in many applications (see (Gáspár et al. 2007; Tóth and Fodor 2004) and Rugh and Shamma (2000) for examples). At the same time, many pitfalls are present for unexperienced users. To illustrate one of these pitfalls, consider

$$\frac{d}{dt}x = x^2 - 1, \quad (7.16)$$

and represent this differential equation in a LPV form

$$\frac{d}{dt}x = px, \quad \text{where } p = x - \frac{1}{x}. \quad (7.17)$$

Seemingly, the two differential equations are equivalent. However, the resulting behaviors are different for $x(t) = 0$. Thus using the LPV model (7.17), to design a stabilizing LPV controller for the original NL system is dangerous as it is unpredictable how the closed loop system will behave when x approaches 0.

C. Velocity based scheduling technique

The velocity based method of Leith and Leithhead (1998a,b) associates a linear system with every operating point of a NL system, rather than just the equilibrium

points or pre-specified reference points. This is called *local linear equivalence* in Leith and Leithhead (1996). Assume that a representation of the NL system is given in the form

$$\frac{d}{dt}x = Ax + Bu + \check{f}(\gamma(x, u)), \quad (7.18a)$$

$$y = Cx + Du + \check{g}(\gamma(x, u)), \quad (7.18b)$$

where (A, B, C, D) are constant matrices, $\check{f} : \mathbb{R}^n \rightarrow \mathbb{R}^{n \times}$, $\check{g} : \mathbb{R}^n \rightarrow \mathbb{R}^{n \nu}$ are partially differentiable nonlinear functions, and the function γ is given by

$$\gamma(x, u) = E_x x + E_u u, \quad (7.19)$$

where $E_x \in \mathbb{R}^{n \times n \times}$ and $E_u \in \mathbb{R}^{n \times n \nu}$. This reformulation of (7.2a-b) can always be achieved. Introduce $p = \text{col}(x, u)$ as the scheduling signal. Differentiating equations (7.18a-b) gives the following alternative reformulation:

$$\frac{d^2}{dt^2}x = \left(A + \frac{\partial}{\partial \gamma} \check{f}(\gamma(p)) E_x \right) \frac{d}{dt}x + \left(B + \frac{\partial}{\partial \gamma} \check{f}(\gamma(p)) E_u \right) \frac{d}{dt}u, \quad (7.20a)$$

$$\frac{d}{dt}y = \left(C + \frac{\partial}{\partial \gamma} \check{g}(\gamma(p)) E_x \right) \frac{d}{dt}x + \left(D + \frac{\partial}{\partial \gamma} \check{g}(\gamma(p)) E_u \right) \frac{d}{dt}u. \quad (7.20b)$$

By restricting the behavior of (7.2a-b) to signals that are differentiable, the set of signals satisfying (7.20a-b) is equivalent with the solution set of (7.2a-b) for appropriate initial conditions. Substitution by $\check{x} = \frac{d}{dt}x$, $\check{u} = \frac{d}{dt}u$, and $\check{y} = \frac{d}{dt}y$ delivers a quasi-LPV form of (7.20a-b), suggesting the conclusion that every nonlinear system (7.18a-b) can be reformulated in this way as an quasi-LPV SS representation. However, by masking differentiation of the system signals into new variables, the behavior of the resulting quasi-LPV system is different. Additionally, in the practical use of the suggested LPV description, if instead of $\frac{d}{dt}u$ and $\frac{d}{dt}y$, only the measurements of u and y are available in the physical system, the amplification of noise is inevitable by the differentiation of u and y . Such a phenomenon can have serious impact on identification or control of the underlying system. Moreover, there is little hope of controlling the original NL system only via its differentiated description.

D. Function substitution

Another way of quasi-LPV model generation leads through the idea of approximating the nonlinear functions f and g in (7.2a-b) by a linear combination of scheduling dependent functions multiplied by x and u . To decompose nonlinear functions in this form, an equilibrium point is used, with the result that the generated LPV model is strongly dependent on this single reference point. The formulation is as follows:

Consider the NL system described by the state-equation

$$\frac{d}{dt}x = A(x_1)x + B(x_1)u + f(x_1), \quad (7.21)$$

where $x = \text{col}(x_1, x_2)$. To perform the substitution method, choose an equilibrium point $(\bar{x}_1, \bar{x}_2, \bar{u})$ and transform the variables as

$$\check{x}_1 = x_1 - \bar{x}_1, \quad \check{x}_2 = x_2 - \bar{x}_2, \quad \check{u} = u - \bar{u}. \quad (7.22)$$

Using these new variables, (7.21) can be rewritten as

$$\frac{d}{dt} \begin{bmatrix} \check{x}_1 \\ \check{x}_2 \end{bmatrix} = A(x_1) \begin{bmatrix} \check{x}_1 \\ \check{x}_2 \end{bmatrix} + B(x_1)u + \check{f}(x_1), \quad (7.23)$$

where

$$\check{f}(x_1) = A(x_1) \begin{bmatrix} \bar{x}_1 \\ \bar{x}_2 \end{bmatrix} + B(x_1)\bar{u} + f(x_1). \quad (7.24)$$

The next step is to reformulate \check{f} into a PV functional form such that

$$\check{f}(x_1) \approx \Gamma(p)\check{x}_1, \quad (7.25)$$

where $p = x_1$ and Γ is an unknown matrix function. Then, the goal of the modeling approach is to determine Γ such that the approximation (7.25) is adequate for every trajectory of x_1 . It is obvious that solutions of (7.25) are not unique since this is an under-determined problem. In many applications of this idea like Tan (1997); Tan et al. (2000); Shin et al. (2002); and Marcos and Balas (2004), Γ is calculated based on a particular functional parameterization, to minimize the approximation error of (7.25) on the entire operating envelope \mathbb{X}_1 . The solution of this minimization problem is obtained by linear programming. Then, the final quasi-LPV approximation of (7.21) is given as

$$\frac{d}{dt} \check{x} = (A(p) + \begin{bmatrix} \Gamma(p) & 0 \end{bmatrix}) \check{x} + B(p)\check{u} \quad (7.26)$$

with $p = x_1$. The behavior of (7.26) can approximate the behavior of the original NL representation if (7.25) is satisfied adequately. A disadvantage of this method is the strong dependence on the equilibrium point (with different reference points different representations can be obtained) and that the model may not capture the local stability of the original NL model at other equilibrium points. In Shin (2007), an improved version of the method has been developed to preserve local stability over the entire operation envelope. In this modified approach, the search for Γ is formulated as a bilinear-matrix-inequality based optimization problem including stability constraints.

7.3.4 Automated model transformation

Automated model transformation is based on the exploration of all possible ways of reformulating the NL system as a quasi-LPV model with the smallest possible conservatism. Such a technique can also be seen as a substitution method. Recently the approach of Kwiatkowski et al. (2006) has appeared in this context, formulating the basic idea of this approach as an algorithm. The proposed procedure consists of the following steps:

Algorithm 7.1 (Automated model transformation) (Kwiatkowski et al. 2006)

Step 1. Write (7.2a) as a summation of additive nonlinear terms (summands) for each row separately. This refers to the symbolic separation of nonlinear terms that add together to form for example the i^{th} row of f as:

$$[f(x, u)]_i = \sum_{j=1}^{n_i} f_{ij}(x, u). \quad (7.27)$$

Step 2. Each summand is written in a rational form and the numerator is factorized as the product of powers of state and input elements and a coefficient γ_{ij} that is a non-factorizable function of x and u .

$$f_{ij}(x, u) = \frac{\gamma_{ij}(x, u) \prod_{k=1}^{n_x} x_k^{n_{1k}} \prod_{l=1}^{n_u} u_l^{n_{2l}}}{\varphi(x, u)}. \quad (7.28)$$

Step 3. The summands are distinguished based on that their numerators are factorizable, i.e. not all powers n_{1k} and n_{2l} in (7.28) are zero.

Step 4. Summands are assigned to state-space matrices A and B . If the summand is non-factorizable, then it is multiplied by $\frac{1}{x_k}$ or $\frac{1}{u_l}$ to be able to write it for example as

$$f_{ij}(x, u) = \frac{f_{ij}(x, u)}{x_k} x_k. \quad (7.29)$$

The obtained expression (7.29) is assigned to the k^{th} state as a coefficient $\alpha_{ijk}(x, u) = \frac{f_{ij}(x, u)}{x_k}$ in the i^{th} row and k^{th} column of A . This assignment gives $n_x + n_u$ possibilities depending on which component of x or u is used to make the division in (7.29).

If the summand f_{ij} is factorizable, then it can be divided by any element x_k or u_l which has nonzero power in (7.28), in order to assign it to a state-matrix. For example if $n_{21} > 0$ in (7.28), then by dividing f_{ij} with u_1 the resulting function is

$$\beta_{ij1}(x, u) = \frac{f_{ij}(x, u)}{u_1} = \frac{\gamma_{ij}(x, u) \prod_{k=1}^{n_x} x_k^{n_{1k}} \prod_{l=2}^{n_u} u_l^{n_{2l}}}{\varphi(x, u)} u_1^{n_{21}-1}. \quad (7.30)$$

This function can be assigned to u_1 as a coefficient in the i^{th} row and the 1^{th} column of B . For each summand, this gives as many assignment possibilities as the number of states and input components in the product expression with non-zero power.

Step 5. Each of the assigned coefficient functions, i.e. $\{\alpha_{ijk}\}$ and $\{\beta_{ijk}\}$, are associated with a virtual scheduling signal p_l . The SS matrices are formed as the linear combination of these virtual scheduling signals (direct assignment). To avoid a large number of virtual scheduling signals associated directly

with $\{\alpha_{ijk}\}$ and $\{\beta_{ijk}\}$, alternatively the linear combination of these function expressions in each element of the resulting A and B is recognized as a virtual scheduling signal (superposition). This results in a LPV state-space representation.

Step 6. By using all assignment possibilities, a set of LPV-SS representations are generated, each corresponding to (7.2a). These representations are tested for complexity and the most adequate LPV description is selected by the user. The exact way of this test and the selection of the most suitable assignment is not formulated in the approach. Thus, these tests remain to the intuition of the user.

The same procedure can be executed for the output equation (7.2b) as well. The whole approach depends on how well the simplification of the nonlinear terms can be archived. As simplification of symbolic terms is not unique in general, the complexity of the resulting model can vary with different symbolic solvers (see Hecker and Varga (2006) for an overview of the required symbolic manipulation techniques). A more serious problem, which has been already mentioned in the linearization part, arises when non-factorizable terms are divided by signal components to achieve the form (7.29). Such operations can result in the alteration of the behavior around the origin. It can also happen that no element of u can be lifted out from any summands in the form of (7.28) and thus the generation procedure results in an autonomous quasi-LPV description.

Another technique that falls into this category develops an automated transformation of a nonlinear model to an *Linear Fractional Transform* (LFT) form by using symbolic manipulation techniques (see (Hecker and Varga 2006; Varga et al. 1998)). A big disadvantage of this method is that it assumes the nonlinear model to be in the form (7.11a-b). In this way it avoids the crucial part of the modeling, namely the generation of the quasi-LPV form (7.11a-b). This technique shows resemblance with other multiple modeling techniques and implements a particular way of model reduction with respect to LFT forms.

7.3.5 Summary of existing techniques

In conclusion, the existing techniques for transformation of NL systems to a quasi-LPV form are either based on linearization-based approximation or substitution techniques. Linearization techniques are commonly easily applicable for this purpose, but they suffer from serious disadvantages in terms of non-eliminatable affine reminder terms, pitfalls of interpolation, selection of adequate linearization points, and the loss of general representation of the nonlinear dynamics. On the other hand, substitution techniques are based on mathematical manipulations that are only applicable for some class of NL systems. Commonly they preserve the original dynamic behavior, however for the general class of NL systems they may result in loss of validity or even stability (e.g. division by signal elements).

A common feature of all approaches is that they use a SS representation of the system as a starting point, thus they try to achieve good approximation with respect to a prior chosen state variable. As a consequence the scheduling variable of the resulting LPV description is composed from the priori chosen state and input variables. This restriction can severely reduce the search-space where an adequate LPV representation of the original NL behavior can be found as rewriting (7.2a-b) to another state-basis may result in a simplified/better transformation to a LPV form.

All of the approaches do not pay attention how the scheduling variable is chosen and what kind of effects a particular choice of p has on the obtained LPV behavior. Seemingly it does not matter that components of x which are inner variables or components of u which are free variables are used for p .

As a general conclusion, existing transformation possibilities to a LPV form are conservative, non-unique, and the validity of the resulting model is based on the skill of the user. On the other hand, to support LPV identification of physical systems, the LPV modeling phase must be accomplished carefully, exploring the best possibility of transformation of the first principle laws into an LPV form, without ad hoc selection of state signals and scheduling variables. Based on this conclusion, in the next section, the possibilities to accomplish this task are investigated and a model transformation procedure is proposed, that can tackle this problem using the powerful theoretical framework of the developed LPV behavioral approach.

7.4 Translation of first principle models to LPV systems

As a next step, a transformation method is investigated that converts first principle laws represented by (7.1) into a LPV *kernel* (KR) representation. The procedure gives the freedom to consider all possibilities of transformation, not restricted by preselected state or IO partition or particular formulation of the nonlinear dynamical relationship like a SS representation. In fact, the method explores all possible transformations that are applicable for general NL dynamical systems, to convert the specific NL behavior into an LPV behavior. Then the obtained LPV-KR representations are categorized by complexity and transformed to an LPV-SS or IO realization based on the equivalence transformation theory of Chapter 3. To assist LPV model structure selection, the discretization theory developed in Chapter 6 is applied to obtain DT descriptions of the original behavior.

The developed transformation mechanism is based on similar concepts like the approach of Kwiatkowski et al. (2006), however the proposed method is constructed in a more structured way, where the validity of the transformation is guaranteed in the applied formulas. In the following, a brief outline of the procedure is presented to give insight into the theoretical concept instead of technicalities. First we define the exact problem setting we consider.

7.4.1 Problem statement

Consider a NL dynamical system $\mathcal{G}_{\text{NL}} = (\mathbb{R}, \mathbb{W}, \mathfrak{B})$ with signal space $\mathbb{W} = \mathbb{R}^{n_{\text{w}}}$ and behavior $\mathfrak{B} \subseteq \mathbb{W}^{\mathbb{T}}$, where \mathfrak{B} is represented by (7.1). Assume that f is a meromorphic function: $f \in \mathcal{R}^{n_{\text{r}} \times 1}$. Then as a short hand notation, introduce

$$f \diamond w = f \left(w, \frac{d}{dt}w, \frac{d^2}{dt^2}w, \dots, \frac{d^n}{dt^n}w \right), \quad (7.31)$$

as the evaluation of f along the signal trajectory $w \in \mathfrak{B}$. In this way, we associate variables of f with specific signal elements of w and their derivatives, similar to the mechanism of Chapter 3. Furthermore, assume that each element of the variable w is of prime interest to the user (they are non-latent variables) and the functional relation described by f can not be simplified without changing the behavior \mathfrak{B} . The latter assumption means that (7.1) is minimal in the sense that no equation can be eliminated from (7.1) by simple row operations like addition or multiplication by functional terms, similar to left-side unimodular transformations in the LPV case. Additionally, if for any $i \in \mathbb{I}_1^{n_{\text{w}}}$ there exists a $\hat{f} \in \mathcal{R}^{n_{\text{r}} \times 1}$, a partition $w = \text{col}(w_1, w_2)$ with $\dim(w_2) = n_2$ and a invertible holomorphic function $g : \mathbb{R}^{n_{\text{w}}} \rightarrow \mathbb{R}^{n_2}$ such that

$$f \diamond w = \hat{f} \diamond \text{col}(w_1, g(w)), \quad (7.32)$$

for all $w \in \mathfrak{B}$ and \hat{f} is a less complicated function than f , then redefine w_2 as $g(w)$ to achieve simplification of f . This operation is similar to right-side unimodular transformations in the LPV case. By applying such a simplification, the resulting behavior is isomorphic with \mathfrak{B} . Now we define our transformation problem as follows:

Problem 7.1 (Translation of dynamic NL systems to LPV systems) *For a given NL dynamical system $\mathcal{G}_{\text{NL}} = (\mathbb{R}, \mathbb{R}^{n_{\text{w}}}, \mathfrak{B})$ with signal variable w , find an LPV system $\mathcal{S}' = (\mathbb{R}, \mathbb{P}', \mathbb{W}', \mathfrak{B}')$ with signal variable w' and scheduling variable p' such that there exist selector matrices $S_{\text{p}}, S_{\text{w}} \in \mathbb{R}^{n_{\text{r}} \times n_{\text{w}}}$ satisfying $w' = S_{\text{w}}w$ and $p' = S_{\text{p}}w$ and it holds that*

$$w \in \mathfrak{B} \cap \mathcal{C}^{\infty}(\mathbb{R}, \mathbb{W}) \Leftrightarrow (w', p') \in \mathfrak{B}' \cap \mathcal{C}^{\infty}(\mathbb{R}, \mathbb{W}' \times \mathbb{P}').$$

Based on this problem setting, we are looking for such an LPV system that has a behavior equal to the behavior of the original NL system.

7.4.2 The transformation algorithm

In the following, an algorithm is applied on the simplified differential equation to explore all possibilities of its transformation to an LPV form and in this way to solve Problem 7.1. We follow a similar strategy as the algorithm of Kwiatkowski et al. (2006) but in a different setting. First we separate the rows of f into summands. Then we factorize the nominator of these summands in a specific way to

lift out signal variables in a product form. Next we collect all factorization possibilities and their associated coefficients in terms of factors into a decision tree. By selecting a route in the resulting tree we assign elements of w to signals or scheduling variables and use their associated coefficients to form a LPV-KR representation. In the process we assume that all summands are factorizable. This assumption is relaxed later. The proposed algorithm reads as follows:

Algorithm 7.2 (Translation to LPV-KR representations)

Step 1. Write f as a summation of additive functional terms (summands) for each row separately. The i^{th} row is written as

$$[f \diamond w]_i = \sum_{j=1}^{n_i} f_{ij} \diamond w, \quad (7.33)$$

where each $f_{ij} \in \mathcal{R}$ is not separable to further summands. This assumes that ideal symbolic recognition of additive terms is available. The results of this operation are unique up to multiplication by a constant. Store the summands in a graph structure, as shown in Figure 7.1 where each node represents a specific summand or a row of f .

Step 2. Each summand is written in the form of

$$f_{ij} = \frac{\hat{g}_{ij}}{\check{g}_{ij}}, \quad (7.34)$$

where $\hat{g}_{ij}, \check{g}_{ij} : \mathbb{R}^{(n+1)n_w} \rightarrow \mathbb{R}$ are coprime holomorphic functions with n denoting the highest derivative order in (7.31). Such a formulation is again unique up to multiplication by a constant.

Step 3. For each $i \in \mathbb{I}_1^{n_r}$, $j \in \mathbb{I}_1^{n_i}$, $k \in \mathbb{I}_1^{n_w}$, and $l \in \mathbb{I}_0^n$, it is investigated if the summand f_{ij} is factorizable to the form

$$f_{ij} \diamond w = \left(\frac{\check{g}_{ijkl}}{\check{g}_{ij}} \diamond w \right) \frac{d^l}{dt^l} w_k, \quad (7.35)$$

where $\check{f}_{ijkl} : \mathbb{R}^{n_w} \rightarrow \mathbb{R}$ is holomorphic. Contrary to Algorithm 7.1, factorization in this case only involves first-order product terms, as any higher order relation is not interesting for the further procedure. Denote

$$\check{f}_{ijkl} = \frac{\check{g}_{ijkl}}{\check{g}_{ij}}. \quad (7.36)$$

Note that $\check{f}_{ijkl} \in \mathcal{R}$. Assume for the moment that each f_{ij} can be factorized by at least one $\frac{d^l}{dt^l} w_k$. The results of the factorization are stored in the graph structure of Figure 7.1. In this graph each node representing a summand f_{ij}

gets a leaf for each $\frac{d^l}{dt^l} w_k$ it can be factorized with. The edges, that connect the leaves to their associated summand, receive a label, which is the set of the specific variables $\{w_1, \dots, w_n\}$ that are involved in the remaining \check{f}_{ijkl} expression. All other edges of the graph get a label of an empty set. Note that leaves with an edge having an empty set label are the linear terms of the nonlinear equation. The resulting graph describes a decision tree.

Step 4. As a next step, possible LPV-KR representations are generated based on the previously developed decision tree. All possible routes in this graph are considered, which involve all nodes and a single leaf for each node if it has one. Routes are only considered to be different if they consist of different leaves. This yields all realization possibilities of (7.1) as a PV differential equation in the following way. For a specific route (see Figure 7.1), compute the union of the sets of variables associated with a label along the edges of the route. This gives a subset of all variables $\{w_1, \dots, w_{n_W}\}$. These variables are recognized as scheduling signals and denoted as $\{p_1, \dots, p_{n_P}\}$ where $n_P \leq n_W$. Define $p = [p_1 \dots p_{n_P}]$ as the scheduling variable for the specific route. Additionally, let \mathbb{P} be the projected subspace of \mathbb{W} with respect to p . Consider all leaves in the route. Define index sets \mathcal{I}_{ikl} , containing all indexes $j \in \mathbb{I}_1^{n_i}$ for which the node, associated with the summand f_{ij} , has a leaf of $\frac{d^l}{dt^l} w_k$ in the considered route. For each leaf in the route, collect the remainder terms $\{\check{f}_{ijlk}\}$ of the factorization into meromorphic coefficient functions $r_l \in \mathcal{R}^{n_r \times n_W}$, $l \in \mathbb{I}_0^n$ where

$$[r_l]_{ik} = \sum_{j \in \mathcal{I}_{ikl}} \check{f}_{ijlk}, \quad \forall (i, k) \in \mathbb{I}_1^{n_r} \times \mathbb{I}_1^{n_W}. \quad (7.37)$$

With the resulting coefficients $\{r_i\}_{i=1}^n$ the NL differential equation (7.1) is formulated as an LPV-KR representation:

$$\left(R \left(\frac{d}{dt}\right) \diamond p\right) w = \sum_{i=0}^n (r_i \diamond p) \frac{d^i}{dt^i} w = 0, \quad (7.38)$$

where $R \in \mathcal{R}[\xi]^{n_r \times n_W}$. Now define \check{w} as the vector containing the subset of the variables $\{w_1, \dots, w_{n_W}\}$, such that for each variable w_i in \check{w} , there is a leaf in the route where the label of the leaf contains w_i or its derivative. Those signals that do not satisfy this property are simply presented with 0 weights in (7.38), thus they do not participate in the signal relation as variables. To eliminate such superfluous terms, (7.38) is rewritten in terms of \check{w} by deleting from R the zero columns associated with the additional variables. Furthermore the signal space associated with \check{w} is defined as the projected subspace of \mathbb{W} with respect to the variables presented in \check{w} .

Step 5. As a result of the previous step, numerous PV differential equation forms of (7.1) are formulated based on all possible routes in the graph structure. However, it is not guaranteed that all of them preserve the dynamical aspects of the original nonlinear behavior \mathfrak{B} . To ensure validity of the transformation, the freedom of the remaining signal variables \check{w} for each PV descrip-

tion has to be checked. If for every IO partition $\check{w} = (\check{u}, \check{y})$ of the resulting LPV-KR representation $\mathfrak{R}_K(\mathcal{S})$, there exists an IO partition $w = (u, y)$ for the original NL system such that $\check{y} = y$ and the elements of \check{u} are a subset of u and the maximal order of derivatives of y in each row of $\mathfrak{R}_K(\mathcal{S})$ are the same as in f , then the LPV representation can be considered as a valid transform of the original system. Otherwise alteration of the dynamical behavior occurred during the process by masking essential dynamics into coefficients. If it is also true for every IO partition of $\mathfrak{R}_K(\mathcal{S})$, that $u = \text{col}(p, \check{u})$, meaning that all elements of p are free variables of the original system and they are independent from \check{u} , then the model corresponds to a true LPV system \mathcal{S} , not just a quasi-LPV, and it is a prime candidate for representing the original system behavior.

Step 6. The resulting LPV representations can be ranked based on the corresponding routes in the graph. Representations which involve the smallest cost in terms of the number of variables associated with scheduling signals give the simplest models of the NL system. From these candidates, representations with free scheduling signals have priority. Further distinction can be the maximal order of derivatives of the leafs. Based on these, the resulting valid representations can be ordered in terms of complexity, to assist selection by the user.

For each LPV-KR representation, that has been found to be a valid representation of \mathcal{G}_{NL} , the PV behavior can be considered to be equal with the original NL behavior \mathfrak{B} . Then the most attractive representation can be selected by the user based on the complexity ordering derived in Step 6. In this way, a solution for our transformation problem, i.e. for Problem 7.1 is obtained. Next, the behavioral approach is applied on the chosen representation to obtain a full row rank KR representation together with an SS or IO realization of the resulting LPV system. With the introduced discretization theory, this methodology serves as a model selection tool for DT-LPV identification routines.

Example 7.2 (Transformation of an NL model to LPV) Consider the nonlinear system $\mathcal{G}_{NL} = (\mathbb{R}, \mathbb{R}^4, \mathfrak{B})$ with $w^T = [w_1 \ w_2 \ w_3 \ w_4]$ in the form:

$$f \left(w, \frac{d}{dt}w, \frac{d^2}{dt^2}w \right) = 0,$$

where

$$f \diamond w = \left[\begin{array}{c} \overbrace{w_1 \cos^2(w_3)}^{f_{11}} + \overbrace{\sin^2(w_3) \frac{d}{dt}w_1}^{f_{12}} + \overbrace{2w_3w_4}^{f_{13}} + \overbrace{2 \frac{d}{dt}w_2}^{f_{14}} + \overbrace{\left(\frac{d}{dt}w_2 \right) \frac{d}{dt}w_3}^{f_{15}} + \overbrace{w_3 \frac{d^2}{dt^2}w_1}^{f_{16}} \\ \underbrace{w_3 \frac{d}{dt}w_1}_{f_{21}} + \underbrace{w_2}_{f_{22}} \end{array} \right].$$

Note that for this nonlinear system the only available IO partition is $y = \text{col}(w_1, w_2)$ and $u = \text{col}(w_3, w_4)$. This is easy to show by writing the equation in the second row as

$$w_2 = -w_3 \frac{d}{dt} w_1,$$

and substituting it into the first row of f . Then a differential equation results where only the derivatives of w_1 appear. Thus w_1 is an obvious output of the system and therefore w_2 is also an output as its trajectory is described by the used substitution rule. The remaining variables w_3 and w_4 are free in the resulting description and thus they are the obvious inputs of the system. However, the second equation written as

$$w_3 = -w_2 / \frac{d^2}{dt^2} w_1,$$

cannot be used for substitution as it would exclude trajectories of w_1 with $\frac{d}{dt} w_1 = 0$. Hence w_3 cannot be the output of the system instead of w_2 .

Additionally, the nonlinear equations of the above given representation have already been separated to minimal summand terms and it can be shown that no further symbolic simplification of the equations is possible. A further property is that all summand terms are factorizable. By applying the decision tree generation procedure described in the previous part, the resulting tree is presented in Figure 7.1. This completes Step 1 to Step 3 of the proposed algorithm.

In terms of Step 4, now we generate all possible routes that contain all nodes and one leaf for each node. There are $2^5 = 32$ possibilities. One of these routes is given by bold lines in Figure 7.1. By using this specific route, a LPV-KR representation is generated in terms of Step 4. The resulting scheduling variable is the collection of variables in the labels along the route: $p = w_3$ and the new signal variable is the collection of variables of the leafs along the route: $\tilde{w} = [w_1 \ w_2 \ w_4]$. Then by these choices, the LPV-KR representation has the following form

$$\begin{bmatrix} \cos^2(p_1) & 0 & 2p_1 \\ 0 & 1 & 0 \end{bmatrix} \tilde{w} + \begin{bmatrix} \sin^2(p_1) & 2 + \frac{d}{dt} p_1 & 0 \\ p_1 & 0 & 0 \end{bmatrix} \frac{d}{dt} \tilde{w} + \begin{bmatrix} p_1 & 0 & 0 \\ 0 & 0 & 0 \end{bmatrix} \frac{d^2}{dt^2} \tilde{w} = 0.$$

Note that the IO partition of the obtained LPV-KR representation is $y = [w_1 \ w_2]$ and $u = w_4$, and the maximal order of the derivatives of w_1 and w_2 in the representation is the same as in f , thus it corresponds a valid LPV model of the original nonlinear system. As the chosen scheduling variable is a free variable in the original system and is independent from \tilde{w} , the obtained representation corresponds to a true (non-quasi) LPV system. This completes Step 5 of the proposed algorithm.

Another choice of route is similar to the previous one except taking the right branch at f_{16} . The resulting scheduling variable is $p = [w_3 \ w_1]$ and the signal variable is $\tilde{w} = [w_1 \ w_2 \ w_3 \ w_4]$. Then by these choices, the following LPV-KR representation results:

$$\begin{bmatrix} \cos^2(p_1) & 0 & \frac{d^2}{dt^2} p_2 & 2p_1 \\ 0 & 1 & 0 & 0 \end{bmatrix} \tilde{w} + \begin{bmatrix} \sin^2(p_1) & 2 + \frac{d}{dt} p_1 & 0 & 0 \\ p_1 & 0 & 0 & 0 \end{bmatrix} \frac{d}{dt} \tilde{w} = 0.$$

A valid IO partition of the obtained LPV-KR representation is $y = \text{col}(w_1, w_2)$ and $u = (w_3, w_4)$, the IO partition of the original nonlinear system. However, the maximal order of derivatives with respect to w_1 is 1. This means that the dynamics of f has been simplified, i.e. masked into coefficient dependence, during the transformation process. Thus the resulting LPV representation is not a valid representation of the nonlinear system.

A third choice is to use the route given with bold lines but to take the left branch at f_{13} . The resulting scheduling variable is $p = [w_3 \ w_4]$ and the signal variable is $\tilde{w} = [w_1 \ w_2 \ w_3]$. Then by these choices, the following LPV-KR representation results:

$$\begin{bmatrix} \cos^2(p_1) & 0 & 2p_2 \\ 0 & 1 & 0 \end{bmatrix} \tilde{w} + \begin{bmatrix} \sin^2(p_1) & 2 + \frac{d}{dt} p_1 & 0 \\ p_1 & 0 & 0 \end{bmatrix} \frac{d}{dt} \tilde{w} + \begin{bmatrix} p_1 & 0 & 0 \\ 0 & 0 & 0 \end{bmatrix} \frac{d^2}{dt^2} \tilde{w} = 0.$$

Note that the resulting LPV-KR representation with IO partition $y = (w_1, w_2)$ and $u = w_3$ is a valid representation of the nonlinear system similarly as the representation associated with the bold lines, but with an increased scheduling dimension and a free but not independent scheduling variable p .

The remaining choices of available routes are the combinations of the previous ones with no interesting further property. Thus in conclusion, the best choice of LPV-KR representation of the system follows through the decision route indicated by bold lines in Figure 7.1. This concludes the final step of the algorithmic scheme.

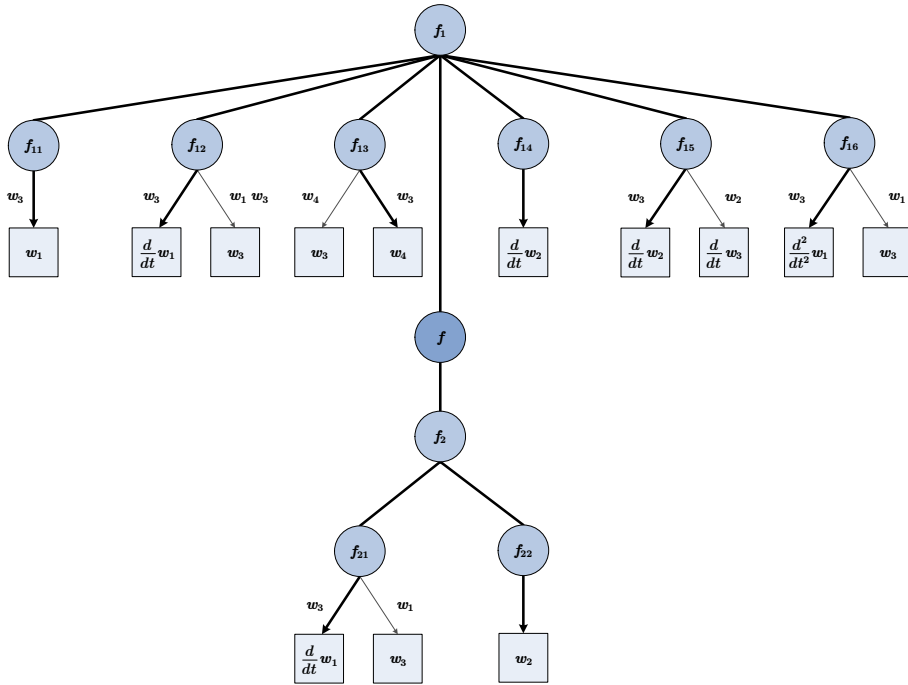


Figure 7.1: Decision tree of NL model transformation to LPV-KR representations

7.4.3 Handling non-factorizable terms

Now we investigate the case, when not all summand terms $\{f_{ij}\}$ are factorizable. In that case, there is little chance for the elimination of these terms and to enable the use of the previously introduced mechanism without any approximation. Variable substitution to eliminate these terms (see Example 7.3) generally does not work, as the substitution must satisfy the equation for all derivative relations of the substituted variables. This may result in ad hoc operations, cancelations of terms and alteration of the behavior. This unfortunate phenomenon even holds for constant terms in general (see Example 7.3).

Example 7.3 (Elimination of non-factorizable terms) Consider the case when $f_{ij} = 1$. Then this constant term is a non-factorizable expression in the nonlinear differential equation described by f . If f reads as

$$f \diamond w = w_2 \frac{d}{dt} w_1 + w_1 + 1,$$

then the non factorizable term 1 can be eliminated by substituting w_1 with $\check{w}_1 = w_1 + 1$, which gives

$$w_2 \frac{d}{dt} \check{w}_1 + \check{w}_1 = 0.$$

Such an expression contains only factorizable summands thus the previously described procedure can be applied on this new differential equation to obtain an LPV representation in terms of (\check{w}_1, w_2) . However, if f is

$$f \diamond w = \begin{bmatrix} w_2 \frac{d}{dt} w_1 + w_1 + 1 \\ w_1 + \frac{d}{dt} w_2 \end{bmatrix},$$

then this elimination cannot be applied on the upper equation as it would introduce a nonfactorizable term -1 in the lower one. In case of other non-factorizable terms, it is generally true that elimination through variable substitution can be applied if it satisfies all the equations without introducing new non-factorizable terms.

A sound possibility is however to approximate the non-factorizable terms in the following way:

1. Let f_{ij} be a non-factorizable summand. Let \mathcal{I}_{ij} be an index set containing all indexes $(k, l) \in \mathbb{I}_1^{n_w} \times \mathbb{I}_0^n$ such that f_{ij} is dependent on $\frac{d^l}{dt^l} w_k$.
2. For each $(k, l) \in \mathcal{I}_{ij}$, try to approximate the function f_{ij} as

$$(f_{ij} \diamond w)(t) \approx \left((\check{f}_{ijkl} \diamond w) \frac{d^l}{dt^l} w_k \right)(t) \quad \forall w \in \mathfrak{B} \quad \forall t \in \mathbb{R}, \quad (7.39)$$

where $\check{f}_{ijkl} \in \mathcal{R}$.

3. If such approximation exists for some $(k, l) \in \mathcal{I}_{ij}$, then treat them as valid factorizations of f_{ij} and proceed with the original algorithm, else transformation to a PV form does not exist with the given precision.

The resulting LPV representation can be considered as the approximation of the original NL system if the conditions described in Step 5 are satisfied. Note that what is considered to be an appropriate approximation is highly dependent on the intended accuracy. For some specific non-factorizable functions like $\sin(\cdot)$, such an approximation can be carried out even in an exact sense (see Example 7.4). If the non-factorizable term is a constant $f_{ij} = \gamma \in \mathbb{R} \setminus \{0\}$, then no sound approximation exists and one may risk to either use an approximation $f_{ij} = \frac{\gamma}{w_k} w_k$ or multiply the i^{th} row of f with w_k and restart the transformation procedure from the first step. Both approaches may result in alteration of the original NL behavior.

Note that in the LPV behavioral approach, the terminology of almost everywhere equivalence has been introduced to handle singularities of the coefficient functions that result or change due to transformations in $\mathcal{R}[\xi]$. One can sense that in case of non-factorizable terms, we face the same situation as by dividing with a w_i any non-factorizable term can be turned to a factorized relation. However, the price to be paid is an almost everywhere equivalence of the resulting representation if w_i is a free signal. However in case w_i is non-free, division by w_i can destabilize the origin of the signal-space, critically altering the dynamical behavior of the system.

Example 7.4 (Approximation of non-factorizable terms) Consider the case, when the non-factorizable term is $\sin(w)$. Then by writing this term as

$$\sin(w) = \text{sinc}(w)w,$$

where $\text{sinc}(w) = \frac{\sin(w)}{w}$ and $\text{sinc}(0) = 1$, we get an exact factorization. However in case of $\cos(w)$,

$$\cos(w) = \frac{\cos(w)}{w}w,$$

where $\lim_{x \rightarrow 0} \frac{\cos(x)}{x} = \infty$. Thus this form can only be considered a factorization if w is a non-zero signal. As an alternative, a finite Taylor expansion of $\cos(\cdot)$ is suggested

$$\cos(w) = 1 + \frac{1}{2}w^2 + \frac{1}{24}w^4 + \dots$$

where if the non-factorizable term 1 can be eliminated, then the remaining tail contains only factorizable parts. This holds for all common functions like trigonometric, exponential, logarithmic, etc. It holds in general that approximation problems of non-factorizable terms relate to the question, how constant terms can be eliminated or approximated with a factorized expression.

7.4.4 Properties of the transformation procedure

It can be concluded that the proposed method can transform a wide class of NL systems satisfying Definition 7.1. An advantage of the method is that it provides a systematic way of conversion, examining all possibilities of an equivalent LPV realization. By checking validity of the derived LPV representation with respect to the behavior of the original NL system, it provides a successful tool to solve Problem 7.1. Additionally, the algorithm gives a structured selection of the scheduling variable p highlighting when not only a quasi-LPV but a true LPV formulation is possible.

However, the approach has disadvantages as well. One of them is the heavy dependence on symbolic recognition of summands and possible ways of factorization. Thus the performance of the algorithm is clearly limited by the available symbolic computational tools. Another disadvantage is that investigating all possible LPV-KR representations that can be obtained from the generated decision tree can be quite demanding in case of large signal dimensions or a complicated f . Moreover, in case of large scale systems, computing and comparing the possible IO partitions of the resulting LPV descriptions is hopeless.

It may also happen for some cases that no valid transformation of the NL dynamic system is available via the proposed algorithm. Commonly, there is little chance of any ad-hoc transformation to succeed if the proposed method does not work as the original system description is minimal and all possibilities are investigated. That means that some sort of approximation technique must be applied in advance. Alternatively, signal relations can be replaced by virtual variables in the original expression to simplify the structure and the model transformation process can be executed on the substituted relations. However, such a substitution by virtual variables may result in the masking of dynamical aspects of the system. Thus, the substituted terms must be identified or modeled separately in order to represent the original behavior. Such an approach is ad hoc and out of the scope of the current process as it is assumed that all signals are important for the modeling purpose. Moreover, it must be accepted that not every NL system can be appropriately transformed to an LPV form, which is especially true for systems not satisfying Definition 7.1. Examples for such dynamical relations are systems with delays, hysteresis, or non-functional signal relations like if-then rules. In such cases, the LPV framework may be inappropriate for dealing with the system dynamics without considerable approximation.

Comparing the proposed approach of model transformation to the available approaches presented in Section 7.3, it can be concluded that this method gives adequate transformation for a much wider class of NL systems. The selection of the scheduling variable follows a more structured procedure, without the ad hoc selection of input, output, or latent variables. This gives the flexibility to find the most efficient form of transformation. In case of non-factorizable terms, approximation is inherently involved in the transformation, similar to the methods of Section 7.3, which result in an approximation of the original behavior up to a specific precision.

7.5 Summary

In this chapter, modeling of physical systems described by nonlinear differential equations has been studied in the LPV framework. Our motivation has been to derive tools that can assist model structure selection LPV identification.

First in Section 7.2, general questions of LPV modeling have been investigated. One of the major conclusions has been that instead of the transformation of a given mathematical description of the NL system to a LPV description, the modeling problem needs to be approached from the perspective of a search for a LPV system with equal behavior. This also implies that there is a prime emphasis on the selection of the scheduling vector, i.e. which variables of the original system are used as a scheduling in order to find an equivalent LPV description.

Next in Section 7.3, existing LPV modeling techniques have been studied and compared. In this overview, it has been shown that available approaches use a state-space representation of the NL system as a starting point. Thus, instead of the representation or approximation of the original behavior they aim at the LPV formulation of the state-equation of the assumed representation. Such a starting point has the danger that the prespecified state variable, which is only a latent variable of the original system, can seriously lower the realization possibilities in the LPV system class. The available approaches have been categorized into groups, based on the used linearization or substitution concept. The former concept aims at the approximation of the NL-SS representation and it originates from the gain-scheduling principle: linearization of the SS representation at given points of the signals space and then interpolation of the resulting LTI models. The latter concept formulates the modeling problem as a transformation of a subclass of NL-SS representations to a LPV form without any approximation. It has been shown that for the linearization based methods any local transformation of the obtained linearized models can seriously alter the result of their interpolation, i.e. the behavior of the obtained LPV description may not even resemble the original NL system.

By showing the open problems of LPV modeling, in Section 7.4 a transformation algorithm has been proposed that aims at the exploration of all possible LPV systems that are equivalent with respect to a given dynamical NL system. The algorithm, using the concepts of Kwiatkowski et al. (2006), converts the NL

differential equation, which defines the behavior of the NL system, into possible LPV-KR representations. During the process, it automates the choice of the scheduling vector, distinguishing the cases when an exact (non quasi) LPV realization is possible. In the derived approach, all possibilities of transformation are investigated with the applied strategy. By comparing IO partitions of the resulting LPV representations and the maximal order of derivatives with respect to the non-free variables, it can be expected that no alteration of the behavior has resulted. In this way, the results of the modeling procedure are validated. The valid solutions are ordered in terms of complexity to assist the user to choose the most adequate representation. For the case, when no exact transformation is possible, approximation possibilities of the troublesome parts of the NL description have been discussed.

The developed technique is a crucial contribution for the general LPV framework as it can assist the identification methods of the field with structural information about the plant. The procedure is also a necessary ingredient of the identification approach of this thesis as it can assist the choice of OBFs based model structures.

Optimal selection of OBFs

In this chapter, selection of the optimal basis, i.e. the basis with the fastest convergence rate, for the series-expansion of LPV systems is investigated. In fact, we consider the situation when information about the system is only available in terms of measured data records of the frozen signal behavior. Solution of this problem is crucial to provide a model structure selection tool for LPV identification based on truncated series-expansion models. In case of an optimal basis, a fast convergence rate of the expansion representation implies that only the estimation of a few expansion coefficients is necessary for a good approximation of the system. By using the concept of Kolmogorov n -width optimality of the basis with respect to the frozen behaviors, we derive a practically applicable algorithm, that provides optimal basis selection based on fuzzy clustering of estimated “frozen” poles. The pole estimates are the results of LTI identification of the system with constant scheduling trajectories. To consider the effect of noise on the estimation of the frozen poles, a robust version of the algorithm is also developed using the strong relation between Kolmogorov n -width theory and hyperbolic geometry.

8.1 Perspectives of OBFs selection

The concept of modeling discrete-time asymptotically stable LPV systems with OBFs based truncated series expansions has been introduced in Chapter 5 to develop an effective model structure for LPV identification. However, practical application of this concept requires the selection of basis functions that guarantees a fast convergence rate of the LPV expansion representation of a system. The reason is that using a truncated expansion with a fast convergence rate, i.e. only a finite number of OBFs from the basis sequence, a model results that approximates the system well with only a few expansion coefficients.

In Section 5.4, it has been motivated that to achieve a fast convergence rate of the LPV expansion representation, a necessary condition is to use a basis which

has optimal convergence rate with respect to $\mathfrak{F}_{\mathbb{P}}$, the set of transfer functions of the frozen system set for the considered IO partition. In order to characterize optimality of the convergence rate with respect to a given transfer function set, like $\mathfrak{F}_{\mathbb{P}}$, we have introduced the worst-case concept of the *Kolmogorov n -width* (KnW) theory in Section 2.4. However, to use this concept to choose an n -width optimal basis, it is required to know the pole locations of $\mathfrak{F}_{\mathbb{P}}$, i.e. the region $\Omega_{\mathbb{P}}$, which contains the points where not all transfer functions in $\mathfrak{F}_{\mathbb{P}}$ are analytic. In an identification scenario, such knowledge might not be available. This underlines that in order to accommodate an effective model structure selection for the identification of LPV systems with truncated expansion models, a practically applicable approach is needed to choose KnW optimal OBFs.

In Chapter 7, we have introduced a modeling procedure, which provides an LPV representation of a NL system based on first principle information. If the parameters of the original system are considered to be known, such a procedure can be used to calculate the pole locations $\Omega_{\mathbb{P}}$ of $\mathfrak{F}_{\mathbb{P}}$. Then by solving the min-max problem of (2.173), optimal basis selection in the KnW sense can be achieved for the system, which provides an efficient model structure selection for its identification. If no first-principle information is available or the uncertainty of the parameters is large, selection of the basis must be based on measured data records of the system. In this chapter, we consider the situation when data records of some frozen behaviors of the LPV system are available. Estimating LTI models based on these data records, gives pole samples of $\Omega_{\mathbb{P}}$. Based on these sample poles, we aim at the derivation of a basis selection mechanism, that is capable to accomplish the following objectives:

- Reconstruction of $\Omega_{\mathbb{P}}$ based on the sample pole locations.
- Determination of the set of OBFs, that are optimal in the KnW sense with respect to $\Omega_{\mathbb{P}}$.

The proposed method solves these objectives simultaneously by the fusion of the KnW theory and the *Fuzzy c -Means* (FcM) clustering approach (see Section 2.5). These theories are applied together to derive KnW optimal basis functions by the clustering of the sample pole locations. The resulting mechanism guarantees optimality in the KnW sense for the obtained basis functions with poles at the cluster centers, in case the fuzzyness parameter approaches infinity. In this way it provides a trade off between the optimality of the chosen basis and the complexity of the optimization. The introduced method characterizes the model structure selection phase of the identification cycle in our approach. The chapter is organized as follows:

To assist the formulation of the basis selection as a clustering problem, in Section 8.2, the KnW concept is revisited to highlight important details of the theory with respect to LPV systems. Then in Section 8.3, both the reconstruction problem of $\Omega_{\mathbb{P}}$ and the KnW problem with respect to $\Omega_{\mathbb{P}}$ are formulated as a clustering problem of the sample pole locations. To solve the clustering problem, a modified FcM algorithm is developed and its properties are investigated in terms of optimality of the solution, numerical convergence, calculation issues, and termination

conditions. Furthermore, the use of adaptive cluster-merging is investigated for the introduced algorithm, showing that it provides an effective tool to choose the width of the KnW problem in which the optimal basis is searched for. In order to handle the effect of pole uncertainties that result during the estimation of the sample pole locations, in Section 8.4 a robust formulation of the introduced basis selection approach is developed. To do so, first important connections of hyperbolic geometry and the KnW theory are explored which give effective tools to handle the basis selection with respect to pole uncertainty regions on the complex plain. In both the robust and non-robust cases, simulation examples are given to show the effectiveness of the proposed approaches.

8.2 Kolmogorov n -width optimality in the frozen sense

As a first step, we investigate the KnW optimality concept of orthonormal basis functions with respect to a LPV system in a frozen sense. To do so we revisit the KnW theory presented in Section 2.4 and we highlight properties that are important for the discussion of the basis selection mechanism. As the presented KnW theory is formulated in the SISO case, we restrict the discussion to SISO asymptotically stable LPV systems in the following. The basis selection problem for MIMO LPV systems is postponed till Chapter 9.

Let $\mathfrak{F}_{\mathbb{P}}$ denote the set of transfer functions corresponding to $\mathcal{F}_{\mathbb{P}}$ for a given IO partition of the LPV system \mathcal{S} . In Section 2.4 it has been already discussed that the KnW concept provides the selection of n_g poles of an inner function $G \in \mathcal{H}_{2-}(\mathbb{E})$, such that the Hambo basis sequence $\Phi_{n_g}^{\infty}$ generated by G is optimal in the $n = n_g(n_e + 1)$ -width sense with respect to a given transfer function set. This optimality means that among all Hambo bases, the linear combination of the set of $n_g(n_e + 1)$ functions $\Phi_{n_g}^{n_e}$ has the smallest worst-case representation error (in the \mathcal{H}_2 norm). In this sense, optimality means also the fastest worst-case convergence rate ρ of the expansion of these transfer functions with the basis sequence $\Phi_{n_g}^{\infty}$. In other words, a KnW optimal basis for $\mathfrak{F}_{\mathbb{P}}$ provides series-expansion representations of all frozen systems $\mathcal{F}_{\mathbb{P}}$, such that the convergence rate of the coefficients is optimal for the considered width. Note that n , i.e. the width in which the optimality of the basis is considered represents a particular freedom. In fact, it is a trade of between ρ and the number of poles required for G to achieve it. By using a KnW optimal basis where both the optimal convergence rate ρ and the width n is small, it is guaranteed that truncated expansion representations of all $\mathcal{F}_{\mathbb{P}}$ need only a few expansion coefficients to approximate each frozen behavior adequately. This means that beside finding n -width optimal OBFs for a fixed n , it is also important to search for an adequate n . The latter problem indirectly refers to the question how many basis functions are required for the truncated expansion representation to achieve a good approximation.

Introduce the pole manifest set

$$\Omega_{\mathbb{P}} = \{ \lambda \in \mathbb{C} \mid \exists \bar{p} \in \mathbb{P}, \text{ such that } \lambda \text{ is a pole of } F_{\bar{p}} \in \mathfrak{F}_{\mathbb{P}} \}, \quad (8.1)$$

the collection of pole locations belonging to $\mathfrak{F}_{\mathbb{P}}$. For a given $\Omega_{\mathbb{P}}$ and a fixed $n = n_g$, the KnW basis selection problem with respect to $\mathfrak{F}_{\mathbb{P}}$ comes down to the inverse Kolmogorov problem (see Section 2.4): finding the best fitting hull of $\Omega_{\mathbb{P}}$ in the form

$$\Omega(\Lambda_{n_g}, \rho) := \{z \in \mathbb{C} \mid |G(z^{-1})| \leq \rho\}, \quad (8.2)$$

where G is defined by the poles $\Lambda_{n_g} = [\lambda_1 \ \dots \ \lambda_{n_g}]$ and $\rho > 0$ is as small as possible. Then, in terms of Proposition 2.1, the inner function G , associated with the best fitting $\Omega(\Lambda_{n_g}, \rho)$, generates the n -width optimal basis functions with respect to $\mathfrak{F}_{\mathbb{P}}$. For a given inner function G with pole set Λ_{n_g} , define

$$\kappa_{n_g}(z, \Lambda_{n_g}) := |G(z^{-1})| = \prod_{j=1}^{n_g} \left| \frac{z - \lambda_j}{1 - z\lambda_j^*} \right|, \quad (8.3)$$

the so called *Kolmogorov cost*. Then for a given $n_g > 0$, the solution of the inverse Kolmogorov problem is equivalent with the min-max problem (2.173), formulated in this case as an optimization:

$$\begin{aligned} &\text{minimize} \quad \rho = \max_{z \in \Omega_{\mathbb{P}}} \kappa_{n_g}(z, \Lambda_{n_g}), \\ &\text{such that} \quad \Lambda_{n_g} = [\lambda_1 \ \dots \ \lambda_{n_g}] \in \mathbb{D}^{n_g}. \end{aligned} \quad (8.4)$$

The minimizer of (8.4), is a set of pole locations Λ_{n_g} which defines the best inner function, i.e. Hambo basis in the KnW sense. If the resulting $\Omega(\Lambda_{n_g}, \rho)$ is equal to $\Omega_{\mathbb{P}}$, then in terms of Proposition 2.1, the generated basis is also optimal in the kn_g -width sense for any $k \in \mathbb{N}$. Otherwise, higher width optimality of the basis does not hold in the general case (see Example 8.1). This underlines that to find an optimal OBF set for $\Omega_{\mathbb{P}}$, an optimal choice of n_g is also needed. We will see that by using powerful results in hyperbolic geometry, in some cases, an optimal choice of the width is available. The latter result is an important contribution of this thesis.

Example 8.1 (Optimal n -widths) *In this example, we show that a basis sequence which is optimal in the KnW sense is not necessary optimal in the $2n$ -width or other higher width cases. Let an inner function G be given with poles*

$$\Lambda_4 = \{0.55 \pm 0.55i, 0.25 \pm 0.25i\}.$$

For $\rho = 0.1$, G defines the complex region $\Omega(\Lambda_4, \rho)$ whose perimeter is given with a blue line in Figure 8.1. Any strictly proper transfer function (and associated LTI system) with all poles in $\Omega(\Lambda_4, \rho)$ has a series-expansion in terms of the inner function G generated Hambo basis Φ_4^∞ with a worst-case convergence rate 0.1. Denote by $\Omega_{\mathbb{P}} = \Omega(\Lambda_4, \rho)$, the region for which we would like to find optimal OBFs in the KnW sense. It is obvious that in the 4-width sense, the Hambo functions Φ_4^0 are optimal with respect to $\Omega_{\mathbb{P}}$ and the convergence rate is 0.1.

Now we would like to derive a 2-width optimal basis with respect to $\Omega_{\mathbb{P}}$. By applying nonlinear optimization in terms of (8.4), the resulting optimal Hambo functions Φ_2^0 are associated with the pole locations

$$\Lambda_2 = \{0.2995 \pm 0.3318i\}.$$

In this case, the convergence rate, i.e. the minimal $\rho > 0$ such that $\Omega_{\mathbb{P}} \subseteq \Omega(\Lambda_2, \rho)$ is 0.5333. With this ρ , the perimeter bound of $\Omega(\Lambda_2, \rho)$ is given with a red line in Figure 8.1.

Now we can see that series-expansion of any strictly proper transfer function with all poles in $\Omega_{\mathbb{P}}$ has a convergence rate 0.1 in case of the 4-width optimal basis Φ_4^∞ and 0.5333 in case of the 2-width optimal basis Φ_2^∞ . This clearly shows that the worst-case decay rate of a Hambo basis Φ_4^∞ generated by an inner function with

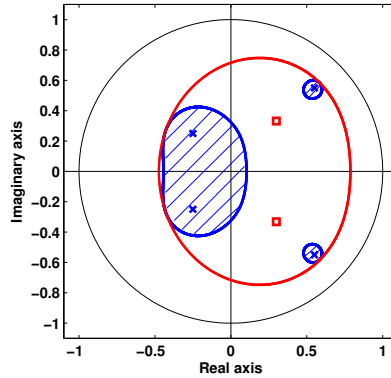


Figure 8.1: Kolmogorov 2-width optimal basis functions Φ_2^0 with poles Λ_2 (denoted by red \square) and Kolmogorov 4-width optimal basis functions Φ_4^0 with poles Λ_4 (denoted by blue \times) with respect to the pole manifest region $\Omega_{\mathbb{P}}$ (shaded blue area). The perimeter of the associated minimal regions $\Omega(\Lambda_2, 0.5333)$ (red line) and $\Omega(\Lambda_2, 0.1)$ (identical to $\Omega_{\mathbb{P}}$) is indicated with contour lines.

poles $\Lambda_4' = \{\Lambda_2, \Lambda_2\}$ (repetition of the 2-width optimal poles) has a convergence rate $(0.5333)^2 = 0.2844$. Comparing this to the convergence rate 0.1 of Φ_4^0 it is clear that the Hambo functions Φ_4^0 are not optimal in the 4-width sense. In general it is true that higher width optimality is only guaranteed for basis functions with $\Omega(\Lambda, \rho) = \Omega_{\mathbb{P}}$. From Figure 8.1 it follows that this is not the case for Λ_2 . However in case of Λ_4 , this equivalence is satisfied, thus with respect to $\Omega_{\mathbb{P}}$, Φ_4^1 is optimal in the 8-width sense, Φ_4^2 is optimal in the 12-width sense, etc.

If $\Omega_{\mathbb{P}}$ is known, then a solution of (8.4) for a fixed n_g can be obtained via the gradient-search based method of Heuberger et al. (2005). However, in case of an identification scenario, when $\Omega_{\mathbb{P}}$ is not available, the gradient approach is not applicable unless $\Omega_{\mathbb{P}}$ is reconstructed from some estimated samples. The method that is proposed solves both objectives (reconstruction and KnW optimization) and gives a practical solution for the basis selection step. This method also enables an effective choice of the number OBFs, i.e. in which width-sense it is best to search for KnW optimal OBFs, by the use of adaptive cluster merging.

8.3 The Fuzzy-Kolmogorov c -Max clustering approach

In the following we propose a particular data clustering algorithm as the extension of the conventional FcM approach, which can effectively handle the reconstruction problem of $\Omega_{\mathbb{P}}$ jointly with the solution of (8.4). To do so, first in section 8.3.1 we formulate the exact problem setting for the clustering approach to interpret our basis selection goal. Then, we characterize the optimal solution of the clustering problem and introduce the extension of the FcM algorithm (Algorithm

2.1) to calculate it. As a next step, in Section 8.3.2 we show how the derived optimal solution provides an answer for the original basis selection problem of Section 8.2. Numerical properties of the derived algorithm are investigated together with practical aspects, like the use of *Adaptive Cluster Merging* (ACM) in this setting. At last, a simulation example is presented to show the effectiveness of the introduced basis selection mechanism.

8.3.1 The pole clustering algorithm

Let $n_c > 1$ be the number of clusters (pole regions) to be used to reconstruct $\Omega_{\mathbb{P}}$. Note that due to the uniform frozen asymptotic stability of $\mathcal{F}_{\mathbb{P}}$, it is guaranteed that $\Omega_{\mathbb{P}} \subseteq \mathbb{D}$, i.e. all sample poles \mathbf{z}_k are in \mathbb{D} . Thus, let \mathbb{D} be the clustering space, i.e. $\mathbb{V} = \mathbb{D}$, and let $Z = \{\mathbf{z}_k\}_{k=1}^{N_z} \subset \mathbb{D}$, be the set of observed poles for clustering. Similar to the FcM case, we introduce membership functions $\mu_i : \mathbb{D} \rightarrow [0, 1]$ that determine the “degree of membership” to the clusters for all $z \in \mathbb{D}$. By using a *threshold value* ε , we can obtain a set

$$\Omega_\varepsilon = \{z \in \mathbb{D} \mid \exists i \in \mathbb{I}_1^{n_c}, \mu_i(z) \geq \varepsilon\}. \quad (8.5)$$

This set characterizes the region approximated by the clusters for the minimal membership level ε . Now we formulate the clustering problem that is considered.

Problem 8.1 (Pole clustering problem) *For a set of sampled pole locations Z and for a given number of clusters n_c , find a set of cluster centers $\{v_i\}_{i=1}^{n_c}$, a set of membership functions $\{\mu_i\}_{i=1}^{n_c}$, and the maximum of ε , such that*

- Ω_ε contains Z .
- With respect to Ω_ε , the OBFs, with poles Λ_{n_c} in the cluster centers $\{v_i\}_{i=1}^{n_c}$, are optimal in the KnW sense, where $n = n_c$.

The solution is based on finding clusters in accordance with the KnW concept and subsequently finding a maximal value for ε , such that all sampled poles are inside Ω_ε . The latter is equivalent to minimizing ρ in the optimization problem of (8.4). Note that optimality of the OBFs is considered with $n_e = 0$. According to the principle of KnW theory, this might result in repetitive optimal poles and therefore similar clusters. In the following we focus on finding n -width-based clusters. Additionally, in case $n_c \geq N_z$, the solution of Problem 8.1 is trivial: the cluster centers are associated with the sample poles. Thus only the case when $n_c < N_z$ is considered in the sequel.

Similar to the FcM case, denote $V = [v_i]_{i=1}^{n_c}$ the vector of cluster centers and introduce the membership matrix $U = [\mu_{ik}]_{n_c \times N_z}$, where μ_{ik} is the degree of membership of \mathbf{z}_k to cluster i , i.e. $\mu_{ik} := \mu_i(\mathbf{z}_k)$. Furthermore, distances d_{ik} are introduced between v_i and \mathbf{z}_k to measure dissimilarity of Z with respect to each candidate cluster. The distance is formulated in terms of the 1-width version of the n -width Kolmogorov cost (2.172), which is also called the *Kolmogorov Measure*:

Definition 8.1 (Kolmogorov measure)

$$\kappa_1(\mathbf{x}, \mathbf{y}) := \left| \frac{\mathbf{x} - \mathbf{y}}{1 - \mathbf{xy}^*} \right| : \mathbb{D} \times \mathbb{D} \rightarrow \mathbb{R}_0^+, \quad (8.6)$$

is called the Kolmogorov measure (KM) on \mathbb{D} .

Later we show that κ_1 is a metric in \mathbb{D} . As notation,

$$d_{ik} = \kappa_1(v_i, \mathbf{z}_k), \quad (8.7)$$

is introduced. In the following discussion it is shown how the KM relates the FcM clustering asymptotically to the KnW theory, and in this way to the solution of Problem 8.1. In order to uniquely associate each d_{ik} with a membership level μ_{ik} , the set of membership functions is restricted to satisfy $\sum_{i=1}^{n_c} \mu_i(z) = 1$, which requires that $U \in \mathcal{U}_{n_c}^{N_z}$ (see (2.175)).

The fuzzy-functional $J_m(U, V) : \mathcal{U}_{n_c}^{N_z} \times \mathbb{V}^{n_c} \rightarrow \mathbb{R}_0^+$, for Problem 8.1 is formulated as

$$J_m(U, V) := \max_{k \in \mathbb{I}_1^{N_z}} \sum_{i=1}^{n_c} \mu_{ik}^m d_{ik}. \quad (8.8)$$

This functional defines the cost function, i.e. the criterion of the expected solution for Problem 8.1. It can be observed that (8.8) corresponds to a *worst-case (max) sum-of-error* criterion, contrary to the *mean-squared-error* criterion of the original FcM, see Section 2.5. Hence, we call the algorithm that minimizes the fuzzy-functional (8.8) *Fuzzy-Kolmogorov c-Max (FKcM)* clustering. The exact relation of (8.8) with the KnW optimality of a partition (U, V) is explained later (see Theorem 8.2). The design parameter $m \in (1, \infty)$, which is called the fuzzyness, determines the sharpness of the separation in the global minima of (8.8). This means that for low values of m , the clusters in the optimal partition (U, V) are separated, i.e. even for a low value of ε they contribute disjoint regions to Ω_ε . For large values of m , the contribution of the regions are indistinguishable in almost every point of \mathbb{D} . This gives the intuition that for low m , we try to achieve the reconstruction of $\Omega_{\mathbb{P}}$ with the clusters in an “individual” sense, while for large m in a “cooperative” sense. Based on this, the following theorem yields the ingredients to solve Problem 8.1:

Theorem 8.1 (Optimal Partition) *Let $m > 1$, a data set $Z \subset \mathbb{D}$ with $N_z > 0$, and a fuzzy partition $(U, V) \in \mathcal{U}_{n_c}^{N_z} \times \mathbb{D}^{n_c}$ be given. Denote $[V]_i = v_i$ and $[U]_{ij} = \mu_{ij}$. Define $\gamma_i(v, U)$ as the minimal value of $\tau \in [0, 1]$ fulfilling the quadratic constraints:*

$$\left[\begin{array}{c} |1 - \mathbf{z}_k^* v|^2 \\ \mu_{ik}^m \cdot (\mathbf{z}_k - v)^* \end{array} \right] \geq 0, \quad \forall \mathbf{z}_k \in Z, \quad (8.9)$$

where $v \in \mathbb{D}$. Additionally, let $d_{ik} = \kappa_1(v_i, \mathbf{z}_k)$ be the dissimilarity measure of \mathbf{z}_k with respect to V and $\mathcal{I}_k^\emptyset = \{i \in \mathbb{I}_1^{n_c} \mid d_{ik} = 0\}$ be the singularity set of \mathbf{z}_k with $\text{card}(\mathcal{I}_k^\emptyset) = n_k^\emptyset$ (number of elements). Then (U, V) is a local minimum of J_m , if for any $(i, k) \in$

$\mathbb{1}_1^{n_c} \times \mathbb{1}_1^{N_z}$:

$$\mu_{ik} = \begin{cases} \left[\sum_{j=1}^{n_c} \left(\frac{d_{jk}}{d_{jk}} \right)^{\frac{1}{m-1}} \right]^{-1} & \text{if } \mathcal{I}_k^\emptyset = \emptyset; \\ \frac{1}{n_k^\emptyset} & \text{if } i \in \mathcal{I}_k^\emptyset; \\ 0 & \text{if } i \notin \mathcal{I}_k^\emptyset \neq \emptyset; \end{cases} \quad (8.10a)$$

$$v_i = \arg \min_{\nu \in \mathbb{D}} \gamma_i(\nu, U). \quad (8.10b)$$

The proof is given in Appendix A.3. Using the approach of the FcM case, minimization of (8.8) subject to (2.175) is tackled by alternating optimization (Picard iteration), steering the solution towards a settling partition in the sense of Theorem 8.1. For the FKcM, this yields Algorithm 8.1, which is based on the same mechanism as Algorithm 2.1 in the FcM case.

Algorithm 8.1 (FKcM clustering)

- | | |
|----------------------------------|---|
| 0. Initialization: | Fix n_c and m ; and initialize $V_0 \in \mathbb{D}^{n_c}$, $l = 0$. |
| 1. Membership update: | With (8.10a), solve $U_{l+1} = \arg \min_{U \in \mathcal{U}_{n_c}^{N_z}} J_m(U, V_l)$. |
| 2. Cluster center update: | With (8.10b), solve $V_{l+1} = \arg \min_{V \in \mathbb{D}^{n_c}} J_m(U_{l+1}, V)$. |
| 3. Check of convergence: | If $J_m(U_{l+1}, V_{l+1})$ has converged, then stop, else $l = l + 1$ and goto Step 1. |
-

8.3.2 Properties of the FKcM

Next, we investigate the properties of the introduced algorithm, showing that KnW optimality of the resulting cluster centers (if the solution is the global minima of (8.8)) holds in an asymptotic sense ($m \rightarrow \infty$). It is also discussed how Algorithm 8.1 can be implemented in practice, how convergence of the solution can be detected, and how numerical conditioning problems can be avoided.

Asymptotic property

In order to explain the specific choices for the fuzzy functional (8.8) and the dissimilarity measure d_{ik} , we use the following theorem.

Theorem 8.2 (Asymptotic property of J_m) *Given a data set $Z \subset \mathbb{D}$ with $N_z > 0$, and a vector of cluster centers $V \in \mathbb{D}^{n_c}$, with $n_c > 0$, such that $d_{ik} = \kappa_1(v_i, z_k) \neq 0$ for all $(i, k) \in \mathbb{1}_1^{N_z} \times \mathbb{1}_1^{n_c}$ (no singularity). Define U_m as a membership matrix of V satisfying (8.10a) for $m > 1$. Then*

- a. $\lim_{m \rightarrow 1} J_m(U_m, V) = \max_{k \in \mathbb{I}_1^{N_z}} \min_{i \in \mathbb{I}_1^{n_c}} \{d_{ik}\}$, which corresponds to the hard partitioning of Z , i.e. $\mu_{ik} \in \{0, 1\}$, $\forall (i, k) \in \mathbb{I}_1^{n_c} \times \mathbb{I}_1^{N_z}$.
- b. $J_2(U_2, V) = \max_{k \in \mathbb{I}_1^{N_z}} [\sum_{i=1}^{n_c} d_{ik}]^{-1}$, which is the maximum of the harmonic-means-based distance of each z_k with respect to the clusters.
- c. $J_m(U_m, V) = n_c^{1-m} \max_{k \in \mathbb{I}_1^{N_z}} [\prod_{i=1}^{n_c} d_{ik}]^{1/n_c} + \mathcal{O}(e^{-m})$. Furthermore, $J_m(U_m, V)$ decreases monotonically with m , and $J_\infty(U_\infty, V) = 0$.

The proof is presented in Appendix A.3. Theorem 8.2 shows that the value of m has great impact on what the minimization of the fuzzy-functional (8.8) represents. If $m = 1$, each sample pole is assigned exactly to one cluster. Thus, minimizing the KM distance of the cluster center with respect to only the assigned poles yields that the resulting cluster center is the pole of the 1-width optimal basis function with respect to the assigned sample poles. In this way, the optimal partition corresponds to a collection of 1-width optimal basis functions with respect to each separated groups of the sample poles. In case $m > 1$, each of the sample poles belongs to all clusters with different membership levels. Thus minimizing the KM distance of each cluster center with respect to the sample poles with these membership weights (see (8.8)), yields a set of pole locations that approximates the poles of the KnW optimal solution. If $m \rightarrow \infty$, then these weights/memberships become equal, and all cluster centers try to decrease the KM distance for all sampled poles in a cooperative manner, which is equivalent with the KnW optimization problem (8.4). In this way, the minimization of J_m corresponds to a close approximation of (8.4) for large m . This property enables the FKcM to solve Problem 8.1 directly and explains all the particular choices (dissimilarity measure, modified fuzzy-functional) we made during its introduction. In this way, as a clustering mechanism, the algorithm solves the reconstruction of the possible Ω_P and at the same time it solves the optimization problem (8.4) in an approximative manner.

It should be noted that, in case $m \rightarrow \infty$, $\mu_{ik} \rightarrow 1/n_c$ for all $(i, k) \in \mathbb{I}_1^{n_c} \times \mathbb{I}_1^{N_z}$ in the optimal partition, which can cause numerical problems in the minimization of (8.10b). Therefore m acts as a trade-off parameter: to obtain a well approximating solution of Problem 8.1, an appropriately large value of $m \in (1, \infty)$ should be used, but at the same time m must be as low as possible to reduce the complexity of the optimization. Based on experience in the application of the algorithm, $m \in [5, 10]$ usually yields satisfactory results.

For $m > 1$, the FKcM-functional (8.8) is a bounded ($0 \leq J_m \leq 1$) monotonically decreasing function both in $\{d_{ik}\}$ and U , which allows Algorithm 8.1 to converge in practice¹. The convergence point, which directly depends on the initial V_0 , can either be a local minimum or a saddle point of J_m , fulfilling Theorem 8.1. Therefore, just like for FcM clustering, it is advisable to repeat the algorithm multiple times with different initial choices for V_0 and then select the best resulting set of

¹For the standard FcM, convergence to a local minimum can be shown Bezdek (1981), but the underlying reasoning does not hold for the FKcM case as J_m is discontinuous on $\mathcal{U}_{n_c}^{N_z}$.

OBFs. The performance comparison of the resulting clusters is available by computing the Kolmogorov cost (8.3), i.e. associated decay rate, $\check{\rho}$ of the cluster centers with respect to the sample poles:

$$\check{\rho} := \max_{z \in \Omega} \kappa_{n_g}(z, \Lambda_{n_g}) = \max_{z \in Z} \prod_{i=1}^{n_c} \left| \frac{z - v_i}{1 - zv_i^*} \right|, \quad (8.11)$$

and by visual inspection of the boundary region $\Omega(\check{\rho}, \Lambda_{n_c} = V)$ (see (8.1)) with respect to Z . In practice, uniformly random choices for V_0 are suggested. Initial partitions based on the distribution of Z can also be used (V_0 chosen as random elements of Z , V_0 is given as the points of a circle around the mean of Z , etc.) however they limit the possibilities to explore all local minima, while random initialization based on a uniform distribution gives equal probability.

In the rare case of singularity of the resulting partition (some $d_{ik} = 0$), Theorem 8.2 does not hold. Such a phenomenon can only happen in extreme situations when for example $n_c \approx N_z$. In that case, an optimal partition can contain some clusters whose cluster center is equal to sample pole locations. Singularity of the partition can also result if the samples of $\Omega_{\mathbb{P}}$ do not describe any data coherency, suggesting that $\Omega_{\mathbb{P}}$ is not a region but a finite set of isolated points. In such cases, the best solution in the KnW sense is to assign a dedicated OBF with respect to some sampled poles. However, when $\Omega_{\mathbb{P}}$ is a region, this solution should be avoided, as the reconstruction of $\Omega_{\mathbb{P}}$ is required based on the pole samples before choosing the basis functions. Thus, to assist the validity of the reconstruction, n_c must be chosen a priori such that it correctly describes the separated pole regions of $\Omega_{\mathbb{P}}$. This can be achieved by visual inspection of the sampled poles or by trial-and-error.

Optimization and numerical conditioning

While Step 2 in Algorithm 8.1, i.e. the membership update, can be analytically computed through (8.10a), Step 3, i.e. the cluster center update, requires the solution of (8.10b). The optimization defined by (8.10b) is a minimization problem with *Quadratic Constraints* (QC)s, where γ is the optimization variable and ν is the decision variable. Based on Scherer and Hol (2006), it is possible to derive *Sum-of-Squares* (SoS) relaxations of such constraints, through which (8.9) is turned into a *Linear Matrix Inequality* (LMI). The resulting convex minimization of γ , based on these constraints, is a *Linear Semi Definite Programming* (LSDP) problem that can be efficiently solved by a variety of (interior-point-based) solvers like SeDuMi (Sturm 1999) or CSDP etc. Alternatively, bisection-based recursive search (see Atkinson (1989)) can also be used to obtain the minimization of $\{\gamma_i\}$ with respect to (8.9). In each step of this bisection-based minimization, every QC with a fixed τ is rewritten as a LMI constraint. Checking feasibility of the constraints indicates how to proceed with the minimization of γ_i .

For high values of m , the QCs (8.9) become numerically ill-conditioned, which

can be avoided by the normalization of $\{\mu_{ik}^m\}_{k=1}^{N_z}$:

$$\bar{\mu}_{ik} = \frac{\mu_{ik}^m}{\check{\mu}_i}, \quad \text{with} \quad \check{\mu}_i = \sum_{k=1}^{N_z} \mu_{ik}^m. \quad (8.12)$$

Termination criterion

In Algorithm 8.1, the cost function J_m “flattens” when m increases. This yields that for high values of m , J_m is almost constant for all points of $\mathcal{U}_{n_c}^{N_z} \times \mathbb{D}^{n_c}$ except in the close neighborhood of its local minima where its value decreases quickly. To avoid unnecessary termination of the algorithm on the flat surface of the cost function, the relative evolution of J_m , in each iteration step l , has to be checked in a windowed sense:

$$1 - \frac{\max_k [J_m(U_k, V_k) - J_m(U_{k-n}, V_{k-n})]}{\max_k J_m(U_k, V_k)} < \varepsilon_t \quad (8.13)$$

where $k \in \mathbb{I}_{l-n}^l$, $n > 0$ is the length of the window, and $0 \ll \varepsilon_t < 1$ is a user defined termination constant. If in step l (8.13) is satisfied, then the relative evolution of J_m has been small in the considered window, so the optimization is terminated. Experience has shown, that for $m \in [5, 10]$, the threshold $\varepsilon_t = 0.99$ with $n = 3$ usually works well.

Cluster merging

The determination of the number of “natural” pole groups in Z , i.e. the best suitable n_c for clustering, is important for the successful application of the FKcM method. Similarity-based *Adaptive Cluster Merging* (ACM) can be effectively used for this purpose (see Section 2.5). Starting from a large n_c , the use of the ACM strategy in the FKcM algorithm gives the possibility to choose the number of clusters to describe the region $\Omega_{\mathbb{P}}$, associated with the samples Z , “adequately”. In the considered problem setting, adequateness means that for the reconstructed region Ω_ε , in which width sense we search for KnW optimal OBFs, where the basis functions are associated with the cluster centers. If the available information, the sampling of $\Omega_{\mathbb{P}}$, is dense, then in the optimal solution of Problem 8.1: $\Omega_\varepsilon \approx \Omega_{\mathbb{P}}$. This implies that the ACM provides an effective choice of the width, i.e. the value of n in which the KnW basis is searched for $\Omega_{\mathbb{P}}$ with the proposed algorithm. However in terms of Proposition 2.1, the setting of Problem (8.1) implies that repetitive basis poles can also be part of the optimal solution. With ACM, these solutions are not accessible as repetitive poles result in perfectly similar clusters which are immediately joined. As a result, the ACM only yields convergence to partitions with distinct cluster centers. This means that the choice of the adequate width in the KnW sense is restricted such that the optimal basis poles for the adequate width must be distinct.

8.3.3 Simulation example

To allow insight into the basis selection method an extensive example is studied.

The data generating system

Consider an asymptotically stable discrete-time SISO LPV system \mathcal{S} with IO partition (u, y) and scheduling signal p . Let a minimal IO representation of \mathcal{S} , $\mathfrak{R}_{\text{IO}}(\mathcal{S})$ be given as:

$$\sum_{i=0}^5 (a_i \diamond p) q^i y = (b_4 \diamond p) q^4 u, \quad (8.14)$$

with $\mathbb{P} = [0.6, 0.8]$ and coefficients

$$\begin{aligned} a_0 \diamond p &= -0.003, & a_3 \diamond p &= \frac{61}{110} - 0.2 \sin(q^5 p), \\ a_1 \diamond p &= \frac{12}{125} - 0.1 \sin(q^5 p), & a_4 \diamond p &= -\frac{511+192q^5 p^2 - 258(\cos(q^5 p) - \sin(q^5 p))}{860}, \\ a_2 \diamond p &= -\frac{23}{85} + 0.2 \sin(q^5 p), & a_5 \diamond p &= 0.58 - 0.1q^5 p, \\ b_4 \diamond p &= \cos(q^5 p). \end{aligned}$$

In Figure 8.2a, the pole manifest set $\Omega_{\mathbb{P}}$ of $\mathfrak{R}_{\text{IO}}(\mathcal{S})$ is presented with a solid red line, while in Figure 8.2b the first 15 Markov parameters of the frozen impulse responses of $\mathfrak{R}_{\text{IO}}(\mathcal{S})$ are given for all constant scheduling trajectories $p(k) = \bar{p}$. These frozen impulse responses are associated with the behaviors of the frozen system set $\mathcal{F}_{\mathbb{P}}$ of \mathcal{S} for the considered IO partition. These pictures show that the dynamic changes of \mathcal{S} are quite heavy for different constant scheduling trajectories.

By using constant scheduling signals with values $\{0.6; 0.6 + \tau; \dots; 0.8\}$, where $\tau = 0.02$, 11 frozen LTI representations of \mathcal{S} are obtained, whose pole locations are samples of $\Omega_{\mathbb{P}}$. These samples are given with yellow \star in Figure 8.2a. In our basis selection approach, these LTI representation are considered to be the results of identification of \mathcal{S} with constant p .

FKcM clustering of the sample poles

By using the obtained $N_z = 11 \cdot 5$ sample pole locations as a data set Z , the FKcM algorithm has been executed with different values of m and both with a fixed number of clusters and also with the application of ACM starting from $n_c^{(0)} = 27 \approx N_z/2$. In the fixed case, $n_c = 8$ is used and the obtained solution is denoted as $m2n_c8$ for a fuzzyness $m = 2$. In case of ACM, if the algorithm has resulted in $n_c = 11$ clusters for a fixed m , like $m = 8$, then the solution is denoted by $m8ad11$. Note that in the fixed case we use the particular choice of 8 clusters as this number of clusters agrees with the number of sets by visual inspection (two times 3 sets for the complex and 2 sets for the real poles). It is shown in the sequel that this number of clusters is also selected by the ACM.

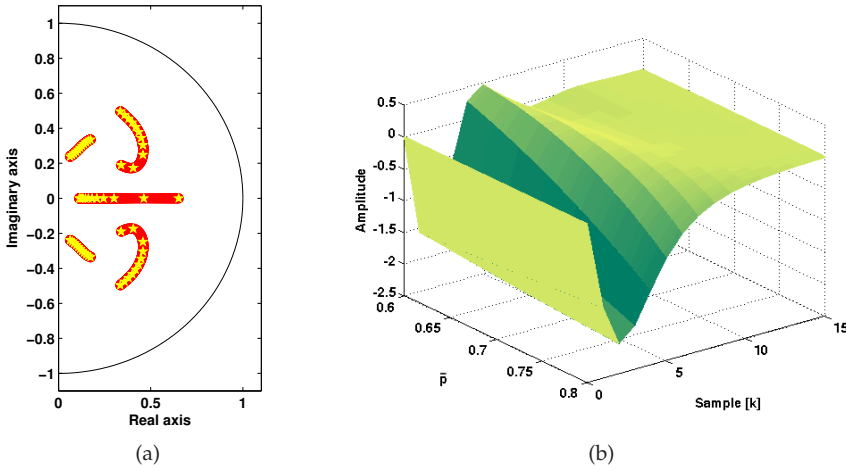


Figure 8.2: (a) The pole manifest set $\Omega_{\mathbb{P}}$ (solid red line) of the LPV-IO representation $\mathfrak{R}_{\text{IO}}(\mathcal{S})$. Sampled pole locations are denoted by \star . (b) First 15 Markov parameters of the impulse responses of $\mathfrak{R}_{\text{IO}}(\mathcal{S})$ with respect to all constant scheduling trajectories $p(k) = \bar{p}$.

The results of the algorithm are presented in Table 8.1 and in Figure 8.3. The comparison in Table 8.1 is presented in terms of N_{av} , the average number of iterations based on 10 runs of the algorithm starting from random V_0 ; n_c , the number of obtained clusters; S_e , the Normalized Entropy (see (2.181)); χ , the Xie-Beni validity index (see (2.178)); $\check{\rho}$, the achieved decay rate (see (8.11)); and $\epsilon_{\text{max}}^{n_e}$, the worst-case absolute error of the impulse responses of the truncated series-expansion representation of each $\mathcal{F}_{\bar{p}} \in \mathcal{F}_{\mathbb{P}}$ in terms of the resulting OBFs with n_e repetitions. In Figure 8.3, the resulting basis poles are given by blue \times for each solutions together with the sampled poles (red \circ). By using the cluster centers as basis poles, $\Lambda_{n_c} = V$, the resulting boundary of $\Omega(\Lambda_{n_c}, \check{\rho})$ is also given in Figure 8.3. Based on these, the following observations can be made:

Analysis of the results

- The values of N_{av} , which are based on the results of 10 runs starting from random V_0 , are relatively low, but they are growing with m . Explanation lies in Theorem 8.2, by which $J_m \rightarrow 0$ as $m \rightarrow \infty$. This property introduces both increased computational error and flat shapes of membership surfaces for large m (compare Fig. 8.4a to 8.4b). Flat surfaces give smaller improvements towards the minimum of J_m in each iteration of Algorithm 8.1, than the smooth slope of the $m = 2$ case.
- The FKcM with ACM ($\epsilon_s = -15\text{dB}$), starting from $n_c^{(0)} = N_z/2$, converges to a 8-cluster-based partition for low m , but in case of higher values of m , the optimization has different attractive solutions, like the *m8ad8* and

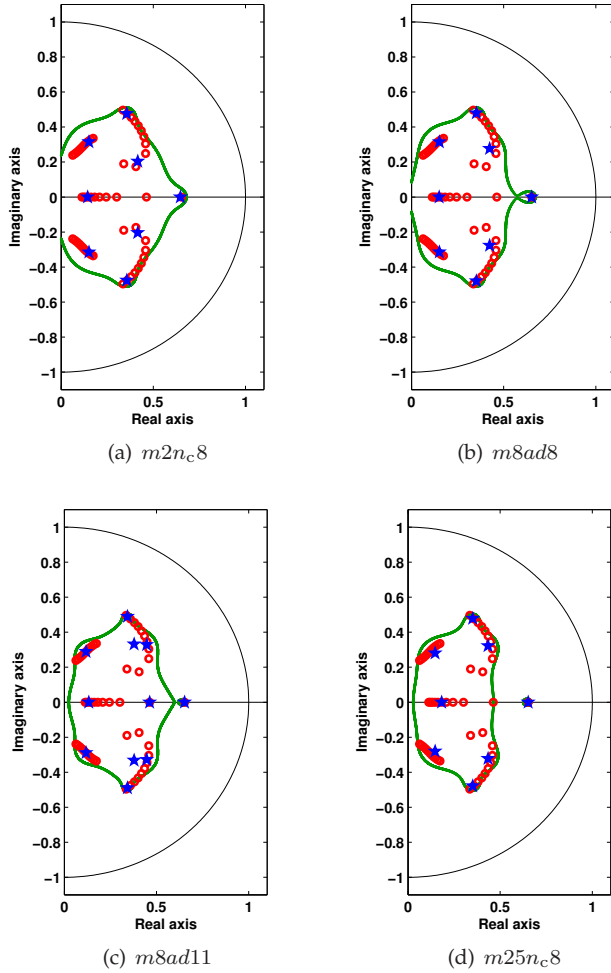
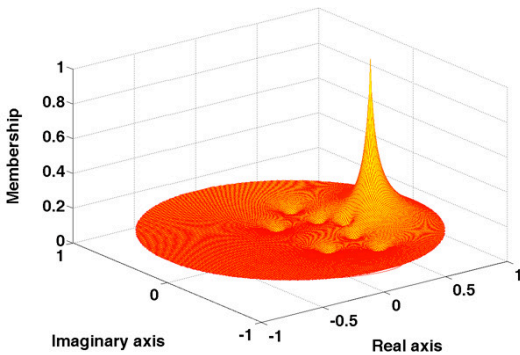


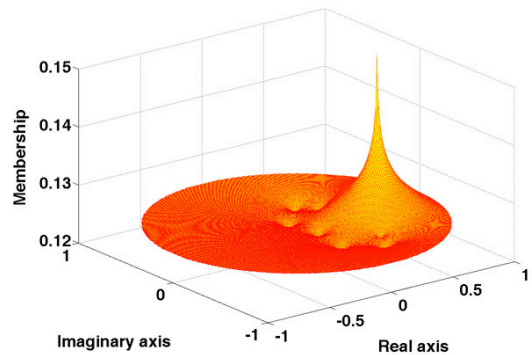
Figure 8.3: Results of FKcM clustering in the considered cases: sampled poles (red o), resulting cluster centers (blue \star), and boundaries of $\Omega(\Lambda_{n_c}, \check{\rho})$ (green bold lines).

Table 8.1: Comparison of algorithmic results in terms of N_{av} , the average number of iterations based on 10 runs of the algorithm starting from random V_0 ; n_c , the number of obtained clusters; S_e , the Normalized Entropy; χ , the Xie-Beni validity index; $\check{\rho}$, the achieved decay rate; and $\epsilon_{\max}^{n_e}$, the worst-case absolute error of the impulse responses of the truncated series-expansion representation of each $\mathcal{F}_{\mathbb{P}} \in \mathcal{F}_{\mathbb{P}}$ in terms of the cluster centers generated OBFs with n_e repetition.

Test case	N_{av}	n_c	χ (dB)	$\check{\rho}$ (dB)	S_e	$\epsilon_{\max}^{n_e=1}$ (dB)	$\epsilon_{\max}^{n_e=3}$ (dB)
$m2n_c8$	21	8	-17.49	-55.86	1.79	-43.73	-146.61
$m8ad8$	37	8	-12.42	-58.38	2.41	-46.90	-171.41
$m8ad11$	65	11	-8.44	-83.11	2.94	-77.33	-249.63
$m25n_c8$	56	8	-13.20	-61.36	2.43	-45.34	-168.83

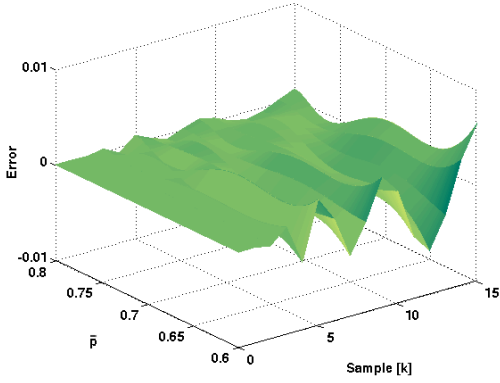


(a) $m = 2, n_c = 8$

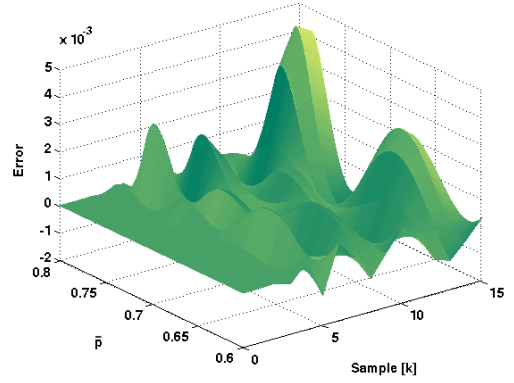


(b) $m = 25, n_c = 8$

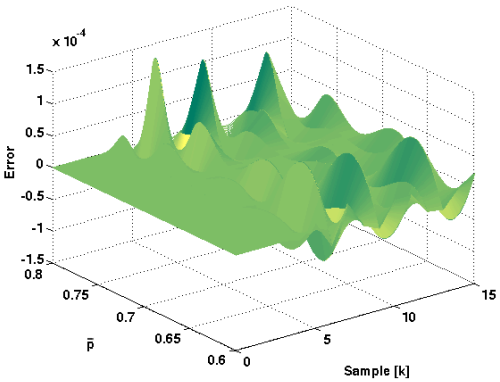
Figure 8.4: Membership functions of the 8th cluster for different m . In the second case the point corresponding to v_8 is not shown due to the peaking nature of the function to 1 (only a straight line to 1 from a flat surface would be presented).



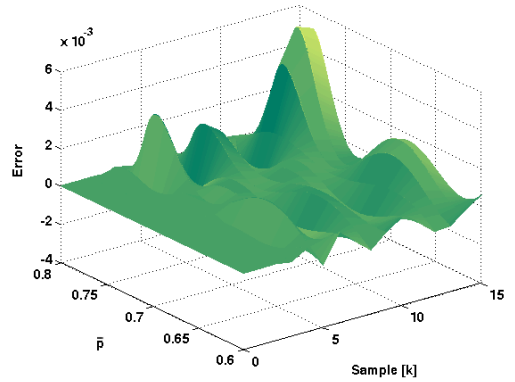
(a) $m2n_c8$



(b) $m8ad8$



(c) $m8ad11$



(d) $m25n_c8$

Figure 8.5: Approximation error of the frozen impulse responses of $\mathfrak{R}_{10}(\mathcal{S})$ by the impulse responses of the truncated expansion representations of each $\mathcal{F}_{\bar{p}} \in \mathcal{F}_{\mathcal{P}}$ in terms of the FKcM clustering obtained OBFs.

$m8ad11$ cases. Here both the 8 and the 11 cluster-based partitions are attractive, depending on the initial position of the cluster centers. However, $m8ad8$ achieves a lower entropy S_e than $m8ad11$, suggesting that $m8ad8$ corresponds better to the natural data structure. As different initial conditions can drive the FKcM with ACM to converge to partitions with different n_c , it is suggested to the user to choose the one with the lowest S_e , as it most likely yields the “best” partition (see Chapter 2.5).

- χ is small in all cases, showing that each partition represents the underlying structure well. However, χ is not comparable for different m . χ has a decreasing tendency with growing n_c and an increasing tendency for growing m , therefore the fact that $\chi_{m25n_c8} < \chi_{m8ad8}$ supports that $m25n_c8$ corresponds better to the underlying data structure in the KnW sense than $m8ad8$. However, such a comparison can not be made with respect to the $m8ad11$ -case.
- The region $\Omega(\Lambda_{n_c}, \check{\rho})$ describes the pole locations of all transfer functions that have a series-expansion with a worst-case convergence rate of $\check{\rho}$ in terms of the Λ_{n_c} associated OBFs. For the resulting cluster centers, the boundary of $\Omega(\Lambda_{n_c}, \check{\rho})$ is relatively tight in all cases except for $m2n_c8$ and it also includes $\Omega_{\mathbb{P}}$ (see Figure 8.2). This means that the convergence rate of the basis has been focused/optimized for LTI systems with transfer functions that have poles close to the frozen poles of $\mathfrak{R}_{\text{IO}}(\mathcal{S})$. $\check{\rho}$ is also acceptable, which means small modeling error, i.e. fast convergence rate if the corresponding poles generated orthonormal basis are used for the series-expansion representation of the frozen behaviors of \mathcal{S} . In terms of Section 5.4, this implies fast convergence rate of the series-expansion of \mathcal{S} with respect to the derived basis. In the $m8ad11$ -case, $\check{\rho}$ is the best, which is the consequence of the larger ($n_c = 11$) number of OBFs only. By repeating both the obtained pole sets in the Hambo generation of the basis functions, i.e. using $n_e > 0$, such that the number of generated basis functions are equal, comparison of the KnW performance of these cases becomes available. Based on such a comparison, it follows that $m25n_c8$ is better in the KnW sense, which is in agreement with Theorem 8.2. The partition $m2n_c8$ is the worst among these results, which suggests that only larger values of m can ensure the quality of the obtained solution.
- Figure 8.5 and Table 8.1 show the representation errors of the frozen impulse responses of $\mathfrak{R}_{\text{IO}}(\mathcal{S})$ by the impulse responses of the truncated series-expansion representation of each $\mathcal{F}_{\check{\mathbb{P}}} \in \check{\mathcal{F}}_{\mathbb{P}}$ in terms of the OBFs generated by the cluster centers with n_e repetitions. From these results it follows that the obtained set of OBFs has negligible representation error with respect to $\check{\mathfrak{F}}_{\mathbb{P}}$, which has been our main objective (see Section 8.3.1). Among the solutions with 8 basis functions, surprisingly $m8n_c8$ has the lowest representation error of the frozen impulse responses instead of $m25n_c8$. Based on the previous results, one would expect that the representation error of the frozen impulse responses is less for OBFs generated with higher m , however this is not the case here, due to the fact that $\Omega_{\mathbb{P}}$ is sampled. Even if

$m25n_c8$ delivers a better choice with respect to the sampled pole locations, it is not guaranteed that the reconstruction of $\Omega_{\mathbb{P}}$, based on the sample poles, resulted in a better estimate than in the other cases. By comparing the results in terms of S_e , such a phenomenon is clearly indicated. The quality of the information, i.e. how well the pole samples describe $\Omega_{\mathbb{P}}$ is highly significant in establishing optimality between the sampled-poles-based OBFs and the original system.

In conclusion, the FKcM solutions for the considered example are converging relatively fast to optimal partitions in terms of Theorem 8.1. In accordance with Theorem 8.2, as m increases, these partitions give better solutions of Problem 8.1. ACM also ensures proper selection of an efficient number of OBFs in the KnW sense, if the different settling partitions are compared in terms of S_e . Furthermore, validity of the derived partitions is supported by low χ in all cases.

Comparison of results to solutions obtained by the gradient search method (Heuberger et al. 2005, Ch. 11), is only possible if the number of available samples of $\Omega_{\mathbb{P}}$ is so high that there is no need for the reconstruction of $\Omega_{\mathbb{P}}$. Thus an advantage of the FKcM approach is that it gives a solution for the practical case when only few samples of $\Omega_{\mathbb{P}}$ are available. In the unrealistic case, when $\Omega_{\mathbb{P}}$ is known, both algorithms converge to similar solutions, but with a lower computational time in the FKcM case. The two algorithms also have similar properties in the sense that they only yield convergence to local minima. As online selection of the efficient number of OBFs is very difficult to implement into the gradient search method, the FKcM approach, with strategies like the ACM, has a second advantage over gradient approaches.

8.4 Robust extension of the FKcM approach

During the development of the FKcM approach, we have assumed that some samples of $\Omega_{\mathbb{P}}$ are given. These samples have been used as a data set, i.e. a source of information on which the developed basis selection tool is based on. We have motivated that such samples are available in practice either based on first principle information or as the poles of model estimates of the frozen system set $\mathcal{F}_{\mathbb{P}}$. These model estimates are considered to be the result of LTI identification of the LPV system with constant scheduling signals. However, system identification is in practice always affected by noise, thus the pole locations of the estimated models are the realizations of an underlying probability function of the frozen poles. This means that selecting basis functions, based on estimated poles, carries the risk that the result of the basis selection by the FKcM method is significantly effected by the noise. In this section, we aim to provide a robust solution of the previously considered basis selection problem by reformulating the developed FKcM approach, such that it takes into account the uncertainty of the pole estimates.

8.4.1 Questions of robustness

In prediction-error identification, each estimated pole can be associated with an uncertainty region in the complex plain for a certain level of confidence. In the classical literature, ellipsoidal regions are quantified that are the results of the linearization of the map from parameters θ to pole locations $\{\lambda\}$. In Section 2.3.6, an alternative approach of Vuerinckx et al. (2001) has been introduced that characterizes pole uncertainty regions of the model estimates without linearization. The approach leads to a (possibly disconnected) uncertainty region $\mathcal{P}(\mathcal{Q}_\theta, \alpha) \subset \mathbb{C}$ for which it holds that

$$\hat{\lambda}_1, \dots, \hat{\lambda}_n \in \mathcal{P}(\mathcal{Q}_\theta, \alpha), \quad \text{with probability } \geq \alpha \quad (8.15)$$

where $\{\hat{\lambda}_1, \dots, \hat{\lambda}_n\}$ are the poles of the model estimate. Note that this uncertainty concept is still necessarily conservative as it disregards covariance of the pole estimates. However, later it will be shown that the locations of the possible pole estimates, i.e. possible poles of a transfer function set, are formulated in the same worst-case sense as the KnW theory. Based on this, it is clear that by using the uncertainty regions provided by this approach as data objects in both the reconstruction problem of $\Omega_{\mathbb{P}}$ and the KnW optimization problem, the basis selection task can be solved in a robust sense.

In the original problem of FKcM clustering, the samples of $\Omega_{\mathbb{P}}$ form a finite set of points Z in \mathbb{D} . Because of the fact that the set Z is finite, both the reconstruction problem and the minimization of (8.4) can be analytically computed and solved via the proposed algorithm. However, if Z is not a finite set but a collection of complex regions, i.e. uncertainty sets, it is not trivial how to calculate ρ in (8.4) with respect to these regions or how to obtain the worst-case KM distance involved in the FKcM as the dissimilarity measure d_{ik} . Subsequently the problem rises how to solve the selection problem of the OBFs poles by using the FKcM mechanism.

To provide answers for these questions, in Section 8.4.2 we first show that by using results of hyperbolic geometry, (8.3) and its 1-width version, the so called Kolmogorov measure, can be analytically computed if the regions in Z are hyperbolic circles or hyperbolic segments. However, shapes of uncertainty regions can vary arbitrary, thus to use the developed hyperbolic results, the regions must be covered by a collection of hyperbolic circles or hyperbolic segments. Thus, in Section 8.4.2 also a practically applicable multistep procedure is developed that covers complex regions with the union of hyperbolic circles. In this way, the KnW optimization problem (8.4) and also the reconstruction problem of $\Omega_{\mathbb{P}}$ by the clustering of pole uncertainty regions can be solved along a similar line of reasoning as in Section 8.3. This robust extension of the FKcM clustering is developed in Section 8.4.4 and its properties are investigated again in terms of optimality of the solution, numerical convergence, etc. Based on this, it is shown that the resulting algorithm provides the selection of asymptotically optimal OBFs in the KnW sense for the local behaviors of \mathcal{S} even in case of significant measurement noise. This property is also illustrated through an example.

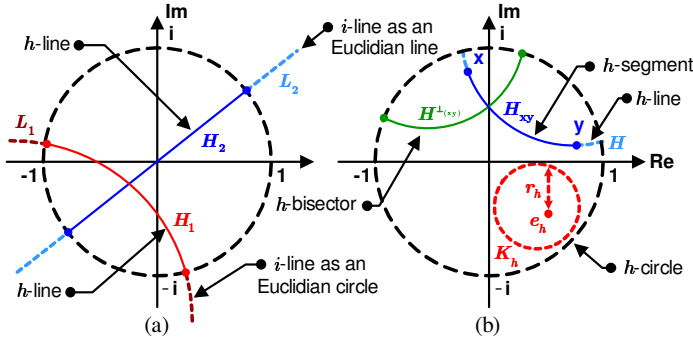


Figure 8.6: Hyperbolic objects of the Poincaré disc model.

8.4.2 Basic concepts of hyperbolic geometry

In order to develop the required geometrical tools, the basic aspects of the 2-dimensional *Poincaré disc model* of hyperbolic geometry are introduced in the sequel. Based on new results, it is also shown that hyperbolic geometry generalizes results of the KnW theory.

The 2-dimensional Poincaré model provides a conformal disc model, where points of the geometry are in a complex disc. The lines are segments of circles that lie inside the disc, where the circles themselves are orthogonal to the boundary of the disc, or the segments are part of a diameter of the disc (see Figure 8.6). Before defining these objects, it is motivated why this geometric model has important relations to the KnW theory.

We have already discussed that the Kolmogorov measure (see Definition 8.1) is equal to the cost function of the 1-width Kolmogorov problem ($n_g = 1$) (see (8.3)). Based on this property, the KM had an important role as a dissimilarity measure in the FKcM algorithm to formulate KnW optimality of the obtained solution in an asymptotic sense. Additionally, this observation has an important consequence for geometrical objects in \mathbb{D} which are convex in terms of the KM. Namely, that in the $n_g = 1$ case, the solution of (8.4) with respect to regions equivalent with these objects can be found through LMI's based optimization. We will see that this property provides an efficient way to solve the heavy nonlinear optimization problem that (8.4) represents and is also the key ingredient to handle the robust basis selection problem. In the following, we first introduce some simple convex objects in the KM sense and additional geometrical tools that are required in the second part to develop three key results for the above mentioned property.

The most simplest of the convex objects in the KM sense are the segments of hyperbolic lines which are introduced through the concept of i -lines (see Figure 8.6.a) and their orthogonality in \mathbb{C} :

Definition 8.2 (i-line) (Brannan et al. 1999) *In \mathbb{C} , an i -line L is either an Euclidian*

line E :

$$L = E(\mathbf{e}, \mathbf{r}) := \left\{ z \in \mathbb{C} \mid \begin{array}{ll} \text{if } \mathbf{r} < \infty, & \text{Im}(z) = \mathbf{r}\text{Re}(z) + \mathbf{e} \\ \text{else,} & \text{Re}(z) = \mathbf{e} \end{array} \right\}, \quad (8.16)$$

with y -intercept $\mathbf{e} \in \mathbb{C}$ and slope $\mathbf{r} \in \mathbb{R}_0^+ \cup \{\infty\}$, or Euclidian circle K

$$L = K(\mathbf{e}, \mathbf{r}) := \{z \in \mathbb{C} \mid |z - \mathbf{e}| = \mathbf{r}\}, \quad (8.17)$$

with center $\mathbf{e} \in \mathbb{C}$ and radius $\mathbf{r} \in \mathbb{R}^+$, such that $L \cap \mathbb{D} \neq \emptyset$.

Definition 8.3 (Orthogonality) (Brannan et al. 1999) *Two i -lines L_1 and L_2 are orthogonal, iff*

L_1	L_2	$L_1 \perp L_2$
line	line	Euclidian orthogonality
circle	line	if $L_1 = K(\mathbf{e}_1, \mathbf{r}_1)$, then $\mathbf{e}_1 \in L_2$
circle	circle	$\forall z \in L_1 \cap L_2 \neq \emptyset$, the radii of L_1 and L_2 through z are orthogonal

Now it is possible to define hyperbolic lines and segments (see Figure 8.6):

Definition 8.4 (h-line & h-segment) (Brannan et al. 1999) *A hyperbolic line (h-line) is defined as $H = L \cap \mathbb{D}$, where L is an i -line, $L \perp \mathbb{J}$ (orthogonal to the unit circle), and \mathbb{D} is the unit disc. The section of H between $\mathbf{x}, \mathbf{y} \in H$ is denoted as $H_{\mathbf{x}\mathbf{y}}$ and called a hyperbolic segment (h-segment).*

Lemma 8.1 (Uniqueness of h-lines) (Brannan et al. 1999) *If $\mathbf{x} \neq \mathbf{y}$ and $\mathbf{x}, \mathbf{y} \in \mathbb{D}$, then there is a unique h-line H such that $\mathbf{x}, \mathbf{y} \in H$.*

Hence h-lines are part of Euclidean circles orthogonal to the unit circle or part of Euclidian lines through the origin, where the part is strictly inside \mathbb{D} . The concept of h-bisectors of h-segments (see Figure 8.6.b) is also important to develop connections of Euclidian and hyperbolic geometry.

Definition 8.5 (h-bisector) (Brannan et al. 1999) *The h-bisector of the h-segment $H_{\mathbf{x}\mathbf{y}}$ (segment of h-line H), is an h-line $H^{\perp(\mathbf{x}\mathbf{y})}$ containing the midpoint (in the KM sense) of $H_{\mathbf{x}\mathbf{y}}$ and $H^{\perp(\mathbf{x}\mathbf{y})} \perp H$, meaning that their corresponding i -lines are orthogonal.*

Circles are convex geometrical objects in Euclidian geometry. Their counterpart in hyperbolic geometry (see Figure 8.6.b) is defined as follows:

Definition 8.6 (h-circle & h-disc) (Brannan et al. 1999) *A hyperbolic circle (h-circle) $K_h(\mathbf{e}_h, \mathbf{r}_h)$ and a hyperbolic disc (h-disc) $D_h(\mathbf{e}_h, \mathbf{r}_h)$ with h-center $\mathbf{e}_h \in \mathbb{D}$ and h-radius $\mathbf{r}_h \in (0, 1)$ are defined as*

$$K_h(\mathbf{e}_h, \mathbf{r}_h) := \{z \in \mathbb{D} \mid \kappa_1(z, \mathbf{e}_h) = \mathbf{r}_h\}, \quad (8.18a)$$

$$D_h(\mathbf{e}_h, \mathbf{r}_h) := \{z \in \mathbb{D} \mid \kappa_1(z, \mathbf{e}_h) \leq \mathbf{r}_h\}. \quad (8.18b)$$

To establish connection with the Euclidian geometry, the following lemmas are important:

Lemma 8.2 (h-circle equivalence) (Brannan et al. 1999) *For any Euclidian circle $K(\mathbf{e}, \mathbf{r}) \subset \mathbb{D}$ with $\mathbf{r} > 0$, there exists a unique h-circle $K_h(\mathbf{e}_h, \mathbf{r}_h)$, such that $K_h(\mathbf{e}_h, \mathbf{r}_h) = K(\mathbf{e}, \mathbf{r})$ and \mathbf{e}_h is strictly inside $K(\mathbf{e}, \mathbf{r})$, i.e. $|\mathbf{e}_h - \mathbf{e}| < \mathbf{r}$.*

Lemma 8.3 (h-center relation) *For any h-circle $K_h(\mathbf{e}_h, \mathbf{r}_h)$ and its Euclidian equivalent $K(\mathbf{e}, \mathbf{r})$, there exists a $\varphi_h \in \mathbb{R}$, such that $\mathbf{e} = \varphi_h \mathbf{e}_h$.*

The proof of Lemma 8.3 is given in Appendix A.3. From Lemma 8.2, it follows that the same equivalence holds between discs and h-discs. Furthermore, Lemma 8.3 states that the h-center and the Euclidian center of a circle or a disc lie on the same Euclidian line connecting them to the origin. Note that hyperbolic circles are defined through the KM measure. Therefore, based on (2.173) and Proposition 2.1, for any circular pole region $\Omega = D_h(\mathbf{e}_h, \mathbf{r}_h)$, the optimal Λ_n in the Kolmogorov n -width sense is $\Lambda_n = [\mathbf{e}_h, \dots, \mathbf{e}_h]_{1 \times n}$ with $\rho = \mathbf{r}_h^n$. This important consequence generalizes the result of Pinkus (1985) for the pulse basis (see Section 2.4):

Theorem 8.3 (K_nW optimal OBFs for circular regions of non-analyticity) *For the class of stable transfer functions analytical outside the disc $D_h(\mathbf{e}_h, \mathbf{r}_h)$, the set of (complex) OBFs*

$$\left\{ \frac{\sqrt{1 - |\mathbf{e}_h|^2}}{z - \mathbf{e}_h} G^i(z) \right\}_{i=0}^{n-1}, \quad \text{with } G(z) = \frac{1 - z\mathbf{e}_h^*}{z - \mathbf{e}_h}, \quad (8.19)$$

are optimal in the K_nW sense.

The proof of Theorem 8.3 is trivial from the previously described motivation. To utilize this property of h-circles in the sequel, the following concepts are crucial:

Definition 8.7 (Angle of h-lines) (Brannan et al. 1999) *Let H_1 and H_2 be two h-lines intersecting in point \mathbf{x} and let H_3 be an h-line intersecting H_1 in \mathbf{y} and H_2 in \mathbf{z} . Then the angle γ_h between H_1 and H_2 is defined by the cosine rule:*

$$\sin(\kappa_1(\mathbf{x}, \mathbf{y})) \sin(\kappa_1(\mathbf{x}, \mathbf{z})) \cos(\gamma_h) = \cos(\kappa_1(\mathbf{x}, \mathbf{y})) \cos(\kappa_1(\mathbf{x}, \mathbf{z})) - \cos(\kappa_1(\mathbf{y}, \mathbf{z})),$$

By convention, γ_h is the acute angle between H_1 and H_2 (if $\gamma_h > \frac{\pi}{4}$, then $\gamma_h := \frac{\pi}{2} - \gamma_h$).

Definition 8.8 (h-inversion) (Brannan et al. 1999) $\mathfrak{h}_H : \mathbb{D} \rightarrow \mathbb{D}$ *is called an inversion with respect to the h-line H , iff \mathfrak{h}_H maps h-lines to h-lines, preserves angles between h-lines, and $\mathfrak{h}_H(z) = z$ for $\forall z \in H$.*

The following properties are immediate:

Lemma 8.4 (h-inversion uniqueness) (Brannan et al. 1999) For $\forall \mathbf{x} \in \mathbb{D}$, there exists an h-inversion \mathfrak{h}_H , such that $\mathfrak{h}_H(\mathbf{x}) = 0$ and $\mathfrak{h}_H(0) = \mathbf{x}$. If $\mathbf{x} \neq 0$, then the h-line H associated with \mathfrak{h}_H is unique and $H = H^{\perp(\mathbf{x},0)}$, otherwise H can be any h-line through the origin.

In the sequel, the notation \mathfrak{h}_x is used to denote the h-inversion associated with x .

Lemma 8.5 (Hyperbolic group) (Brannan et al. 1999) The h-inversions generate a hyperbolic group \mathcal{D} whose elements $\mathfrak{h} : \mathbb{D} \rightarrow \mathbb{D}$ are called hyperbolic transformations. Each $\mathfrak{h} \in \mathcal{D}$ is a conformal mapping of \mathbb{D} .

These give the following crucial observations:

Lemma 8.6 (h-circle transformation) (Brannan et al. 1999) For any $\mathfrak{h} \in \mathcal{D}$ and h-circle $K_h(\mathbf{e}_h, \mathbf{r}_h)$,

$$\mathfrak{h}(K_h(\mathbf{e}_h, \mathbf{r}_h)) = K_h(\mathfrak{h}(\mathbf{e}_h), \mathbf{r}_h). \quad (8.20)$$

Corollary 8.1 (κ_1 -invariance) (Brannan et al. 1999) $\kappa_1(x, y)$ is invariant under \mathcal{D} , meaning that $\kappa_1(x, y) = \kappa_1(\mathfrak{h}(x), \mathfrak{h}(y))$, for all $\mathfrak{h} \in \mathcal{D}$ and $x, y \in \mathbb{D}$.

Now it is possible to develop three key results that are used for the robust solution of the basis selection problem.

Theorem 8.4 (κ_1 -metric) The Kolmogorov measure κ_1 is a metric on \mathbb{D} .

The proof is given in Appendix A.3. This shows that KM is a natural “distance²” on \mathbb{D} .

Theorem 8.5 (h-segment worst-case distance) Given $x, y \in \mathbb{D}$, $x \neq y$, defining the h-segment H_{xy} , then for any $v \in \mathbb{D}$

$$\max_{z \in H_{xy}} \kappa_1(v, z) = \max_{z \in \{x, y\}} \kappa_1(v, z). \quad (8.21)$$

The proof is given in Appendix A.3. This shows (see Figure 8.7a), that the worst-case KM of any point in \mathbb{D} with respect to an h-segment can be calculated as the maximum of the KMs with respect to the endpoints of the segment. In Section 8.4.4, this result is used in the solution of the KnW optimization problem for calculating the worst-case cost of basis pole candidates with respect to uncertainty regions associated with real pole estimates.

Theorem 8.6 (h-disc worst-case distance) Let $D_h(\mathbf{e}_h, \mathbf{r}_h)$ be an h-disc and $v \in \mathbb{D}$. Denote by $K_h(\mathbf{e}_h, \mathbf{r}_h)$ the perimeter circle of $D_h(\mathbf{e}_h, \mathbf{r}_h)$ and by H the unique h-line through v and \mathbf{e}_h . Then,

$$\max_{z \in D_h} \kappa_1(v, z) = \begin{cases} \max_{z \in \{x, y\}} \kappa_1(v, z), & \text{if } v \neq \mathbf{e}_h; \\ \mathbf{r}_h, & \text{if } v = \mathbf{e}_h; \end{cases} \quad (8.22)$$

²Note that KM is not a distance on \mathbb{D} in the geometrical sense; only $2\text{arctanh}(\kappa_1(x, y))$ bears this property and is called the *Poincaré distance* (Brannan et al. 1999).

confidence level α) contains segments of the real axis. Therefore, these segment parts of $\mathcal{P}(\Omega_\theta, \alpha)$ can be associated with h-segments without the need of any approximation. In case $F(q, \hat{\theta}_{N_d})$ has a complex pole pair, then $\mathcal{P}(\Omega_\theta, \alpha)$ contains complex regions which come in complex conjugate pairs. Depending on the uncertainty of the model estimate, these complex regions can merge into one another, and can also encircle parts of \mathbb{D} which seemingly do not contain any of the estimated or original pole locations (see Section 2.3.6). Thus complex pole uncertainty regions can occur in complicated shapes. However, with a simple methodology, quite effective coverage of such shapes can be achieved by h-discs.

Let Ω be a separate, complex region in $\mathcal{P}(\Omega_\theta, \alpha)$. Due to the method of Tóth et al. (2008c), the separated regions are distinguished during the calculation of $\mathcal{P}(\Omega_\theta, \alpha)$. Assume that an equidistant gridding of \mathbb{D} is given with step size $\tau \in \mathbb{R}^+$ and the set of grid points is denoted by Q . Let $Q_+ = \Omega \cap Q$ be the grid points in Ω and let $Q_- = Q \setminus Q_+$. Next, define \mathcal{D}_0 as a collection of equidistant Euclidian discs with centers at each point of Q_+ and with radii $r = \frac{\sqrt{2}}{2}\tau$. In this way, a coverage of Ω is obtained by an unnecessary large number of Euclidian discs determining uniquely their h-disc counterparts. This is used as the initialization of the iterative optimization procedure of Algorithm 8.2 to find an efficient disc-coverage based on a fixed number of n discs with unequal radii.

In Step 1 of this algorithm, a disc is selected from the coverage which is the furthest from the points of Q_- and its radii can be increased by $\frac{\sqrt{2}}{2}\tau$, without causing the discs to contain any point of Q_- . In case of a tie, an arbitrary disc is selected from the possible choices. The radius of the selected disc is increased with $\frac{\sqrt{2}}{2}\tau$ in Step 2. If a disc contains other discs after its radius was increased, then those discs are removed from the coverage in Step 3. The procedure is repeated till there is no disc whose radius can be increased by $\frac{\sqrt{2}}{2}\tau$ without containing a point of Q_- . The optimization results in a h-disc coverage that gives an “optimal” coverage for the grid-points Q_+ with a minimal number of circles, however this number can be much larger than desired. Therefore a second optimization is initiated in Step 5, which gives a suboptimal approximation of this coverage by a predefined number of discs n . In Step 6, two discs that have the smallest dissimilarity in terms of $\varepsilon_{ij} = |e_j - e_i| + |r_j - r_i|$, where e_j, e_i are the Euclidean centers and r_j, r_i the Euclidian radiuses of the discs, are selected. These discs are merged in Step 7 by increasing the radii of the larger disc with ε_{ij} . If a disc contains other discs after merging, then the contained discs are removed from the coverage. Merging is repeated till the desired number of circles is achieved. Example 8.2 shows how the method works in practice.

Example 8.2 (Hyperbolic coverage of pole-uncertainty regions) *Continue Example 2.1 by computing the hyperbolic coverage of the pole uncertainty regions with Algorithm 8.2 using $\tau = 10^{-3}$. For regions associated with different confidence levels, the results are given in Figure 8.8. As can be seen, even the complicated butterfly region is rather well approximated with a small number of h-discs.*

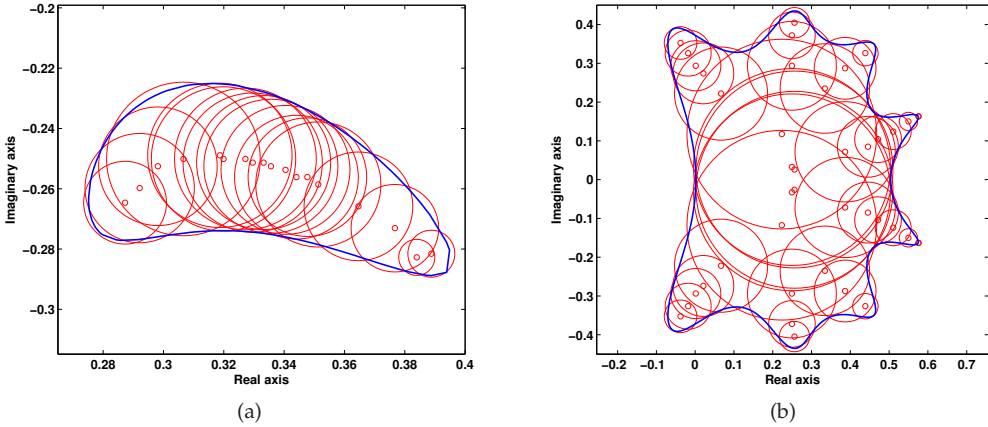


Figure 8.8: (a) 20 h-discs based coverage of a non-connected uncertainty region of Figure 2.6 with confidence level 1%. The overfit in area is 4.55%. (b) 40 h-discs based coverage of a connected uncertainty region of Figure 2.6 with confidence level 99%. The overfit in area is 4.35%.

Algorithm 8.2 (Disc coverage of complex regions)

- | | |
|---------------------------------|---|
| 0. Initialization: | Let $\mathcal{D}_0 := \{D(\mathbf{e}, \frac{\sqrt{2}}{2}\tau)\}_{\mathbf{e} \in \mathcal{Q}_+}$ be a disc coverage of Ω based on the step size $\tau > 0$. Let $n > 0$ and $l := 0$. |
| 1. Furthest h-discs: | Find a $D(\mathbf{e}, r) \in \mathcal{D}_l$ such that $\min_{\mathbf{v} \in \mathcal{Q}_-} \min_{\mathbf{z} \in D(\mathbf{e}, r)} \mathbf{v} - \mathbf{z} $ is maximal on \mathcal{D}_l and $D(\mathbf{e}, r + \frac{\sqrt{2}}{2}\tau) \cap \mathcal{Q}_- = \emptyset$. Let $\hat{D}_l = D(\mathbf{e}, r + \frac{\sqrt{2}}{2}\tau)$ otherwise $\hat{D}_l = \emptyset$. |
| 2. h-disc extension: | If such D exists, then $\mathcal{D}_{l+1} = (\mathcal{D}_l \setminus D) \cup \hat{D}_l$. |
| 3. Remove discs: | Remove all D from \mathcal{D}_{l+1} which satisfy $D \subseteq \hat{D}_l$. |
| 4. Check of convergence: | If $\hat{D}_l \neq \emptyset$, then set $l := l + 1$ and goto Step 1. |
| 5. Check of cardinality: | If $\text{card}(\mathcal{D}_{l+1}) \leq n$, then stop, else set $l := l + 1$ and continue with Step 6. |
| 6. Most similar h-discs: | Find $D_i(\mathbf{e}_i, \mathbf{r}_i), D_j(\mathbf{e}_j, \mathbf{r}_j) \in \mathcal{D}_l$ such that $D_i \neq D_j$, $\mathbf{r}_i \geq \mathbf{r}_j$, and $\varepsilon_{ij} = \mathbf{e}_j - \mathbf{e}_i + \mathbf{r}_j - \mathbf{r}_i $ is minimal. |
| 7. Merging: | $\hat{D}_l = D(\mathbf{e}_i, \mathbf{r}_i + \varepsilon_{ij})$ and $\mathcal{D}_{l+1} = (\mathcal{D}_l \setminus \{D_i, D_j\}) \cup \hat{D}_l$. Perform Step 3 and goto Step 5. |
-

8.4.4 The robust pole clustering algorithm

In the following, the robust extension of the original FKcM approach is discussed. As the mechanism of the clustering remains the same in the robust extension, we will follow the same line of reasoning as in Section 8.3. However, we investigate and derive these results in a different problem setting.

Let $\{\hat{F}_{\bar{p}_i}\}_{i=1}^{n_{loc}}$ be a set of $n_{loc} \geq 1$ estimated frozen transfer functions of the LPV system \mathcal{S} identified for constant scheduling signals: $\bar{p}_i \in \mathbb{P}$ and IO partition (u, y) . Each $\hat{F}_{\bar{p}_i}$ is associated with a pole uncertainty region $\mathcal{P}_{\bar{p}_i}$ containing a number of regions in \mathbb{D} . Let $\{\Omega_k\}_{k=1}^{N_z}$ denote the collection of these regions and introduce \mathcal{Z}_k as the set of hyperbolic objects describing/approximating each Ω_k , as has been discussed in Section 8.4.3. If Ω_k is a segment on the real axis (real pole), then associate \mathcal{Z}_k with an h-segment being equal to Ω_k , else associate it with a union of h-discs covering Ω_k (complex case). Denote $Z = \{\mathcal{Z}_k\}_{k=1}^{N_z}$ and call it the data set. Similar to the original FKcM algorithm, introduce $1 < n_c < N_z$ as the number of clusters or data groups, $v_i \in \mathbb{D}$ as the cluster centers, and $\mu_i : \mathbb{D} \rightarrow [0, 1]$ as the membership functions of the clusters for all $z \in \mathbb{D}$. By using the threshold value ε , we again obtain the set

$$\Omega_\varepsilon = \{z \in \mathbb{D} \mid \exists i \in \{1, \dots, n_c\}, \mu_i(z) \geq \varepsilon\}, \quad (8.23)$$

which is used to formulate the robust variant of Problem 8.1:

Problem 8.2 *For a set of pole uncertainty regions $\{\mathcal{P}_{\bar{p}_i}\}_{i=1}^{n_{loc}}$, described by a set of hyperbolic objects Z , and for a given number of clusters n_c , find a set of cluster centers $\{v_i\}_{i=1}^{n_c}$, a set of membership functions $\{\mu_i\}_{i=1}^{n_c}$, and the maximum of ε , such that*

- Ω_ε contains Z .
- With respect to Ω_ε , the OBFs, with poles Λ_{n_c} in the cluster centers $\{v_i\}_{i=1}^{n_c}$, are optimal in the KnW sense, where $n = n_c$.

Again, the solution is based on finding clusters in accordance with the KnW concept and subsequently finding a maximal value for ε , such that all uncertainty regions are inside Ω_ε . It is obvious that the only difference between the robust and non-robust clustering problem is in terms of the data objects, which are points (poles) of the complex plane in the non-robust case and regions of the complex plane in the robust case.

Denote $V = [v_i]_{i=1}^{n_c}$ and $U = [\mu_{ik}]_{n_c \times N_z}$, where $\mu_{ik} = \max_{z \in \mathcal{Z}_k} \mu_i(z)$ is the degree of membership of \mathcal{Z}_k to cluster i . Furthermore, “distances” d_{ik} between v_i and \mathcal{Z}_k are also introduced to measure dissimilarity of Z with respect to each cluster. To derive an algorithmic solution of Problem 8.2, this dissimilarity measure is defined as the Kolmogorov measure, the cost function of the 1-width version of (8.4), but instead of pointwise, it is defined with respect to each \mathcal{Z}_k in a worst-case sense:

$$d_{ik} = \max_{z \in \mathcal{Z}_k} \kappa_1(v_i, z). \quad (8.24)$$

Note that by applying Theorems 8.5 and 8.6, d_{ik} can be computed analytically with respect to each $\mathcal{Z}_k \in \mathcal{Z}$. If \mathcal{Z}_k is a h-segment between points $\mathbf{z}_{k1}, \mathbf{z}_{k2} \in (-1, 1)$, then d_{ik} is the maximum of the Euclidian distance between v_i and these end-points. In case \mathcal{Z}_k is a union of h-discs, then first the intersection points are computed for each disc between the perimeter of the disc and the h-line connecting its h-center with v_i . Then d_{ik} results by calculating the maximum of the KM between these points and v_i . In all cases $d_{ik} > 0$, as the worst-case “distance” over regions can never drop to zero. In the sequel, it is shown that similar to the original FKcM approach, this specific choice of dissimilarity measure relates the FcM asymptotically to the KnW theory, and in this way to the solution of Problem 8.2. In order to uniquely associate each d_{ik} with a membership level μ_{ik} the set of membership function is restricted to satisfy $\sum_{i=1}^{n_c} \mu_i(z) = 1$, which requires again that $U \in \mathcal{U}_{n_c}^{N_z}$ (see (2.175))

In the robust FKcM case, the fuzzy-functional $J_m(U, V)$ is formulated as

$$J_m(U, V) := \max_{k \in \mathbb{1}_1^{N_z}} \sum_{i=1}^{n_c} \mu_{ik}^m d_{ik} = \max_{k \in \mathbb{1}_1^{N_z}} \max_{z \in \mathcal{Z}_k} \sum_{i=1}^{n_c} \mu_{ik}^m \kappa_1(v_i, z), \quad (8.25)$$

where the design parameter $m \in (1, \infty)$ determines the fuzziness of the resulting partition. This functional defines the cost function, i.e. the criterion of the expected solution for Problem 8.2. The intuition behind the choice of m is similar as in the non-robust case. (8.25) also corresponds to a *worst-case (max) sum of error* criterion and its relation with the KnW optimality of (U, V) is the same as in the FKcM algorithm except that here the KnW problem is considered for regions and not for points of \mathbb{D} . Based on these, the following theorem yields the solution of Problem 8.2:

Theorem 8.8 (Optimal Robust Partition) *Let $m > 1$, a fuzzy partition $(U, V) \in \mathcal{U}_{n_c}^{N_z} \times \mathbb{D}^{n_c}$, and a data set $Z = \{\mathcal{Z}_k\}_{k=1}^{N_z}$ be given, where \mathcal{Z}_k is either an h-segment between points $\mathbf{z}_{k1}, \mathbf{z}_{k2} \in (-1, 1)$ or a union of n_k h-discs with h-centers $\{\mathbf{e}_{kl}\}_{l=1}^{n_k}$ and h-radial $\{\mathbf{r}_{kl}\}_{l=1}^{n_k}$. Denote $[V]_i = v_i$ and $[U]_{ij} = \mu_{ij}$. Define $\gamma_i(\nu, U)$ as the minimal value of $\tau \in [0, 1]$ fulfilling the quadratic constraints:*

$$\begin{bmatrix} |1 - \mathbf{z}^* \nu|^2 & \mu_{ik}^m \cdot (\mathbf{z} - \nu) \\ \mu_{ik}^m \cdot (\mathbf{z} - \nu)^* & \tau^2 \end{bmatrix} \succeq 0, \quad \forall \mathbf{z} \in \mathcal{Z}_k, \quad (8.26)$$

for all $k \in \mathbb{1}_1^{N_z}$, where $\nu \in \mathbb{D}$. Additionally, let $d_{ik} = \max_{z \in \mathcal{Z}_k} \kappa_1(v_i, z)$ be the dissimilarity measure of \mathcal{Z}_k with respect to V . Then (U, V) is a local minimum of J_m , if for any $(i, k) \in \mathbb{1}_1^{n_c} \times \mathbb{1}_1^{N_z}$:

$$\mu_{ik} = \left[\sum_{j=1}^{n_c} \left(\frac{d_{jk}}{d_{jk}} \right)^{\frac{1}{m-1}} \right]^{-1}, \quad (8.27a)$$

$$v_i = \arg \min_{\nu \in \mathbb{D}} \gamma_i(\nu, U). \quad (8.27b)$$

The proof is given in Appendix A.3. Similar to the FcM case, minimization of

(8.25), subject to (2.175), is tackled by alternating optimization which yields the same algorithm as Algorithm 8.1, except in Step 2 and Step 3 the solutions are obtained via (8.27a) and (8.27b).

8.4.5 Properties of the robust FKcM

As a next step we investigate the properties of the robust extension of the FKcM algorithm. It is shown that KnW optimality of the resulting cluster centers (if the solution is the global minima of (8.25)) holds again in an asymptotic sense ($m \rightarrow \infty$). Practical implementation of the algorithm is also discussed together with how the conservatism of the used pole uncertainty concept influences the procedure.

Asymptotic property

We use the asymptotic properties of J_m to explain the specific choices for the fuzzy functional (8.25) and the dissimilarity measure (8.24).

Theorem 8.9 (Asymptotic property of J_m in the robust FKcM) *Given a data set $Z = \{\mathcal{Z}_k\}_{k=1}^{N_z}$, $N_z > 0$, and a set of cluster centers $V \in \mathbb{D}^{n_c}$, $n_c > 0$. Define U_m as a membership matrix of V satisfying (8.27a) for $m > 1$. Then*

$$J_m(U_m, V) = n_c^{1-m} \max_{k \in \{1, \dots, N_z\}} \left[\prod_{i=1}^{n_c} d_{ik} \right]^{1/n_c} + \mathcal{O}(e^{-m}) \quad (8.28)$$

Furthermore, $J_m(U_m, V)$ decreases monotonically with m , and $J_\infty(U_\infty, V) = 0$.

As the proof is not affected by the specific choice of d_{ik} , the same proof can be exploited as in the original FKcM case (see Theorem 8.2). Based on Theorem 8.9, for large m and for a U satisfying (8.27a), J_m corresponds to

$$J_m(U, V) \approx n_c^{1-m} \max_{k \in \{1, \dots, N_z\}} \max_{z \in \mathcal{Z}_k} \left[\prod_{i=1}^{n_c} \kappa_1(v_i, z) \right]^{1/n_c}, \quad (8.29)$$

thus its minimization gives a close approximation of (8.4), enabling the FKcM to solve Problem 8.2 directly. However, if $m \rightarrow \infty$, then again numerical problems can occur in the minimization of (8.27b). Therefore, to obtain a well approximating solution of Problem 8.2, an appropriately large value of $m \in (1, \infty)$ should be used. Just like for the original FKcM, $m \in [5, 10]$ usually yields satisfactory results.

Similar to the previous case, for $m > 1$ the FKcM-functional (8.25) is a bounded ($0 \leq J_m \leq 1$) monotonically decreasing function both in $\{d_{ik}\}$ and U , which allows Algorithm 8.1 to converge in practice in the same sense as has been discussed in the non-robust case. By using different initial choices of V_0 , all local minima of (8.25) can be explored. From these multiple runs, the best set of the obtained OBFs

can be selected by comparison of the achieved decay rate, which is formulated in the robust case as:

$$\check{\rho} = \max_{k \in \mathbb{I}_1^{N_z}} \max_{z \in \mathcal{Z}_k} \prod_{i=1}^{n_c} \left| \frac{z - v_i}{1 - z v_i^*} \right|. \quad (8.30)$$

Comparison can also be made by visual inspection of the boundary region of $\Omega(\Lambda_{n_c}, \check{\rho})$. In practice, uniformly random choices for V_0 are suggested.

Optimization

In order to derive an algorithmic solution of Problem 8.2 in terms of Theorem 8.8, it is important to define the regions \mathcal{Z}_k as inequality constraints. Such form would enable to use (8.26) as a quadratic constraint and apply the same LMIs based optimization as in the FKcM case. Using the hyperbolic geometry, each uncertainty region can be represented in the following way:

- If \mathcal{Z}_k is an h-segment then for $z \in \mathcal{Z}_k$ it holds that

$$z_{k1} \leq z \leq z_{k2}. \quad (8.31)$$

- If \mathcal{Z}_k is the union of h-disks then for a $z \in \mathcal{Z}_k$ there exists a $l \in \mathbb{I}_1^{n_k}$ such that

$$\begin{bmatrix} |1 - z^* e_{kl}|^2 & z - e_{kl} \\ z^* - e_{kl}^* & r_{kl}^2 \end{bmatrix} \succeq 0. \quad (8.32)$$

As the resulting descriptions define an inequality (see 8.31) or a set of quadratic constraints (see 8.32) thus (8.27b) is equivalent with a minimization problem with QCs where γ is the optimization variable and ν is the decision variable. As the structure of these constraints is similar as in the non-robust case, it is possible to derive SoS relaxations through which (8.26) and (8.31) turn into LMIs. The resulting LSDP can be efficiently solved by LMI solvers. Alternatively, bisection-based recursive search can be used to obtain the minimization of γ_i in (8.27b). Also numerical conditioning of U_l can relax the computational need of the LMI's based optimization and the termination criterion of the overall algorithm can be established similar to the original FKcM method. For details on these items see Section 8.3.2. Similarity-based ACM (see Section 2.5) can also be used for the determination of the number of "natural" groups in Z , i.e. the best suitable n_c for clustering, which is also important for the successful application of the robust FKcM method.

Conservatism of the pole uncertainty concept

The approach of calculating pole uncertainty regions, presented in Section 2.3.6, projects ellipsoidal uncertainty regions of parameter estimates to regions in the complex plane. It has been already explained in Section 2.3.6 that these regions represent the set of possible pole locations of the model with respect to the parameter uncertainties with the given confidence level. However, the covariance

of the poles, i.e. which poles occur together in the model estimate with the given confidence level, is disregarded in this representation. Thus, the projection is inherently conservative as for a pole uncertainty region \mathcal{P} of a 5th order system it is not guaranteed that for any 5 arbitrary chosen points $\{\lambda_1, \dots, \lambda_5\}$ in \mathcal{P} there exists a parameter vector θ in the ellipsoidal parameter uncertainty region such that the model associated with θ has poles $\{\lambda_1, \dots, \lambda_5\}$. In other words, neglecting the covariance between the pole estimates introduces conservatism. However, it is true that for any point in \mathcal{P} it is guaranteed that there exist 4 other points in \mathcal{P} , such that these 5 points correspond to the pole locations of a model whose parameters are in the ellipsoidal parameter uncertainty region. This means that the pole uncertainty regions obtained by this method contain all possible, including the worst-case pole locations that can occur due to the uncertainty of the obtained model. However, such worst-case conservatism completely matches the worst-case concept of the KnW theory (see Section 2.4). Thus the conservatism of the projection does not affect the basis selection mechanism. This is an important observation which underlines the validity of the presented approach.

8.4.6 Simulation example

In the following an example is given to visualize the applicability of the robust basis selection mechanism and to enable comparison with the original FKcM method. In this example it is shown that disregarding pole uncertainties during the basis selection process can result in a lower worst-case convergence rate of the obtained basis functions.

Data generation

Consider again the asymptotically stable SISO LPV system \mathcal{S} given by the LPV-IO representation (8.14). By using constant scheduling signals with values $\{0.6; 0.6 + \tau; \dots; 0.8\}$, where $\tau = 0.04$, 6 local LTI-IO representations of \mathcal{S} are obtained, whose pole locations are samples of $\Omega_{\mathcal{P}}$ (see Figure 8.2a). We use fewer constant scheduling points in this case than before, to make the results and the figures more transparent. The LTI models, associated with constant scheduling signals, in this example are estimated. The identification of each frozen model has been based on a OE parametrization and 250 samples long measured IO signals of the system. The measurements contained additive white output noise ϵ with normal distribution $\mathcal{N}(0, 0.1)$ and a white input signal u with uniform distribution $\mathcal{U}(-1, 1)$. Using the pole uncertainty concept of Section 2.3.6, the pole uncertainty regions $\{\mathcal{P}_i\}_{i=1}^6$ of the estimated models have been calculated with confidence level $\alpha = 99\%$. The resulting uncertainty regions consist of $N_z = 6 \cdot 5$ complex regions $\{\Omega_k\}_{k=1}^{N_z}$ which are presented in Figures 8.9a-b. In Figure 8.9a, the estimated frozen poles are denoted by \circ with a color indicating the constant scheduling trajectory they are associated with (deep red $\bar{p}_1 = 0.6 \leftrightarrow$ yellow $\bar{p}_6 = 0.8$). The perimeter lines of the pole uncertainty regions are given in Figure 8.9b with a color indicating which poles they are associated with. Based on these figures, the resulting uncertainty regions are relatively large, prognosticating that using

only the estimated poles by the non-robust algorithm can result in a serious performance degradation of the obtained solution. In order to derive an OBF set for \mathcal{S} based on the robust FKcM mechanism, a hyperbolic coverage $\{\mathcal{Z}_k\}_{k=1}^{N_z}$ has been generated with respect to each region Ω_k , using gridding step size 0.01 and 20 h-discs per complex region. The average overfit in area has been 4.5% of the resulting coverage (see Section 8.4.3 for details on this algorithm).

Robust and non-robust pole clustering

For the identified pole locations, the non-robust FKcM algorithm has been applied with $m = 8$ and $n_c = 8$ (denoted by $m\delta n_c\delta$), while for the obtained hyperbolic coverage, the robust FKcM with the same fuzzyness m and number of clusters n_c has been executed (denoted by $rob\text{-}m\delta n_c\delta$). Note that $m = 8$ has been used to guarantee close approximation of the asymptotic case similar to the choices of the example presented in Section 8.3.3. Moreover, $n_c = 8$ has been used in both algorithms to enable comparison to the previous example. Note that the estimated poles form more or less 8 groups in this case as well (see Figure 8.9a), however this is not true for their associated uncertainty regions where only 5 groups can be detected (see Figure 8.9b). The results of the clustering are presented in Figures 8.10a-b and also in Table 8.2. In these figures, the resulting cluster centers are given by blue \times . To visualize the performance of the associated OBFs, the perimeter of their $\Omega(\Lambda_{n_c}, \check{\rho})$ region with respect to the uncertainty regions/pole estimates is given with a green bold line. Additionally, to compare the performance of the resulting OBFs the achieved $\Omega(\Lambda_{n_c}, \check{\rho}_{id})$ regions (green bold line) of the basis functions with worst-case convergence rate $\check{\rho}_{id}$ are given in Figures 8.11a-b with respect to the estimated pole locations. The performance is also compared in terms of their achieved $\Omega(\Lambda_{n_c}, \check{\rho}_{unc})$ regions given with respect to the uncertainty regions in Figures 8.12a-b, and also in terms of their achieved $\Omega(\Lambda_{n_c}, \check{\rho}_{true})$ regions given with respect to the true frozen poles in Figures 8.13a-b. These figures have been generated for comparison purposes to show why the use of the robust FKcM clustering delivers a better basis for the frozen behaviors than the non-robust solution. In Table 8.2, the comparison of the results is presented in terms of the previously used indicators like χ , the Xie-Beni validity index and S_e , the normalized entropy together with the achieved decay rate with respect to the estimated pole locations: $\check{\rho}_{id}$, to the uncertainty regions: $\check{\rho}_{unc}$, and to the true pole location of the local systems: $\check{\rho}_{true}$. Additionally, $\epsilon_{\max}^{n_e}$, the worst-case absolute error of the impulse responses of the truncated series-expansion representation of each $\mathcal{F}_{\bar{p}} \in \mathcal{F}_{\mathbb{P}}$ in terms of the generated OBFs with n_e repetitions, is also given. Based on these and the previous results of Section 8.3.3, the following observations can be made:

Analyzing the results

The resulting partitions of the non-robust ($m\delta n_c\delta$) and the robust FKcM clustering ($rob\text{-}m\delta n_c\delta$) solve the basis selection problem for the identified pole locations / pole uncertainty regions. This follows from the tight fit of the resulting boundary regions (see Figures 8.10a-b) with respect to the data sets and the achieved

Table 8.2: Comparison of algorithmic results in terms of χ , the Xie-Beni validity index; S_e , the Normalized Entropy; the achieved decay rate with respect to the estimated pole locations: $\check{\rho}_{id}$, to the uncertainty regions: $\check{\rho}_{unc}$, and to the true pole location of the local systems: $\check{\rho}_{true}$; and $\epsilon_{max}^{n_e}$, the worst-case absolute error of the impulse responses of the truncated series-expansion representation of each $\mathcal{F}_{\bar{p}} \in \mathcal{F}_{\mathbb{P}}$ in terms of the cluster centers generated OBFs with n_e repetition. All results are given in dB.

Test case	χ	$\check{\rho}_{id}$	$\check{\rho}_{unc}$	$\check{\rho}_{true}$	S_e	$\epsilon_{max}^{n_e=1}$	$\epsilon_{max}^{n_e=3}$
<i>rob-m8n_c8</i>	38.958	-52.444	-43.695	-47.012	2.830	-37.326	-140.919
<i>m8n_c8</i>	-5.003	-62.809	-32.165	-44.052	2.828	-32.165	-131.207

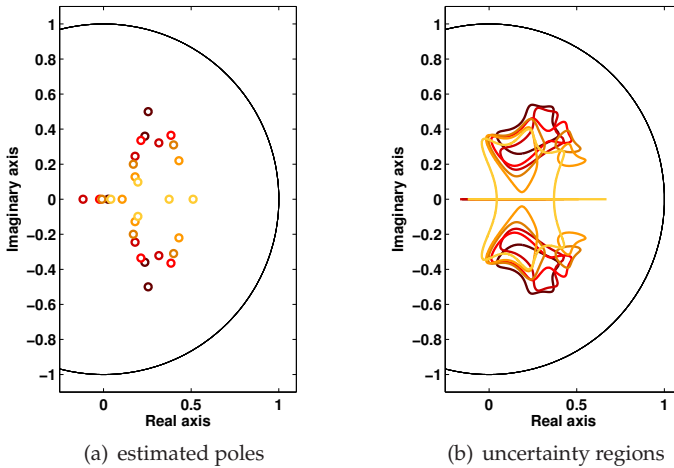


Figure 8.9: Estimated frozen poles of $\mathfrak{N}_{IO}(S)$ and their associated uncertainty regions. The poles are denoted by \circ in subfigure (a) with a color indicating the constant scheduling trajectory they are associated with (deep red $\bar{p}_1 = 0.6 \leftrightarrow$ yellow $\bar{p}_6 = 0.8$). The perimeter lines of the pole uncertainty regions are given in subfigure (b) with a color indicating that which estimated poles they are associated with.

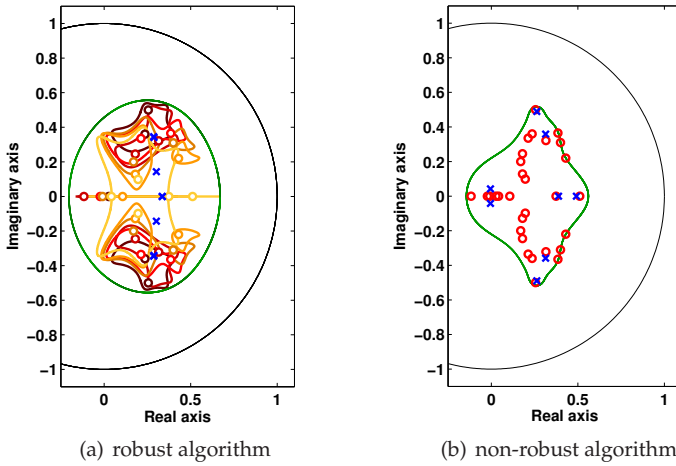


Figure 8.10: Resulting cluster centers (blue \times) of robust FKcM clustering of the pole uncertainty regions (deep red for $\bar{p}_1 = 0.6 \leftrightarrow$ light orange for $\bar{p}_6 = 0.8$) and non-robust FKcM clustering of the estimated poles (red \circ). To visualize the performance of the cluster centers associated OBFs, the perimeter of their $\Omega(\Lambda_{n_c}, \check{\rho})$ region with respect to the uncertainty regions/pole estimates is given with green bold line.

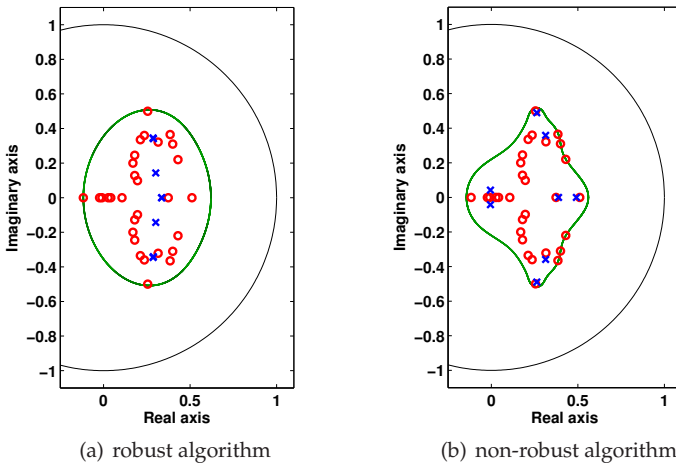


Figure 8.11: Performance comparison of the resulting cluster centers (blue \times) associated OBFs in terms of the perimeter of their $\Omega(\Lambda_{n_c}, \check{\rho}_{id})$ region (green bold line) with respect to the estimated frozen poles (red \circ) of $\mathfrak{R}_{IO}(\mathcal{S})$.

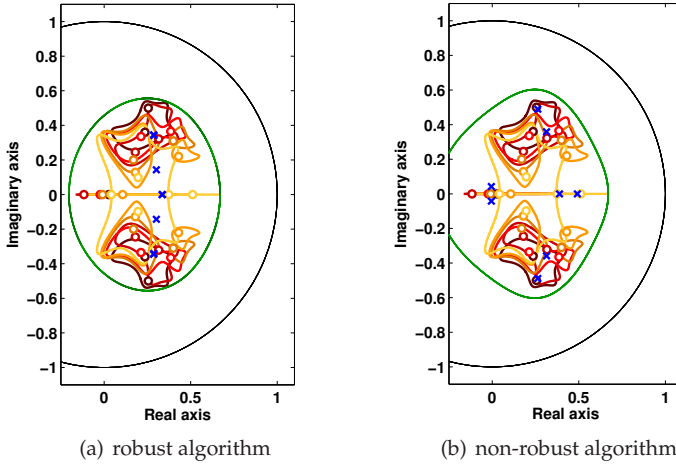


Figure 8.12: Performance comparison of the resulting cluster centers (blue \times) associated OBFs in terms of the perimeter of their $\Omega(\Lambda_{n_c}, \check{\rho}_{unc})$ region (green bold line) with respect to the uncertainty regions of the estimated frozen poles.

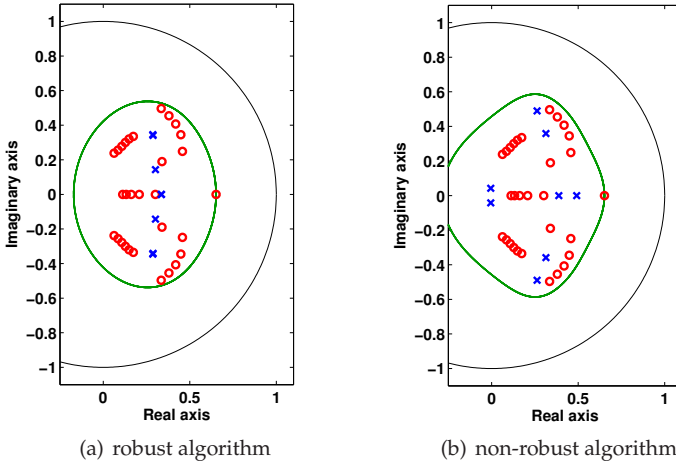


Figure 8.13: Performance comparison of the resulting cluster centers (blue \times) associated OBFs in terms of the perimeter of their $\Omega(\Lambda_{n_c}, \check{\rho}_{true})$ region (green bold line) with respect to the true frozen poles (red \circ) of $\mathfrak{F}_{IO}(\mathcal{S})$.

small value of the worst-case convergence rate with respect to the used estimated poles/uncertainty regions (see $\check{\rho}_{\text{unc}}$ for $rob\text{-}m\delta n_c\delta$ and $\check{\rho}_{\text{id}}$ for $m\delta n_c\delta$ in Table 8.2). However, the OBFs represented by the $rob\text{-}m\delta n_c\delta$ partition are better basis functions for \mathcal{S} than the $m\delta n_c\delta$ solution, as the worst-case convergence rate ($\check{\rho}_{\text{true}}$) of the basis poles with respect to the true frozen pole locations is smaller in the former case. This is also shown in Figure 8.13a, where the $rob\text{-}m\delta n_c\delta$ solution achieves a relatively tight $\Omega(\Lambda_{nc}, \check{\rho}_{\text{true}})$ on the true pole locations, while the $m\delta n_c\delta$ case has quite high performance degradation resulting in a loose bound (see in Figure 8.13b). This yields a smaller representation error if the $rob\text{-}m\delta n_c\delta$ OBFs are used for a truncated series-expansion representation of \mathcal{S} , which is proved by comparing the worst-case impulse response representation errors ($\varepsilon_{\text{max}}^{n_e}$) in Table 8.2. The reason why $rob\text{-}m\delta n_c\delta$ outperforms the $m\delta n_c\delta$ solution, comes from the fact that the $m\delta n_c\delta$ solution is based on only one realization of the *probability density function* (pdf) associated with the pole estimation, while $rob\text{-}m\delta n_c\delta$ is based on pole regions associated with a level set of the pdf through the pole uncertainty concept of Section 2.3.6. Therefore, if the realization, i.e. the estimated poles, is far from the true pole locations, then there is no guarantee about the true performance of the non-robust OBF selection ($\check{\rho}_{\text{true}} > \check{\rho}_{\text{id}}$). Contrary, the robust solution obtains guaranteed performance for any realization inside the used uncertainty regions, giving a high probability in terms of α , that this guaranteed performance is the upper bound of the achieved performance with respect to the true pole locations. This is clearly shown by comparing $\check{\rho}_{\text{true}}$ to $\check{\rho}_{\text{unc}}$ in the robust case. Obviously, the optimal performance of the non-robust solution with respect to the true pole locations, $\check{\rho}_{\text{true}} = -58.38$ dB (see Table 8.1) can be achieved in the noiseless case only.

χ is quite high in the $rob\text{-}m\delta n_c\delta$ case and also moderately high in the $m\delta n_c\delta$ case, showing that each partition represents the underlying structure inefficiently. Moreover, the relatively high value of S_e in both cases suggests also that a smaller number of clusters is more suitable to describe the underlying data structure, which agrees with the visual inspection of the almost colliding cluster centers (see Figure 8.10). This phenomenon is due to the noise uncertainty: the originally required 8 clusters (see Section 8.3.3) to describe the samples of $\Omega_{\mathbb{P}}$ are more than the number of clusters suggested by the identified poles, i.e. their associated uncertainty regions. Using the ACM, the solution converges to a partition that consist of 7 clusters in the non-robust case and 5 clusters in the robust case which agrees with visual inspection. By comparing properties of clustering with varying m , the same conclusions can be drawn as in the non-robust case Section 8.3.3, except that the computation time increases more rapidly with increasing m .

8.5 Summary

In this chapter, optimal basis selection for series-expansion of LPV systems has been investigated in the case when only measured data records of the frozen signal behavior are available. The solution of this problem is crucial to provide a practical model structure selection tool for LPV identification based on truncated

series-expansion models. In case of an optimal basis, a fast convergence rate of the expansion representation implies that only the estimation of a few coefficients is necessary for a good approximation of the system.

It has been shown previously that Kolmogorov n -width optimality of the basis with respect to the transfer functions associated with the frozen behaviors is a necessary condition for fast convergence rate of the global expansion. Thus, it has been motivated, that a prime objective of the developed model selection is to find a KnW optimal basis in the frozen sense for the unknown LPV system. However, the KnW theory is formulated on the fact that the set of pole locations of the frozen behaviors associated transfer functions is known. As this pole manifest set is generally unknown in practice, it must be reconstructed from measured data. It has been proposed that, using measured data records of the frozen behaviors, some samples of the pole manifest set can be estimated from which reconstruction of the whole pole set is possible through data clustering algorithms, like FcM. This has lead to the conclusion that solving these objectives: reconstruction of the pole manifest set and finding the KnW optimal basis with respect to the reconstructed set are both required for a practically applicable basis selection tool.

To develop this tool, in Section 8.2 the KnW theory has been revisited, showing how the underlying optimality concept corresponds to the adequate approximation quality of truncated series-expansion models in the frozen sense. It has been motivated that beside finding an optimal basis for a fixed n -width, it is also of crucial importance to find an adequate n . While the former objective corresponds to the optimal worst-case approximation error of the truncated series-expansion, the latter determines how many basis functions, i.e. expansion coefficients, are required for that. Thus to provide an efficient selection of a truncated expansion model structure for the identification of LPV systems, both questions must be considered.

In Section 8.3, both the reconstruction problem and the KnW problem with respect to the frozen transfer function set have been formulated as a clustering problem of the sample pole locations. It has been shown that this clustering problem can be efficiently solved by a modified Fuzzy c -Means algorithm. The developed algorithm, the so called *Fuzzy-Kolmogorov c -Max* (FKcM) clustering, has been shown to give KnW optimal selection of the basis on the reconstructed pole manifest set if the fuzzyness m tends to infinity. In this way, the method involves m as a user defined trade-off between the optimality of the solution and the required computational load. It has also been motivated that the alternating optimization on which the algorithm is based always converges in practice, even if proof of this property is still need to be found. Additionally, we have explored that the optimization steps of the FKcM approach can be formulated as *Linear Matrix Inequalities* (LMIs), which can be solved efficiently in practice based on the available interior point methods. Besides other practical aspect, it has been also discussed that the use of adaptive cluster-merging provides an effective tool to choose the width of the KnW problem. In this way, this contribution of the thesis has been shown to provide an effective basis selection tool for truncated expansion model selection of LPV system identification.

In order to handle the effect of pole uncertainties that result during the esti-

mation of the sample pole locations, in Section 8.4 a robust formulation of the introduced basis selection approach has been introduced. However, to develop the tools that are needed for this extension, first important connections of hyperbolic geometry and the KnW theory have been explored in Section 8.4.2. The main message has been that hyperbolic concepts generalize the results of the Kolmogorov n -width theory with respect to OBFs and also provide simple and efficient ways of solving the underlying optimization problem with respect to specific regions, like hyperbolic segments or disks. As a contribution, a theory has been developed in this section to prove this connection and to provide the ingredients for the robust solution of the basis selection problem in the LPV case. It has been shown that the Kolmogorov n -width optimality result of the pulse basis with respect to circular regions of non-analyticity around the origin can be extended. The extended theory proves the optimality of general orthonormal basis functions with respect to any circular region or h -segment of the unit-disk. As an additional ingredient of the robust basis selection tool, an algorithm has been developed which provides efficient coverage of pole uncertainty regions with h -discs.

Using the hyperbolic geometry results, the robust formulation of the FKcM approach has been developed showing that the main difference of the two problem setting lies in the fact that clustering of uncertainty regions is required in the robust case instead of just the estimated poles. It has been shown, that the robust algorithm has the same properties in terms of KnW optimality, numerical convergence, etc. as the original FKcM algorithm. However, the robust formulation provides optimal selection of the basis even in case of considerable measurement noise, i.e. pole uncertainty. The latter property has been illustrated in a simulation example.

The algorithms, developed in this chapter, provide effective tools for model structure selection for LPV identification based on truncated series-expansion models.

LPV identification via OBFs

All the theory that has been introduced so far has served the sole purpose of providing tools to formulate identification of general LPV systems in a well-established manner. Finally in this chapter, the identification approach of this thesis is proposed, which is based on model structures that originate from truncated OBF expansion representations of LPV systems. By assuming static dependence of the expansion coefficients, two identification methods, a local and global one, are developed for the introduced model structures. While the local approach uses the gain-scheduling principle: identification with constant scheduling signals and interpolation of the resulting LTI models, the global approach provides a direct LPV model estimate via linear regression based on data records with varying scheduling trajectories. The introduced approaches are analyzed in terms of variance, bias, consistency, and validation of the model estimates is also investigated. To enable the estimation of modes with dynamic coefficient dependencies, a modified feedback-based OBF model structure is proposed, which, by using static dependence, is able to represent a truncated series-expansion with coefficients having dynamic dependence. Estimation of the parameters of such a model structure is formulated through a separable least-squares strategy and the resulting approach is analyzed in terms of its properties.

9.1 Introduction

In the previous chapters we have built up an extensive LPV system theoretical framework to provide understanding of model structures and to develop tools for their analysis. Based on this framework it has been shown that a series-expansion representation of discrete-time asymptotically stable LPV systems is available in terms of *Orthonormal Basis Functions* (OBFs). By the motivation given in Chapter 1, we have set up our research goal to use finite truncations of such representations as models for the identification of LPV systems. We aim to fulfill this goal

here, by formulating finite truncation based expansion model structures and by developing approaches and algorithms that solve the estimation problem of these models in the classical *Least-Squared* (LS) setting (see Section 2.3).

First in Section 9.2, we show that truncated OBF expansion model structures have many advantages over the model structures used in the state-of-the-art of LPV system identification (see Section 1.3). In fact we motivate that the developed structures provide an easily scalable trade-off between model complexity and accuracy of the estimate; simplify control design and identification; do not suffer from locally changing system order; and that they extend the results of LTI system identification. As a major contribution, we also formulate the prediction-error setting for LPV identification, analyzing the one-step-ahead predictor and possible noise model concepts. This provides the final tools in order to compare identification algorithms of the LPV identification field.

It has already been shown that the convergence rate of a LPV series-expansion is directly influenced by the used basis. Hence the number of terms required in a truncated expansion to achieve a good approximation of the system (low bias) is dependent on the basis. In this way, there is a prime emphasis on appropriate selection of the basis for these model structures. In Chapter 7 we have developed an algorithm to assist this selection task based on first principle information, while in Chapter 8, a basis selection mechanism has been introduced that solves this problem based on measured data. In this chapter, we treat these approaches as the part of the model structure selection phase of our identification approach, and in the sequel we continue the discussion by searching solutions for the remaining steps of the identification cycle.

In Section 9.3, we develop discrete-time identification algorithms for the proposed model structures in the LS setting. We motivate that the freedom of dynamic dependence, which is required in all model structures for the representation of general LPV systems, is too vast to handle black-box identification effectively. Additionally, static dependence of the identified system models is most often assumed by the currently available LPV control design tools. Thus, to narrow the search space and to provide models directly applicable for control, the coefficient functions of the OBF model structures are restricted to have static dependence in the developed approaches of Section 9.3. Based on this restricted model class and the LS setting, two identification approaches, a local and a global one, are introduced. The local method uses the gain-scheduling type of identification strategy: for some constant scheduling trajectories, LTI truncated expansion models of the system based on a fixed set of OBFs are identified and then the expansion coefficients of the estimated models are interpolated on the scheduling space \mathbb{P} . It is shown that in comparison with other gain-scheduling based identification approaches, the interpolation problem is well formulated in this case. The global method uses a data record collected from the system for a varying scheduling trajectory, and formulates the estimation of the expansion coefficients by a linear regression. To do so, the expansion coefficients in this case are assumed to be linear in the parameters, i.e. to be the linear combination of a prior chosen set of meromorphic functions. The introduced approaches are analyzed in terms of variance, bias, consistency, and validation of the model estimates is also investigated.

To enable the estimation of truncated expansion models with dynamic coefficient dependencies, but at the same time still provide applicable models for control, feedback-based OBF model structures are proposed in Section 9.4. It is shown that, by using static dependence, the introduced models are able to represent truncated expansion models with dynamic coefficient dependencies. For the identification of such feedback-based model structures, the previously developed global approach is extended, formulating the parameter estimation through a separable least-squares approach. Finally, in Section 9.5, the extension of the introduced approaches to MIMO systems is investigated, which concludes the chapter.

The aim of this chapter is to give a set of identification approaches that are capable to deliver theoretically well-founded model estimates in the LPV framework, accomplishing the primary objective of this thesis. Here we do not pursue the proper exploration of the other two steps of the identification cycle: experiment design and model validation, though some basic results about these issues are briefly covered in the analysis of the identification approaches. The proper treatment of these steps is reserved for further studies. Our intention is to open a new sound alternative of the existing identification literature and to give further possibilities for the development of a future generation of LPV identification approaches.

9.2 OBFs based LPV model structures

LPV model structures based on truncated OBF expansion representations are introduced in this section. The structures are defined by using the concepts of the classical prediction error setting. Thus first, characterization of this setting is developed in the LPV case. Due to the absence of a transfer function type of description of LPV systems, the process and noise models are formulated based on their impulse response presentation. This gives the possibility to develop one-step-ahead predictors in this framework. As a next step, the proposed model structures, as truncated OBF expansion representations are formulated with *Output-Error* (OE) type of noise models. Based on the fact that the coefficients can appear on the left or on the right-side of the basis functions in the expansion, different type of model structures can be introduced. Finally, important properties of the proposed model structures are investigated and compared to other model structures of the LPV identification field. Similarity of the introduced structures to nonlinear Wiener and Hammerstein models is also explored.

9.2.1 The LPV prediction error framework

As a starting point, we assume that a non-autonomous, SISO, asymptotically stable LPV system $\mathcal{S} = (\mathbb{Z}, \mathbb{P}, \mathbb{W}, \mathfrak{B})$ is given in *discrete-time* (DT) with scheduling signal p . We aim at the identification of this system based on a predefined *input-output* (IO) partition (u, y) . We suppose that \mathcal{S} is equivalent with the deterministic part of the data generating physical system (i.e. the deterministic part of the physical system corresponds to an LPV system with the considered scheduling signal).

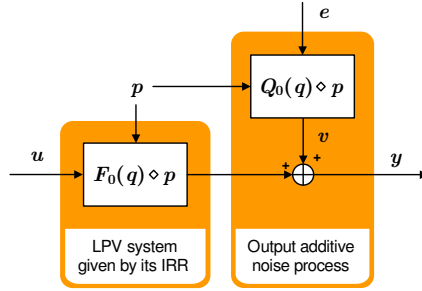


Figure 9.1: Data generating system in the LPV prediction error framework.

Based on first principles information, it is possible in practice to select scheduling variables for a plant that yield an LPV equivalent (see the procedure developed in Section 7.4).

Prediction error setting

First we clarify the identification setting in which we position our models. Using the concept of the classical prediction system error identification (see Section 2.3), it is assumed that the data generating system, illustrated in Figure 9.1, is given as

$$y = (F_0(q) \diamond p)u + v, \quad (9.1)$$

where the process part, i.e. the LPV system \mathcal{S} , is represented in an impulse response form $\mathfrak{R}_{\text{IM}}(\mathcal{S})$:

$$F_0(q) \diamond p = \sum_{i=0}^{\infty} (\mathbf{g}_i \diamond p)q^{-i}, \quad (9.2)$$

with $\mathbf{g}_i \in \mathcal{R}$. Note that due to the asymptotic stability assumption, every considered discrete-time LPV system has a *Impulse Response Representation* (IRR) (see Section 5.3). The reason why we use the IRR to define the data generating equation (9.1) is due to the fact that a transfer function form of the dynamic relation, like in the LTI counterpart (2.135), is not available for LPV systems. Additionally, the noise part of (9.1) is given as v , satisfying

$$(Q_{A_0}(q) \diamond p)v = (Q_{B_0}(q) \diamond p)e, \quad (9.3)$$

where e is a zero-mean white noise process with variance σ_e^2 and $Q_{A_0}, Q_{B_0} \in \mathcal{R}[\xi]$ are polynomial functions such that $\deg(Q_{A_0}) \geq \deg(Q_{B_0})$. Similar to the LTI case, it is assumed that the IO representation (9.3) defines an asymptotically stable system in the deterministic sense, otherwise the identification of F_0 in (9.1) is not meaningful. Under this assumption, the representation of the noise structure (9.3)

has a pulse basis series-expansion, which is denoted by $Q_0(q)$ and satisfies

$$v = (Q_0(q) \diamond p)e \quad \text{with} \quad Q_0(q) = \sum_{i=0}^{\infty} (h_i \diamond p)q^{-i}, \quad (9.4)$$

where $h_i \in \mathcal{R}$.

One-step-ahead prediction of v

Similar to the LTI case, to formulate a one-step-ahead predictor with respect to y , it is required to clarify how we can predict $v(k)$ at a given time step k , if we have observed $v(\tau)$ for $\tau \leq k-1$. A crucial property of (9.4) what we will impose to enable an answer to this question is that it should be invertible, i.e. there exists a stable inverse $Q_0^\dagger(q, p)$ of $Q_0(q, p)$, where $Q_0^\dagger(q, p)$ is a convergent LPV series-expansion and

$$e = (Q_0^\dagger(q) \diamond p)v. \quad (9.5)$$

Note that by taking $Q_{B_0}, Q_{A_0} \in \mathbb{R}[\xi]$, which is a subspace of $\mathcal{R}[\xi]$, Q_0 is equivalent with a transfer function and Q_0^\dagger is its stable inverse. This results in the LTI case discussed in Section 2.3.

As a next step, write (9.4) as

$$v(k) = (h_0 \diamond p)(k)e(k) + \sum_{i=1}^{\infty} (h_i \diamond p)(k)e(k-i). \quad (9.6)$$

Now the knowledge of $\{v(\tau)\}_{\tau \leq k-1}$ and a given trajectory of p implies the knowledge of $\{e(\tau)\}_{\tau \leq k-1}$ in the view of (9.6). Based on this relation, there are many ways to define the prediction of $v(k)$, like the maximum a posteriori prediction or the mean value of the distribution in question, etc. The classical approach we use in the following is to view the prediction of $v(k)$ as the conditional expectation of $v(k)$ based on $\{e(\tau)\}_{\tau \leq k-1}$ and a fixed trajectory of $p \in \mathfrak{B}_{\mathbb{P}}$:

$$\hat{v}(k|k-1) := \mathcal{E} \{v(k) \mid \{e(\tau)\}_{\tau \leq k-1}, \{p(\tau)\}_{\tau \in \mathbb{Z}}\}, \quad (9.7)$$

where \mathcal{E} is the expectation operator. Assume that p is deterministic and $h_0 = 1$, which also implies that the feedthrough term in Q_0^\dagger is 1. Then the conditional expectation of $v(k)$ is given as

$$\hat{v}(k|k-1) = \sum_{i=1}^{\infty} (h_i \diamond p)(k)e(k-i). \quad (9.8)$$

It is also easy to establish that the conditional expectation minimizes the mean-squared error of the prediction:

$$\min_{\hat{v}(k)} \mathcal{E} \{v(k) - \hat{v}(k)\}^2 \Rightarrow \hat{v}(k) = \hat{v}(k|k-1), \quad (9.9)$$

where the minimization is carried out over all functions $\hat{v} \in \mathbb{R}^Z$ (see Ljung (1999)). Additionally, using (9.5) we can write

$$\hat{v} = ((Q_0(q) \diamond p) - 1)e = (1 - (Q_0^\dagger(q) \diamond p))v, \quad (9.10)$$

which gives the classical one-step-ahead predictor result of v . In case p is a stochastic process, it is a difficult problem to establish conditional expectation of $v(k)$, as each Markov parameter h_i can be a nonlinear function of $p(k-l)$ where $l \in Z$, i.e. it contains forward and backward samples of p . Due to this fact, in the future analysis p is considered to be a deterministic signal.

One-step-ahead prediction of y

As a next objective, we develop the one-step-ahead prediction of $y(k)$ based on $\{y(\tau)\}_{\tau \leq k-1}$, $\{u(\tau)\}_{\tau \leq k}$ and a given scheduling trajectory $p \in \mathfrak{B}_P$. Since

$$v(k) = y(k) - \sum_{i=0}^{\infty} (g_i \diamond p)(k)u(k-i), \quad (9.11)$$

this means that also $v(\tau)$ is known for $\tau \leq k-1$. We would like to predict the value of $y(k)$ based on this information. Using the reasoning of the previous discussion, the conditional expectation $\hat{y}(k|k-1)$ of $y(k)$ is

$$\begin{aligned} \hat{y} &= (F_0(q) \diamond p)u + \hat{v} \\ &= (F_0(q) \diamond p)u + (1 - (Q_0^\dagger(q) \diamond p))v \\ &= (F_0(q) \diamond p)u + (1 - (Q_0^\dagger(q) \diamond p))(y - (F_0(q) \diamond p)u) \\ &= ((Q_0^\dagger(q)F_0(q)) \diamond p)u + (1 - (Q_0^\dagger(q) \diamond p))y. \end{aligned} \quad (9.12)$$

This gives that in the view of the developed IRR representation of LPV systems, the classical result of the one-step-ahead predictor also holds in the LPV case, giving a powerful tool to develop and analyze identification methods.

Prediction error models

Following a similar reasoning as in the LTI case, we can introduce the parameterized model

$$(F(q, \theta), Q(q, \theta)), \quad (9.13)$$

where $\theta \in \mathcal{R}^n$ represents the “parameter vector”, the collection of meromorphic coefficients associated with F and Q (in case Q is not dependent on p , then θ contains the real constant coefficients of Q). Note that these coefficients are not necessarily associated with Markov parameters. So θ can correspond to the coefficients of the process and the noise models given in a SS or IO representation. Then, these parameterized structures are represented in a series-expansion form by F and Q . The parameterized model of (9.13) leads to the following one-step-ahead

parameter-varying (PV) predictor based on (9.12):

$$\hat{y}_\theta := (1 - Q^\dagger(q, \theta) \diamond p)y + (Q^\dagger(q, \theta) \diamond p)(F(q, \theta) \diamond p)u. \quad (9.14)$$

In this case, the allowed parameter space is $\Theta \subseteq \mathcal{R}^n$. Now again, we are looking for an estimate of θ such that \hat{y}_θ is a good approximation of y , i.e. the *prediction error*:

$$\epsilon(k, \theta) := y(k) - \hat{y}_\theta(k), \quad (9.15)$$

is minimized. Just like in the LTI case, it is possible to apply the LS criterion (2.140) for this purpose based on an available data record $\mathcal{D}_{N_d} = \{y(k), u(k), p(k)\}_{k=0}^{N_d-1}$.

9.2.2 The Wiener and the Hammerstein OBF models

In the introduced prediction error setting, we aim to develop model structures in which the process model F is a finite truncation of a OBF expansion representation and the noise model Q is equal to identity. The motivation is similar as in the LTI case (see Section 2.3.5), namely that with this particular choice of the process and noise models the coefficients of F appear linearly in (9.14) and the noise model Q is parameterized independently from F . The model structures that can be deduced from this choice are the key elements for the identification approaches of this thesis.

Assume that we are given a set of Hambo orthonormal basis functions $\Phi_{n_g}^\infty$, defined as

$$\Phi_{n_g}^\infty := \{\phi_j(z)G^i(z)\}_{j=1, \dots, n_g}^{i=0, \dots, \infty}, \quad (9.16)$$

where G is an inner function in $\mathcal{H}_2(\mathbb{E})$. Note that $\Phi_{n_g}^\infty$ can be arbitrary or chosen by a basis selection mechanism, as described in Chapter 8. In terms of these basis functions, a series-expansion representation of \mathcal{S} , i.e. the process part of (9.1), is available in the form of (5.19), implying that:

$$y = e + (w_{00} \diamond p)u + \sum_{i=0}^{\infty} \sum_{j=1}^{n_g} (w_{ij} \diamond p)\phi_j(q)G^i(q)u, \quad (9.17)$$

where $w_{ij} \in \mathcal{R}$ and the feedthrough-term $w_{00} \in \mathcal{R}$ are meromorphic coefficient functions. As a next step, we define model structures as the finite truncation of the series-expansion in (9.17). Here, one should realize that (9.17) can be formulated in an alternative way, where the expansion coefficients appear *after* the basis functions. Since multiplication by the time operator q is non-commutative with respect to w_{ij} (see Section 3.1.3), a finite truncation of that alternative form would lead to a model with different approximation capabilities. To show that the alternative formulation of (9.17) exists, consider (5.3). It is obvious that this pulse basis expansion can be also written as

$$y = (g_0 \diamond p)u + q^{-1}(\overrightarrow{g}_1 \diamond p)u + q^{-2}(\overrightarrow{g}_2 \diamond p)u + \dots \quad (9.18)$$

where $\overrightarrow{\cdot}$ is the forward-shift operator on \mathcal{R} (see Definition 3.13). Using this al-

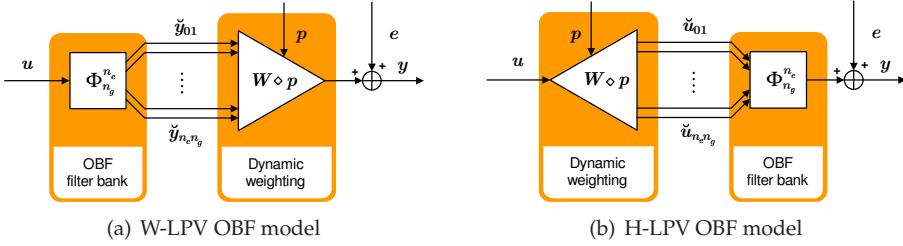


Figure 9.2: IO signal flow graph of (a) the W-LPV OBF model described by (9.21) and (b) the H-LPV OBF model described by (9.24) with $W = [w_{01} \dots w_{n_e n_g}]$ and without a feedthrough term ($w_{00} = 0$).

ternative formulation of (5.3) to derive OBF expansions of asymptotically LPV systems via the substitution rule (5.10), leads to

$$y = e + (w_{00} \diamond p)u + \sum_{i=0}^{\infty} \sum_{j=1}^{n_g} \phi_j(q) G^i(q) (w_{ij} \diamond p)u. \quad (9.19)$$

Note that in (9.19), the coefficient functions $\{w_{ij}\}$ are generally not equal to the coefficients of (9.17) due to the non-commutativity of q .

Now consider the finite truncation of the Hambo basis $\Phi_{n_g}^{\infty}$:

$$\Phi_{n_g}^{n_e} := \{\phi_j(z) G^i(z)\}_{j=1, \dots, n_g}^{i=0, \dots, n_e}, \quad (9.20)$$

with $n_e \leq \infty$. In terms of this truncation, (9.17) or (9.19) provide an approximation of the data generating system (9.1), i.e the LPV system \mathcal{S} . The resulting structures, presented in Figure 9.2a-b, can be viewed as a filter bank of OBFs, which is a LTI system, followed or preceded by a meromorphic weighting function set with dynamic dependence on p . Thus, these structures have some resemblance with *nonlinear Wiener* (NW) and *nonlinear Hammerstein* (NH) models, important model classes for chemical, biological, and sensor/actuator systems (Billings and Fakhouri 1982). An LTI model with static nonlinearity on its output is called a Wiener model (see Figure 9.3a) while an LTI model with static nonlinearity on its input is called a Hammerstein model (see Figure 9.3b). The consequences of this similarity are investigated later on, but for the time being, to respect this relation, the introduced structures are called a *Wiener LPV OBF model* (W-LPV OBF) and a *Hammerstein LPV OBF model* (W-LPV OBF). These model structures are formally defined as follows:

- Wiener LPV OBF model (W-LPV OBF)

$$F(q, \theta) \diamond p = w_{00} \diamond p + \sum_{i=0}^{n_e} \sum_{j=1}^{n_g} (w_{ij} \diamond p) \phi_j(q) G^i(q), \quad Q(q, \theta) = 1, \quad (9.21)$$

with $\theta = [w_{00} \ w_{01} \ \dots \ w_{n_e n_g}]^T \in \mathcal{R}^{1+(n_e+1)n_g}$ and $p \in \mathfrak{B}_p$, where \mathfrak{B}_p

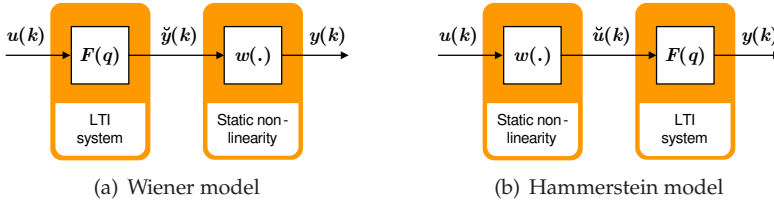


Figure 9.3: IO signal flow graph of (a) nonlinear Wiener models and (b) nonlinear Hammerstein models.

is considered to be known. This model, given in Figure 9.2a, is called the W-LPV OBF model and denoted by $\mathfrak{M}_W(\Phi_{n_g}^{n_e}, \theta, \mathfrak{B}_P)$. Based on (9.21), the predictor model reads as

$$\hat{y}_\theta = (w_{00} \diamond p) \underbrace{u}_{\check{y}_{00}} + \sum_{i=0}^{n_e} \sum_{j=1}^{n_g} (w_{ij} \diamond p) \underbrace{\phi_j(q) G^i(q)}_{\check{y}_{ij}} u. \quad (9.22)$$

Let (A, B, C, D) be a minimal balanced LTI *state-space* (SS) realization of $\Phi_{n_g}^{n_e}$. Using this realization, the SS equivalent representation of (9.22), is given by

$$qx = Ax + Bu, \quad (9.23a)$$

$$\hat{y}_\theta = (W \diamond p)x + (w_{00} \diamond p)u, \quad (9.23b)$$

where $x = [\check{y}_{01} \dots \check{y}_{n_e n_g}]^\top$ and $W = [w_{01} \dots w_{n_e n_g}]$.

- Hammerstein LPV OBF model (H-LPV OBF)

$$F(q, \theta) \diamond p = w_{00} \diamond p + \sum_{i=0}^{n_e} \sum_{j=1}^{n_g} \phi_j(q) G^i(q) (w_{ij} \diamond p), \quad Q(q, \theta) = 1, \quad (9.24)$$

with $\theta = [w_{00} \ w_{01} \ \dots \ w_{n_e n_g}]^\top \in \mathcal{R}^{1+(n_e+1)n_g}$ and $p \in \mathfrak{B}_P$, where \mathfrak{B}_P is considered to be known. This model, given in Figure 9.2b, is called the H-LPV OBF model and denoted by $\mathfrak{M}_H(\Phi_{n_g}^{n_e}, \theta, \mathfrak{B}_P)$. In this case, the predictor reads as

$$\hat{y}_\theta = \underbrace{(w_{00} \diamond p)u}_{\check{u}_{00}} + \sum_{i=0}^{n_e} \sum_{j=1}^{n_g} \phi_j(q) G^i(q) \underbrace{(w_{ij} \diamond p)u}_{\check{u}_{ij}}. \quad (9.25)$$

The SS equivalent representation of (9.25), is given by

$$qx = Ax + (W \diamond p)^\top u, \quad (9.26a)$$

$$\hat{y}_\theta = Cx + (w_{00} \diamond p)u, \quad (9.26b)$$

where $[\check{u}_{01} \dots \check{u}_{n_e n_g}]^\top = (W \diamond p)^\top u$.

These model structures are the PV forms of the (A, B) and the (A, C) invariant

Hambo OBFs based model parameterizations in the LTI case (see Section 2.2). Those LTI model parameterizations are considered to be equivalent in a SISO setting, as their coefficients are equivalent up to a linear transformation (Section 2.3.5). However, this does not hold in the LPV case due to the absence of the transposition property (Section 4.1.4), therefore the coefficients $\{w_{ij}\}_{j=1,\dots,n_g}^{i=0,\dots,n_e}$ are generally not equivalent in (9.21) and (9.24). Thus, these model structures are distinguished in the sequel.

9.2.3 Properties of Wiener and the Hammerstein OBF models

As a next step, important properties of the introduced models are investigated from the viewpoint of system identification. First we prove that the W-LPV OBF and H-LPV OBF models are general approximators of LPV systems, so by these models, LPV systems can be approximated with arbitrary precision. Then we explore how a locally changing McMillan degree of the system, which is a crucial problem in the interpolation-based identification methods, affects these model structures. Next we show why these model structures are beneficial in the prediction error setting and how estimates in these structural forms can be used for control design, i.e. that these models are compatible with the existing LPV control theory.

General approximation property

It has been shown in Chapter 5 that an asymptotically stable discrete-time LPV system has a series-expansion representation in terms of an arbitrary basis for $\mathcal{RH}_{2-}(\mathbb{E})$. For such an approximation-free representation, infinitely many basis functions, $\Phi_{n_g}^\infty$, are required in the general case. This implies that using a finite number of basis functions, $\Phi_{n_g}^{n_e}$, restricts the class of realizable LPV systems. Thus, it is important to investigate the approximation capabilities of these models.

In the work of Boyd and Chua (1985), it has been proved for nonlinear Wiener models that, if the LTI part is an OBF filter bank, then such models are general approximators of nonlinear systems with fading memory (NL dynamic systems with convolution representation). This means that, if the number of the OBFs in the filter bank tends to infinity, then the best achievable approximation error of the output trajectories in terms of the choice of the static nonlinearity converges to zero in an arbitrary norm.

Now consider the LPV case. In Chapter 5 it has been shown that the series-expansion of asymptotically stable LPV systems in terms of an orthonormal basis $\Phi_{n_g}^\infty$ is convergent. It has also been highlighted, that such series expansions in general only exist, if the expansion coefficients have dynamic dependence. Furthermore, it has been shown that the expansion coefficients yield a sequence, which converges to zero for each scheduling trajectory. For a given basis sequence $\Phi_{n_g}^\infty$,

the worst-case approximation error of a truncated expansion representation is

$$\sup_{(y,u,p) \in \mathfrak{B}} \left\| \sum_{i=n_e+1}^{\infty} \sum_{j=1}^{n_g} (w_{ij} \diamond p) \phi_j(q) G^i(q) u \right\|. \quad (9.27)$$

Based on the previous, it holds that this worst-case approximation error satisfies that

$$\lim_{n_e \rightarrow \infty} \sup_{(y,u,p) \in \mathfrak{B}} \left\| \sum_{i=n_e+1}^{\infty} \sum_{j=1}^{n_g} (w_{ij} \diamond p) \phi_j(q) G^i(q) u \right\| = 0. \quad (9.28)$$

W-LPV and H-LPV OBF models are formulated based on finite truncation of LPV expansion representations, thus (9.28) proves the following property:

Property 9.1 (General LPV approximation) *W-LPV and H-LPV OBF models are general approximators of LPV systems.*

This result means that, by extending the basis function set of these models, approximation of general LPV systems can be achieved with arbitrary precision. An additional property is that, in practice, careful selection of the basis functions can ensure almost error free representation of the frozen transfer function set $\mathfrak{F}_{\mathbb{P}}$ of \mathcal{S} with a limited number of OBFs (see Chapter 8). Such a basis function set has fast convergence rate in the series-expansion of \mathcal{S} . This provides the conclusion that with the general approximator property, the proposed model structures offer an efficient approximation structure for identification.

There is also an important difference with respect to the previously mentioned nonlinear counterpart of this result. In the nonlinear case, a necessary condition for the general approximator property is that the static nonlinearity must contain all possible combinations of the products of the output signals \check{y}_{ij} of the filter bank. Due to the linear signal relation of the LPV setting, this condition is not required for Property 9.1, i.e. the linear combination of \check{y}_{ij} with meromorphic PV coefficients is sufficient.

McMillan degree property

An additional property of the introduced model structures is that they are well structured against changes of the McMillan degree in the frozen system set $\mathcal{F}_{\mathbb{P}}$ of \mathcal{S} . It is generally true that, if for a constant scheduling signal $p(t) = \bar{p}$ the associated $\mathcal{F}_{\bar{p}} \in \mathcal{F}_{\mathbb{P}}$ has a lower McMillan degree than the rest of the systems in $\mathcal{F}_{\mathbb{P}}$, then this does not imply that any of the coefficient functions $\{w_{ij}\}$ of the OBF series-expansion is zero for \bar{p} . This shows that these model parameterizations are not affected by problems that are common for LPV-SS or IO representations based model structures (see Chapter 1).

Linear in the coefficients property

The third, but equally important property of W-LPV OBF and H-LPV OBF models is that they are linear in the coefficients θ , i.e. both in predictor equations (9.22) and (9.25) the coefficients $\{w_{ij}\}$ appear linearly. This means that for a LS identification criterion and with a linear parametrization of $\{w_{ij}\}$, the estimation problem of these coefficient functions has an analytic solution.

Models for control

The proposed models are also efficiently applicable for LPV control design. Through (9.23a-b) and (9.26a-b), a SS realization of the estimated models is available and therefore the existing LPV control approaches, which are exclusively formulated for SS representations, can be directly applied. Due to the fact, that both in (9.23a) and (9.26a) the matrix A is constant, optimal control design greatly simplifies with respect to these model estimates. The reason is that global dynamic stability of models with constant A can be always expressed by a Lyapunov equation with non-parameter dependent, i.e. constant P (see Section (3.3.2)). The only disadvantage is that many control approaches assumes static dependence of the matrices. This implies, that dependence of $\{w_{ij}\}$ must be restricted to static dependence, i.e. $w_{ij} \in \mathcal{R}|_{n_{\mathbb{P}}}$, to provide models to which these control solutions can be applied. However, for the general approximator property, dynamic dependence of the coefficients is required, which means that the restriction to static dependence reduces the representation capabilities of the models. This issue is explored further in Section 9.3 and 9.4.

9.2.4 OBF models vs other model structures

The prediction-error setting with the one-step-ahead predictor (9.14) enables the comparison with other model structures used in the LPV identification literature. Hence in the following, the properties of LPV-IO and SS models, introduced in Chapter 1, are discussed in the prediction-error setting and compared to OBFs models. As we will show, there are hidden assumptions in these LPV model structures in terms of the noise models.

Comparison to LPV-IO models

Consider

$$y = - \sum_{i=1}^{n_a} (a_i \diamond p) q^{-i} y + \sum_{j=0}^{n_b} (b_j \diamond p) q^{-j} u + e, \quad (9.29)$$

the LPV-IO filter model of the IO identification approaches (see Chapter 1). The parameter vector for this ARX model consists of the coefficients in (9.29):

$$\theta = [a_1 \quad \dots \quad a_{n_a} \quad b_0 \quad \dots \quad b_{n_b}],$$

where each coefficient has static dependence. It can be easily shown that the one-step-ahead predictor of y reads as

$$\hat{y}_\theta = - \sum_{i=1}^{n_a} (a_i \diamond p) q^{-i} y + \sum_{j=0}^{n_b} (b_j \diamond p) q^{-j} u, \quad (9.30)$$

if the noise model Q is chosen in a way that

$$Q^\dagger(q, \theta) \diamond p = 1 + \sum_{i=1}^{n_a} (a_i \diamond p) q^{-i}. \quad (9.31)$$

Note that, similar to the OBF models, this model structure is also linear in the coefficients, but its noise model is not independently parameterized from the processes part, as it is well-known for the LTI case. However, the suggested noise model

$$e = v + \sum_{i=1}^{n_a} (a_i \diamond p) q^{-i} v, \quad (9.32)$$

reveals that

$$Q(q, \theta) \diamond p = 1 - \sum_{i=1}^{n_a} (a_i \diamond p) q^{-i} + \left(\sum_{i=1}^{n_a} (a_i \diamond p) q^{-i} \right) \left(\sum_{i=1}^{n_a} (a_i \diamond p) q^{-i} \right) - \dots$$

This shows that, even if each a_i has static dependence, the noise model $Q(q, \theta)$ has dynamic dependence, i.e. v is dependent on the entire past of the scheduling signal p . Thus the assumed noise structure of an ARX model is rather artificial, implying much more conservatism than in the LTI case. It must be noted, that in the cited works (Wei and Del Re 2006; Wei 2006; Bamieh and Giarré 2000, 1999), only the estimation problem (9.29) has been solved in the LS setting, while the assumed noise model of this model structure and its effects have not been investigated.

Comparison to LPV-SS models

In the SS case, the model structure of the global identification methods, like the global subspace techniques and gradient methods, is given by

$$qx = (A \diamond p)x + (B \diamond p)u + (E_1 \diamond p)e, \quad (9.33a)$$

$$y = (C \diamond p)x + (D \diamond p)u + (E_2 \diamond p)e, \quad (9.33b)$$

where the matrices (A, B, C, D) define a DT-LPV-SS representation, $E_1, E_2 \in \mathcal{R}^{n_x \times 1}$, and e is a vector of independent zero-mean white noise processes (see Chapter 1). Commonly it is assumed that all coefficients of the model has static dependence. In the SISO case, by applying pulse basis expansion on this model, the process model F and the noise model Q trivially follow:

$$F(q, \theta) = D + \sum_{i=1}^{\infty} C \left(\prod_{j=1}^{i-1} A^{[j]} \right) B^{[i]} q^{-i}, \quad (9.34a)$$

$$Q(q, \theta) = E_2 + \sum_{i=1}^{\infty} C \left(\prod_{j=1}^{i-1} A^{[j]} \right) E_1^{[i]} q^{-i}, \quad (9.34b)$$

where $\cdot^{[j]}$ denotes that the backward-shift operator (see Definition 3.13) applied j -times on the matrix. Note that the noise model (9.34b) involves all matrices of the process part, thus it is obvious that its not independently parameterized from F and it depends on the entire past of scheduling signal p . Furthermore, the coefficients, i.e. the matrices, do not appear linearly in (9.34a). Thus, the model (9.33a-b) can be efficiently used in the prediction error identification setting by either applying a (complicated) nonlinear estimation procedure, like gradient search (Lee (1997); Lee and Poolla (1996); Verdult et al. (2002) and Verdult et al. (2003)) or in the unrealistic case, when the state signals x are measurable. In the latter case, prediction of the state and output signals becomes linear in the coefficients, thus in a LS setting, linear regression can be used to derive a model estimate (see Nemani et al. (1995); Lovera et al. (1998); Lovera (1997)). Based on this, LPV-SS models are commonly estimated in a non-prediction error setting like the subspace approaches of van Wingerden et al. (2007); Felici et al. (2006) and Verdult and Verhaegen (2005).

Comparison of the proposed model structures with the considered model structures underlines that the introduced OBFs-based series-expansion models are attractive candidates in the prediction-error identification setting of LPV systems as they are linear in the coefficients and their noise model is independently parameterized from the process part and independent from the scheduling.

Similarity to the nonlinear Wiener and Hammerstein models

By comparing NW and NH models to the introduced structures (see Figure 9.2 and 9.3), the structural similarity is immediate. However, there are some fundamental differences:

- In the NW and NH case, a static nonlinearity is assumed on the output/input of the LTI part. In the W-LPV and H-LPV OBF case, the “nonlinearity” is entering through a dynamic dependence on p , which can be composed of external (strict LPV systems) and internal (quasi-LPV systems) variables alike. Assuming that p is equal to u or y , NW and NH models can be viewed as special cases of W-LPV and H-LPV OBF models. This is illustrated by Example 9.1
- LTI parts of W-LPV and H-LPV OBF are *single-input multiple-output* (SIMO) and *multiple-input single-output* (MISO) systems as opposed to the SISO LTI part of NW and NH models¹.

¹Originally both Wiener and Hammerstein proposed their models with SIMO and MISO LTI parts, but because of the complexity of the problem, the LTI part has been simplified to be SISO (Billings and Fakhouri 1982; Ljung 1999).

Example 9.1 (NW as a special case of W-LPV OBF) Given a nonlinear Wiener model defined by an asymptotically stable LTI transfer function F and static nonlinearity $w(y) = \sin(y)$. F can be viewed as a linear combination of basis functions $\Phi_{n_g}^{n_e}$ with coefficients $\{w_{01}, \dots, w_{n_e n_g}\}$. If we can write the static nonlinearity $w(y)$ as $w(y) = f(y)y$ where f is meromorphic, then the NL model can be transformed to a W-LPV OBF model with $p = y$. Similar to Example 7.4, we can rewrite the considered nonlinearity as

$$w(y) = \text{sinc}(p)y \quad \text{with } p = y.$$

This leads to a W-LPV OBF structure, which is characterized by the basis functions $\Phi_{n_g}^{n_e}$ and the parameter-varying coefficients

$$\{w_{01} \text{sinc}(p), \dots, w_{n_e n_g} \text{sinc}(p)\}$$

However, if the output nonlinearity is $\cos(y)$, then the previous mechanism cannot be applied as

$$\lim_{y \rightarrow 0} \frac{\cos(y)}{y} = \infty.$$

In such cases, it is advisable to convert the NL model through its differential equation description to a LPV form. This procedure might result only in an approximation of the original model (see Chapter 8).

9.2.5 Identification of W-LPV and H-LPV OBF models

In the following, a general outline of LPV identification based on W-LPV and H-LPV OBF models is presented. The major steps of the identification cycle: model structure selection, identification criterion selection, and estimation are considered. Our aim is to set the stage for the upcoming discussion of the identification approaches of this thesis, which are based on particular choices with respect to these steps.

OBF selection

In case of W-LPV and H-LPV OBF models, there is a primal emphasis on the model structure selection step of the identification cycle. This is due to the fact that selection of the finite OBF set, that defines the structure, effects the approximation capabilities in terms of the convergence rate of the series-expansion with respect to these basis. With an adequate selection of the basis functions, i.e. with high convergence rate, negligible approximation error, i.e. bias can be achieved.

Tools to provide adequate selection of the basis functions have been already worked out. In Chapter 7, an algorithm has been proposed to assist basis selection based on first principle information. By using this algorithm, the set of frozen pole locations of the system can be characterized, and based on this pole set, the optimal choice of a orthonormal basis follows in the Kolmogorov n -width (K_nW) sense. Additionally, in Chapter 8, a clustering algorithm has been introduced, that solves the K_nW optimal basis selection problem based on measured data. The latter approach is useful in a black-box identification scenario, where no useful structural information about the LPV system/physical plant is presented. This practically applicable tool, which accomplishes the model structure selection in terms of the basis functions can be summarized in the following algorithm:

Algorithm 9.1 (OBFs based LPV identification, model structure selection)

- Step 1.** Estimation of samples of the pole manifest set $\Omega_{\mathbb{P}}$ associated with the LPV system \mathcal{S} . The estimation is accomplished by LTI identification of each $F_{\bar{p}_i} \in \mathcal{F}_{\mathbb{P}}$ of \mathcal{S} for a given set of scheduling points $\{\bar{p}_i\}_{i=1}^{N_{\mathbb{P}}} \subset \mathbb{P}$.
- Step 2.** Based on FKcM clustering of the sample poles, determination of an adequate (optimal) OBF set $\Phi_{n_g}^{n_e} \subset \mathcal{RH}_{2-}(\mathbb{E})$ with respect to \mathcal{S} .
-

Parameterization of coefficient dependencies

Beside the selection of basis functions, model structure selection with respect to W-LPV and H-LPV OBF also contains an equally important part: the parametrization of the functional dependence of the coefficients w_{ij} on the scheduling signal p :

$$w_{ij} = \psi_{ij}(\theta), \quad (9.35)$$

where $\psi_{ij} \in \mathcal{R}$ is meromorphic with constant parameters $\theta \in \mathbb{R}^n$. Then the aim of the identification is to estimate θ based on a measured data record. If first principle information is available which is transformed into an LPV form, then series-expansion of this LPV model in terms of the chosen basis functions can provide vital information about the structure of $\{\psi_{ij}\}$. Considering that the class of meromorphic functions \mathcal{R} presents degrees of freedom in terms of the order of dynamic dependence and in terms of functions, any structural information about the coefficients can considerably reduce the search space for an optimal choice of $\{\psi_{ij}\}$. In case of a black-box scenario, the choice of ψ_{ij} can be arbitrary. One can consider all ψ_{ij} to be rational functions or polynomials with a fixed degree and a fixed order of dynamic dependence.

Criteria selection and estimation

Based on the predictor form (9.14), many different classical identification criteria can be applied for the selected model structure. A particularly interesting choice is the *Least-Squared* (LS) prediction error criterion

$$\mathcal{W}_{N_d}(\theta, \mathcal{D}_{N_d}) = \frac{1}{N_d} \sum_{k=0}^{N_d-1} \epsilon^2(k, \theta). \quad (9.36)$$

where the residual ϵ is given by (9.15). If the parametrization of the coefficients is linear, e.g. w_{ij} is a linear combination of fixed meromorphic functions $\psi_{ijl} \in \mathcal{R}|_{n_{\mathbb{P}}}$:

$$w_{ij} = \sum_{l=0}^{n_{ij}} \theta_{ijl} \psi_{ijl}, \quad (9.37)$$

then with respect to (9.36), the estimation of $\{\theta_{ijl}\}$, similar to the LTI case, reduces to a linear regression problem for the W-LPV and H-LPV OBF models. In other cases, when parameterization of the coefficients is nonlinear, e.g. rational dependence, then estimation corresponds to a nonlinear optimization problem.

9.3 Identification with static dependence

In the previous part, we have developed truncated OBF expansion models, as the basic ingredients of a well-posed LPV identification approach. As a next step, we show how these model structures can be efficiently identified in the prediction error setting, such that the obtained models are directly applicable for control design. First, we clarify the exact identification setting (parameterization, identification criterion, etc.) in which we aim to derive the model estimates. Then we develop our approaches using either the gain-scheduling type of identification strategy (local approach) or a linear regression based strategy with varying scheduling trajectory (global approach). We only treat the SISO case. The MIMO extension of the developed approaches is covered later. The methods are analyzed in terms of variance, bias, consistency and validation of the model estimates is also investigated. Finally, a simulation example is studied to visualize the performance of the approaches.

9.3.1 The identification setting

In the previous parts, we have seen that a common problem of all LPV model structures, either based on SS, IO, or series-expansion representations, is that to represent general LPV systems they need dynamic dependence in the parameterization of their coefficients. However, LPV control design approaches require static dependence of the model estimate and it is also hard to handle the extra degree of freedom that dynamic dependence constitutes in an estimation problem. This gives the motivation to investigate identification in the special case, when the coefficients of W-LPV and H-LPV OBF model structures are parameterized with static dependence, i.e. in (9.35) the chosen structural dependence ψ_{ij} is only dependent on the instantaneous value of p . To make a clear distinction when we talk about static and respectively dynamic dependence, we use $w(p)$ to express evaluation of a static coefficient dependence along a scheduling trajectory p , contrary to $w \diamond p$.

We have already motivated that using a linear parametrization of the expansion coefficients (see (9.37)), estimation of the parameters can be formulated as a linear regression if the LS identification criterion (9.36) is used. Based on this, in this section we aim at the identification of LPV systems by the $\mathfrak{M}_W(\Phi_{n_g}^{n_e}, \theta, \mathfrak{B}_P)$ and $\mathfrak{M}_H(\Phi_{n_g}^{n_e}, \theta, \mathfrak{B}_P)$ model structures, where the process part F is parameterized as:

$$F(q, \theta) \diamond p = \underbrace{\sum_{l=0}^{n_{00}} \theta_{00l} \psi_{00l}(p)}_{w_{00} \diamond p} + \sum_{i=0}^{n_e} \sum_{j=1}^{n_g} \underbrace{\sum_{l=0}^{n_{ij}} \theta_{ijl} \psi_{ijl}(p) \phi_{ij}(q)}_{w_{ij} \diamond p}, \quad (9.38a)$$

in the Wiener case and

$$F(q, \theta) \diamond p = \underbrace{\sum_{l=0}^{n_{00}} \theta_{00l} \psi_{00l}(p)}_{w_{00} \diamond p} + \sum_{i=0}^{n_e} \sum_{j=1}^{n_g} \phi_{ij}(q) \underbrace{\sum_{l=0}^{n_{ij}} \theta_{ijl} \psi_{ijl}(p)}_{w_{ij} \diamond p}. \quad (9.38b)$$

in the Hammerstein case, where $\theta_{ijl} \in \mathbb{R}$, $\psi_{ijl} \in \mathcal{R}|_{n_{\mathbb{P}}}$, and $\Phi_{n_g}^{n_e} = \{\phi_{ij}\}_{j=1, \dots, n_g}^{i=0, \dots, n_e}$. In these parameterizations, the basis functions $\Phi_{n_g}^{n_e}$ are considered to be the result of a basis selection and hence they are fixed, while the functions ψ_{ijl} are either chosen by the user, or derived from first-principle information (like by the use of the approach given in Chapter 7). This yields that in this case the unknowns in the model are the real parameters $\{\theta_{ijl}\}$ which appear linearly in the structures. Thus by using the LS criterion they can be identified by linear regression. Here we do not consider the identification or optimal choice of the functions ψ_{ijl} , which remains an subject for future research.

9.3.2 LPV identification with fixed OBFs

Based on the choice of linear parametrization with static dependence and the LS criterion, two pragmatcal approaches are available for the identification of the LPV system \mathcal{S} via W-LPV and H-LPV OBF models:

Local approach Identify $w_{ij} = \sum_l^{n_{ij}} \theta_{ijl} \psi_{ijl}(\bar{p})$ for several $\bar{p} \in \mathbb{P}$ and interpolate the obtained estimates to calculate $\{\theta_{ijl}\}$. This gives the freedom to choose the functions $\psi_{ijl}(\bar{p})$ based on the local estimates w_{ij} . However, an apparent disadvantage is that many experiments with different constant scheduling trajectories are needed for successful interpolation.

Global approach Using a data record with varying p , formulate a linear regression problem with respect $\{\theta_{ijl}\}$. The resulting problem has an analytic solution, giving a direct estimate of the parameters without the need of interpolation.

In the following the detailed description of these approaches is presented. The approaches are formulated by assuming that the basis selection phase has been already accomplished, so we pick up the line of reasoning right after Step 2 in Section 9.2.5. Figure 9.4 illustrates the basic steps of the approaches. For reasons of simplicity, we assume that no feedthrough term is present, $w_{00} = 0$, however later, the estimation of w_{00} is also investigated for both algorithms.

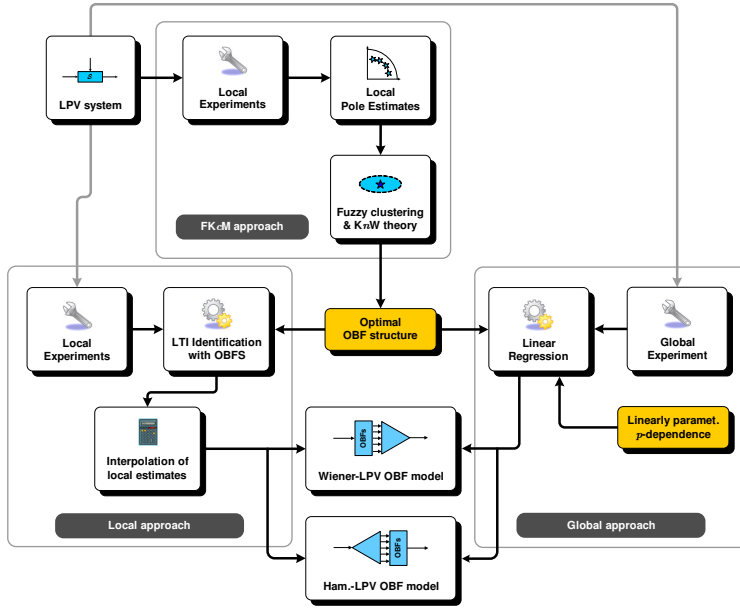


Figure 9.4: Block diagram of local and global identification methods

9.3.3 Local approach

Assume that a set of constant scheduling points $P = \{\bar{p}_\tau\}_{\tau=1}^{N_{loc}} \subset \mathbb{P}$, with $N_{loc} \in \mathbb{N}$, is given for \mathcal{S} , where it is assumed that \mathbb{P} is well covered, meaning that $\max_i \min_{j \neq i} |\bar{p}_i - \bar{p}_j|$, $i, j \in \mathbb{I}_1^{N_{loc}}$ is small enough. This is required for successful interpolation by most numerical methods. Assume also that measured data records $\mathcal{D}_{N_d, \bar{p}_\tau} = \{y(k), u(k), \bar{p}\}_{k=0}^{N_d-1}$ with length $N_d \in \mathbb{N}$ are available with u that is PE with the required order. Then the identification of \mathcal{S} is solved as (continuing from Step 2 in Section 9.2.5):

Algorithm 9.2 (OBFs based LPV identification, local method)

Step 3a. For a given OBF set $\Phi_{n_g}^{n_e} = \{\phi_{ij}\}_{j=1, \dots, n_g}^{i=0, \dots, n_e}$, scheduling points $P = \{\bar{p}_\tau\}_{\tau=1}^{N_{loc}} \subset \mathbb{P}$, and identification criterion \mathcal{W} , identify each frozen system $F_{\bar{p}_\tau} \in \mathcal{F}_P$, $\tau \in \mathbb{I}_1^{N_{loc}}$ based on the LTI-OBF model structure:

$$F_{\bar{p}_\tau}(q, \theta) = \sum_{i=0}^{n_e} \sum_{j=1}^{n_g} w_{ij\tau} \phi_{ij}(q), \quad Q(q, \theta) = 1, \quad (9.39)$$

and data records $\mathcal{D}_{N_d, \bar{p}_\tau}$ of \mathcal{S} collected with constant scheduling trajectories. This results in a set of estimated coefficients

$$\{\hat{w}_{ij\tau}\}_{i=0, j=1, \tau=1}^{n_e, n_g, N_{loc}} \subset \mathbb{R}, \quad (9.40)$$

where $\{\hat{w}_{ij\tau}\}_{i=0,j=1}^{n_e,n_g}$ describes the coefficients of $\Phi_{n_g}^{n_e}$ with respect to $\mathcal{F}_{\bar{p}_\tau}$.

Step 4a. Interpolation of the frozen OBF coefficients $\{\hat{w}_{ij\tau}\}$. For each $(i, j) \in \mathbb{I}_0^{n_e} \times \mathbb{I}_1^{n_g}$, choose a set of interpolation functions

$$\{\hat{\psi}_l\}_{l=0}^{n_{ij}}, \quad (9.41)$$

being a set of meromorphic functions over \mathbb{P} , i.e. $\hat{\psi}_\tau \in \mathcal{R}|_{n_{\mathbb{P}}}$, and a set of constants $\{\hat{\theta}_{ijl}\}_{l=0}^{n_{ij}}$ such that

$$\hat{w}_{ij\tau} = \sum_l^{n_{ij}} \hat{\theta}_{ijl} \hat{\psi}_l(\bar{p}_\tau), \quad \forall \tau \in \mathbb{I}_1^{N_{loc}}. \quad (9.42)$$

In this way the estimate of the expansion coefficients results as

$$\hat{w}_{ij} := \sum_{l=0}^{n_{ij}} \hat{\theta}_{ijl} \hat{\psi}_l. \quad (9.43)$$

In general, any interpolation technique can be used to approximate the coefficient functions $\{w_{ij}\}$, however most commonly polynomial, rational, or Chebyshev interpolation provides adequate results (see Sakhnovich (1997)). Of course specific choices of the interpolation functions result in different estimates of (9.43). Validation of the model estimate is required to verify these choices.

9.3.4 Global approach

Opposite to the local approach, the global approach utilizes only one data set which is collected from \mathcal{S} with varying scheduling, i.e. one global experiment. Assume that measured IO data of \mathcal{S} as $\mathcal{D}_{N_d} = \{y(k), u(k), p(k)\}_{k=0}^{N_d-1}$ is available and informative for \mathcal{S} . Informative means in this case that with the considered parametrization (9.38a-b), a unique model in the model class can be found such that (9.36) is minimal. Using this data set, the global identification of \mathcal{S} is solved in the W-LPV OBF case as

Algorithm 9.3 (OBFs based LPV identification, global method, Wiener case)

Step 3b. For a given OBF set $\Phi_{n_g}^{n_e} = \{\phi_{ij}\}_{j=1,\dots,n_g}^{i=0,\dots,n_e}$ and data record \mathcal{D}_{N_d} , generate $\check{y} = [\check{y}_{ij}]_{j=1,\dots,n_g}^{i=0,\dots,n_e}$ with $\check{y}_{ij} = \phi_{ij}(q)u$. Denote by (A, B, C, D) the minimal balanced SS realization of $\Phi_{n_g}^{n_e}$. By computing the state evolution (9.23a) in the time interval $[0, N_d - 1]$ with respect to $\{u(k)\}_{k=0}^{N_d-1}$ and $x(0) = 0$, the signal \check{y} on $[0, N_d - 1]$ follows as $\check{y} = x$.

Step 4b. Choose a row vector of meromorphic functions $\Psi = [\psi_l]_{l=0}^{n_\psi}$ for the parameterization of each w_{ij} in (9.21) as $w_{ij} = \sum_{l=0}^{n_\psi} \theta_{ijl} \psi_l$ where $\{\theta_{ijl}\}$ are real unknown parameters, $\psi_l \in \mathcal{R}|_{n_{\mathbb{P}}}$, and $\psi_0 = 1$.

Step 5b. Based on the data set \mathcal{D}_{N_d} , estimate the parameter set $\{\theta_{ijl}\}_{i=0, j=1, l=1}^{n_e, n_g, n_\psi}$ by linear regression. Based on the predictor (9.22), define the regressors as

$$\gamma^\top(k) = \check{y}^\top(k) \otimes \Psi(p(k)), \quad \forall k \in [0, N_d - 1], \quad (9.44)$$

with \otimes denoting the Kronecker tensor product. Collect the data into

$$\begin{aligned} \Gamma_{N_d} &= [\gamma(0), \dots, \gamma(N_d - 1)]^\top, \\ Y_{N_d} &= [y(0), \dots, y(N_d - 1)]^\top. \end{aligned}$$

Arrange the parameters to be estimated into a column vector

$$\theta = [\theta_{010} \dots \theta_{01n_r} \dots \theta_{n_e n_g n_\psi}]^\top. \quad (9.45)$$

Then, to minimize the LS prediction error criterion

$$\mathcal{W}_{N_d}(\theta, \mathcal{D}_{N_d}) = \frac{1}{N_d} \|Y_{N_d} - \Gamma_{N_d} \theta\|_2^2, \quad (9.46)$$

the analytic solution is obtained by

$$\hat{\theta}_{N_d} = \left[\frac{1}{N_d} \Gamma_{N_d}^\top \Gamma_{N_d} \right]^{-1} \left[\frac{1}{N_d} \Gamma_{N_d}^\top Y_{N_d} \right]. \quad (9.47)$$

In this way the estimates of the expansion coefficients result in the form of:

$$\hat{w}_{ij} := \sum_{l=0}^{n_\psi} \hat{\theta}_{ijl} \psi_l. \quad (9.48)$$

In the H-LPV OBF case, the identification procedure is similar. However, the formulation of the regressor is more complicated as the coefficients appear linearly at the input side. Next, it is described how Γ_{N_d} can be formulated for the H-LPV OBF case. The first step is the calculation of the parameter-varying Toeplitz matrix of the predictor (9.25-b):

$$\hat{Y}_{N_d} = \begin{bmatrix} 0 & 0 & \dots \\ CW(p(0)) & 0 & \dots \\ CAW(p(0)) & CW(p(1)) & \dots \\ \vdots & \vdots & \ddots \end{bmatrix} U_{N_d}, \quad (9.49)$$

where $\hat{Y}_{N_d} = [\hat{y}_\theta(0) \ \dots \ \hat{y}_\theta(N_d - 1)]^\top$ is the stacked predicted output vector of the H-LPV OBF structure. By simple rearrangement it follows that

$$\hat{Y}_{N_d} = \underbrace{\begin{bmatrix} 0 & 0 & \cdots \\ CIu(0) & 0 & \cdots \\ CAIu(0) & CIu(1) & \\ \vdots & \vdots & \ddots \end{bmatrix}}_{\hat{H}_{N_d}} \begin{bmatrix} W(p(0)) \\ W(p(1)) \\ \vdots \end{bmatrix}. \quad (9.50)$$

Let δ be the Kronecker delta function, i.e. pulse input at $k = 0$. Now define $h = [h_{ij}]_{j=1 \dots n_g}^{i=0, \dots, n_e}$ as the state evolution of

$$qh = A^\top h + C^\top \delta, \quad (9.51)$$

on the interval $[0, N_d - 1]$ with $h(0) = 0$. Then h is used to calculate the columns of the previously derived transition matrix \hat{H}_{N_d} . By combining each column of H_{N_d} in a Kronecker product with Ψ , the parameters $\{\theta_{ijl}\}$ to be estimated are separated, giving the regressor matrix as

$$\Gamma_{N_d} = [\hat{H}_0 \ \dots \ \hat{H}_{n_p}] \quad (9.52)$$

where

$$\hat{H}_l = \sum_{k=0}^{N_d-1} H_k u(k) \psi_l(p(k)), \quad (9.53)$$

and

$$H_k = [0 \ \dots \ 0 \ h^\top(0) \ \dots \ h^\top(N_d - k - 1)]^\top \in \mathbb{R}^{N_d \times n_g(n_e+1)}. \quad (9.54)$$

Algorithm 9.3 can also be extended for both model structures to estimate a direct feedthrough term. The extension is obtained by defining $w_{00} = \sum_{l=0}^{n_\psi} \theta_{00l} \psi_l$ and formulating the regressor matrix as

$$\Gamma'_{N_d} = \left[\begin{array}{c} u(0) \otimes \psi(p(0)) \\ \vdots \\ u(N_d - 1) \otimes \psi(p(N_d - 1)) \end{array} \middle| \Gamma_{N_d} \right]. \quad (9.55)$$

Including $\{\theta_{00l}\}$ into θ implies that the estimate follows via (9.47).

9.3.5 Properties

In this part the properties of the introduced identification approaches are investigated. First we analyze the restriction of the used linear parametrization with static dependence in the identification of general LPV systems and we characterize that subclass of LPV systems where no bias results. Then we show convergence

and consistency of the parameter estimates. By using similarity of the identification methods with respect to LTI prediction error identification, we characterize basic results about variance and bias of the estimates. Finally, (in)validation issues are discussed in the introduced framework together with the estimation of initial conditions.

Representation capabilities via static dependence

It is important to investigate the effects of the linear parametrization with static dependence on the representation capabilities of the models. From the SS representation form of the models (see (9.23a-b) and (9.26a-b)) it is obvious that the assumption of static dependence restricts the class of representable LPV systems to systems which have a SS representation with static p -dependence only in the C (see (9.23a-b)) or in the B (see (9.26a-b)) system matrices. This means that systems that have no representation that satisfies these conditions are not in the model class. Hence, due to parametrization, a modeling error inevitably occurs during the identification process in these cases. Additionally, the linear parametrization of the expansion coefficients (see (9.38a-b)) implies that systems that are identifiable in the considered way are further restricted to have a SS representation where only the C (or B) matrix depends on p and the functional dependence is the linear combination of the used $\psi_{i,j}$ functions. This underlines that selection of these functions based on prior information is an important part of the model structure selection process. Note that the NL model conversion tool, developed in Section 7.4 provides a practically applicable method to assist this selection.

A second consequence of the parametrization (9.38a-b) rises with respect to the general approximator property of the W-LPV and H-LPV OBF models. We have seen in the general case that increasing n_e lowers the achievable approximation error with these models. However, in case of static dependence, increasing n_e enlarges $\text{span}\{\Phi_{n_g}^{n_e}\}$ which means that the worst-case representation error in the KnW sense is lowered with respect to the frozen system set of the data generating system. However, an increase in n_e may not lower the representation error of the LPV system in a global sense as the modeling error can be significantly dominated by the missing non-static p -dependence of the expansion coefficients. This destroys the general approximator property, meaning that the approximation capability of the model is restricted by the absence of dynamic coefficient dependence. Thus increasing n_e in the hope of better accuracy can easily result in over-parametrization in this case.

We will see that despite the theoretically presented restrictions of the applied parametrization, commonly in a practical situation, adequate approximation of the data generating system can be achieved by the resulting model estimates. It is an important remark that the global method is also applicable in the situations where the coefficients of the W-LPV and H-LPV OBF model structures are not assumed to be static. As the estimation algorithm is independent from the choice of the $\psi_{i,j}$ functions, these functions can be considered with dynamic dependence. Then with a data record containing sufficiently exciting p , estimation of the parameters is similarly available as in the static case. Unfortunately, this property

does not apply for the local method, as in that case, interpolation with dynamic dependence based on frozen estimates is an ill-conditioned problem.

Consistency and convergence

Similar to the classical LTI identification framework, it is possible to show that under minor conditions, the parameter estimates by both approaches are convergent and consistent. Convergence means that for $N_d \rightarrow \infty$ the parameter estimate $\hat{\theta}_{N_d}$ converges, i.e. $\hat{\theta}_{N_d} \rightarrow \theta^*$ with probability 1, while consistency means that the convergence point θ^* is equal with the parameters of the data generating system (9.1). Obviously, the latter property requires that the data generating system is in the model class of the $\mathfrak{M}_W(\Phi_{n_g}^{n_e}, \theta, \mathfrak{B}_P)$ and $\mathfrak{M}_W(\Phi_{n_g}^{n_e}, \theta, \mathfrak{B}_P)$ structures. For a given OBF set $\Phi_{n_g}^{n_e}$ and LPV system \mathcal{S} , this means that for the considered IO partition, \mathcal{S} has a series-expansion in terms of $\Phi_{n_g}^\infty$ where only the first $(n_e + 1)n_g$ expansion coefficients are not zero. Furthermore these expansion coefficients $\{w_{ij}^o\}_{j=1, \dots, n_g}^{i=0, \dots, n_e}$, appearing on the left (or the right) side of the basis functions, are the linear combination of the functions $\{\psi_{ijl}\}$ used in the parametrization (9.38a-b):

$$w_{ij}^o = \sum_{l=0}^{n_{ij}} \theta_{ijl}^o \psi_{ijl}. \quad (9.56)$$

Collect these true parameters $\{\theta_{ijl}^o\}$ into the parameter vector θ_0 . Then, consistency means that $\hat{\theta}_{N_d} \rightarrow \theta_0$ with probability 1.

In the local case, assume that in the measurements $\mathcal{D}_{N_d}^{\bar{p}}$, the noise is uncorrelated with u and $\mathcal{D}_{N_d}^{\bar{p}}$ is informative with respect to the considered model set. Then, convergence and consistency of the estimated LTI models with parameters $\{\bar{w}_{ij\tau}\}$ is well-known (Heuberger et al. 2005; Ljung 1999). This implies the following theorem:

Theorem 9.1 (Convergence and consistency, local method) *Given a model structure $\mathfrak{M}_W(\Phi_{n_g}^{n_e}, \theta, \mathfrak{B}_P)$, with OBFs $\Phi_{n_g}^{n_e}$ and coefficient parametrization (9.38a), where $\theta_{ijl} \in \mathbb{R}$ and each $\psi_{ijl} : \mathbb{P} \rightarrow \mathbb{R}$ is a Lipschitz continuous function. Consider the estimate $\hat{\theta}_{N_d}$ determined by the local method for N_d long informative data records gathered for N_{loc} frozen scheduling signals. If $N_{loc} \rightarrow \infty$ and $N_d \rightarrow \infty$ then $\hat{\theta}_{N_d} \rightarrow \theta^*$ where θ^* is the minimizing argument of the expected value of the squared residual error, $\theta^* = \arg \min_{\theta \in \Theta} \bar{E}\{\epsilon^2(\theta)\}$. Furthermore, if \mathcal{S} is in the model class with parameters θ_0 , then $\theta^* = \theta_0$.*

Theorem (9.1) similarly holds in the H-LPV OBF case. This theorem implies that the asymptotic parameter estimate is independent from the particular noise realization in the data sequence and identification of the true system is possible if it is in the model class. Proof of the theorem follows from the consistency and convergence of the local model estimates together with the convergence of the interpolation in case of Lipschitz continuous functions (for the latter property see Atkinson (1989)).

Consider the global approach. Assume that the available data record is informative with respect to the considered model. Then based on the OE structure of the W-LPV and H-LPV OBF models and the applied linear parametrization of the coefficient functions, it is well-known in the nonlinear case (see Ljung (1999)), that under these conditions, the least-squares estimate of θ is strongly convergent and consistent. So the following theorem obviously holds:

Theorem 9.2 (Convergence and consistency, global method) *Consider the estimate $\hat{\theta}_{N_d}$ determined by (9.47) with respect to the model structure $\mathfrak{M}_W(\Phi_{n_g}^{n_e}, \theta, \mathfrak{B}_F)$ or $\mathfrak{M}_H(\Phi_{n_g}^{n_e}, \theta, \mathfrak{B}_F)$. Assume that the data record \mathcal{D}_∞ is informative. If $N_d \rightarrow \infty$, then $\hat{\theta}_{N_d} \rightarrow \theta^*$ with probability 1 where θ^* is the minimizing argument of the expected value of the squared residual error, $\theta^* = \arg \min_{\theta \in \Theta} \bar{E}\{\epsilon^2(\theta)\}$. Furthermore, if \mathcal{S} is in the model class with parameters θ_0 , then $\theta^* = \theta_0$.*

The concept of variance and bias

Estimation errors of the resulting model estimates can be decomposed into variance and bias parts:

$$F_0(q) - F(q, \hat{\theta}_{N_d}) = \underbrace{F_0(q) - F(q, \theta^*)}_{\text{bias}} + \underbrace{F(q, \theta^*) - F(q, \hat{\theta}_{N_d})}_{\text{variance}}. \quad (9.57)$$

where $F_0(q)$ is the pulse basis expansion of the process part of the data generating system (9.1), while $F(q, \hat{\theta}_{N_d})$ corresponds to the truncated OBF expansion form of the estimated model $\mathfrak{M}_W(\Phi_{n_g}^{n_e}, \hat{\theta}_{N_d}, \mathfrak{B}_F)$ or $\mathfrak{M}_H(\Phi_{n_g}^{n_e}, \hat{\theta}_{N_d}, \mathfrak{B}_F)$. Similar to the LTI case, the *bias* part corresponds to the structural error, i.e. the modeling error introduced by the finite truncation of the expansion and the applied coefficient parametrization, while the *variance* corresponds to the error which is due to the noise contribution on the data.

Variance

In case of the local approach, the concepts of variance and bias can be formulated in the frozen sense. By viewing the result of each frozen identification as a LTI model estimate in terms of the considered basis functions, all results of the LTI framework apply in terms of variance and bias (see Section 2.3.5). However, due to interpolation of these local model estimates through their expansion coefficients, there is a little hope to characterize the variance and the bias of the resulting LPV model estimate. In terms of the bias, the main difficulty is that the number of frozen models, i.e. the number of interpolation points has a significant, but not well understood effect on the bias. For the variance, the problem is that, by knowing the distribution of $\{\hat{w}_{ij\tau}\}$, it is a difficult problem in general to deduce the distribution of $\{\hat{\theta}_{ijl}\}$ in (9.42). Based on these, variance and bias are only characterized in the frozen sense with respect to the estimates by the local method.

In the global case, we face a different situation. We have already shown that the parameter estimates in this case are consistent. Let \mathcal{D}_∞ be informative with respect to \mathcal{S} . Then due to the prediction-error setting of the estimation, the classical result of the LTI framework holds:

Theorem 9.3 (Asymptotic variance, global method) *Consider the estimate $\hat{\theta}_{N_d}$ determined by (9.47) with respect to the model structure $\mathfrak{M}_W(\Phi_{n_g}^{n_e}, \theta, \mathfrak{B}_P)$ or $\mathfrak{M}_H(\Phi_{n_g}^{n_e}, \theta, \mathfrak{B}_P)$. Assume that the data record \mathcal{D}_∞ is informative. Due to the convergence of $\hat{\theta}_{N_d}$, there exists a $\theta^* \in \Theta$ such that $\hat{\theta}_{N_d} \rightarrow \theta^*$ with probability 1 if $N_d \rightarrow \infty$. Then*

$$\sqrt{N_d}(\hat{\theta}_{N_d} - \theta^*) \rightarrow \mathcal{N}(0, \Omega_\theta) \quad \text{as } N_d \rightarrow \infty, \quad (9.58)$$

where

$$\Omega_\theta = \lim_{N_d \rightarrow \infty} N_d \cdot \mathcal{E} \left\{ \left[\frac{\partial}{\partial \theta} \mathcal{W}_{N_d}(\theta^*, \mathcal{D}_{N_d}) \right] \left[\frac{\partial}{\partial \theta} \mathcal{W}_{N_d}(\theta^*, \mathcal{D}_{N_d})^\top \right] \right\}$$

Note that the proof follows similarly as in the LTI case Ljung (1999), due to the fact that the considered model sets correspond to asymptotically stable models with respect to all $\theta \in \Theta$, the estimates of θ are convergent, and the considered prediction error framework is equivalent with the classical formulation. This basic result on the variance of the parameter estimates provides some insights, however further properties in terms of asymptotic model order or frequency characterization of the variance are hard to derive due to the parameter-varying nature of the plant. Developing more informative expression for the asymptotic variance are the aims of future research.

Bias

Consider the bias of the estimated models $\mathfrak{M}_W(\Phi_{n_g}^{n_e}, \hat{\theta}_{N_d}, \mathfrak{B}_P)$ and $\mathfrak{M}_H(\Phi_{n_g}^{n_e}, \hat{\theta}_{N_d}, \mathfrak{B}_P)$. In the global case it holds that, if the data record \mathcal{D}_{N_d} is informative and the data generating system is in the model class, then the classical results of prediction error identification imply that the estimate $\hat{\theta}_{N_d}$ of the parameters θ is unbiased. In case the process part F_0 , i.e. the LPV system \mathcal{S} , in (9.1) is not in the model class, i.e. either in the series-expansion of \mathcal{S} by $\Phi_{n_g}^\infty$ the coefficients $\{w_{ij}^o\}$ are non-zero in the truncated part ($w_{ij} \neq 0$ for $i > n_e$), or the coefficients have different dependence than the used parametrization (9.38a-b), then for the asymptotic estimate θ^* it holds that for a given $p \in \mathfrak{B}_P$

$$\begin{aligned} (F_0(q) - F(q, \theta^*)) \diamond p &= \underbrace{\sum_{i=0}^{n_e} \sum_{j=1}^{n_g} \left[\left(w_{ij}^o - \sum_{l=0}^{n_{ij}} \theta_{ijl}^* \psi_{ijl} \right) \diamond p \right] \phi_{ij}(q)}_{\text{parametrization bias}} \\ &+ \underbrace{\sum_{i=n_e+1}^{\infty} \sum_{j=1}^{n_g} [w_{ij} \diamond p] \phi_{ij}(q)}_{\text{truncation bias}}, \end{aligned} \quad (9.59)$$

where $\{w_{ij}^o\}$ are the expansion coefficients of \mathcal{S} in terms of $\Phi_{n_e}^\infty$ and $\theta^* = [\theta_{ijl}^*]_{i=0, j=1, l=0}^{n_e, n_g, n_{ij}}$. The first part in expression (9.59) describes bias due to improper assumptions on the scheduling dependence while the right side describes bias due to the non-considered tail of the series-expansion. Based on (9.59), it can be concluded that by extending the basis functions, i.e. increasing n_e , the truncation bias can be arbitrary decreased. However, increasing n_e means that more coefficients appear in the parametrization associated bias, which results in an eventual increase of this term. This underlines that choosing a good coefficient dependence in terms of $\{\psi_{ijl}\}$ is equally important to the choice of a OBF set with fast convergence rate. Fortunately, due to the model transformation approach of Chapter 7, first principle information can be used to assist the adequate choice of ψ_{ijl} with respect to a given basis $\Phi_{n_g}^{n_e}$.

(In)validation

In general, reliable (in)validation of LPV model estimates is a theoretically hard task. One problem is that uncertainty of the model estimates has not been investigated in the LPV framework and on the other hand, it is difficult to judge how the estimated model relates or fits to the available first principle knowledge.

In general, only (in)validation through the simulation of the model is available, comparing the model output with respect to measured data records which are assumed to be informative. Here the richness of p in terms of excitation has a prime importance, as with slowly varying scheduling trajectories, model estimates with significantly different transient behavior can seem to be both valid models of the plant. Error measures like MSE, BFT, VAF introduced in Section 2.3.7, can be successfully used to accommodate comparison of the simulated and measured signals and to decide on the validity of the model estimates. However, in case of an invalidated model estimate, it is hard to give any indication about how to identify the system with a better end result (reconfiguration of the model structure, more exciting (u, p) , other type of identification method, etc.).

Additionally, for the introduced models, (in)validation can also be accomplished based on the residual signal ϵ in the one-step-ahead prediction error (9.14). The residual can be easily computed for the proposed models as the inverse of the noise model is 1. Applying residual analysis, similar to the LTI case, the hypothesis that ϵ is white noise or ϵ is uncorrelated with the past inputs can be tested. If these hypothesis tests result in rejection, then the deficiency of the applied model structure is implied. The only problem is that due to the approximative nature of the applied model structure (both in terms of the finite series-expansion and in terms of the assumption of static dependence), some unmodeled dynamics of the system always contribute to the residual term. This implies that based on residual analysis, the models are most likely to be rejected. Thus in the following, we only consider (in)validation in terms of simulations and error measures.

Initial conditions

In practice, slow dynamics of the system, safety considerations, or high costs of long measurements often result in data records which are collected with non-zero initial conditions of the plant. For these data sets, the initial conditions need to be estimated during the identification process. In the LTI case, the identification framework of OBFs supports estimation of initial conditions (Heuberger et al. 2005), which can be efficiently applied in the local algorithm to estimate initial conditions of the frozen systems of \mathcal{S} . Therefore, further investigation of initial condition estimation is only interesting for the global identification approach.

In the global method, the SS form of the H-LPV OBF model structure, can be used to formulate an extended data matrix which involves the initial condition $x(0)$ of the model. The extended data matrix \hat{Y}'_{N_d} is introduced as

$$\hat{Y}'_{N_d} = \begin{bmatrix} Cx(0) \\ \vdots \\ CA^{N_d-1}x(0) \end{bmatrix} + \hat{Y}_{N_d}. \quad (9.60)$$

where \hat{Y}_{N_d} satisfies (9.49), i.e. it is the predicted output of $\mathfrak{M}_H(\Phi_{n_g}^{n_e}, \theta, \mathfrak{B}_P)$ with zero initial condition. By extending θ with $x(0)$ as parameters and including $[C^\top \ A^\top \ C^\top \ \dots]^\top$ into Γ_{N_d} , estimation of $x(0)$ becomes available through linear regression. In the W-LPV OBF case, the extended data matrix is

$$\hat{Y}'_{N_d} = \begin{bmatrix} W(p(0))x(0) \\ \vdots \\ W(p(N_d))A^{N_d-1}x(0) \end{bmatrix} + \hat{Y}_{N_d}. \quad (9.61)$$

Based on (9.61), simultaneous estimation of θ and $x(0)$ is a bilinear optimization problem for the LS criterion. This optimization is solvable by the application of a separable least-squares strategy (see Golub and Pereyra (1973)), however the obtained solutions are only local minima of the involved cost function.

(Quasi) LPV system identification

There is an important aspect of the proposed identification methods if the data generating system is a quasi LPV system. For quasi LPV systems, generally, p cannot be held constant, as the scheduling is an internal signal of the system like elements of the state or output variables. Thus for this case, only the global method is applicable, as the local approach needs identification of the system with respect to constant scheduling trajectories.

Similarity to nonlinear identification methods

In Chapter 1 it has been discussed that the attractive properties of truncated OBF expansion representations inspired some identification approaches of the NL and

the fuzzy field. In order to position the developed approaches with respect to these methods, i.e. to clarify the connection or the dissimilarities, the following properties are important:

- In the nonlinear case, the method of Gómez and Baeyens (2004) uses Wiener and Hammerstein type of models where the LTI part is the linear combination of a filter bank of OBFs. We have already shown that these models result as “special cases” of W-LPV and H-LPV OBF models in the quasi-LPV case. In Sbárbaro and Johansen (1997), the used model structure contains fuzzy membership functions associated with a (Laguerre) basis function in the filter bank.
- In our approach, the OBFs, the backbone of the model structures, are optimized for \mathcal{S} , while in the methods of Sbárbaro and Johansen (1997) and Gómez and Baeyens (2004) they are assumed to be chosen by the user.
- In Gómez and Baeyens (2004), the LTI part is parameterized and estimated as a linear combination of the chosen basis simultaneously with the estimation of the static nonlinearity. Similarly in Sbárbaro and Johansen (1997), both the LTI part and the fuzzy part are identified together. In our approach, the parametrization is focused on the expansion coefficients while the LTI part is fixed, thus the complicated estimation structure of the fuzzy and NL methods is not required in this case.
- Both the proposed and the NL/fuzzy approaches use the least-squares criterion for the identification of the system, however, the proposed LPV approach is simpler as it solves the estimation problem by linear regression.

9.3.6 Examples

In this section, the applicability of the introduced identification methods is shown in three different examples.

SS example with invariant (A, B)

As a first example, consider an asymptotically stable LPV system \mathcal{S}_1 , with an $\mathfrak{R}_{\text{SS}}(\mathcal{S}_1)$ equal to

$$\left[\begin{array}{c|c} A & B \\ \hline C \diamond p & 0 \end{array} \right] = \left[\begin{array}{ccc|c} 0.3 & 0.2 & 0.4 & 1 \\ -0.1 & 0.2 & 0.2 & 1 \\ 0.4 & -0.1 & 0.5 & 1 \\ \hline 2p & -p^2 & \sin(p) & 0 \end{array} \right],$$

and $\mathbb{P} = [-1, 1]$. Note that in this representation, only C depends on p and the underlying dependence is static. Using the poles of A to generate Hambo basis functions Φ_3^0 , the resulting OBFs are complete with respect to the frozen transfer function set $\mathfrak{F}_{\mathbb{P}}$ of $\mathfrak{R}_{\text{SS}}(\mathcal{S}_1)$. As only C is dependent on p and Φ_3^0 is complete,

Table 9.1: Validation results of 100 identification experiments by the global and local methods using the W-LPV and H-LPV OBF model structures in the considered examples. The results are given in terms of the MSE and the average BFT and VAF of the simulated output signals of the model estimates.

Model	Case	MSE (dB)	BTF (%)	VAF (%)
W-LPV \mathcal{S}_1	loc.	-94.99	99.84%	99.99%
	glob.	-62.35	98.54%	98.98%
H-LPV \mathcal{S}_2	loc.	-95.90	99.71%	99.99%
	glob.	-62.78	98.39%	99.97%
W-LPV \mathcal{S}_3	loc.	-18.01	75.82%	94.12%
	glob.	-31.03	86.34%	98.23%
H-LPV \mathcal{S}_3	loc.	-10.16	62.13%	85.69%
	glob.	-26.41	82.11%	96.18%

the system lies in the model class of the W-LPV OBF structure with these basis functions. Furthermore, the expansion coefficients of $\mathfrak{R}_{\mathcal{S}\mathcal{S}}(\mathcal{S}_1)$ in terms of the basis functions Φ_3^0 have static dependence, thus choosing the parametrization of the W-LPV OBF model with static dependence still implies that the system lies in the model class.

Based on the OBF set Φ_3^0 and 100 experiments with varying p , global identification of \mathcal{S} with the W-LPV OBF structure has been carried out 100 times. In each experiment, a $N_d = 500$ sample long data record of the system has been generated, based on white u and p with uniform distribution $\mathcal{U}(-1, 1)$. For each data record, a white output noise e with distribution $\mathcal{N}(0, 0.5)$ has been added, which matches with the noise concept of the prediction error setting (see Section 9.2.1). The resulting *Signal-to-Noise Ratio* (SNR) has been 29.5 dB, while the relative signal-to-noise amplitude has been 26 %. Using the same conditions in the local case, $\mathcal{D}_{N_d, \bar{p}}$ data records have been collected 100 times with constant scheduling points $P_{11} = \{-1 + 0.2\tau\}_{\tau=0}^{10}$. Based on these data records, 11 local estimates of $\mathfrak{R}_{\mathcal{S}\mathcal{S}}(\mathcal{S})$ have been produced using an LTI-OBF model structure with Φ_3^0 . The resulting “frozen” basis coefficients have been interpolated in each of the 100 cases. In both the global and local methods, a 2nd-order polynomial based parametrization has been used in the estimation of W (see (9.38a) with $\psi_{i,jl}(p) = p^j$ and $n_{ij} = 2$).

In the first row of Table 9.1, the (in)validation results of the resulting 100 model estimates are shown in both the local and global cases. The (in)validation results are given in terms of MSE and *average* BFT and VAF of the simulated output signals of the models (see Section 2.3) for realizations of u and p that are different from the ones used during the identification. In Figure 9.5, a typical plot of the simulated output signals and the resulting output-error of the models are presented. As expected, both approaches identified the system with adequate validation results. This underlines, that with respect systems that are in the considered W-LPV OBF model class, both approaches provide reliable estimates even in case of significant output noise. By further investigating the results it is obvious that

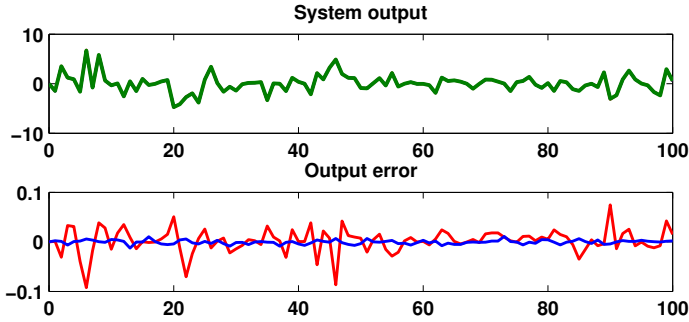


Figure 9.5: Comparison of the identified models of \mathcal{S}_1 by their responses for white u, p with distribution $\mathcal{U}(-1, 1)$: $\mathfrak{R}_{\text{SS}}(\mathcal{S})$ (green), W-LPV OBF local (blue), W-LPV OBF global (red).

the global approach has produced a slightly worse result than the local approach. Explanation of this phenomena lies in the much larger amount of data ($11 \cdot N_d$) available in the local case.

SS example with invariant (A, C)

As a second example, consider an asymptotically stable LPV system \mathcal{S}_2 , with an $\mathfrak{R}_{\text{SS}}(\mathcal{S}_2)$ equal to the transpose of $\mathfrak{R}_{\text{SS}}(\mathcal{S}_1)$:

$$\left[\begin{array}{c|c} A_2 & B_2 \\ \hline C_2 & 0 \end{array} \right] = \left[\begin{array}{c|c} A_1^\top & C_1^\top \\ \hline B_1^\top & 0 \end{array} \right].$$

Note that $\mathfrak{R}_{\text{SS}}(\mathcal{S}_1)$ and $\mathfrak{R}_{\text{SS}}(\mathcal{S}_2)$ are not equivalent. However, the OBF set Φ_3^0 of the previous example is still complete with respect to the frozen transfer function set $\mathfrak{F}_{\mathbb{P}}$ of $\mathfrak{R}_{\text{SS}}(\mathcal{S}_2)$. So also in this case, the true system lies in the model class of the H-LPV OBF structure with the basis functions Φ_3^0 and with static coefficient dependence. By using the same setting of data sequences and local model estimates as in the previous example, identification of \mathcal{S}_2 has been accomplished by the H-LPV OBF model structure with Φ_3^0 . The (in)validation results in terms of simulation are shown in Figure 9.6 and in the second row of Table 9.1. As expected, both approaches identified the system adequately just like in the previous example.

IO example

As a third example, the asymptotically stable LPV system \mathcal{S}_3 for which OBF selection has been extensively studied in Section 8.3.3 is identified. Consider the IO representation $\mathfrak{R}_{\text{IO}}(\mathcal{S}_3)$ defined by (8.14) and with $\mathbb{P} = [0.6, 0.8]$. Using the poles obtained via the FKcM algorithm with fuzzyness $m = 25$ and $n_c = 8$, a OBF set Φ_8^0 has resulted, which has been found adequate for the truncated series-expansion

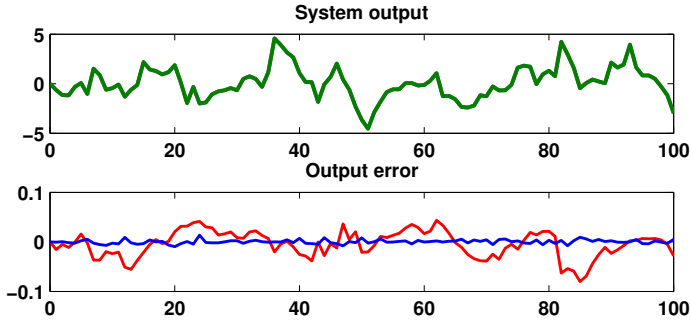


Figure 9.6: Comparison of the identified models of S_2 by their responses for white u, p with distribution $\mathcal{U}(-1, 1)$: $\mathfrak{R}_{SS}(S_2)$ (green), H-LPV OBF local (blue), H-LPV OBF global (red).

based approximation of the system. Using this basis function set and the proposed identification algorithms, we show that quite accurate estimated models of the system can be derived.

Based on Φ_8^0 and a 2nd-order polynomial based parametrization of the coefficients, identification of S_3 with both methods and structures has been accomplished 100 times. The used data sequences have been based on the same setting and conditions as in the previous examples, except p has been generated with a distribution $\mathcal{U}(0.6, 0.8)$. The resulting SNR has been 20 dB in the resulting data records with a relative signal-to-noise amplitude of 25 %. Calculation time of the algorithms has been a few seconds on a Pentium 4, 2.8 GHz PC.

In Figure 9.7 and 9.8 and in the last two rows of Table 9.1, the (in)validation results are shown for different realizations of u, p than used during the identification. As expected, the W-LPV and H-LPV OBF structures based on coefficients with static dependence could not fully cope with the variations in the $\{a_i\}_{i=0}^5$ parameters. However, the global W-LPV OBF identification provided quite acceptable results for such a heavily nonlinear system. The explanation why the H-LPV OBF structure gave a worse result lies in the different approximation capabilities of these models. By computing the left-side expansion coefficients of (8.14) in terms of the used basis, which corresponds to the true coefficients of the system with respect to the W-LPV OBF model structure, the resulting expansion coefficients have a dominant part with static dependence. This means that a good approximation of the system can be found among the used W-LPV OBF models with static dependence (both the parametrization and truncation bias are small). On the other hand, the right-side expansion coefficients of (8.14) in terms of Φ_8^∞ have a dominant part with dynamic dependence. This means that the parametrization bias of H-LPV OBF models with static dependence must be larger than in the previous case. This implies that with the considered parametrization, W-LPV OBF model structures are generally better for systems with a IO representation where the dynamics are dominated by the variation of the $\{a_i\}$ coefficients, while H-LPV OBF model structures are better for the cases, where $\{b_j\}$ are dominant.

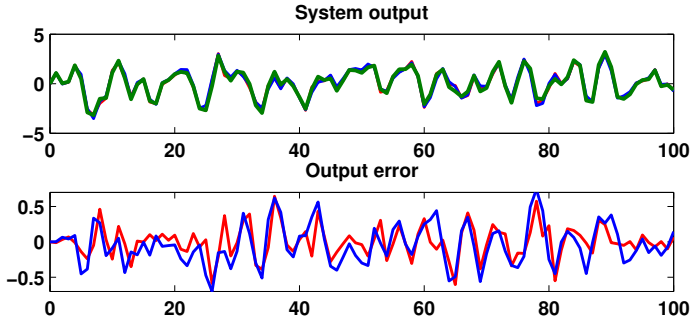


Figure 9.7: Comparison of the identified models of \mathcal{S}_3 by their responses for white (u, p) with distribution $(\mathcal{U}(-1, 1), \mathcal{U}(0.6, 0.8))$: \mathcal{S}_3 (green), W-LPV OBF global (red), H-LPV OBF global (blue).

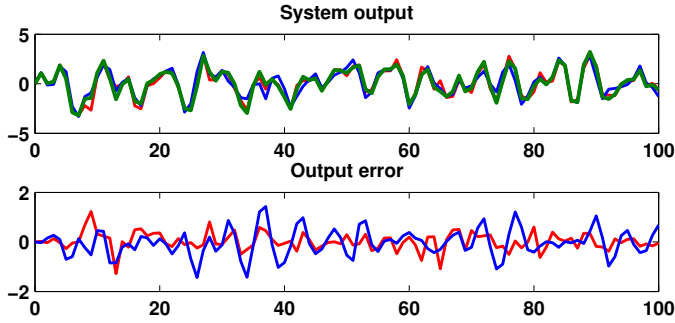


Figure 9.8: Comparison of the identified models of \mathcal{S}_3 by their responses for white (u, p) with distribution $(\mathcal{U}(-1, 1), \mathcal{U}(0.6, 0.8))$: \mathcal{S}_3 (green), W-LPV OBF local (red), H-LPV OBF local (blue).

In this example global methods are prevailed, because they have been able to capture the transient dynamics of the system between frozen scheduling points of \mathbb{P} , while in the local case the 11 local model estimates have been not enough for correct interpolation. By using $N_{loc} > 11$, the local method quickly improves. Note, that in the asymptotic sense (in N_{loc}), the local and global method converge to the same optimal model in the utilized model class. Extension of Φ_8 with $n_e = 1, 2, \dots$ has not improved the results as Φ_8 is well chosen with respect to \mathcal{S}_3 , i.e. the local modeling error is negligible due to the optimal choice by the FKcM. Therefore, the error in Table 9.1 is mainly governed by the modeling error of the used parametrization (9.59). Using higher order polynomials in Ψ produces a 2-5% percentage improvement in the results of Table 9.1, but in order to achieve full representation with the proposed models, incorporation of dynamic dependence on p is needed.

9.4 Approximation of dynamic dependence

In the previous part, OBFs-based model structures have been introduced for the identification of LPV systems, with the main intention to give flexible models that are able to describe general LPV systems, simplify identification, are useful for control, and are unaffected by the difficulties present in the identification of LPV-SS or IO models. It has been shown that to describe any LPV system, the coefficients of the W-LPV and H-LPV OBF models, similar to the coefficients of other LPV models, need to have dynamic dependence on p . We have motivated, that dynamic dependence presents an extra freedom of the parametrization and is not supported by the existing control approaches. To overcome this problem, in Section 9.3 the coefficients have been restricted to static dependence. This assumption led to a novel and efficient identification approach of W-LPV and H-LPV OBF model structures based on the LS criterion. However, the drawback of the assumption has been also pointed out: it limits the class of representable LPV systems. In this section, an alternative of LPV truncated OBF expansion models and its identification approach is introduced with the intention to improve the representation capabilities of the previously considered model structures and parametrization, but without the use of dynamic dependence. In fact the idea that we will apply is the introduction of an additional feedback-loop around each basis component of the W-LPV and H-LPV OBF model structures with a gain incorporating also static dependence (see Figures 9.9 and 9.10). In this way, the filter bank of OBFs as a dynamical LTI system is “reused” to provide dynamic expansion coefficients. This implies that these modified structures can approximate a much wider class of LPV systems, than W-LPV and H-LPV OBF models with static dependence. The introduction of feedback-based weighting leads to two new model structures given in Figure 9.9 and 9.10, which we call *Wiener Feedback* (WF) and *Hammerstein Feedback* (HF) LPV OBF models.

9.4.1 Feedback-based OBF model structures

Again we consider the prediction-error setting of Section 9.2.1. Let $\Phi_{n_g}^{n_e}$ be a set of Hambo basis functions in $\mathcal{RH}_{2-}(\mathbb{E})$. Denote the input and output of each basis function in $\Phi_{n_g}^{n_e}$ by \check{u}_{ij} and \check{y}_{ij} satisfying:

$$\check{y}_{ij} = \phi_j(q)G^i(q)\check{u}_{ij}. \quad (9.62)$$

Additionally, let $(A_{ij}, B_{ij}, C_{ij}, D_{ij})$ be the minimal balanced SS realization of each basis function $\phi_j G^i$ and introduce $A = \text{diag}(A_{01}, \dots, A_{n_e n_g})$. Similarly define B and C . Denote $\check{u} = [\check{u}_{01} \ \dots \ \check{u}_{n_e n_g}]^\top$ and $\check{y} = [\check{y}_{01} \ \dots \ \check{y}_{n_e n_g}]^\top$. Then, the SS form of the IO relations (9.62) is

$$qx = Ax + B\check{u}, \quad (9.63a)$$

$$\check{y} = Cx. \quad (9.63b)$$

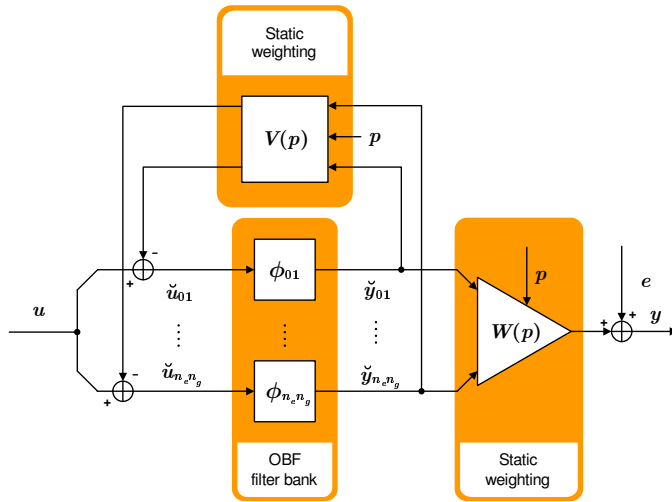


Figure 9.9: IO signal flow graph of WF-LPV OBF models with feedback coefficients $V = [v_{01} \dots v_{n_e n_g}]$ and output-side coefficients $W = [w_{01} \dots w_{n_e n_g}]$ without a feedthrough term. All coefficients are considered with static dependence.

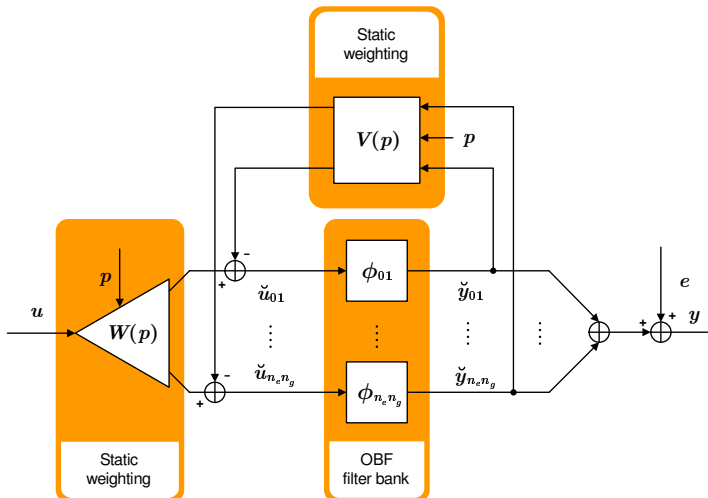


Figure 9.10: IO signal flow graph of HF-LPV OBF models with feedback coefficients $V = [v_{01} \dots v_{n_e n_g}]$ and input-side coefficients $W = [w_{01} \dots w_{n_e n_g}]$ without a feedthrough term. All coefficients are considered with static dependence.

Note that this is a non-minimal SS representation, but it is needed to introduce the feedback loops around each basis function separately (see Figures 9.9 and 9.10).

Let \mathcal{S} be an asymptotically stable SISO LPV system with scheduling space $\mathbb{P} \subseteq \mathbb{R}^{n_{\mathbb{P}}}$, scheduling signal p , and IO partition (u, y) . Then the feedback model structures of Figures 9.9 and 9.10 are formulated as follows:

- Wiener feedback LPV OBF model (WF-LPV OBF)

$$\check{y}_{ij} = \phi_j(q)G^i(q)u - \phi_j(q)G^i(q)v_{ij}(p)\check{y}_{ij}, \quad (9.64a)$$

$$y = e + w_{00}(p)u + \sum_{i=0}^{n_e} \sum_{j=1}^{n_g} w_{ij}(p)\check{y}_{ij}, \quad (9.64b)$$

with $p \in \mathfrak{B}_{\mathbb{P}}$, where $\mathfrak{B}_{\mathbb{P}}$ is considered to be known and with

$$\theta = \begin{bmatrix} w_{00} & w_{01} & \dots & w_{n_e n_g} & v_{01} & \dots & v_{n_e n_g} \end{bmatrix}^{\top} \in (\mathcal{R}|_{n_{\mathbb{P}}})^{1+2(n_e+1)n_g}.$$

This model, given in Figure 9.9, is called the WF-LPV OBF model and denoted by $\mathfrak{M}_{\text{WF}}(\Phi_{n_g}^{n_e}, \theta, \mathfrak{B}_{\mathbb{P}})$. As \check{y}_{ij} is independent from e (u and p are assumed to be deterministic), the one-step-ahead predictor in this case reads as

$$\check{y}_{ij} = \phi_j(q)G^i(q)u - \phi_j(q)G^i(q)v_{ij}(p)\check{y}_{ij}, \quad (9.65a)$$

$$\hat{y}_{\theta} = w_{00}(p)u + \sum_{i=0}^{n_e} \sum_{j=1}^{n_g} w_{ij}(p)\check{y}_{ij}. \quad (9.65b)$$

Denote $W = \text{diag}(w_{01}, \dots, w_{n_e n_g})$ and V accordingly and let $E = [1 \dots 1]$. Then, the SS equivalent of (9.65a-b) is given by

$$qx = [A - BV(p)C]x + BE^{\top}u, \quad (9.66a)$$

$$\hat{y}_{\theta} = W(p)Cx + w_{00}(p)u. \quad (9.66b)$$

- Hammerstein feedback LPV OBF model (HF-LPV OBF)

$$\check{u}_{ij} = w_{ij}(p)u - v_{ij}(p)\phi_j(q)G^i(q)\check{u}_{ij}, \quad (9.67a)$$

$$y = e + w_{00}(p)u + \sum_{i=0}^{n_e} \sum_{j=1}^{n_g} \phi_j(q)G^i(q)\check{u}_{ij}. \quad (9.67b)$$

with $p \in \mathfrak{B}_{\mathbb{P}}$, where $\mathfrak{B}_{\mathbb{P}}$ is considered to be known and with

$$\theta = \begin{bmatrix} w_{00} & w_{01} & \dots & w_{n_e n_g} & v_{01} & \dots & v_{n_e n_g} \end{bmatrix}^{\top} \in (\mathcal{R}|_{n_{\mathbb{P}}})^{1+2(n_e+1)n_g}.$$

This model, given in Figure 9.10, is called the HF-LPV OBF model and denoted by $\mathfrak{M}_{\text{HF}}(\Phi_{n_g}^{n_e}, \theta, \mathfrak{B}_{\mathbb{P}})$. As \check{u}_{ij} is independent from e , the one-step-ahead

predictor reads as

$$\check{u}_{ij} = w_{ij}(p)u - v_{ij}(p)\phi_j(q)G^i(q)\check{u}_{ij}, \quad (9.68a)$$

$$\hat{y}_\theta = w_{00}(p)u + \sum_{i=0}^{n_e} \sum_{j=1}^{n_g} \phi_j(q)G^i(q)\check{u}_{ij}. \quad (9.68b)$$

Following a similar formulation as in the Wiener case, the SS equivalent of (9.68a-b) is given by

$$qx = [A - BV(p)C]x + BW(p)u, \quad (9.69a)$$

$$\hat{y}_\theta = ECx + w_{00}(p)u, \quad (9.69b)$$

Note that the weighting functions $\{w_{ij}\}$, $\{v_{ij}\}$ are not necessarily equivalent in (9.64a-b) and (9.67a-b). Thus similar to the previous case, these model structures are distinguished in the sequel.

9.4.2 Properties of Wiener and Hammerstein feedback models

Representation of dynamic dependence

First, an important property of the introduced feedback based model structures is discussed:

Property 9.2 (Representation of dynamic dependence) *Let S be an asymptotically stable LPV system and $\Phi_{n_g}^\infty \subset \mathcal{RH}_{2-}(\mathbb{E})$ be a Hambo basis. Given a Wiener-feedback model $\mathfrak{M}_{\text{WF}}(\Phi_{n_g}^{n_e}, \theta, \mathfrak{B}_{\mathbb{F}})$ or Hammerstein-feedback model $\mathfrak{M}_{\text{HF}}(\Phi_{n_g}^{n_e}, \theta, \mathfrak{B}_{\mathbb{F}})$ of S with truncation $n_e > 0$ and coefficients $w_{ij}, v_{ij} \in \mathcal{R}|_{n_{\mathbb{F}}}$ having static dependence. If $\mathfrak{M}_{\text{WF}}(\Phi_{n_g}^{n_e}, \theta, \mathfrak{B}_{\mathbb{F}})$ ($\mathfrak{M}_{\text{HF}}(\Phi_{n_g}^{n_e}, \theta, \mathfrak{B}_{\mathbb{F}})$) is asymptotically stable, then its process model (deterministic part) has a convergent series-expansion in terms of $\Phi_{n_g}^\infty$. If there is an $(i, j) \in \mathbb{I}_0^{n_e} \times \mathbb{I}_1^{n_g}$ such that v_{ij} is dependent on p , i.e. not all feedback terms are constant, then the coefficients of the series-expansion have dynamic dependence otherwise all expansion coefficients have static dependence.*

For a proof see Appendix A.4. Note that in terms of Property 9.2, a WF-LPV or a HF-LPV OBF model can be considered to be equivalent with a W-LPV or a H-LPV OBF model with dynamic coefficient dependence. However, the converse does not hold in general. Thus, through feedback-based static weighting functions $w_{ij}, v_{ij} \in \mathcal{R}|_{n_{\mathbb{F}}}$ the feedback based OBF models can approximate general LPV systems. It is trivial that such an approximation is more adequate than using W-LPV and H-LPV OBF models with static coefficient dependence. In fact, those models are special cases of the WF-LPV OBF and HF-LPV OBF structures. Equations (9.66a-b) and (9.69a-b) imply that the WF-LPV and HF-LPV OBF structures can approximate static scheduling dependence in the A matrix as well as static scheduling dependence in the autoregressive part, see (9.64a-b) and (9.67a-b). However, this improved representation capability comes at a price, namely that due to the feedback, stability of the model is not internally guaranteed like in the W-LPV or the H-LPV OBF case.

General approximation property

Based on the previous part, a WF-LPV or a HF-LPV OBF model can only approximate and not represent an arbitrary LPV system S . So the general approximator property does not hold in this case as it would require dynamic dependence of W and V . However, these models have a series-expansion representation with coefficients incorporating dynamic dependence, thus they give better approximation of general LPV systems than W-LPV and H-LPV OBF models restricted to have static dependence.

Loss of linearity in the coefficients

The second price to be paid is that by the introduction of the feedback loop, the linear-in-the-coefficients property of the original series-expansion structure is lost. The resulting predictors (9.65a-b) and (9.68a-b) are bilinear in the coefficients.

McMillan degree property

Due to the fact, that the introduced feedback based structures are still based on truncated series expansions, just like the W-LPV and H-LPV OBF models, they are well structured against changes of the McMillan degree in the frozen system set $\mathcal{F}_{\mathbb{P}}$ of S .

Models for control

The existing approaches of LPV control theory are also directly applicable for estimates with the introduced model structures. Through (9.66a-b) and (9.69a-b), immediate SS realizations of estimated models are available where all dependencies are static. Opposite to the previous case, in (9.66a) and (9.69a) the resulting A matrix is dependent on p , thus control design does not simplify for these models. However, the specific structure of the dependence may be exploited during control design.

9.4.3 Identification by dynamic dependence approximation

In the following, an approach is proposed for the identification with the introduced WF-LPV and HF-LPV OBF model structures based on a LS criterion. This identification approach is the extension of the global method of Section 9.3. Again we consider the parametrization of each w_{ij} and v_{ij} as

$$w_{ij} = \sum_{l=0}^{n_w} \theta_{ijl}^w \psi_l^w, \quad v_{ij} = \sum_{l=0}^{n_v} \theta_{ijl}^v \psi_l^v, \quad (9.70)$$

where $\{\theta_{ijl}^w\}$ and $\{\theta_{ijl}^v\}$ are real-valued unknown coefficients and $\psi_l^w, \psi_l^v \in \mathcal{R}|_{n_{\mathbb{P}}}$, with $\psi_0^w = \psi_0^v = 1$, are given meromorphic functions with static dependence.

We also assume that no feedthrough term is present, $w_{00} = 0$, however later, the estimation of w_{00} is also investigated for the algorithm. Similar to the previous case, the approach is formulated by assuming that the basis selection phase has already been accomplished, so we pick up the line of reasoning right after Step 2 in Section 9.2.5.

Similar to the global approach of Section 9.3, the estimation phase of the identification approach based on WF-LPV and HF-LPV OBF model structures uses only one data set $\mathcal{D}_{N_d} = \{y(k), u(k), p(k)\}_{k=0}^{N_d-1}$ which is collected from \mathcal{S} with varying scheduling and it is assumed to be informative. Note that due to the linear parametrization of the coefficients, the unknown parameters $\{\theta_{ijl}^v\}$ and $\{\theta_{ijl}^w\}$ appear in a bilinear relationship in the predictors (9.65a-b) and (9.68a-b). This implies that by using the LS criterion (9.36) as an identification criterion with residual (9.15), the minimization of (9.36) can be tackled by a separable least squares algorithm. In each step of this iterative solution, either $\{\theta_{ijl}^v\}$ or $\{\theta_{ijl}^w\}$ is fixed, while the other parameter set is estimated by linear regression. This iterative scheme is repeated, till (9.36) converges. The procedure for the Wiener case is given in detail as follows:

Algorithm 9.4 (OBFs based LPV identification, Wiener-Feedback case)

Step 3c. Given an OBF set $\Phi_{n_g}^{n_e} = \{\phi_{ij}\}_{j=1, \dots, n_g}^{i=0, \dots, n_e}$ and data record \mathcal{D}_{N_d} of \mathcal{S} . Parameterize each w_{ij} and v_{ij} of (9.64a-b) according to (9.70) where $\psi_l^w, \psi_l^v \in \mathcal{R}|_{n_{\mathcal{P}}}$ are meromorphic functional dependencies chosen by the user with $\psi_0^w = \psi_0^v = 1$. Collect these functions as

$$\begin{aligned}\Psi^w &= [\psi_0^w \ \dots \ \psi_{n_w}^w], \\ \Psi^v &= [\psi_0^v \ \dots \ \psi_{n_v}^v],\end{aligned}$$

and also the real parameters, associated with the parametrization (9.70), into the vectors:

$$\begin{aligned}\theta^w &= [\theta_{010}^w \ \theta_{011}^w \ \dots \ \theta_{n_e n_g n_w}^w]^\top, \\ \theta^v &= [\theta_{010}^v \ \theta_{011}^v \ \dots \ \theta_{n_e n_g n_v}^v]^\top.\end{aligned}$$

Step 4c. Choose an initial set of values for the parameters $\{\theta_{ijl}^v\}$, like $\theta_{ijl}^v = 0$.

Step 5c. Based on \mathcal{D}_{N_d} , compute $\check{y} = [\check{y}_{ij}]_{j=1, \dots, n_g}^{i=0, \dots, n_e}$ via (9.64a) with respect to the OBF set $\Phi_{n_g}^{n_e}$.

Step 6c. Estimate the parameter set $\{\theta_{ijl}^w\}_{i=0, j=1, l=0}^{n_e, n_g, n_\psi}$ by linear regression with respect to fixed $\{\theta_{ijl}^v\}_{i=0, j=1, l=0}^{n_e, n_g, n_\psi}$. This is done by defining the regressors as

$$\gamma^\top(k) = \check{y}(k) \otimes \Psi^w(p(k)), \quad k \in [0, N_d - 1], \quad (9.73)$$

Collect the data into

$$\begin{aligned}\Gamma_{N_d} &= [\gamma(0) \dots \gamma(N_d - 1)]^\top, \\ Y_{N_d} &= [y(0) \dots y(N_d - 1)]^\top.\end{aligned}$$

Then, to minimize the prediction error criterion (9.46), the analytic solution θ is obtained via (9.47).

Step 7c. Fix $\{\theta_{ijl}^v\}$ to $\hat{\theta}_{N_d}^v$ and estimate the parameters $\{\theta_{ijl}^v\}$ in the following iterative way. In each iteration step we calculate an update for each $\theta_{ij}^v = [\theta_{ij0}^v \dots \theta_{ijn_v}^v]$ and choose that estimate which gives the best improvement on the prediction error of the model. This is formalized in the following steps:

1. For each basis function $\phi_j G^i$, compute

$$\tilde{y}_{ij} = \frac{1}{w_{ij}(p)} \left[y - \sum_{k=0, k \neq i}^{n_e} \sum_{l=1, l \neq j}^{n_g} w_{kl}(p) \check{y}_{kl} \right]. \quad (9.75)$$

If $w_{ij}(p(k)) = 0$ for some k , then do not consider those time instants in the further procedure.

2. Collect each \tilde{y}_{ij} into $\tilde{Y}_{N_d}^{(ij)}$ and u into U_{N_d} similar to Y_{N_d} . Let H_{ij} be the lower triangular Toeplitz matrix of the Markov parameters associated with (A_{ij}, B_{ij}, C_{ij}) :

$$H_{ij} = \begin{bmatrix} 0 & 0 & \dots & \dots \\ C_{ij} B_{ij} & 0 & \dots & \dots \\ C_{ij} A_{ij} B_{ij} & C_{ij} B_{ij} & 0 & \dots \\ \vdots & \vdots & \vdots & \ddots \end{bmatrix}. \quad (9.76)$$

Define

$$\gamma_{ij}^\top(k) = \check{y}_{ij}(k) \otimes \psi^v(p(k)), \quad k \in [0, N_d - 1], \quad (9.77)$$

and collect it into $\Gamma_{N_d}^{(ij)}$. Then, based on (9.66a-b), it holds that

$$\hat{Y}_{N_d}^{(ij)} = H_{ij} U_{N_d} - H_{ij} \Gamma_{N_d}^{(ij)} \theta_{ij}^v, \quad (9.78)$$

where

$$\hat{Y}_{N_d}^{(ij)} \left[\hat{y}_\theta^{(ij)}(0) \quad \hat{y}_\theta^{(ij)}(1) \quad \dots \quad \hat{y}_\theta^{(ij)}(N_d - 1) \right]^\top \quad (9.79)$$

is the predicted output of the basis function $\phi_j G^i$. Estimation of θ_{ij}^v can be formulated as a linear regression, similarly as in Step 6.c, to minimize the residual of $\tilde{Y}_{N_d}^{(ij)} - \hat{Y}_{N_d}^{(ij)}$. The regressor in this case is $H_{ij} \Gamma_{N_d}^{(ij)}$ and the data matrix is $H_{ij} U_{N_d} - \tilde{Y}_{N_d}^{(ij)}$.

3. For each $\hat{\theta}_{ij}^v$, compute the prediction error with only this element updated in θ^v . Choose the $\hat{\theta}_{ij}^v$ which renders the smallest error and only

update the value of θ^v with this element.

4. If the overall prediction error did not converge, then goto Step 7.c.1.

Step 8c. If the prediction error converged with respect to both $\{\theta_{ijl}^w\}$ and $\{\theta_{ijl}^v\}$, then stop, else goto 5.c.

In the HF-LPV OBF case, the identification procedure is similar. However, the formulation of the regressor is accomplished differently just like in Section 9.3. Based on (9.69a-b), for $x(0) = 0$ and $w_{00} = 0$, the predicted output of the HF-LPV OBF model

$$\hat{Y}_{N_d} = [\hat{y}_\theta(0) \quad \hat{y}_\theta(1) \quad \dots \quad \hat{y}_\theta(N_d - 1)]^\top$$

satisfies

$$\hat{Y}_{N_d} = \begin{bmatrix} 0 & 0 & \dots \\ ECBW(p(0)) & 0 & \dots \\ EC[A - BV(p(1))C]BW(p(0)) & ECBW(p(1)) & \dots \\ \vdots & \vdots & \ddots \end{bmatrix} U_{N_d}.$$

By simple rearrangement it follows that

$$\hat{Y}_{N_d} = \underbrace{\begin{bmatrix} 0 & 0 & \dots \\ ECBIu(0) & 0 & \dots \\ EC[A - BV(p(1))C]BIu(0) & ECBIu(1) & \dots \\ \vdots & \vdots & \ddots \end{bmatrix}}_{\hat{H}_{N_d}} \begin{bmatrix} W(p(0)) \\ W(p(1)) \\ \vdots \end{bmatrix}$$

Now similar to the global method of Section 9.3, formulation of the regressor can be accomplished based on \hat{H}_{N_d} and the estimate of $\{\theta_{ijl}^w\}$ follows via linear regression.

The other difference occurs in Step 7.c.1 where due to the Hammerstein structure of the model, (9.75) simplifies to

$$\tilde{y}_{ij} = y - \sum_{k=0, k \neq i}^{n_e} \sum_{l=1, l \neq j}^{n_g} \check{y}_{kl}. \quad (9.80)$$

Furthermore, (9.78) is translated to

$$\hat{Y}_{N_d}^{(ij)} = H_{ij} \hat{U}_{N_d}^{(ij)} - H_{ij} \Gamma_{N_d}^{(ij)} \theta_{ij}^v, \quad (9.81)$$

where

$$\hat{U}_{N_d}^{(ij)} = [w_{ij}(p(0))u(0) \quad w_{ij}(p(1))u(1) \quad \dots \quad w_{ij}(p(N_d - 1))u(N_d - 1)]^\top.$$

The procedure can also be extended to estimate a direct feedthrough in the same way as discussed in Section 9.3.

9.4.4 Properties

In the following important properties of the introduced identification approach of WF-LPV and HF-LPV OBF models are investigated. It is motivated that the separable least-squares estimation scheme is convergent and the obtained parameter estimates are local minima or saddle point of the LS criterion.

Convergence of the iterative estimation scheme

In the proposed identification scheme, the coefficients w_{ij} and v_{ij} are parameterized linearly via (9.70), resulting in a set of unknown parameters $\{\theta_{ijl}^w\}$ and $\{\theta_{ijl}^v\}$. Due to the bilinear relationship in which these parameters appear in the one-step-ahead predictors (9.65a) and (9.68a), a separable-least squares algorithm is applied to tackle the minimization of the LS criterion. It is a cardinal question if this iterative scheme is convergent, i.e. is it guaranteed that the value of the LS criterion decreases in each consecutive iteration step. In each iteration cycle of this scheme, one set of the parameters is fixed, $\{\theta_{ijl}^w\}$ or $\{\theta_{ijl}^v\}$, in order to form a linear regression based estimation of the other set by minimizing the mean squared error of the residual. This results in a steepest descend type of iterative optimization in the search for the optimal LS prediction error. For such a separable least squares strategy, it is well known that it is convergent and the convergence point is a saddle point or a local minimum of the cost function (Golub and Pereyra 1973). The exact convergence point is characterized by the initial choice of $\{\theta_{ijl}^v\}$ in Step 3c. The estimates converge to that point of the parameter space Θ whose associated region of attraction, based on the given data set, contains the initial choice of $\{\theta_{ijl}^v\}$. Similar to the numerical optimization schemes of LTI OE or Box-Jenkins models, the global optimum of (9.36) can only be obtained by starting the iterative search from different initial values and comparing the results (Ljung 1999).

Unstable model estimates

A further problem may arise in cases where the resulting model estimate is unstable, even if \mathcal{S} is asymptotically stable. This phenomenon is due to the fact that the feedback weighting is tuned on a particular, finite scheduling trajectory. As this feedback tuning can be thought of as the reoptimization of the basis with respect to \mathcal{D}_{N_d} , the finite data length and the excitation capabilities of the input and scheduling signals directly effect the estimation. Thus, even if the resulting model is stable with respect to the scheduling trajectory in \mathcal{D}_{N_d} it is not guaranteed that it is stable for any other $p \in \mathfrak{B}_{\mathbb{P}}$.

Practical use and (in)validation

Local minima and the possibility of unstable model estimates do not necessarily create problems in practice. If the resulting model passes the validation test it should be an acceptable model (Ljung 1999). The problem is that the only theoretically sound (in)validation approach of the model estimates is based on simulation. By computing error measures of the difference of simulated and measured outputs, the qualities of the model estimates can be compared. As is shown in the example of Section 9.4.5, the proposed method quickly converges in practice and provides a reliable estimate of LPV systems.

Consistency, variance, and bias of the estimates

In the previous section, the linear-in-the-parameter property of the used model structures in the one-step-ahead predictor enabled results on the consistency, variance, and bias of the resulting model estimates. In the feedback case, the linear-in-the-parameter property is lost, due to the bilinear relationship of the coefficients. Thus the previously developed results do not hold in this case. In nonlinear system identification, there are many results on the consistency, variance, and bias of model estimates obtained via different types of separable least-squares strategies. However, none of these results seems to apply to the considered model structures and estimation strategies used here. Investigation of consistency, variance, and bias of the estimation mechanism remains the subject of future research for the feedback based model structures.

9.4.5 Example

In this section, applicability of WF-LPV OBF model structure and identification approach for the approximation of general LPV systems is shown through an example. Comparison is made with the static-coefficient-function based Wiener OBF model structure to show that by using the proposed feedback structure, better performance of the model estimates can be achieved.

As in the previous case, the asymptotically stable LPV system S_3 is considered which has been studied in Section 8.3.3. The IO representation of S_3 , $\mathfrak{R}_{IO}(S_3)$ is defined by (8.14). This system has been also identified in Section 9.3.6 by using the basis functions set Φ_8^0 obtained via the FKcM algorithm with fuzzyness $m = 25$ and $n_c = 8$.

Here we aim at the identification of S_3 with the WF-LPV and W-LPV OBF model structures. To ensure fair comparison of the results, both model structures are used with basis functions Φ_8^0 and the coefficients in W are parameterized as 2nd-order polynomials in p . In the feedback case, the coefficients in V are parameterized as 3rd-order polynomials. These orders have been found optimal after several trial and error experiments.

Identification of S_3 with the global approach has been accomplished 100 times in 4 different noise settings with both the Wiener and the Wiener-feedback model

Table 9.2: Validation results of 100 identification experiments with the Wiener (W) and the Wiener Feedback (WF) model structures. The results are given in terms of the MSE and the average BFT and VAF of the simulated output signals of the model estimates.

	Validation by multisine					
	MSE (dB)		BFT (%)		VAF (%)	
SNR	W	WF	W	WF	W	WF
no noise	-18.23	-31.32	85.39	94.04	97.84	99.55
35 dB	-18.21	-31.30	85.38	93.64	97.82	99.53
20 dB	-17.81	-21.60	85.17	89.30	97.75	98.52
10 dB	-20.68	-22.60	86.27	88.44	98.47	98.98

	Validation by uniform noise + multisine					
	MSE (dB)		BFT (%)		VAF (%)	
SNR	W	WF	W	WF	W	WF
no noise	-34.96	-39.75	90.04	92.40	99.00	99.42
35 dB	-34.77	-39.17	89.92	92.15	98.99	99.39
20 dB	-32.75	-35.01	88.69	90.06	98.71	99.00
10 dB	-31.81	-32.38	87.73	88.15	98.19	98.59

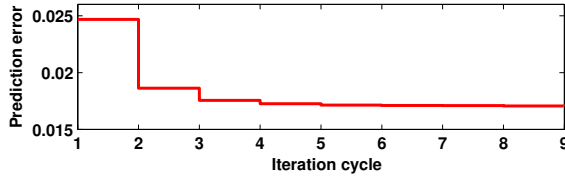


Figure 9.11: Typical convergence plot of the prediction error in terms of (9.36) for the iterative WF-LPV OBF identification algorithm.

structures. The data records for each identification have been generated by a white (u, p) with uniform distribution $\mathcal{U}(-0.5, 0.5), \mathcal{U}(0.65, 0.75)$ superimposed on random multisines (3 sines with random phase in $[0, \pi]$ and frequency in $[0, \pi/5]$ and with overall amplitude of 0.5 and 0.05). The reason why this particular excitation has been used is explained later. For each data record, the identification has been accomplished in a noiseless setting and also with additive zero mean white output noise with normal distribution and variance $\sigma_e^2 = 0.01, 0.1, \text{ and } 0.5$. The resulting SNR has been 35 dB, 20 dB, and 10 dB, while the relative noise amplitude has been 7%, 25%, and 54% in average for the three noise cases. For the $\sigma^2 = 0.5$ noise case $N_d = 1000$, and in the other cases $N_d = 500$ samples long data records have been used. In the iterative identification method, the feedback weights have been initialized at zero. The iterative identification method converged in an average of 14 iterations for the 4×100 runs. A typical convergence plot is given in Figure 9.11 and the typical output trajectories of the resulting estimates are shown in Figure 9.12. Calculation time for each data set has been approximately 2 minutes with the WF-LPV OBF structure and only a few seconds with the W-LPV OBF structure on a Pentium 4, 2.8 GHz PC. In Table 9.2, the (in)validation results are shown for multisine (u, p) with random frequencies and phases and also for uniform noise superimposed on random multisine, similarly generated like the identification data. As expected, both approaches identified the system with adequate MSE and average BFT, VAF even in case of extremely heavy output noise, which underlines the effectiveness of the proposed OBF identification philosophy. For all measures, validation signals, and noise cases, the WF-LPV OBF model provided better estimates than the pure static dependence based W-LPV OBF model estimate. This clearly shows the improvement in the approximation capability due to the approximation of dynamic dependence with feedback-based weighting. Additional extension of Φ_8^0 with $n_e = 1, 2, \dots$ has not improved the results as Φ_8^0 is well chosen with respect to \mathcal{S} , i.e. the local modeling error is negligible due to the FKcM (see Section 8.3.3). Even in the SNR= 10dB case, the model estimates proved to be accurate, showing that the proposed identification scheme is applicable even in the presence of significant measurement noise.

It has been observed that by using multisines superimposed on the realization of a noise sequence for the excitation of the system, the results have been better with the feedback-based structures in the presence of output additive noise. Explanation lies in the presence of the feedback gain of the model structure. In case significant noise is present in short data records, it is possible that the feedback weights are fitted to the noise process during the iterative optimization. By using

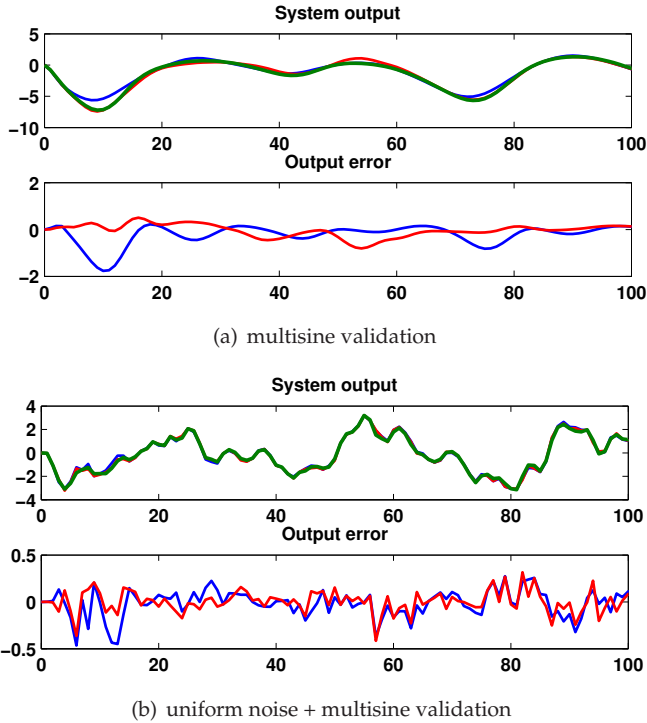


Figure 9.12: Typical validation results of identified WF-LPV OBF (red) and W-LPV OBF (blue) models in the SNR = 20dB case. The response of the true system is given in green.

multisines that emphasizes certain frequencies in the input and the scheduling signal, this effect can be attenuated. This underlines that much more understanding of feedback-based OBF models, especially in terms of sufficient excitation, is needed to achieve high quality model estimates. This remains the target of future research.

9.5 Extension towards MIMO systems

Next, we investigate how the developed approaches and model structures can be used for identification in the MIMO case. We show that by different choices of the basis (scalar or multivariable) different extensions of the previously studied approaches are available.

Extension by using scalar basis

For asymptotically stable MIMO LPV systems, the formulation of the W-LPV and H-LPV OBF model structures follows similarly as in Section 9.2. In Section 5.3,

the OBF expansion representation of asymptotically stable LPV systems has been introduced also for the MIMO case. These representations are based on the expansion of the IO map of the system in terms of scalar basis functions. This implies that by using the concept of truncation of multivariable expansion representations based on scalar basis functions, the MIMO W-LPV OBF structure like (9.21) or a MIMO H-LPV OBF model like (9.24) can be formulated with $w_{ij} \in \mathcal{R}^{n_v \times n_w}$. By assuming static dependence of these coefficients, identification follows by applying the algorithms of Section 9.3 with some extra book keeping due to the multidimensional input and output signals. Additionally, the basis selection algorithm of Chapter 8 is also applicable in this case, by selecting the scalar basis with respect to the pole manifest set of the MIMO frozen systems of \mathcal{S} .

Note, that a multidimensional p results in a multidimensional interpolation in the local case or the use of multidimensional $\psi(p)$ in the global case. Multidimensional interpolation problems are hard to be solved and they require many interpolation points, i.e. many local experiments. Therefore, the global method is practically applicable for large scheduling dimensions. Note that the global approach is even applicable for significantly large scheduling dimensions which is an advantageous property with respect to LPV subspace identification methods due to the serious increase of block dimensions in such cases.

Extension by using multivariable basis

Due to the scalar basis sequence, it can happen that a MIMO series-expansion converges fast with respect to specific input-output channels, but quite slow for others just like in the LTI case (see Section 2.2.2). As a result, some elements of the resulting coefficient matrices can have negligibly small amplitudes over all trajectories of the scheduling behavior $\mathfrak{B}_{\mathbb{P}}$. This implies that their estimation can result in a considerable variance. To overcome this effect, series-expansion of asymptotically stable multivariable LPV systems can be introduced using a MIMO basis of $\mathcal{RH}_{2-}(\mathbb{E})$. Again, the key idea is to use MIMO basis functions that are composed from scalar basis sequences (see Section 2.2.2):

$$\check{\phi}_l(q) := \begin{bmatrix} \phi_{l11}(q) & \dots & \phi_{l1n_w}(q) \\ \vdots & \ddots & \vdots \\ \phi_{ln_v1}(q) & \dots & \phi_{ln_vn_w}(q) \end{bmatrix}, \quad (9.82)$$

where each $\{\phi_{lij}\}_{i=1}^{\infty}$ corresponds to a basis of $\mathcal{RH}_{2-}(\mathbb{E})$. Then, in terms of Theorem 5.2, an asymptotically stable LPV system, with respect to a given IO partition, can be represented as

$$y = (W_0 \diamond p)u + \sum_{i=0}^{\infty} \left[(W_i \diamond p) \odot \check{\phi}_i(q) \right] u, \quad (9.83)$$

where $W_i \in \mathcal{R}^{n_v \times n_w}$ and \odot denotes the element-by-element matrix product. By choosing the basis sequences appropriately, a fast convergence rate can be achieved for each IO channel. The basis selection can follow by applying the OBF selection

procedure of Chapter 8, with respect to each input-output channel separately. This means that the method is applied for a set of pole samples that are associated with the set of SISO systems describing the frozen behavior of \mathcal{S} restricted to the considered IO channel. As a next step, we formulate these model structures for a given MIMO basis sequence $\Phi_n = \{\check{\phi}_i\}_{i=1}^n$ composed from these scalar elements. Note that in this case, each basis sequence $\{\phi_{lij}\}_{l=1}^\infty$ is generated with a different inner function, thus Φ_n denotes the first n functions in each sequence.

- MIMO Wiener LPV-OBF model, $\mathfrak{M}_W(\Phi_n, \theta, \mathfrak{B}_P)$

$$F(q, \theta) \diamond p = W_0 \diamond p + \sum_{i=0}^n (W_i \diamond p) \odot \check{\phi}_i(q), \quad Q(q, \theta) = I, \quad (9.84)$$

where $W_i \in \mathcal{R}^{n_y \times n_u}$ and e in this case is a vector of independent zero mean white noise processes. The parameter vector of the coefficients is

$$\theta = [W_0 \ ; \ W_1 \ ; \ \dots \ ; \ W_n]^\top. \quad (9.85)$$

The one-step-ahead predictor is formulated in this case as

$$\hat{y}_\theta = (W_0 \diamond p)u + \sum_{i=0}^n [(W_i \diamond p) \odot \check{\phi}_j(q)] u. \quad (9.86)$$

Let $E = [1 \ \dots \ 1]^\top$ and introduce $\check{y}_i : \mathbb{Z} \rightarrow \mathbb{R}^{n_y \times n_u}$ defined as

$$\check{y}_i = \check{\phi}_j(q) \odot (Eu^\top). \quad (9.87)$$

These signals are the multidimensional counterparts of the output signals of the filter bank part of the model structures in the SISO case (see Figure 9.2).

- MIMO Hammerstein LPV-OBF model, $\mathfrak{M}_H(\Phi_n, \theta, \mathfrak{B}_P)$

$$F(q, \theta) \diamond p = W_0 \diamond p + \sum_{i=0}^n \check{\phi}_i(q) \odot (W_i \diamond p), \quad Q(q, \theta) = I, \quad (9.88)$$

where $W_i \in \mathcal{R}^{n_y \times n_u}$. The one-step-ahead predictor is formulated in this case as

$$\hat{y}_\theta = (W_0 \diamond p)u + \sum_{i=0}^n [\check{\phi}_j(q) \odot (W_i \diamond p)] u. \quad (9.89)$$

Additionally, the multidimensional $\check{u}_i : \mathbb{Z} \rightarrow \mathbb{R}^{n_y \times n_u}$ (see Figure 9.3) are introduced as

$$\check{u}_i = (W_i \diamond p) \odot (Eu^\top). \quad (9.90)$$

By assuming static dependence of the matrix coefficients $\{W_i\}$ and introducing a parametrization of $\{W_i\}$ in terms of linear combination of predefined functions:

$$W_i = \sum_{l=0}^{n_i} \theta_l \odot \psi_l \quad (9.91)$$

where $\theta_l \in \mathbb{R}^{n_y \times n_u}$ and $\psi_l \in (\mathcal{R}|_{n_{\mathbb{F}}})^{n_y \times n_u}$, identification follows by applying the algorithms of Section 9.3 with an extended matrix regressor γ and a stacked output record Y_{N_d} formulated as

$$Y_{N_d} = [y_1(0) \quad \dots \quad y_{n_y}(0) \quad y_1(1) \quad \dots \quad y_{n_y}(N_d - 1)]^{\top}. \quad (9.92)$$

All results in this case about consistency, bias, variance, etc. obviously extend to the MIMO case.

Extension by using multivariable basis in the feedback case

In case of the feedback structures of Section 9.4, the MIMO version of the model structures based on a given MIMO basis sequence Φ_n composed from scalar elements can also be formulated.

- MIMO WF-LPV OBF model, $\mathfrak{M}_{\text{WF}}(\Phi_n, \theta, \mathfrak{B}_{\mathbb{F}})$

$$\check{y}_i = \check{\phi}_i(q) \odot (E_y u^{\top}) - \check{\phi}_i(q) \odot (V_i \diamond p) \odot \check{y}_i \quad (9.93a)$$

$$y = e + (W_0 \diamond p)u + \sum_{i=0}^n [(W_i \diamond p) \odot \check{y}_i] E_u, \quad (9.93b)$$

where $E_y \in \mathbb{R}^{n_y}$, $E_y = [1 \dots 1]^{\top}$ and $E_u \in \mathbb{R}^{n_u}$, $E_u = [1 \dots 1]^{\top}$. Furthermore, each $\check{y}_i : \mathbb{Z} \rightarrow \mathbb{R}^{n_y \times n_u}$ is a multidimensional signal, $W_i, V_j \in \mathcal{R}^{n_y \times n_u}$ and e is a vector of independent zero-mean white noise processes. Again as each \check{y}_i is independent from e , the one-step-ahead predictor reads as

$$\hat{y}_{\theta} = (W_0 \diamond p)u + \sum_{i=0}^n [(W_i \diamond p) \odot \check{y}_i] E_u, \quad (9.94)$$

- MIMO HF-LPV OBF model, $\mathfrak{M}_{\text{HF}}(\Phi_n, \theta, \mathfrak{B}_{\mathbb{F}})$

$$\check{u}_i = (W_i \diamond p) \odot (E_y u^{\top}) - (V_i \diamond p) \odot \check{\phi}_i(q) \odot \check{u}_i, \quad (9.95a)$$

$$y = e + (W_0 \diamond p)u + \sum_{i=0}^n (\check{\phi}_i(q) \odot \check{u}_i) E_u. \quad (9.95b)$$

where each $\check{u}_i : \mathbb{Z} \rightarrow \mathbb{R}^{n_v \times n_u}$ is a multidimensional signal, $W_i, V_j \in \mathcal{R}^{n_v \times n_u}$. The one-step-ahead predictor reads as

$$\hat{y}_\theta = (W_0 \diamond p)u + \sum_{i=0}^n (\check{\phi}_i(q) \odot \check{u}_i)E_u. \quad (9.96)$$

Assume that each element of the coefficient matrix functions of these structures is parameterized as a linear combination of functions with static dependence. Then the specific structure of the used MIMO forms enables the application of the separable least-squares algorithm for the estimation of the coefficient functions. Note that the crucial point of the algorithm is the propagation of the error backwards to the output of a basis function (see (9.75) or (9.80)). The propagated error can be computed for each element of the basis function matrix separately. As each OBF has a separate feedback via (9.95a) or (9.93a), thus re-optimization of each feedback weight on a output channel can be done in parallel.

General remarks on the MIMO extension

Similar to the LTI case, OBFs based identification of MIMO LPV systems has a much larger freedom than the LTI case. There are different approaches that can be applied to derive a MIMO basis expansion, to formulate MIMO version of W-LPV and H-LPV OBF models, and to develop identification algorithms that can deliver the estimate. We have taken here specific choices in order to be able to apply the introduced estimation mechanisms of Section 9.3 and 9.4 without any modification or reformulation. However, there are numerous possibilities that may be interesting for further investigation. For example, by considering left or right side placement of the expansion coefficients for specific IO channels, like mixing the structures of H-LPV OBF and W-LPV OBF models, or using other formulation of MIMO orthonormal basis functions, like presented in Section 2.2.2.

In conclusion, it can be stated that the introduced identification approaches of this thesis can be directly applied to MIMO LPV systems without the need of any modification or further assumptions. This implies that the proposed identification scheme in terms of model structure selection, parametrization, and estimation offers an effectively and easily applicable identification scheme for a wide variety of LPV systems.

9.6 Summary

In this chapter we have introduced OBF based model structures and identification methods in discrete-time to solve the primary objective of this thesis: the development of an efficient identification approach of LPV systems.

By using the concept of series-expansion of LPV systems in terms of OBFs we have first introduced model structures in Section 9.2 that approximate the system dynamics based on a truncation of the expansion representation. As it is possible

to formulate LPV expansions with coefficients on the right and on the left side of the basis functions, finite truncation of such expansions results in different model structures. Due to the non-commutativity of the multiplication with the time-shift operator in the expansion representations, such models have different approximation capabilities. The resulting structures can be seen as a LTI filter bank followed or preceded by a weighing functions set with dynamic dependence on the scheduling, thus the introduced structures are named as Wiener and Hammerstein LPV-OBF models. It has been shown that similar to their nonlinear counterparts, these structures can approximate any LPV system with arbitrary accuracy if the coefficients have dynamic dependence. Furthermore, these models are not effected by changing McMillan degree of the frozen aspects of the LPV system, which represents a significant difficulty for the identification of other type of LPV model structures. We have motivated that the introduced models are effectively applicable for control as they have a direct state-space realization, however to satisfy assumptions of the control approaches, their coefficient dependencies must be restricted to be static.

As a significant contribution, we have extended the classical prediction error setting to the LPV framework. Due to the absence of a transfer function type of description of LPV systems, the process and noise models are formulated based on their impulse response presentation. This has been used to define the one-step ahead predictor in this framework for both the proposed model structures and other LPV model types. We have analyzed the notion of noise model in this setting showing that to formulate the predictor in the classical sense, the scheduling variable must be a deterministic signal. It has been also shown that the introduced model structures are linear-in-the coefficients with respect to the predictor and the noise model is independently parameterized from the process model. These imply that similar to the LTI case, estimation of the coefficients is available through linear regression if the least-squared error criterion is used. Additionally, it has been discussed how other LPV model structures, used in the literature, are formulated in the prediction error setting and how their associated noise models influence the parameter estimation in this setting.

Using the previously derived properties and the prediction error framework, we have developed in Section 9.3 discrete-time identification algorithms for the proposed model structures in the least-squares setting. To narrow the search space and to provide models directly applicable for control, the coefficient functions of the OBF model structures have been restricted to have static dependence in developed approaches of Section 9.3. Based on the linear and static parametrization of the model coefficients (each coefficient is a linear combination of a priori chosen set of meromorphic functions with static dependence) and by the use of the least-squares prediction-error setting, two identification approaches: a local and a global one are introduced for the SISO case. The local method uses the gain-scheduling type of identification strategy: for some constant scheduling trajectories, LTI truncated expansion models of the system based on a fixed set of OBFs are identified and then the expansion coefficients of the resulting models are interpolated on the scheduling space \mathbb{P} . It has been shown that in comparison with other gain-scheduling-based identification approaches the interpolation problem

is well formulated in this case. The global method uses a data record collected from the system for a varying scheduling trajectory, and formulates the estimation of the parameters of the coefficients by a linear regression. The introduced approaches are analyzed in terms of variance, bias, and consistency.

To enable the estimation of truncated expansion models with dynamic coefficient dependencies, but at the same time still provide applicable models for control, feedback-based OBF model structures have been proposed in Section 9.4. It has been shown, that by using static dependence, the introduced model structure is equivalent to OBF expansion models with dynamic coefficient dependencies. For the identification with such feedback-based model structures, the previously developed global approach is extended, formulating the parameter estimation through a separable least-squares approach. Finally, in Section 9.5, the extension of the introduced approaches to MIMO systems is investigated. It has been concluded, that for OBF models, based on MIMO functions composed from scalar basis sequences, the developed approaches and results are applicable.

This concludes that, by the developed identification algorithms, the research objective of this thesis is completed, giving an alternative, practically applicable approach for identification of LPV systems as models of an underlying physical process.

Conclusions and Recommendations

In this thesis, we have aimed at the development of a framework and structural approach for the identification of general LPV systems as models of an underlying physical process. This chapter is dedicated to the main conclusions of the presented research and to investigate which aspects of the aimed objectives have been fulfilled. In addition, suggestions for future research are given.

10.1 Conclusions

This thesis has been motivated by the research goal to develop an improved framework and approach for the identification of *Linear Parameter-Varying* (LPV) systems. LPV systems can incorporate and describe both *nonlinear* (NL) and *time-varying* (TV) aspects of physical phenomena and the framework of LPV control is well worked out and industrially reputed. However, identification of such systems is still in an immature state. Thus, development of an improved LPV identification approach could provide models which fulfill the increasing expectations of industrial applications. In view of the state-of-the-art LPV identification, the motivation for improvement has been based on the following observations:

- The LPV identification field is dispersed, as available methods focus mainly on estimation in specific model structures while the steps of the classical identification cycle often remain uninvestigated.
- The main obstacles in the analysis of methods and model structures are the gaps of LPV system theory. Dynamic dependence seems to play a crucial role, but its formalization and effects have not been investigated yet.
- The use of *Orthonormal Basis Functions* (OBF)s-based model structures for LPV identification is promising, due to their attractive parametrization, wide representation capabilities, and easy application for control. Identification,

based on these structures, might avoid problematic issues connected to the use of other LPV model structures.

Based on these observations, we have established several sub-objectives (see Section 1.6) which had to be investigated to fulfill our primary research goal. In the research plan, that has been followed throughout this thesis, emphasis has been laid on the investigation of identification using OBF model structures as prime candidates to fulfill our primary objective. A major conclusion of this thesis is that truncated OBF expansion models and the associated identification approaches give an attractive and useful way of identifying LPV systems in practice. In this final chapter, we summarize the results of our research, the achieved contributions, and the conclusions that we have developed in our work and which have led to the above stated result.

Subgoal 1: Model structure selection

In the scope of our first research goal, we have investigated LPV model structures and how model-structure selection can be accomplished. We observed that the main obstacles to answer these questions are the missing system theoretical concepts, like transformation theory of LPV representations, equivalence classes, canonical forms, etc. and a clear understanding how NL differential equations translate to LPV models. Based on the similarity with the *Linear Time-Varying* (LTV) system theory, the question was raised whether it would be necessary to introduce dynamic dependence on the scheduling variable to enable equivalence relations between representations of an LPV system.

In Chapter 3, we have shown that dynamic dependence is the key ingredient to establish a well founded system theory. We have developed the LPV *behavioral approach*, which enables comparison of LPV model structures and their analysis. A major conclusion has been that LPV model structures need dynamic coefficient dependence to enable approximation of general LPV systems. We have defined representations of LPV systems, formalized their equivalence classes, and investigated their general properties in terms of stability and state-observability and reachability. We have used the concepts of LTV system theory to characterize our framework, formulating algebraic structures and concepts that made the extension of these theories to the LPV case possible. We have also shown that the introduced framework is compatible with the existing results of LPV system theory.

In Chapter 4, we have introduced state-space canonical forms and equivalence transformations between SS and IO representations. It has been shown that for the LPV formulation of the classical canonical forms, which are the gateways of equivalence transformations, the concept of structural state-observability and reachability is the key concept instead of complete state-observability and reachability. The theory on equivalence transformations between SS and IO representations enabled the comparison of model structures, which has been subgoal 1.a of our research plan. We have also concluded that equality of behaviors must be understood in an *almost-everywhere sense*. It has been proven that several relations of LTI system theory, like canonical form construction, realization theory, etc. do

not hold in the LPV case, showing that the intuitive use of LTI theory in the LPV identification field can result in unexpected errors.

In Chapter 5 we have shown that an asymptotically stable LPV system has a series-expansion representation in terms of LTI basis functions. This has directly answered our research question 1.c, implying that truncated versions of such model structures can be used for the identification of LPV systems. We have also motivated that a fast convergence rate of this expansion can be achieved, by choosing the basis functions such that they are optimal with respect to the frozen transfer function set of the LPV system. This proved to be the key concept to facilitate model-structure selection based on OBF models for the LPV case.

In the scope of research goal 1.b, we have studied in Chapter 6 discretization approaches of LPV-SS representations in a *zero-order-hold* (ZOH) setting and derived criteria to choose an adequate discretization step-size. A major conclusion has been that the ZOH setting for the scheduling variable is only adequate for the discretization of SS representations with static dependence. A higher-order hold setting has been proposed for the discretization of representations with dynamic dependence.

In the ZOH case, there is a trade-off between accuracy of the discretization and the resulting complexity of the coefficient dependence. This has motivated the introduction of approximative methods that provide less complicated DT realizations. It has been also shown that numerical stability and preservation of the frozen stability of the original system are equivalent in case of single-step discretization methods.

In Chapter 7, our research goal 1.b has been fulfilled by developing a model transformation approach that converts first-principle knowledge, given in terms of NL differential equations, to a LPV description. It was shown that the selection of scheduling variables is restricted if predefined state-signals, inputs or outputs, or representations are considered. We have developed an approach that investigates all possible conversions to a *parameter-varying* (PV) differential equation form. Using the behavioral framework, the resulting PV description (if it exists) can be realized as an arbitrary model representation and assist the model-structure-selection phase of the identification cycle.

In order to deal with research objective 1.c, it has been shown in Chapter 8 that adequate selection of basis functions for OBF model structures can be accomplished by the combined use of fuzzy clustering and the *Kolmogorov n-width* (KnW) theory. If the pole locations of the frozen transfer functions of the LPV system are known, then an OBF set can be derived which achieves the smallest possible upperbound on the representation error with respect to the frozen transfer function set. This also holds if the region of pole locations, associated with the frozen transfer functions, can be reconstructed based on experimental data. For this purpose we have developed the *Fuzzy Kolmogorov c-Max* (FKcM) clustering approach and showed that both reconstruction and optimal basis selection can be solved simultaneously by this approach. To take the effect of noise and disturbances into account, we have developed also a robust extension of the FKcM procedure via the use of hyperbolic geometry.

Subgoal 2: LPV prediction error framework

Using the developed concept of series-expansions of LPV systems in terms of the pulse basis, we have introduced in Chapter 9 a LPV prediction-error framework, establishing research objective 2. It has been shown that, due to the absence of a transfer function description of LPV systems, series-expansion representations are crucial to formulate this framework. An important conclusion has been that the scheduling signal must be deterministic to enable the definition of output predictors.

With respect to noise models in the LPV setting we have observed that a prime advantage of OBFs-based models is that the assumed noise model is independent of the scheduling and that the models are linear-in-the-coefficients. For ARX models, often used in LPV-IO identification, the noise model does depend on the scheduling, which is quite unrealistic from a practical point of view. As other model structures are not linear-in-the-coefficients, we have concluded that OBF expansion models are attractive candidates for LPV prediction-error identification.

Subgoal 3: Improved LPV identification approach

Finally, in Chapter 9, the LPV identification procedure, intended to fulfill the primary research objective and hence sub-objective 3, has been formalized. Model structures in terms of OBFs-based series-expansions have been formally defined and analyzed. The similarity of these structures with respect to nonlinear Wiener and Hammerstein models has been explained, and as a dual of the nonlinear result, it has been proven that OBF models are general approximators of LPV systems. Furthermore, it has been shown that it is straightforward to derive a SS realization of these models, enabling the application of LPV control approaches. Concepts to identify OBF models have been derived in a two-step procedure, where first the OBFs are selected for the model structure, based on first-principle information or the FKcM mechanism. As a second step, the parameterization of the model coefficients is chosen and the estimates are obtained. The estimation phase has been explored by using both a gain-scheduling type of identification mechanism (local approach) and linear regression in the prediction-error framework (global approach), yielding answers to sub-objectives 3.a-b.

The developed approaches have been formulated by assuming static dependence of the coefficients, which has been motivated both from a control and a parametrization perspective. Convergence and consistency of the estimates have been investigated proving that both approaches are consistent under minor conditions. Asymptotic variance and bias expressions of the model estimates have been derived for the global approach, showing that the introduced mechanism generalizes the classical asymptotic results of the LTI framework.

To overcome the restrictions of static dependence, a new model structure based on feedback has been proposed, which, by using only static dependence, is capable to approximate series-expansion models with dynamic dependence. The basic

issues and properties of this modeling concept have been analyzed and an identification approach has been given based on separable least-squares. These models can approximate general LPV system better than expansion models with static dependence and they are also easily applicable for control. However, due to the feedback structure, stability of the model estimates is not guaranteed and results on consistency, variance and bias are hard to be drawn. Finally, it has been shown that all introduced approaches can easily be extended to the MIMO case.

Based on these observations, it can be concluded that the developed identification framework and approaches of this thesis fulfill the primary objective: development of a low-complexity and reliable identification mechanism of LPV systems as models of physical plants, where the model estimates are directly applicable for control.

10.2 Contributions to the state-of-the-art

As solutions for the presented research objectives, the main contributions of this thesis are the following:

Unified LPV system theory

- A unified system theoretical framework of LPV systems is developed, where notions of representation, equivalency and minimality can be defined through the concepts of behaviors and dynamic dependence (Chapter 3). A transformation theory between IO and SS representations is established and a new state-construction algorithm is introduced which delivers a minimal SS representation in the SISO case (Chapter 4). Concepts of state-observability, state-reachability, stability, and canonical forms are also reformulated in this setting, yielding a common basis for the analysis of LPV system representations. The presented theoretical framework enables the comparison and analysis of model estimates and identification algorithms in the LPV context.
- Discretization theory of LPV systems is worked out in a zero-order-hold setting with respect to models with static dependence (Chapter 6). Criteria are given to choose a discretization step size, guaranteeing stability preservation or a specific approximation error. The concepts of discretization of general LPV systems with dynamic dependence are also established. This contribution enables the use of first-principle information about continuous-time dynamics of the system in the model-structure selection of discrete-time identification methods.
- The modeling capabilities of LPV systems with respect to NL systems are studied and a new method for automatic model conversion of NL differential equations to LPV models is given (Chapter 7). The procedure formulates an effective way of modeling NL systems in the LPV framework and the use of first-principle knowledge in model-structure selection.

LPV-OBF expansion model structures

- It is shown, in Chapter 7, that asymptotically stable LPV systems have series-expansion representations in terms of OBFs.
- In Chapter 9, OBFs based LPV model structures are introduced and analyzed in terms of representation and properties, with the conclusion that in many aspects these model structures are attractive for LPV identification.

The LPV prediction-error setting

- An LPV prediction-error setting is formalized, based on the concepts of the classical identification framework (Chapter 9). This includes the definition of predictors and noise models and the analysis of these concepts for the LPV case.
- A comparison of LPV model structures in the introduced prediction-error framework is carried out, showing that OBF models are attractive as they are linear-in-the-coefficients and their noise model is independently parameterized and does not depend on the scheduling. This enables an efficient estimation of OBF models by linear regression.

LPV identification based on OBF models

- Two novel approximative LPV identification approaches, a local and a global approach, are proposed, based on OBFs models with static-scheduling dependence. The methods extend the concept of LTI prediction-error identification and can also be applied for the identification of MIMO systems. The local method exploits the principle of gain-scheduling to formulate the LPV identification as a well-posed interpolation problem of identified LTI models with constant scheduling signals. The global method relies on a prior chosen parameterization of the scheduling dependence to provide a global estimate via linear regression and a varying scheduling signal.
- Feedback-based model structures are introduced, which can approximate dynamic dependence of the coefficients of LPV series-expansions by using static dependence. The identification problem with these structures is solved via a separable least-squares strategy.
- A novel OBFs-selection mechanism and its robust extension are developed. These mechanisms provide the basis selection, i.e. the model-structure selection, phase for the proposed OBFs-based LPV identification approach (Chapter 8).
- By using the concepts of hyperbolic geometry, the Kolmogorov n -width optimality result of the pulse basis with respect to circular regions of non-analyticity around the origin is extended. This contribution gives more insight in the understanding of Kolmogorov n -width optimality of OBFs with

respect to specific regions of non-analyticity and enables the robust extension of the basis-selection tool.

10.3 Recommendations for future research

As a continuation of the presented results and in view of our research goals the following problems/challenges are suggested for future research:

- In the LTI behavioral framework, a considerable amount of theory is dedicated to the investigation of observability and reachability of behaviors and system representations. Such notions are inevitable to formulate and understand control in the behavioral concept. In this thesis, such notions have been left unexplored as they have been not necessary ingredients for the developed theory. However, to achieve a complete foundation of the LPV behavioral approach, such notions must be worked out as well. This investigation might be based on the compatible theories of Zerz (2006) and Ilchmann and Mehrmann (2005).
- Beside the proposed cut & shift procedure, the development of a state construction mechanism for the realization of LPV-SS representations with minimal complexity of coefficient dependence can also be important from a number of aspects. It would establish the concept of minimality both in terms of state dimensions and complexity of the coefficient dependence. Furthermore, it would provide the most simple realization of a given model in a SS representation, making comparison and further use much more efficient.
- In this thesis, series-expansions representations of LPV models have been established in terms of LTI basis functions. It is an interesting question whether such basis functions can be defined in a parameter-varying sense. Such a mathematical concept might enable the full extension of the theory on orthonormal basis functions with respect to LPV systems.
- The developed discretization theory focuses on static dependence of the coefficients in a zero-order-hold setting. Foundations for discretization of representations with dynamic dependence are given in a higher-order-hold setting. However, for a well-established theory, further investigation of this setting is needed. The performance of the methods in a higher-order-hold setting together with the derivation of criteria to assist the step-size selection could be an interesting target of future research.
- Instead of the isolated discretization concept, treated in this thesis, the development of discretization procedures that focus on preservation of the closed-loop performance, would provide valuable tools for the LPV control community.

- In the proposed transformation mechanism of NL models to LPV descriptions, the approximation of non-factorizable terms leaves a considerable amount of freedom. By analyzing and categorizing efficient approximation of common non-factorizable nonlinear terms, a fully automatized model conversion tool could result.
- Strong concepts of identifiability, persistency of excitation, and validation of the proposed model structures and LPV systems in general have been left unanswered. General results about the asymptotic variance and bias of the estimates have been derived, but developing more informative expressions remains a subject for future research. The exploration and analysis of these issues, together with an experiment-design theory, are inevitable to accomplish the identification cycle and give a complete theory of LPV modeling and identification.
- Further investigation of relations of hyperbolic geometry, pole uncertainties, and the Kolmogorov theory also presents an interesting objective. These investigations may provide a better understanding of model uncertainties or define well-established metrics for investigating similarity or distance of LTI models.
- In the proposed identification scheme, one of the major difficulties is the decision about the parameterization of coefficient dependencies both in terms of functional and dynamic dependence, in the absence of structural information. In the NL case, especially for Wiener models (Hagenblad 1999), recently some theories appeared to choose appropriate functional forms for the coefficients, based on measured data sequences. Due to the similarity of the proposed model structures to this system class, such results could be useful to solve similar questions in the LPV case as well.
- Commonly, unstable systems are identified in a closed-loop setting. Considering that the primary objective of control is stabilization of such systems, the identification of unstable phenomena is also a vital problem in the LPV case. Based on this, investigation of LPV closed-loop identification with series-expansion model structures is proposed as one of the most crucial objectives of future research.
- Finally, testing the developed approaches and theories in practice is required for verification of their usefulness. Establishing model estimates based on measured data and synthesizing LPV control with these models are essential steps to be taken. This may lead to further insight and experience to develop the LPV identification field into a well-established framework.

Proofs

In this appendix, the proofs of the theories and lemmas of this thesis are presented. The proofs rely heavily on the notation and concepts introduced in the previous chapters.

A.1 Proofs of Chapter 3

Proof: (Field property of \mathcal{R} , Lemma 3.1) To prove that \mathcal{R} is a field the following properties have to be satisfied by the operators \boxplus and \boxminus .

- *Closure of \mathcal{R} under \boxplus and \boxminus .*
We need to prove that

$$(\forall r_1, r_2 \in \mathcal{R}) \Rightarrow (r_1 \boxplus r_2 \in \mathcal{R}) \quad \text{and} \quad (r_1 \boxminus r_2 \in \mathcal{R}). \quad (\text{A.1})$$

Let $r_1, r_2 \in \mathcal{R}$ such that $r_1 \in \bar{\mathcal{R}}_i$ and $r_2 \in \bar{\mathcal{R}}_j$ with $i \geq j \geq 0$. Let $r'_2 \in \mathcal{R}_i$ such that $\mathcal{U}_*(r'_2) = r_2$. Note that r'_2 is unique. In \mathcal{R}_i it holds that $r_1 + r'_2 \in \mathcal{R}_i$ and $r_1 \cdot r'_2 \in \mathcal{R}_i$. Furthermore the results of these operators are unique in \mathcal{R}_i . For any $r \in \mathcal{R}_i$ it also trivially holds that $\mathcal{U}_*(r) \in \mathcal{R}$ and it is unique. These imply that $r_1 \boxplus r_2 \in \mathcal{R}$ and $r_1 \boxminus r_2 \in \mathcal{R}$ and the results of these operators are also unique in \mathcal{R} . This proves (A.1).

- *Commutativity of \boxplus and \boxminus .*
This property follows from the commutativity of the Euclidean operators.
- *Associativity of \boxplus and \boxminus .*
We need to prove that for all $r_1, r_2, r_3 \in \mathcal{R}$

$$r_1 \boxplus (r_2 \boxplus r_3) = (r_1 \boxplus r_2) \boxplus r_3 \quad \text{and} \quad r_1 \boxminus (r_2 \boxminus r_3) = (r_1 \boxminus r_2) \boxminus r_3.$$

Due to the fact that $+$ and \cdot are associative in \mathcal{R}_n for $n \geq 0$, it is enough to show that $\mathcal{U}_*(r_1 + r_2) = \mathcal{U}_*(r_1) \boxplus \mathcal{U}_*(r_2)$ and $\mathcal{U}_*(r_1 \cdot r_2) = \mathcal{U}_*(r_1) \boxminus \mathcal{U}_*(r_2)$. As for all $r \in \mathcal{R}$ it holds that $r = \mathcal{U}_*(r)$ these properties are trivially satisfied.

- Operation \square is distributive over \boxplus .

We need to prove that for all $r_1, r_2, r_3 \in \mathcal{R}$

$$r_1 \square (r_2 \boxplus r_3) = (r_1 \square r_2) \boxplus (r_1 \square r_3).$$

Due to the fact that \cdot is distributive over $+$ in \mathcal{R}_n for $n \geq 0$, the argument that proves this property is similar to the previous case.

- *Existence of additive identity.*

Due to construction (3.12), the additive identity in \mathcal{R} is unique and equal to $0 \in \mathbb{R}$. This is proved by the following argument. In \mathcal{R}_n for $n \geq 0$, the zero element r_0 is unique and satisfies $r_0 + r = r$ for all $r \in \mathcal{R}_n$. It also holds that r_0 is not in $\bar{\mathcal{R}}_n$ except for $n = 0$ because $\mathcal{U}_*(r_0) = 0 \in \mathbb{R}$.

- *Existence of multiplicative identity.*

Due to construction (3.12), the multiplicative identity in \mathcal{R} is unique and equal to $1 \in \mathbb{R}$. This is proved by a similar argument as in the previous case.

- *Existence of additive/multiplicative inverse.*

For any $r \in \mathcal{R}_n$, there exists a unique $-r \in \mathcal{R}_n$ such that $r + (-r) = r_0$ where r_0 is the zero element in \mathcal{R}_n . If $\mathcal{U}_*(r) = r$, then it trivially implies that $\mathcal{U}_*(-r) = -r$. Thus for all $r \in \bar{\mathcal{R}}_n$, it holds that its additive inverse exists in $\bar{\mathcal{R}}_n$ and it is unique. This proves the existence of additive inverse in \mathcal{R} which is also unique. Similar arguments hold for the multiplicative inverse.

□

Proof: (State-kernel form, Theorem 3.2) The concept of the proof is based on Rapisarda and Willems (1997). To simplify the discussion, we prove only the so called *Markovian case* as the state case follows trivially from this concept due to the linearity and time-invariance of LPV systems. We call the continuous-time LPV system $\mathcal{S} = (\mathbb{R}, \mathbb{P}, \mathbb{W}, \mathfrak{B})$ Markovian, if for all $p \in \mathfrak{B}_p$

$$(w_1, w_2 \in \mathfrak{B}_p) \wedge (w_1, w_2 \text{ continuous at } 0) \wedge (w_1(0) = w_2(0)) \Rightarrow (w_1 \underset{0}{\wedge} w_2) \in \mathfrak{B}_p.$$

In case of a discrete-time \mathcal{S} , i.e. $\mathbb{T} = \mathbb{Z}$, the definition is similar except continuity of w_1 and w_2 is not required at 0. In the following, we prove that \mathcal{S} is Markovian, iff there exist matrices $r_0, r_1 \in \mathcal{R}^{n_r \times n_w}$ such that \mathfrak{B} has the kernel representation:

$$r_0 w + r_1 \xi w = 0. \tag{A.2}$$

For the sake of simplicity we consider only the continuous-time case as the DT case follows similarly. For $\mathbb{T} = \mathbb{R}$, $\xi = \frac{d}{dt}$, the “if” part is trivial. To show the “only if” case, assume that a KR representation of \mathcal{S} is given with $R \in \mathcal{R}[\xi]^{n_r \times n_w}$ for which the solutions of (3.17) satisfy the above given connectability condition. Without loss of generality it can be assumed that R is full row rank. Also, there exists a unimodular $M \in \mathcal{R}[\xi]^{n_r \times n_r}$ such that $R' = MR$ is in a row reduced form, meaning that the matrix formed by the coefficient functions of the highest powers

in ξ of the rows $R'(\xi)$ has full row rank. Due to the fact that M is a left-side unimodular transformation, the behaviors of R and R' are equivalent.

We show now that $\deg(R') = 1$. Assume the contrary and write R' in the IO form:

$$(R_1 \left(\frac{d}{dt}\right) \diamond p)w_1 = (R_2 \left(\frac{d}{dt}\right) \diamond p)w_2, \quad (\text{A.3})$$

where $\text{col}(w_1, w_2) = w$ corresponds to an IO partition and $\deg(R_1) \geq \deg(R_2)$. The assumption that $\deg(R') > 1$ implies that $\deg(R_1) > 1$. Similarly, the assumption of $(R' \left(\frac{d}{dt}\right) \diamond p)w = 0$ is Markovian implies that $(R_1 \left(\frac{d}{dt}\right) \diamond p)w_1 = 0$ is Markovian.

Now let w'_1, w''_1 be the solutions of $(R_1 \left(\frac{d}{dt}\right) \diamond p)w_1 = 0$ for a $p \in \mathfrak{B}_{\mathbb{P}}$ with $w'_1(0) = w''_1(0)$. Since (w_1, w_2) is an IO partition of \mathcal{S} , thus $\text{col}(w'_1, 0)$ and $\text{col}(w''_1, 0)$ are also solutions of $(R' \left(\frac{d}{dt}\right) \diamond p)w = 0$ and due to Markovian property, they are connectable. This implies that in order to obtain contradiction it suffices to prove contradiction for autonomous systems. Let $n_\xi = \deg(R_1)$ and by assumption $n_\xi > 1$. Introduce auxiliary variables \check{w}_{ij} defined as

$$\check{w}_{ij} := \frac{d^i}{dt^i} w_j, \quad (i, j) \in \mathbb{I}_0^{n_\xi} \times \mathbb{I}_1^{n_w}, \quad (\text{A.4})$$

where $w = [w_1 \dots w_{n_w}]^\top$. Collect these variables in a column vector

$$\check{w} = \left[\check{w}_{01} \quad \check{w}_{02} \quad \dots \quad \check{w}_{0n_w} \quad \check{w}_{11} \quad \dots \quad \check{w}_{n_\xi n_w} \right]^\top. \quad (\text{A.5})$$

Now consider the system with latent variable \check{w} as

$$\frac{d}{dt} \check{w} = (r \diamond p) \check{w}, \quad (\text{A.6a})$$

$$w_j = \check{w}_{0j}, \quad \forall j \in \mathbb{I}_1^{n_w}. \quad (\text{A.6b})$$

where the coefficient $r \in \mathcal{R}^{(n_\xi n_w) \times (n_\xi n_w)}$ is determined from the coefficients of $R_1(\xi)$ and the definition (A.4). The manifest behavior of (A.6a) is equivalent with the manifest behavior of $R_1(\xi)$, which can be checked by elimination of the latent variables of (A.6a-b). However, the manifest behavior can not be Markovian as (A.6a-b) has exactly one solution (w, \check{w}) for each initial condition $\check{w}(0)$ and scheduling trajectory $p \in \mathfrak{B}_{\mathbb{P}}$. This contradicts Markovianity, since two solutions (w, \check{w}) and (w', \check{w}') with $\check{w}_{0j}(0) = \check{w}'_{0j}(0), \forall j \in \mathbb{I}_1^{n_w}$ cannot be connected unless also $\check{w}_{ij}(0) = \check{w}'_{ij}(0), \forall (i, j) \in \mathbb{I}_1^{n_\xi-1} \times \mathbb{I}_1^{n_w}$. \square

A.2 Proofs of Chapter 5

Proof: (LPV series expansion, pulse basis, Theorem 5.1) In the introduced LPV behavioral framework it has been shown that any discrete-time non-autonomous LPV system $\mathcal{S} = (\mathbb{Z}, \mathbb{P} \subseteq \mathbb{R}^{n_p}, \mathbb{R}^{n_w}, \mathfrak{B})$ has non-unique IO representations. Denote the scheduling variable of \mathcal{S} as p . For a given IO partition with output dimension n_y and input dimension n_u , a IO representation of \mathcal{S} is characterized by the

polynomials $R_u \in \mathcal{R}[\xi]^{n_y \times n_u}$ and full row rank $R_y \in \mathcal{R}[\xi]^{n_y \times n_y}$. Among the IO representations that belong to the equivalence class of S for this IO partition, there exists a subset of representations where R_y and R_u are coprime. Those representations are called minimal. Among these minimal representations the representation with monic R_y is unique. Consider this unique, minimal IO representation of S and denote its polynomials with R_y and R_u . Then the dynamic relation reads as

$$q^{n_a} y + \sum_{i=0}^{n_a-1} (a_i \diamond p) q^i y = \sum_{j=0}^{n_b} (b_j \diamond p) q^j u, \quad (\text{A.7})$$

where $a_i \in \mathcal{R}^{n_y \times n_y}$, $i \in \mathbb{I}_0^{n_a-1}$ and $b_j \in \mathcal{R}^{n_y \times n_u}$, $j \in \mathbb{I}_0^{n_b}$ are the coefficients of R_y and R_u . Due to the maximum freedom of u in the IO partition, it holds that $\deg(R_y) = n_a \geq n_b = \deg(R_u)$.

Assume that S is asymptotically stable. Multiply the expression (A.7) with q^{-n_a} which according to the non-commutative multiplication rules in discrete time (see Definition 3.13) results in

$$y = - \sum_{i=0}^{n_a-1} ([a_i]^{n_a} \diamond p) q^{i-n_a} y + \sum_{j=0}^{n_b} ([b_j]^{n_a} \diamond p) q^{j-n_a} u, \quad (\text{A.8})$$

where $[\cdot]^{n_a}$ denotes the backward shift operator applied on the coefficient function for n_a times. We call (A.8) the filter form of (A.7). Now substitute $q^{-1}y$ in (A.8) by the left-hand side of (A.8) multiplied by q^{-1} . This results in the following expression:

$$\begin{aligned} y &= -[a_{n_a-1}]^{n_a} \left(- \sum_{i=0}^{n_a-1} ([a_i]^{n_a+1} \diamond p) q^{i-1-n_a} y + \sum_{j=0}^{n_b} ([b_j]^{n_a+1} \diamond p) q^{j-1-n_a} u \right) \\ &\quad - \sum_{i=0}^{n_a-2} ([a_i]^{n_a} \diamond p) q^{i-n_a} y + \sum_{j=0}^{n_b} ([b_j]^{n_a} \diamond p) q^{j-n_a} u, \end{aligned} \quad (\text{A.9})$$

Notice that in (A.9), the smallest time-shift of y has the order of -2 and that all coefficient relations with (A.8) are uniquely determined. Note that (A.7) represents \mathfrak{B} restricted to signals y and u with left compact support. Thus, by applying this procedure recursively on $q^{-2}y$, $q^{-3}y$, etc., there exists a $n \in \mathbb{N}$ for every $(u, y, p) \in \mathfrak{B}$ such that y vanishes after substitution of $q^{-n}y$. This yields, that the recursive procedure results in a Laurent-like series expansion of (A.7).

Denote by g_i the resulting expressions of the coefficients of R_y and R_u associated with each $q^{-i}u$ in (A.9). It is obvious that $g_i \in \mathcal{R}^{n_y \times n_u}$. However, it is not obvious how this coefficient sequence behaves for increasing i and if it is convergent or not. As a next step, we investigate this property.

Due to the asymptotic stability of S , it holds that for all $p \in \mathfrak{B}_{\mathbb{P}}$ and $k \in \mathbb{Z}$

$$\lim_{i \rightarrow \infty} (g_i \diamond p)(k) = 0. \quad (\text{A.10})$$

Otherwise there exists a $k_0 \in \mathbb{Z}$, and an input signal

$$u(k) = \begin{cases} 1, & \text{if } k = k_0; \\ 0, & \text{else.} \end{cases} \quad (\text{A.11})$$

such that the associated output trajectory y in terms of the IO representation does not converge to the origin when $k \rightarrow \infty$, which contradicts with the asymptotic stability. This implies that

$$\lim_{i \rightarrow \infty} (\mathbf{g}_i \diamond p) = 0 \quad \forall p \in \mathfrak{B}_p, \quad (\text{A.12})$$

meaning that the coefficient sequence of the expansion converges to the zero function on \mathfrak{B}_p . In this way, the limit of the function sequence $\{\mathbf{g}_0, \mathbf{g}_1, \mathbf{g}_2, \dots\}$ can be considered zero.

Asymptotic stability of S also implies BIBO stability in the ℓ_∞ norm:

$$\sup_{k \geq 0} \|u(k)\| < \infty \Rightarrow \sup_{k \geq 0} \|y(k)\| < \infty.$$

In the view of ℓ_∞ BIBO stability, the resulting series expansion form satisfies

$$\sup_{k \geq 0} \|y(k)\| = \sup_{k \geq 0} \|(\mathbf{g}_0 \diamond p)(k)u(k) + (\mathbf{g}_1 \diamond p)(k)u(k-1) + \dots\|.$$

As $\sup_{k \geq 0} \|u(k)\| < \infty$ and $\sup_{k \geq 0} \|y(k)\| < \infty$, the above equation implies that

$$\sup_{k \geq 0} \sum_{i=0}^{\infty} \|(\mathbf{g}_i \diamond p)(k)\| < \infty. \quad (\text{A.13})$$

These properties prove that

$$y = \sum_{i=0}^{\infty} (\mathbf{g}_i \diamond p) q^{-i} u, \quad (\text{A.14})$$

exists and it is satisfied for all $(u, y, p) \in \mathfrak{B}$ with left compact support. In this way, an asymptotically stable discrete-time LPV system has a unique, convergent series expansion in terms of the LTI pulse basis $\{1, q^{-1}, q^{-2}, \dots\}$ with expansion coefficients in $\mathcal{R}^{n_y \times n_u}$. \square

Proof: (LPV series expansion, OBFs, Theorem 5.2) In the LTI theory, it is proven that any pulse basis function z^{-i} , $i > 0$, has a unique series expansion in terms of a arbitrary basis sequence $\Phi_\infty = \{\phi_i\}_{i=1}^\infty$ in $\mathcal{RH}_{2-}(\mathbb{E})$ (Heuberger et al. 2005). This implies that

$$\begin{bmatrix} q^{-1} \\ q^{-2} \\ q^{-3} \\ \vdots \end{bmatrix} = \begin{bmatrix} \mathbf{w}_{11} & \mathbf{w}_{12} & \mathbf{w}_{13} & \dots \\ \mathbf{w}_{21} & \mathbf{w}_{22} & \mathbf{w}_{23} & \dots \\ \mathbf{w}_{31} & \mathbf{w}_{32} & \mathbf{w}_{33} & \dots \\ \vdots & \vdots & \vdots & \ddots \end{bmatrix} \begin{bmatrix} \phi_1(q) \\ \phi_2(q) \\ \phi_3(q) \\ \vdots \end{bmatrix}, \quad (\text{A.15})$$

where $w_{ij} \in \mathbb{R}$, $i, j \in \mathbb{I}_1^\infty$, are the expansion coefficients. It holds for all $i \in \mathbb{I}_1^\infty$, that the sequence $\{w_{ij}\}_{j=1}^\infty$ is an ℓ_2 sequence (Heuberger et al. 2005). The same property also holds for each sequence $\{w_{ij}\}_{i=1}^\infty$.

Based on Theorem 5.1, there exists a pulse basis series expansion of any discrete-time asymptotically stable LPV system $\mathcal{S} = (\mathbb{Z}, \mathbb{P}, \mathbb{W}, \mathfrak{B})$ with IO partition (u, y) . This series expansion can be written in the form of

$$y = g_0 u + \left(\begin{bmatrix} g_1 & g_2 & g_3 & \dots \end{bmatrix} \diamond p \right) \begin{bmatrix} q^{-1} \\ q^{-2} \\ q^{-3} \\ \vdots \end{bmatrix} u. \quad (\text{A.16})$$

Now by substituting (A.15) into (A.16) it follows that

$$y = g_0 u + \left(\begin{bmatrix} w_1 & w_2 & w_3 & \dots \end{bmatrix} \diamond p \right) \begin{bmatrix} \phi_1 \\ \phi_2 \\ \phi_3 \\ \vdots \end{bmatrix} u, \quad (\text{A.17})$$

where

$$\begin{bmatrix} w_1 & w_2 & w_3 & \dots \end{bmatrix} = \begin{bmatrix} g_1 & g_2 & g_3 & \dots \end{bmatrix} \begin{bmatrix} w_{11} & w_{12} & w_{13} & \dots \\ w_{21} & w_{22} & w_{23} & \dots \\ w_{31} & w_{32} & w_{33} & \dots \\ \vdots & \vdots & \vdots & \ddots \end{bmatrix}. \quad (\text{A.18})$$

Due to the fact that $\{g_i\}_{i=1}^\infty$ converges to zero and it satisfies (A.13) for all $p \in \mathfrak{B}_\mathbb{P}$ and each $\{w_{ij}\}_{i=1}^\infty$ is an ℓ_2 sequence, each $w_i \in \mathcal{R}^{n_y \times n_u}$ is unique and well defined. On the other hand, zero convergence of each $\{w_{ij}\}_{j=1}^\infty$ implies that

$$\lim_{i \rightarrow \infty} (w_i \diamond p) = 0 \quad \forall p \in \mathfrak{B}_\mathbb{P}, \quad (\text{A.19})$$

meaning that the new coefficient sequence converges to the zero function on $\mathfrak{B}_\mathbb{P}$. This provides that (A.17) is a unique, convergent series expansion of the LPV system in terms of $\Phi_\infty \subset \mathcal{RH}_{2-}(\mathbb{E})$. As in the considered system class any system has a convergent series expansion in terms of the pulse basis, therefore any of these systems has a convergent series expansion in terms of an arbitrary $\Phi_\infty \subset \mathcal{RH}_{2-}(\mathbb{E})$ basis. \square

A.3 Proofs of Chapter 8

Proof: (Optimal Partition, Theorem 8.1) The proof is given in an alternating minimization sense. First, fix V and define $\hat{J}_m(U) = J_m(U, V)$, for $U \in \mathcal{U}_{n_c}^{N_z}$. Since the membership values $[\mu_{ik}]_{i=1}^{n_c}$ of z_k to the fixed clusters are not depending on

the memberships of other data points, therefore the columns of U are degenerate to each other (decoupled) in the minimization of $\hat{J}_m(U)$, therefore:

$$\min_{U \in \mathcal{U}_{n_c}^{N_z}} \hat{J}_m(U) = \min_{U \in \mathcal{U}_{n_c}^{N_z}} \max_{k \in \mathbb{1}_1^{N_z}} \sum_{i=1}^{n_c} \mu_{ik}^m d_{ik} = \max_{k \in \mathbb{1}_1^{N_z}} \min_{U \in \mathcal{U}_{n_c}^{N_z}} \sum_{i=1}^{N_z} \mu_{ik}^m d_{ik}. \quad (\text{A.20})$$

Denote $\hat{J}_m^{(k)}(U) = \sum_{i=1}^{n_c} \mu_{ik}^m d_{ik}$. To introduce the constraints $\mathcal{U}_{n_c}^{N_z}$, the Lagrangian $\Delta_k(\delta_k, U)$ of $\hat{J}_m^{(k)}(U)$ is defined for each $k \in \mathbb{1}_1^{N_z}$ as

$$\Delta_k(\delta_k, U) = \sum_{i=1}^{n_c} \mu_{ik}^m d_{ik} - \delta_k \left[\left(\sum_{i=1}^{n_c} \mu_{ik} \right) - 1 \right]. \quad (\text{A.21})$$

Assume that $\mathcal{I}_k^\emptyset = \emptyset$, then (δ_k, U) is a stationary point for Δ_k , only if

$$\frac{\partial}{\partial(\delta, U)} \Delta_k(\delta_k, U) = (0^{N_z}, 0^{n_c \times N_z}), \quad (\text{A.22})$$

for all $k \in \mathbb{1}_1^{N_z}$. Setting all of these gradients equal to zero yields that

$$\frac{\partial \Delta_k(\delta_k, U)}{\partial \delta_k} = \sum_{i=1}^{n_c} \mu_{ik} - 1 = 0, \quad (\text{A.23a})$$

$$\frac{\partial \Delta_k(\delta_k, U)}{\partial \mu_{ik}} = m \mu_{ik}^{m-1} d_{ik} - \delta_k = 0, \quad (\text{A.23b})$$

for every $k \in \mathbb{1}_1^{N_z}$ and $i \in \mathbb{1}_1^{n_c}$. From (A.23b), it follows that

$$\mu_{ik} = \left(\frac{\delta_k}{m d_{ik}} \right)^{\frac{1}{m-1}}. \quad (\text{A.24})$$

Moreover, by substitution of (A.24) into (A.23a):

$$0 = \sum_{l=1}^{n_c} \left(\frac{\delta_k}{m} \right)^{\frac{1}{m-1}} \left(\frac{1}{d_{lk}} \right)^{\frac{1}{m-1}} - 1 \quad (\text{A.25a})$$

$$\left(\frac{\delta_k}{m} \right)^{\frac{1}{m-1}} = \left[\sum_{l=1}^{n_c} \left(\frac{1}{d_{lk}} \right)^{\frac{1}{m-1}} \right]^{-1}. \quad (\text{A.25b})$$

If (A.25b) is substituted back into (A.24), then

$$\mu_{ik} = \frac{\left(\frac{1}{d_{ik}} \right)^{\frac{1}{m-1}}}{\sum_{l=1}^{n_c} \left(\frac{1}{d_{lk}} \right)^{\frac{1}{m-1}}} = \frac{1}{\sum_{l=1}^{n_c} \left(\frac{d_{lk}}{d_{ik}} \right)^{\frac{1}{m-1}}}. \quad (\text{A.26})$$

In this way we have proved that in a local minima of $J_m(U, V)$, all μ_{ik} has to satisfy (8.10a). If $\mathcal{I}_k^\emptyset \neq \emptyset$, then (A.26) is singular. In this situation, choosing μ_{ik} as given by (8.10a) results in $\hat{J}_m^{(k)}(U) = 0$, because the non-zero weights are placed on zero

distances, while positive distances with nonzero weights would increase $\hat{J}_m^{(k)}(U)$, contradicting to minimality. As the zero-distances can have arbitrary weights, for the sake of simplicity equal weights are considered fulfilling (8.10a). Note, that such singularity hardly occurs in reality, since machine round-off prevents its encounter.

To establish (8.10b), fix $U \in \mathcal{U}_{n_c}^{N_z}$ and define $\check{J}_m(V) = J_m(U, V)$. Minimization of $\check{J}_m(V)$ is unconstrained on \mathbb{D}^{n_c} , and it is decoupled for each v_i . Therefore

$$\min_{V \in \mathbb{D}^{n_c}} \check{J}_m(V) = \min_{V \in \mathbb{D}^{n_c}} \max_{k \in \mathbb{I}_1^{N_z}} \sum_{i=1}^{n_c} \mu_{ik}^m d_{ik} = \sum_{i=1}^{n_c} \min_{V \in \mathbb{D}^{n_c}} \check{J}_m^{(i)}(V), \quad (\text{A.27})$$

where $\check{J}_m^{(i)}(V) = \max_{k \in \mathbb{I}_1^{N_z}} \mu_{ik}^m d_{ik}$, depending only on v_i . This means that

$$v_i = \arg \min_{V \in \mathbb{D}^{n_c}} \check{J}_m^{(i)}(V) = \arg \min_{v_i \in \mathbb{D}} \max_{k \in \mathbb{I}_1^{N_z}} \mu_{ik}^m d_{ik}. \quad (\text{A.28})$$

Optimization (A.28) can be formulated as a matrix inequalities constrained minimization problem. Denote

$$\gamma_i = \check{J}_m^{(i)}(V) = \max_{k \in \mathbb{I}_1^{N_z}} \mu_{ik}^m d_{ik}, \quad (\text{A.29})$$

then the solution of (A.28) can be obtained by solving

$$\begin{aligned} & \text{minimize} && \gamma_i \geq 0, \\ & \text{subject to} && \mu_{ik}^m \left| \frac{\mathbf{z}_k - v}{1 - \mathbf{z}_k^* v} \right| \leq \gamma_i, \quad \forall k \in \mathbb{I}_1^{N_z}, \\ & && v \in \mathbb{D}. \end{aligned}$$

The constraints of this minimization can be written for each k as

$$\mu_{ik}^m \left| \frac{\mathbf{z}_k - v}{1 - \mathbf{z}_k^* v} \right| \leq \gamma_i, \quad (\text{A.30a})$$

$$\mu_{ik}^{2m} |\mathbf{z}_k - v|^2 |1 - \mathbf{z}_k^* v|^{-2} \leq \gamma_i^2. \quad (\text{A.30b})$$

From the Schurr-complement of (A.30b) it follows that (A.30a) holds iff

$$\begin{bmatrix} |1 - \mathbf{z}_k^* v|^2 & \mu_{ik}^m (\mathbf{z}_k - v) \\ \mu_{ik}^m (\mathbf{z}_k - v)^* & \gamma_i^2 \end{bmatrix} \succeq 0, \quad \forall k \in \mathbb{I}_1^{N_z}, \quad (\text{A.31})$$

where $v \in \mathbb{D}$. Then a sufficient but not necessary condition for (U, V) being local minima of J_m is to satisfy (A.26) and (A.28). This concludes the proof. It is important to remark that $J_m(U, V)$ has more stationary points than what can be reached through alternating minimization, however all points fulfilling Theorem 8.1 are stationary points of $J_m(U, V)$. \square

Proof: (Asymptotic property of J_m , Theorem 8.2) As the cluster centers of V are assumed to be “nonsingular” with respect to Z , i.e. $d_{ik} > 0$ for all $(i, k) \in \mathbb{I}_1^{n_c} \times \mathbb{I}_1^{N_z}$, thus based on the optimality of U_m , substitution of (A.26) into (8.8) implies, that for $m > 1$:

$$\begin{aligned} J_m(U_m, V) &= \max_{k \in \mathbb{I}_1^{N_z}} \sum_{i=1}^{n_c} \mu_{ik}^m d_{ik} = \max_{k \in \mathbb{I}_1^{N_z}} \sum_{i=1}^{n_c} \mu_{ik} \mu_{ik}^{m-1} d_{ik} = \\ &= \max_{k \in \mathbb{I}_1^{N_z}} \sum_{i=1}^{n_c} \mu_{ik} \frac{d_{ik}}{d_{ik} \left[\sum_{l=1}^{n_c} \left(\frac{1}{d_{lk}} \right)^{\frac{1}{m-1}} \right]^{m-1}} = \\ &= \max_{k \in \mathbb{I}_1^{N_z}} \left[\sum_{l=1}^{n_c} (d_{lk})^{\frac{1}{1-m}} \right]^{1-m}, \end{aligned}$$

holds as $\sum_{i=1}^{n_c} \mu_{ik} = 1$. Now introduce

$$\bar{J}_\tau^{(k)}(V) = \left[\sum_{i=1}^c \frac{1}{c} (d_{ik})^\tau \right]^{1/\tau}, \quad (\text{A.32})$$

with $\tau = \frac{1}{1-m}$. Then

$$J_m(U_m, V) = J_{\frac{\tau-1}{\tau}}(U_{\frac{\tau-1}{\tau}}, V) = n_c^{1/\tau} \max_{k \in \mathbb{I}_1^{N_z}} \bar{J}_\tau^{(k)}(V). \quad (\text{A.33})$$

Equation (A.32) is called the *Hölder* or *generalized mean* (Bullen 2003) of d_{ik} . Based on the properties of the generalized mean in terms of τ , the following hold:

Case $m \rightarrow 1 \Leftrightarrow \tau \rightarrow -\infty \Rightarrow \bar{J}_\tau^{(k)}(V) \rightarrow \min_{i \in \mathbb{I}_1^{n_c}} \{d_{ik}\}$ for all $k \in \mathbb{I}_1^{N_z}$. Since $n_c^{1-m} \rightarrow 1$, the minimum over $\mathbb{I}_1^{n_c}$ is unique for each k :

$$\lim_{m \rightarrow 1} J_m(U_m, V) = \max_{k \in \mathbb{I}_1^{N_z}} \min_{i \in \mathbb{I}_1^{n_c}} \{d_{ik}\}. \quad (\text{A.34})$$

Case $m = 2 \Leftrightarrow \tau = -1$. Then $\bar{J}_{-1}^{(k)}(V)$ is the harmonic mean of $\{d_{ik}\}_{i=1}^{n_c}$ for each $k \in \mathbb{I}_1^{N_z}$, so

$$J_2(U_2, V) = \frac{1}{n_c} \max_{k \in \mathbb{I}_1^{N_z}} \frac{n_c}{\sum_{i=1}^{n_c} \frac{1}{d_{ik}}}. \quad (\text{A.35})$$

Case $m \rightarrow \infty \Leftrightarrow \tau \rightarrow 0$. Then, the asymptotic convergence of the generalized mean to the geometric mean yields: $\bar{J}_\tau^{(k)}(V) = [\prod_{i=1}^{n_c} d_{ik}]^{1/n_c} + \mathcal{O}(e^{\frac{1}{\tau}})$, which gives

$$J_m(U_m, V) = n_c^{1-m} \max_{k \in \mathbb{I}_1^{N_z}} \left[\prod_{i=1}^{n_c} d_{ik} \right]^{\frac{1}{n_c}} + \mathcal{O}(e^{-m}), \quad (\text{A.36})$$

and since $n_c^{1-m} \rightarrow 0$, therefore

$$\lim_{m \rightarrow \infty} J_m(U_m, V) = 0. \quad (\text{A.37})$$

□

Proof: (h-center relation, Lemma 8.3) From Lemma 8.2 we obtain that for any $K_h(e_h, r_h)$, there exists a $K(e, r)$, such that all $z \in K_h(e_h, r_h)$ satisfies both

$$\left| \frac{z - e_h}{1 - z^* e_h} \right| = r_h, \quad |z - e| = r. \quad (\text{A.38})$$

Straightforward calculus leads to

$$e = \frac{1 - r_h^2}{1 - r_h^2 |e_h|^2} e_h, \quad r = \frac{1 - |e_h|^2}{1 - r_h^2 |e_h|^2} r_h, \quad (\text{A.39})$$

concluding that

$$\varphi_h = \frac{1 - r_h^2}{1 - r_h^2 |e_h|^2} \in \mathbb{R} \quad \Rightarrow \quad e = \varphi_h e_h. \quad (\text{A.40})$$

□

Proof: (κ_1 -metric, Theorem 8.4) In order to prove that KM is a metric on \mathbb{D} , the following 3 properties have to be verified for all $x, y, z \in \mathbb{D}$:

(i) *Zero metricity:* $\kappa_1(x, x) = 0$. By substitution:

$$\kappa_1(x, x) = \left| \frac{x - x}{1 - x^* x} \right| = \left| \frac{0}{1 - |x|^2} \right| = 0, \quad \forall x \in \mathbb{D}. \quad (\text{A.41})$$

(ii) *Symmetry:* $\kappa_1(x, y) = \kappa_1(y, x)$. Let $x, y \in \mathbb{D}$ be arbitrary, then:

$$\kappa_1(x, y) = \frac{|x - y|}{|1 - x^* y|} = \frac{|-(y - x)|}{|(1 - (x^* y))^*|} = \kappa_1(y, x). \quad (\text{A.42})$$

(iii) *Triangular inequality:* $\kappa_1(x, y) \leq \kappa_1(z, x) + \kappa_1(z, y)$. Assume that $x, y \in \mathbb{D}$ and $z \in H_{xy}$ (see Figure A.1.a). If $x = y$, then (iii) holds trivially as $\kappa_1(x, x) = 0 \leq 2\kappa_1(z, x)$. Moreover, if $z = x$ or $z = y$ then (iii) holds with equality as $\kappa_1(x, y) = \kappa_1(x, x) + \kappa_1(x, y) = \kappa_1(x, y)$ or $\kappa_1(x, y) = \kappa_1(y, y) + \kappa_1(x, y) = \kappa_1(x, y)$. Now assume that x, y, z are distinct points. Define $\hat{x} = \mathfrak{h}_z(x)$ and $\hat{y} = \mathfrak{h}_z(y)$, where \mathfrak{h}_z is the h-inversion that maps $z \rightarrow 0$. Then, $\mathfrak{h}_z(H_{xy}) = H_{\hat{x}\hat{y}}$ is a segment of an Euclidian line, a diameter of \mathbb{J} (blue line in Figure A.1.a). Let \tilde{H} be the diameter line (also an h-line) bisecting the angle between $H_{0\hat{x}}$ and the real axis. Then $\mathfrak{h}_{\tilde{H}}(\hat{x}) = \tilde{x}$ and $\mathfrak{h}_{\tilde{H}}(\hat{y}) = \tilde{y}$ are points of the real axis and $\mathfrak{h}_{\tilde{H}}(H_{\hat{x}\hat{y}}) = H_{\tilde{x}\tilde{y}} \subset (-1, 1)$ with $0 \in H_{\tilde{x}\tilde{y}}$ (green in Figure A.1.a). As $\mathfrak{h}_{\tilde{H}} \circ \mathfrak{h}_z \in \mathcal{D}$, then by Corollary 8.1, (iii) can be written as $\kappa_1(\tilde{x}, \tilde{y}) \leq$

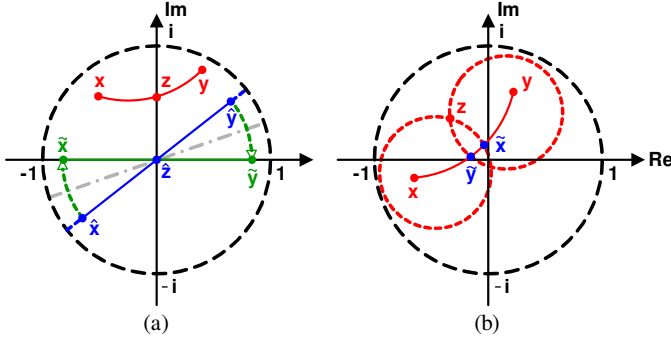


Figure A.1: Inversion of h-lines and points proving the Triangular equality.

$\kappa_1(0, \tilde{x}) + \kappa_1(0, \tilde{y})$. Assuming that \tilde{x} and \tilde{y} are ordered as $\tilde{x} \in (-1, 0)$ and $\tilde{y} \in (0, 1)$, then

$$\begin{aligned} \frac{|\tilde{x} - \tilde{y}|}{|1 - \tilde{x}^* \tilde{y}|} &\leq -\tilde{x} + \tilde{y}, \\ \frac{\tilde{y} - \tilde{x}}{1 + |\tilde{x}| \tilde{y}} &\leq \tilde{y} - \tilde{x}, \\ 1 &\leq 1 + |\tilde{x}| \tilde{y}, \\ 0 &\leq |\tilde{x}| \tilde{y}. \end{aligned}$$

In the second part of the proof assume that $z \notin H_{xy}$. Define h-circles $K_{h1}(x, r_{h1})$ and $K_{h2}(y, r_{h2})$ such that $z \in K_{h1}, K_{h2}$ (red in Figure A.1.b). Note that $\kappa_1(z, x) = r_{h1}$ and $\kappa_1(z, y) = r_{h2}$. If $\max(r_{h1}, r_{h2}) \leq \kappa_1(x, y)$, then $K_{h1} \cap H_{xy} = \tilde{x}$ and $K_{h2} \cap H_{xy} = \tilde{y}$ exist (blue in Figure A.1.b). Since $\tilde{x}, z \in K_{h1}$, therefore $\kappa_1(\tilde{x}, x) = \kappa_1(z, x)$ and since $\tilde{y}, z \in K_{h2}$, therefore $\kappa_1(\tilde{y}, y) = \kappa_1(z, y)$. Moreover, $\kappa_1(\tilde{x}, x) > \kappa_1(\tilde{y}, x)$ and $\kappa_1(\tilde{y}, y) > \kappa_1(\tilde{x}, y)$, otherwise $K_{h1} \cap K_{h2} = \emptyset$. Then, $\kappa_1(x, y) \leq \kappa_1(\tilde{x}, x) + \kappa_1(\tilde{x}, y)$, which gives $\kappa_1(x, y) \leq \kappa_1(z, x) + \kappa_1(\tilde{y}, y)$ implying (iii). If $\max(r_{h1}, r_{h2}) > \kappa_1(x, y)$, then either $\tilde{x} \notin H_{xy}$ or $\tilde{y} \notin H_{xy}$. $\tilde{x} \notin H_{xy}$ means that the circle K_{h1} is containing the circle $K_h(x, \kappa_1(x, y))$, so $\kappa_1(x, y) < r_{h1} = \kappa_1(z, x)$. This implies that (iii) holds. The case of $\tilde{y} \notin H_{xy}$ analogously follows.

□

Proof: (h-segment worst-case distance, Theorem 8.5) Define $\hat{x} = \eta_v(x)$, $\hat{y} = \eta_v(y)$, $H_{\hat{x}\hat{y}} = \eta_v(H_{xy})$. As $\eta_v(v) = 0$, then $\kappa_1(0, \hat{z}) = |\hat{z}|$ for all $\hat{z} \in H_{\hat{x}\hat{y}}$. Moreover, η_v keeps distances in the Kolmogorov sense (Corollary 8.1), therefore

$$\max_{z \in H_{xy}} \kappa_1(v, z) = \max_{\hat{z} \in H_{\hat{x}\hat{y}}} |\hat{z}|. \tag{A.43}$$

In accordance to this, the most distant point of $H_{\hat{x}\hat{y}}$ in the Euclidian sense from the origin represents the furthest point of H_{xy} in the Kolmogorov sense from v . Based

on the Euclidian geometry:

$$\max_{\hat{z} \in H_{\hat{x}\hat{y}}} |\hat{z}| = \max(|\hat{x}|, |\hat{y}|) = \max(\kappa_1(\mathbf{x}, \mathbf{v}), \kappa_1(\mathbf{y}, \mathbf{v})). \quad (\text{A.44})$$

□

Proof: (h-disc worst-case distance, Theorem 8.6) Define $\hat{\mathbf{e}}_h = \mathfrak{h}_v(\mathbf{e}_h)$, then due to Lemma 8.6, $\mathfrak{h}_v(D_h(\mathbf{e}_h, \mathbf{r}_h)) = D_h(\hat{\mathbf{e}}_h, \mathbf{r}_h)$. As $\mathfrak{h}_v(\mathbf{v}) = 0$, thus $\kappa_1(0, \hat{z}) = |\hat{z}|$ for every $\hat{z} \in D_h(\hat{\mathbf{e}}_h, \mathbf{r}_h)$. Due to Corollary 8.1:

$$\check{z} = \arg \max_{z \in D_h(\mathbf{e}_h, \mathbf{r}_h)} \kappa_1(\mathbf{v}, z) = \mathfrak{h}_v(\arg \max_{\hat{z} \in D_h(\hat{\mathbf{e}}_h, \mathbf{r}_h)} |\hat{z}|). \quad (\text{A.45})$$

Assume that $\mathbf{v} = \mathbf{e}_h$, then $\hat{\mathbf{e}}_h = 0$ and $\mathfrak{h}_v(D_h(\mathbf{e}_h, \mathbf{r}_h))$ is equal to the Euclidean disc $D(0, \mathbf{r}_h)$. Then

$$\arg \max_{\hat{z} \in D(0, \mathbf{r}_h)} |\hat{z}| = K(0, \mathbf{r}_h), \quad (\text{A.46})$$

and $\check{z} = \mathfrak{h}_v(K(0, \mathbf{r}_h)) = K_h(\mathbf{e}_h, \mathbf{r}_h)$, i.e. all the perimeter points of $D_h(\mathbf{e}_h, \mathbf{r}_h)$, with

$$\max_{z \in D_h(\mathbf{e}_h, \mathbf{r}_h)} \kappa_1(\mathbf{v}, z) = \mathbf{r}_h. \quad (\text{A.47})$$

If $\mathbf{v} \neq \mathbf{e}_h$, then due to Lemma 8.3, $\hat{\mathbf{e}}_h$ and the Euclidian center of $D_h(\hat{\mathbf{e}}_h, \mathbf{r}_h)$ are on the same Euclidian line from the origin. Therefore, based on the Euclidian geometry:

$$\check{z} = \mathfrak{h}_v(\arg \max_{\hat{z} \in \{\hat{z}_1, \hat{z}_2\}} |\hat{z}|) \quad (\text{A.48})$$

where $\{\hat{z}_1, \hat{z}_2\} = E(0, \hat{\mathbf{r}}) \cap K_h(\hat{\mathbf{e}}_h, \mathbf{r}_h)$ with $E(0, \hat{\mathbf{r}})$, the Euclidian line connecting the origin with $\hat{\mathbf{e}}_h$. Furthermore,

$$\max_{z \in D_h(\mathbf{e}_h, \mathbf{r}_h)} \kappa_1(\mathbf{v}, z) = \max(|\hat{z}_1|, |\hat{z}_2|). \quad (\text{A.49})$$

Moreover as $\mathfrak{h}_v(E(0, \hat{\mathbf{r}})) = H_{\mathbf{v}\mathbf{e}_h}$ the h-line connecting \mathbf{v} with \mathbf{e}_h , therefore $H_{\mathbf{v}\mathbf{e}_h} \cap K_h(\mathbf{e}_h, \mathbf{r}_h) = \{\mathfrak{h}_v(\hat{z}_1), \mathfrak{h}_v(\hat{z}_2)\}$. □

Proof: (Convexity, Theorem 8.7) Any conformal mapping in \mathbb{D} preserves convexity of subsets of \mathbb{D} (Blair 2000). As any \mathfrak{h}_e , with $\mathbf{e} \in \mathbb{D}$, is a conformal mapping, therefore \mathfrak{h}_e preserves convexity of sets in \mathbb{D} (convexity preservation in the KM sense). Let an arbitrary h-segment H_{xy} be given. Then $\mathbf{e} = H_{xy} \cap H^{\perp(xy)}$ is the midpoint of H_{xy} and $H_{\hat{x}\hat{y}} = \mathfrak{h}_e(H_{xy})$ is the part of a diameter of \mathbb{D} . Then based on the convexity of Euclidian lines, for any $\mathbf{z}_1, \mathbf{z}_2 \in H_{\hat{x}\hat{y}}$ and $\mathbf{r} \in [0, 1]$ it holds that $\mathbf{r}\mathbf{z}_1 + (1 - \mathbf{r})\mathbf{z}_2 \in H_{\hat{x}\hat{y}}$. Therefore convexity holds for H_{xy} in the KM sense. Furthermore, for any $D_h(\mathbf{e}_h, \mathbf{r}_h)$, there exists an equivalent Euclidian disc $D(\mathbf{e}, \mathbf{r})$. Based on the convexity of Euclidian discs, the convexity of $D_h(\mathbf{e}_h, \mathbf{r}_h)$ is straight-

forward. \square

Proof: (Optimal Robust Partition, Theorem 8.8) Similar to the proof of Theorem 8.1 an alternating minimization approach is utilized. First, fix V and define $\hat{J}_m(U) = J_m(U, V)$, for $U \in \mathcal{U}_{n_c}^{N_z}$. Since the minimization of $\hat{J}_m(U)$ does not depend on the actual computation of $\{d_{ik}\}$, therefore the first part of the proof deriving the condition (8.27a) is the same as given for the proof of Theorem 8.1 with the exception, that in this case no singularity can occur as $d_{ik} > 0$ for all $(i, j) \in \mathbb{I}_1^{n_c} \times \mathbb{I}_1^{N_z}$. See Section 8.3 for details. To establish (8.27b), fix $U \in \mathcal{U}_{n_c}^{N_z}$ and define $\check{J}_m(V) = J_m(U, V)$. Minimization of $\check{J}_m(V)$ is decoupled for each v_i , therefore

$$\min_{V \in \mathbb{D}^c} \check{J}_m(V) = \min_{V \in \mathbb{D}^{n_c}} \max_{k \in \mathbb{I}_1^{N_z}} \sum_{i=1}^{n_c} \mu_{ik}^m d_{ik} = \sum_{i=1}^{n_c} \min_{V \in \mathbb{D}^{n_c}} \check{J}_m^{(i)}(V), \quad (\text{A.50})$$

where $\check{J}_m^{(i)}(V) = \max_{k \in \mathbb{I}_1^{N_z}} \mu_{ik}^m d_{ik}$, depending only on v_i . As the elements of V are degenerate to each other (decoupled) in the minimization of $\check{J}_m^{(i)}(V)$, the minimizer of $\check{J}_m^{(i)}$ is obtained as

$$v_i = \arg \min_{v_i \in \mathbb{D}} \max_{k \in \mathbb{I}_1^{N_z}} \max_{z_k \in \mathcal{Z}_k} \mu_{ik}^m \kappa_1(v_i, z_k). \quad (\text{A.51})$$

Optimization (A.51) can be formulated as a QCs' constrained minimization problem. Denote

$$\gamma_i = \check{J}_m^{(i)}(V) = \max_{k \in \mathbb{I}_1^{N_z}} \mu_{ik}^m d_{ik}, \quad (\text{A.52})$$

then the solution of (A.51) can be obtained by solving

$$\begin{aligned} & \text{minimize} && \gamma_i \geq 0, \\ & \text{subject to} && \mu_{ik}^m \left| \frac{z - \nu}{1 - z^* \nu} \right| \leq \gamma_i, \forall k \in \mathbb{I}_1^{N_z}, \forall z \in \mathcal{Z}_k \\ & && \nu \in \mathbb{D}. \end{aligned}$$

Moreover, the constraints of the minimization can be rewritten for each k as (A.30a-b). The same holds for the h-discs induced constraints. From the Schurr-complement it follows that (A.30a) holds iff (8.26) is fulfilled and the h-disc coverage induced constraints hold iff (8.32) is fulfilled. Then a sufficient but not necessary condition for (U, V) being a local minimum of J_m is to satisfy (8.27a) and (8.27b). \square

A.4 Proofs of Chapter 9

Proof: (Representation of dynamic dependence, Property 9.2) Let \mathcal{S} be an asymptotically stable SISO LPV system and $\Phi_{n_g}^\infty \subset \mathcal{RH}_{2-}(\mathbb{E})$ be a Hambo basis. For a $n_e > 0$, consider the Wiener-feedback model $\mathfrak{M}_{\text{WF}}(\Phi_{n_g}^{n_e}, \theta, \mathfrak{B}_P)$. The process model

of $\mathfrak{M}_{\text{WF}}(\Phi_{n_g}^{n_e}, \theta, \mathfrak{B}_{\mathbb{F}})$ has the representation:

$$\check{y}_{ij} = \phi_j(q)G^i(q)u - \phi_j(q)G^i(q)v_{ij}(p)\check{y}_{ij}, \quad (\text{A.53a})$$

$$y = w_{00}(p)u + \sum_{i=0}^{n_e} \sum_{j=1}^{n_g} w_{ij}(p)\check{y}_{ij}, \quad (\text{A.53b})$$

where $w_{ij}, v_{ij} \in \mathcal{R}|_{n_{\mathbb{F}}}$ are meromorphic coefficients with static dependency. S is asymptotically stable which implies that (A.53a-b) has a convergent series expansion in terms of $\Phi_{n_g}^{\infty}$. By substituting (A.53a) into (A.53b) recursively, this series expansion reads as:

$$\begin{aligned} y &= w_{00}(p)u + \sum_{i=0}^{n_e} \sum_{j=1}^{n_g} w_{ij}(p)\phi_j(q)G^i(q)u \\ &\quad - \sum_{i=0}^{n_e} \sum_{j=1}^{n_g} w_{ij}(p)\phi_j(q)G^i(q)v_{ij}\phi_j(q)G^i(q)u + \dots \end{aligned}$$

From this expression it follows that

$$w_{ij}(p)\phi_j(q)G^i(q)v_{ij}(p) = (f_{ij} \diamond p)\phi_j(q)G^i(q), \quad (\text{A.54})$$

where $f_{ij} \in \mathcal{R}$ has dynamic dependence. This implies that the resulting expansion coefficients of $\phi_j(q)G^i$, with $i > n_e$, have dynamic dependence. If each v_{ij} is constant, then in (A.54) $f_{ij} = w_{ij}$, which means that the resulting expansion coefficients of $\phi_j(q)G^i$, $i > n_e$ have static dependence. This concludes the proof in the WF-LPV OBF case. With respect to HF-LPV OBF models, the proof follows similarly. □

Bibliography

- Anderson, B. D. O. (1982). Internal and external stability of linear time-varying systems. *SIAM Journal on Control and Optimization* **20**, 408–413.
- Angelis, G. Z. (2001). *System Analysis, Modelling and Control with Polytopic Linear Models*. Ph. D. thesis, Eindhoven University of Technology.
- Apkarian, P. (1997). On the discretization of LMI-synthesized linear parameter-varying controllers. *Automatica* **33**(4), 655–661.
- Apkarian, P. and R. J. Adams (1998). Advanced gain-scheduling techniques for uncertain systems. *IEEE Trans. on Control Systems Technology* **9**(1), 21–32.
- Apkarian, P. and P. Gahinet (1995). A convex characterization of gain-scheduled \mathcal{H}_∞ controllers. *IEEE Trans. on Automatic Control* **40**(5), 853–864.
- Åström, K. J. and B. Wittenmark (1989). *Adaptive Control*. Addison-Wesley.
- Atkinson, K. E. (1989). *An Introduction to Numerical Analysis*. John Wiley and Sons.
- Backer, E. and A. K. Jain (1981). A clustering performance measure based on fuzzy set decomposition. *IEEE Trans. on Pattern Analysis and Machine Intelligence* **3**, 66–75.
- Balas, G., J. Bokor and Z. Szabó (2003). Invariant subspaces for LPV systems and their applications. *IEEE Trans. on Automatic Control* **48**(11), 2065–2069.
- Bamieh, B. and L. Giarré (1999). Identification of linear parameter varying models. In *Proc. of the 38th IEEE Conf. on Decision and Control*, Phoenix, Arizona, USA (Dec.), pp. 1505–1510.
- Bamieh, B. and L. Giarré (2000). Identification for a general class of LPV models. In *Proc. of the 11th IFAC Symposium on System Identification*, Santa Barbara, California, USA (June).
- Bamieh, B. and L. Giarré (2002). Identification of linear parameter varying models. *Int. Journal of Robust and Nonlinear Control* **12**, 841–853.
- Banks, S. P. and S. K. Al-Jurani (1996). Pseudo-linear systems, Lie’s algebra, and stability. *IMA Journal of Mathematical Control and Information* **13**, 385–401.

- Beauzamy, B. (1988). *Introduction to Operator Theory and Invariant Subspaces*. North-Holland.
- Becker, G., A. Packard, D. Philbrick and G. Balas (1993). Control of parametrically-dependent linear systems: A single quadratic Lyapunov function approach. In *Proc. of the American Control Conf.*, San Francisco, California, USA (June), pp. 2795–2799.
- Bezdek, J. C. (1981). *Pattern Recognition with Fuzzy Objective Function Algorithms*. Plenum Press.
- Bianchi, F. D., H. De Battista and R. J. Mantz (2007). *Wind Turbine Control Systems; Principles, modeling and gain scheduling design*. Springer-Verlag.
- Billings, S. and S. Fakhouri (1982). Identification of systems containing linear dynamic and static nonlinear elements. *Automatica* **18**(1), 15–26.
- Blair, D. E. (2000). *Inversion Theory and Conformal Mapping*, Volume 9 of *Student Mathematical Library*. American Mathematical Society.
- Bos, R., X. Bombois and P. M. J. Van den Hof (2005). Accelerating simulations of first principle models of complex industrial systems using quasi linear parameter varying models. In *Proc. of the 44th IEEE Conf. on Decision and Control*, Seville, Spain (Dec.), pp. 4146–4151.
- Boyd, S. and L. O. Chua (1985). Fading memory and the problem of approximating nonlinear operators with Volterra series. *IEEE Trans. on Circuits and Systems* **32**(11), 1150–1161.
- Boyd, S., L. E. Ghaoui, E. Feron and V. Balakrishnan (1994). *Linear Matrix Inequalities in System and Control Theory*. SIAM Press.
- Brannan, D. A., M. F. Esplen and J. J. Gray (1999). *Geometry*. Cambridge university press.
- Brockett, R. W. (1970). *Finite Dimensional Linear Systems*. John Wiley and Sons.
- Bullen, P. S. (2003). *Handbook of Means and Their Inequalities*. Kluwer Academic Publishers.
- Callier, F. M. and C. A. Desoer (1991). *Linear System Theory*. Springer-Verlag.
- Carter, L. H. and J. S. Shamma (1996). Gain-scheduled bank-to-turn autopilot design using linear parameter varying transformations. *Int. Journal of Control* **19**(5), 1056–1063.
- Chon, P. M. (1971). *Free Rings and their relations*. Academic Press.
- Chyzak, F. and B. Salvy (1998). Non-commutative elimination in Ore algebras proves multivariate identities. *Journal of Symbolic Computation* **26**, 187–227.
- Cook, M. V. (1997). *Flight Dynamics Principles*. Springer.

- Davies, D. I. and D. W. Bouldin (1979). A cluster separation measure. *IEEE Trans. on Pattern Analysis and Machine Intelligence* **1**(2), 95–104.
- Dettoni, M. and C. W. Scherer (2001). LPV design for a CD player: An experimental evaluation of performance. In *Proc. of the 40th IEEE Conf. on Decision and Control*, Orlando, Florida, USA (Dec.), pp. 4711–4716.
- dos Santos, P. L., J. A. Ramos and J. L. M. de Carvalho (2007). Identification of linear parameter varying systems using an iterative deterministic-stochastic subspace approach. In *Proc. of the European Control Conf.*, Kos, Greece (July), pp. 4867–4873.
- Douma, S. G. and P. M. J. Van den Hof (2005). Relations between uncertainty structures in identification for robust control. *Automatica* **41**(3), 439–457.
- Evans, L. C. (1998). *Partial Differential Equations*. American Mathematical Society, Providence.
- Felici, F., J. W. van Wingerden and M. Verhaegen (2006). Subspace identification of MIMO LPV systems using a periodic scheduling sequence. *Automatica* **43**(10), 1684–1697.
- Felici, F., J. W. van Wingerden and M. Verhaegen (2007). Dedicated periodic scheduling sequences for LPV system identification. In *Proc. of the European Control Conf.*, Kos, Greece (July), pp. 4896–4902.
- Gáspár, P., Z. Szabó and J. Bokor (2005). A grey-box continuous-time parameter identification for LPV models with vehicle dynamics applications. In *Proc. of the 13th Mediterranean Conf. on Control and Automation*, Limassol, Cyprus (June), pp. 393–397.
- Gáspár, P., Z. Szabó and J. Bokor (2007). A grey-box identification of an LPV vehicle model for observer-based side-slip angle estimation. In *Proc. of the American Control Conf.*, New York City, USA (July), pp. 2961–2965.
- Giarré, L., D. Bauso, P. Falugi and B. Bamieh (2006). LPV model identification for gain scheduling control: An application to rotating stall and surge control problem. *Control Engineering Practice* **14**, 351–361.
- Ginnakis, G. B. and E. Serpedin (2001). A bibliography on nonlinear system identification. *Signal Processing* **81**(3), 533–580.
- Glover, K. (1984). All optimal Hankel norm approximations of linear multivariable systems and their L_∞ -error bound. *Int. Journal of Control* **39**(6), 1115–1193.
- Gohberg, I., M. A. Kaashoek and L. Lerer (1992). *Time-Variant Systems and Interpolation*, Chapter : Minimality and Realization of Discrete Time-Varying Systems, pp. 261–296. Birkhäuser Verlag.
- Golub, G. H. and V. Pereyra (1973). The differentiation of pseudo-inverses and nonlinear least squares problems whose variables are separate. *SIAM Journal on Numerical Analysis* **10**(2), 413–432.

- Gómez, J. C. and E. Baeyens (2004). Identification of block-oriented nonlinear systems using orthonormal bases. *Journal of Process Control* **14**, 685–697.
- Gooderal, K. R. and R. B. Warfield (1989). *An introduction to Noncommutative Noetherian Rings*. Cambridge University Press.
- Gray, R. M. and D. L. Neuhoff (1998). Quantization. *IEEE Trans. on Information Theory* **44**(6), 2325–2383.
- Guidorzi, R. and R. Diversi (2003). Minimal representations of MIMO time-varying systems and realization of cyclostationary models. *Automatica* **39**(11), 1903–1914.
- Guidorzi, R. P. (1981). Invariants and canonical forms for systems structural and parametric identification. *Automatica* **17**(1), 117–133.
- Guillaume, P., J. Schoukens and R. Pintelon (1989). Sensitivity of roots to errors in the coefficient of polynomials obtained by frequency-domain estimation methods. *IEEE Trans. on Instrumentation and Measurement* **38**(6), 1050–1056.
- Hagenblad, A. (1999). *Aspects of identification of Wiener models*. Ph.D. thesis, Linköping university.
- Hakvoort, R. G. and P. M. J. Van den Hof (1997). Identification of probabilistic system uncertainty regions by explicit evaluation of bias and variance errors. *IEEE Trans. on Automatic Control* **42**(11), 1516–1528.
- Halanay, A. and V. Ionescu (1994). *Time-Varying Discrete Linear Systems: Input-Output Operators, Riccati Equations, Disturbance Attenuation*. Birkhäuser Verlag.
- Hallouzi, R., M. Verhaegen and S. Kanev (2006). Model weight estimation for FDI using convex fault models. In *Proc. of the 6th IFAC Symposium on Fault Detection, Supervision and Safety of Technical Processes*, Beijing, China (Aug.), pp. 847–852.
- Hanselmann, H. (1987). Implementation of digital controllers - A survey. *Automatica* **23**(1), 7–32.
- Hecker, S. and A. Varga (2006). Symbolic manipulation techniques for low order LFT-based parametric uncertainty modelling. *International Journal of Control* **79**(11), 1485–1494.
- Heuberger, P. S. C. (1990). *On Approximate System Identification with System Based Orthonormal Functions*. Ph. D. thesis, Delft University of Technology.
- Heuberger, P. S. C., P. M. J. Van den Hof and Bo Wahlberg (2005). *Modeling and Identification with Rational Orthonormal Basis Functions*. Springer-Verlag.
- Heuberger, P. S. C., P. M. J. Van den Hof and O. H. Bosgra (1995). A generalized orthonormal basis for linear dynamical systems. *IEEE Trans. on Automatic Control* **40**(3), 451–465.
- Hunt, K. J., R. Haas and R. Murray-Smith (1997). Design analysis of gain-scheduled local controller networks. *Int. Journal of Control* **66**(5), 619–651.

- Hyde, R. A. and K. Glover (1993). The application of scheduled \mathcal{H}_∞ controllers to a VSTOL aircraft. *IEEE Trans. on Automatic Control* **38**, 1021–1039.
- Ilchmann, A. and V. Mehrmann (2005). A behavioral approach to time-varying linear systems. Part 1: General theory. *SIAM Journal of Control Optimization* **44**(5), 1725–1747.
- Jain, A. K. and R. C. Dubes (1988). *Algorithms for Clustering Data*. Prentice Hall.
- Kailath, T. (1980). *Linear Systems*. Prentice Hall.
- Kalman, R. E. (1963). Mathematical description of linear dynamical systems. *SIAM Journal on Control* **1**, 152–192.
- Kamen, E. W., P. P. Khargonekar and K. R. Poolla (1985). A transfer-function approach to linear time-varying discrete-time systems. *SIAM Journal of Control and Optimization* **23**(4), 550–565.
- Kanev, S. (2006). Polytopic model set generation for fault detection and diagnosis. Technical report, Delft University of Technology, Delft Center for Systems and Control.
- Kaymak, U. and M. Setnes (2002). Fuzzy clustering with volume prototypes and adaptive cluster merging. *IEEE Trans. on Fuzzy Systems* **10**(6), 705–711.
- Kiriakidis, K. (2007). Nonlinear modeling by interpolation between linear dynamics and its application in control. *Journal of Dynamic Systems, Measurement, and Control* **129**(6), 813–824.
- Korba, P. (2000). *A Gain-Scheduling Approach to Model-Based Fuzzy control*. Ph. D. thesis, Universität Duisburg.
- Korba, P. and H. Werner (2001). Counter-example to ad-hoc off-equilibrium linearisation methods in gain-scheduling. In *Proc. of the 40th IEEE Conf. on Decision and Control*, Orlando, Florida, USA (Dec.), pp. 1342–1347.
- Krantz, S. G. (1999). *Handbook of Complex Variables*. Birkhäuser Verlag.
- Krishnapuram, R. and J. M. Keller (2000). A probabilistic approach to clustering. *IEEE Trans. on Fuzzy Systems* **1**, 98–110.
- Kulcsár, B., J. Bokor and J. Shinar (2008). Unknown input reconstruction for LPV systems. *Provisionally accepted to the IFAC International Journal of Robust and Nonlinear Control*.
- Kwiatkowski, A., H. Werner and M. T. Boll (2006). Automated generation and assessment of affine LPV models. In *Proc. of the 45th IEEE Conf. on Decision and Control*, San Diego, California, USA (Dec.), pp. 6690–6695.
- Lam, T. Y. (2000). On the equality of row rank and column rank. *Expositiones Mathematicae* **18**, 161–164.

- Lawrence, D. A. and W. J. Rugh (1995). Gain scheduling dynamic linear controllers for a nonlinear plant. *Automatica* **3**(31), 381–390.
- Lee, L. H. (1997). *Identification and Robust Control of Linear Parameter-Varying Systems*. Ph. D. thesis, University of California, Berkely.
- Lee, L. H. and K. R. Poolla (1996). Identification of linear parameter-varying systems via LFTs. In *Proc. of the 35th IEEE Conf. on Decision and Control*, Kobe, Japan (Dec.), pp. 1545–1550.
- Lee, L. H. and K. R. Poolla (1997). Identifiability issues for parameter-varying and multidimensional linear systems. In *Proc. of the ASME Design, Engineering Technical Conference*, Sacramento, California (Sep.).
- Leith, D. J. and W. E. Leithhead (1996). Appropriate realization of gain-scheduled controllers with application to wind turbine regulation. *International Journal of Control* **65**(2), 223–248.
- Leith, D. J. and W. E. Leithhead (1998a). Gain-scheduled controller design: An analytic framework directly incorporating non-equilibrium plant dynamics. *Int. Journal of Control* **70**, 249–269.
- Leith, D. J. and W. E. Leithhead (1998b). Gain-scheduled nonlinear systems: Dynamic analysis by velocity based linearization families. *Int. Journal of Control* **70**, 289–317.
- Leith, D. J. and W. E. Leithhead (1999). Comments on the prevalence of linear parameter varying systems. Technical report, Department of Electronic and Electrical Engineering, University of Strathclyde, Glasgow, Scotland.
- Lescher, F., J. Y. Zhao and A. Martinez (2006). Multiobjective $\mathcal{H}_2/\mathcal{H}_\infty$ control of a pitch regulated wind turbine for mechanical load reduction. In *Proc. of the European Wind Energy Conf.*, Athens, Greece (Feb.).
- Liu, K. (1997). Identification of linear time varying systems. *Journal of Sound and Vibration* **206**(4), 487–505.
- Ljung, L. (1999). *System Identification, theory for the user*. Prentice Hall.
- Ljung, L. (2006). *System Identification Toolbox, for use with Matlab*. The Mathworks Inc.
- Lovera, M. (1997). *Subspace Identification methods: theory and applications*. Ph. D. thesis, Department of Electronics and Information, Politecnico di Milano.
- Lovera, M. and G. Mercère (2007). Identification for gain-scheduling: a balanced subspace approach. In *Proc. of the American Control Conf.*, New York City, USA (July), pp. 858–863.
- Lovera, M., M. Verhaegen and C. T. Chou (1998). State space identification of MIMO linear parameter varying models. In *Proc. of the Int. Symposium on the Mathematical Theory of Networks and Systems*, Padova, Italy (July), pp. 839–842.

- Luenberger, D. G. (1967). Canonical forms of linear multivariable systems. *IEEE Trans. on Automatic Control* **12**(3), 290–293.
- Mäkilä, P. M. and J. R. Partington (1993). Robust approximate modeling of stable linear systems. *Int. Journal of Control* **58**(3), 665–683.
- Marcos, A. and G. J. Balas (2004). Development of linear-parameter-varying models for aircraft. *Journal of Guidance, Control and Dynamics* **27**(2), 218–228.
- Marcovitz, A. B. (1964). *Linear time-varying discrete time systems*. Lancaster, PA.: The Franklin Institute.
- Mårtensson, J. and H. Hjalmarsson (2007). Variance error quantification for identified poles and zeros. *Automatica*. Provisionally accepted.
- Mason, S. J. (1956). Feedback theory, further properties of signal flow graphs. *Proc. of the IRE* **44**(8), 920–926.
- Matz, G. and F. Hlawatsch (1998). Extending the transfer function calculus of time-varying linear systems: a generalized underspread theory. In *Proc. of the 23rd IEEE Int. Conf. on Acoustics, Speech, and Signal Processing*, Seattle, Washington, USA (May.), pp. 2189–2192.
- Mazzaro, M. C., E. A. Movsichoff and R. S. S. Pena (1999). Robust identification of linear parameter varying systems. In *Proc. of the American Control Conf.*, San Diego, California, USA (June), pp. 2282–2284.
- Middleton, R. H. and G. C. Goodwin (1990). *Digital Control and Estimation - A Unified Approach*. Prentice-Hall.
- Milanese, M. and A. Vicino (1991). Optimal estimation theory for dynamic systems with set membership uncertainty : An overview. *Automatica* **27**(6), 997–1009.
- Mizutani, K. and S. Miyamoto (2005). *Modeling Decisions for Artificial Intelligence*, Chapter : Possibilistic Approach to Kernel-Based Fuzzy *c*-Means Clustering with Entropy Regularization, pp. 144–155. Springer.
- Murray-Smith, R. and T. A. Johansen (1997). *Multiple Model Approaches to Modeling and Control*. Taylor and Francis.
- Murray-Smith, R., T. A. Johansen and R. Shorten (1999a). On the interpretation of local models in blended multiple model structures. *Int. Journal of Control* **72**(7-8), 620–628.
- Murray-Smith, R., T. A. Johansen and R. Shorten (1999b). On transient dynamics, off-equilibrium behavior and identification in blended multiple model structures. In *Proc. of the European Control Conf.*, Karlsruhe, Germany (Aug.).
- Nemani, M., R. Ravikanth and B. A. Bamieh (1995). Identification of linear parametrically varying systems. In *Proc. of the 34th IEEE Conf. on Decision and Control*, New Orleans, Louisiana, USA (Dec.), pp. 2990–2995.

- Neuman, C. P. and C. S. Baradello (1979). Digital transfer functions for microcomputer control. *IEEE Trans. on Systems, Man, and Cybernetics* **SMC-9**(12), 856–860.
- Nichols, R. A., R. T. Reichert and W. J. Rugh (1993). Gain scheduling for \mathcal{H} -infinity controllers: A flight control example. *IEEE Trans. on Control Systems Technology* **1**(2), 69–79.
- Niedźwiecki, M. (2000). *Identification of Time-Varying processes*. John Wiley and Sons.
- Ninness, B. and G. C. Goodwin (1995). Estimation of model quality. *Automatica* **31**(12), 1771–1797.
- Ninness, B. M. and J. C. Gómez (1996). Asymptotic analysis of MIMO systems estimates by the use of orthonormal basis. In *Proc. of the 13th IFAC World Congress*, San Francisco, California, USA (July), pp. 363–368.
- Ninness, B. M. and F. Gustafsson (1997). A unifying construction of orthonormal bases for system identification. *IEEE Trans. on Automatic Control* **42**(4), 515–521.
- Nobakhti, A. and N. Munro (2002). Eigenfitting: An alternative LPV modeling technique. In *Proc. of the 10th Mediterranean Conf. on Control and Automation*, Lisbon, Portugal (July).
- Oliveira e Silva, T. (1996). A n -width result for the generalized orthonormal basis function model. In *Proc. of the 13th IFAC World Congress*, Sydney, Australia (July), pp. 375–380.
- Packard, A. (1994). Gain scheduling via linear fractional transformations. *System Control Letters* **22**(2), 79–92.
- Packard, A. and G. Becker (1992). Quadratic stabilization of parametrically-dependent linear system using parametrically-dependent linear, dynamic feedback. *Advances in Robust and Nonlinear Control Systems* **DSC**(43), 29–36.
- Paijmans, B., W. Symens, H. Van Brussel and J. Swevers (2006). A gain-scheduling-control technique for mechatronic systems with position dependent dynamics. In *Proc. of the American Control Conf.*, Minneapolis, Minnesota, USA (June), pp. 2933–2938.
- Paijmans, B., W. Symens, H. Van Brussel and J. Swevers (2008). Interpolating affine LPV identification for mechatronic systems with one varying parameter. *European Journal of Control* **14**(1).
- Papageorgiou, G. (1998). *Robust Control System Design, \mathcal{H}_∞ Loop shaping and Aerospace Application*. Ph. D. thesis, University of Cambridge.
- Papageorgiou, G., K. Glover, G. D’Mello and Y. Patel (2000). Taking robust LPV control into flight on the VAAC Harrier. In *Proc. of the 39th IEEE Conf. on Decision and Control*, Sydney, Australia (Dec.), pp. 4558–4564.

- Park, B. P. and E. I. Verriest (1990). Canonical forms for linear time-varying multi-variable discrete systems. In *Proc. of the 28th Annual Allerton Conf. on Communication, Control, and Computers*, Urbana, Illinois, USA (Oct.).
- Peters, M. A. and P. A. Iglesias (1999). A spectral test for observability and reachability of time-varying systems and the Riccati difference equation. *SIAM Journal on Control and Optimization* **37**(5), 1330–1344.
- Pinkus, A. (1985). *n-Widths in Approximation Theory*. Springer-Verlag.
- Pintelon, R. and J. Schoukens (2001). *System Identification, A Frequency Domain Approach*. IEEE press.
- Polderman, J. W. and J. C. Willems (1991). *Introduction to Mathematical Systems Theory, A Behavioral Approach*. Springer.
- Pommaret, J. F. (2001). *Partial Differential Control Theory, vol. I, Mathematical tools*. Kluwer Academic Publishers.
- Prempain, E., I. Postlethwaite and A. Benchaib (2002). Linear parameter variant \mathcal{H}_∞ control design for an induction motor. *Control Engineering Practice* **10**(6), 663–644.
- Previdi, F. and M. Lovera (1999). Identification of a class of linear models with nonlinearly varying parameters. In *Proc. of the European Control Conf.*, Karlsruhe, Germany (Aug.).
- Previdi, F. and M. Lovera (2001). Identification of a class of nonlinear parametrically varying models. In *Proc. of the European Control Conf.*, Porto, Portugal (Sep.), pp. 3086–3091.
- Previdi, F. and M. Lovera (2003). Identification of a class of non-linear parametrically varying models. *Int. Journal on Adaptive Control and Signal Processing* **17**, 33–50.
- Previdi, F. and M. Lovera (2004). Identification of nonlinear parametrically varying models using separable least squares. *Int. Journal of Control* **77**(12), 1382–1392.
- Qin, W. and Q. Wang (2007). An LPV approximation for admission control of an internet web server: Identification and control. *Control Engineering Practice* **15**, 1457–1467.
- Rapisarda, P. and J. C. Willems (1997). State maps for linear systems. *SIAM Journal on Control and Optimization* **35**(3), 1053–1091.
- Raviv, R., K. M. Nagpal and P. P. Khargonekar (1991). \mathcal{H}_∞ control of linear time-varying systems: A state-space approach. *SIAM Journal on Control and Optimization* **29**(6), 1394–1413.
- Rosenbrock, H. H. (1963). The stability of linear time-dependent control systems. *Journal of Electronic Control* **15**, 73–80.

- Rugh, W. and J. Shamma (2000). Research on gain scheduling. *Automatica* **36**(10), 1401–1425.
- Rugh, W. J. (1991). Analytical framework for gain scheduling. *IEEE Control Systems Magazine* **11**(1), 79–84.
- Sakhnovich, L. A. (1997). *Interpolation theory and its applications*. Kluwer Academic, Dordrecht.
- Sbárbaro, D. and T. A. Johansen (1997). Multiple local Laguerre models for modeling nonlinear dynamic systems of the Wiener class. *IEEE Process Control Theory Applications* **144**(5), 375–380.
- Schalkoff, R. J. (1992). *Pattern Recognition: Statistical, Structural and Neural Approaches*. John Wiley and Sons.
- Scherer, C. W. (1996). Mixed $\mathcal{H}_2/\mathcal{H}_\infty$ control for time-varying and linear parametrically-varying systems. *Int. Journal of Robust and Nonlinear Control* **6**(9–10), 929–952.
- Scherer, C. W. (2001). LPV control and full block multipliers. *Automatica* **37**(3), 361–375.
- Scherer, C. W. and C. W. J. Hol (2006). Matrix sum-of-squares relaxations for robust semi-definit programs. *Mathematical Programming* **107**(1), 189–211.
- Setnes, M. (1999). Supervised fuzzy clustering for rule extraction. In *Proc. of the IEEE Int. Conference on Fuzzy Systems*, Seoul, South Korea (Aug.), pp. 1270–1274.
- Setnes, M. and R. Babuška (2001). Rule based reduction: some comments on the use of orthogonal transforms. *IEEE Trans. on Systems, Man and Cybernetics* **31**(2), 199–206.
- Shamma, J.S. and M. Athans (1992). Gain scheduling: potential hazards and possible remedies. *IEEE Control Systems Magazine* **12**(3), 101–107.
- Shamma, J. S. (1990). Analysis of gain scheduled control of nonlinear plants. *IEEE Trans. on Automatic Control* **35**(8), 898–907.
- Shamma, J. S. and M. Athans (1990). Analysis of gain scheduled control for nonlinear plants. *IEEE Trans. on Automatic Control* **35**(8), 898–907.
- Shamma, J. S. and M. Athans (1991). Guaranteed properties of gain-scheduled control for nonlinear-plants. *Automatica* **27**, 559–564.
- Shamma, J. S. and J. R. Cloutier (1993). Gain-scheduled missile autopilot design using linear-parameter varying transformations. *AIAA Journal of Guidance, Control and Dynamics* **16**(2), 256–263.
- Shin, J. Y. (2000). *Worst-Case Analysis and Linear Parameter-Varying Gain-Scheduled Control of Aerospace Systems*. Ph. D. thesis, University of Minnesota, Minneapolis.

- Shin, J. Y. (2007). Quasi-linear parameter varying representation of general aircraft dynamics over non-trim region. Technical report, NASA: Langley Research Center.
- Shin, J. Y., G. Balas and M. A. Kaya (2002). Blending methodology of linear parameter varying control synthesis of F-16 aircraft system. *Journal of Guidance, Control, and Dynamics* **25**(6), 1040–1048.
- Silverman, L. M. (1966). Transformation of time-variable systems to canonical (phase-variable) form. *IEEE Trans. on Automatic Control* **11**(2), 300–303.
- Silverman, L. M. (1971). Realization of linear dynamical systems. *IEEE Trans. on Automatic Control* **16**(6), 554–567.
- Silverman, L. M. and H. E. Meadows (1965). Degrees of controllability in time-variable systems. In *Proc. of the National Electronics Conf.*, Volume 21, Chicago (Oct.), pp. 689–693.
- Silverman, L. M. and H. E. Meadows (1967). Controllability and observability in time-variable linear systems. *SIAM Journal on Control* **5**, 64–73.
- Silverman, L. M. and H. E. Meadows (1969). Equivalent realizations of linear systems. *SIAM Journal on Applied Mathematics* **17**(2), 393–408.
- Skoog, R. A. and C. G. Lau (1972). Instability of slowly varying systems. *IEEE Trans. on Automatic Control* **17**(1), 86–92.
- Spong, M. (1987). Modeling and control of elastic joint robots. *Journal of dynamic systems, measurement, and control* **109**(4), 310–319.
- Sreedhar, N. and S. N. Rao (1968). Stability of linear time-varying systems. *Int. Journal of Control* **7**(6), 591–594.
- Stein, G. (1980). *Applications of Adaptive Control*, Chapter : Adaptive flight control - A pragmatic view. New York: Academic.
- Steinbuch, M., R. van de Molengraft and A. van der Voort (2003). Experimental modeling and LPV control of a motion system. In *Proc. of the American Control Conf.*, Denver, Colorado, USA (June), pp. 1374–1379.
- Stevens, B. L. and F. L. Lewis (2003). *Aircraft Control and Simulation*. John Wiley and Sons.
- Stilwell, D. J. and W. J. Rugh (2000). Stability preserving interpolation methods for synthesis of gain scheduled controllers. *Automatica* **36**(5), 665–671.
- Sturm, J. (1999). Using SeDuMi 1.02, a matlab toolbox for optimization over symmetric cones. *Optimization Methods and Software* **11-12**, 625–653.
- Sznaier, M., C. Mazzaro and T. Inanc (2000). An LMI approach to control oriented identification of LPV systems. In *Proc. of the American Control Conf.*, Chicago, Illinois, USA (June), pp. 3682–3686.

- Tan, W. (1997). Application of linear parameter-varying control theory. Master's thesis, University of California, Berkeley.
- Tan, W., A. Packard and G. Balas (2000). Quasi-LPV modeling and LPV control of a generic missile. In *Proc. of the American Control Conf.*, Chicago, Illinois, USA (June), pp. 3692–3696.
- Tóth, R., F. Felici, P. S. C. Heuberger and P. M. J. Van den Hof (2007). Discrete time LPV I/O and state space representations, differences of behavior and pitfalls of interpolation. In *Proc. of the European Control Conf.*, Kos, Greece (July), pp. 5418–5425.
- Tóth, R., F. Felici, P. S. C. Heuberger and P. M. J. Van den Hof (2008). Crucial aspects of zero-order-hold LPV state-space system discretization. In *Proc. of the 17th IFAC World Congress*, Seoul, Korea (July), pp. 3246–3251.
- Tóth, R. and D. Fodor (2004). Speed sensorless mixed sensitivity linear parameter variant H_∞ control of the induction motor. In *Proc. of the 43rd IEEE Conf. on Decision and Control*, Atlantis, Paradise Island, Bahamas (Dec.), pp. 4435–4440.
- Tóth, R., P. S. C. Heuberger and P. M. J. Van den Hof (2006a). Optimal pole selection for LPV system identification with OBFs, a clustering approach. In *Proc. of the 14th IFAC Symposium on System Identification*, Newcastle, Australia (Mar.), pp. 356–361.
- Tóth, R., P. S. C. Heuberger and P. M. J. Van den Hof (2006b). Orthonormal basis selection for LPV system identification, the Fuzzy-Kolmogorov c -Max approach. In *Proc. of the 45th IEEE Conf. on Decision and Control*, San Diego, California, USA (Dec.), pp. 2529–2534.
- Tóth, R., P. S. C. Heuberger and P. M. J. Van den Hof (2007). LPV system identification with globally fixed orthonormal basis functions. In *Proc. of the 46th IEEE Conf. on Decision and Control*, New Orleans, Louisiana, USA (Dec.), pp. 3646–3653.
- Tóth, R., P. S. C. Heuberger and P. M. J. Van den Hof (2008a). Asymptotically optimal orthonormal bases functions for LPV system identification. *Provisionally accepted for Automatica*.
- Tóth, R., P. S. C. Heuberger and P. M. J. Van den Hof (2008b). Flexible model structures for LPV identification with static scheduling dependency. *Accepted for the 47th IEEE Conf. on Decision and Control*.
- Tóth, R., P. S. C. Heuberger and P. M. J. Van den Hof (2008c). On the calculation of accurate uncertainty regions for estimated system poles and zeros. *Submitted*.
- van der Voort, A. (2002). *LPV control based on a pick-and-place unit*. Ph. D. thesis, Delft University of Technology.
- van Donkelaar, E. T. (2000). Improvement of efficiency in identification and model predictive control of industrial processes. Technical report, Delft University of Technology, Delft Center for Systems and Control.

- van Wingerden, J. W., F. Felici and M. Verhaegen (2007). Subspace identification of MIMO LPV systems using a piecewise constant scheduling sequence with hard/soft switching. In *Proc. of the European Control Conf.*, Kos, Greece (July), pp. 927–934.
- Varga, A., G. Looye, D. Moorman and G. Grübel (1998). Automated generation of LFT-based parametric uncertainty descriptions from generic aircraft models. *Mathematical and Computer Modelling of Dynamical Systems* **4**, 249–274.
- Verdult, V. (2002). *Nonlinear system identification: a state-space approach*. Ph. D. thesis, University of Twente.
- Verdult, V., N. Bergoer and M. Verhaegen (2003). Identification of fully parameterized linear and non-linear state-space systems by projected gradient search. In *Proc. of the 13th IFAC Symposium on System Identification*, Rotterdam, The Netherlands (Aug.), pp. 737–742.
- Verdult, V., L. Ljung and M. Verhaegen (2002). Identification of composite local linear state-space models using a projected gradient search. *Int. Journal of Control* **75**(16-17), 1125–1153.
- Verdult, V., M. Lovera and M. Verhaegen (2004). Identification of linear parameter-varying state space models with application to helicopter rotor dynamics. *Int. Journal of Control* **77**(13), 1149–1159.
- Verdult, V. and M. Verhaegen (2002). Subspace identification of multivariable linear parameter-varying systems. *Automatica* **38**(5), 805–814.
- Verdult, V. and M. Verhaegen (2004). Subspace identification of piecewise linear systems. In *Proc. of the 43rd IEEE Conf. on Decision and Control*, Atlantis, Paradise Island, Bahamas (Dec.), pp. 3838–3843.
- Verdult, V. and M. Verhaegen (2005). Kernel methods for subspace identification of multivariable LPV and bilinear systems. *Automatica* **41**(9), 1557–1565.
- Verhaegen, M. (1994). Identification of the deterministic part of MIMO state space models given in innovations form from input-output data. *Automatica* **30**(1), 61–74.
- Verhaegen, M. and P. Dewilde (1992). Subspace model identification Part 1: The output-error state-space model identification class of algorithms. *Int. Journal of Control* **56**(5), 1187–1210.
- Verhaegen, M. and X. Yu (1995). A class of subspace model identification algorithms to identify periodically and arbitrary time-varying systems. *Automatica* **31**(2), 201–216.
- Vuerinckx, R., R. Pintelon, J. Schoukens and Y. Rolain (2001). Obtaining accurate confidence regions for the estimated zeros and poles in system identification problems. *IEEE Trans. on Automatic Control* **46**(4), 656–659.

- Wassink, M. G., M. van de Wal, C. W. Scherer and O. Bosgra (2004). LPV control for a wafer stage: Beyond the theoretical solution. *Control Engineering Practice* **13**, 231–245.
- Wei, X. (2006). *Adaptive LPV techniques for Diesel Engines*. Ph. D. thesis, Johannes Kepler University, Linz.
- Wei, X. and L. Del Re (2006). On persistent excitation for parameter estimation of quasi-LPV systems and its application in modeling of diesel engine torque. In *Proc. of the 14th IFAC Symposium on System Identification*, Newcastle, Australia (Mar.), pp. 517–522.
- Weiss, G. (2005). Memoryless output nullification and canonical forms, for time varying-systems. *Int. Journal of Control* **78**(15), 1174–1181.
- Whatley, M. J. and D. C. Pot (1984). Adaptive gain improves reactor control. *Hydrocarbon Processing*, 75–78.
- Wijnheijmer, F., G. Naus, W. Post, M. Steinbuch and P. Teerhuis (2006). Modeling and LPV control of an electro-hydraulic servo system. In *Proc. of the IEEE International Conf. on Control Applications*, Munich, Germany (Oct.), pp. 3116–3120.
- Willems, J. C. (2007). The behavioral approach to open and interconnected systems. *IEEE Control Systems Magazine* **27**(6), 2–56.
- Wood, G. D., P. J. Goddard and I. Glover (1996). Approximation of linear parameter-varying systems. Kobe, Japan (Dec.), pp. 406–411.
- Wu, F. and K. Dong (2006). Gain-scheduling control of LFT systems using parameter-dependent Lyapunov functions. *Automatica* **42**(1), 39–50.
- Xie, X. L. X. and G. Beni (1991). A validity measure for fuzzy clustering. *IEEE Trans. on Pattern Analysis and Machine Intelligence* **13**(8), 841–847.
- Yaz, E. and X. Niu (1989). Stability robustness of linear discrete-time systems in the presence of uncertainty. *Int. Journal of Control* **50**(1), 173–182.
- Yen, J. and L. Wang (1999). Simplifying fuzzy rule-based models using orthogonal transformation methods. *IEEE Trans. on Systems, Man and Cybernetics* **29**(1), 13–24.
- Young, J. (2002). *Gain scheduling for geometrically nonlinear flexible space structures*. Ph. D. thesis, Massachusetts Institute of Technology.
- Zenger, K. and R. Ylinen (2005). Pole placement of time-varying state space representations. In *Proc. of the 44th IEEE Conf. on Decision and Control*, Seville, Spain (Dec.), pp. 6527–6532.
- Zerz, E. (2006). An algebraic analysis approach to linear time-varying systems. *IMA Journal of Mathematical Control and Information* **23**, 113–126.
- Zhou, K. and J. C. Doyle (1998). *Essentials of Robust Control*. Prentice-Hall.

Summary

The constant need to improve efficiency of plants and processes in terms of performance or energy consumption challenges the system identification field to provide simple but more accurate models of physical/chemical phenomena. This leads to the need of system descriptions of nonlinear/time-varying plants that go beyond the framework of *Linear Time-Invariant* (LTI) systems. The model class of *Linear Parameter-Varying* (LPV) systems provides an attractive candidate for this purpose. The philosophy of LPV systems is to represent the physical reality as a set of LTI systems from which one is selected at every time instance to describe the continuation of the signal trajectories. This selection is based on the variation of an external signal of the system called the *scheduling variable*. The LPV system class has a wide representation capability of physical processes and is supported by a well worked-out and industrially reputed control theory.

Despite the advances of the LPV control field, identification/modeling of plants in an LPV form based on measured data is still not well-developed. The main problem is that a unified view on LPV system identification is missing as most methods only focus on the estimation of models in particular model structures. The question whether the used model structure is an adequate choice for the plant is commonly left unanswered. Furthermore, it is not well understood how a given nonlinear system can be efficiently described by a LPV model. Often extensions of classical LTI identification methods are used for the LPV case, but these approaches are applied as an optimization tool instead of estimation in a stochastic sense. Most methods have significant computational load, that makes their practical use difficult. There is even not a well-accepted definition of the concept of an LPV system. The question whether different LPV model representations are equivalent or how they are related is generally left unanswered due to the lack of a well-founded LPV system theory.

The aim of this thesis is to find solutions for these problems by focusing on the development of an LPV identification framework that provides reliable LPV model estimates with low computational load. In order to establish such a framework, it is first necessary to understand how different model structures relate to each other and what type of dynamical relation they describe. When analyzing system equivalence between different models and system representations it turns out that time-shifted versions/derivatives of the scheduling signal (dynamic dependence) need to be taken into account.

In order to construct a parametrization-free description of LPV systems, a behavioral approach is introduced in this thesis that serves as a solid basis for specifying system theoretic properties. This behavioral setting yields a framework that enables a unified view on the concepts of LPV identification and control. LPV systems are defined as the collection of valid trajectories of system variables (like inputs and outputs) and scheduling variables. Kernel, input-output, and state-space representations are introduced as well as appropriate equivalence transformations between these representations, both in discrete and continuous time. Using the developed framework it is shown that - similar to LTI systems - asymptotically stable LPV systems have a convergent series expansion representation in terms of *Orthonormal Basis Functions* (OBFs). This observation supports the use of such models for identification purposes.

In order to understand how nonlinear first-principle models can be used to facilitate LPV model structure selection in discrete-time, based on prior information, the discretization of LPV systems is investigated in a zero-order-hold setting. Complete and approximative methods are explored together with criteria to choose adequate sampling times. As a major contribution, an algorithm is developed to convert nonlinear differential equations into LPV system representations. The algorithm induces the selection of suitable scheduling signals.

Building on the previously introduced tools and concepts, an identification framework is introduced in a well-established sense that uses truncated LPV series expansions in terms of OBFs as model structures. Such models have attractive properties in identification and they are general approximations of nonlinear systems with fading memory. Identification approaches based on several different OBF model structures are developed and analyzed in an LPV prediction-error framework. The general idea of OBFs based identification results in a two-step procedure, where first the OBFs are selected, based on measured data or first-principle information. This basis selection is accomplished by a combination of fuzzy clustering of estimated pole locations. For the estimation two approaches are proposed:

- A local method, using locally identified LTI models (constant scheduling) followed by interpolation of the resulting model coefficients.
- A global approach, based on linear regression using varying scheduling signals.

The developed framework provides an efficient (in terms of reliability and complexity) LPV identification approach from model structure selection till delivering the model estimate. Issues of variance and bias are investigated, extending the classical results of the LTI framework. Besides the practical investigation of the presented results, exploration of the other steps of the identification cycle, like experiment design and validation is targeted for future research in the LPV framework.

Samenvatting

De hedendaagse systeem en regeltechniek wordt gekenmerkt door een voortdurende vraag naar efficiëntieverhoging van de beschouwde processen en systemen in termen van prestatie of energieverbruik. Voor het gebied van de systeemidentificatie betekent dit een vraag naar meer accurate, maar tegelijkertijd eenvoudige, modellen van fysisch/chemische processen. Het klassieke raamwerk van *Lineaire Tijd-Invariante* (LTI) systemen dient daartoe te worden uitgebreid om ook niet-lineaire en tijdvariërende processen accuraat te kunnen beschrijven. De klasse van *Lineaire Parameter-Variërende* (LPV) systemen vormt een aantrekkelijke kandidaat voor deze uitbreiding. Het idee achter deze klasse van modellen is de weergave van de fysische realiteit als een verzameling LTI systemen, waaruit op elk moment één wordt gekozen voor de beschrijving van de systeemdynamica. Deze keuze is gebaseerd op een extern systeemsignaal, aangeduid als de *scheduling variabele*. Met deze klasse van LPV systemen kan een breed spectrum van fysische processen op adequate wijze beschreven worden. Daarbij is van belang dat er een uitgebreide en goed gefundeerde theorie beschikbaar is voor het regelen van deze systemen.

Daartegenover staat dat de theorie rond het modelleren en identificeren van deze systemen nog niet goed ontwikkeld is. De gebruikte methodieken zijn meestal generalisaties van LTI identificatiemethoden en focussen vaak op zeer specifieke modelstructuren, zonder afdoende motivatie en inzicht in de onderliggende problematiek. Daarnaast wordt nauwelijks aandacht besteed aan de vraag hoe en in hoeverre een niet-lineair proces op efficiënte wijze gemodelleerd kan worden als een LPV systeem. Diverse methoden vergen een grote rekentechnische inspanning, wat praktische toepassing belemmert. Een fundamenteel probleem is dat er geen algemeen aanvaarde definitie van LPV systemen voorhanden is en dat het onduidelijk is in hoeverre de gebruikte definities en representaties met elkaar overeenkomen of juist niet. In feite ontbreekt het aan een goede gefundeerde LPV systeemtheorie.

Het doel van dit proefschrift is om oplossingen voor deze problematiek aan te dragen, waarbij de aandacht met name ligt op het ontwikkelen van een goed gestructureerd LPV identificatie-raamwerk, waarmee betrouwbare LPV modellen kunnen worden bepaald met een beperkte rekentechnische inspanning. Hiervoor is het essentieel om inzicht te verkrijgen in de relaties tussen de verschillende modelstructuren en de dynamica die door deze structuren beschreven wordt. Uit de analyse van deze problematiek volgt dat equivalentie tussen de verschillende

model- en systeemrepresentaties alleen mogelijk is indien er wordt uitgegaan van zogenaamde dynamische afhankelijkheid van het scheduling signaal. Dit betekent dat niet alleen de instantane waarde van dit signaal van belang is, maar ook afgeleiden, dan wel in de tijd verschoven waarden een rol spelen.

In dit proefschrift wordt een niet-parametrische beschrijving van LPV systemen, de zogenaamde *behavioral approach*, geïntroduceerd en geanalyseerd. Dit leidt tot een solide raamwerk voor het beschrijven van systeemtheoretische eigenschappen en maakt het mogelijk om te komen tot een algemene theorie van identificatie en regeling van LPV systemen. Deze systemen worden in dit raamwerk beschreven als een verzameling van alle mogelijk signalen (zoals input-, output- en scheduling signalen). Er worden diverse representaties geïntroduceerd en geanalyseerd, zowel in het continue als discrete tijddomein en de transformaties tussen deze representaties worden beschreven. Met dit raamwerk wordt aangetoond dat LPV systemen beschreven kunnen worden door middel van een reeksontwikkeling in termen van *Orthogonale Basis Functies* (OBF's). Dit resultaat maakt het mogelijk om efficiënte modelstructuren te ontwikkelen die toegepast kunnen worden bij het identificeren van LPV systemen.

Cruciaal bij de keuze van een LPV modelstructuur is inzicht in de mogelijke vertaling van niet-lineaire relaties en modelbeschrijvingen, mogelijk in continue tijd, naar een LPV vorm. In dit kader is de discretisatie van LPV systemen onderzocht, waarbij zowel complete als benaderende methoden zijn verkend en criteria voor adequate sampletijden zijn afgeleid. Een belangrijke bijdrage is een algoritme waarmee niet-lineaire differentiaalvergelijkingen worden getransformeerd naar een LPV formulering, inclusief de keuze van de scheduling signalen.

Met behulp van de ontwikkelde concepten is een raamwerk ontwikkeld voor de identificatie van LPV systemen, dat gebruik maakt van modelstructuren gebaseerd op reeksontwikkelingen in termen van OBF's. Deze structuren hebben aantrekkelijke eigenschappen en zijn tevens geschikt voor het benaderen van een brede klasse van niet-lineaire systemen. Er zijn meerdere identificatiealgoritmes op basis van deze modestructuren ontwikkeld en geanalyseerd. Deze methoden worden gekenmerkt door een aanpak in 2 stappen. Hierbij worden eerst de basisfuncties geselecteerd op basis van meetdata, voorkennis of fysisch inzicht. Deze selectiestap maakt gebruik van fuzzy clustering technieken. In de tweede stap worden modellen geschat. Daarbij worden twee aanpakken onderscheiden:

- Een locale aanpak, waarbij eerst een aantal LTI modellen geschat wordt voor contante scheduling signalen. Door middel van interpolatie van de modelcoëfficiënten wordt vervolgens een LPV model bepaald.
- Een globale methode, waarbij de relatie van de modelcoëfficiënten met de scheduling variabele eerst op lineaire wijze wordt geparametriseerd, en waarbij de resulterende parameters worden geschat op basis van globale meetdata, met een variërend scheduling signaal.

Dit raamwerk resulteert in een efficiënte LPV identificatieprocedure, vanaf de keuze van modelstructuur tot het schatten van modellen. Toekomstig onderzoek zal gericht zijn op de praktische toepassing van de ontwikkelde concepten, evenals op andere belangrijke onderdelen van het identificatieproces, zoals experimentontwerp en modelvalidatie.

List of Symbols

Operators

q	Forward time shift
$\frac{d}{dt}$	Differentiation
ϱ_-	Shift and cut
ϱ_+	Inverse shift and cut
Σ_-	Shift map
\diamond	Function evaluation along a trajectory
\oplus	Direct sum
\odot	Element by element product
\boxplus	Addition on \mathcal{R}
\boxtimes	Multiplication on \mathcal{R}
$\langle \cdot, \cdot \rangle$	Inner product
$[\cdot]_{ij}$	Element of the i -th row and j -th column
\cdot^T	Transposition
\cdot^*	Complex conjugate
\cdot^{-1}	Inverse
$\succ, (\succeq)$	Positive (semi)-definite
$\succ, (\preceq)$	Negative (semi)-definite
Re	Real part
Im	Imaginary part
inf	Infinum
sup	Supremum
min	Minimum
max	Maximum
var	Variance
$\mathcal{E}\{\cdot\}$	Mean/Expectation
$\bar{\mathcal{E}}\{\cdot\}$	Generalized expectation

\dim	Dimension
\det	Determinant
adj	Matrix adjoint
diag	Diagonal matrix operator
span	Algebraic span
$\text{span}_{\mathbb{R}}^{\text{row}}$	Row span on the ring $\mathbb{R}[\xi]$, subspace in $\mathbb{R}[\xi]^{\times}$.
$\text{span}_{\mathcal{R}}^{\text{row}}$	Row span on the ring $\mathcal{R}[\xi]$, subspace in $\mathcal{R}[\xi]^{\times}$.
$\text{span}_{\mathcal{R}}^{\text{col}}$	Column span on the ring $\mathcal{R}[\xi]$, subspace in $\mathcal{R}[\xi]^{\times}$.
grad	Gradient
card	Cardinality
col	Column composition
deg	Degree
rank	Rank
$\text{module}_{\mathbb{R}[\xi]}$	Left module in $\mathbb{R}[\xi]^{\times}$.
$\text{module}_{\mathcal{R}[\xi]}$	Left module in $\mathcal{R}[\xi]^{\times}$.
\bigwedge_t	Concatenation of signals at time instant t
\mathcal{L}	Laplace transformation
\mathcal{Z}	Z-transformation

Geometrical objects

E	Euclidian line
L	i-line
H	h-line
K	Euclidian circle
K_h	Hyperbolic circle
D	Euclidean disc
D_h	Hyperbolic disc
\mathcal{D}	Set of Euclidian discs
e	Euclidian center
r	Euclidian radius
e_h	Hyperbolic center
r_h	Hyperbolic radius
x, y, z, u, v	Points
φ_h	Hyperbolic coefficient
γ_h	Hyperbolic angle
\mathfrak{h}_H	Hyperbolic inversion with respect to H
\mathfrak{h}_x	Hyperbolic inversion s.t. $\mathfrak{h}_x(z) = 0$

\mathcal{Z} Hyperbolic coverage

Dynamical systems

\mathcal{G} Dynamical system
 \mathcal{G}_L Dynamical system with latent variables
 \mathcal{G}_{NL} Nonlinear dynamical system
 \mathcal{G}_P Parameter-varying dynamical system
 \mathcal{G}_{PL} Parameter-varying dynamical system with latent variables
 \mathcal{S} LPV system
 \mathcal{F} LTI system
 \mathcal{F} LTI system set
 \mathcal{F}_P Frozen system set of an LPV system

Behaviors

\mathfrak{B} Behavior
 \mathfrak{B}_L Latent Behavior
 \mathfrak{B}_{SS} State-space Behavior
 $\mathfrak{B}_{\bar{p}}$ Frozen behavior for constant scheduling \bar{p}
 \mathfrak{B}_P Scheduling behavior (projected)
 \mathfrak{B}_w Signal behavior (projected)
 \mathfrak{B}_x Sate signal behavior (projected)
 \mathfrak{B}_p Projected behavior on a scheduling trajectory

Representations and models

$\mathfrak{R}_{SS}(\cdot)$ State-space system representation
 $\mathfrak{R}_{SS}^\top(\cdot)$ Transpose of a state-space system representation
 $\mathfrak{R}_{SS}^O(\cdot)$ State-space representation, observability
 $\mathfrak{R}_{SS}^R(\cdot)$ State-space representation, reachability
 $\mathfrak{R}_{SS}^{Oc}(\cdot)$ State-space representation, companion-observability
 $\mathfrak{R}_{SS}^{Rc}(\cdot)$ State-space representation, companion-reachability
 $\mathfrak{R}_{SS}^{OLTI}(\cdot)$ State-space representation, observability, generated via LTI rules
 $\mathfrak{R}_{SS}^{RLTI}(\cdot)$ State-space representation, reachability, generated via LTI rules
 $\mathfrak{R}_{IO}(\cdot)$ Input-output representation
 $\mathfrak{R}_K(\cdot)$ Kernel representation
 $\mathfrak{R}_{IM}(\cdot)$ Impulse response representation
 $\mathfrak{R}_{OBF}(\cdot)$ OBF expansion representation
 $\mathfrak{M}_W(\cdot)$ Wiener LPV OBF model

$\mathfrak{M}_H(\cdot)$	Hammerstein LPV OBF model
$\mathfrak{M}_{WF}(\cdot)$	Wiener feedback LPV OBF model
$\mathfrak{M}_{HF}(\cdot)$	Hammerstein feedback LPV OBF model

Equivalence classes, transformations

\mathcal{E}	Equivalence class, LTI
\mathcal{E}^{n_P}	Equivalence class, LPV
\mathcal{E}_{IO}	Equivalence class of IO representations, LTI
$\mathcal{E}_{IO}^{n_P}$	Equivalence class of IO representations, LPV with $\dim(\mathbb{P}) = n_P$
\mathcal{E}_{SS}	Equivalence class of SS representations, LTI
$\mathcal{E}_{SS}^{n_P}$	Equivalence class of SS representations, LPV with $\dim(\mathbb{P}) = n_P$
\mathcal{E}_{can}	Set of canonical representations, LTI
$\mathcal{E}_{can}^{n_P}$	Set of canonical representations, LPV with $\dim(\mathbb{P}) = n_P$
\sim	Equivalence relation, LTI
$\overset{n_P}{\sim}$	Equivalence relation, LPV with $\dim(\mathbb{P}) = n_P$
T	State-transformation
T_o	State-transformation, observability
T_{co}	State-transformation, companion-observability
T_r	State-transformation, reachability
T_{cr}	State-transformation, companion- reachability

Signals and variables

w	System signal
w_L	Latent system signal
u	Input signal
y	Output signal
x	State signal
p	Scheduling variable
x_o	State signal (observability canonical)
x_r	State signal (reachability canonical)
u_d, y_d, x_d, p_d	Discretized signals
h	Impulse response
\bar{p}	Point of the scheduling space
ξ	Indeterminate variable, time operator
ζ	Indeterminate variable, scheduling dependence
ω	Frequency
Δ	Lagrangian

δ	Lagrangian variable
ϵ	Noise/error/residual
v, e	Noise, stochastic process
$\mathcal{C}_y, \mathcal{C}_{yu}$	(Cross)-covariance
$\Phi_y(e^{i\omega}), \Phi_{yu}(e^{i\omega})$	(Cross)-power spectral densities
ϵ_k	Local unit truncation error (k^{th} -interval)
η_k	Global error (k^{th} -interval)
ϵ_*	Maximal local unit truncation error
η_*	Maximal global error
ϵ_{\max}	Acceptable maximal local unit truncation error
η_{\max}	Acceptable maximal global error

Functions

R, P, X	Polynomial matrix functions
M	Polynomial matrix function, unimodular
R_u	Polynomial matrix function, input side
R_y	Polynomial matrix function, output side
R_L	Polynomial matrix function, latent side
R_{com}	Common divisor of polynomial matrix functions
R_A, \dots, R_F	Polynomial functions, classical model parameterization
F	Transfer function
F_0	Transfer function of the nominal model
Q	Transfer function associated with noise
Q_0	Transfer function of the noise part of the nominal model
G	Inner function
M	Transfer function vector
\mathfrak{F}	Transfer functions set
$\mathfrak{F}_{\mathbb{F}}$	Transfer functions set of frozen behaviors
$\mathfrak{A}(\cdot, \cdot)$	Transition matrix
\mathcal{V}	Lyapunov function
J	Cost-function
ϕ	Orthonormal basis function
Φ_n	Orthonormal basis function set with n elements
$\Phi_{n_g}^{n_e}$	Hambo functions generated by a G with n_g poles and n_e extensions
μ	Membership function
\mathcal{W}	Criterion function
ψ	Functionals defining coefficient dependency in a model parametrization

Ψ	Set of functionals defining coefficient dependency
g	Scheduling function
$1(\cdot)$	Unit step (Heaviside) function

Spaces and fields

\mathbb{T}	Time axis
\mathbb{V}	Clustering space
\mathbb{W}	Signal space
\mathbb{W}_L	Latent signal space
\mathbb{R}	Set of real numbers
$\mathbb{R}^+, \mathbb{R}^-, \mathbb{R}_0^+, \mathbb{R}_0^-$	Positive (negative) real numbers with or without zero
\mathbb{Z}	Set of integers
$\mathbb{Z}^+, \mathbb{Z}^-, \mathbb{Z}_0^+, \mathbb{Z}_0^-$	Positive (negative) integers with or without zero
\mathbb{C}	Set of complex numbers
\mathbb{N}	Set of natural numbers
\mathbb{D}	Unit disk
\mathbb{J}	Unit circle
\mathbb{E}	Exterior of the unit disk
\mathbb{X}	State-space
\mathbb{U}	Input-space
\mathbb{Y}	Output-space
$\mathbb{I}_{n_1}^{n_2}$	Index set $[n_1, \dots, n_2]$
\mathbb{P}	Scheduling domain
$\mathbb{W}^{\mathbb{T}}$	Collection of all maps from \mathbb{T} to \mathbb{W}
$\mathbb{P}^{\mathbb{T}}$	Collection of all maps from \mathbb{T} to \mathbb{P}
$(\mathbb{W} \times \mathbb{P})^{\mathbb{T}}$	All signals and schedulings
\mathcal{M}	Subspace
$\check{\mathcal{M}}$	Optimal Subspace
\mathcal{M}	Set of subspaces with the same dimension
\mathcal{U}	Membership space
\mathcal{I}^{\emptyset}	Singularity set, set of indices
\mathcal{I}	Set of indices
\mathcal{D}	Hyperbolic group
\mathcal{H}_2	Space of proper functions square integrable on \mathbb{J}
\mathcal{H}_{2-}	Space of strictly proper functions square integrable on \mathbb{J}
\mathcal{H}_2^{\perp}	Complementer of \mathcal{H}_2
$\mathcal{H}_2(\mathbb{E})$	Space of all \mathcal{H}_2 functions that are analytic in \mathbb{E}

$\mathcal{H}_2(\mathbb{C}^+)$	Space of all \mathcal{H}_2 functions that are analytic in \mathbb{C}^+
$\mathcal{H}_{2-}(\mathbb{E})$	Space of all \mathcal{H}_{2-} functions that are analytic in \mathbb{E}
$\mathcal{RH}_{2-}(\mathbb{E})$	Space of all real \mathcal{H}_{2-} functions that are analytic in \mathbb{E}
\mathcal{R}_n	Field of meromorphic functions with n variables
$\bar{\mathcal{R}}_n$	Subset of \mathcal{R}_n , non-eliminatable n^{th} variable
\mathcal{R}	Field of meromorphic functions with finite many variables
$\mathcal{R} _{n_{\mathbb{P}}}$	Field of meromorphic functions with maximum $n_{\mathbb{P}}$ variables
$\mathbb{R}[\xi]$	Ring of polynomials in indeterminant ξ
$\mathcal{R}[\xi]$	Ring of polynomials with meromorphic coefficients
\mathcal{C}^∞	Space of infinity differentiable functions
L_1^{loc}	Space of locally integrable functions
$\mathcal{U}(n_1, n_2)$	Uniform distribution on interval $[n_1, n_2]$
$\mathcal{N}(n_1, n_2)$	Normal distribution with mean n_1 and variance n_2

Poles and Eigenvalues

σ	Singular value
$\bar{\sigma}$	Maximal singular value
$\underline{\sigma}$	Minimal singular value
λ	System pole
Ω	Pole region
$\Omega_{\mathbb{P}}$	Pole manifest region
\mathcal{P}	Pole uncertainty region
Λ	Set of poles
\check{R}	characteristic polynomial

Measures and Norms

$\ \cdot\ _n$	n^{th} vector norm
$\ell_n(\cdot)$	n^{th} -signal norm
S_s	Similarity measure
S_e	Normalized entropy
χ	Xie-Beni validity measure
π	Kolmogorov distance
κ_1	Kolmogorov measure
κ_n	Kolmogorov cost n -width
d	Dissimilarity measure
$d_{\mathcal{H}_2}$	Distance on \mathcal{H}_2

Coefficients, constants, and rates

A, B, C, D	State-space matrices
A_o, B_o, C_o, D_o	State-space matrices, observability canonical
A_r, B_r, C_r, D_r	State-space matrices, reachability canonical
$A_{co}, B_{co}, C_{co}, D_{co}$	State-space matrices, companion-observability canonical
$A_{cr}, B_{cr}, C_{cr}, D_{cr}$	State-space matrices, companion-reachability canonical
A_d, B_d, C_d, D_d	Discretized state-space matrices
α, β	State-space matrix elements
α^o, β^o	State-space matrix elements, observability canonical
α^r, β^r	State-space matrix elements, reachability canonical
α^{co}, β^{co}	State-space matrix elements, companion-observability canonical
α^{cr}, β^{cr}	State-space matrix elements, companion-reachability canonical
a, b	IO representation coefficients
R	Reachability gramian
O	Observability gramian
O_n	Observability matrix, n -step
\mathcal{R}_n	Reachability matrix, n -step
o	Observability matrix element
r	Reachability matrix element
θ	Parameter vector
θ_0	Parameter vector associated with the true system
θ^*	Asymptotic parameter vector estimate
$\hat{\theta}_{N_d}$	Parameter vector estimate, based on N_d samples
Θ	Parameter vector space
\mathcal{E}	Ellipsoidal parameter uncertainty region
g, h	Markov parameters (of the noise model)
H	Hankel/Toeplitz matrix
T_d	Discretization time
\check{T}_d	Stability upperbound of T_d
\hat{T}_d	Performance upperbound of T_d
m	Fuzzyness
\mathcal{O}	Rate of convergence
ρ	Convergence rate of the series expansion
$\check{\rho}$	Worst-case convergence rate of the series expansion
γ	Regressor vector
Γ	Regressor matrix
i	Imaginary unit

$M^{(n)}$	N-sensitivity constant, n -th order
M_x^{\max}	Maximal amplitude of x over all trajectories
k_s	Spring constant
S_u, S_y, S_w, S_x, S_p	Selector matrices
Z	Data for clustering
v	Cluster center
V	Vector of cluster centers
U	Membership matrix
w	Coefficient in OBF models / expansion coefficient
v	Coefficient in OBF models (feedback)
W, V	Coefficient matrices in OBF models
Q	Set of grid points
Q_+	Set of grid points inside a region
Q_-	Set of grid points outside a region
ε	Threshold value
ε_s	Similarity threshold
ε_a	Adaptive threshold
ε_t	Termination threshold
α	Confidence level

Dimensions

n_w	Signal dimension
n_u	Input dimension
n_y	Output dimension
n_x	State dimension
n_p	Scheduling dimension
n_r	Dimension of a differential equation (number of equations)
n_L	Dimension of the latent variables
n_ξ	Maximal power of ξ
n_ζ	Maximal power of ζ
n_g	Inner function dimension
n_e	Number of bases extension
n_a	Order of the denominator polynomial
n_b	Order of the nominator polynomial
n_c	Number of clusters
n_θ	Parameter vector dimension
n_{loc}	Number of local models

n_ψ	Number of used functions in dependency parameterization
n_w	Dimension of w
n_v	Dimension of v
n^\emptyset	Number of singularity points
N_z	Number of data points for clustering
N_{av}	Average number of iterations
N_d	Data record length
N_p	Number of linearization/scheduling points (basis selection)
N_{loc}	Number of linearization / scheduling points (identification)

Data sets

P	Linearization points/ identification points
\mathcal{D}	Data record

List of Abbreviations

ACM	Adaptive Cluster Merging
ARMAX	Auto-Regressive Moving-Average model with eXogenous variable
ARX	Auto-Regressive model with eXogenous variable
BFT	Best Fit Rate
BIBO	Bounded-Input Bounded-Output (stability)
BJ	Box-Jenkins (model)
CT	Continuous Time
DE	Differential Equation
DF	Difference Equation
DT	Discrete Time
FcM	Fuzzy <i>c</i> -Means
FIR	Finite Impulse Response
FKcM	Fuzzy Kolmogorov <i>c</i> -Max
GOBF	General Orthonormal Basis Function
H-LPV OBF	Hammerstein Linear Parameter-Varying OBF (model)
HF-LPV OBF	Hammerstein Feedback Linear Parameter-Varying OBF (model)
IIR	Infinite Input Response
IRR	Impulse Response Representation
IO	Input-Output
KM	Kolmogorov Metric
K_nW	Kolmogorov <i>n</i> -Width
KR	Kernel Representation
LFT	Linear Fractional Transform

LMI	Linear Matrix Inequalities
LPV	Linear Parameter-Varying
LS	Least Squares (criterion)
LSDP	Linear Semidefinite Programming
LTI	Linear Time-Invariant
LTV	Linear Time-Varying
LUT	Local Unit Truncation (error)
MSE	Mean Squared Error
MIMO	Multiple-Input Multiple-Output
MISO	Multiple-Input Single-Output
MOESP	Multivariable Output Error State-Space (algorithm)
NH	Nonlinear Hammerstein (model)
NL	Nonlinear
NW	Nonlinear Wiener (model)
OBF	Orthonormal Basis Function
ODE	Ordinary Differential Equation
OE	Output Error (model)
PE	Persistency of Excitation
pdf	Probability Density Function
PV	Parameter-Varying
QC	Quadratic Constraint
ROC	Region of Convergence
SISO	Single-Input Single-Output
SIMO	Single-Input Multiple-Output
SNR	Signal to Noise Ratio
SoS	Sum of Squares
SS	State-Space
TS	Takagi-Sugeno (model)
TV	Time-Varying
VAF	Variance Accounted For
W-LPV OBF	Wiener Linear Parameter-Varying OBF (model)
WF-LPV OBF	Wiener Feedback Linear Parameter-Varying OBF (model)
ZOH	Zero-Order-Hold

List of Publications

Accepted journal papers

- R. Tóth, P. S. C. Heuberger, and P. M. J. Van den Hof (2008). Asymptotically Optimal Orthonormal Bases Functions for LPV System Identification. *Provisionally accepted for Automatica*.
- R. Tóth and D. Fodor (2006). Speed Sensorless Mixed Sensitivity Linear Parameter Variant H_∞ Control of the Induction Motor. *Journal of Electrical Engineering*. **6(4)**, 12–000.
- R. Tóth (2004). Simulation results on the asymptotic periodicity of compartmental systems with lags. *Functional Differential Equations*. **11(1-2)**, 195–202.

Conference proceedings

- R. Tóth, P. S. C. Heuberger, and P. M. J. Van den Hof (2008). Flexible model structures for LPV identification with static scheduling dependency. *Accepted to the 47th IEEE Conf. on Decision and Control*, Cancun, Mexico (Dec.).
- R. Tóth, F. Felici, P. S. C. Heuberger, and P. M. J. Van den Hof (2008). Crucial Aspects of Zero-Order Hold LPV State-Space System Discretization. *Proc. of the 17th IFAC World Congress*, Seoul, Korea (July), pp. 3246–3251.
- R. Tóth, P. S. C. Heuberger, and P. M. J. Van den Hof (2007). LPV System Identification with Globally Fixed Orthonormal Basis Functions. *Proc. of the 46th IEEE Conf. on Decision and Control*, New Orleans, Louisiana, USA (Dec.), pp. 3646–3653.
- R. Tóth, F. Felici, P. S. C. Heuberger, and P. M. J. Van den Hof (2007). Discrete time LPV I/O and State Space Representations, Differences of Behavior and Pitfalls of Interpolation. *Proc. of the European Control Conf.*, Kos, Greece (July), pp. 5418–5425.
- R. Tóth, P. S. C. Heuberger, and P. M. J. Van den Hof (2007). (In)equivalence of discrete time LPV state-space and input/output representations. *Proc. of the 26th Benelux Meeting*, Lommel, Belgium (Mar.), pp. 34.

- R. Tóth, P. S. C. Heuberger, and P. M. J. Van den Hof (2006). Orthonormal basis selection for LPV system identification, the Fuzzy-Kolmogorov c -Max approach. *Proc. of the 45th IEEE Conf. on Decision and Control*, San Diego, California, USA (Dec.), pp. 2529–2534.
- R. Tóth, P. S. C. Heuberger, and P. M. J. Van den Hof (2006). Optimal Pole Selection for LPV System Identification with OBFs, A Clustering Approach. *Proc. of the 14th IFAC Symposium on System Identification*, Newcastle, Australia, (Mar.), pp. 356–361.
- R. Tóth, P. S. C. Heuberger, and P. M. J. Van den Hof (2006). Robust and optimal selection of OBFs based model structures. *Proc. of the 25th Benelux Meeting*, Heeze, The Netherlands (Mar.), pp. 27.
- R. Tóth, P. S. C. Heuberger, and P. M. J. Van den Hof (2005). Identification of LPV systems using orthonormal basis functions. *Proc. of the 24th Benelux Meeting*, Houffalize, Belgium (Mar.), pp. 70.
- R. Tóth and D. Fodor (2004). Speed Sensorless Mixed Sensitivity Linear Parameter Variant H_∞ Control of the Induction Motor. *Proc. of the 43rd IEEE Conf. on Decision and Control*, Atlantis, Paradise Island, Bahamas (Dec.), pp. 4435–4440.

Curriculum Vitae

Roland Tóth was born on September 7, 1979 in Miskolc, Hungary. He started his secondary education in 1994 at the Vetési Albert Secondary Grammar School in Veszprém, Hungary, and finished it in 1998. He specialized in computer science and received a software operator license. As a student, he worked for the Virus Buster Company as an Assembly programmer in 1996.

From 1998 to 1999, he studied at the Auburn University of Montgomery (AUM) in Alabama, USA, as a beneficiary of the International Scholarship for Foreign Students. During the period 1999-2004, he continued his studies at the University of Pannonia in Veszprém, Hungary, where he followed a 5-year MSc. program in Information Technology in parallel with a 3-year BSc. program in Electrical Engineering. He graduated from both programs with summa cum laude. His theses dealt with the design and implementation of Linear Parameter-Varying (LPV) optimal control on induction motor drives in a speed sensorless setting and were recognized by national prizes of the Scientific Society for Measurement, Automation and Informatics (MATE) and the Foundation for Technological Progress in Industry (IMFA). He also had the honor of receiving twice the second prize with his papers at the National Scientific Students' Associations Conference in Informatics in Hungary, which resulted in international publications.

In 2004, he started working as a Ph.D. student at the Delft Center for Systems and Control research group, Delft University of Technology, the Netherlands. With his supervisors P. M. J. Van den Hof and P. S. C. Heuberger, he worked on identification and modeling of LPV systems, in a project supported by the Netherlands Organization for Scientific Research (NWO). During the period 2004-2005, he took graduate courses at the Dutch Institute of Systems and Control (DISC), and received the DISC certificate.

In 2005 he married Andrea, the most admirable woman, who made his life complete and they lived happily ever after. In 2006 their son Sándor was born, who has shown incredible interest towards sports cars and Hungarian folklore music since his birth. They wonder what he is going to choose. In 2008, they were also gifted by a daughter, Lujza, who has been an admirable little lady since her birth.

In his spare time, Roland likes to listen to music and read. He also has a long-standing affection towards role-playing games and model building.